The effect of material properties on the compactability of some untreated roadbuilding materials

by

Christiaan Johan Semmelink

A dissertation submitted as fulfilment for the degree

Doctor of Philosophy
in the Department of Civil Engineering
Faculty of Engineering
University of Pretoria

Pretoria

October 1991

SUMMARY

The proper densification of the separate pavement layers forms an integral part of road construction. Many problems, are, however, experienced in this area. Because of a lack of knowledge the compaction of untreated roadbuilding materials in problem situations is usually approached on a "trial and error" basis rather than basing possible solutions on scientific evidence of the collective influence of the material properties and site conditions.

The purpose of the study was to place the compaction of untreated roadbuilding materials on a more scientific basis. An investigation was therefore launched to determine the effect of measured material properties on their compactability. A non-standard vibratory compaction test was used to compact the samples in one layer. New test parameters to quantify the shape and texture of the material were also developed, namely the shakedown bulk density and the shape factor. The CBR values of the materials at moulding moisture content were determined for each material for a range of densities and moisture contents. The maximum dry densities (MDD) (vibratory and mod. AASHTO) and optimum moisture content (OMC) (vibratory and mod. AASHTO) were also determined.

The measured values were then evaluated in terms of the following physical properties of the materials: grading, Atterberg limits, linear shrinkage, shakedown bulk density (SBD), loose bulk density (LBD), shape factor (SF) and specific rugosity (S_{rv}). In the extensive laboratory study of 21 different untreated roadbuilding materials, varying from TRB classes A-7-6 to A-1, it was found that both the maximum dry densities and moisture regimes can be quantified in terms of the grading, liquid limit and linear shrinkage of the materials. These relations were modelled by means of regression analysis.

Besides this a general bearing capacity model was found for all these materials where the CBR is a function of the dry density and moisture content of the material. This model was further refined to take account of the influence of shape and texture of the particles so that it is possible to determine reasonable estimates of the bearing capacity for a range of densities and moisture contents from the grading, Atterberg limits, linear shrinkage, shakedown bulk density and shape factor.

This investigation has shown that physical laws govern both the compactability and bearing capacity of untreated roadbuilding materials, irrespective of their composition or nature, making it possible to approach the compaction of untreated roadbuilding materials in a more generalised manner.

SAMEVATTING

Die behoorlike verdigting van die afsonderlike plaveiselllae vorm 'n integrale deel van padkonstruksie. Baie probleme word egter op die gebied ondervind. As gevolg van 'n gebrek aan kennis word die verdigting van onbehandelde padboumateriale in probleemsituasies gewoonlik op 'n "probeer en tref" basis benader in plaas van om moontlike oplossings op wetenskaplike getuienis van die gesamentlike invloed van die materiaaleienskappe en terreintoestande te baseer.

Die doel van die studie was om die verdigting van onbehandelde padboumateriale op 'n meer wetenskaplike basis te plaas. 'n Ondersoek is dus geloods om die effek van die gemete materiaaleienskappe op hulle verdigbaarheid te bepaal. 'n Nie-standaard vibrasie verdigtingstoets is gebruik om die monsters in 'n enkellaag te verdig. Nuwe toets parameters wat die vorm en tekstuur van die materiaal kwantifiseer, is ook ontwikkel, naamlik die skudbrutodigtheid en vormfaktor. Die KDV waardes van die materiale by verdigtings-voggehalte is ook bepaal vir elke materiaal vir 'n reeks digthede en voggehaltes. Die maksimum droë digtheid (MDD) (vibreer en gew. AASHTO), optimum voggehalte (OVG) (vibreer en gew. AASHTO) is ook bepaal.

Die gemete waardes is toe geëvalueer in terme van die volgende fisiese eienskappe van die materiale: gradering, Atterberggrense, lineêre krimping, skudbrutodigtheid (SBD), los bruto digtheid (LBD), vormfaktor (SF) en kliptekstuur "specific rugosity" (S_{rv}). In die uitgebreide laboratoriumondersoek van 21 onbehandelde padboumateriale, wat gewissel het van TRB klas A-7-6 tot A-1, is daar bevind dat beide die maksimum droë digthede en die vogregimes gekwantifiseer kan word in terme van die gradering, vloeigrens en lineêre krimping van die materiale, Hierdie verbande is gemodelleer deur middel van regressie analise.

Hierbenewens is gevind dat daar 'n algemene dravermoë model bestaan vir al hierdie materiale waar die KDV 'n funksie is van die droë digtheid en voginhoud van die materiaal., Hierdie model is verder verfyn om die invloed van vorm en tekstuur van die partikels in aanmerking te neem, sodat dit moontlik is om redelike skattings van die dravermoë te maak vir 'n reeks digthede en voggehaltes vanaf die gradering, Atterberggrense, lineêre krimping, skud bruto digtheid en vormfaktor.

Hierdie ondersoek het getoon dat fisiese wette die verdigbaarheid en dravermoë van onbehandelde padboumateriale beheer, wat dit gevolglik moontlik maak om die verdigting van onbehandelde padboumateriale op 'n meer wetenskaplike manier te benader.

ACKNOWLEDGEMENTS

I would like to thank the following persons and organisations for their aid and contributions:

Dr C R Freeme, director of the Division of Roads and Transport Technology (DRTT) of the CSIR for his permission to publish and submit this dissertation, which is based on research that was performed at the Division.

The Department of Transport and the provincial road authorities of South Africa for their funding, support and assistance of this research.

Prof. A T Visser for his tremendous support and supervision of this thesis.

The research team members Wynand Brink, Joseph Meadows, Joseph Marima, Nathanael Masango, Reuben Rakabe and John Matabane for their loyalty, support and hard work in executing the extensive laboratory research programme as well as other persons, both DRTT colleagues and others, who assisted with the research in one way or another.

All the persons, both DRTT colleagues and others, who helped with the drawings and the typing of this thesis, in particular Mrs Trudie Hübener and Mrs Bets Diering.

All my colleagues and others for their interest, moral support and assistance, in particular Dan Silcock, Coen Coetzee and Chris van der Merwe.

My wife Noëlla and daughters, Hannelie and Corine, for their interest, encouragement, support and prayers.

My late mother, my brothers and sisters, and other family and friends for their interest, encouragement, support and prayers.

Above all I would like to thank God who carried and guided me throughout the investigation and gave me the insight I lacked so that I could complete this investigation successfully.

"You are worthy, our Lord and God,
to receive glory and honour and power,
for You created all things,
and by your will they were created
and have their being." Revelations 4:11 (NIV)

CONTENTS

LIST OF ABBREVIATIONS

AASHO	=	American Association of State Highway Officials
AASHTO	=	American Association of State Highway and Transportation Officials
AD	=	Apparent density (= 10 x ARD)
ARD	=	Apparent relative density
BPR	=	Bureau for Public Roads
BRD	=	Bulk relative density
CBR	=	California bearing ratio
CBR:CMC	=	CBR at critical moisture content (CMC) (%)
CBR:decrease	=	Percentage decrease in strength of CBR due to moisture content deviation from CMC (% CBR:CMC)
CMC	=	Critical moisture content
DBD	=	Dry bulk density (= 100 x BRD)
DD	=	Dry density
EMC	=	Equilibrium moisture content
GF	=	Grading factor (see p 98 for definition)
IGF	=	Ideal grading factor for "ideal" grading
LBD	=	Loose bulk density
LL	=	Liquid limit
LS	=	Linear shrinkage
MAMC	=	Maximum allowable moisture content
MC	=	Moisture content
MDD	=	Maximum dry density
mod. AASHTO	=	Modified AASHTO compaction effort
OMC	=	Optimum moisture content
PI	=	Plasticity index
PL	=	Plastic limit
PRA	=	Public Roads Administration
SBD	=	Shakedown bulk density
SCMC	=	Standardised critical moisture content
SD	=	Solid density (expressed as percentage of AD for non-porous materials) or solid density (expressed as percentage of DBD for porous materials)
SF	=	Shape factor

SOMC	=	Standardised optimum moisture content
S_{rv}	=	Specific rugosity
std. AASHTO	=	Standard AASHTO compaction effort
SZAVMC	=	Standardised zero air voids moisture content
T_n	=	Outlier coefficient (see p 88)
vib	=	Vibratory compaction effort
ZAVD	=	Zero air voids density
ZAVMC	=	Zero air voids moisture content

CHAPTER 1
INTRODUCTION, PURPOSE AND STRUCTURE OF PROJECT

1.1 Introduction

Before it is possible to study the subject it is necessary to have a clear understanding of the term "compactability" or "compactibility". The word is made up in two parts namely by the verb "compact" and the suffix "ability" or "ibility".

From the definitions listed in Appendix A the meaning of the term "compactability" in terms of roadbuilding materials is clearly the "capacity of the material to consolidate and densify through the loss of internal pore space in response to the exertion of some form of compaction energy". The amount of densification that takes place is dependent on the amount and type of compaction energy applied and the insitu moisture content of the material. For a given compaction energy there is a maximum level of density. Furthermore there is an ultimate level of density beyond which the material cannot be compacted. If more energy is applied this normally leads to dedensification due to the degradation of the material.

The compactability of roadbuilding materials is usually described in terms of the dry density that could be achieved for a certain amount of compaction effort being exerted on the soil in a specific manner (ie std. AASHTO, mod. AASHTO or vibratory compaction). Besides the amount of compaction energy it has long been known that the grading of material has an important influence on the levels of density that could be achieved and that a well-graded material can be compacted better than a poorly-graded or uniformly-graded material. The particle size of the largest particles also has a tremendous effect on the level of density and bearing capacity that can be achieved. Other material properties, such as the general shape and texture of the individual particles as well as the Atterberg limits and the linear shrinkage all have an effect on the compactability of a material and have subjectively been included in specifications.

The problem is that it is still not known to what extent these properties, separately and collectively, influence the compactability of untreated roadbuilding materials. Because of this lack of knowledge the compaction of untreated roadbuilding materials is still more an "art" than a "science" in that it cannot rightly be explained why certain results are achieved. Because of this lack of knowledge, engineers tend to be conservative in their decisions; sometimes demanding the impossible by specifying density levels that cannot be achieved. On the other hand, sometimes being overly lenient, with detrimental consequences for the

projects involved. At the same time most "problem" situations are approached on a "trial and error" basis rather than basing possible solutions on scientific evidence of the collective influence of the material properties and site conditions.

For the compactability of untreated roadbuilding materials to change from an "art" to a "science", it will be necessary to quantify the influence of each of the properties on the compactability of untreated roadbuilding materials. Once these relationships have been established, it will be possible to deal with the compaction of untreated roadbuilding materials in a far more effective manner than is presently possible.

1.2 Purpose of the research project

The purpose of the research is to quantify the effects of material properties on the compactability of untreated roadbuilding materials in general by means of a structured research programme. For this reason a range of vastly different materials, ranging from a black clay (A-7-6) to several crushed rock materials (A-1) used for G1-base construction were chosen. The material properties which are included in defining a particular material are the following:

- the grading (percentages passing 75 mm, 63 mm, 53 mm, 37,5 mm, 26,5 mm, 19 mm, 13,2 mm, 4,75 mm, 2 mm, 0,425 mm and 0,075 mm) (normal indicator sieve range used in South Africa)
- the Atterberg limits (LL, PL and PI)
- the linear shrinkage (LS)
- factors to define the shape and surface texture of the particles (eg the specific rugosity or particle index)
- the maximum dry density and optimum moisture content for the vibratory compaction table
- the maximum dry density and optimum moisture content for the mod. AASHTO compactive effort
- the CBR values of the compacted materials immediately after compaction for a range of dry densities and moulding moisture contents (not soaked)

The specific aims of the research project are as follows:

- To develop models by means of which the maximum achievable dry density and moisture requirements can be predicted from the previously mentioned material

properties.

- To develop a model by means of which the bearing capacity of the material can be predicted from the previously mentioned material properties for a range of densities and moisture contents.

Achievement of these goals will give engineers a much better appreciation of how the inherent material properties as quantified by the indicator tests influence the maximum dry density, the moisture regime and the bearing capacity of the material and change the compaction process from an "art" to a "science". Apart from this it could lead to a substantial reduction of required laboratory compaction tests on sites and savings in project costs due to more optimal compaction procedures as well as an improvement in pavement performance.

1.3 Structure of document

The layout of this dissertation is shown diagrammatically in Figure 1.1.

The literature survey on the influence of material properties and other factors on compactability covers the following:

- the theory of compaction
- the influence of density
- the influence of moisture content
- the influence of the grading
- the influence of particle shape and texture
- the influence of the Atterberg limits and the linear shrinkage
- the influence of the crushing strength of the material
- the influence of the bearing capacity of the underlying layers
- the bearing capacity of materials.

In the chapter on laboratory procedures followed to determine the material properties the data collection procedures followed as far as the density, moisture content and bearing capacity (CBR at moulding moisture content) are discussed. Standard test procedures are not discussed, but modification of standard test procedures are presented, for example the procedure followed to compact samples on the vibratory compaction table, the weighted CBR value, the shape factor (SF) (modification of the specific rugosity) and the shakedown bulk density (SBD).

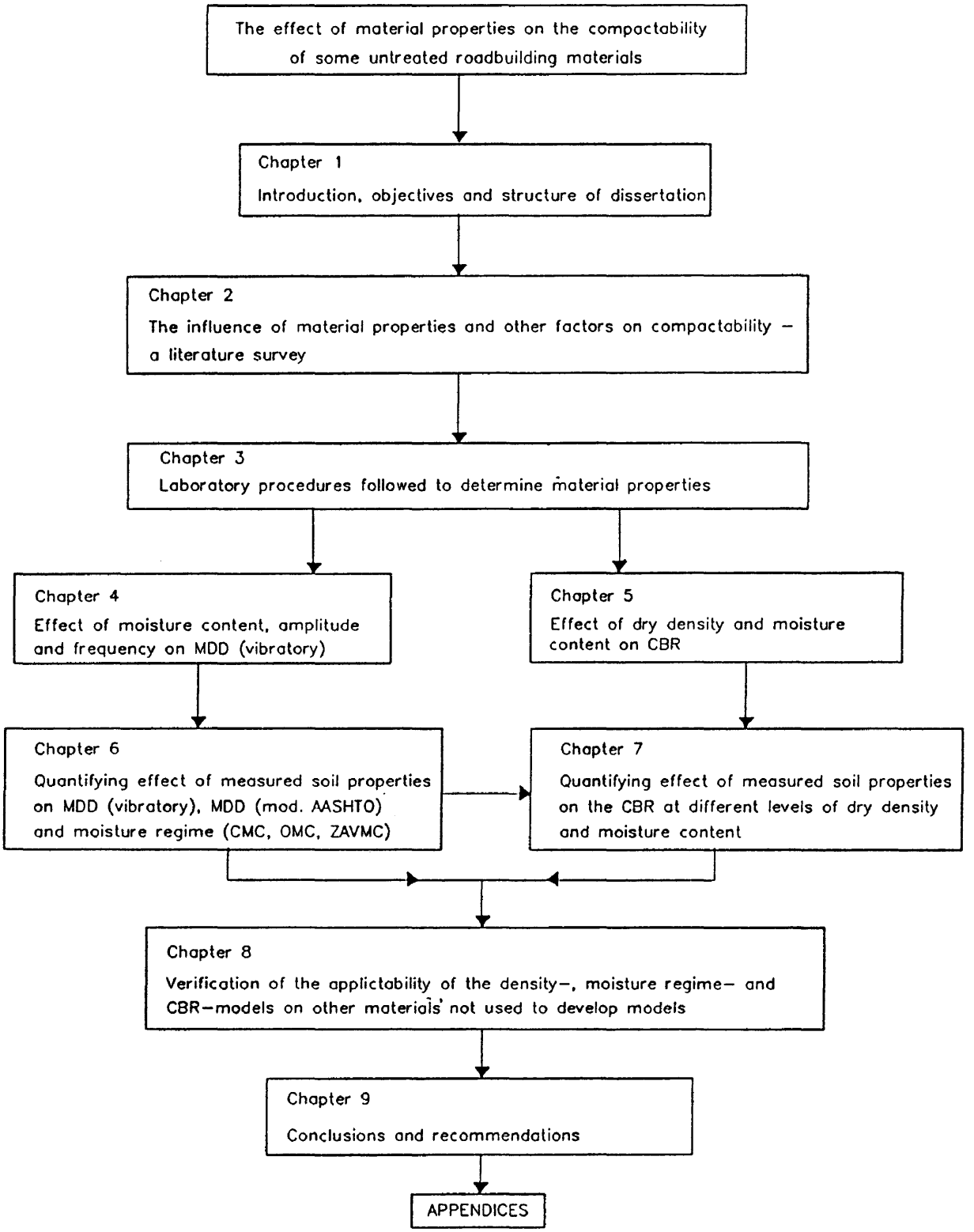

FIGURE 1.1 LAYOUT OF THIS DISSERTATION

Chapter 4 deals with the effect of moisture content and frequency - amplitude combination on the maximum dry density (MDD) (vibratory) as well as a comparison between MDD (vibratory) and MDD (mod. AASHTO).

This is followed by a discussion of the effect of dry density and moisture content on the CBR of materials for a range of densities (90 %, 93 %, 95 %, 97 %, 100 % and 100+ % mod. AASHTO) and a range of moisture contents (on both sides of OMC). The observation of a critical moisture content (CMC) for each material as well as the development of a general bearing capacity model where the insitu CBR is a function of the dry density and the absolute difference between the CMC and MC of the material are also discussed.

The next chapter deals with the quantification of MDD (vibratory), OMC (vibratory), ZAVMC (vibratory), CMC, MDD (mod. AASHTO), OMC (mod. AASHTO) and ZAVMC (mod. AASHTO) in terms of the grading, Atterberg limits and linear shrinkage of the materials.

This is followed by the quantification of the moulding CBR (equivalent to the insitu CBR) for a range of densities and moisture contents in terms of the grading, Atterberg limits, linear shrinkage, the shakedown bulk density (SBD) and the shape factor (SF) of the materials.

The penultimate chapter deals with the verification of the applicability of the density-, moisture regime- and CBR-models on other materials not used to develop these models by comparing the theoretical results with the actual results obtained.

The final chapter, Chapter 9, contains the conclusions and recommendations on how this knowledge could be applied effectively in practice as well as needs for further research.

The following information is listed in the Appendices.

Appendix A	List of word definitions to define "compactability".
Appendix B	Calibration of the vibratory compaction table.
Appendix C	List of MDDs, OMCs and ZAVDs for materials for different frequency-amplitude combinations on the vibratory compaction table (Chapter 4).
Appendix D	Listing of CBR, DD, MC results of original materials and regression analysis results and remaining figures of original CBR-models as a function of DD, CMC and OMC (Chapter 5).

Appendix E Listing of material properties used to model MDDs (vibratory and mod. AASHTO), OMC (vibratory and mod. AASHTO), ZAVMCs (vibratory and mod. AASHTO) and CMC as well as regression analysis results of these models (Chapter 6).

Appendix F Listing of the shakedown bulk density (SBD), loose bulk density (LBD), shape factor (SF) and specific rugosity (S_{rv}) values of the original materials and regression analysis results of CBR:CMC and CBR:decrease models in terms of DD, SBD (LBD), SF (S_{rv}), CMC and MC as well as regression analysis results of updated models for MDDs and moisture regime which include SBD and SF as variables (Chapter 7).

Appendix G Listing of CBR, DD, MC results used for verification of the compactability and CBR-models, and regression analysis results of models for MDD (vib) and moisture regime for "coarse" graded materials as well as regression analysis results of the final revision of the MDD and moisture regime models for "fine" graded materials with and without the SBD and SF as input variables (Chapter 8).

1.4 Contribution envisaged

Through the quantification of the influence of each of the indicator test values on the maximum dry density (MDD), moisture regime (CMC, OMC and ZAVMC) and the bearing capacity (CBR) at different levels of dry density and moisture content, it will be possible to handle compaction procedures in a more scientific manner, rather than handling compaction problems on the basis of past experience of approximately similar situations or trial and error basis.

Engineers will also be able to get reasonable estimates of the MDD, the moisture regime (CMC, OMC and ZAVMC) and bearing capacity (CBR) at different levels of dry density and moisture content, without having to perform a vast number of tests in the laboratory. This will lead to benefits both in the planning and construction phases of projects.

During the planning phase the identification and selection of suitable roadbuilding materials can be done much more rapidly and effectively, leading to substantial savings in time and effort. During the construction phase the actual compaction procedures can also be approached in a more scientific manner. The movement will be away from method specifications toward end result specifications. Each individual compaction situation can be clearly defined by determining the MDD and the moisture regime from the indicator tests and

comparing them with the measured values in the field. For instance if it is found that the field moisture content is above the estimated ZAVMC of the material, the material will have to be dried out before proper compaction can take place. This applies to all roadbuilding material containing a substantial amount of fines. The only exceptions to this rule is possibly rockfill and crushed stone base material due to their free draining nature.

The material should, however, never be seen in isolation, but one should also take account of the effect of procedures on the already completed construction work. For instance it will usually be impossible to effectively compact a layer properly if the support of the underlying layer is weak. Wherever possible, the support of the underlying layer should be improved as far as possible (possibly by draining or drying out) before placing and compacting the next layer. Similarly slushing of crushed stone bases should preferably only be done if the subbase is stabilised as the water drains downward and may weaken the subbase if not stabilised. To prevent this from happening the Cape Provincial Administration slush very short sections (100 m) of the crushed stone base at a time when the subbase is not stabilised.

The all too familiar phenomena on construction sites of "over rolling" can hopefully be eliminated as engineers and their construction teams will now appreciate the detrimental consequences of an over-application of energy, which leads to excessive degradation of the material and therefore dedensification of the layer. This will not only lead to savings in construction costs but should also improve the performance of the materials themselves thereby leading to improved life expectancy of roads, and in the long run the specification of more optimal design standards for compacted layer work.

CHAPTER 2
THE INFLUENCE OF MATERIAL PROPERTIES AND OTHER FACTORS ON COMPACTABILITY - A LITERATURE SURVEY

It has long been known that the material's physical properties such as grading, Atterberg limits, linear shrinkage and shape and texture of individual particles have an influence on the compactability of the material and have therefore featured in the design specification. The exact influence of each of the properties on the compactability have, however, never been quantified.

Apart from the material's physical properties, the work of Proctor and others showed that factors such as the moisture content, the magnitude and the manner in which the compactive effort was being applied, as well as the reactive support of the underlying material during the compaction process all had an important influence on the results that could be achieved.

2.1 Theory of compaction

In the work by Proctor and others general trends in the reaction of untreated roadbuilding materials were observed when being compacted. If a particular material with a particular grading is compacted with a certain application of compactive energy (eg standard AASHTO (Proctor) or modified AASHTO) at a particular moisture content, approximately the same level of density is invariably achieved for the same compactive effort. If the moisture content of this material is changed and the same compactive effort is applied a different level of density will be achieved than before. For a range of moisture contents a range of density levels will be achieved, reaching a maximum level at a particular moisture content (Figure 2.1). The moisture content at which the dry density of the material reaches a maximum level is called the optimum moisture content (OMC) because optimal densification of the particular material is achieved at this moisture content for the particular compactive effort.

Because the in-situ moisture content of a material varies from point to point and changes with changes in the environmental conditions, density is always expressed in terms of solid material contained in a unit volume (ie kg/m^3). The dry density at the point where the maximum density level is achieved is referred to as the maximum dry density (MDD).

The MDD and OMC values of a material will vary with the nature and size of the compactive effort. Within limits, an increase in compactive effort normally leads to an increase in the MDD and a decrease in the OMC for the same roadbuilding material (see Figure 2.1).

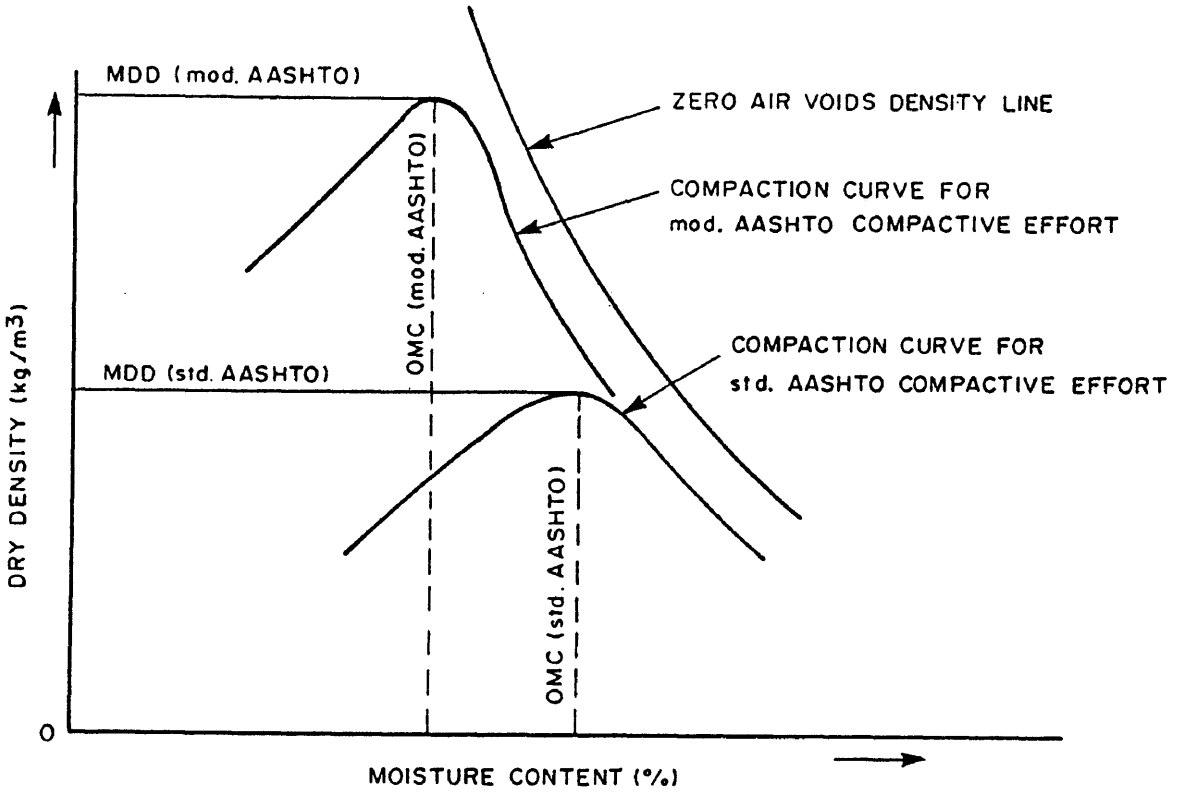

FIGURE 2.1 GENERAL RELATION BETWEEN THE DRY DENSITY OF UNTREATED ROADBUILDING MATERIALS AND THE MOISTURE CONTENT AT THE TIME OF COMPACTION

Similarly the MDD and OMC of the material will vary with the composition of the material itself. Materials consisting of a wide range of particle sizes, ranging from coarse to fine, always have higher MDDs and lower OMCs than materials with a limited range of particle sizes such as fine-graded roadbuilding materials.

The relative density of the "solids" of the materials also plays a role in that the mass per unit volume will be greater for a particular grading as the value of the apparent relative density

(ARD) or bulk relative density (BRD) of the "solids" of the material increases. This fact has extremely important consequences in practice as the geological composition of materials vary tremendously from point to point on a construction site as well as from one borrow pit to another, even though the materials appear to be similar. This has lead to the practice in South Africa of expressing the density in terms of the space occupied by the "solid" material per unit volume (ie solid density (SD) expressed as a percentage of apparent density (% AD) or percentage of dry bulk density (% DBD)) particularly as far as the higher quality crushed stone materials used in the upper layers of the pavement structure are concerned. This was done because the impact compaction tests were found to be unsuitable for the determination of the MDD and OMC of coarse granular materials.

The American Society for Testing Materials (ASTM) specify the density in terms of relative density, where the relative density D_d is defined as follows:

$$D_d = \frac{e_{max} - e}{e_{max} - e_{min}} \times 100$$

or

$$D_d = \frac{\gamma_{max}(\gamma - \gamma_{min})}{\gamma(\gamma_{max} - \gamma_{min})} \times 100$$

where D_d = relative density (%)
e_{max} = maximum void content at minimum density γ_{min}
e_{min} = minimum void content at maximum density γ_{max}
e = actual void content at measured density γ
γ_{min} = minimum density (kg/m^3)
γ_{max} = maximum density for specific compactive effort (kg/m^3)
γ = measured density (kg/m^3)

2.2 Influence of density

2.2.1 Reasons for controlling density

Although there seems to have been a general understanding in the early years that an increase in the maximum dry density of a material generally improved the bearing capacity

of the material as well, usually only metalled or paved surfaces were compacted in some manner. Generally in the early part of this century roads tended to follow the topography of the landscape and cuts and fills were limited to the absolute minimum. Fills were then constructed by end-dumping the loose material without benefit of compaction as filling progressed. The settlement of the fill was usually considered largely to be a function of time. Paving was delayed until the fill had sufficient time to settle without exactly knowing when settlement of the fill would be complete.[1]

The coming of motorized vehicles increased the demand for better roads, with better alignment; cuts and fills became much larger, and the time delays for proper settlement of the fills could no longer be afforded.

> "This resulted in materials being placed in layers, in some instances moistened, and either compacted by distribution of hauling equipment or "thoroughly compacted" by rolling in order to prevent settling. Controversy often arose over what constituted adequate compaction under the requirement "thoroughly compacted", "thoroughly rolled", or rolled "to the satisfaction of the engineer." This resulted in demands for controls for use in checking the results of the contractors' operations in highway construction" [1].

2.2.2 Development of density tests

The first work along these lines was done by the California Division of Highways in 1929. From an extensive series of tests they developed field equipment and a method of compacting material samples to determine the maximum dry density (MDD) and optimum moisture content (OMC) requirements before construction. Subsequently these values were used for control purposes of the actual constructed layer work. This test used a 3-in. diameter cylinder, a 10-lb. rammer having a 2-in. diameter striking face, and an 18-in. free-drop of the rammer[1].

A test along similar lines, developed by Proctor for use in earth dam construction, was reported in 1933. The original apparatus consisted of a cylindrical mould about 4 in. in diameter and 5 in. high. The material was compacted in three layers; each layer was compacted by 25 firm 12-in. strokes of a 5,5-lb rammer with a striking face 2 in. in diameter. This test was accepted by the American Association of State Highway Officials (AASHO) in 1938 (AASHO designation: T99-38) and by the American Society for Testing Materials (ASTM) in 1942 (ASTM designation: D698-42T). In standardizing the test, the original 25 firm 12-in. strokes became 25 blows from the rammer dropping free from a height of 12 in. above the surface elevation of the soil on each of the three layers[1]. This test was generally termed the standard AASHO or standard Proctor test.

However it was very soon realised that the MDD Proctor (ie MDD (standard AASHO)) did not present the ultimate density to which a material could be compacted. During the construction of air bases in the United States of America and elsewhere during World War II, the U.S. Army Corps of Engineers developed what became known as the modified AASHO method of compaction for use in preparing specimens for the California bearing ratio (CBR) test. This test employed a 6-in. diameter mould, and compacted a sample 5 in. high, in 5 layers, subjecting each layer to 55 blows of a 10-lb rammer, with a 2-in. diameter striking face, dropping free from a height of 18 inches. During 1957 AASHO standardized the Modified test under AASHO Designation: T180. The ASTM subsequently also accepted the modified test as a standard (ASTM D1557)[1]. This test was generally termed the modified AASHO or modified Proctor test.

The name of the American Association of State Highway officials (AASHO) has since been changed to the American Association of State Highway and Transportation Officials (AASHTO) and therefore names of the compaction tests have also been changed to the standard AASHTO and modified AASHTO compaction tests.

Although the standard AASHTO and modified AASHTO compaction test methods are the most universally used compaction tests, engineers have since the late fifties realised that these tests are not suitable to determine the MDD of all types of materials. To name but one, the MDDs of these tests for coarse granular material did not tie in with the actual densities that could be achieved in practice. These shortcomings caused engineers to look for more suitable laboratory compaction techniques, such as static compaction (seldom used), kneading compaction and vibratory compaction. For untreated roadbuilding materials vibratory compaction tests were found to be suitable and relatively inexpensive in comparison with the kneading compaction tests.

In the field of vibratory compaction tests two approaches were followed namely where the sample is compacted either on a vibratory table with a surcharge on top of the sample practically covering the whole surface area of the sample (TMH1: (1986) Method A11T, ASTM Method D4253-83) or similar to the British test (BS1372: 1967) where use is made of a vibrating hammer fitted with a special tamping foot, which practically covers the whole surface area of the sample.

Fairly early in the research on compaction it was already noted that materials with high MDDs have lower OMCs than materials with low MDDs. This phenomenon was implemented by Woods et al[2], when they developed a classification system for untreated roadbuilding

materials (for use in the Mississippi basin where soils are very uniform over large areas) which was purely based on the MDD that could be achieved. The system reported in 1938, was developed by classifying and averaging data on 1383 Ohio soils (see Figure 2.2)[2]. Curves of constant air voids for a material with an apparent relative density of 2,70 have been superposed on Woods' curves. The figure clearly shows that on the right-hand-side all the curves approach the saturation line (better known as the zero air voids density (ZAVD) line) and the peaks all occur at an air voids content of approximately five per cent. The average curves are all rather similar in shape. Generally a flat curve denotes a uniformly graded soil; a curve with a pronounced peak denotes a well-graded material. Woods' system simply divides soils into groups as shown in Table 2.1[3].

Table 2.1 COMPACTION CLASSIFICATION ACCORDING TO THE OHIO MOISTURE-DENSITY CURVES [3]

MDD (lb/ft^3)	MDD** (% AD)	General value as a foundation	Approximate BPR Class
>130	>77	excellent	A-1, A-2, A-3
120-130	71-77	good	A-1, A-2, A-3
110-120	65-71	fair	A-4
100-110	59-65	poor	A-6, A-7
90-100	53-59	very poor	A-5, A-8
70-90	42-53	unsatisfactory	-

**MDD expressed in % AD for apparent relative density (ARD) of 2,70 (as for Figure 2.2)

The original work of Woods and Litehiser on the so-called Ohio typical moisture-density curves method was extended on the basis of 10149 tests to develop a set of 26 typical curves similar to those in Figure 2.2 except that wet density was plotted against moisture content. These curves apply to materials with an apparent relative density (ARD) of approximately 2,67. Together with the curves a table of MDDs and OMCs for these curves were given. (See Table 2.2)[4, 5].

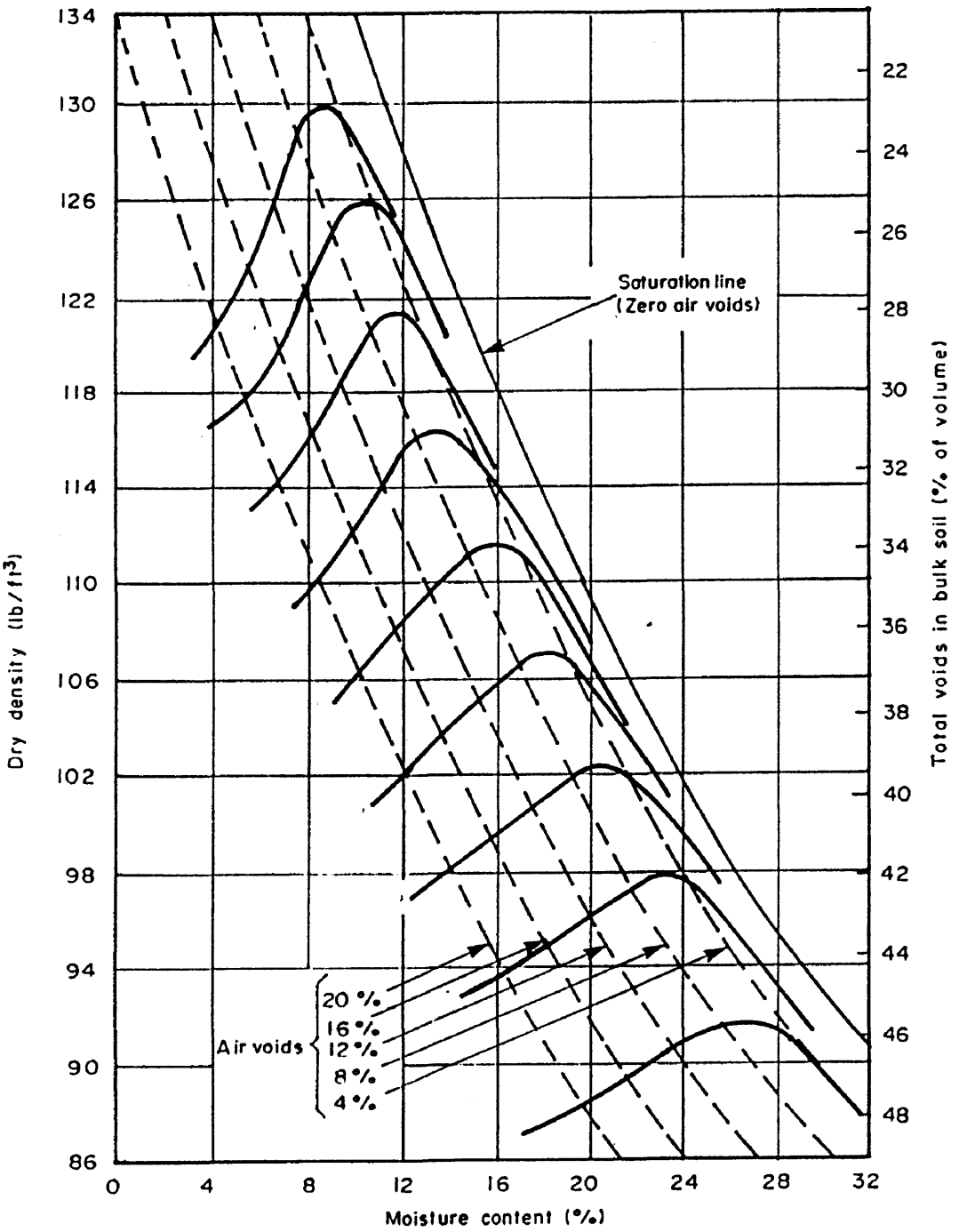

FIGURE 2.2 **AVERAGE RELATION BETWEEN DRY DENSITY AND MOISTURE CONTENT FOR SOILS HAVING MAXIMUM DRY DENSITIES DIFFERING BY 5 LB/FT^3**

(Based on experimental data by K B Woods covering 1 383 soils)

Table 2.2 THE MDDs AND OMCs FOR THE EXTENDED OHIO MOISTURE-DENSITY CURVES [4].

Curve designation	MDD (lb/ft^3)	OMC (%)	MDD* (% AD)
A	141,8	6,6	85,1
B	139,1	7,2	83,5
C	136,3	7,9	81,8
D	134,1	8,5	80,5
E	132,0	9,0	79,2
F	129,3	9,7	77,6
G	126,6	10,5	76,0
H	124,2	11,2	74,5
I	121,7	11,9	73,0
J	119,3	12,7	71,6
K	117,0	13,5	70,2
L	114,6	14,6	68,8
M	112,0	15,8	67,2
N	109,6	16,9	65,8
O	107,1	18,1	64,3
P	104,7	19,2	62,8
Q	102,4	20,3	61,5
R	99,9	21,5	60,0
S	97,4	22,7	58,5
T	94,6	24,4	56,8
U	92,1	25,8	55,3
V	89,9	27,4	54,0
W	87,5	29,5	52,5
X	85,0	30,5	51,0
Y	83,0	31,5	49,8
Z	81,1	32,5	48,7

*MDD expressed in % AD for apparent relative density (ARD) of 2,67 [5]

The Casagrande classification system (1942) also gave an indication of the MDDs and void ratios of the different classes of material (see Table 2.3) [6].

Table 2.3 THE MDDs AND VOID RATIOS FOR CASAGRANDE SOIL CLASSIFICATION[6]

Group Symbol	MDD+ (lb/ft^3)	Void ratio e	Porosity n (%)*	MDD* (% AD)
GW	>125	<0,35	<25,9	>74,1
GC	>130	<0,30	<23,1	>76,9
GU	>110	<0,50	<33,3	>66,7
GP	>115	<0,45	<31,0	>69,0
GF	>120	<0,40	<28,6	>71,4
SW	>120	<0,40	<28,6	>71,4
SC	>125	<0,35	<25,9	>74,1
SU	>100	<0,70	<41,2	>58,5
SP	>100	<0,70	<41,2	>58,8
SF	>105	<0,60	<37,5	>62,5
ML	>100	<0,70	<41,2	>58,8
CL	>100	<0,70	<41,2	>58,8
OL	>90	<0,90	<47,4	>52,6
MI++	>100	<0,70	<41,2	>58,8
CI++	>95	<0,80	<44,4	>55,6
OI++	>95	<0,80	<44,4	>55,6
MH	>100	<0,70	<41,2	>58,8
CH	>90	<0,90	<47,4	>52,6
OH	>100	<0,70	<41,2	>58,8

\+ Applies to soils with apparent relative density (ARD) between 2,65 and 2,75.

* n = e/(1+e).100

** MDD (% AD)=100-n

++ These groups have fallen away in the more recently used Unified Classification System (see ASTM D2487-69)

The compaction tests were originally developed with the concept that they could serve as flexible tools (by varying the compaction effort) to produce MDDs that would reduce settlement and increase strength, as well as assist in the control of soil properties within a given practical range for construction equipment. Some engineers erroneously accepted the MDDs and OMCs (as determined by the standard procedures) as fixed values which could not be exceeded. Because of this misunderstanding, these engineers in positions of authority have felt that it was not good practice to specify that contractors compact materials to more than 100 per cent, as this would be asking for the impossible to be achieved. This reluctance is still prevalent today in some instances.

It is appropriate to note the difference between "density" and "relative compaction." Marek et al[7] had the following to say:

> "There is a distinctive difference between density and compaction. Unfortunately, this difference is often overlooked or ignored. Two aggregate base materials may have the same density, but different degrees of compaction. That is, a material with one gradation of aggregate that is well compacted may have the same unit weight (density) as another aggregate, with another different gradation, that is poorly compacted. The difference must be recognized and dealt with effectively to ensure good base performance. Good compaction always results in good performance, whereas, high density may or may not result in good performance depending on the degree of compaction achieved.
>
> The degree of compaction of any material can only be measured in terms of the materials density after compaction relative to the "maximum" density attainable for the same material, utilizing specific equipment and procedures. Comparing "field" density to "laboratory" density as a measure of compaction is only correct when (1) the material tested in the laboratory is identical to the field materials in gradation, specific gravity, moisture content, etc., and when (2) the same equipment and procedures are utilized to achieve compaction. Changes in factors such as aggregate gradation, construction equipment, and construction procedure will significantly change the density and thereby render the calculated "percent compaction" as meaningless."

The maximum particle size for both AASHTO compaction tests is 19mm (0,75 in). The test methods state that aggregate retained on the 19,0 mm sieve is to be crushed lightly by means of a steel tamper (or laboratory crusher) to pass the 19,0 mm sieve and added to the portion passing the sieve. Some states of the USA do the compaction test only on the material passing the 19,0 mm sieve and then correct the MDD for the presence of oversize particles.

The formula[8] used is as follows:

$$MDD\ calculated = \frac{(MDD_f)\ (AD_c)}{(MDD_f . P_c + AD_c . P_f)}$$

where MDD (calculated) = calculated maximum dry density (kg/m^3)
MDD_f = maximum dry density of -19 mm material (kg/m^3)
AD_c = apparent density of +19 mm material (kg/m^3)
P_c = fraction of +19 mm material in total sample
P_f = fraction of -19 mm material in total sample (=1-P_c)

In the case of porous coarse aggregate the formula[8] is as follows:

$$MDD\ calculated = \frac{(MDD_f)\ (DBD_c)}{(MDD_f(1+A) . P_c + DBD . P_f)}$$

where A = water absorption of the +19 mm material expressed as a fraction
DBD = dry bulk density of the +19 mm material

These formulas are based on the assumption that the coarse aggregate in a compacted mixture acts as a displacer only. In other words all voids between the coarse aggregate particles are always filled with fine aggregate particles. The value of the calculated MDD will therefore vary on a straight line between MDD_f (ie 0 % coarse) to AD_c or DBD_c (ie 100 % coarse) (ie the whole space is occupied by one solid piece of material). This latter assumption is wrong as there will always be voids in the coarse aggregate.

Other methods such as the US Bureau of Reclamation have tried to correct for this last error. According to Marek et al[7] many specifications make little or no mention of the adjustment, if any, that should be made. In South Africa no correction is made presently for this adjustment in aggregate grading; the MDD of the minus 19 mm material taken is to be the correct value of the MDD (mod. AASHTO). Noorany[9] commented:

> "The oversize correction is particularly significant and arises from the elimination of the soil's coarse fraction in the laboratory compaction test, thereby resulting in a lower "maximum" unit weight or IUW than for the total soil sample. Various available oversize correction procedures such as those recommended by CALTRANS and ASTM, AASHTO, or Navy Manual may provide reasonable satisfactory corrections for low gravel contents, but are not accurate enough for gravel contents more than 30 or 40

% depending on the soil type and gradation."

The best answer is obtained by using the entire sample if at all possible, or staying as close as possible to original composition of the material. The maximum aggregate size for compaction tests is normally said to be 0,25D where D is the diameter of the mould.

Marek et al[7] state that all elements of a flexible pavement system should be compacted to a density during construction that will be capable of carrying imposed traffic loads and repetitions of loads, and withstand environmental effects without further densification. If "compacted" materials further densify after construction, permanent deformation of the pavement surface will result and this may be detrimental to satisfactory pavement performance. They concluded that short-sighted economy in compaction procedures, may result in large increases in maintenance costs.

There is, however, one perplexing phenomena, for which no logical explanation has been found as yet, and this is the difficulty that contractors experience to obtain the required field density for silty and clayey soils, and on the other hand the relative ease to obtain the required density for sandy and granular soils when using the modified AASHTO test for determining the MDD.

2.3 Influence of the moisture content of the material

The influence of the moisture content on the compactability of the material has always been recognised as a major factor. The major function of the compaction tests have always been to determine the MDD and the OMC at which this density could be achieved.

If the dry density values are plotted against their respective moisture contents on a moisture-density curve it is found that the MDD values always plot near to the zero air voids density (ZAVD) line on the graph. If the moisture content is higher than the OMC the density starts decreasing parallel to the ZAVD line (see Figure 2.1). From this it is clear to see that the MDD is normally achieved at a state when the material is nearly saturated, that is nearly all voids present are filled with moisture. If more water is added the density starts decreasing because more voids are filled with water which cannot be effectively expelled by compaction due to the reactive nature of the pore pressure which lowers the effective stress levels.

Proctor[10] saw the water as a lubricating agent which coats the surface of the soil grains, reducing the frictional resistance between these soil grains and permitting the compacting

force to become more efficient in arranging the soil fines into the voids between the larger grains. If the moisture content is not sufficient to produce adequate lubrication, the density of the compacted mass will be relatively low. As the moisture content (lubricant) is increased, a point will be reached where the compacting force will overcome this resistance and maximum density will be obtained.

> "As the moisture content is increased beyond this point, the compacting force compresses the small volume of entrapped air in the soil mass. This compression gives rise to hydrostatic pressure, which tends to separate the soil grains by partial flotation; thereby causing a reduction in density"[10].

Hogentogler[10] advanced a multilayer theory on water in the soil, particularly the fine grained cohesive soils. The water in the jackets is attracted by the minerals of the soil grains and has different characteristics in the innermost and outermost layers of the films; the innermost layers are seen to be extremely cohesive and the cohesiveness decreases as the distance from the soil surface increases and gradually grades out to the properties of free water.

Hogentogler's theory indicated that, if the moisture content is low and the moisture films very thin, there will be high resistance between the soil grains as the films are extremely cohesive. As the moisture is increased, the films become thicker and less cohesive, enabling them to serve as lubricants. At the maximum density, these films reach a thickness which gives a cohesive strength at the points of contact that just fails to balance the compacting force used.

> "As the optimum moisture is exceeded the increase in film thickness causes a corresponding increase in the separation of the soil grains and, consequently a decrease in density. Also, as the films thicken, their strength is decreased, resulting in decreased stability of the compacted mass ....." [10].

Research by Turnbull et al[11] on crusher run, Lee et al[12] on clays, sand, sand-clay mixtures and shale, Pike[13] on crushed stone materials and Poulos[14] on clean medium sand (containing some gravel) showed that a totally dry material can very often be compacted to a higher density than a material which contains a low amount of moisture. Pike[13] defined the moisture content at which the minimum dry density was achieved on the dry side of OMC as the "pessimum" moisture content.

Pike[13] agrees with Olson[15] that the concave portion of density versus moisture curves on the dry side of OMC is governed by "negative pore-water pressure". The formation of pore-water menisci between soil particles at their points of contact cause an increase in effective stress from the surface tension of the pore fluid which reduces the effectiveness of the compactive

forces due to higher internal forces which oppose the particle reorientation. The "pessimum" moisture content occurs when all the menisci are fully developed. Beyond this point flattening of the menisci reduces the pressure differential across the surface, whereupon lubrication and double water layers contribute to higher densities.

In postulating his theory of compaction Arquié[16] concluded that for all materials in a crumbled state there is a "critical moisture content" (CMC) (ie W_c on Figure 2.3) at which the cohesion will be a maximum value. If the material is only moistened slightly, the suction stresses are high, the material absorbs the water eagerly and local bonds develop between the particles. The cohesion increases, but not all possible bonds have developed. At the CMC the material is moistened in such a way that moisture is present at all points of particle contact. If the moisture content is higher than the CMC the cohesion starts decreasing because the suction stresses become smaller until the cohesion becomes zero when the material is saturated, because the suction stresses have now been neutralized.

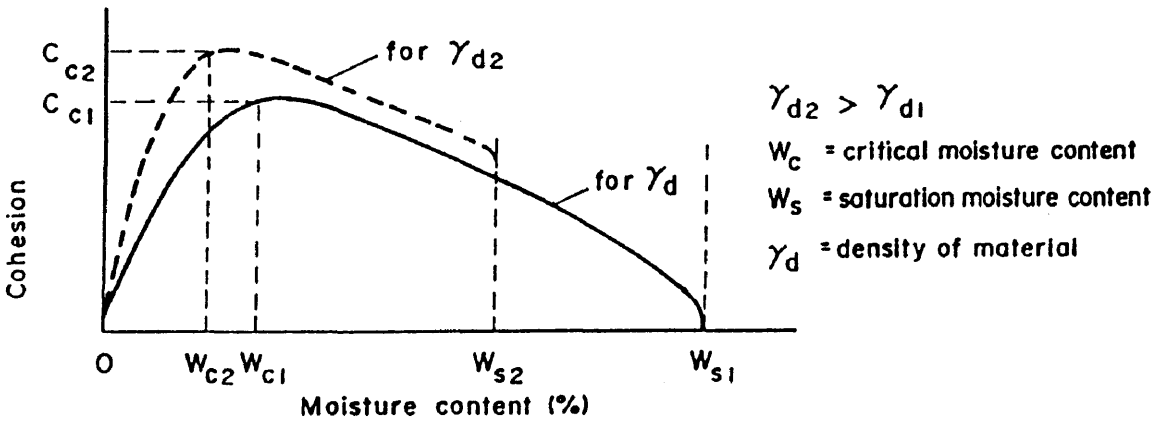

FIGURE 2.3 REAL VARIATION OF COHESION WITH VARYING MOISTURE CONTENT FOR DIFFERENT DENSITIES IN A CRUMBLED SOIL.

Arquié also concluded that both the values of the CMC and saturation moisture content will decrease and that the cohesion would increase with increasing density for the same material. Although not explained it seems his reasoning was that because the particles are packed closer the number of interparticle contacts would be greater, but that the amount of moisture

required would therefore be less due to closer packing of the particles leading to a reduced moisture film thickness required at the CMC (see Figure 2.3).

According to Arquié the other important factor which is influenced by the moisture content is the pore pressure. As long as the material is not saturated the pore pressure is nearly zero, but as soon as the material becomes saturated the pore pressure builds up making it impossible to densify the material any further.

He developed the following partial differential equation:

$$(dD_d /dW) = -a.(dC/dW) + b.(dp/dW)$$

where D_d = density of the material
W = moisture content of the material
C = cohesion in the material
p = pore pressure in the material
a = positive constant
b = positive constant

From the equation it is clear that for a crumbled material as the moisture content increases from zero to CMC (ie $0>W>W_c$) the derivative dC/dW is positive while dp/dW is practically zero, so that D_d decreases for the same compaction effort. In the range between W_c and the zone where the material is virtually totally saturated dC/dW is negative and dp/dW is positive. (The value of p is low for a relatively permeable material). The density D_d therefore increases in this range of moisture contents.

If the material has a high permeability, like coarse granular material, it is even possible to reach the saturation moisture content (ie ZAVD line) because dp/dW is still positive. For materials which are less permeable p will increase rapidly when a critical saturation level is reached (at this point dp/dW will become zero); the material allows itself to be deformed but the density will not increase because dC/dW is also zero.

Arquié's theory therefore ties in with the observations of other researchers that there is a moisture content between zero and OMC at which the material will have a minimum density for a particular compactive effort, after which the density will rise to a maximum at OMC and then once again decrease with increasing moisture contents.

Maree[17] evaluated the performance of granular base materials, both in the laboratory and in the road itself. In the laboratory the material performance was basically assessed by means of repeated loading triaxial compression tests and in the road by means of the performance of the material under the Heavy Vehicle Simulator (HVS) under different conditions.

Maree found that the degree of saturation of the granular base material had a dramatic influence on the shear strength of the material as measured in the triaxial compression test. He found that for the same density (between 87 and 88 % of apparent density) the shear strength more than doubled as the material dried out. He concluded that the suction mainly influences the cohesion. He also concluded that the two factors that have the greatest influence on the shear strength of granular base materials are the density and the moisture content of the material, whereas the stress situation also plays an important role. The modulus of resilience is primarily influenced by the stress situation and the moisture content; the density and plasticity of the fines are the most important secondary factors.

Although the dissertation deals with untreated roadbuilding materials, it is interesting to note that similar tendencies were found for other lubricating agents such as bituminous binders. Lees[18] had the following to say about this:

> "The addition of small quantities of a bituminous binder will, as described by many authors, result in an initial dilation of the aggregate structure with little or no reduction in air voids content..... Further increases in the liquid content, and hence film thickness, are in general accompanied by reduction in viscosity, more complete burial of surface texture irregularities and reduction of surface tension forces at liquid/air interfaces. An accompanying rapid increase in the lubrication effect is common, leading in some cases to the aggregate packing even more densely under the given effort than when compacted alone,...."[18].

2.3.1 Conclusions on the influence of moisture content

The quantity of moisture or other liquid in roadbuilding materials has a tremendous influence on the compactability of all roadbuilding materials. It is, therefore, extremely important to control this parameter to ensure effective compaction. The great variation in the OMCs of materials due to their different gradings (see Table 2.2 and Figure 2.2) also emphasizes the fact why it is impossible to compact highly variable materials properly. For effective compaction it is, therefore, imperative that the material should be as uniform as possible and that the correct amount of moisture or liquid should be added. Because the compactive effort in the field is usually greater than that applied in the laboratory tests, the field moisture content should in most situations not exceed the laboratory OMC. Trying to compact above OMC is

usually a futile and dangerous exercise as it is not only a waste of energy, but normally leads to the degradation of the material as well. The only exceptions to the rule are normally rockfill, crushed stone materials and swelling clays. In the case of rockfill and crushed stone material, this is due to their free-draining properties and in the case of swelling clays to limit swelling (see section on the influence of the Atterberg limits and linear shrinkage on the compactability). Even with the free-draining properties of crushed stone, one should be careful not to add too much water and that the layer is properly "dried out" before the slushing operation is performed to densify the uppermost 50 mm of the layer and rid this layer of excess fines.

2.4 Influence of the grading

2.4.1 Research done on the influence of the grading

The importance of hard, solid, coarse aggregates for building roads was a well known fact through the ages as is evident from the following quotation:

> "Appius Claudius Crassus had urged that the road to Capua be provided with firm foundations and here lay the chief contribution of Rome to the science of road engineering. From the first, heavy vehicles and a large volume of traffic were allowed for, great care being taken to ensure not only a hard-wearing surface but also good drainage. Initially the ground was levelled, then drainage ditches were dug on either side of the route; next a foundation level of heavy stones laid; above this came a stratum of broken bricks or pottery. In other examples the road was excavated to a depth of three feet, the trench filled with loose stones, and above this was laid the surface of well-fitting hexagonal blocks of volcanic stone."[19]

In the eighteenth century roads in France constructed by Pierre Frésaguet

> "consisted of three layers contained by large upright stones at either edge. The foundation was of large heavy stones set on a cambered footing; above this came the 'base course' of somewhat smaller stones, and the surface was composed of small graded stones. Although flush with the surrounding topsoil, this was sure of adequate drainage because of its own cambered surface and the cambering of the levels beneath it."[20]

In England in the first half of the nineteenth century Thomas Telford was well known for his superior roads.

> "The base of his roads was formed of large blocks of stone wedged together with stone chips, giving a cambered layer 9 in. thick at the edges and 15 in. thick in the

middle. This was covered with 6 in. small broken stones followed by a wearing surface of 3 in. of gravel." [21]

Another road engineer, John Loudon MacAdam, also left his mark during the same period.

"He made the subsoil of his roads very firm and shaped to the finished camber; side ditches were also dug for draining the road bed. His road then consisted of a layer one foot thick of small broken stones as cubical as possible, able to pass through a ring 2,5 in. in diameter but not passing a 2 in. ring. No large stones, loose earth or other binding material was allowed. The wheels of the coaches ground the stones together and the dust so made filled the interstices." [22]

All these construction methods were geared for manual construction and were therefore not suitable for mechanical construction. When mechanical construction techniques came to the fore, it was therefore necessary to determine new requirements that would suit these construction techniques.

According to Casagrande[23], the first classification of soils according to their grain-size was developed by M Whitney in 1895 for the US Bureau of Soils. In 1913 the International Society of Soil Science accepted a group division of soil grains recommended by Atterberg. Both these classifications were mainly developed for agricultural purposes.

The first studies with coarse materials to evaluate the effect of aggregate size and grading on their performance involved the proportioning of concrete. Experiments were undertaken by Fuller and others in the United States of America and the findings were reported in the Proceedings of the American Society of Civil Engineers. Although the applicability of these findings to untreated roadbuilding materials may, therefore, be disputed, they are widely used in this field as well as in the field of asphalt mix design. Some of the conclusions[24] were the following:

"1. Stone of the largest size makes the strongest concrete under both compression and transverse loading ie, a graded aggregate in which the maximum size of the stone is 2,25 in. in diameter gives stronger concrete than a graded aggregate with 1-in. maximum size, and the 1-in. stone gives a stronger concrete than 0,50-in. stone.....

2. The largest stone makes the densest concrete. Concrete made with graded stone having a maximum diameter of 2,25 in. is noticeably denser than that with 1-in. stone, and this is denser than that with 0,50-in. stone.

6. Aggregates in which particles have been specially graded in sizes so as to give, when water and cement are added, an artificial mixture of greatest density, produce

concrete of higher strength than mixtures of cement and natural material in similar proportions.....

7. The strength and density of concrete is affected but slightly, if at all, by decreasing the quantity of the medium size stone of the aggregate and increasing the quantity of the coarsest stone. An excess of stone of medium size, on the other hand, appreciably decreases the density and strength of the concrete.

12. In ordinary proportioning with a given sand and stone and a given percentage of cement, the densest and strongest mixture is attained when the volume of the mixture of sand, cement and water is so small as just to fill the voids in the stone. In other words, in practical construction, use as small a proportion of sand and as large a proportion of stone as is possible without producing visible voids in the concrete.

13. The best mixture of cement and aggregate has a mechanical analysis curve resembling a parabola, which is a combination of a curve approaching an ellipse for the sand portion and a tangent straight line for the stone portion. The ellipse runs to a diameter of one-tenth of the diameter of the maximum size of stone, and the stone from this point is uniformly graded.

15. The form of the best analysis curve for any given material is nearly the same for all sizes of stone, that is, the curve for 0,50-in., 1-in., and 2,25-in. maximum stone may be described by an equation with the maximum diameter as the only variable. In other words, suppose a diagram in which the left ordinate is zero, and the extreme right ordinate corresponds to 2,25-in. stone, with the best curve for this stone drawn upon it. If, now, on this diagram the vertical scale remains the same, but the horizontal scale is increased two and a quarter times, so that the diameter of 1-in. stone will be very nearly the one already drawn for the 2,25-in. stone. The chief difference between the two is that the larger size of stone requires a slightly higher curve in the fine sand portion."

In 1923, Talbot et al[25] published their well known formula:

$$p = (d/D)^n . 100$$

where p = percentage passing a sieve size with opening d
D = maximum stone size
n = a constant

This formula was also derived from work done on concrete.

In 1929 Hogentogler and Terzaghi[26] published the U S Bureau of Public Roads classification which divides the materials into different classes according to their grading and observed performance. The grading was described in general terms such as coarse, fine, well graded,

poorly graded, etcetera.

In Germany, George Rothfuchs was looking for asphalt mixes with the highest density possible.

The result of his empirical research[27] gave the following formula

$$P = (d/D)^{0,5}.100$$

where p = percentage passing a sieve size with opening d
D = maximum stone size

It is interesting to note that Huang et al[25], in their investigation into the influence of the shape, angularity and surface texture of the aggregate particles found that there was one gradation according to the Talbot equation which consistently gave the highest density with all aggregates; this was the grading with the exponent n equal to 0,5 (maximum stone size used was 19 mm). It seems that for larger stone sizes this grading is usually difficult to compact and the ASTM specification is therefore based on n equal to 0,45.

The important influence of the grading on the compactability of untreated roadbuilding materials was and still is not always appreciated as is evident from the following remark:

> "Fitting of mechanical analysis curves to curves with known equations, such as the probability integral curve or half of the probability curve, is one possible approach. Such a fitting method allows the expression of the grain-size distribution by two parameters but, although this procedure is interesting, it has little practical value. Simple methods based on the same principle merely describe two points on the curve, and several choices have been proposed.
>
> The best known of these methods is that used by Allan Hazen"[28].

This is the well known uniformity coefficient, U, which was developed in 1892.

$$U = d_{60}/d_{10}$$

where d_{60} and d_{10} are the particle diameters at 60 % and 10 % respectively of the cumulative particle size distribution.

High values for U normally indicate well-graded materials which compact well and usually have high densities. Low values for U normally indicate uniformly-graded or poorly-graded materials which are difficult to compact and have lower densities. The original work was done on filter sands.

In the forties[6] the Casagrande classification system, and the Civil Aeronautics Administration classification system were both developed for the design and construction of runways and taxiways; both required the grading as part of their classification system. Similar to the US Bureau of Public Roads classification system (presently known as the TRB-PRA classification system), the grading requirements were, also, very limited in that they basically divided the material into three fractions namely gravel, sand, cohesive materials (silt and clay). This was most probably due to the fact that all three systems were developed for the classification of natural sources. Materials that were artificially produced through the crushing of rock were not really included.

Where crushed rock was used it would seem that "crusher run" was used and no mention is made of grading requirements. It would seem, however, that with time the requirements which Fuller and Talbot laid down for producing a dense concrete were verified for crushed stone layers as well and incorporated into the specification requirements of crushed stone layers. This was done in the first place to ensure that crushing plant would produce aggregate within certain grading limits. Presently the only untreated roadbuilding materials in South Africa with fixed grading requirements[29] are graded crushed stone (G1, G2 and G3), waterbound macadam (WM) and processed and/or modified natural gravel (G4).

The grading requirements for natural gravel (G5 and G6) are that the maximum particle size should be the lesser of 63 mm or two-thirds of the compacted layer thickness, and minimum grading modulus of 1,5 (G5) and 1,2 (G6) should be obtained.

The grading modulus (GM) is calculated as follows:

$$GM = (300 - (P_{2,00\ mm} + P_{0,425\ mm} + P_{0,075mm}))/100$$

where $P_{2,00mm}$ = percentage passing 2,00 mm sieve size
$P_{0,425mm}$ = percentage passing 0,425 mm sieve size
$P_{0,075mm}$ = percentage passing 0,075 mm sieve size

The grading requirements for gravel-soil (G7) are that the maximum particle size in place, after

compaction should not be greater than two-thirds of the compacted layer thickness and a minimum grading modulus of 0,75 should be obtained. Gravel-soil (G8, G9 and G10) have no grading requirements at all.

The debate on the effect of the aggregate grading on the compactability of roadbuilding materials has still not been concluded. In a fairly recent paper on the rational design of aggregate gradings for dense asphaltic compositions written by Lees[18], the author was rather critical in his views on the existence of an "ideal grading curve" for maximum density. He refers to the work by Fuller and Talbot stating:

> "Historically the best known of all systems of continuous grading is that known as the Fuller curve and is due to Fuller and Thompson (1907). These authors made up gradings of a wide variety of types, and derived a 'maximum density curve' from consideration of their results. As observed by Hveem (1940), this curve follows the two equations
>
> $$p = 100\,(d/D)^{0,2} \qquad \ldots\ldots\ldots\ldots\ldots\ldots\ldots\ldots\ldots\ldots\ldots\ldots (7)$$
>
> and
>
> $$p = 100\,(d/D)^{0,5} \qquad \ldots\ldots\ldots\ldots\ldots\ldots\ldots\ldots\ldots\ldots\ldots\ldots (8)$$
>
> Many authors however, seem to have neglected the first "elliptical" section and assumed equation (9) as synonymous with the Fuller grading
>
> Equations (7) and (8) are special forms of the equation
>
> $$p = 100\,(d/D)^{n} \qquad \ldots\ldots\ldots\ldots\ldots\ldots\ldots\ldots\ldots\ldots\ldots\ldots (9)$$
>
> previously given. Other authors, notably Talbot and Richart (1923), have investigated a wide range of continuously graded systems of this type with varying values of the exponent n.
>
> All approaches of this nature however whether they follow the Fuller tradition, one of Talbot and Richart's curves or arbitrary curves or envelopes such as those of the Asphalt Institute, etc., etc., suffer from the unjustified assumption that some one grading curve is the best to use, regardless of the packing properties of the aggregate or variations in these packing properties from size to size, and regardless of the effort to be applied and of any boundary restraints."[18]

Lees proposed a totally different approach whereby the voids are determined for both the 'coarse' and 'fine' aggregates. From these values it is then possible to determine the percentage of fine aggregate which should be added to the coarse aggregate to give the lowest void content. The aggregate does not necessarily have to be divided into two fractions only, but can also be determined from the separate sieve fractions starting from the coarse side. The important point that Lees makes in this method is that the smaller particle size is consecutively used to fill up as much of the void space between the larger particles.

He pointed out that the porosity of a single size aggregate is not only dependent on the particle shape, but is also influenced by the compactive effort, boundary effects (ie container size or layer thickness versus particle size) and surface lubricating or adhesive effects. He states:

> "..... it is obvious that the porosity of a given aggregate is higher at its loosest state than at its densest. It is not so generally recognised however, that the proportions in which to mix two components for maximum density can change appreciably with the compactive effort applied, WITHOUT ANY ALTERNATION IN TYPES OF AGGREGATE EMPLOYED."[18]

This implies that if the compactive effort is too low to properly compact the coarse and fine fraction to their minimum porosities a greater amount of fines will be required in the mix. The difference in the percentage fines will be

> "the same amount as if the difference in porosity had been caused by different shape at constant effort instead of by constant shape at varying effort"[18].

Lees did experimental work with a variety of aggregate combination over a wide range of size ratios (ie size of "fines" divided by size of "coarse aggregate"). From the results he concluded that the relationship between percentage fines for minimum voids and all other relevant factors could be expressed as follows:

$$\% \text{ fines (by volume)} = f(P_{coarse}, P_{fines}, \text{size ratio})$$
$$= f(P_{average}, P_{difference}, \text{size ratio})$$

where P_{coarse} = porosity of coarse aggregate fraction

P_{fines} = porosity of fines fraction

$P_{average}$ = $(P_{coarse} + P_{fines})/2$

$P_{difference}$ = $P_{coarse} - P_{fines}$

He also compared the reduction in bulk volume on mixing the two components at their optimum proportions in comparison with the sum of their separate bulk volumes (ie relative contraction). He concluded from his experimental work that the relative contraction was independent of $P_{average}$ but dependent upon the size ratio and upon $P_{difference}$ (but irrespective of its sign).

He concluded from his investigation

> "that there can be no such thing as a unique ideal maximum grading curve"

and further observed

> "proponents of the continuous type grading, eg Andreasen and Anderson (1929) extend, probably without justification, the observation that the porosity of a 2-component mix can be reduced by the insertion of a quantity of an intermediate size, into such statements as "one can hardly expect greater density from systems existing of a few sizes fitted together, than from systems in which all sizes are represented in appropriate amount" ..... "[18].

However, in discussing his results on the designs of component gap graded mixtures, designed for minimum void content, Lees admitted that the porosity of the five component mix was 1,5 to 2 per cent lower than that of the three component mix.

In discussing Lees' paper McLeod stated that densely graded mixtures in Canada tend to conform to Fuller grading curves based on "n" equal to 0,5. He also pointed out that Lees' design actually approximated the corresponding Fuller curve. He concluded that

> "from a practical point of view, there seems to be a substantial amount of evidence to support the use of the Fuller curve to the 0,5 power as a guide to the grading curve of maximum density....."[18].

But he also concurred

> "while this can serve as a useful rough guide, it is realized that there can be exceptions, and Dr Lees' paper may provide the reason for these"[18].

Not all researchers are convinced that the grading of the material has a definite effect on the maximum dry density that can be achieved. Sweere[30] investigated the performance of unbound granular base materials. In his laboratory study he used the British Vibrating Hammer Density Test, the Modified Proctor Density Test (ie mod AASHTO density test) and the Single

Point Proctor Density Test (using std. AASHTO density effort). In the case of the vibrating hammer and the Single Point Proctor density tests the material grading was left unchanged with maximum particle sizes of 45 mm and 40 mm respectively. However, in the case of the modified Proctor density test the grading was changed to a maximum particle size of 22,4 mm. He did a regression analysis of the density results of the different compaction tests against one another.

He concluded

> "Noting that the compaction effort applied in the Vibrating Hammer Test and the Modified Proctor Compaction Test is similar, the influence of scaling down the grading on the dry density obtained appears to be small."[30]

He also found that the density results of the single point Proctor density test were generally lower than the density results of to modified Proctor density test and the vibrating hammer density test. He concluded:

> "Since the compaction energy applied in the Single Point Proctor Compaction Test is significantly lower than the energy applied in the two other tests, the conclusion can be drawn that the influence of compaction energy appears to dominate the influence of scaling down the grading. This conclusion is only tentative. A more detailed investigation involving, for instance, the same compaction test on different gradings would be required to substantiate it."[30]

2.4.2 Conclusion on the influence of the grading

A number of researchers, quite independent from one another, came to the conclusion that the Fuller or Talbot equation to the power of 0,5 gives the densest aggregate mix. It is interesting to note that this applies to both untreated material, such as crushed stone material, and treated material, such as portland cement concrete or asphalt mixtures. This confirms that the aggregate packing pattern basically stays the same irrespective of how it is being used.

In the field of untreated roadbuilding materials, this ideal grading is never found in the material in its natural state. But using material with a wide range of particle sizes will always produce a denser mix than material consisting of a uniform particle size. This confirms the positive benefits of mechanical soil stabilization where different materials, with different particle sizes are mixed together for improved density and higher stability than when used separately.

2.5 Influence of particle shape and texture

2.5.1 Research done on the influence of shape and texture

Particle shape and texture have received relatively little attention in research. This is most probably due to the fact that it is extremely difficult to find a single parameter to quantify the influence of shape and texture on the compactability of the material. It is often assumed that higher angularity means better interlocking and higher strength. However, the shape and texture factors that resist shearing also resist compaction, which may be considered as a controlled shearing process. The Oxford Dictionary defines the term "interlock" as "to engage with each other by partial overlapping or interpenetration of alternative projections and recesses". For aggregate particles to "shear" at their contact faces therefore requires that the soil must either increase in volume or break off the interlocking pieces. Therefore, the closer the particles are interlocked, the higher the shear force required in order to shear, as it becomes more difficult to increase in volume due to the lower void content.

Similarly, the particle interlock at points of interparticle contact is much greater for particles with a harsh surface texture than for particles with a smooth surface texture. Higher compactive efforts are therefore required to compact aggregate with a harsh surface texture to the same density as an aggregate with a smooth surface texture. This was already found by Fuller et al[24] as can be seen from the following conclusions.

> "3. Round material like gravel, under similar conditions, gives a denser concrete than broken stone.
>
> 4. Sand produces a denser concrete than screenings of similar sized grains.
>
> 5. A concrete with an angular coarse aggregate, such as broken stone, is stronger than one with a rounded coarse aggregate, like gravel, and the same sand and cement - although the rounded aggregate produces greater density - thus indicating a stronger adhesion of cement to broken stone than to gravel. However, if the sand is also angular, like screenings, but with its grains of the same sizes as the sand, the concrete with rounded coarse and fine aggregate is the stronger, probably because of its greater density."[24]

In his research Lees[31] also investigated the influence of the particle shape on the compactability of the material. He classified particle according to the flatness ratio, p, and the elongation ratio, q, where they are defined as follows:

p = (shortest length)/(intermediate length)

q = (intermediate length)/(greatest length)

Using these two parameters he divided particles into four categories as shown in the following table.

Table 2.4: Classification of particles according to shape used by Lees

3-Dimensional shape	p	q
Equidimensional	> 0,67	> 0,67
Disc	< 0,67	> 0,67
Rod	> 0,67	< 0,67
Blade	< 0,67	< 0,67

He concluded that sieves are not able to efficiently

> "sort particles according to size when the particles are of different shapes. Were the distribution of shapes in aggregate always the same, this might not matter so much, but where one shape predominates, the effect in practice would be that an aggregate composed mainly of Rods would be effectively a complete size coarser in grading than an aggregate of Discs of identical sieve analysis"[31].

As far as the use of the flakiness index is concerned, he concluded

> "It is therefore clearly not sufficient to specify that for a particular engineering purpose the Flakiness Index shall not exceed a prescribed value without also indicating the distribution of (p) and (q) values. It is even more certain that a single criteria for flakiness cannot be applied indiscriminately to all usages."[31]

A substantial amount of research has been done into the influence of shape and texture of different aggregates on their strength by means of triaxial compression test and the shear box test.

Vallerga et al[32] did research on uniformly graded, angular and subrounded material from the same source with a maximum size of approximately 0,2 inch (5 mm) in diameter. Their conclusions were as follows:

> "1. For the void ratios and lateral pressures used in this investigation, the angle of friction of uniformly graded materials up to about 0,2 inch in diameter does not appear to be affected by particle size.

2. For a given value of void ratio, the angle of friction of a granular material appears to increase considerably if the angularity of the particles is increased by crushing, although part of this increase may be due to an increase in surface roughness; however, for samples prepared using equal compactive efforts an increase in angularity of particles appears to cause only a slight increase in angle of internal friction.

3. For uniformly graded aggregates up to 0,2 inch in diameter the effect of particle shape on strength appears to be independent of particle size.

4. The strength characteristics of a granular material are considerably affected by a change in surface roughness of the aggregate particles...."[32]

Gur et al[33] compared the properties of crushed graded materials of which the course fraction was either flaky or non-flaky. They evaluated the performance of these graded aggregates by comparing the amount of breakdown occurring during compaction and their CBR values as well as evaluating the performance of these materials under a laboratory wheel tracking test and determining the triaxial shear-strength factors, c and ϕ, for a single-cycle series and a four-cycle series. They also determined the Aggregate Crushing Values and Los Angeles Abrasion values for different proportions of flaky material in the grading. They concluded amongst others:

"(3) Flaky material is inferior to non-flaky material in mechanical quality. An increase in the flakiness index results in a drop in the abrasion value and in a smaller drop in the crushing value.

(4) Breakage under different modes of compaction is higher in flaky than in non-flaky material. Breakage increases as the compaction energy and compaction stress increase, and as initial particle displacement is impeded by the mode of testing and alignment.

(5) In the test range in question, flakiness has only a slight effect on the strength of graded aggregate.

(6) Specific alignment of the particles does not produce marked strength anisotropy.

(7) Material with a flaky coarse fraction shows a slightly lower horizontal bearing capacity in the absence of vertical support.

The principal conclusion is that, for graded aggregate in ordinary road-building practice, no technological significance attaches to the flakiness of the coarse material used for lower courses. The suitability of graded crushed aggregate in the test range as base-course material for a flexible pavement is not impaired by flakiness. It is doubtful, however, whether flaky material is suitable as aggregate for the surface course."[33]

Pike[34] used a large shear-box test to evaluate the performance of aggregates from 17 sources. The materials had various gradings that ranged from 100 per cent passing the 38 mm sieve to a certain percentage passing the 0,075 mm sieve. The shear-box was 300 mm square in plan, with a capacity of 250 kN shear force and 100 kN normal force. The normal load for tests involving shape was 200 kN per square meter.

He concluded amongst others:

> "3. The degree of compaction, grading and moisture content of aggregates all influence their shear strength; the scale of influence can be assessed via the relation between changes in density caused by these variables and a parameter of shear strength (tan ϕ). An increase in dry density of 1 per cent caused by an improvement in grading leads to an average increase of shear strength of 1 to 2 per cent but the same change in dry density caused by increased compactive effort or optimising of moisture content leads to an average increase of about 5 per cent in shear strength.
>
> 4. An increase in particle angularity or roughness generally leads to a decrease in dry density at a given level of compactive effort but also to an increase in shear strength at low and intermediate levels of normal stress. A three per cent increase in strength was found for a 1 per cent decrease in dry density attributable to an increase in angularity. Limestones as a group, however, exhibit higher levels of compactibility (and hence of shear strength) than would be expected from simple measurements of the angularity of their coarser particles."[34]

Holubec et al[35] evaluated the effect of particle shape on the engineering properties of granular soils. They evaluated four granular materials with particles in the medium to fine sand range. The materials consisted of glass beads and three sands from different sources with different degrees of angularity. Both the maximum and minimum void ratios were determined; the minimum void ratio was determined for two different methods of compaction namely by vibration by horizontal tapping of the mould until no further settlement was observed, and by using the modified Proctor (ie mod AASHTO) compaction method. The latter method generally produced higher densities except for the glass beads. They therefore proposed that maximum density should be determined by method based on compaction rather than on vibration alone. They also found that the particle shape has a major influence on the maximum void ratio (ie minimum density); the void ratio difference therefore, diverges markedly with increase in angularity.

The stress-strain characteristics of the four materials were determined by drained triaxial tests on saturated 2-inch diameter by 4-inch long specimens. The specimens were tested at constant cell pressure and at constant diameter. A miniature penetration test was used to

investigate qualitatively the effect of particle shape on resistance to dynamic penetration.

They found that

> "the shear strength and deformability as given by the strain at failure and strain produced in one-dimensional compression, increase with the increase in angularity of the particles. These effects of particle shape are as great as differences caused by large changes in relative density. The tests showed that the deformability of sands having the same gradation and relative density increased with increasing angularity. This suggests that the common assumption cohesionless soils with high shear strength are less deformable is not always valid.....
>
> The tests performed with the model penetration test apparatus suggest that the Standard Penetration Test (SPT) is also affected by particle shape..... Therefore, SPT correlations with relative density obtained from a particular sand are not necessarily applicable to sands with different particle shape...."[35]

They concluded

> "that the particle shape has a significant effect on the engineering properties of cohesionless soils, and it should be considered as an index property in correlations of properties of granular soils.....
>
> The variation of the engineering properties due to particle shape can be of the same order of magnitude as the variation of the properties due to changes in relative density. Therefore, the use of existing correlations of relative density with engineering properties to predict soil behaviour should be undertaken with caution and with full understanding of the assumptions and limitations of current published correlations for granular soils."[35]

It should be pointed out that the "relative density" mentioned is the ASTM definition of density in terms of maximum and minimum void content in the material (see section on theory of compaction).

Holtz et al[36] did a series of tests on free-draining sand-gravel mixtures to determine the relations between shear resistance and (1) density, (2) amount of gravel, (3) gradation, (4) maximum particle size, and (5) particle shape. They used triaxial compression tests. Four sizes of specimens were selected for studying the effect of specimen size on measured shear strength. The diameter and length dimensions were 1,375 by 3 inches, 3,25 by 8,125 inches, 6 by 15 inches, and 9 by 22,5 inches.

They used sand-gravel mixtures containing various amounts of 0,1875 inch to 0,75 inch, and 1,5-inch, and 3-inch gravel to obtain specific gradations. The sand and gravel was obtained

from a river deposit and the particles were of subangular to subrounded shape. A second group of materials were tested in connection with the design of a rockfill structure. These materials consisted of very sharp angular particles obtained from rock quarry operations. The samples were compacted to different levels of relative density (ASTM approach) ranging from 50 to 70 per cent for the sand-gravel mixtures and 50 to 90 per cent for the quarry rock. The specimens were prepared with the material in a moist condition and were saturated by percolating water through them after application of the chamber pressure but prior to loading axially.

They concluded amongst others:

> "(c) The "initial placement" relative density of the sand or sand-gravel mixtures had appreciable effect on the shear strength. The lowest computed friction value ($\tan \phi = 0,65$) was obtained on the river sand material placed at 50 per cent relative density while the highest value ($\tan \phi = 0,98$) was obtained on the quarry material having 82 per cent gravel sizes and placed at 90 per cent relative density.
>
> (d) While the size of the gravel particles above 0,75 inch itself had no appreciable effect on shear strength because they were few in number, the amount of gravel in the mixture had a very significant effect. The shear strength appears to increase appreciably as the gravel content is increased up to 50 to 60 per cent, depending on the maximum size. After this point is reached the material becomes less well-graded and the actual density does not increase (for constant relative density) and likewise the shearing resistance does not increase, or even may become less.
>
> (e) The shape of the particles affected the friction of the material significantly. An increase in shear strength was observed for the angular quarry material over the subrounded to subangular river materials and density appeared to have a particularly significant effect on the friction of the angular materials."[36]

Marachi et al[37] evaluated the properties of rockfill materials. They tried to assess the effects of modelling of the gradation curves on the strength and deformation characteristics of rockfill materials and investigated the possibility of predicting the angle of internal friction of the actual rockfill material in a dam with a satisfactory degree of accuracy and confidence from the results of tests performed on modelled materials.

They evaluated the rockfill material from three dam sites with particle shapes ranging from very angular to rounded and subrounded. The tests consisted of three series of isotropically consolidated, drained triaxial compression tests on each of these materials. Each series consisted of at least four test specimens having diameters of 36, 12 and 2,8 inches

respectively. The four tests for each specimen size were performed using effective confining pressures of 30 psi, 140 psi, 420 psi and 650 psi. The grading curves of the materials used for the different specimen sizes were similar in shape and had the shape of the Fuller curve with a maximum particle size equal to one sixth of the diameter of the specimen.

They concluded amongst others:

> "3. ..... In comparing the volume change characteristics of the different rockfill types, it appears that under similar testing conditions particle shape has a much greater effect on the volume change characteristics during shear than mineralogy.
>
> 4. Although the general trend of the results seem to indicate that the axial strain at failure increases as the particle size increases, this trend is not pronounced. Again, comparing the rockfill types, particle shape seems to have a much greater effect than mineralogy.....
>
> 7. A comparison of the rockfill materials of various types supports Casagrande's conclusion that materials composed of well-graded and well-rounded particles are superior in their mechanical properties to uniformly-graded angular rockfill materials and thus are more suitable for use in high dams."[37]

Koerner[38] evaluated the effect of particle characteristics on soil strength. The soil characteristics that were studied were:

1. Particle shape, evaluated by varying the sphericity (ratio of projected particle area to area of smallest circumscribing sphere) and angularity.

2. Particle size, evaluated by varying the effective size, d_{10}, of the particles.

3. Gradation, evaluated by varying the coefficient of uniformity of the soil mass.

All soils were tested in triaxial compression using lubricated end platens and samples measuring approximately 4 inch high and 4 inch in diameter. The two types of tests performed were drained and undrained pore pressure tests.

He found amongst others that:

1. The principal stress ratio, σ_1/σ_3, increases with increasing density.

2. Strain at failure decreases with increasing density.

3. There was always an initial volume decrease which becomes less as density increases.

He concluded amongst others that:

> "1. .....Soils with more angular particles and lower sphericities had significantly higher shearing angles than the more rounded particles; the difference was between 6 to 8 degrees.
>
> 2. The friction angle increased with decreasing effective particle size, d_{10}, in the effective size range from fine gravel (2,60 mm) through to clay sizes (0,001 mm). This increase is significant with particle sizes less than 0,06 mm (medium sand and finer).
>
> 3. The effect of varying coefficient of uniformity, U, in the range from 1,25 to 5,0, was negligible on the shearing and friction angles in quartz soils, but on feldspar and calcite soils an increasing U gave higher shearing and friction angles. However, in the latter two mineral soils, large degradations were noted which had the effect of lowering d_{10} of the samples, thus increasing the friction angle (see Conclusion 2). It was, therefore, concluded that, at a given relative density, or void ratio, gradation has a relatively minor effect on the friction angle."[38]

Marsal[39] did large scale triaxial tests on rockfill materials. the maximum particle size was 200 mm and the coefficients of uniformity, U, of the three materials were 19, 14 and 2,5 respectively. One of his main conclusions was that

> "the shear strength is larger in well-graded materials with a low void ratio, whether of alluvial origin or the product of quarry blasting...."

George et al[40] investigated the dilatancy of granular media in triaxial shear. Two contrasting granular materials were used, namely a natural gravel and a crushed limestone. Four continuous gradings were used; all had a maximum particle size of 25,4 mm but the respective minimum particle sizes were 0,15 mm, 2,0 mm, 3,17 mm and 6,37 mm. The granular aggregates were tested in triaxial compression using samples of approximately 100 mm in diameter by 200 mm in height. Complete saturation was ensured before testing. This was necessary to monitor volume changes during loading.

They divided the material characteristics that govern the strength and dilatancy of granular materials into two groups: intrinsic factors, such as surface texture, shape, size and elastic properties of grains, and extrinsic factors, such as grading and porosity or packing of aggregations.

They concluded

> "that between the two factors, shape and texture, the former primarily controls the dilatancy characteristics whereas the latter influences the undrained shear strength."

They stated that the drained shear strength, ϕ_d, is constituted of the following four components

> "(a) strength arising from surface friction, ϕ_μ;
>
> (b) strength due to interlocking (which increases with density of the mix), ϕ_i;
>
> (c) strength corresponding to the energy spent in remoulding (which is zero in a dense mix), ϕ_r; and
>
> (d) strength equivalent to the energy spent in dilating the sample against confining pressure, ϕ_δ."

Some of the other conclusions were the following:

> "1. The main cause of strain in granular materials is relative movement (sliding and rolling) between particles.
>
> 3. The dilatancy during failure increases with decreasing values of physical (solid) friction of the grains.
>
> 4. The strength and dilatancy of granular aggregates depend not on the stiffness of the constituent particles but on the shape and surface texture of the grains.
>
> 5. Crushed gravels of elongated (platey) particles undergo a decrease in volume in contrast to chunky subrounded aggregates, which tend to dilate at failure.....
>
> 6. Dilatancy increases with increasing effective size (d_{10}) - more so in the rounded natural gravel.
>
> 7. Increasing the coefficient of uniformity produces a negligible effect on ϕ_d, doing so, however, decreases the dilatancy component in both gravels."[40]

Barksdale et al[41] investigated the influence of aggregate shape on unbound base materials by means of slow triaxial shear tests and cycle load triaxial tests. They concluded amongst others that:

> "2. Aggregate characteristics including shape, angularity, surface roughness and roundness have an important influence upon the resilient and permanent response of an unbound aggregate. Methods are presented for evaluating

these aggregate properties. The permanent deformation characteristics of disc-shaped granitic gneiss, blade-shaped limestone, and blade-shaped shale aggregates were all very similar for the same gradation and level of compaction. The general appearance of these aggregates were, however, quite different. A blade-shaped quartzite appeared to be slightly more susceptible to rutting than the other crushed aggregates. A cubic-shaped, rounded river gravel with smooth surfaces was over two times more susceptible to rutting than the crushed aggregates"[41].

In his tests on the performance of granular base materials Maree[17] found that the cohesion and friction components of the shear strength were greater for freshly crushed material than that of weathered material. He also found that the friction component increases for harsh surface textures and that better particle interlock is achieved with angular material.

2.5.2 Laboratory methods to quantify shape and texture

Various empirical methods of quantifying the shape, and texture of roadbuilding materials exist and those that have been related to compactability are described below.

2.5.2.1 Angularity Number[42]

The angularity number is determined from the proportion of voids in a sample of aggregate subjected to light compaction with a tamping rod. The least angular (most rounded) aggregates were found to have about 33 per cent voids and the angularity number is defined as the amount by which the percentage of voids exceeds 33. The sample of single sized aggregate is compacted by a 100 blows of a tamping rod which is dropped from approximately 50 mm above the aggregate. The size of the cylinder is approximately 0,003 m^3 in volume (approx 150 mm dia x 150 mm high) and the volume is determined accurately.

The angularity number = 67 - (100.M)/(C.ARD)

where M = mass of aggregate to fill cylinder (g)
C = volume of cylinder (ml)
ARD = apparent relative density of the aggregate

The angularity number ranges from zero for smooth rounded aggregate to about 12 for very angular aggregate. For graded aggregate the angularity number is the weighted average of the angularity number of the separate fractions passing 19 mm and being retained on 4,75 mm.

2.5.2.2 Particle Index[25]

The particle index is determined in a manner similar to the angularity number. The material is placed in 3 layers; each layer is lightly compacted with a tamping rod which is dropped 50 mm onto the aggregate. The test is carried out twice with 10 and 50 blows per layer respectively. The percentage of voids in the aggregate after 10 and 50 blows per layer are determined accurately. The test is also performed on single sized aggregate. The particle index I_a is then determined by the following formula:

$$I_a = 1{,}25\ V_{10} - 0{,}25\ V_{50} - 32{,}0$$

where V_{10} = percentage voids in aggregate for 10 blows per layer

V_{50} = percentage voids in aggregate for 50 blows per layer

For graded aggregate the particle index is the weighted average of the particle index of the separate fractions passing 19 mm and being retained on 4,75 mm.

2.5.2.3 Specific Rugosity[43]

The specific rugosity is determined by comparing the bulk densities (% AD) of aggregate fractions with the bulk density (% AD) of glass spheres of similar diameter. This is done by pouring the aggregate through a funnel with a certain pouring height and overfilling a container which is then levelled off with a straight edge and the mass of the aggregate determined. Five readings are taken for each aggregate fraction. Different funnel orifice diameters, pouring heights, container sizes and glass bead sizes are used for different aggregate fractions. The mass of the glass beads required to fill the container is determined in a similar manner.

The specific rugosity S_{rv} is given by the following equation:

$$S_{rv} = 100.(1-G_A/G_B)$$

where G_A = bulk density of aggregate (% AD)

G_B = bulk density of glass beads (% AD)

and $G_A = (100.M_A)/(ARD_A.V)$

$G_B = (100.M_B)/(ARD_B.V)$

where M_A = average mass of aggregate to fill container (g)
ARD_A = apparent relative density of aggregate
V = volume of container (ml)
M_B = average mass of glass beads to fill container (g)
ARD_B = apparent relative density of glass beads

In the case of graded aggregate the specific rugosity is the weighted average of the specific rugosity of the separate fractions.

Although this test yields good results it is rather cumbersome in that large quantities of graded aggregate have to be sieved to obtain enough material for the pouring tests on each fraction and that different funnels, pouring heights and container sizes are required for the separate fractions. Similarly minimum quantities of glass beads of different sizes are also required. The original test by Ishai et al[43] was done on material smaller than 16 mm. In his research into the compaction of crushed stone bases Van der Merwe[44] extended the test to aggregate sizes smaller than 37,5 mm.

2.5.2.4 Flakiness Index[29, 42]

The only parameter on shape of the aggregate which features in South Africa specification presently, is the flakiness index. It is only stipulated in the specification requirements for graded crushed stone (G1, G2) and waterbound macadam (WM). The specification requirement states that the weighted average flakiness index determined on the -26,5 +19,0 mm and -19,0 mm +13,2 mm fractions should not exceed 35 %.

2.5.3 General conclusions on influence of shape and texture

Pike[13] found that there was a linear relationship between the dry density (%AD) and the angularity number for different aggregate types with the same grading, and that more angular aggregates gave lower dry densities (%AD). Huang et al[25] also found that higher particle indexes resulted in lower densities. The relationship was also linear for a particular grading, but varying from one grading to another; the variation was larger for coarser gradings than for finer gradings. Van der Merwe[44] also found that there was a decrease in density for an increase in the specific rugosity. He also found that the variations were larger for coarser gradings than for finer gradings. However the relationship between dry density (% AD) and the specific rugosity was not linear but parabolic.

There is general agreement amongst researchers that both the shape and the texture of the aggregate particles have a definite effect on the performance of granular materials. At the same porosity "angular" materials are superior in strength to "rounded and subrounded" materials, however, it also requires more compactive effort to compact the "angular" material to a specific level of porosity than is the case with "rounded or subrounded" materials. The shape primarily controls the dilatancy characteristics and the texture the shear strength. At the same time materials with high values of physical friction between particles tend to dilate less than materials with low values of physical friction between particles.

Excessive flakiness causes low density, due to reduced packability, which in turn causes a reduction in strength. Low density, combined with inferior mechanical quality also causes excessive settlement due to fracture under load with time. However, a limited amount of flaky material only leads to a slight reduction in strength and is therefore allowable in most cases. The surface course should preferably not contain any flaky material.

Shape and texture should, however, not be seen in isolation, but should be evaluated together with the other properties such as maximum particle size and grading. Materials composed of well-graded and well-rounded particles are superior in strength to uniformly-graded angular materials.

The main cause of strain in granular materials is relative movement (sliding and rolling) between particles. Proper compaction is therefore not only necessary from a strength point of view, but also to prevent unnecessary deformation of the pavement layers.

Although a lot of work has already been done to evaluate the effect of particle shape and texture on the compactability of a material, more work is still required to quantify the effect of particle shape and texture on the compactability and bearing strength of the material more accurately.

2.6 Influence of the Atterberg limits and linear shrinkage

Plasticity is a major characteristic of the so-called "cohesive" soils. This property enables a material to suffer deformation without noticeable elastic recovery and without cracking or crumbling.

The test which is used by engineers to describe the plastic properties of a soil are the so-called Atterberg limits, namely the plastic limit (PL), liquid limit (LL) and plasticity index (PI).

This test was originally developed by Atterberg for agricultural purposes but in the twenties[45] they were already being used to classify subgrade soils.

Although the Atterberg limits are generally associated with the Casagrande classification system, other classification systems also incorporated them. The Public Roads Administration (PRA) classification system also required the shrinkage limit. This is not the same test as the linear shrinkage (LS) because it measured volume change in the total sample whereas the linear shrinkage is a test on the minus 0,425-mm fraction only.

The linear shrinkage test is a test which was developed by California Highways Department in conjunction with the Atterberg limits to quantify the linear shrinkage of the minus 0,425-mm fraction.

It is clear that the engineers appreciated the serious influence of the cohesive fraction in the material on the overall performance of the material. However this was done more from a strength point of view than from a density point of view, although some researchers[46, 47] have looked at the effect of the Atterberg limits on density.

In looking at the Atterberg limits and linear shrinkage it should be remembered that they are determined on the portion of the material grading which passes the 0,425-mm sieve, thus the fine sands, silt and clay in the material.

At this point it is appropriate to point out that clayey soils at the same dry density react differently depending on whether they have been compacted to the dry side or wet side of OMC, and the method of compaction that was used (static or dynamic). Lambe[48] noted that this is mainly due to the particle orientation, which is more random on the dry side of OMC and parallel on the wet side of OMC. The random orientation on the dry side results in greater cohesive forces, and therefore greater strength at the same dry density than the same material on the wet side of OMC. The random structure on the dry side also causes greater swelling upon wetting, as well as being more permeable. Increasing the compaction effort reduces the permeability of clay since it both increases the compacted density and the orientation of particles[48].

In compacting clays it is therefore important that the engineer should determine the variation of properties of a clay with placement conditions and then select those conditions which most nearly give him the properties desired. The author is of the opinion that this would generally mean that clayey soils should be compacted at OMC or just above OMC to limit swelling of

the subgrade, which is normally the biggest problem as far as roads are concerned. In very arid conditions where the clay is totally dried out, it is allowable to compact at 0 % moisture content provided the embankments are protected against sudden wetting which could lead to wash-aways due to the high permeability of the soil structure due to random particle orientation on the dry side. Partial wetting of clays in arid conditions are detrimental in that they increase the cohesive force, making it more difficult to compact (see section on the influence of moisture content of the material).

2.6.1 Conclusions on the influence of the Atterberg limits and linear shrinkage

Presently the influence of the Atterberg limits and linear shrinkage on the compactability and bearing capacity is only subjective. Although engineers have placed limits on their values for each category of material, their influence has not been quantified. The "linear shrinkage" has in actual fact recently been scrapped as a required indicator value in South Africa. This is unfortunate, because research results presented later have shown that the "linear shrinkage" plays an important role in quantifying the effect of the soil fines on the compactability and bearing strength of all untreated roadbuilding materials.

2.7 Influence of the crushing strength of the material

According to Scott[49] the magnitude of normal stresses applied to a soil by most engineering structures is far below that required to produce crushing of the grains. He mentions that customary stresses are in the range of 0 to 10 000 psf (480 kPa) as compared to stresses of around 500 000 psf (23,95 MPa) leading to crushing. In general engineers have therefore not considered this to be a serious problem and one gets the impression that the crushing strength is specified to limit the weathering of the material particles.

Pinto[50] investigated the performance of rockfill materials for rockfill dams. In his investigation he also looked at the influence of the strength of the rock material and to interparticle contact forces. He mentioned that

> "According to Marsal (1973) contact forces between particles roughly comply with a statistical distribution of a normal law type....."[50]

Based on his own research and the work of Marsal he concluded that the mean contact force $\overline{P}$ is equal to:

$$\overline{P} = 0,6 . d^{1,96}$$

where $\bar{P}$ = mean contact force for an external load of 1 kgf/cm^2

d = particle diameter (cm)

He observed that

> "The contact force may vary from 1 gf to 1 tf as one goes from a granular medium composed of sand grains to a granular medium formed of rockfill blocks."[50]

According to Pinto, Marsal (1969) also concluded that

> "the crushing strength of particles in a granular medium also complies with a statistical distribution of the normal law type. For its mean value to he obtained an equation of the type
>
> $$P_a = \eta \cdot d^{\lambda}$$
>
> That is to say, the crushing strength is also proportional to the diameter of the particles."[50]

Marsal proposed a very simple test to determine η and λ. In the test three aggregate particles of about the same size are placed between two fairly thick steel plates in a press. A load is then applied and the force at which any one of the three particles yields by crushing is recorded. This value is divided by the number, N_c, which corresponds to the least number of contacts of the particles with each plate, giving the crushing strength of the aggregate, P_a.

Both the research of Marsal and that reported by Pinto satisfied the equation

$$P_a = \eta \cdot d^{\lambda}$$

and showed that the value of λ usually varies between 1,2 and 1,8, with a mean value of 1,5 while the value for η varied between 80 to 140 kgf/cm$^{\lambda}$.

Because λ, the exponent for the crushing strength of particles is smaller than the value of 1,96, the exponent for the mean contact force Pinto concluded that

> "with the increase of the size of the particles we can expect to obtain an increase of fracturing of rock elements and thus a decrease of shear strength and growing deformability..... In addition to the size, the fracturing of particles depends on crushing

strength, void ratio and state of stress."[50]

Pinto concluded that

> "If high crushing strength between elements can be guaranteed, it is of interest to give such a shape to those elements as they may display high mutual interlocking in order to obtain maximum stability. If fracturing, however, prevails over the sliding of particles one must give a more regular shape to those elements to obtain maximum strength."[50]

The principal finding of the research by Marsal and Pinto that contact pressures increase with particle size support the necessity to specify a minimum strength (ACV or 10 % FACT) for the higher class roadbuilding materials which normally contain larger particles.

However, it is not only the crushing strength of the material at the time of construction that is important, but also the crushing strength of the material with time. Spangler et al[51] mentioned that

> "In recent years a number of high "rock-fill" embankments built with shale failed after being in service for a period of years, due to the physical weathering of shale back to soil. In these instances the granular, interlocking character of this rock gradually has been lost, changing the classification and allowing the road embankments to fail...."[51]

From his tests on granular base materials Maree[52] concluded that the inherent strength of the material is very important. A material with a low durability will usually not give very angular material during the crushing process. Furthermore its grading may change during the compaction process or later on due to traffic loading. The maximum particle size may decrease, too much fines may be produced, the fines may be plastic in nature, the surface texture of the aggregate particles may become smooth and the particles become more rounded in shape. According to Maree all these factors contribute towards a reduction in shear strength with time.

For this reason the weathered strength of material should also be determined.

In South Africa the specifying of crushing strength criteria is limited to graded crushed stone (G1, G2 and WM)[29]. The specification requirement states that the minimum 10 % FACT is 110 kN or the maximum ACV is 29 %. Where calcrete is used the minimum 10 % FACT should be 80 kN. In certain cases, such as for evaluating tillites, a 10 % FACT on wet material (24 hours soaking followed by draining) is also specified in which case the wet value should be at least 75 % of the dry value.

2.7.1 Conclusions on the influence of the crushing strength of the material

The crushing strength of material is generally not a very serious problem in roadbuilding materials as the particles are generally fairly small and, according to the equations by Marsal and Pinto, the contact pressures will normally be much lower than the crushing strength of the material. However, the 10 % FACT test (wet and dry) does give an indication of the durability of the material which should very definitely be considered as the failure to do so can have very serious consequences. This is particularly the case with mudrocks as mentioned by Spangler et al. Specific tests have been developed by Venter[53] for this purpose.

2.8 Influence of the bearing capacity of the underlying layers

The degree to which a layer can be compacted properly, is not only dependent on the condition of the material in the layer itself (ie its grading, Atterberg limits, LS, MC, shape and texture) and the compactive effort applied, but is very strongly dependent on the reactive response of the underlying layers to the compactive effort. If the underlying layers are firm the density to which a material can be compacted will be greater than the density to which the material can be compacted when the underlying layers are weak and spongy. The latter conditions should be avoided as far as possible as they cause inherent weaknesses in pavements, because layers which have not been compacted properly, lead to excessive deformation and premature failure of pavements. In the Standard Specifications for Road and Bridge Works[54] the draining of the roadbed or the removal of unsuitable materials from the roadbed is specified precisely for this reason (see Clauses 3305(e) and 3305(a)).

One should therefore keep in mind that it is only possible to come close to the MDDs under ideal circumstances. On the other hand it is imperative to compact each layer to the highest practically achievable density. This will ensure better pavement performances on the whole. For this reason proof-rolling of the roadbed by means of an impact roller is often specified in South Africa (see Clause 3305(b))[54].

Casagrande[55] noted

> "In constructing an embankment, the soil, which has consolidated perhaps for thousands or millions of years, is broken up and disturbed thoroughly. The best compaction often could not replace the original state of the earth, and it takes a long time before such a highway fill has come to a complete rest. In making a cut, one disturbs the equilibrium which again has been built up during a long period."

Although the disturbance of the material cannot be avoided when constructing fills, the unnecessary disturbance of the roadbed by "ripping and recompacting", which is often specified, should therefore be avoided wherever possible. Organic material should, however, always be removed before proofrolling of the roadbed.

By comparing the field dry density with the MDD achieved in the laboratory one can get a very good indication of how successful the compaction process is, as well as the amount of consolidation that is likely to take place with time if not properly compacted to MDD.

2.8.1 Conclusions on the influence of the bearing capacity of the underlying layers

The restraint of the underlying material is very often the factor that limits the densities that can be obtained during construction; this is particularly true of poor roadbed conditions or the material being too wet. The consequences of this can be serious on the overall performance of the road. Wherever possible it is in the interest of the performance of the road that all layers should be compacted as densely as practically possible as these densities do not only influence the densities of the layers on top but also the overall performance of the road.

2.9 Bearing capacity of materials

Although the bearing capacity is not normally considered to be a factor which influences the compactability, they are inter-related. Because the California bearing ratio (CBR) test was used in this investigation as one of the parameters, it is briefly discussed.

The CBR test was devised in 1929 by the California Highways Department in an attempt to eliminate some of the objections to field loading tests and to provide a quick method for comparing the relative strengths of materials.

According to Porter[56] the samples are firstly compacted

> "to approximate the density ultimately produced by traffic in good subgrade and base materials. This procedure eliminates to a large degree the consolidation deformation which often influences static load tests made in the field. The compacted specimens are next soaked under a surcharge representing the weight of the pavement, to permit the specimen to swell and reach the adverse state of moisture which is usually present in the subgrade under normal drainage and climatic conditions. A penetration test is then made on the specimen to determine the resistance to lateral displacement, thus measuring the combined influence of cohesion and internal friction."

Although very wet pavement conditions may be prevalent in California and elsewhere, they are not really applicable to most pavements in South Africa. In an extensive study by Emery[57] into the in situ moisture content in pavements in South Africa it was found that the "equilibrium moisture content" (EMC) is in most cases below the OMC and that soaked conditions are rather the exception than the rule. Emery[57] found that the EMC was influenced by amongst others the MDD, OMC, the liquid limit, the linear shrinkage and the percentage passing the 0,425-mm sieve.

The author therefore decided to determine the CBR-values of the compacted samples at the moulding moisture contents of the samples immediately after compaction. These moisture contents varied from relatively dry to totally saturated materials. This would therefore not only show the bearing capacity in a soaked condition, but also at other moisture contents as well. Although not customary, this approach has been followed by a number of other researchers. (see Figures 2.4[58] and 2.5[59]). Lubking et al[58] remarked:

> "Additional laboratory CBR-tests in a Proctor cylinder proved the importance of the apparent cohesion in partly saturated fine sand samples. The tests were carried out with different moisture contents and densities;...."

Although the CBR test has been widely used not all researchers, and for that matter engineers in practice, are convinced that the CBR test gives a valid impression of the bearing capacity of the materials. Sweere[30] had the following to say about the CBR:

> "Although the Dutch standards for road building materials incorporate the CBR test for determination of "Bearing capacity of embankment and granular base course material", the test standard itself prescribes the test to be carried out on material with particle diameter d < 4 mm. For granular materials with a nominal 0/40 mm grading such testing does not make sense. On the other hand, testing of the full 0/40 mm grading in the 152,4 mm diameter CBR mould also is of little use. Therefore, in testing the 0/40 mm materials of group C and R, a grading scaled down to 0-22,4 mm (as used in the Maximum Modified Proctor Compaction Tests) was used. The sands of Group S were - of course - tested at their full grading."[30]

Elsewhere in his dissertation Sweere[60] has the following to say about the scaling down of the grading of the material.

> "This approach is quite classical: in standard test procedures like the CBR-test the grading of the material to be tested is also adjusted to the relatively small specimen size. AASHTO T193-72 for instance prescribes the scaling down of the grading of a granular material to 0-19 mm before CBR-testing in the 152,4 mm cylindrical mould.

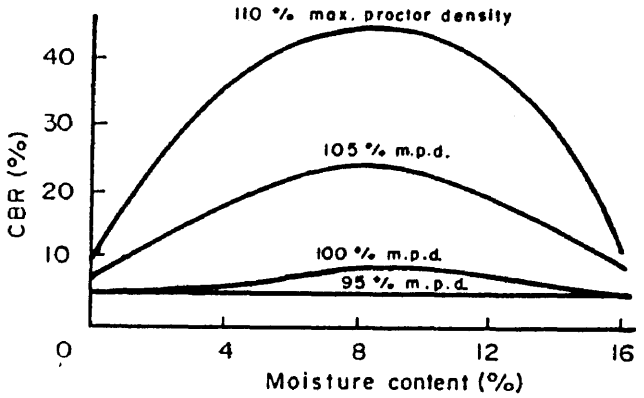

FIGURE 2.4 RELATION BETWEEN CBR AT MOULDING MOISTURE CONTENT AND MOULDING MOISTURE CONTENT FOR DIFFERENT DENSITIES FOR SAND[58]

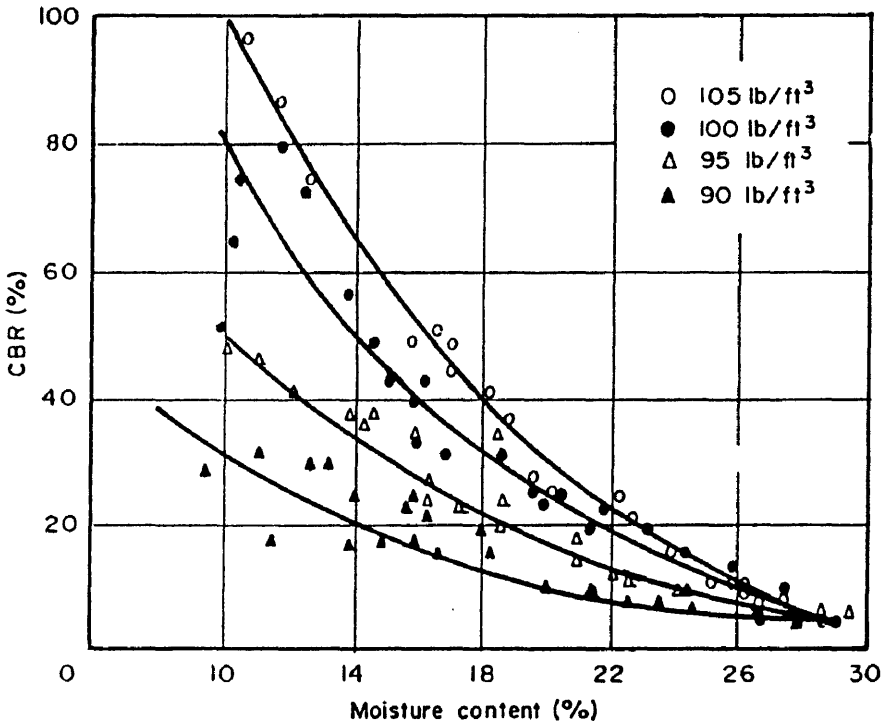

FIGURE 2.5 RELATION BETWEEN CBR AT MOULDING MOISTURE CONTENT AND MOULDING MOISTURE CONTENT FOR DIFFERENT DENSITIES FOR A HEAVY CLAY[59]

> It should be noted that when grading is scaled down, another material is in fact tested. As discussed in Paragraph 2.5.3.1, scaling down the grading of a granular material has been shown to result in a decrease in elastic stiffness. The resilient properties for instance of a 0-19 mm material can therefore only be indicative of the same properties of the original 0/40 mm material. Although often necessitated by the limitation of the available testing equipment, the scaling down of the material grading is in fact incompatible with one of the requirements of fundamentally sound testing, being that the material should be tested at the same grading as applied in-situ."[60]

Note that "0/40 mm material" refers to minus 40 mm material and "0-19 mm material" refers to minus 19 mm material, etc.

2.9.1 Conclusions on bearing capacity of materials

The CBR is the universal test used to express the bearing capacity of roadbuilding materials. The general way in which it is presently performed, namely soaking the samples for four days prior to testing and only using particle sizes smaller than 19 mm bears no direct relationship to the way the material performs in the pavement itself, as is rightly pointed out by Sweere.

For this reason the author decided to determine the CBRs of the materials with a maximum particle size of 37,5 mm at their moulding moisture contents with the moisture contents ranging from fairly dry to totally saturated. The materials were also compacted to different density levels for this range of moisture contents to determine the effect of both density and moisture content on the CBRs.

2.10 Concluding remarks and needs for further investigation

Engineers clearly have a good understanding of the material properties and their factors that influence their compactability. For instance, Maree[61] concluded from his research on crusher run materials that the following changes in the material properties all led to an increase in the shear strength of granular base materials:

(i) an increase in density
(ii) the change of the exponent n in the Talbot grading equation from 0,5 to 0,33
(iii) an increase in the maximum particle size
(iv) an increase in the amount of fines from one per cent to nine per cent (the strength decreased for a fines content between nine and fifteen per cent)
(v) a drop in the plasticity of the fines
(vi) the material was a crushed stone instead of a gravel

(vii) the inherent strength of the stone was greater

(viii) the particle shapes changed from rounded to angular

(ix) the surface texture of the particles changed from smooth to harsh

(x) the added binder changed from a natural sand to crusher dust.

However, none have succeeded up till now in quantifying the compactability of untreated roadbuilding materials in terms of these properties. Spangler et al[62] state:

> "Because of the obvious dependence on soil type, a number of investigators have attempted to predict maximum density and optimum moisture content from various other soil properties such as particle gradation, plasticity, or shrinkage data, or all three. However, none of the formulas yet derived has been found to have a universal application."

Unfortunately no references are given to the work of these investigators and none were traced during the literature survey except for instance References 46 and 47.

The likely interrelation between the material properties and the moisture regime have also not been established as yet.

It is clear from all this that there is great need for quantifying the maximum dry density and optimum moisture content as well as the bearing capacity in terms of these properties as this would be the first step in changing the determination of the compactability of untreated roadbuilding materials from an "art" to a "science". The more precise our estimates are the better we will be able to make the correct decisions to ensure that optimal performance of the material is achieved during the service life of the road.

It is very necessary that these interrelations between the material properties and the moisture content be established in a quantitative manner, as the total performance of the material in a road pavement is dependent on the conditions in which we place and keep the material during the service life of the road. Only when the detrimental consequences of under-compaction or an unnecessary high moisture content is quantified in terms of strength-loss or as a percentage loss of obtainable effective service life of the road, will engineers pay the necessary attention to ensure that each layer is compacted to highest practically achievable density and see to it that the pavement structure is protected through proper surface and sub-surface drainage (where required).

CHAPTER 3

THE DEVELOPMENT OF THE TESTING PROCEDURES

3.1 Introduction

The literature survey showed that the grading of the material, the cohesive properties of the fines, the inherent strength of the material itself, the shape and texture of the aggregate particles, the compaction moisture content and the type and size of the compactive effort all play a role in final density and bearing capacity that will be achieved.

From the start of this investigation it was realised that if standard testing procedures were followed, it would be unlikely that anything new could be learned above what was already known on this subject. It, therefore, meant that the investigation had to use tests not generally used before.

3.2 The compaction procedure of samples

In practice, layers of 150 mm to 200 mm or even thicker (up to 500 mm) are normally compacted in one operation during construction. Because the aim was to simulate the field compaction process in the laboratory, this meant that the laboratory samples would also have to be compacted in a single layer, and not in five or three thinner layers as is the case with the mod. AASHTO or std. AASHTO test methods respectively. The only compaction method which complied with this test requirement was the vibratory compaction method. The vibratory compaction table used in this investigation and its calibration are discussed in Appendix B. The compaction effort required to compact a sample to its maximum density, is dependent on the sample size. The optimal sample size was, therefore, one which could be compacted to its maximum density in a reasonable time as well as being large enough to quantify the other individual properties which have an effect on the compactability of the material.

To determine the influence of the compaction on the material itself it was also decided to use the actual grading of the material as far as possible. The only exception made, was that the maximum particle size was limited to 37,5 mm, because of the mould size used (152,4 mm in diameter).

In compaction on site the material at a particular position is also not limited by side friction as is the case when compacting a sample in a mould. Lees[18] showed that boundary effects of samples had an important influence on the MDD that could be achieved. To eliminate the

problem of side friction as far as possible, a number of different approaches were investigated. These included plastic lining of the mould and "anti-stick" preparations such as a teflon spray, "Spray and Cook", "Q-20" and "WD 40". Some samples were also compacted without any lining or spray treatment of the mould to determine the effect of the lining or spray treatment. Great problems were experienced with the compaction and extrusion of these latter samples, which clearly emphasize the tremendous influence the wall friction of the mould has on the results that can be achieved. The pretreatment of the moulds and surcharge with a lubricating spray, such as WD-40 or Q-20, gave the best results and this became part of the standard test procedure. A comparison of a number of different materials compacted with and without treating the mould and surcharge with the lubricating spray are shown in Table 3.1.

TABLE 3.1 Density results (% SD) of three types of material compacted with and without treatment of the mould and surcharge with a lubricating spray

	Without WD-40	With WD-40	Ratio (%)
CRUSHED STONE	82,7	86,9	105,1
	82,2	86,9	105,6
	82,9	87,4	105,5
	82,6	87,2	105,5
NATURAL GRAVEL	78,0	79,8	102,3
	78,9	80,0	101,4
	77,8	79,8	102,6
	77,7	80,2	103,2
SANDY CLAY	69,6	71,1	102,1
	69,8	71,4	102,3
	69,7	71,3	102,3
	69,8	70,8	101,4

The sprays also assisted in the extrusion of the samples from the moulds. Where the mould had not been treated with a spray, the samples sometimes had to be broken because they could not be extruded with the manually operated extrusion apparatus developed by Maree[63]. Because of these difficulties a hydraulic extrusion apparatus was built which makes it possible to extrude samples from the split moulds in less than thirty seconds. After extrusion it was found that samples which had been compacted in untreated moulds (without spray), had much greater density gradients through the depth of the samples, with substantially lower densities at the bottom of the of the sample.

3.3 The compaction moulds and surcharge

The basic shape and size of the moulds and surcharge were similar to those used by Maree[63], when he investigated the density and strength characteristics of graded crushed stone base material in earlier research at the Division. Each mould consisted of a single piece of thick walled cylinder with an internal diameter of 152,4 mm, similar to the mould diameter of the mod. AASHTO compaction test method, which is still the standard compaction test for roadbuilding materials in South Africa.

To assist with the extrusion of the samples, the moulds were split on the one side. The height of the moulds was 400 mm. This was done so that there would be no joint between the moulds and loose collar, as was usually the case, which could influence the free movement of the surcharge on top of the sample.

The moulds were bolted tightly to the table top by means of three lugs mounted at 120 degree intervals on the circumference of the moulds. To assist in the rapid fastening and unfastening in bolting the moulds to the table and tightening and splitting the moulds, use was made of an air-wrench.

Initially the surcharge consisted of five circular masses slightly smaller than 152,4 mm in diameter, each weighing approximately 10 kg, which were bolted together by means of a long threaded bolt with an eye on the end, for lifting and lowering. To prevent people from being hurt when lifting or lowering the surcharge, use was made of an electrical hoist. The five weights are locked tightly together by means of locknuts at the top end of the surcharge.

With the initial trials, it seemed as though the surcharge was floating on a cushion of air; for this reason the diameter of the surcharge was reduced by 0,7 mm. This did not produce more satisfactory results. It seemed as though it was impossible to achieve uniform compaction results with the same compaction energy; the results were scattered over a wide range without any definite pattern. It was also observed that a portion of the sample fines worked their way up between the surcharge and the mould which seemed to prevent the surcharge from moving up and down freely. The mould lubricating sprays, mentioned earlier, did improve the situation, but not in a consistent manner. Some samples were properly compacted and others not; it was possible to predict whether a sample would be well compacted or not by observing the reaction of the surcharge during the compaction cycle.

To prevent the fines in the soil sample from working their way up between the mould and surcharge a 25 mm thick circular base plate with a very small tolerance on the internal diameter of the moulds was fixed to the base of the surcharge. This definitely improved the results and consistent results were now obtained with medium sized samples (100 mm high at 100 % mod. AASHTO density). As soon as an attempt was made to compact a full sized sample (150 mm high at 100 % mod. AASHTO density) the old problem recurred. The cause of the problem was that the surcharge tended to jam at a slight angle when compacting fairly large samples. This was caused by the horizontal component of the force generated by the single vibration motor. A second circular plate, similar to the base plate, was mounted higher up in the surcharge, to prevent the surcharge from jamming sideways. This had the desired effect and more consistent results were obtained.

Initially it seemed that it would take three to four times as long to compact a sample which would give a sample height of 135 mm at 100 % mod. AASHTO compared to a sample which would give a sample height of 100 mm at 100 % mod. AASHTO (see Figure 3.1). The frequency-amplitude combination used was 30 Hz with the eccentric weight setting k equal to 36 % (see Appendix B for an explanation of the setting k). For this reason it was decided to use a standard sample size which would give 100 mm high samples if compacted to 100 % mod. AASHTO density. Subsequent results have shown that this is not necessarily the case (see Table 3.2). The frequency-amplitude combination used in this case was 30 Hz with the eccentric weight setting k equal to 64 %.

To assist in the free movement of the surcharge, both the sides and the bottom of the base of the surcharge were also sprayed with the lubricant spray, prior to each test. A piece of filter paper was placed in the bottom of the mould on top of the base plate as well as on top of the sample. The filter paper was placed on top to prevent the material from sticking to the surcharge.

3.4 The duration of the vibratory compaction for MDD

To limit the unnecessary degradation of samples it was essential that samples be compacted for as short a time as possible. To determine this period, use was made of a laser measuring apparatus which monitored the settlement of the sample during the compaction procedure.

The laser measuring head was mounted on a wall bracket, which could move up and down as well as turn sideways. In this way it was possible for the laser beam to make contact with the top of the surcharge after it had been lowered onto of the sample by means of the electrical hoist.

TABLE 3.2 Density results of three types of material for three different sample sizes against compaction time

Material	time (min)	h (mm)	DD (% SD)	h (mm)	DD (% SD)	h (mm)	DD (% SD)
Moisture content			(4,50 %)		(4,25 %)		(4,88 %)
Crushed stone	0,5	101,00	82,0	124,50	83,3	140,00	81,3
	1,0	98,38	84,2	121,25	85,5	135,75	83,9
	1,5	97,25	85,2	118,00	87,9	134,50	84,7
	2,0	95,25	87,0	117,50	88,3	134,50	84,7
	2,5	94,75	87,5	117,25	88,4	132,00	86,3
	3,0	94,75	87,5	116,75	88,8	131,50	86,6
	3,5	94,25	87,9			130,25	87,4
	5,0		90,3	114,25			
	5,5	91,75			90,3		
Moisture content			(8,26 %)		(8,71 %)		(7,85 %)
Natural gravel	0,5	91,50	79,0	115,00	78,2	124,50	78,8
	1,0	91,25	79,2	114,50	78,6	122,75	79,9
	1,5	90,00	80,3	114,25	78,8	122,25	80,2
	2,0	90,00	80,3	114,25	78,8	122,00	80,4
	2,5	90,00	80,3	114,00	78,9	121,50	80,7
	3,0	90,00	80,3	113,50	79,3	121,00	81,1
	5,0	90,00	80,3	113,25	79,5	120,00	81,7
	6,0					120,00	81,7

TABLE 3.2 (Continued)

Material	time (min)	h (mm)	DD (% SD)	h (mm)	DD (% SD)	h (mm)	DD (% SD)
Moisture content			(14,08 %)		(14,06 %)		(14,04 %)
Sandy clay	0,5	96,00	70,2	166,75	51,0	170,50	53,8
	1,0	95,50	70,6	119,75	71,1	133,00	68,9
	1,5	95,50	70,6	118,75	71,7	128,75	71,2
	2,0	95,50	70,6	118,25	72,0	128,25	71,5
	2,5	95,50	70,6	118,25	72,0	128,25	71,5
	3,0	95,50	70,6	118,25	72,0	128,25	71,5
	5,0	94,75	71,1	118,25	72,0	128,00	71,6
	7,0	94,75	71,1	118,00	72,1	128,00	71,6

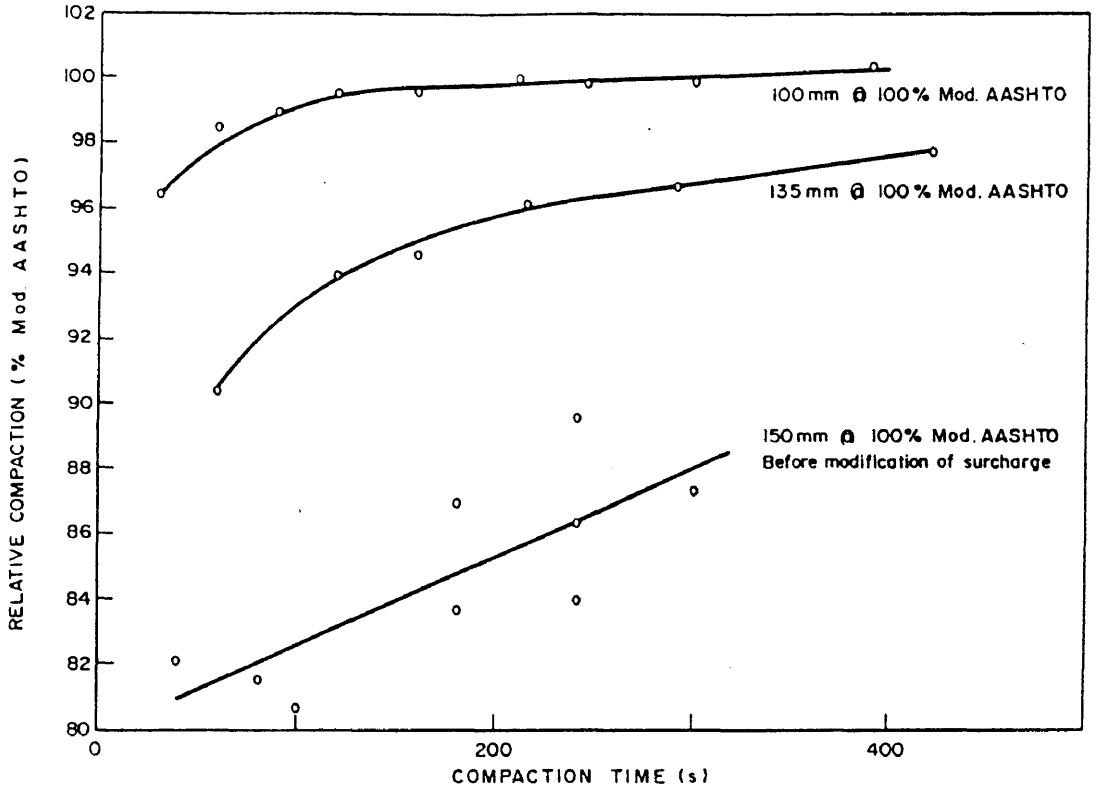

FIGURE 3.1 THE EFFECT OF SAMPLE HEIGHT ON THE COMPACTION TIME USING LARGE SURCHARGE (30 Hz - k = 36 %)

For the determination of the time period a trial sample of the material at OMC (mod. AASHTO) (see list of abbreviations) was used. The sample was compacted for an extended period while the height measurement of the laser gauge was continuously recorded on an analogue cassette recorder. The recorded signal was then fed into a computer by means of an analogue-digital interface and plotted against time. The readings were sampled at a rate of ten readings per second. Because of the up and down movement of the surcharge itself, the moving average of 40 readings was taken to smooth out the plot of the graph (see Figure 3.2). The optimal compaction period was taken to be the point in time when the sample height remained approximately constant,which reflected where the discernible densification of the sample had ceased.

For most materials this point in time was between 120 seconds (2 minutes) and 180 seconds (three minutes). The only material that had a period longer than 180 seconds, was the montmorillonite clay, which took 210 seconds (three and a half minutes) to compact.

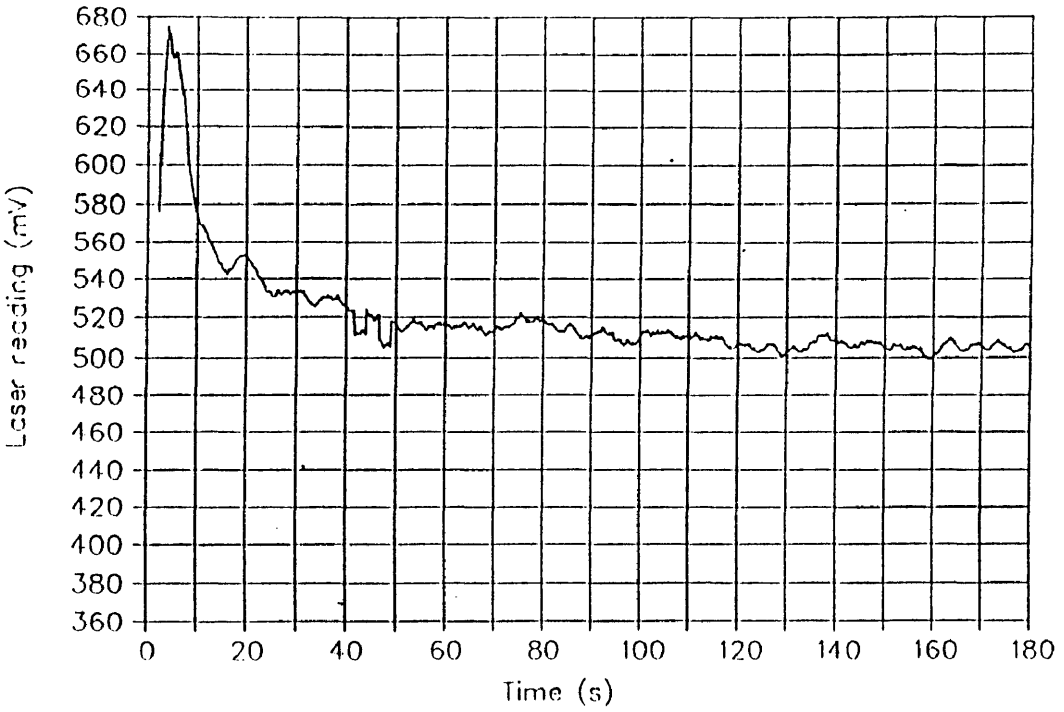

FIGURE 3.2 AN EXAMPLE OF A COMPACTION SETTLEMENT CURVE AS MEASURED WITH THE LASER MEASURING APPARATUS

3.5 Compaction of samples to specified density levels

A standard sized sample was used, namely the amount of dry material which would yield a sample of 100 mm high, if the sample was compacted to 100 % mod. AASHTO density. For this reason, the MDD (mod. AASHTO) and OMC (mod. AASHTO) were always determined first, along with the grading, Atterberg limits and linear shrinkage (all the indicator tests).

For the determination of MDD (vibratory) and OMC (vibratory), the materials were all compacted over a range of moisture contents as is done with the normal compaction tests. The determination of the MDD (vibratory) and OMC (vibratory) of the materials was done for three amplitude-frequency combinations. These combinations were chosen to determine what the effects of amplitude and frequency were on the compactability of untreated roadbuilding materials. The combinations were such that the vibratory table would deliver the same amount of compaction energy to the sample per unit time, irrespective of the amplitude used. The three combinations were chosen to yield a high, medium and low amplitude and are listed in Table 3.3 (see Appendix B for more information).

TABLE 3.3 Amplitude-frequency combinations used in the research

	Eccentric weight setting	Operation frequency
Amplitude	**k (%)***	**f (Hz)**
High	64	30
Medium	47	35
Low	36	40

* see Appendix B.

Further samples of each material with different moisture contents, ranging from nearly dry to very wet, were also compacted to different levels of density. The density levels were 90 %, 93 %, 95 %, 97 % and 100 % mod. AASHTO.

Because a standard sized sample was used, the density level was controlled by means of the sample height. The sample height was controlled by means of an infrared beam triggering system which switched off the vibratory table automatically as soon as the required height had been reached. The infrared beam sensing mechanism was mounted on two pillars which were mounted on opposite sides of the mould on the table top. The infrared beam emitter and sensing units were mounted on sliding units on these pillars and could be locked tightly in any position within a certain height range. Two linear scales for a range of sample heights were fixed to the pillars to assist with the height adjustment. The infrared beam was blocked out by the surcharge on top of the sample as long as the required height had not yet been reached. As soon as the required height was reached, the infrared beam would be picked up by the sensing unit, which then triggered the system to stop the vibratory table automatically.

3.6 Determination of the densities of compacted samples

The sample height of the compacted samples, which is usually kept constant in compaction tests, was not fixed. This was done to avoid unnecessary disturbance of the compacted sample. Instead, the sample volume was determined by measuring the heights of the samples very accurately inside the compaction mould. For this purpose a purpose-made measuring bracket and a digital height gauge, which could read accurately to 0,01 mm, was used.

A sketch of the measuring bracket is shown in Figure 3.3. It was placed over the side-wall of the compaction mould until the inside foot touched the surface of the compacted sample. The bracket was then pressed firmly against the side-wall of the mould so that the measuring

bracket was standing firm and vertical. While held in this manner, the measuring arm of the digital height gauge was lowered onto the measuring foot to take a height reading. Because the height difference between the two feet of the measuring bracket was equal to the thickness of the mould base plates, the height gauge was zeroed with the measuring foot in contact with the polished and hardened steel plate on which the height gauge was mounted.

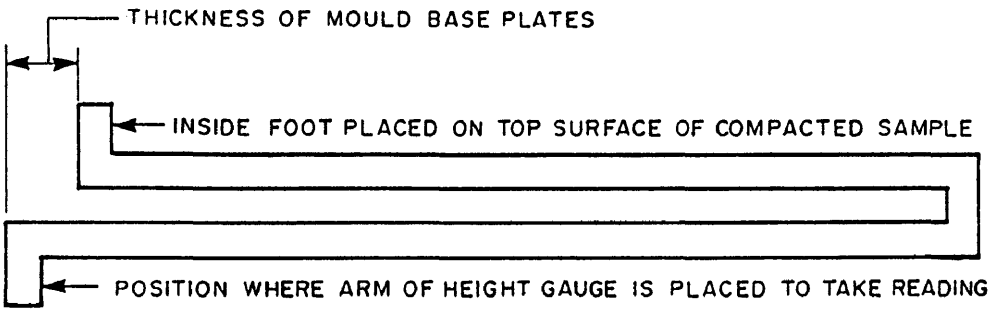

FIGURE 3.3 SCHEMATIC ILLUSTRATION OF PURPOSE-MADE MEASURING BRACKET

Because the surcharge has a slight amount of freeplay within the mould, it means that there is also the possibility that the surcharge can tilt slightly during compaction. This could lead to slightly varying heights around the circumference of the compacted sample. For this reason the sample height of each compacted sample was defined as the average of four height measurements taken at approximately 90° intervals on the circumference of the mould. The number of readings was set at four to ensure that possible measuring errors could easily be identified and corrected.

After the sample height had been determined, the CBR penetration test was performed on the sample inside the compaction mould, with the usual annular surcharge of 5,56 kg ± 50 g on the surface of the sample. Once the CBR penetration loads had been measured, the sample was extruded from the mould by splitting the mould after which its wet mass (M_1) was determined accurately before drying it in an oven at 105 °C to 110 °C to constant mass. When the sample had dried to constant mass it was left to cool down before its dry mass (M_2) was determined.

Because the compaction moulds had been accurately machined to 152,4 mm diameter and their surfaces case-hardened, the diameter of the moulds were assumed to be constant throughout the investigation.

The volume of the sample (m^3) $= (\pi.d^2.h)/(4.1000)$ . . . . . (3.1)

where d = diameter of the mould (= 0,1524 m)
h = average sample height (mm)

The wet density of the sample WD (kg/m^3) $= M_1/\text{volume}$
$= (M_1.4.1000)/(\pi.d^2.h.1000)$
$= (4.M_1)/(\pi.d^2.h)$ . . . . . (3.2)

where M_1 = mass of wet sample (g)
h = average sample height (mm)
d = diameter of mould (= 0,1524 m)

The moisture content MC (%) $= [(M_1 - M_2)/M_2].100$ . . . . . (3.3)
where M_1 = mass of wet sample (g)
M_2 = mass of dry sample (g)

The dry density of the sample DD(kg/m^3) $= WD/(1 + MC/100)$ . . . . . (3.4)
where WD = wet density of the sample (kg/m^3)
MC = moisture content of the sample (%)

The dry densities of the samples were also expressed as percentages of MDD (mod. AASHTO) and Apparent Density (AD) (see Appendix D for listing of compaction and CBR results).

3.7 The determination of the CBR values of the samples

As mentioned in the previous section, the CBR penetration tests were performed on the samples immediately after compaction. This was purposely done to determine the bearing capacity of materials at the time of compaction. Apart from this Emery[57] found that the soaked conditions of the "standard" CBR tests are seldom found in pavements in practice in South Africa. A secondary reason also had an influence in that all the compaction and CBR tests

had to be performed with four compaction moulds, which completely eliminated the possibility of soaking the samples.

The CBR-value was determined for all three standard penetration depths of 2,54 mm (CBR_1), 5,08 mm (CBR_2) and 7,62 mm (CBR_3). Although the values of CBR_1, CBR_2 and CBR_3 are similar in most cases, they tend to differ substantially on particularly coarse granular materials. In South Africa CBR_1 is normally used as the standard value and in the USA the greater of CBR_1 and CBR_2. The author is of the opinion that a value based on all three measured values would be a better reflection of the bearing capacity. The author is also of the opinion that CBR values become more reliable with increasing penetration depths. For the purpose of this investigation the author therefore decided to use a weighted CBR value for each compacted sample.

$$CBR = (CBR_1 + 2.CBR_2 + 3.CBR_3)/6 \quad \ldots\ldots\ldots\ldots\ldots\ldots\ldots\ldots \quad (3.5)$$

3.8 The determination of the specific rugosity (S_{rv}) and shape factor (SF) of the materials

In Section 2.5.2 laboratory methods to quantify shape and texture were discussed. Most of these parameters are empirical quantities obtained by compacting single sized aggregate fractions in a specified manner. For graded aggregates these parameters are usually expressed as the weighted average of the values for the separate sieve fractions passing 19 mm and being retained on the 4,75 mm. However, Van der Merwe[44] successfully extended the specific rugosity particle size range from minus 0,075 mm to material passing the 37,5 mm sieve. As the shape and texture of each fraction contributes to their combined influence on compactability and bearing capacity, the parameters used to quantify the shape and texture of untreated roadbuilding materials should preferably cover as many of the standard sieve sizes as possible. If for instance the size is limited to particles larger than 4,75 mm, one would not be able to quantify the shape and texture of any material passing the 4,75 mm sieve. The author therefore decided to use the specific rugosity as this covered the particle size range from less than 0,075 mm to material passing the 37,5 mm sieve. In principle this could even be extended to larger particles. The maximum particle for this investigation was minus 37,5 mm.

The specific rugosity (S_{rv}) can be expressed as follows :

$$S_{rv} = (100)(1 - G_A/G_B) \quad \ldots\ldots\ldots\ldots\ldots\ldots\ldots\ldots \quad (3.6)$$

where G_A = bulk density of aggregate fraction (% SD)

G_B = bulk density of equivalent spheres (% SD)

"Equivalent spheres" are spheres of the "same size" as the particular aggregate fraction. These "equivalent spheres" were obtained by sieving glass spheres of different sizes through the same sieves as used for the aggregates themselves.

However, instead of sieving large samples of each material to obtain large enough amounts of the separate sieve fractions to do the test according to the method used by Van der Merwe a single previously compacted sample of each material was taken randomly and sieved into separate fractions.

Initially the density of each fraction was determined by pouring the separate fractions into plastic measuring cylinders, determining the poured volume of the sample, dividing the mass of the sample by the volume to get density (kg/m^3) and expressing this as a percentage of the solid density. For the larger particle sizes plastic measuring beakers were used instead of measuring cylinders. The measuring scale was duplicated on four sides of the beakers at 90° intervals and the volume was taken to be the average of the four readings. The same procedure was also followed for glass beads of different sizes. Using the above formula the specific rugosity of each fraction was then determined. The initial results gave the highest values for the fines fraction, which seemed contra to what was expected because in essence the fines are relatively smooth compared to the large stone.

It was therefore decided to tamp each sieved fraction in the measuring cylinder until there was no discernible change in the volume of the sample. For most samples this occurred fairly quickly but for the fines as many as 200 tamping strokes had to be given to get rid of the entrapped air. This procedure was also followed for glass beads of different sizes. Because of the change in test method from the normal "specific rugosity" test it was decided to call this value the "shape factor" (SF).

Comparative volume determinations were also done on a number of samples by sealing the sample fractions in plastic bags under vacuum and then determining the volumes of these vacuumed samples. The values obtained with the vacuumed sample and tamped sample methods compared well with one another. Because plastic measuring cylinders are fairly cheap compared to a vacuum sealer the general approach followed was to determine the densities of the separate fractions by tamping the measuring cylinders. Weighted values of the specific rugosity (S_{rv}) and shape factor (SF) were then determined for the total grading.

Because of uncertainty as to whether the poured volume or tamped volume of each fraction of each material would be more relevant, both were continuously recorded. In the case of particularly the coarse materials, one sometimes had an extremely limited amount of the larger particles which made it impossible to determine a reasonable value. They were then left out when calculating the value of the shape factor. Subsequent evaluation of the research data in modelling the CBR has shown that the tamped values give a better indication of the influence of the shape and texture of aggregate particles than the poured values.

3.9 The determination of the shakedown bulk density (SBD) of the materials

Although the effect of shape and texture of the aggregate particles was quantified by the shape factor (SF), this factor does not really quantify the collective influence of all the particles together. For this reason the author decided to determine the loose bulk density (LBD) and the shakedown bulk density (SBD) of the material as well.

This was done by pouring the total sample into the large plastic measuring beaker, levelling the surface with a spatula and taking four readings on the measuring scales at 90° intervals to get an average volume (V_1) for the loose bulk state. After this the beaker and sample were tamped until there was no further discernible change in volume. The average shakedown bulk volume (V_2) was then determined from the four volume readings on the four measuring scales at 90° intervals. The sample mass (M_1) was determined accurately. The loose bulk density and shakedown bulk density are expressed as a percentage of the space occupied by "solids" as is the case with the determination of the G_A and G_B for the shape factor (SF).

They can therefore be determined as follows:

$$\text{LBD (\% SD)} = (100.M_1)/(V_1.SD) \quad \ldots\ldots\ldots\ldots\ldots\ldots\ldots\ldots\ldots\ldots \quad (3.7)$$

$$\text{SBD (\% SD)} = (100.M_1)/(V_2.SD) \quad \ldots\ldots\ldots\ldots\ldots\ldots\ldots\ldots\ldots\ldots \quad (3.8)$$

In the case of materials with a high content of coarse granular material the SBD was determined slightly differently. The whole sample was sieved through the 4,75 mm sieve. The coarse fraction of the sample (ie larger than 4,75 mm) was then poured into the beaker first and levelled, whereafter the fine fraction was placed on top. The sample was then tamped in the normal manner. This procedure prevented the larger particles from "climbing" out on top of the sample which originally made it difficult to determine the sample volume accurately.

In the case of porous aggregates where there is a substantial difference in the values of the bulk relative density and the apparent relative density of the same aggregate, the dry bulk density (DBD) should be used as the value of SD in the determination of the LBD, SBD, S_{rv} and SF as the internal voids in the aggregate particles do not play an active part. For friable materials such as clays which completely break down in structure the apparent density (AD) should be used as there are no "internal" voids left after compaction.

3.10 Summary of test procedures

The choice of compaction method for this compactability study fell on vibratory compaction. This was done to enable the compaction of the sample in a single layer using the actual grading of the untreated roadbuilding material. The only adjustment to the grading was to limit the maximum particle size to 37,5 mm. A non-standard vibratory table, of which both the frequency and amplitude could be adjusted was used (see Appendix B for more information on the vibratory table and its calibration). Special compaction moulds that could split on one side were used. Their height and diameter were 400 mm and 152,4 mm respectively and they were case-hardened to limit wear. The load was supplied by a special surcharge to ensure free movement of the surcharge as far as possible. To limit wall friction the mould and surcharge were sprayed with a lubricant spray prior to the compaction of a sample. Immediately after compaction the sample height was determined accurately for volume determination purposes, whereafter the CBR penetration test was done on the sample inside the mould. The sample was then removed and the moisture content of the sample determined. Samples were not only compacted to MDD but also to other density levels, namely 90 %, 93 %, 95 %, 97 % and 100 % mod. AASHTO for a whole range of moisture contents. The shape and texture were quantified by the specific rugosity (S_{rv}), shape factor (SF), the loose bulk density (LBD) and shakedown bulk density (SBD). Their methods of determination were discussed.

CHAPTER 4

INFLUENCE OF MATERIAL PROPERTIES AND VIBRATORY TEST PARAMETERS ON THE MAXIMUM DRY DENSITY

To determine the influence of material properties in general on the compactability and bearing capacity of the materials a wide range of materials, ranging from very poor quality to very good quality, were used in this investigation (see Table 4.1). The MDD and OMC results are listed in Appendix C and the indicator test values (ie the grading, Atterberg limits and linear shrinkage) are listed in Appendix E.

TABLE 4.1: List of materials and their basic description

NAME	MATERIAL TYPE	TRB - PRA CLASSIFICATION
BAB	Black clay (montmorillonite)	A-7-6 (17)
SPR2	White sandy clay	A-6 (4)
SPR1	Red sandy clay	A-6 (5)
LABLEN	Red silty sand	A-2-6 (1)
LABDEW	Slightly plastic sand	A-2-4 (0)
OFS1	Windblown sand	A-2-4 (0)
NPAB	Decomposed dolerite	A-2-7 (0)
SIL	Silty sand	A-2-4 (0)
LABD	Red chert soil	A-2-4 (0)
TPA3	Chert gravel	A-2-6 (0)
TPA1	Norite gravel	A-1-a (0)
CPA1	Hornfelz crushed stone (G1)	A-1-a (0)
DENS7	Dolomitic soil	A-2-6 (0)
TPA2	Quartzite gravel	A-2-4 (0)
NPAE	Tillite crushed stone (G1)	A-2-4 (0)
FERR1	Quartzite crushed stone (G1)	A-1-a (0)
OFS2	Weathered dolerite	A-1-a (0)
NPAA	Dolerite crushed stone (G1)	A-1-a (0)
ROSS1	Granite crushed stone (G1)	A-1-a (0)
DENS8	Shale	A-2-6 (0)
OFS3	Dolerite crushed stone (G1)	A-1-a (0)

The standard compaction test used to determine the MDD of untreated roadbuilding material in South Africa is the mod. AASHTO compaction test. In the case of G1 crushed stone materials no compaction test is usually performed but the specified density is expressed as a percentage of the solid density (% SD) of the material to be used. On construction sites many different makes of vibratory rollers, with a range of frequency-amplitude combinations are used. To determine the effect of these different frequency-amplitude combinations on the compactability of untreated roadbuilding materials on site in a reasonable period, was an impossible task as one could not effectively control all the input variables, such as material type, moisture content, frequency-amplitude combination, and the mass of the roller.

For this reason it was decided to use a vibratory compaction table on which both the frequency and amplitude could be adjusted to specific values. For general compaction purposes of this investigation frequency levels used in practice on many rollers were selected namely 30, 35 and 40 Hz. The amplitudes used together with these frequency levels were such that the size of the eccentric force would be exactly the same for each of these frequency amplitude combinations (ie $kmrf^2$ = constant) (see Appendix B).

Because of a lack of knowledge on the separate influences of the frequency and amplitude of the compactive force on the densification process, a limited amount of testing was also done at other "frequency-amplitude" combinations. Only one material type, namely a silty sand was used and the samples were compacted at frequencies of 20, 30 and 40 Hz respectively. For the lowest frequency of 20 Hz the amplitude settings were set at 64 % and 35 % for combinations 1 and 2 respectively (see Table 4.2). To ensure that the samples compacted at 20 Hz received the same number of compaction blows as in the standard situation when the sample is compacted at 30 Hz the time period was extended by fifty per cent. The k-settings for 30 and 40 Hz respectively were selected in such a manner that the vibratory force per unit time would be the same for each of the three combinations ($kmr.f^2$ = constant) (see Table 4.2).

Because the values of the k-settings for 30 and 40 Hz were now lower than 35 % (the part in which the "fixed eccentric moment" was not constant anymore), the k-settings had to be determined from a special table where kmr is given for any value of k between zero and hundred per cent (see Table 4.3).

TABLE 4.2 Amplitude settings for special amplitude frequency combinations

Combination	Frequency	kmr.f^2	kmr (kg-mm)	k (%)
1	20	442640	1106,6	64,00
1	30	442640	491,8	29,25
1	40	442640	276,7	17,25
2	20	242040	605,1	35,00
2	30	242040	268,9	16,50
2	40	242040	151,3	9,75

At the same time the effect of the "surcharge" on top on the frequency-amplitude combination was also evaluated in that the samples were compacted for these frequency-amplitude combinations using both the normal large surcharge (± 53 kg) and a small surcharge (± 30 kg) (see Figures 4.1 to 4.7).

TABLE 4.3 The values for the eccentric moment (kmr) (kg-mm) for any value of k (%) between zero and hundred per cent

k-setting(%)	k-setting(%)				
	+0	+1	+2	+3	+4
0	0,00	14,99	30,12	45,38	60,79
5	76,33	92,00	107,81	123,76	139,85
10	156,07	172,43	188,93	205,57	222,34
15	239,25	256,29	273,47	290,79	308,25
20	325,84	343,57	361,43	379,44	397,58
25	415,85	434,27	452,82	471,51	490,33
30	509,29	528,39	547,63	567,00	586,51
35	606,15	625,94	645,86	665,91	686,11
40	706,44	726,91	747,51	768,25	789,13
45	778,04	795,33	812,62	829,91	847,20
50	864,49	881,78	899,07	916,36	933,65
55	950,94	968,23	985,52	1002,81	1020,10
60	1037,39	1054,68	1071,97	1089,26	1106,55
65	1123,84	1141,13	1158,42	1175,71	1193,00
70	1210,29	1227,58	1244,87	1262,16	1279,45
75	1296,74	1314,02	1331,31	1348,60	1365,89
80	1383,18	1400,47	1417,76	1435,05	1452,34
85	1469,63	1486,92	1504,21	1521,50	1538,79
90	1556,08	1573,37	1590,66	1607,95	1625,24
95	1642,53	1659,82	1677,11	1694,40	1711,69
100	1728,98	*****	*****	*****	*****

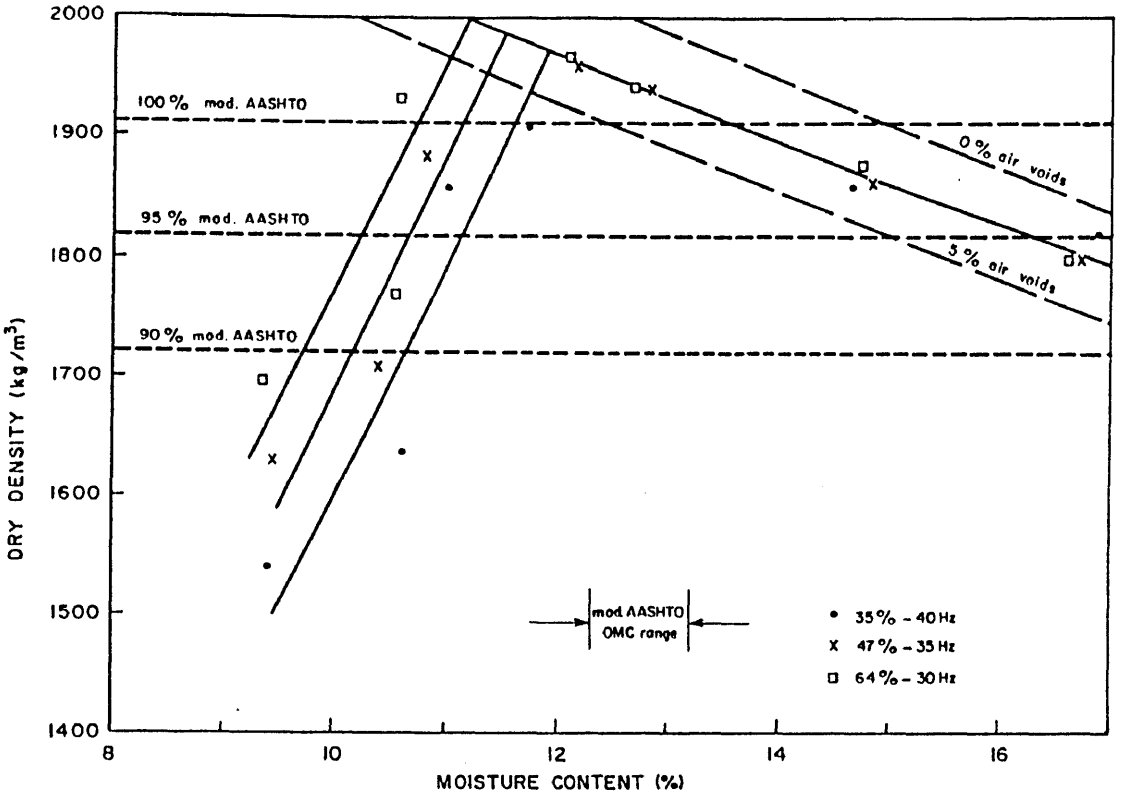

FIGURE 4.1 DRY DENSITY AGAINST MOISTURE CONTENT FOR SILTY SAND FOR LARGE SURCHARGE (FREQUENCY 30-40 Hz) (k_{max} = 64 %)

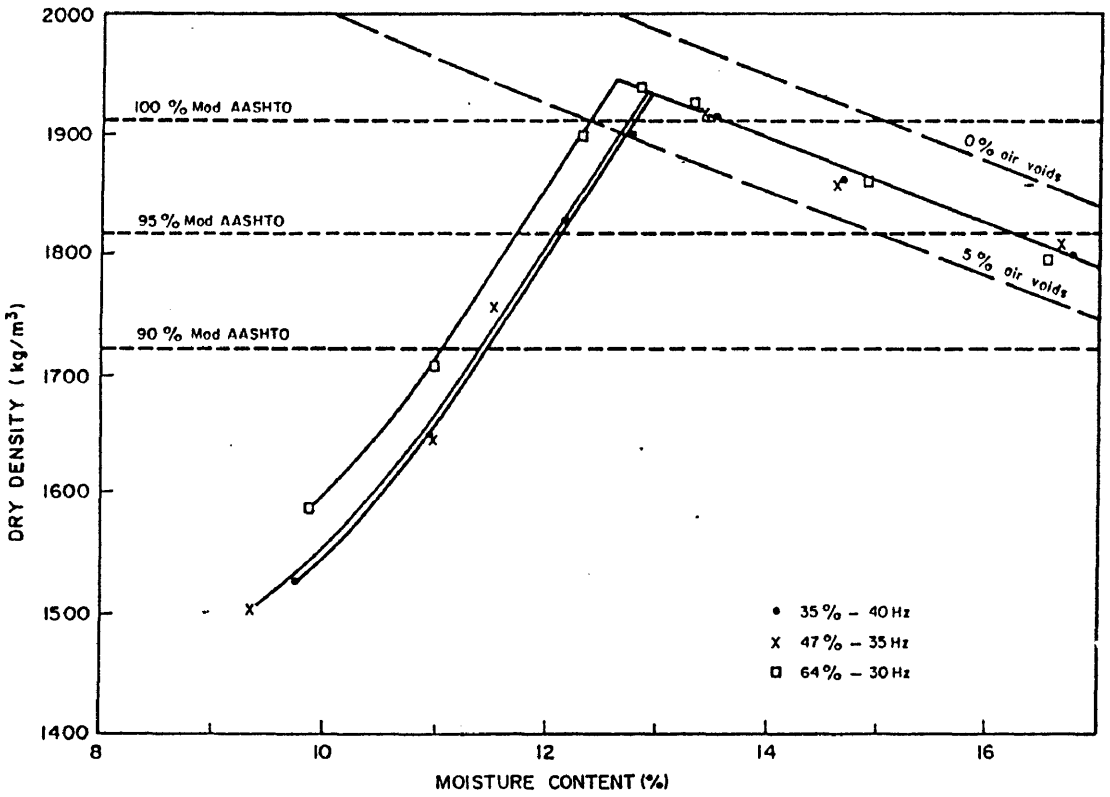

FIGURE 4.2 DRY DENSITY AGAINST MOISTURE CONTENT FOR SILTY SAND FOR SMALL SURCHARGE (FREQUENCY 30-40 Hz) (k_{max} = 64 %)

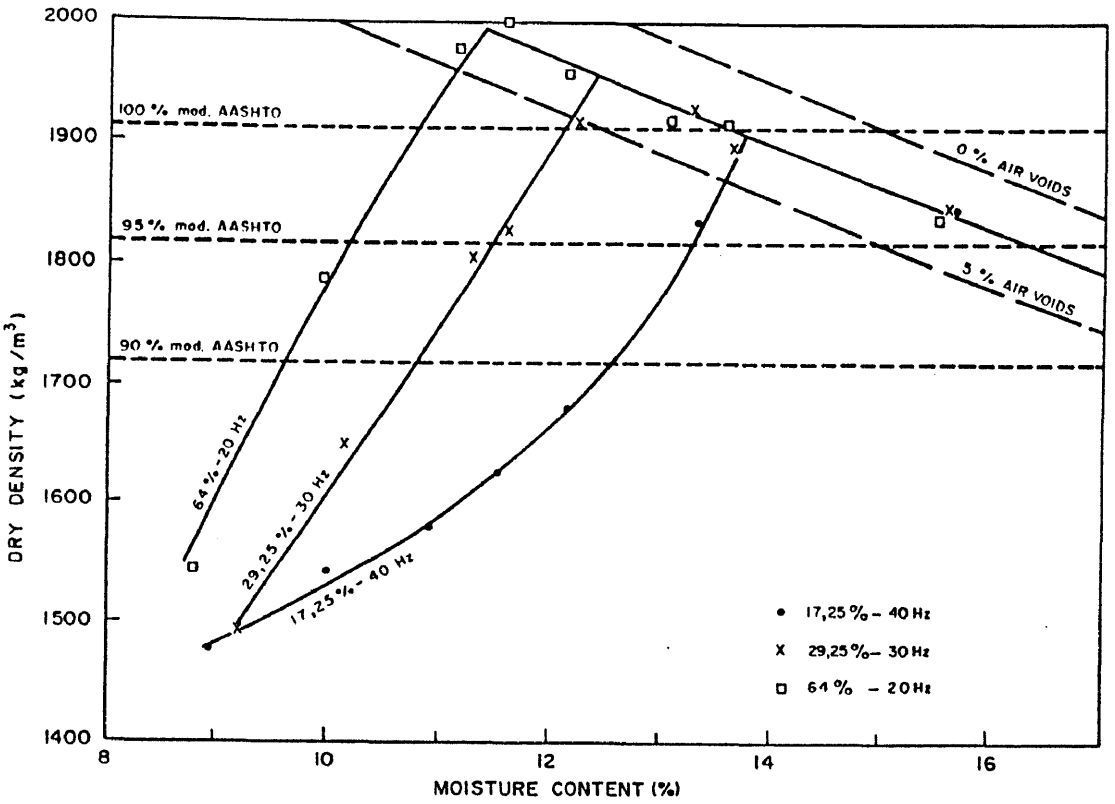

FIGURE 4.3 DRY DENSITY AGAINST MOISTURE CONTENT FOR SILTY SAND FOR LARGE SURCHARGE (FREQUENCY 20-40 Hz) (k_{max} = 64 %)

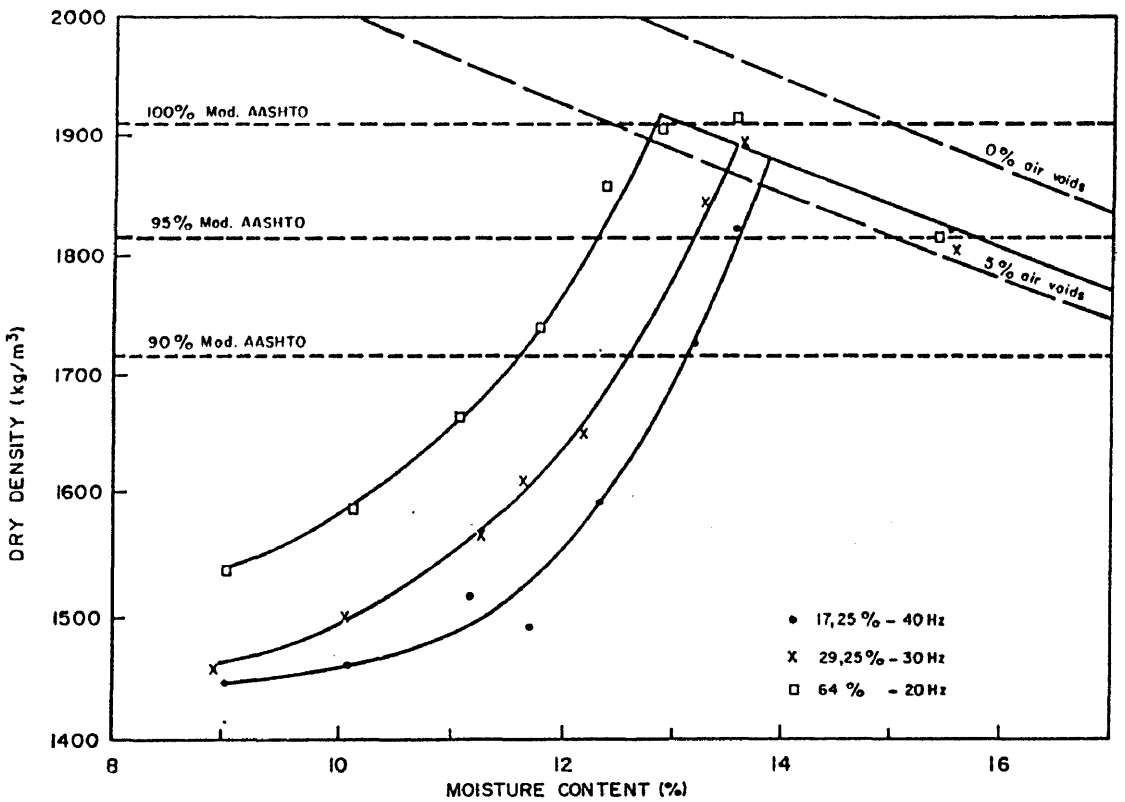

FIGURE 4.4 DRY DENSITY AGAINST MOISTURE CONTENT FOR SILTY SAND FOR SMALL SURCHARGE (FREQUENCY 20-40 Hz) (k_{max} = 64 %)

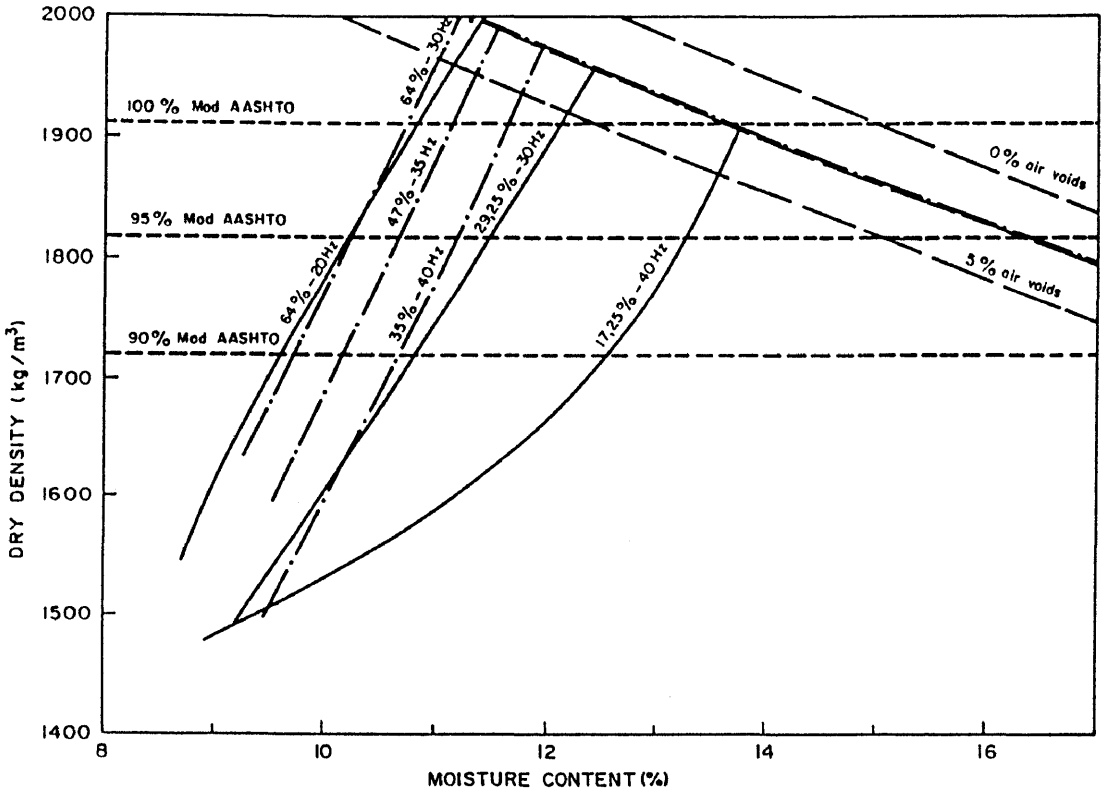

FIGURE 4.5 DRY DENSITY AGAINST MOISTURE CONTENT FOR SILTY SAND FOR LARGE SURCHARGE (FIGURES 4.1 AND 4.3 COMBINED)

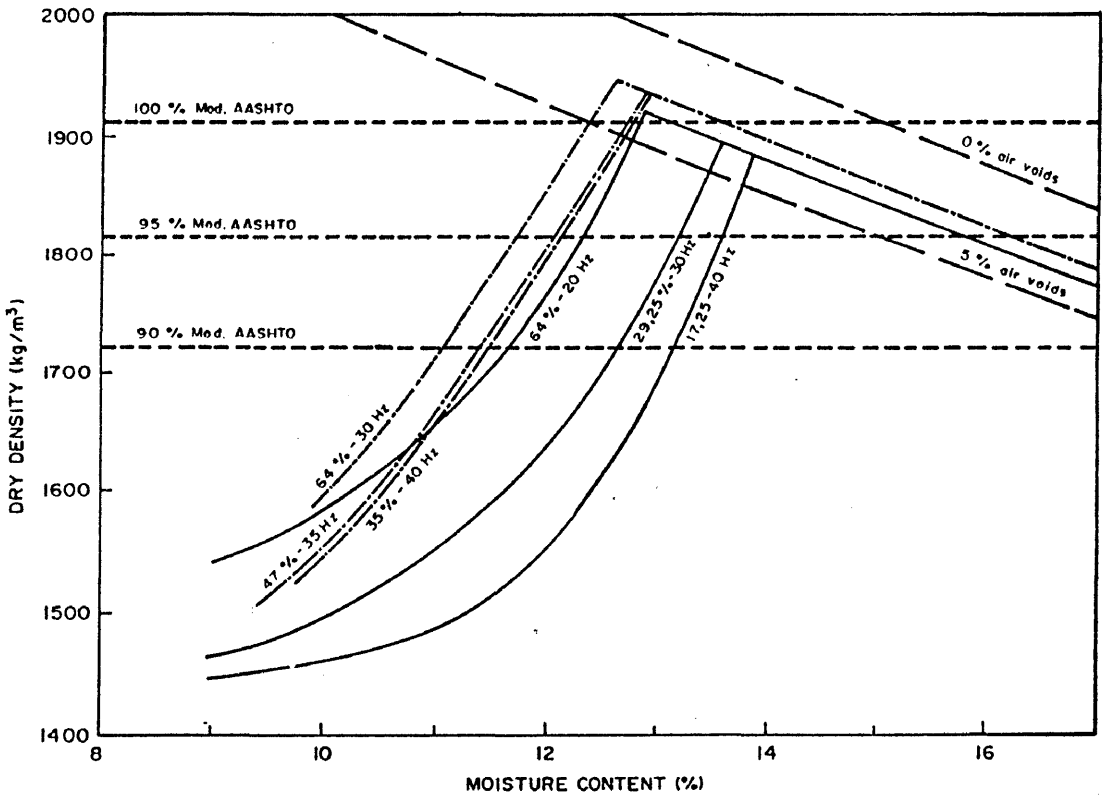

FIGURE 4.6 DRY DENSITY AGAINST MOISTURE CONTENT FOR SILTY SAND FOR SMALL SURCHARGE (FIGURES 4.2 AND 4.4 COMBINED)

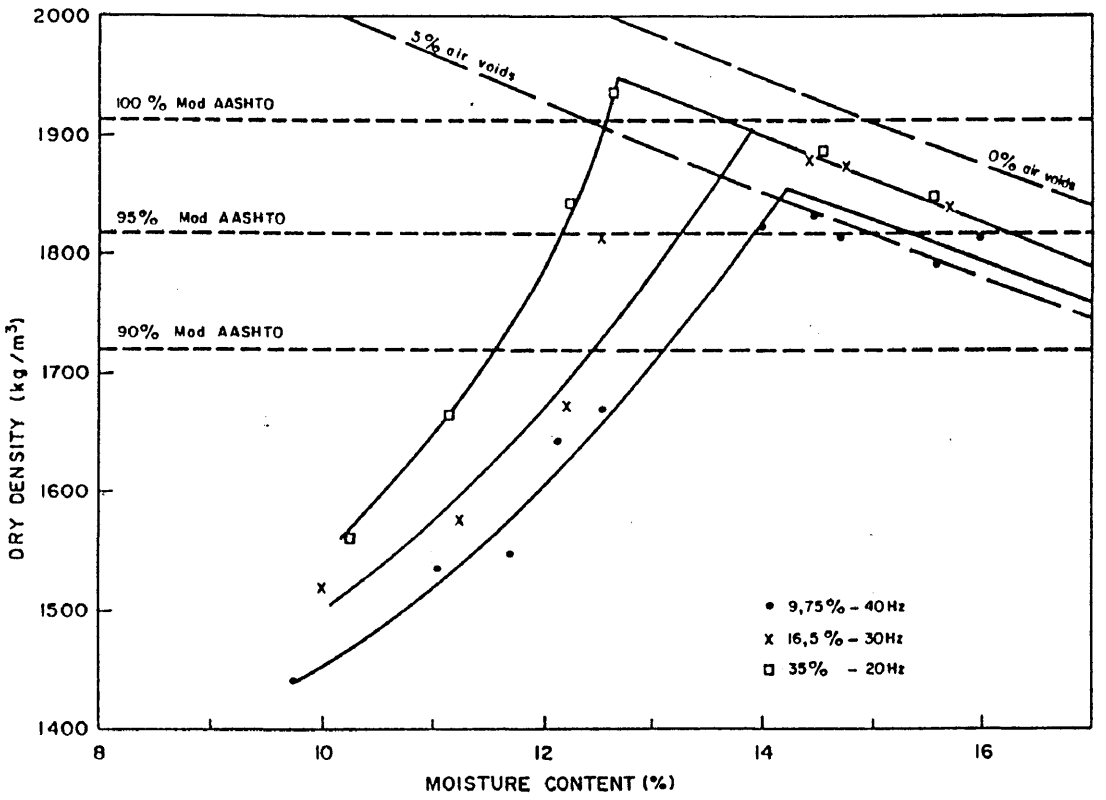

FIGURE 4.7 DRY DENSITY AGAINST MOISTURE CONTENT FOR SILTY SAND FOR LARGE SURCHARGE (k_{max} = 35 %) (Frequency 20-40 Hz)

For some unexplained reason the k-setting of 36 % for the general combination of 40 Hz-36 % was accidently set to 35 % for these early tests. This was the case for both the large as well as the small surcharge. As this was not critical to our observations, the work was not repeated with k equal to 36 %.

As the effect of vibratory compaction on the MDD and OMC values was unknown it was decided to follow the same strategy as that used for the std. AASHTO and mod. AASHTO compaction tests, where five to six samples are prepared at different moisture contents. The OMC and MDD results of the mod. AASHTO compaction test of each material were used for the selection of the different moisture contents (eg 25 %, 50 %, 75 %, 100 %, 125 % and 150 % of OMC (mod. AASHTO)) and sample size of the dry material (ie mass equal to a sample 100 mm high at 100 % mod. AASHTO density).

Once the compaction time for the material had been established (see Chapter 3), each sample was compacted for the same period, to ensure that each sample received the same amount of compaction effort. The sample densities were then determined as mentioned in Chapter 3.

The actual calculations were done using the Lotus 1-2-3 spreadsheet program. In this way the results could also immediately be viewed graphically, which is usually the best way to evaluate data initially. As the SD values of the material were also known, the zero air voids density lines (ZAVD) were also plotted on the graphs.

4.1 Discussion of the results

The results obtained with the different frequency-amplitude combinations on the slightly plastic sand lead to the following observations.

(a) The compaction of material on the dry side of optimum moisture content (OMC) is far more critical than on the wet side. The slope of the compaction curve on the dry side of OMC is approximately four times steeper than on the wet side of OMC (see Figures 4.1 to 4.7).

(b) The compaction curve is not symmetrical, (ie two separate functions) (see Figures 4.1 to 4.7).

(c) The slope of the compaction curve for moisture contents above OMC is parallel to the ZAVD line at about two and a half per cent air voids (see Figures 4.1 to 4.5).

(d) The transition from the compaction curve on the dry side of OMC to the compaction curve on the wet side of OMC is very rapid which points to the very rapid build-up of pore pressure (water and air) which cannot be dissipated (see Figures 4.2 to 4.4).

(e) The compaction curves for the different frequency-amplitude combination, such that $kmr.4\pi^2f^2$ was constant, gave different graphs on the dry side of OMC; the highest density for a given moisture content was achieved for the highest k-settings (k = 64 %) and lowest frequencies. For moisture contents above the OMCs the results obtained for the different amplitude frequency combinations described the same compaction curve parallel to the ZAVD line (ie the same density results were achieved at higher moisture contents) (see Figures 4.1 to 4.5).

(f) Due to the different compaction curves for the different frequency-amplitude combination on the dry side of optimum, the different frequency-amplitude combinations have different OMCs (see Figures 4.1 to 4.7).

(g) The large surcharge gave higher densities on the dry side of OMC than the small surcharge. On the wet side of OMC the density results for the large and small surcharges described the same compaction curve. The OMC values for the same frequency-amplitude combinations but different surcharges therefore also differed (see Figures 4.1 and 4.2 together and Figures 4.3 and 4.4 together).

(h) The fact that compaction curves on the dry side of OMC for a k-setting of 64 % and frequencies of 20 and 30 Hz respectively, virtually coincide for the same number of compaction blows (see Figures 4.5 and 4.6) point to the fact that compaction is more dependent on the amplitude than on the frequency. This is confirmed by the fact that the compaction curves on the dry side of OMC for other frequency-amplitude combinations lie higher in the sequential order of their respective amplitude sizes, namely k = 47 % (f = 35 Hz), k = 35 % (f = 40 Hz), k = 29,25 % (f = 30 Hz) and k = 17,25 % (f = 40 Hz).

(i) The more effective utilization of the compaction energy by a high amplitude in the moisture region below OMC broadens the range of moisture contents at which the material can still effectively be compacted to the specified density requirement (ie 95 % mod. AASHTO) (see Figures 4.1 to 4.7).

(j) In cases where the moisture content is too high (above OMC) it is clear that the higher amplitude can not produce higher densities, because of the build-up of pore pressure due to the excess liquid which cannot be dissipated rapidly. The only effective manner whereby higher densities can be achieved, is by the lowering of the moisture content by desiccation.

(k) Observations (e), (h) and (i) also supply the proof why impact compaction by impact rollers with their very high dynamic loading is generally so successful.

(l) Only in one case for the large surcharge did the kmr-value become low enough for the density curve above OMC not to coincide with the density curves of the other frequency-amplitude combinations (viz k = 9,75 %) (see Figure 4.7), but the curve was once again parallel to the ZAVD line. The air voids in this case amounted to about four per cent while it amounted to about two and a half per cent for the other frequency-amplitude combinations. The compactive force was, therefore, neutralised at a lower pore pressure.

The compaction results of the other materials tested subsequently confirmed these findings (see Table 4.4) in that for most of the soils the frequency-amplitude combination of 30 Hz - 64 % gave the highest MDD and lowest OMC.

TABLE 4.4 The MDD and OMC values for the different materials tested for the general frequency-amplitude combinations

F/A	40/36	35/47	30/64	40/36	35/47	30/64
MATERIAL	MDD (%SD)	MDD (%SD)	MDD (%SD)	OMC (%)	OMC (%)	OMC (%)
BAB2(1+2)	57,52	57,86	59,11	25,35	25,00	23,71
BAB2(2)	58,27	58,32	59,09	24,63	24,58	23,80
SPR2	70,23	73,26	72,77	14,84	12,73	13,05
SPR1	71,62	71,41	71,51	14,68	14,84	14,76
SPR1(2)	71,62	71,44	71,53	14,68	14,84	14,77
LABLEN2	73,67	74,46	79,05	10,62	10,12	7,38
LABDEW1	77,51	78,17	77,96	9,87	9,47	9,59
OFS1	67,60	71,62	70,83	18,60	15,04	15,68
NPAB	74,81	76,44	77,44	11,90	10,90	10,31
SIL1	73,50	73,72	73,21	11,23	11,08	11,42
LABD1	77,61	78,84	79,59	8,93	8,23	7,82
TPA3	77,01	77,15	77,47	9,67	9,58	9,40
TPA1	77,92	79,03	79,11	8,70	8,11	8,06
CPA1	88,73	88,98	90,24	4,61	4,49	3,92
DENS7	82,68	84,07	84,28	7,38	6,69	6,58
TPA2	81,09	80,59	82,14	7,80	8,08	7,22
NPAE	87,47	87,95	88,33	5,43	5,19	5,01
FERR1	85,91	86,26	86,79	5,25	5,08	4,82
OFS2	81,36	83,94	83,96	6,87	5,62	5,61
NPAA	87,92	87,63	88,04	4,60	4,72	4,55
ROSS1	86,14	85,80	86,64	4,34	4,50	4,09
DENS8	75,90	76,07	77,79	11,92	11,81	10,76
DENS8(2)	77,72	76,78	77,81	10,80	11,37	10,74
OFS3	86,24	89,52	88,41	4,25	2,85	3,31

Other findings for these materials are:

(a) For most of the materials tested the MDD- and OMC-values for the three generally used frequency-amplitude combinations were very similar (see Table 4.4).

(b) When expressing the MDDs and zero air voids densities (ZAVDs) as a percentage of the solid density of the respective materials (ie how much of the space is occupied by solids) and plotting these values against their respective OMCs, a very interesting result is obtained (see Figure 4.8). It is interesting to note that the coarse well-graded materials had the highest MDDs and had the lowest OMCs while the other materials had progressively lower MDDs and higher OMCs as the material became finer and more uniform in nature. This is similar to what Woods et al[2] had found for materials with the same solid density (see Figure 2.2).

(c) Expressing the MDDs (mod. AASHTO) as a percentage of the apparent density of the respective materials and plotting these values against their respective MDDs (vibratory) also gives a very interesting result (see Figure 4.9). For all the materials tested except two cohesive materials, namely the shale and the montmorillonite clay, the MDDs (mod AASHTO) are substantially lower than the MDDs (vibratory). This phenomenon was already known for well-graded crushed stone materials in South Africa in that the specification requirement for the density of G1 materials normally specifies a density of 86 % to 88 % AD which agrees with MDD (vibratory). This was also confirmed by the earlier research by Maree[63] on crushed stone base materials.

4.2 General conclusions on the effect of frequency and amplitude of the vibratory force on the compaction of roadbuilding materials

(a) The higher densities generally achieved by the high amplitude vibratory force very clearly points to the important effect of the dynamic component of the vibratory force. Using a high amplitude will therefore usually improve the compaction results obtained as well as extend the range of moisture contents in which materials can still effectively be compacted to the specified density (eg 95 % mod. AASHTO).

(b) Associated with conclusion (a) is the very important effect of the dynamic component of the compactive force which also confirms why impact rollers are so successful.

(c) If the moisture content is too high (above OMC), the higher dynamic force dissipated by the high amplitude vibratory force cannot improve the density, because of the build-up of pore pressure which cannot be dissipated. The only effective manner in which higher densities can be obtained is by lowering the moisture content. It is imperative therefore to properly control the moisture content of materials in order to

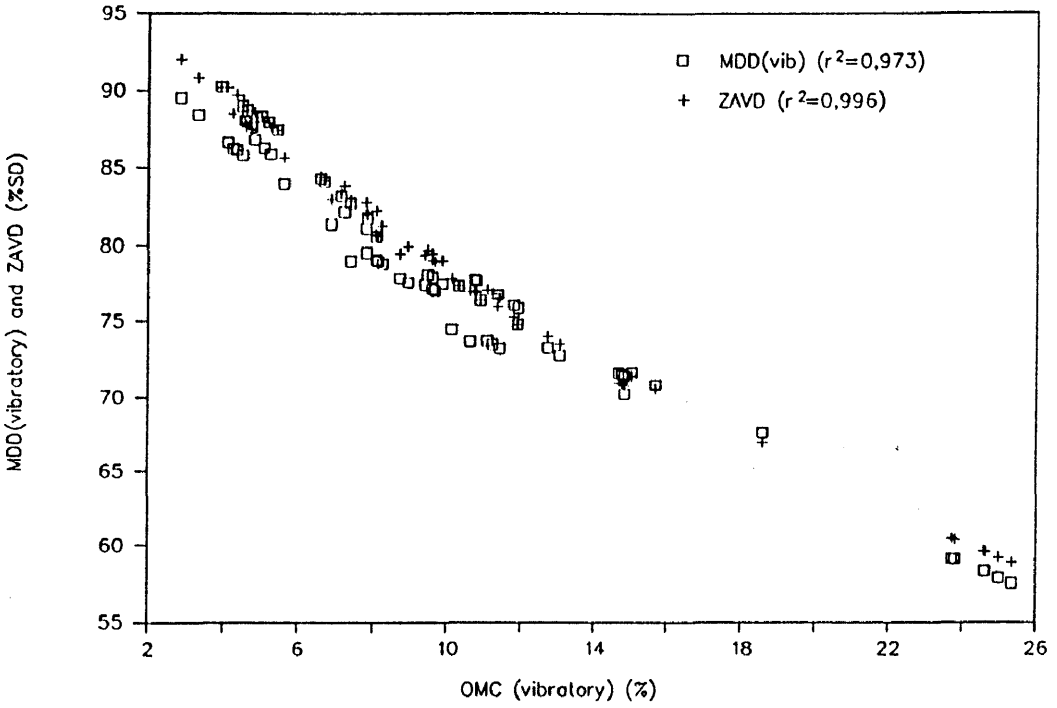

FIGURE 4.8 **MAXIMUM DRY DENSITY (VIBRATORY) (% SD) AND ZERO AIR VOIDS DENSITY (% SD) AGAINST OPTIMUM MOISTURE CONTENT (VIBRATORY) (%) OF THE RESPECTIVE MATERIALS FOR THE GENERALLY USED FREQUENCY-AMPLITUDE COMBINATIONS (40 Hz - 36 %, 35 Hz - 47 %, 30 Hz - 64 %)**

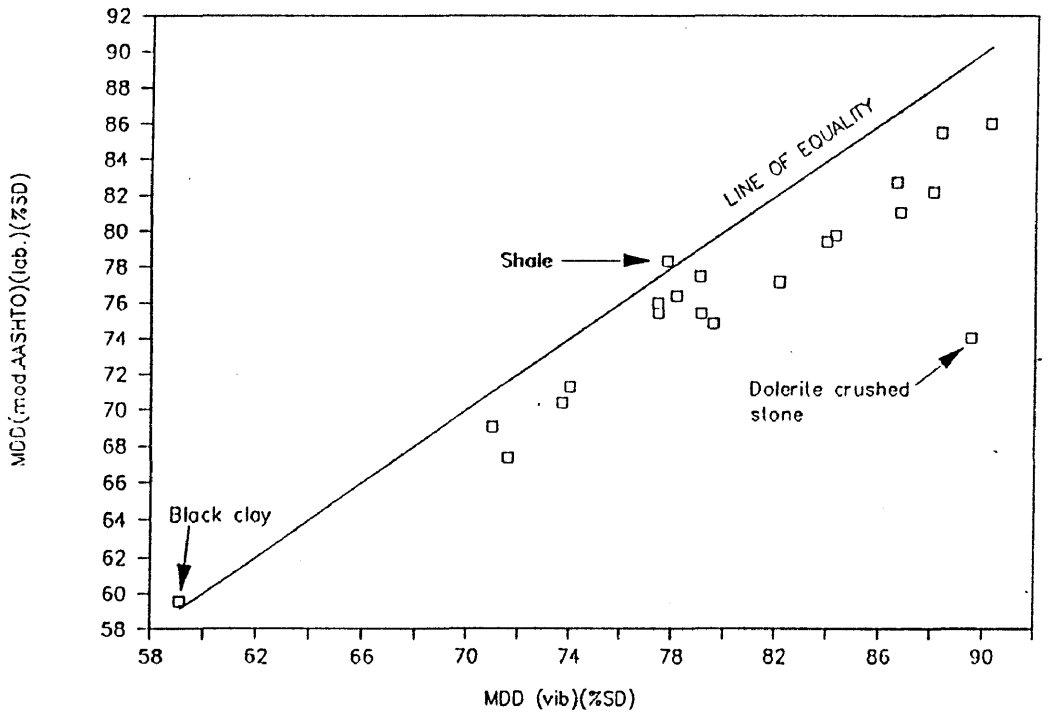

FIGURE 4.9 **MAXIMUM DRY DENSITY (mod. AASHTO) (% SD) AGAINST HIGHEST MAXIMUM DRY DENSITY (VIBRATORY) (% SD) OF THE RESPECTIVE MATERIALS FOR THE GENERALLY USED FREQUENCY-AMPLITUDE COMBINATIONS**

ensure that they can be effectively compacted. Furthermore, if moisture content is poorly controlled the compaction results obtained will be highly variable.

(d) It was found that the MDDs and OMCs for the different frequency-amplitude combinations for the same compactive effort were grouped together fairly closely (see Figures 4.1 to 4.7). In practice this flexibility in choice should be remembered as the compaction of a layer should never be seen in isolation but should take account of the overall situation. For example in the compaction of a crushed stone base on top of a stabilised subbase it is normally recommended to limit the high amplitude compaction to the breakdown pass only of the crushed stone base whereafter the low amplitude should be used. This is done to prevent possible damage to the stabilised subbase by the higher dynamic forces of the "low frequency - high amplitude" combination. At the same time the "high frequency - low amplitude" combination will give more tamping blows per unit distance travelled, which should lead to a smoother surface.

(e) The differences in the dry densities produced by the large and small surcharge for the same frequency-amplitude combinations also clearly point to fact that the increase of the vibratory force alone without increasing the load of the roller on the drum will not necessarily increase the efficiency of the roller. The total load resting on the drum of a vibratory roller has a very important influence on the results that can be obtained.

(f) Figure 4.8 shows that each material has a unique MDD and OMC and that both are only to a certain extent dependent on the nature and size of the compactive force involved (ie approximately the same amount of compaction energy was used to compact all these samples) but very dependent on the actual composition of the material.

(g) Figure 4.8 also shows that the MDD and OMC values of each material are related to one another in that all the MDD values are always found in a position very near to the ZAVD line. This shows that if enough effective compactive energy is applied to an untreated roadbuilding material, the material particles will re-orientate themselves until a state is reached where the voids cannot be reduced anymore. The final amount of voids left is therefore strongly dependent on the particle size distribution. Because the MDD of each material is always found near the ZAVD this means that the OMC of each material is also dependent on the particle size distribution (ie the total space at MDD is very nearly filled with either solids of the material, or water which fills the

voids; a very low percentage (0 - 3 %) of the total space is occupied by air). Some relationship therefore exists between the particle size distribution after compaction and the MDD and OMC of each material. Because the particle size distribution after compaction determines the MDD and OMC, the amount of compaction should be carefully monitored to avoid unnecessary breakdown of the material. Over-rolling (ie over-compaction) should be avoided at all cost as this leads to dedensification of the material due to breakdown of the material.

(h) Figure 4.9 shows that the mod. AASHTO density test generally does not compact materials optimally, as endorsed by the fact that mod. AASHTO densities of all the materials tested, except those of the black clay and shale (both cohesive materials), plotted below the line of equality. There are several reasons for this, amongst others the test requirement that all particles larger than 19 mm must be replaced by material passing the 19 mm sieve, but retained on the 13,2 mm sieve. Another reason is the compaction hammer itself which does not cover the total surface of the sample which often causes the adjacent material to be disturbed by the compaction effort. The important point is, however, that materials are not being compacted optimally in practice due to the misconception that MDD (mod. AASHTO) is the highest density level that can be achieved with materials. The lower the actual density requirement for a layer, the more likely the chance that the layer will be deformed due to an increase in density.

CHAPTER 5
INFLUENCE OF DRY DENSITY AND MOISTURE CONTENT ON CBR

In Chapter 4 it was shown that the size of the dynamic force delivered by the vibrating load has a direct influence on the MDD and OMC. This influence is, however, limited and the MDDs and OMCs of untreated roadbuilding materials are mainly determined by the particle size distribution after compaction. The bearing capacity of the material during the compaction process is influenced by both the dry density level and the moisture content. The general criteria to express the bearing capacity of untreated roadbuilding materials in South Africa is the soaked California bearing ratio or soaked CBR.

As stated by Porter[56] in the literature survey, CBR samples were soaked "to permit the specimen to swell and reach the adverse state of moisture which is usually present in the subgrade under normal drainage and climatic condition". As the main focus of this investigation was on the influence of material properties on the compactability of soils, soaking the samples would not reflect the materials resistance to deformation during compaction at a given moisture content. Apart from this the soaked condition of materials is extremely rare in pavement structures in South Africa in general (see Emery[57]). For these reasons and logistic reasons mentioned in Chapter 3 the CBR values of the compacted samples were always determined on the compacted samples immediately after compaction at moulding moisture content.

5.1 Definition of the California Bearing Ratio (CBR)

The California Bearing ratio of a material is the load in Newtons, expressed as a percentage of the California standard values, required to allow a circular piston of 1935 mm^2 to penetrate the surface of a compacted material at a rate of 1,27 mm per minute to depths of 2,54 mm, 5,98 mm and 7,62 mm. The California standard values for these penetration depths are 13 344, 20 016 and 25 354 N respectively. An annular surcharge weight with a mass of 5,56 kg ± 50 g is placed on the top surface of each sample during the penetration loading of the sample. In South Africa the 2,54 mm penetration value only is used.

5.2 Relationship between CBR, dry density and moisture content of untreated roadbuilding materials

As mentioned earlier, the materials were not only compacted over a range of moisture contents (from fairly dry to very wet) to determine the MDDs and OMCs for different

frequency-amplitude combinations, but the materials were also compacted to approximately 90 %, 93 %, 95 %, 97 % and 100 % mod. AASHTO (where achievable) over a range of moisture contents. These density levels were specifically selected as they are very often used as the specification limits for density for the different structural layers of the road pavement.

The CBR at moulding moisture content of each of these samples was determined immediately after compaction of the sample.

To evaluate the effect of dry density and moisture content on the CBR of untreated roadbuilding materials the following procedure was followed:

(a) All the dry densities (% mod. AASHTO), moisture contents (%) and CBRs (%) for each material were listed.

(b) The list was then rearranged in the order of magnitude of the dry densities.

(c) The CBR values of the samples were then divided in separate categories for densities lower than or equal to 90 % mod. AASHTO, densities from + 90 % to 93 %, + 93 % to 95 %, + 95 % to 97 %, + 97 % to 100 % and + 100 % mod. AASHTO. For some materials the lower density categories were not present, but categories for densities from + 100 % to 105 % and + 105 % to 110 % mod. AASHTO or even higher had to be added. This was particularly applicable for the G1 crushed stone materials. This was done to look at the effect of moisture content on the CBR.

(d) All the CBR values of the different density categories were then plotted together against their respective moisture contents. The CBR values of each density category was given a different symbol. From these plots (see examples in Figures 5.1 to 5.4) it was clear that a definite relation exists between the CBR (%) and the dry density (% mod. AASHTO or % AD or % DBD) and the moisture content (%). When the first material was analysed in this manner the mathematical relation was determined by means of multiple regression techniques. This original model was then tried on the subsequently tested materials. It very soon became quite clear that the same basic reaction model describing the relation of CBR in terms of the dry density and moisture content fitted all the materials used in this investigation (r^2-values varied between 0,70 and 0,95).

(e) The graphs showed that the CBR values of a material tended to reach a maximum at a specific moisture content for all the density levels. This moisture content is called the critical moisture content, after the work by Arquié[16] because the author is of the opinion that this is the point at which maximum cohesive forces are generated (see the section dealing with the influence of moisture content in Chapter 2). The critical moisture content (CMC) of a material is, therefore, defined as that moisture content at which the maximum CBR values are achieved for any level of density for that particular material. It was furthermore found that the CBR for any density level was reduced as the actual moisture content of the material deviated from the CMC. The drop in strength was therefore a function of the moisture content deviation from CMC.

The basic equation (Model A) is the following:

$$CBR = k_5.A + k_6.A^3/Abs(A) + k_7.B + k_8.B^3 + k_9 \quad \ldots\ldots\ldots\ldots\ldots\ldots \quad (5.1)$$

Where $A = k_1.D + k_2.D^2 + k_3.B + k_4$ (first approximation of CBR value)

and where
- D = dry density expressed as a percentage of the MDD (mod. AASHTO) or a percentage of the apparent density (AD) or dry bulk density (DBD)
- B = absolute difference between the sample moisture content and the critical moisture content (CMC) for the particular material
- k_n = regression constant
- $Abs(A)$ = absolute value of A.

The values of the regression constants differed depending on what density standard was used (ie mod. AASHTO or solid density). The choice of density standard really depends on the researcher's preference. At the start of this investigation the author chose the mod. AASHTO density standard as this is the generally accepted standard for road construction in South Africa. However, as the investigation progressed the author changed to solid density to observe the effect of material properties on the bearing capacity.

(f) The general procedure followed was therefore to estimate the CMC from the plots of the data points by maximizing the r^2-value. By comparing the r^2-value of the model for estimated CMC values slightly above or below the original CMC estimate it was

possible to establish the correct CMC value. The correct CMC value was always the moisture content at which the highest r^2-value for the model was achieved.

(g) As with any empirical investigation some outlying results, better known as outliers, were also present. An outlier indicates a data point which is not typical of the rest of the data. It should be submitted to particularly careful examination to see if the reason for its peculiarity can be determined and rectified. This was normally done; where these reasons could not be found these outliers were removed from the population as it seemingly belongs to another population. Ideally one would like to repeat the test. This was, however, not always possible due to time and money constraints. The standard practice for dealing with outlying observations (see ASTM E178-80 (reapproved 1989)) only deals with populations with a single mean. Where the investigation was looking at the effect of the dry density and moisture content over a range of dry densities and moisture contents for each material, the results could not be evaluated by applying these techniques directly. For most of the materials outliers were visually identified from the data plots because they lie three or four standard deviations or further from the mean of the residuals. During the visual assessment of outliers the influence of the removal of a possible outlier on the subsequent r^2-value of the bearing capacity model played a significant role in deciding whether this particular result should be classified as an outlier or not. Once the r^2-value had stabilized, the bearing capacity model was used to determine a predicted mean CBR value for the actual dry density and moisture content of each sample. Using the approach in Section 4 of ASTM E178-80 (reapproved 1989) the T_n-value for each sample was calculated with the following formula:

$$T_n = \text{absolute value of } (x_n - y_n)/S \quad \ldots\ldots\ldots\ldots\ldots\ldots\ldots\ldots \quad (5.2)$$

where T_n = the test value for sample n

x_n = the laboratory value of the CBR for sample n

y_n = the predicted mean value of the CBR for sample n determined with the regression model using the dry density and moisture content of sample n

S = standard error of the regression model

The T_n-value for each sample was then compared with the $T_{(0,050)}$ value, the value of which is dependent on the total number of observations in the population. The values for $T_{(0,050)}$ were obtained from Table 1 in ASTM E178-80. If T_n was larger or

equal to $T_{(0,050)}$ the result was classified as an outlier. For most of the materials there was close agreement between the visually and statistically identified outliers (see Appendix D for the regression analysis results with all data points and minus visually identified outliers as well as for the actual test results used during the regression analysis for the materials used in this investigation showing both the visually and statistically identified outliers).

(h) Once the actual regression constants had been established, the theoretical CBR values for density levels of 90 %, 93 %, 95 %, 97 % and 100 % mod. AASHTO (sometimes higher) were established for the moisture content range of the test results and plotted together with the actual test results (see Figures 5.1 to 5.4 as examples. Figures for other materials are listed in Appendix D). For each material two plots were established namely (i) CBR against dry density for different moisture contents and (ii) CBR against moisture content for different dry densities. The negative and positive values in brackets behind the r^2-values in these figures are the number of outliers deleted from the sample population and sample population size respectively. If there is no negative value, no outliers were deleted.

Vastly different CBR ranges were observed for the different crushed stone materials even though they covered approximately the same density and moisture ranges.

5.3 Conclusions on the influence of dry density and moisture content on CBR

A definite relation exists between the CBR and the dry density and moisture content for each untreated material investigated. Because the basic relation is the same for all the materials investigated (only the values of the regression constants differed) and a wide range of material types ranging from A-1 to A-7-6 were investigated, it is highly likely that the CBRs of other untreated materials not included in this investigation will also be satisfied by the same basic relation. It is also likely that this relation will be universally applicable as the same basic criteria of CBR, dry density and moisture content are also used elsewhere (see Figures 2.4[58] and 2.5[59] as examples of similar relations found elsewhere).

Each material has a unique CMC value at which the CBR values peak. Because the CMC is most likely the moisture content at which maximum cohesive force is achieved, this is also dependent on the physical composition of the material. The particle size distribution (ie grading) of the material most probably has the greatest influence on the CMC. For instance the CMC of crushed stone materials is around 3 per cent and for the black montmorillonite

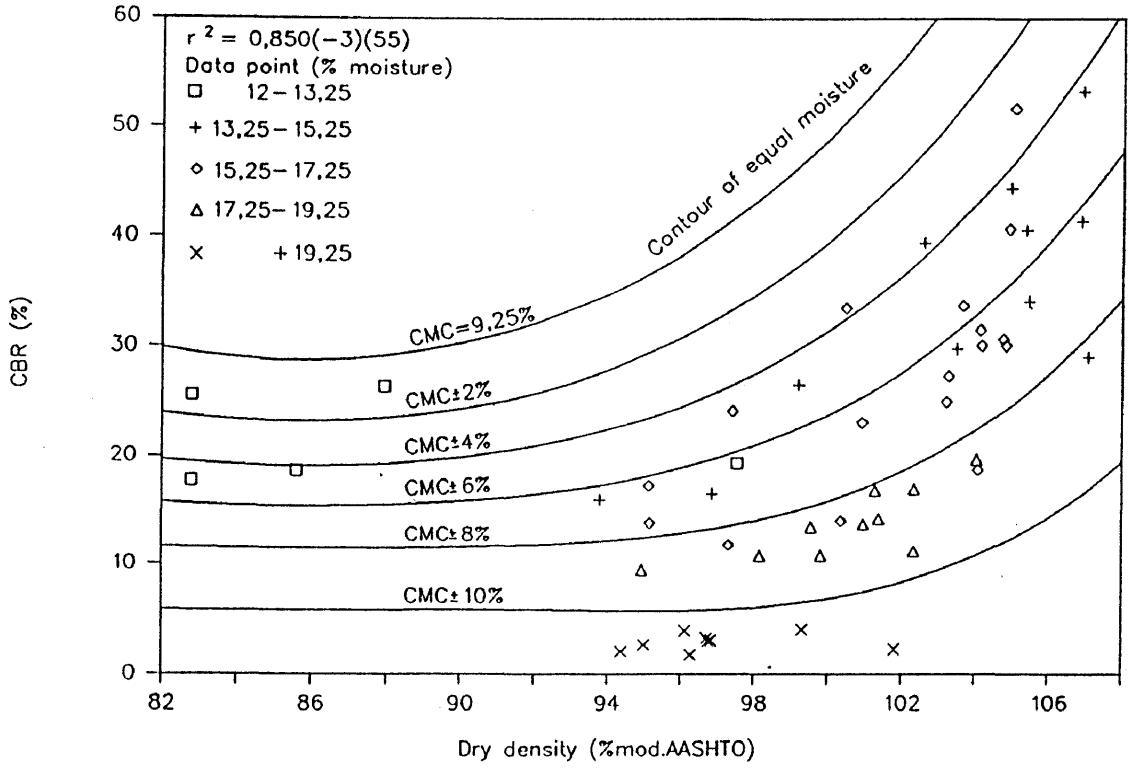

FIGURE 5.1(a) RELATION BETWEEN CBR AND DRY DENSITY FOR DIFFERENT MOISTURE LEVELS (RED SANDY CLAY) (SPR1)

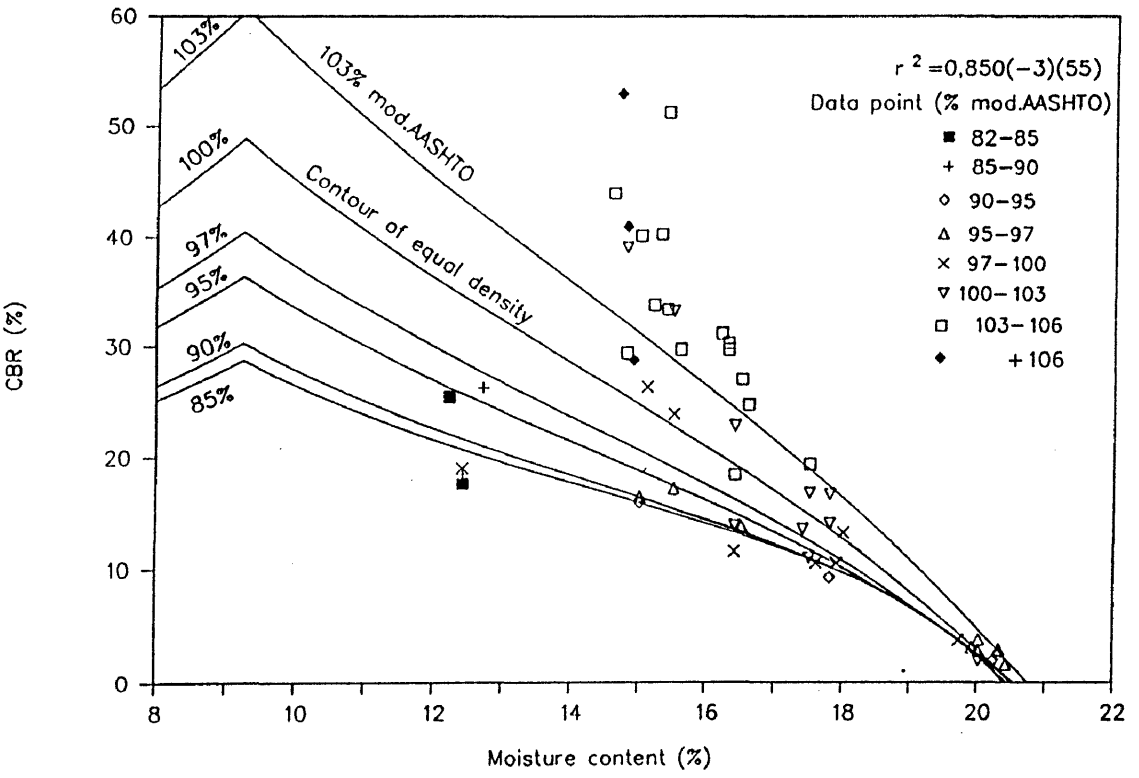

FIGURE 5.1(b) RELATION BETWEEN CBR AND MOISTURE CONTENT FOR DIFFERENT DENSITY LEVELS (RED SANDY CLAY) (SPR1)

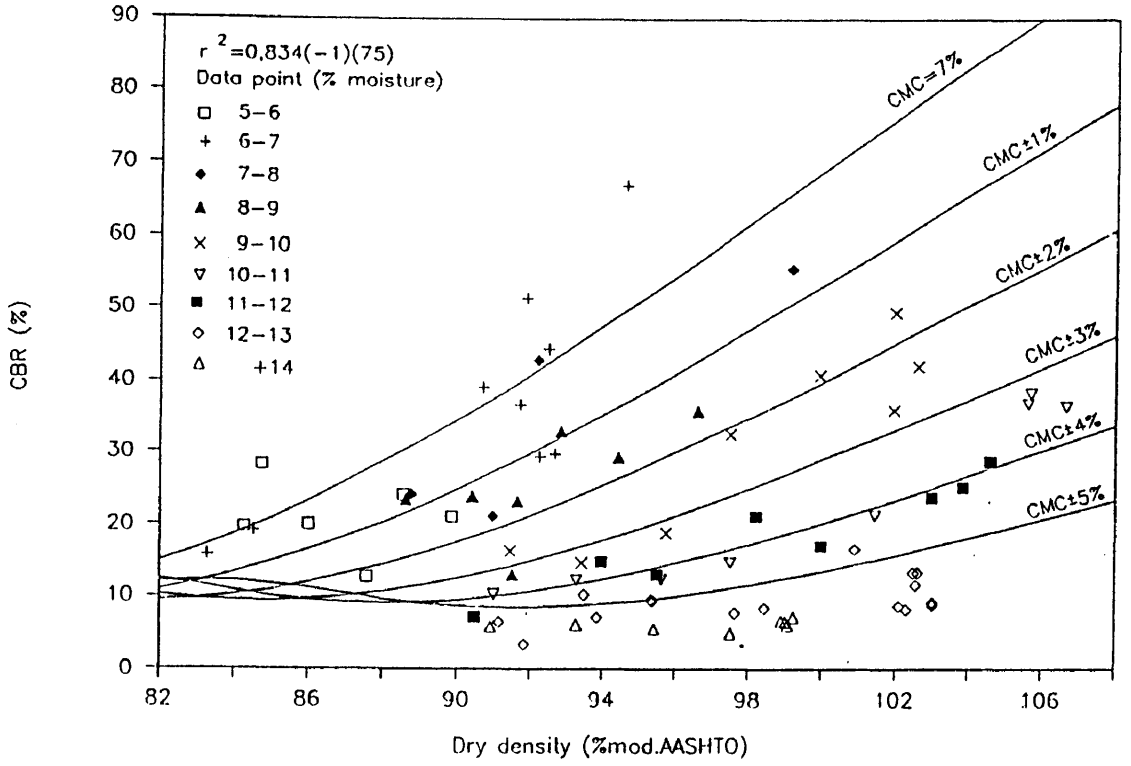

FIGURE 5.2(a) RELATION BETWEEN CBR AND DRY DENSITY FOR DIFFERENT MOISTURE LEVELS (SILTY SAND) (SIL)

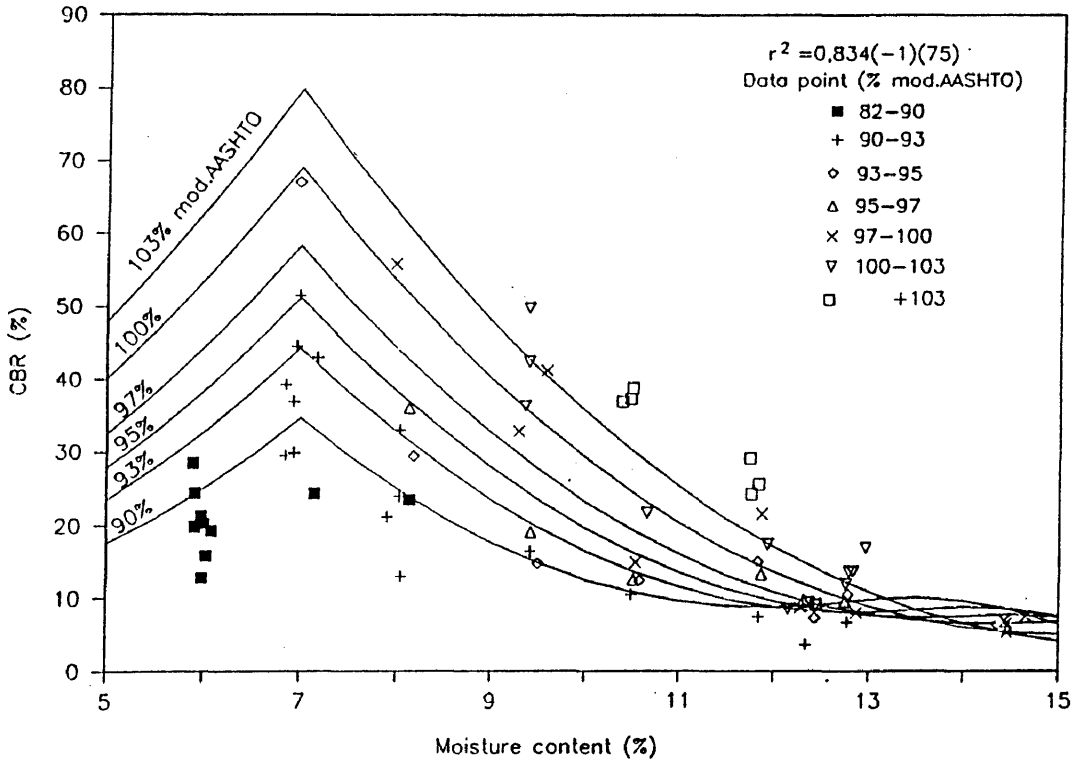

FIGURE 5.2(b) RELATION BETWEEN CBR AND MOISTURE CONTENT FOR DIFFERENT DENSITY LEVELS (SILTY SAND) (SIL)

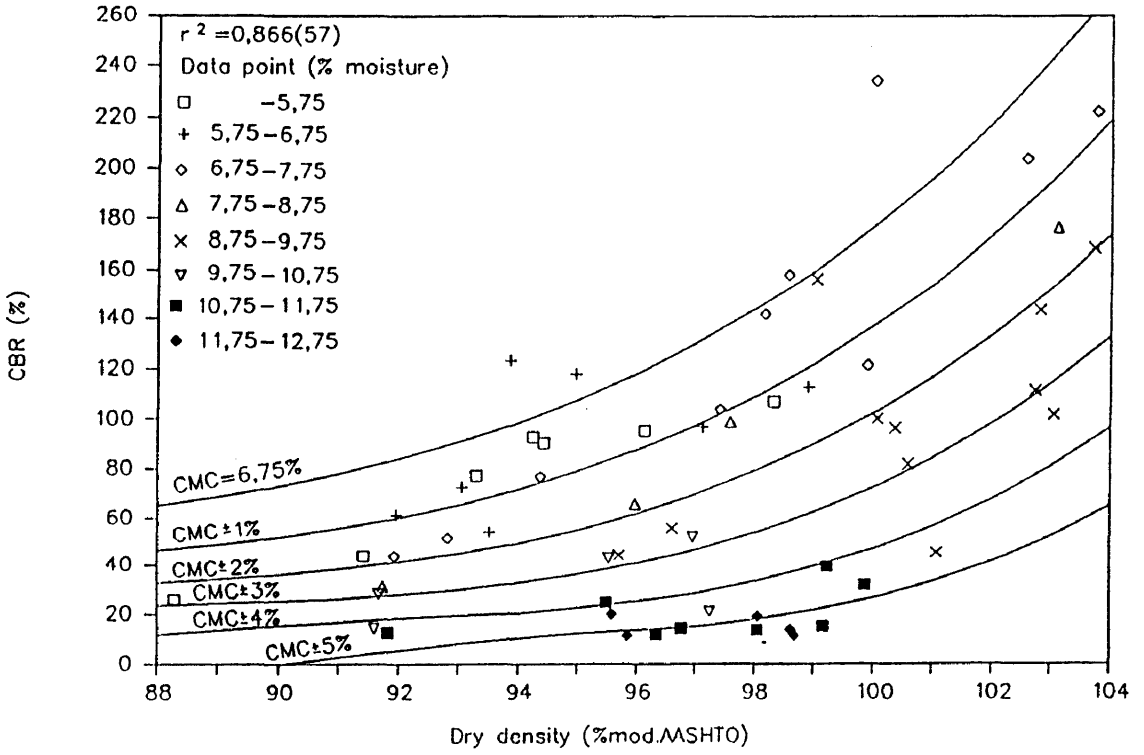

FIGURE 5.3(a) RELATION BETWEEN CBR AND DRY DENSITY FOR DIFFERENT MOISTURE LEVELS (CHERT GRAVEL) (TPA3)

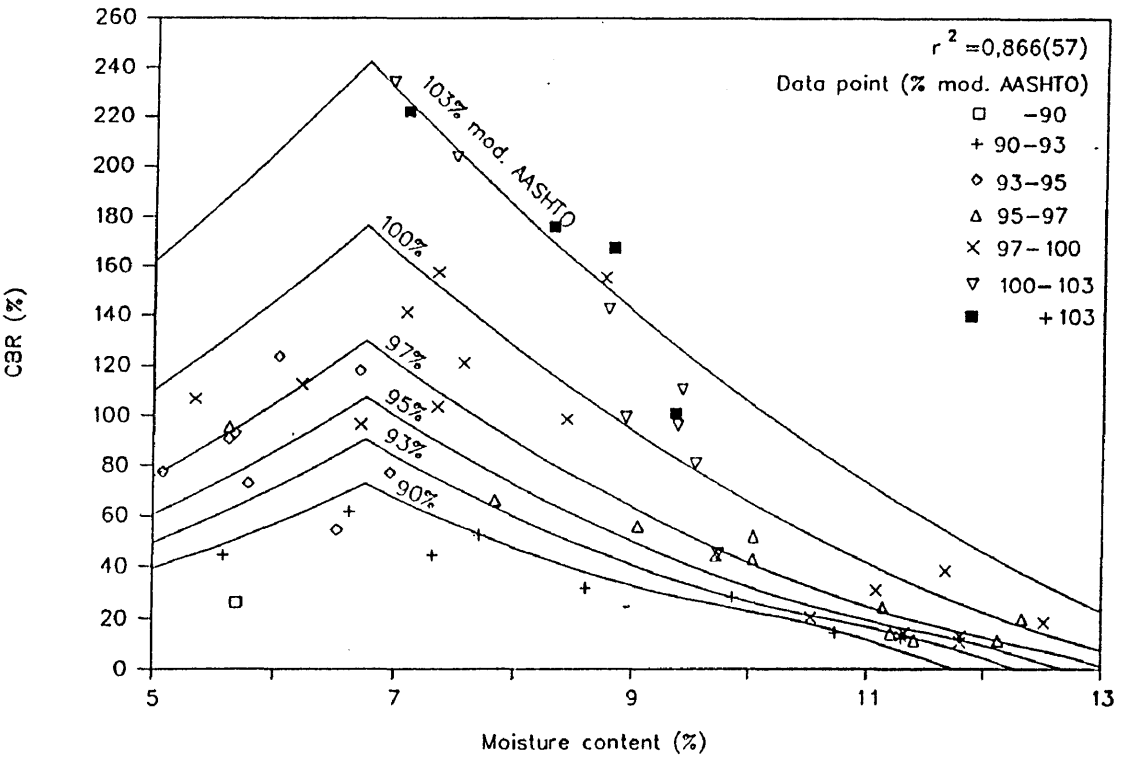

FIGURE 5.3(b) RELATION BETWEEN CBR AND MOISTURE CONTENT FOR DIFFERENT DENSITY LEVELS (CHERT GRAVEL) (TPA3)

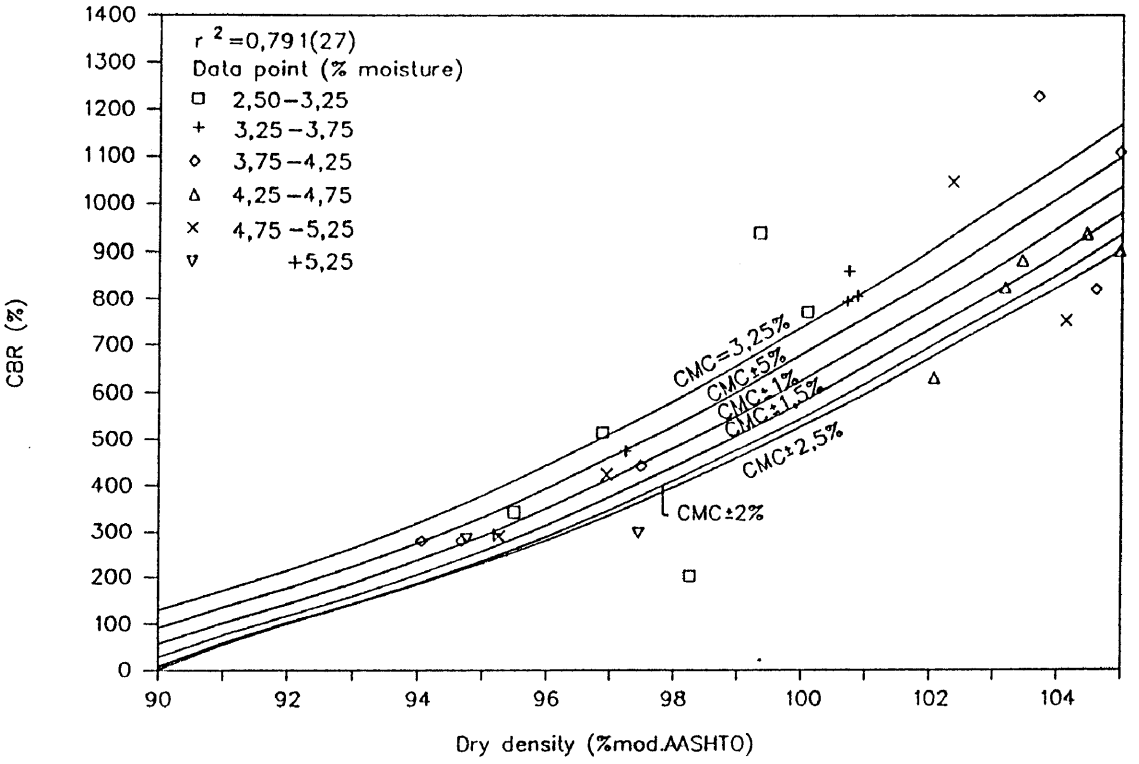

FIGURE 5.4(a) RELATION BETWEEN CBR AND DRY DENSITY FOR DIFFERENT MOISTURE LEVELS (GRANITE CRUSHED STONE) (ROSS1)

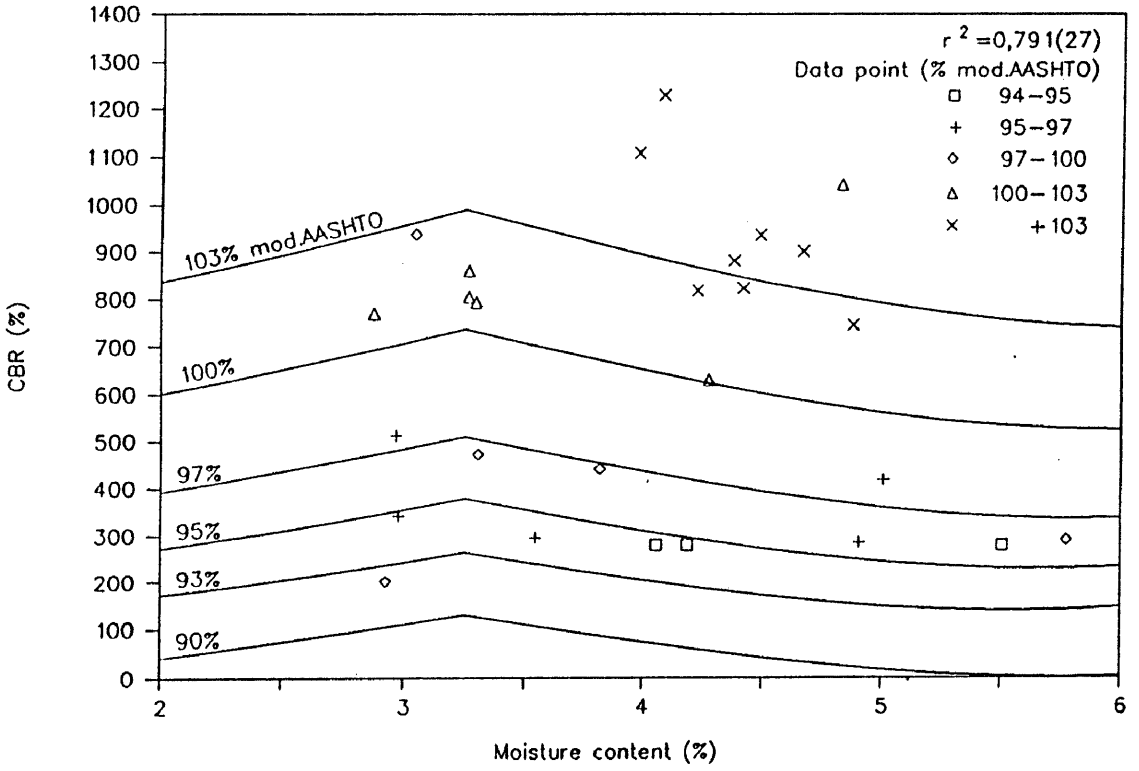

FIGURE 5.4(b) RELATION BETWEEN CBR AND MOISTURE CONTENT FOR DIFFERENT DENSITY LEVELS (GRANITE CRUSHED STONE) (ROSS1)

clay the CMC is 12 per cent, while the natural gravel materials and sandy materials have CMC values somewhere between these values (see Table 5.1). As there is also a relation between the MDD and OMC and both are dependent on the physical composition, as discussed in the previous chapter, it is clear that both the density and moisture regimes are dependent on the physical compositions of the materials themselves. It is therefore almost a foregone conclusion, that some mathematical relation exists whereby it is possible to express both the MDD (vibratory and mod. AASHTO), OMC (vibratory and mod. AASHTO) and CMC of a material in terms of its grading, Atterberg limits and linear shrinkage.

TABLE 5.1 The values of MDD (vib), OMC (vib), ZAVMC (vib) and CMC for the original materials as determined from the test results

SAMPLE	MDD (vib) (% SD)	OMC (vib) (%)	ZAVMC (vib) (%)	CMC (%)
BAB	59,11	23,71	25,10	12,00
SPR2	73,26	12,73	13,23	9,50
SPR1	71,62	14,68	14,68	9,25
LABLEN	79,05	7,38	9,79	7,00
LABDEW	78,17	9,47	10,42	8,75
OFS1	69,53	15,04	16,51	8,50
NPAB	77,44	10,31	10,30	8,00
SIL	73,72	11,08	13,33	7,00
LABD1	79,59	7,82	9,16	7,00
TPA3	77,47	9,40	10,57	6,75
TPA1	79,11	8,06	8,92	6,75
CPA1	90,24	3,92	3,92	2,75
DENS7	84,28	6,58	6,65	5,00
TPA2	82,14	7,22	8,14	4,50
NPAE	88,33	5,01	5,01	4,00
FERR1	86,79	4,82	5,68	4,00
OFS2	83,96	5,61	6,41	3,75
NPAA	88,04	4,55	4,54	3,75
ROSS1	86,64	4,09	5,84	3,25
DENS8	77,81	10,74	10,28	7,25
OFS3	89,52	2,85	3,95	3,00

Contrary to Arquié's theory that the CMC decreases with an increase in density (see Figure 2.3), it would seem that the CMC is not dependent on the density level, because the CBRs of all the materials peaked at a particular moisture content for all density levels. It would seem that the CMC is therefore solely dependent on the physical composition of the material and not on its density. In retrospect this does make sense in that the physical property that has the greatest influence on the CMC is, most likely, the total surface area of the material per unit mass, which is dependent on the physical composition of the material. For the materials investigated the surface areas per unit mass of the crushed stone materials will definitely be the lowest while the surface area per unit mass of the black montmorillonite clay will be the highest, because of their respective particle size distributions. This also suggests that the CMC of each material can possibly be expressed in terms of the grading, Atterberg limits and linear shrinkage of the respective material.

The quantification of the MDD (vibratory and mod. AASHTO), OMC (vibratory and mod. AASHTO), ZAVMC (vibratory and mod. AASHTO) as well as CMC in terms of the grading, Atterberg limits and linear shrinkage, are discussed in Chapter 6.

The fact that vastly different CBRs were measured for the different G1 crushed stone materials at approximately the same density and moisture content points to the fact that the CBR is dependent on other material properties apart from the dry density and the moisture content. These factors are most probably the shape and texture of the individual aggregate particles as well as the interaction between the total particle range of the material. In this investigation an effort was made to quantify these parameters by means of the shape factor (SF) and shakedown bulk density (SBD) (see description in Chapter 3).

Seeing that the CBR of a material is dependent on the density and moisture content of the material, and the shape and texture of the individual particles, it is highly likely that the CBR of a material can also possibly be quantified in terms of its grading, Atterberg limits and linear shrinkage. The quantification of the CBR for different density and moisture content levels in terms of the grading, Atterberg limits and linear shrinkage as well as the SBD and SF is discussed in Chapter 7.

CHAPTER 6

QUANTIFYING THE EFFECT OF MEASURED SOIL PROPERTIES ON MDD (VIBRATORY AND MOD. AASHTO), OMC (VIBRATORY AND MOD. AASHTO) ZAVMC (VIBRATORY AND MOD. AASHTO) AND CMC FOR UNTREATED ROADBUILDING MATERIALS

In Chapter 4 it was shown that the maximum dry density (MDD) and the optimum moisture content (OMC) of all untreated roadbuilding materials covered in this investigation, are related to one another (see Figure 4.8). The fact that materials with high MDDs have low OMCs while materials with low MDDs have high OMCs and that these points are always close to the zero air voids density line (ZAVD), point to the fact that some physical relation exists between these properties and the actual physical composition of these materials.

Similarly it was shown in Chapter 5 that the CBRs for each untreated roadbuilding material peaked at a particular moisture content for all density levels. This unique so-called critical moisture content (CMC) is also dependent on the actual physical composition of the material.

The physical composition of untreated roadbuilding materials in South Africa is normally expressed by the following parameters:

(a) The material by mass passing the 75 mm, 63 mm, 53 mm, 37,5 mm, 26,5 mm, 19 mm, 13,2 mm, 4,75 mm, 2,00 mm, 0,425 mm and 0,075 mm sieves.
(b) The grading modulus
(c) The coarse sand fraction
(d) The fine sand fraction
(e) The Atterberg limits, namely the liquid limit (LL), plastic limit (PL) and plasticity index (PI) (= LL - PL) carried out on the minus 0,425 mm fraction.
(f) The linear shrinkage of the minus 0,425 mm fraction.
(g) TRB classification.

The coarse sand fraction is the material passing the 2,00 mm sieve and retained on the 0,425 mm sieve expressed as a percentage of the material passing the 2,00 mm sieve. The fine sand fraction is the material passing the 0,425 mm sieve and retained on the 0,075 mm sieve expressed as a percentage of the material passing the 2,00 mm sieve.

As this information is normally determined routinely for all untreated roadbuilding materials, the aim was to determine mathematical expressions for MDD (vibratory and mod. AASHTO),

OMC (vibratory and mod. AASHTO), ZAVMC (vibratory and mod. AASHTO) and CMC in terms of these properties, by means of multiple regression techniques.

The vastly different CBRs measured for crushed stone materials at approximately the same density suggest that the CBRs of untreated roadbuilding materials do not only depend on the dry density and moisture content of the material, but also depend on the shape and texture of the aggregate particles. For this reason the weighted values of the specific rugosity (S_{rv}) (loose state) and the shape factor (SF) (shake tamped state) for the different sieve fractions of each of the materials investigated was also determined (see Chapter 3 for method).

Because the particle size distribution also has an effect on the CBR, the loose bulk density (LBD) (% SD) (loose state) and the shakedown bulk density (SBD) (% SD) (shake tamped state) for the total grading of each of the materials, was also determined (see Chapter 3 for method).

6.1 The grading factor (GF)

The fact that the MDDs and OMCs are related to one another and these points are always close to the ZAVD line (see Figure 4.8), suggests that the amount of void space found in a well compacted material is a function of the physical particle size distribution of that material. Similarly the total surface area per unit mass of material which has a direct influence on the CMC of each material. The value of the CMC which is unique for each material is thus also a function of the physical particle size distribution.

The influence of the grading on the MDDs has been known for a very long time. This is borne out by the fact that coefficients such as the grading modulus, and uniformity coefficient (ie d_{60}/d_{10}) have been used for many years to give an indication of the quality and compactability of untreated roadbuilding materials. However, they were only indicative of the quality, and the MDDs can not be determined accurately from them, as they usually take account of limited information from the grading curve. The need for these simplified coefficients is understandable if one recalls that no pocket calculators or personal computers were available until recently. However, since these advanced modes of data processing and calculation are now freely available it does make sense to develop models, which may be fairly complicated, to accurately predict the MDDs, OMCs, ZAVMCs and CMC from the physical composition of the material.

Because all these properties are very strongly dependent on the physical particle size distribution of the materials, and some breakdown of material occurs during the actual compaction procedure (either in the laboratory or on site), it is important to remember that the values of these properties are determined by the grading after compaction.

The best description of the physical particle size distribution is the total grading curve. A new parameter which takes account of the whole grading curve was therefore introduced, namely the so-called grading factor (GF).

> GF = Σ (percentage passing sieve size/nominal sieve size (mm))/100
> for the 75 mm, 63 mm, 53 mm, 37,5 mm, 26,5 mm, 19 mm, 13,2 mm, 4,75 mm, 2,00 mm sieve sizes.

The grading factor (GF) should not be confused with the fineness modulus, as the percentage passing each sieve is divided by that particular sieve size.

Originally the GF also included the 0,425 mm and 0,075 mm sieve sizes. However, it was found by multiple regression during the modelling procedure, that the influence of the fines fraction of each material was more accurately presented by the Atterberg limits and the linear shrinkage which are determined on the material passing the 0,425 mm sieve size. These sieves were therefore eliminated in the calculation of the GF.

6.2 The voids in the soil fines

If a material consisted of single sized spheres, the total amount of voids in the material would be the same for large or small spheres. According to Spangler et al[64] the amount of voids is not dependent on the diameter of the spheres, but on the packing pattern of these spheres.

However, if we had a graded material consisting of different sized spheres the voids would be less, because the void spaces in between the larger spheres will be filled with smaller spheres reducing the amount of void space. The voids in between the smallest sphere size can, however, not be reduced, as smaller spheres are not available. As a material therefore becomes finer the amount of voids in the material tends to increase. This is confirmed by our results where the well graded, course to fine, crushed stone materials were at the one end of the scale with a small amount of void space and the black montmorillonite clay was at the other end of the scale with a high amount of voids.

Because the actual particle size distribution of the particles sizes smaller than 0,075 mm (the cohesive portion of the material) is not determined, it is necessary to express the void content of this fraction of the material in terms of some of the other measured parameters. If the surface area of a fixed mass of large and small spheres of the same material with respective diameters of "D" and "d" were to be compared with one another, it would be found that the ratio of the surface area of the small spheres compared to the large spheres is "D/d" (ie 500 times for D and d equal to 37,5 mm and 0,075 mm respectively). Because the total surface area per unit mass is also a function of the particle sizes, the Atterberg limits seemed the ideal choice. The value of the linear shrinkage also gives an indication of the amount of voids in the soil fines.

Because the amount of soil fines present in the material also has an influence on the total amount of voids per unit volume, the percentage value of the material passing the 0,425 mm sieve also plays a role. During the modelling procedure by means of multiple regression techniques it was found that the liquid limit (LL) gave higher r^2-values than the plasticity index (PI). Apart from this it was found that inclusion of the linear shrinkage (LS) in the model also improved the accuracy of the model (ie increased r^2-value).

6.3 The relationship between MDD, OMC, CMC and ZAVMC

Density of a material in terms of solid density is a function of the void content of the material. This amount of voids is dependent on the particle size distribution. The grading of the material after compaction is therefore extremely important as it is this grading which will determine how much void space will be left in the material.

As far as the moisture regime is concerned, the zero air voids moisture content (ZAVMC) is also a function of the void space in the compacted material, because all the voids at MDD have been filled with water at this moisture content. Similarly, the OMC is found very close to the ZAVMC with a very low percentage of air voids (2 - 3 %) apart from the voids filled with water.

The CMC on the other hand is a function of the total surface area per unit mass of the soil because the maximum cohesive force or capillary action will occur in the region where all the soil particles are just covered by a thin layer of moisture. The surface area of a material per unit mass is also a function of the particle size distribution.

The MDD (vibratory and mod. AASHTO), OMC (vibratory and mod. AASHTO), ZAVMC (vibratory and mod. AASHTO) and the CMC are all influenced by the same material properties. One can therefore use the same basic model to determine the values of all of them.

The model found by means of multiple regression techniques which agreed extremely well with the measured results is as follows (see regression analysis results in Appendix E).

$$\text{MDD (vibratory) (\%SD)} = k_1.(GF)^{0,85} + k_2.C + k_3.(LS) + k_4.C^3 + k_5 \quad \ldots\ldots\ldots\ldots \quad (6.1)$$

(see Figure 6.1)

$$\text{MDD (mod. AASHTO) (\%SD)} = k_6.(GF)^{0,85} + k_7.C + k_8.(LS) + k_9.C^3 + k_{10} \quad \ldots\ldots\ldots \quad (6.2)$$

(see Figure 6.2)

$$\text{OMC (vibratory) (\%)} = k_{11}.(GF)^{0,85} + k_{12}.C + k_{13}.(LS) + k_{14}.C^3 + k_{15} \quad \ldots\ldots\ldots\ldots \quad (6.3)$$

(see Figure 6.3)

$$\text{OMC (mod.AASHTO) (\%)} = k_{16}.(GF)^{0,85} + k_{17}.C + k_{18}.(LS) + k_{19}.C^3 + k_{20} \quad \ldots\ldots\ldots \quad (6.4)$$

(see Figure 6.4)

$$\text{ZAVMC (vibratory) (\%)} = k_{21}.(GF)^{0,85} + k_{22}.C + k_{23}.(LS) + k_{24}.C^3 + k_{25} \quad \ldots\ldots\ldots\ldots \quad (6.5)$$

(see Figure 6.5)

$$\text{ZAVMC (mod. AASHTO) (\%)} = k_{26}.(GF)^{0,85} + k_{27}.C + k_{28}.(LS) + k_{29}.C^3 + k_{30} \quad \ldots\ldots\ldots \quad (6.6)$$

(see Figure 6.6)

$$\text{CMC (\%)} = k_{31}.(GF)^{0,85} + k_{32}.C + k_{33}.(LS) + k_{34}.C^3 + k_{35} \quad \ldots\ldots\ldots\ldots\ldots\ldots \quad (6.7)$$

(see Figure 6.7)

where C = (percentage passing the 0,425 mm sieve/100).$(LL/100)^{0,1}$

GF = grading factor as defined earlier

LL = liquid limit

LS = linear shrinkage

k_n = regression coefficient

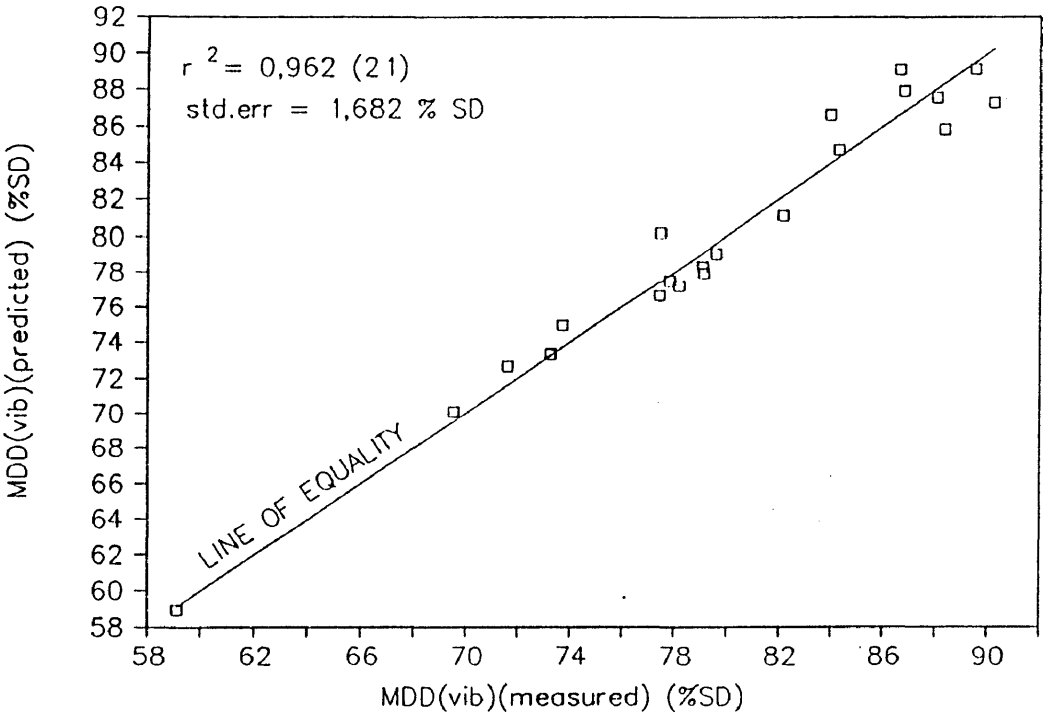

FIGURE 6.1 **RELATION BETWEEN MDD-PREDICTED (VIBRATORY) (% SD) AND MDD-MEASURED (VIBRATORY) (% SD) FOR UNTREATED ROAD-BUILDING MATERIALS**

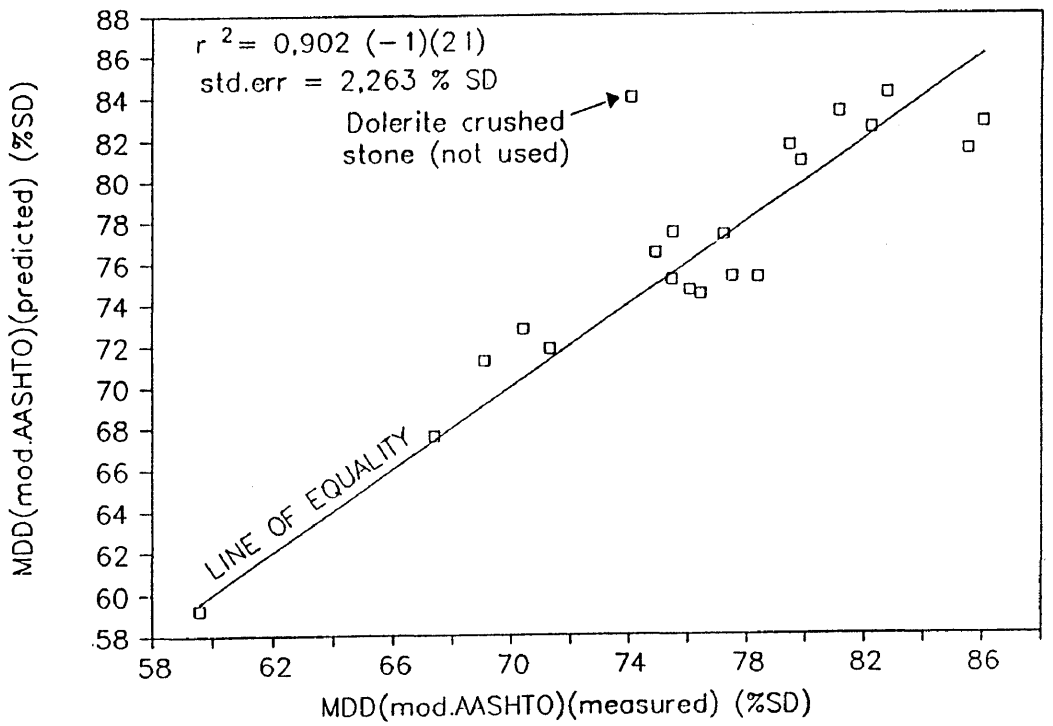

FIGURE 6.2 **RELATION BETWEEN MDD-PREDICTED (MOD. AASHTO) (% SD) AND MDD-MEASURED (MOD. AASHTO) (% SD) FOR UNTREATED ROADBUILDING MATERIALS**

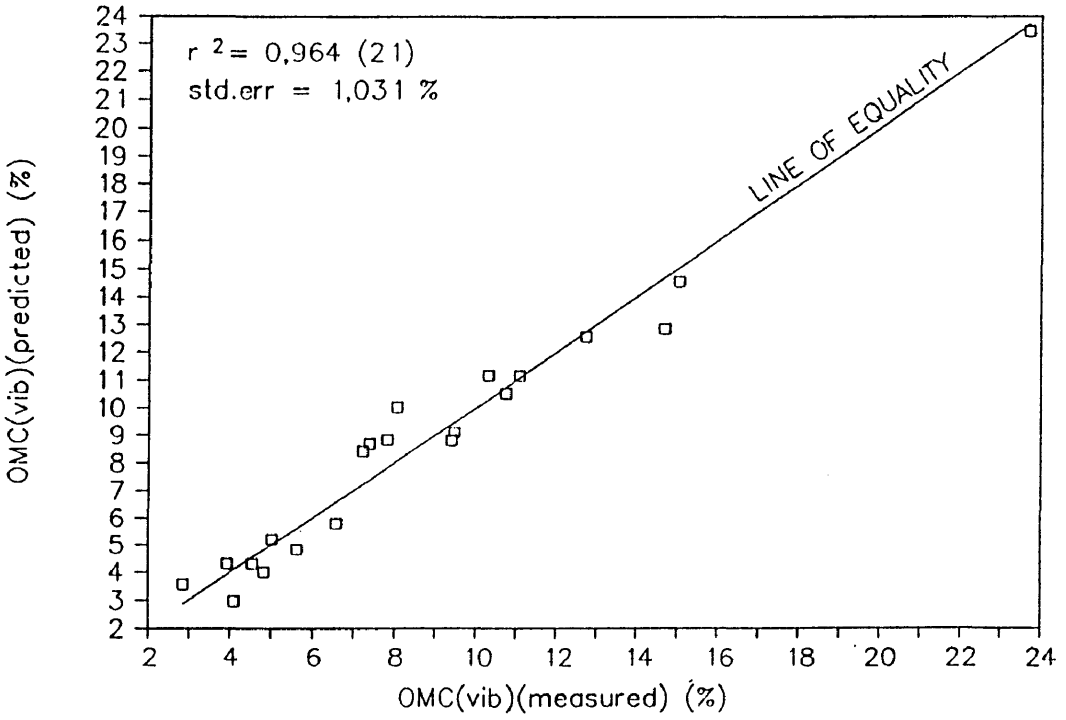

FIGURE 6.3 **RELATION BETWEEN OMC-PREDICTED (VIBRATORY) (%) AND OMC-MEASURED (VIBRATORY) (%) FOR UNTREATED ROADBUILDING MATERIALS**

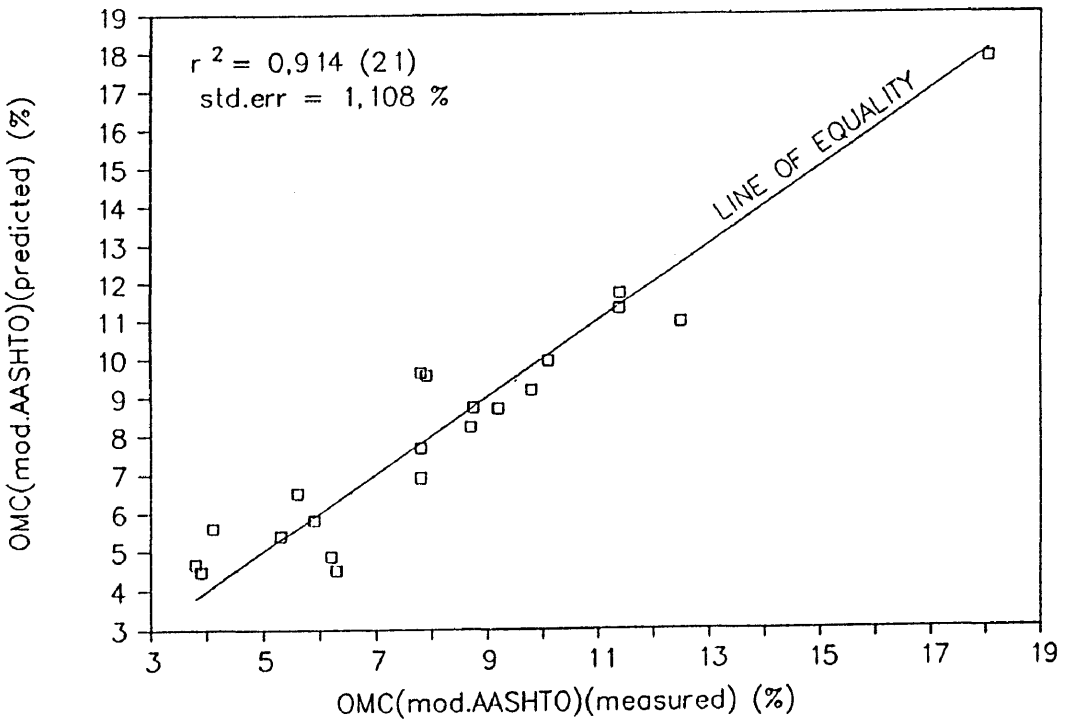

FIGURE 6.4 **RELATION BETWEEN OMC-PREDICTED (MOD. AASHTO) (%) AND OMC-MEASURED (MOD. AASHTO) (%) FOR UNTREATED ROADBUILDING MATERIALS**

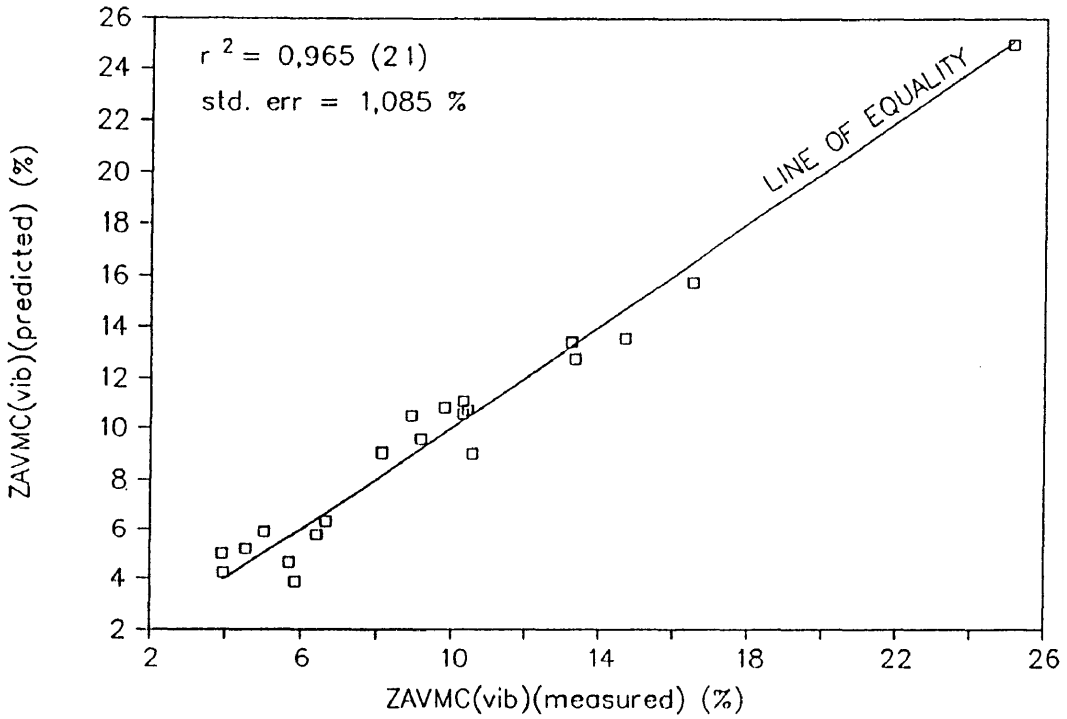

FIGURE 6.5 **RELATION BETWEEN ZAVMC-PREDICTED (VIBRATORY) (%) AND ZAVMC (VIBRATORY) (%) FOR UNTREATED ROAD-BUILDING MATERIALS**

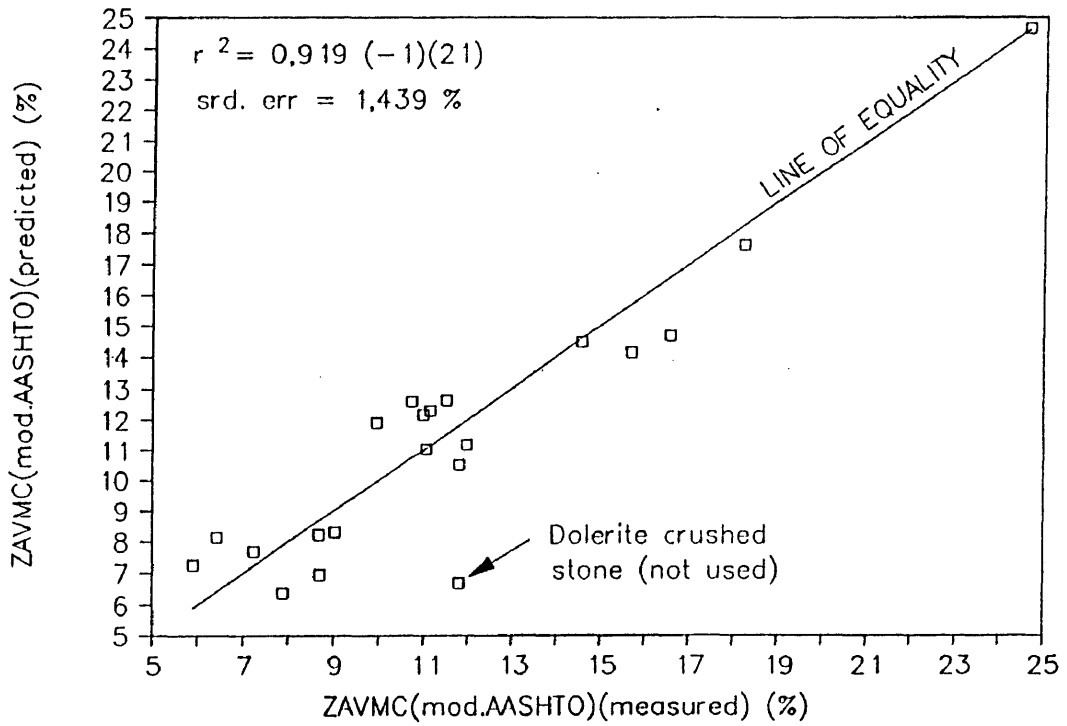

FIGURE 6.6 **RELATION BETWEEN ZAVMC-PREDICTED (MOD. AASHTO) (%) AND ZAVMC (MOD. AASHTO) (%) FOR UNTREATED ROAD-BUILDING MATERIALS**

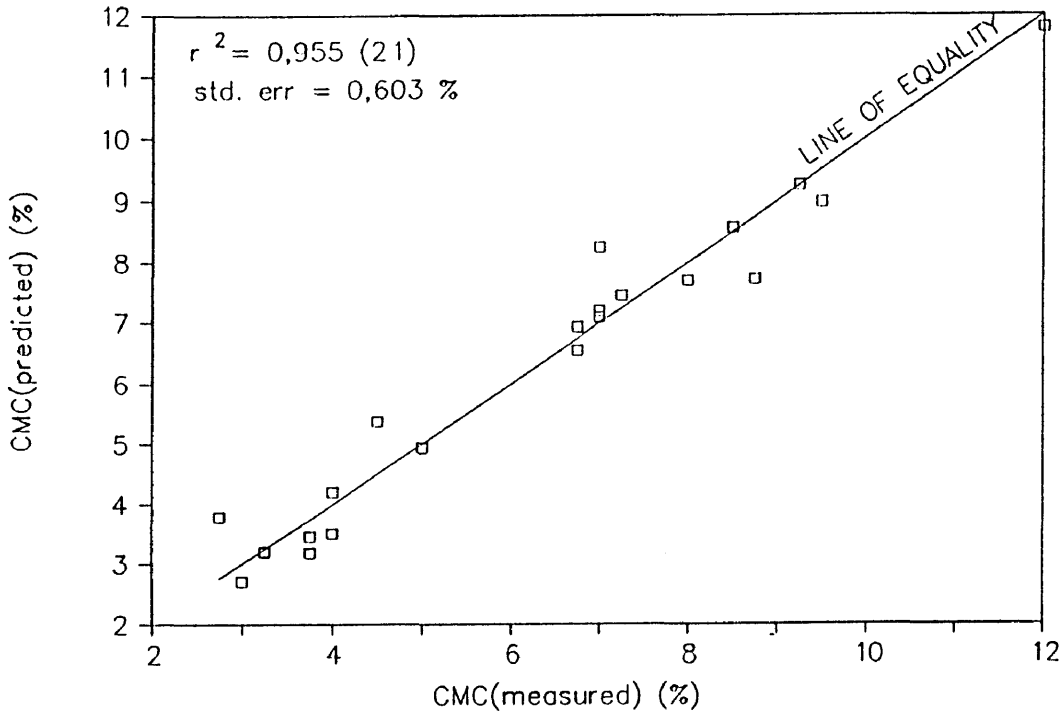

FIGURE 6.7 RELATION BETWEEN CMC-PREDICTED (%) AND CMC (%) FOR UNTREATED ROADBUILDING MATERIALS

6.4 The influence of the effective particle density of the material solids on the density measurements

Equations 6.1 and 6.2 express the MDD (vibratory and mod. AASHTO) in terms of percentage space occupied by material particles (ie % SD). To express these values in terms of kg/m^3 these values have to be multiplied by the solid density of the material particles in terms of kg/m^3. For "solid" roadbuilding materials this value is expressed by the apparent density (AD) (kg/m^3) and is determined by multiplying the apparent relative density (ARD) by 1000.

However, when the roadbuilding material is porous in nature, such as in the case of certain sandstone materials, there are voids present in the larger particles which cannot be filled with fines, although they can be filled with water. The reason why these voids can be filled with water is because the water molecules are many orders smaller than the finest soil fines particles. Although these voids are therefore accessible to water, they are not accessible to soil fines. For this reason these inaccessible voids should be taken account of when determining the solid density of the roadbuilding material. This is done by adding the volume of these internal voids to the volume of the particle solids as determined for the ARD. Because the volume increases for the same mass, the relative density of the material is lower

than the apparent relative density (ARD) and is known as the bulk relative density (BRD) of the material. To express this value in kg/m^3 it is multiplied by 1000 and is known as the dry bulk density (DBD) of the material.

For example these models were applied to sandstone subbase material with an ARD of 2,703 and BRD of 2,510. According to the model the predicted MDD (vib) (% SD) was 83,85, giving values of 2266 kg/m^3 for the ARD and 2105 kg/m^3 for the BRD. Subsequent compaction of the material on the vibratory table gave an MDD value of 2126 kg/m^3, which compares very favourably with the predicted value using the BRD.

A close approximation would be to use the DBD in all cases as the values of the DBD and AD for non-porous materials will approximately be the same. In the case of finer roadbuilding materials or materials which break down completely, the AD value should be used as all the voids in the soil particles are normally accessible to the filled with soil fines.

6.5 The influence of the effective particle density of the material solids on the moisture regime values (OMC, ZAVMC and CMC)

In the case of the moisture regime values (CMC, OMC and ZAVMC), the values are always expressed as a percentage of the dry mass of the material. The ARDs and BRDs for most roadbuilding material are very similar and approximately 2,65. However, one should always remember that the OMC and ZAVMC are dependent on the amount of voids in the material after compaction and the CMC is dependent on the total surface area of material particles.

Where the ARD and BRD values of roadbuilding materials differ vastly from the standard value of about 2,65, the moisture regime values determined with models should be adjusted by multiplying the estimated values by 2,65 and dividing by the respective ARD or BRD value of the particular material. Although this factor was not originally noted in the development of the model and in the determination of the regression constants, this fact should also have been taken into account during the development of the model. In this case the value should have been adjusted in the reverse order by multiplying with the ARD or BRD value and dividing by 2,65. (See Appendix E for regression constants of the standardised OMC (SOMC) (vibratory and mod. AASHTO), the standardised ZAVMC (SZAVMC) (vibratory and mod. AASHTO) and the standardised CMC (SCMC).)

In the case of porous materials a certain amount of water is also absorbed by the porous aggregate and is therefore not freely available for lubrication purposes to enhance the

compactability of the materials. To ensure that enough free water is available for compaction purposes the water absorbtion value (WA) (%), which was determined along with the ARD and BRD of the material, should be multiplied with the fraction larger than 4,75 mm and added to the predicted values by the model for OMC, ZAVMC and CMC.

6.6 Conclusions

The regression coefficients, their standard errors and t-values for all the properties are listed in Table 6.1. Note that in most cases all these factors have a significant influence (ie $t \geq t_{0,050}$). The only exceptions were the constants for C and C^3 for the prediction models of CMC, OMC (mod. AASHTO), SCMC and SOMC (mod. AASHTO).

The regression analysis for these properties were then repeated without taking account of C and C^3. The updated regression constants, their standard errors and t-values for these four properties are listed in Table 6.2. To keep the same regression model throughout for all these properties the values of the regression constants for C and C^3 have been set to zero.

The high r^2-values found for the different maximum dry densities and moisture regimes (ie OMC, ZAVMC and CMC) using the same basic model in terms of GF, C and LS clearly indicate that all these properties are dictated by the particle size distribution.

Considering the high r^2-values it is clear that untreated roadbuilding materials react systematically, proving that there is far more system in God's creation than we as engineers tend to give Him credit for. The fact that basic laws therefore exist, means that it is no longer necessary to follow a trial and error approach to solving compaction problems, but that they can be solved effectively in systematic manner.

TABLE 6.1 **Values of regression coefficients and their standard errors and t-values and r^2-values for the different properties**

PROPERTY		$GF^{0,85}$	C	LS	C^3	Constant	$t_{(0,050)}$	r^2	Degrees of freedom
MDD (vib)	X Coefficient(s)	-39,3373	20,01048	-1,53875	-11,0532	107,8239			
	Std Err of Coef.	3,408744	3,636287	0,157016	4,033739	1,682228			
	t-value	11,54012	5,502999	9,799970	2,740204	64,09589	2,120	0,962	16
OMC (vib)	X Coefficient(s)	23,13580	-15,9000	1,086464	11,15962	-7,63483			
	Std Err of Coef.	2,089120	2,228574	0,096230	2,472161	1,030988			
	t-value	11,07442	7,134641	11,29021	4,514114	7,405351	2,120	0,964	16
ZAVMC (vib)	X Coefficient(s)	23,82679	-15,2362	0,934438	13,38636	-7,09933			
	Std Err of Coef.	2,143341	2,286415	0,098728	2,536324	1,057747			
	t-value	11,11665	6,663824	9,464759	5,277858	6,711752	2,120	0,965	16
CMC	X Coefficient(s)	12,16945	-2,22615	0,495747	-1,83665	-3,09955			
	Std Err of Coef.	1,222593	1,304204	0,056316	1,446756	0,603354			
	t-value	9,953803	1,706907	8,802956	1,269496	5,137210	2,120	0,955	16
MDD (mod. AASHTO)	X Coefficient(s)	-33,7346	19,27655	-1,20764	-12,3063	99,93611			
	Std Err of Coef.	4,723711	4,907930	0,213611	5,567864	2,263200			
	t-value	7,141555	3,927634	5,653466	2,210251	44,15698	2,131	0,902	15
OMC (mod. AASHTO)	X Coefficient(s)	7,175719	0,346294	0,555493	2,861833	0,800098			
	Std Err of Coef.	2,244660	2,394497	0,103395	2,656220	1,107748			
	t-value	3,196795	0,144620	5,372526	1,077408	0,722275	2,120	0,914	16

TABLE 6.1 (Continued)

PROPERTY		$GF^{0,85}$	C	LS	C^3	Constant	$t_{(0,050)}$	r^2	Degrees of freedom
ZAVMC	X Coefficient(s)	22,41750	-14,6602	0,780933	12,59359	-3,87765			
(mod, AASHTO)	Std Err of Coef.	3,003111	3,120229	0,135804	3,539784	1,438835			
	t-value	7,464756	4,698440	5,750430	3,557730	2,694992	2,131	0,919	15
SOMC (vib)	X Coefficient(s)	23,06058	-16,5273	1,146541	11,77833	-7,34696			
	Std Err of Coef.	1,997146	2,130461	0,091994	2,363324	0,985599			
	t-value	11,54676	7,757655	12,46321	4,983797	7,454314	2,120	0,969	16
SZAVMC (vib)	X Coefficient(s)	23,70265	-15,8884	0,992208	14,12369	-6,74470			
	Std Err of Coef.	2,017563	2,152240	0,092934	2,387484	0,995675			
	t-value	11,74815	7,382298	10,67642	5,915722	6,774005	2,120	0,970	16
SCMC	X Coefficient(s)	12,07765	-2,49923	0,533210	-1,74455	-2,85255			
	Std Err of Coef.	1,423187	1,18189	0,065555	1,684130	0,702348			
	t-value	8,486340	1,646192	8,133667	1,035878	4,061457	2,120	0,942	16
SOMC (mod.	X Coefficient(s)	6,967474	-0,06758	0,603192	3,203030	1,185852			
AASHTO)	Std Err of Coef.	2,449756	2,613284	0,112842	2,898920	1,208963			
	t-value	2,844149	0,025861	5,345434	1,104904	0,980882	2,120	0,903	16
SZAVMC (mod.	X Coefficient(s)	22,20080	-15,3738	0,834881	13,35021	-3,35735			
AASHTO)	Std Err of Coef.	2,966392	3,082077	0,134143	3,496502	1,421242			
	t-value	7,484109	4,988147	6,223778	3,818163	2,362265	2,131	0,924	15

TABLE 6.2 **Values of regression coefficients and their standard errors and t-values and r^2-values for the models of CMC, OMC (mod. AASHTO), SCMC and SOMC (mod. AASHTO)**

PROPERTY		$GF^{0,85}$	C	LS	C^3	Constant	$t_{(0,050)}$	r^2	Degrees of freedom
CMC	X Coefficient(s)	9,228955	0,000000	0,369004	0,000000	-1,42919			
	Std Err of Coef.	0,938837	0,000000	0,048379	0,000000	0,732364			
	t-value	9,830193	0,000000	7,627264	0,000000	1,951483	2,101	0,925	18
OMC (mod. AASHTO)	X Coefficient(s)	8,999806	0,000000	0,639039	0,000000	-0,38481			
	Std Err of Coef.	1,421596	0,000000	0,073256	0,000000	1,108952			
	t-value	6,330773	0,000000	8,723269	0,000000	0,347010	2,101	0,902	18
SCMC	X Coefficient(s)	8,944838	0,000000	0,398784	0,000000	-1,09127			
	Std Err of Coef.	1,052807	0,000000	0,054252	0,000000	0,821269			
	t-value	8,496175	0,000000	7,350499	0,000000	1,328764	2,101	0,910	18
SOMC (mod. AASHTO)	X Coefficient(s)	8,607036	0,000000	0,680089	0,000000	0,066340			
	Std Err of Coef.	1,540314	0,000000	0,079374	0,000000	1,201561			
	t-value	5,587842	0,000000	8,568097	0,000000	0,055212	2,101	0,892	18

CHAPTER 7

QUANTIFYING THE EFFECT OF MEASURED SOIL PROPERTIES ON THE CBR AT DIFFERENT LEVELS OF DRY DENSITY AND MOISTURE CONTENT

In Chapter 5 it was shown that there is a basic reaction model for the CBR of untreated roadbuilding materials in terms of the dry density (% mod. AASHTO or % SD) and moisture content of the material (%). It also showed that there is a unique moisture content for each material at which the CBR tends to peak for all levels of density (ie the CMC).

In Chapter 6 it was shown that both the MDD and moisture regime (ie CMC, OMC and ZAVMC) of untreated materials are dependent on the particle size distribution. Models to predict these values from the indicator test values were also developed. The MDD models expressed the density in terms of percentage space filled with "solid" material (ie % SD).

Because the CBR results were originally assessed in terms of dry density (% mod. AASHTO) and moisture content, it was necessary to determine the dry densities in terms of solid density (% SD) before all the CBR results could be evaluated together.

Plotting all the CBR results against dry density (% SD) and moisture content (%) gave the following results (see Figures 7.1 and 7.2). From these figures it is apparent that both the dry density (% SD) and moisture content (%) of the compacted samples have a tremendous effect on the CBR values. The CBRs for instance rapidly increase when a dry density of approximately 75 % SD is reached. Similarly the CBR results peak at a moisture content of approximately 3 %. Because the CBRs of all the materials included in the investigation were determined for a wide range of densities (% SD) and moisture contents (%), the results were scattered.

To properly evaluate the separate effects of dry density (% SD) and moisture content (%) on the bearing capacity it was necessary to assess the CBRs in such a manner that these effects were isolated from one another.

In modelling the CBRs in terms of dry density (% mod AASHTO and % SD) and moisture content (%) it was observed that the results always peaked at a particular moisture content for each material investigated, the so-called CMC. To isolate the effect of dry density the CBR results were therefore all evaluated at the CMC value for each material. This was done by means of the bearing capacity models developed in Chapter 5, by means of which the CBRs at CMC (ie CBR:CMC) at the dry density levels (% SD) of the individual samples were

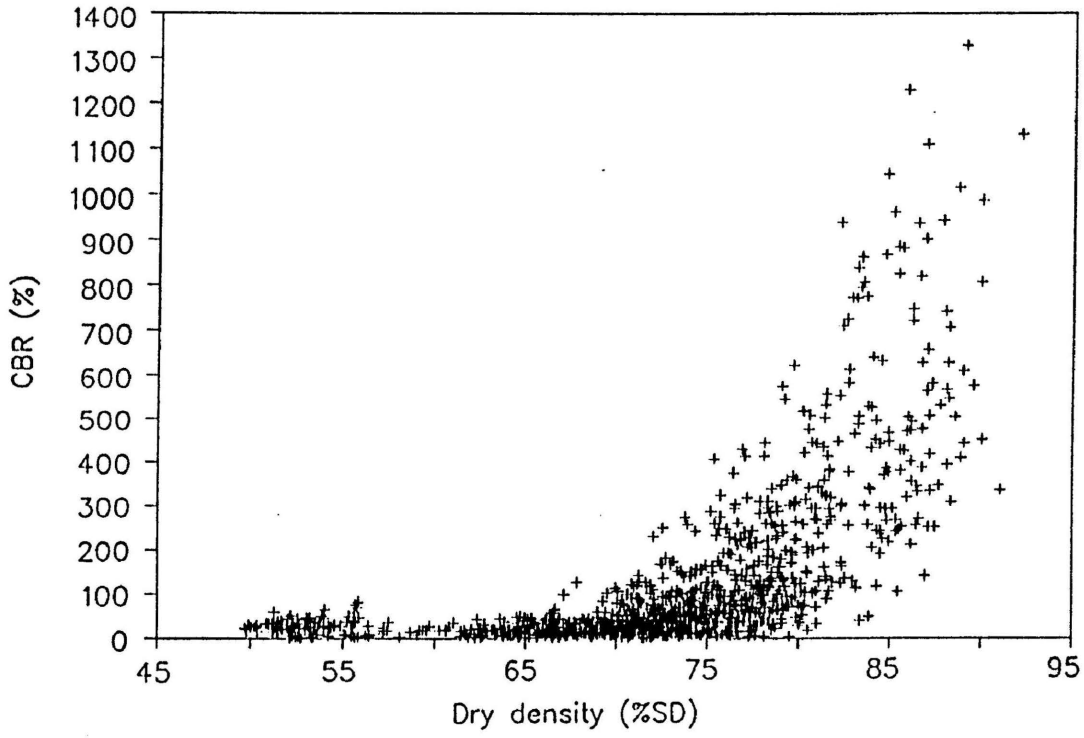

FIGURE 7.1 RELATION BETWEEN CBR (%) AND DRY DENSITY (%SD) FOR UNTREATED ROADBUILDING MATERIALS INVESTIGATED

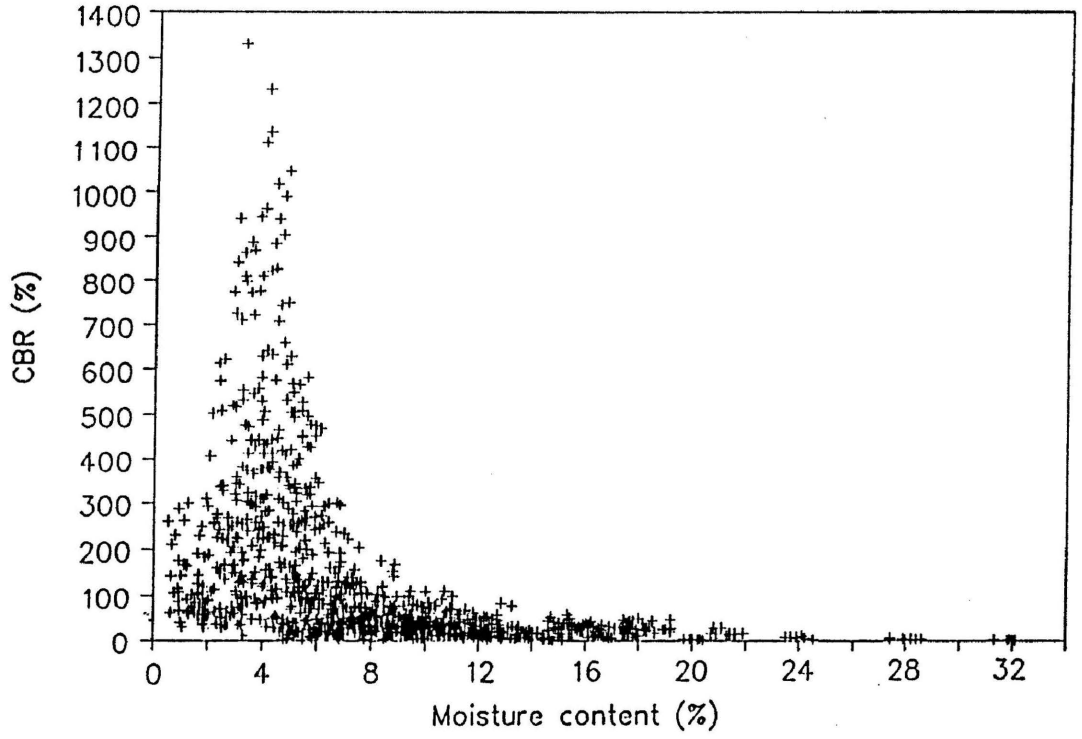

FIGURE 7.2 RELATION BETWEEN CBR (%) AND MOISTURE CONTENT (%) FOR UNTREATED ROADBUILDING MATERIALS INVESTIGATED

calculated. All the densities were converted to solid density to be in line with the compactibility models and to enable the evaluation of all the CBR results together.

To evaluate the effect of moisture content on the CBR the decrease in CBR was expressed as a percentage of CBR:CMC and the moisture content deviation from CMC was expressed as a percentage of CMC (see Figure 7.3). Because the models were symmetrical in shape around the CMC, the absolute difference between the sample moisture contents and the material CMCs were used, whereby the values were always positive.

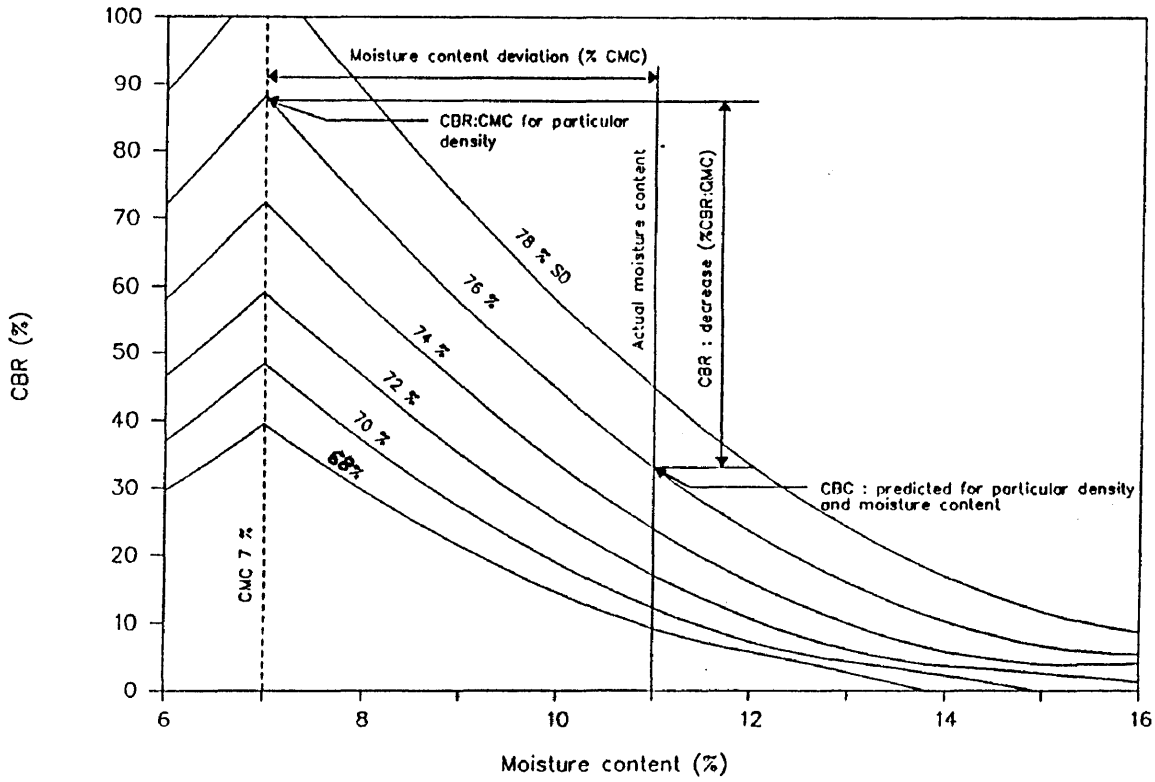

FIGURE 7.3 DETERMINATION OF CBR:DECREASE (% CBR:CMC) IN TERMS OF MOISTURE CONTENT DEVIATION (% CMC) FROM CMC (EXAMPLE)

7.1 Quantification of CBR:CMC

As mentioned in Chapter 5, it was noted, particularly with the better quality crushed stone materials, that the CBRs were not only dependent on the dry density and moisture content of the material, but most likely also dependent on the shape and texture of separate particle fractions as well as their collective influence. These properties were quantified by means of the specific rugosity (S_{rv}), shape factor (SF), loose bulk density (LBD) and shakedown bulk density (SBD) (see Chapter 3 for test methods). To isolate the effect of the individual

properties the following models were used to analyse the CBR:CMC values (see Equations 7.1 to 7.4).

Model 1 : $\log(CBR:CMC) = k_{11}.E + k_{12}.E^2 + k_{13}.F + k_{14}.G + k_{15}.H + k_{16}$ ..... (7.1)

Model 2 : $\log (CBR:CMC) = k_{21}.E + k_{22}.E^2 + k_{23}.F + k_{24}.G + k_{25}$ ..... (7.2)

Model 3 : $\log (CBR:CMC) = k_{31}.E + k_{32}.E^2 + k_{33}.F + k_{34}$ ..... (7.3)

Model 4 : $\log (CBR:CMC) = k_{41}.E + k_{42}.E^2 + k_{43}$ ..... (7.4)

where E = log (dry density (%SD))
F = log (SBD (%SD)) or log (LBD (% SD))
G = log (SF (%)) or log (S_{rv} (%))
H = log (CMC (%))
k_n = regression coefficient

During the regression analysis of these models it became apparent that the shape factor (SF) and the shakedown bulk density (SBD) gave higher r^2-values than the specific rugosity (S_{rv}) and the loose bulk density (LBD). For this reason it is recommended that the shape factor (SF) and shakedown bulk density (SBD) be accepted as standard parameters to quantify the separate and collective influence of the shape and texture of the particles.

The regression coefficients of the CBR:CMC models were evaluated for their significance by means of the t-test. The degrees of freedom are not listed as they are above 100 (see Tables 7.1(a) to 7.1(d)).

Tables 7.1(a) to 7.1(d) show that all these factors contribute significantly towards the CBR:CMC. The only exceptions were the dry density in the case of sandy material and the SBD for all the materials together. This seems highly unlikely and may be due to the interdependency between the DD and SBD. These factors should, therefore, preferably all be taken into account in the determination of CBR:CMC.

TABLE 7.1(a) Listing of regression coefficients, their standard errors and t-values, and r^2-values for model 1 for different material groupings

MATERIALS		logDD (=E)	E^2	logSBD (=F)	logSF (=G)	logCMC (=H)	Constant	$t_{(0,050)}$	r^2
G1 only	X Coefficient(s)	-59,9536	17,94450	7,265313	0,731499	-3,25459	39,29038		
(crushed stone)	Std Err of Coef.	10,42351	2,750026	1,656047	0,206720	0,565659	0,046313		
	t-value	5,751765	6,525212	4,387139	3,538601	5,753625	848,3532	1,972	0,963
NPAB - LABD	X Coefficient(s)	-139,200	39,61879	13,66789	-1,90879	6,819824	95,17697		
(natural gravel)	Std Err of Coef.	16,27516	4,366578	0,239005	0,049708	0,165667	0,035175		
	t-value	8,552954	9,073189	57,18653	38,40002	41,16574	2705,769	1,972	0,979
LABLEN - LABDEW	X Coefficient(s)	-7,69326	3,702538	1,451194	-0,91779	2,018085	0,007049		
(sandy materials)	Std Err of Coef.	14,66805	4,001469	0,147109	0,059872	0,149290	0,068049		
	t-value	0,524491	0,925294	9,864730	15,32915	13,51782	0,103596	1,972	0,835
All except BAB	X Coefficient(s)	-51,8394	15,65623	1,608016	0,325161	-1,62131	42,15851		
(minus black clay)	Std Err of Coef.	9,500547	2,548939	0,187429	0,038353	0,075928	0,135445		
	t-value	5,456469	6,142255	8,579327	8,477979	21,35323	311,2575	1,972	0,914
All materials	X Coefficient(s)	-176,655	48,91816	0,267347	0,352645	-1,82238	161,7910		
	Std Err of Coef.	4,823213	1,323179	0,207472	0,044898	0,088062	0,159110		
	t-value	36,62605	36,97016	1,288593	7,854363	20,69428	1016,846	1,972	0,874

TABLE 7.1(b) Listing of regression coefficients, their standard errors and t-values and r^2-values for model 2 for different material groupings

MATERIALS		logDD (=E)	E^2	logSBD (=F)	logSF (=G)	Constant	$t_{(0,050)}$	r^2
G1 only	X Coefficient(s)	-52,1402	15,92320	-2,05049	-0,45437	48,27211		
(crushed stone)	Std Err of Coef.	10,92757	2,883969	0,367720	0,016781	0,048970		
	t-value	4,771441	5,521280	5,576251	27,07591	985,7344	1,972	0,958
NPAB - LABD	X Coefficient(s)	-73,2694	21,77480	11,37679	0,079896	41,93668		
(natural gravel)	Std Err of Coef.	43,06571	11,55341	0,618046	0,031134	0,093532		
	t-value	1,701340	1,884707	18,40766	2,566148	448,3669	1,972	0,849
LABLEN - LABDEW	X Coefficient(s)	43,58686	-10,5751	0,753324	-0,30698	-43,6710		
(sandy materials)	Std Err of Coef.	18,16973	4,949327	0,176648	0,050371	0,087263		
	t-value	2,398872	2,136674	4,264534	6,094314	500,4473	1,972	0,727
All except BAB	X Coefficient(s)	-42,1963	13,52143	2,866164	-0,35190	28,75397		
(minus black clay)	Std Err of Coef.	11,44319	3,071250	0,214551	0,026019	0,163326		
	t-value	3,687459	4,402582	13,35884	13,52491	176,0526	1,972	0,875
All materials	X Coefficient(s)	-198,772	55,32562	1,493439	-0,41675	177,8976		
	Std Err of Coef.	5,537745	1,514677	0,234108	0,029635	0,187339		
	t-value	35,89415	36,52633	6,379250	14,06250	949,6024	1,972	0,825

TABLE 7.1(c) Listing of regression coefficients, their standard errors and t-values and r^2-values for model 3 for different material groupings

MATERIALS		logDD (=E)	E^2	logSBD (=F)	Constant	$t_{(0,050)}$	r^2
G1 only	X Coefficient(s)	-139,316	38,74522	-1,88508	130,9048		
(crushed stone)	Std Err of Coef.	20,03678	5,292073	0,705475	0,093963		
	t-value	6,953039	7,321368	2,672083	1393,140	1,972	0,845
NPAB - LABD	X Coefficient(s)	-41,9716	13,29600	10,66549	14,44055		
(natural gravel)	Std Err of Coef.	41,71248	11,18074	0,557885	0,094460		
	t-value	1,006214	1,189188	19,11772	152,8743	1,972	0,846
LABLEN - LABDEW	X Coefficient(s)	47,91169	-11,7407	0,916817	-48,3634		
(sandy materials)	Std Err of Coef.	19,28034	5,251936	0,185413	0,092668		
	t-value	2,485001	2,235516	4,944717	521,8964	1,972	0,691
All except BAB	X Coefficient(s)	-50,2036	15,88751	4,561181	32,00755		
(minus black clay)	Std Err of Coef.	12,42110	3,332761	0,189278	0,177521		
	t-value	4,041807	4,767071	24.09766	180,3027	1,972	0,852
All materials	X Coefficient(s)	-223,912	62,31252	3,402784	196,5694		
	Std Err of Coef.	5,687998	1,552832	0,206970	0,203307		
	t-value	39,36571	40,12830	16,44095	966,8603	1,972	0,794

TABLE 7.1(d) Listing of regression coefficients, their standard errors and t-values and r^2-values for model 4 for different material groupings

MATERIALS		logDD (=E)	E^2	Constant	$t_{(0,050)}$	r^2
G1 only	X Coefficient(s)	-142,718	39,66283	130,5236		
(crushed stone)	Std Err of Coef.	20,21910	5,339761	0,095010		
	t-value	7,058582	7,427828	1373,776	1,972	0,841
NPAB - LABD	X Coefficient(s)	68,81246	-15,9990	-70,8046		
(natural gravel)	Std Err of Coef.	62,60729	16,78587	0,143166		
	t-value	1,099112	0,953126	494,5630	1,972	0,644
LABLEN - LABDEW	X Coefficient(s)	66,79872	-16,9411	-63,8506		
(sandy materials)	Std Err of Coef.	19,66295	5,353781	0,096418		
	t-value	3,397186	3,164337	662,2231	1,972	0,664
All except BAB	X Coefficient(s)	-101,965	30,32949	86,63439		
(minus black clay)	Std Err of Coef.	15,36513	4,117519	0,222956		
	t-value	6,636137	7,365962	388,5715	1,972	0,767
All materials	X Coefficient(s)	-209,921	59,06805	187,9870		
	Std Err of Coef.	6,270316	1,717252	0,226671		
	t-value	33,47867	34,39684	829,3357	1,972	0,744

7.2 Quantification of CBR:decrease

In assessing the effect of moisture content on the theoretical CBR value it was found that the drop in CBR expressed as a percentage of CBR:CMC was directly related to the moisture content deviation from the CMC expressed as a percentage of CMC (See Table 7.2 and Figure 7.3). In line with the original models (see Chapter 6) which express the CBR as a function of moisture content and density the following two models were evaluated:

Model 5 : $J = k_1.H + k_2.L + k_3.L^3/abs(L) + k_4$ ..... (7.5)

Model 6 : $J = k_5.H + k_6.L + k_7$ ..... (7.6)

where J = log (CBR:decrease (% CBR:CMC))
H = log (CMC (%))
L = log (absolute moisture content deviation from CMC (% CMC))
abs (L) = absolute value of log (absolute moisture content deviation from CMC (% CMC))
k_n = regression coefficient

The regression coefficients of the CBR:decrease models were evaluated for their significance by means of the t-test. The degrees of freedom are not listed as they are above 100 (see Tables 7.2(a) and 7.2(b)).

Table 7.2 shows that the factors log (CMC) and log (MCdev) (=L) are significant but that the factor L^3/abs (L) is not significant. Table 7.2(b) confirms that both the CMC of the material as well as the moisture content deviation away from the CMC contribute significantly towards the CBR:decrease (% CBR:CMC).

7.3 Combining the models of CBR:CMC and CBR:decrease to estimate CBRs

As a final step the log (CBR-measured) values, as determined on the test samples, were compared with the log (CBR-predicted) values. The predicted CBR results were determined for both the original models from Chapter 5 (CBR as function of density and moisture content) (model A) and the combination of models (CBR:CMC (Model 1) and CBR:decrease (Model 6)) (model B) for the actual densities and moisture content deviations from CMC (See Figures 7.4 to 7.8).

TABLE 7.2(a) Listing of regression coefficients, their standard errors and t-values and r^2-values for model 5 for different material groupings

MATERIALS		logCMC (=H)	logMCdev (=L)	L^3/absL	Constant	$t_{(0,050)}$	r^2
G1 only	X Coefficient(s)	1,203091	0,960898	0,002449	-0,67318		
(crushed stone)	Std Err of Coef.	0,140092	0,024830	0,002245	0,164402		
	t-value	8,587820	38,69793	1,091010	4,094767	1,972	0,985
NPAB - LABD	X Coefficient(s)	1,121915	0,770404	0,068673	-0,77415		
(natural gravel)	Std Err of Coef.	0,146870	0,090798	0,036832	0,176110		
	t-value	7,638799	8,484789	1,864498	4,395859	1,972	0,853
LABLEN - LABDEW	X Coefficient(s)	-0,58758	0,966590	0,002696	0,570880		
(sandy materials)	Std Err of Coef.	0,315104	0,035645	0,003621	0,244386		
	t-value	1,864725	27,11705	0,744670	2,335968	1,972	0,940
All except BAB	X Coefficient(s)	0,150889	1,009676	-0,00124	-0,17347		
(minus black clay)	Std Err of Coef.	0,042586	0,019351	0,001925	0,237888		
	t-value	3,543139	52,17457	0,646236	0,729249	1,972	0,937
All materials	X Coefficient(s)	0,127649	0,991374	0,000264	-0,13591		
	Std Err of Coef.	0,035677	0,018095	0,001817	0,229091		
	t-value	3,577907	54,78531	0,145654	0,593276	1,972	0,936

TABLE 7.2(b) Listing of regression coefficients, their standard errors and t-values and r^2-values for model 6 for different material groupings

MATERIALS		logCMC (=H)	logMCdev (=L)	Constant	$t_{(0,050)}$	r^2
G1 only						
(crushed stone)	X Coefficient(s)	1,178208	0,986691	-0,69168		
	Std Err of Coef.	0,138271	0,007596	0,164459		
	t-value	8,520961	129,8817	4,205809	1,972	0,984
NPAB - LABD	X Coefficient(s)	1,085141	0,933824	-0,82473		
(natural gravel)	Std Err of Coef.	0,146180	0,023813	0,176884		
	t-value	7,423314	39,21467	4,662557	1,972	0,852
LABLEN - LABDEW	X Coefficient(s)	-0,61633	0,990730	0,568200		
(sandy materials)	Std Err of Coef.	0,312484	0,014812	0,244195		
	t-value	1,972384	66,88544	2,326829	1,972	0,940
All except BAB	X Coefficient(s)	0,150996	0,998355	-0,16016		
(minus black clay)	Std Err of Coef.	0,042573	0,008221	0,237819		
	t-value	3,546708	121,4374	0,673488	1,972	0,937
All materials	X Coefficient(s)	0,127356	0,993750	-0,13852		
	Std Err of Coef.	0,035604	0,007837	0,228990		
	t-value	3,576956	126,7871	0,604944	1,972	0,936

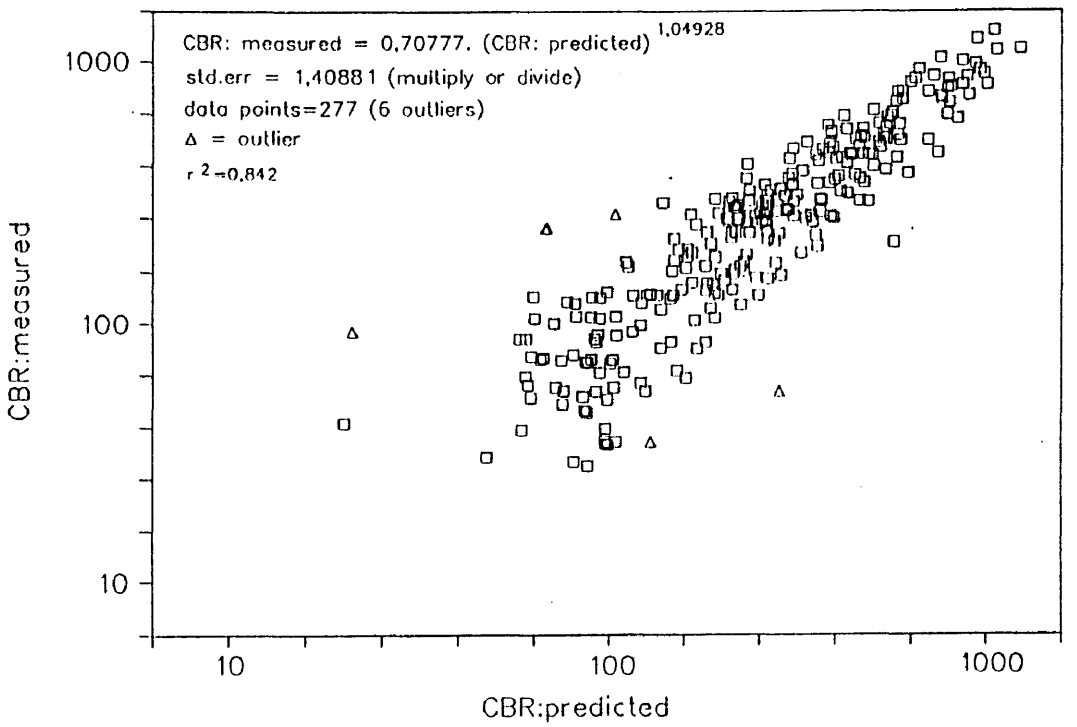

FIGURE 7.4(a) **RELATION BETWEEN LOG (CBR:MEASURED) AND LOG (CBR:PREDICTED) (MODEL A) FOR CRUSHED STONE (G1)**

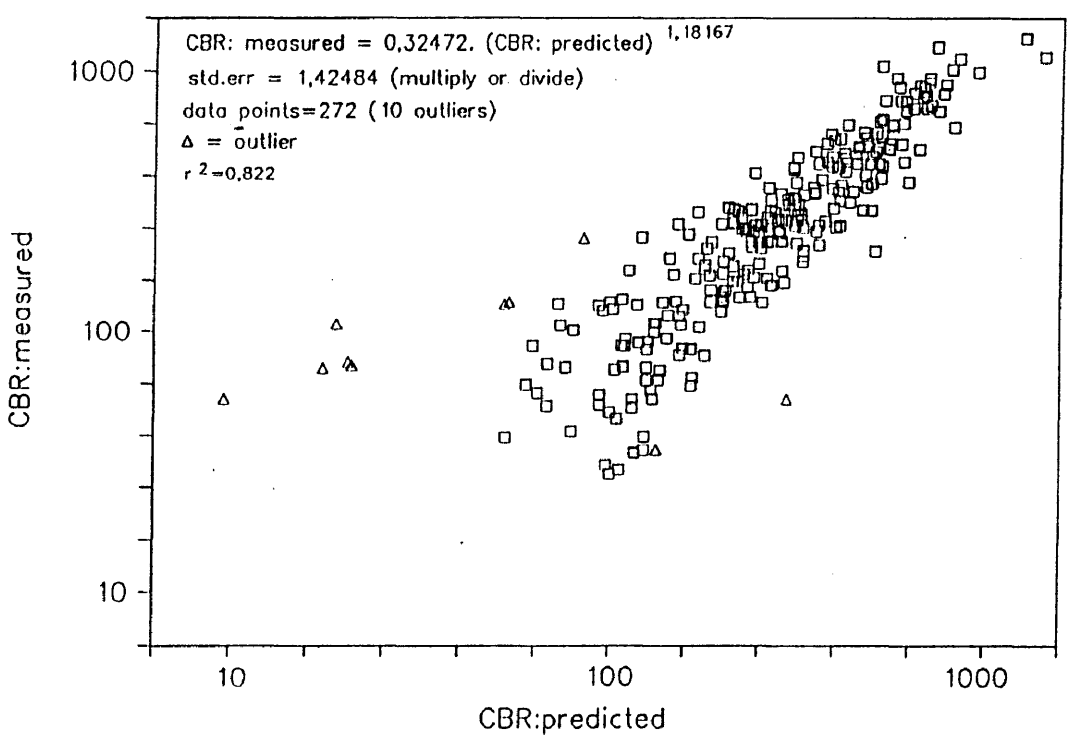

FIGURE 7.4(b) **RELATION BETWEEN LOG (CBR:MEASURED) AND LOG (CBR:PREDICTED) (MODEL B) FOR CRUSHED STONE (G1)**

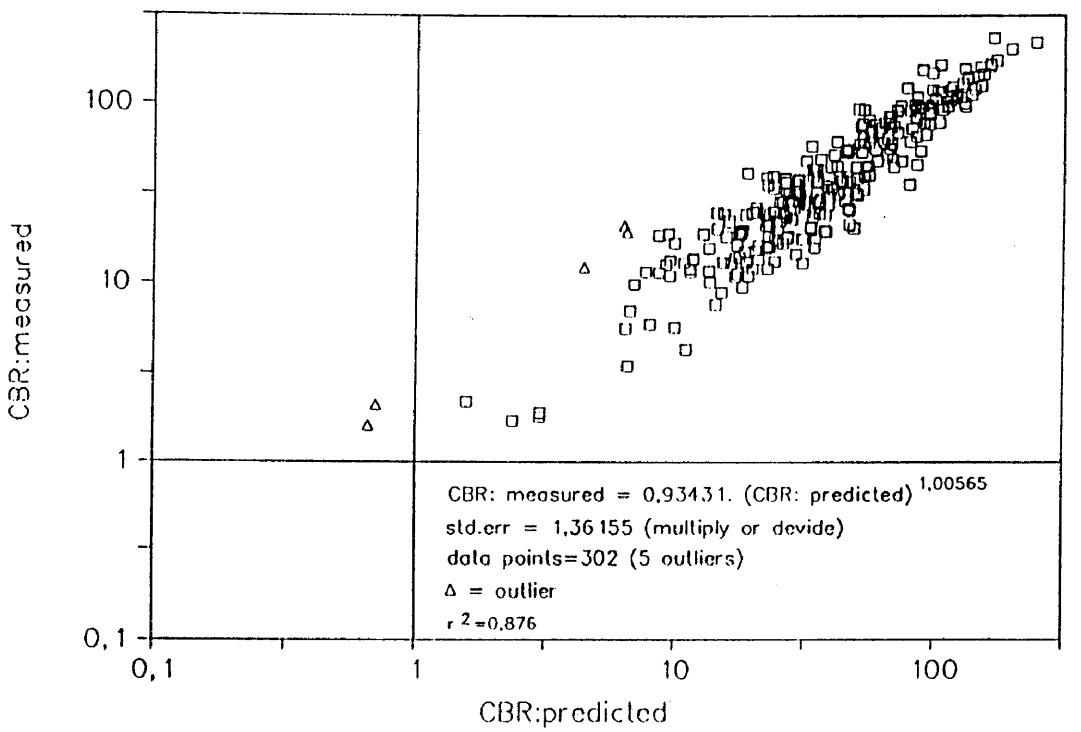

FIGURE 7.5(a) **RELATION BETWEEN LOG (CBR:MEASURED) AND LOG (CBR:PREDICTED) (MODEL A) FOR NATURAL GRAVELS**

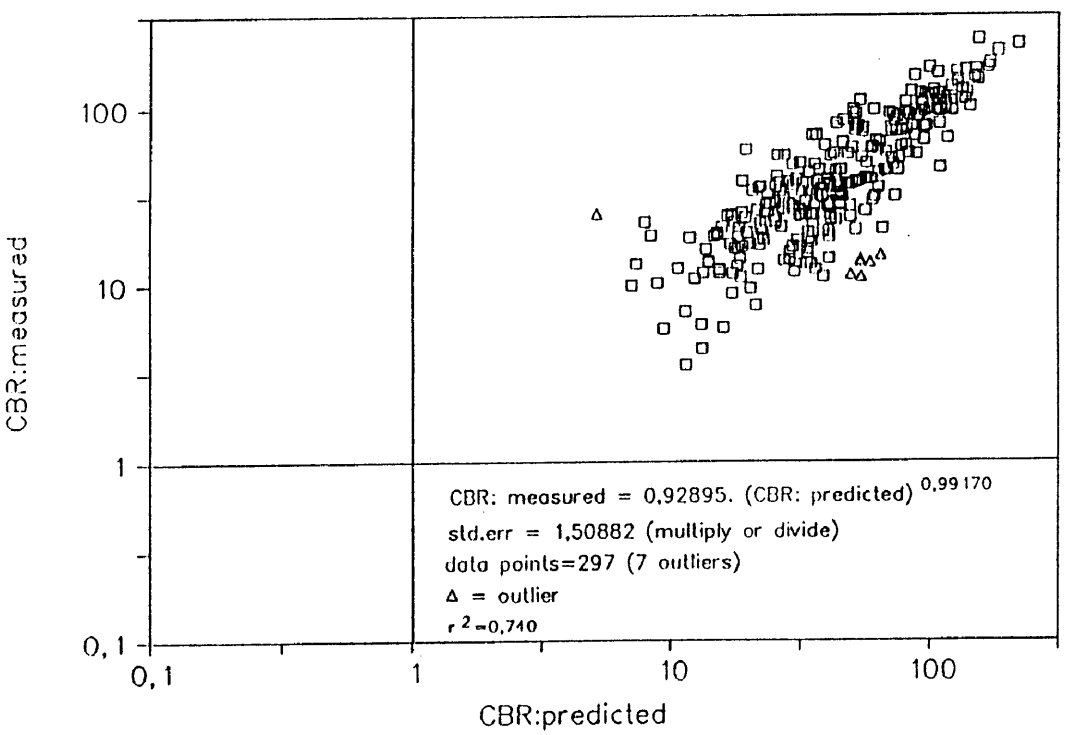

FIGURE 7.5(b) **RELATION BETWEEN LOG (CBR:MEASURED) AND LOG (CBR:PREDICTED) (MODEL B) FOR NATURAL GRAVELS**

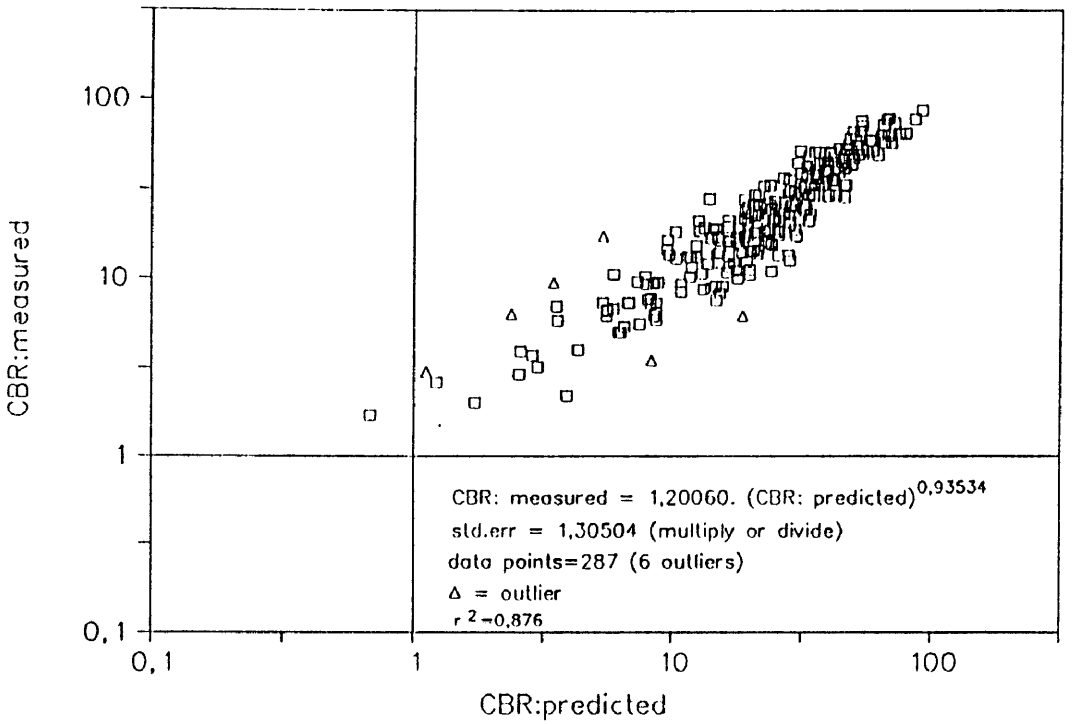

FIGURE 7.6(a) **RELATION BETWEEN LOG (CBR:MEASURED) AND LOG (CBR:PREDICTED) (MODEL A) FOR SANDY MATERIALS**

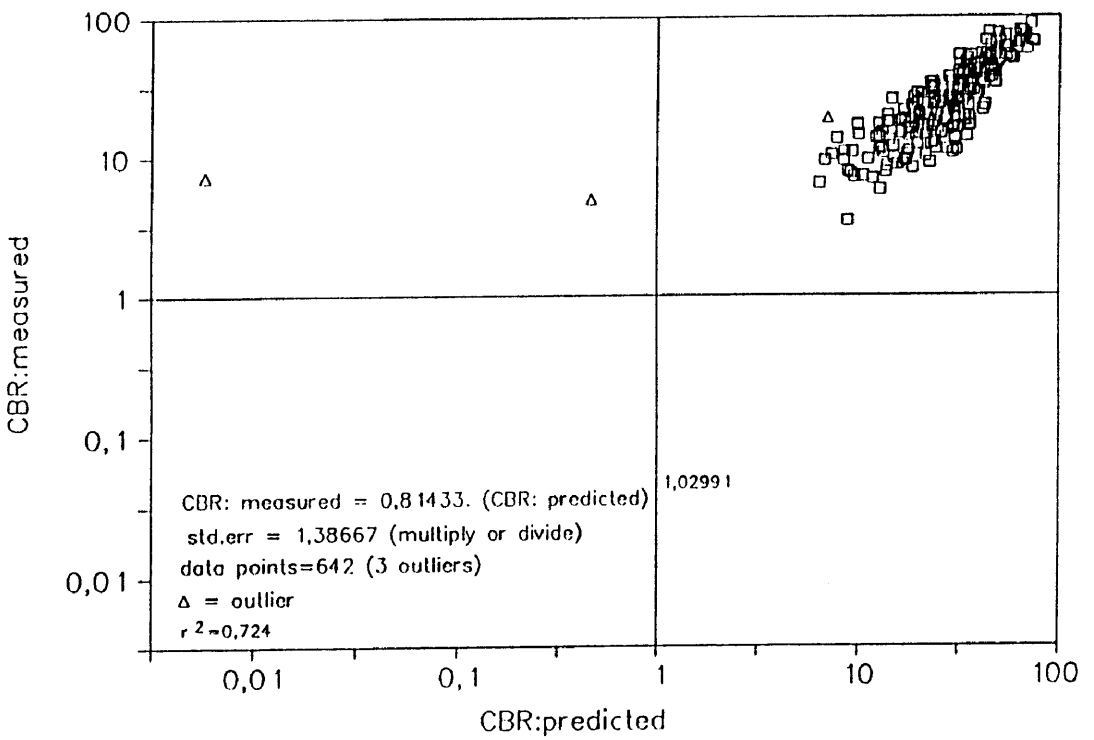

FIGURE 7.6(b) **RELATION BETWEEN LOG (CBR:MEASURED) AND LOG (CBR:PREDICTED) (MODEL B) FOR SANDY MATERIALS**

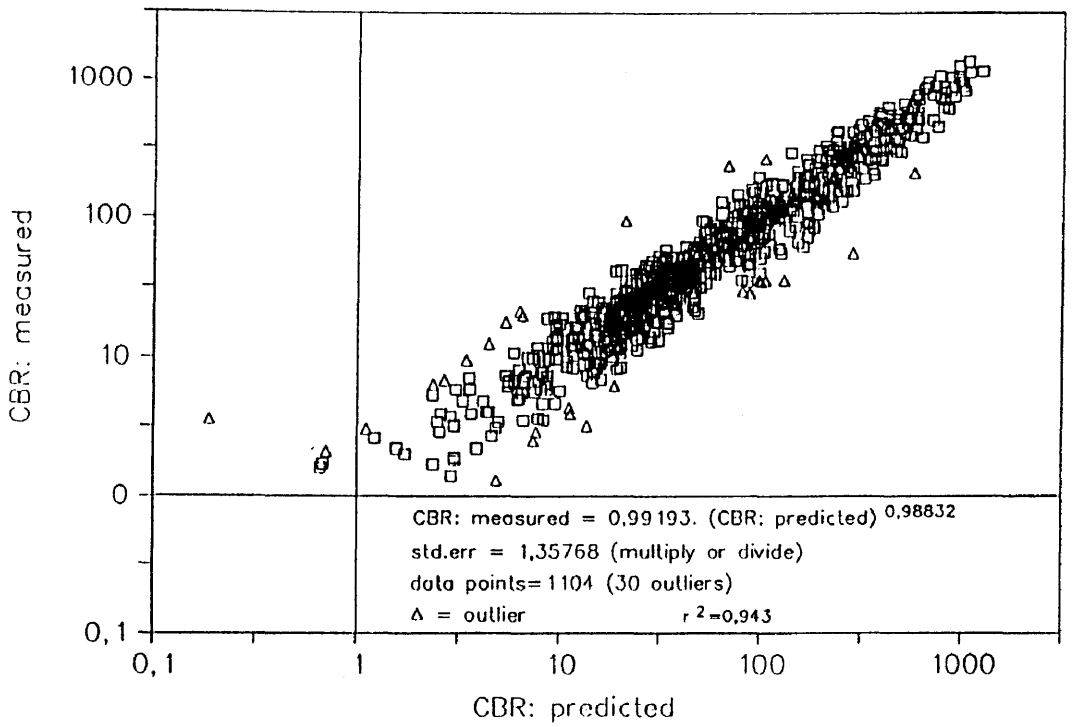

FIGURE 7.7(a) **RELATION BETWEEN LOG (CBR:MEASURED) AND LOG (CBR:PREDICTED) (MODEL A) FOR ALL MATERIALS**

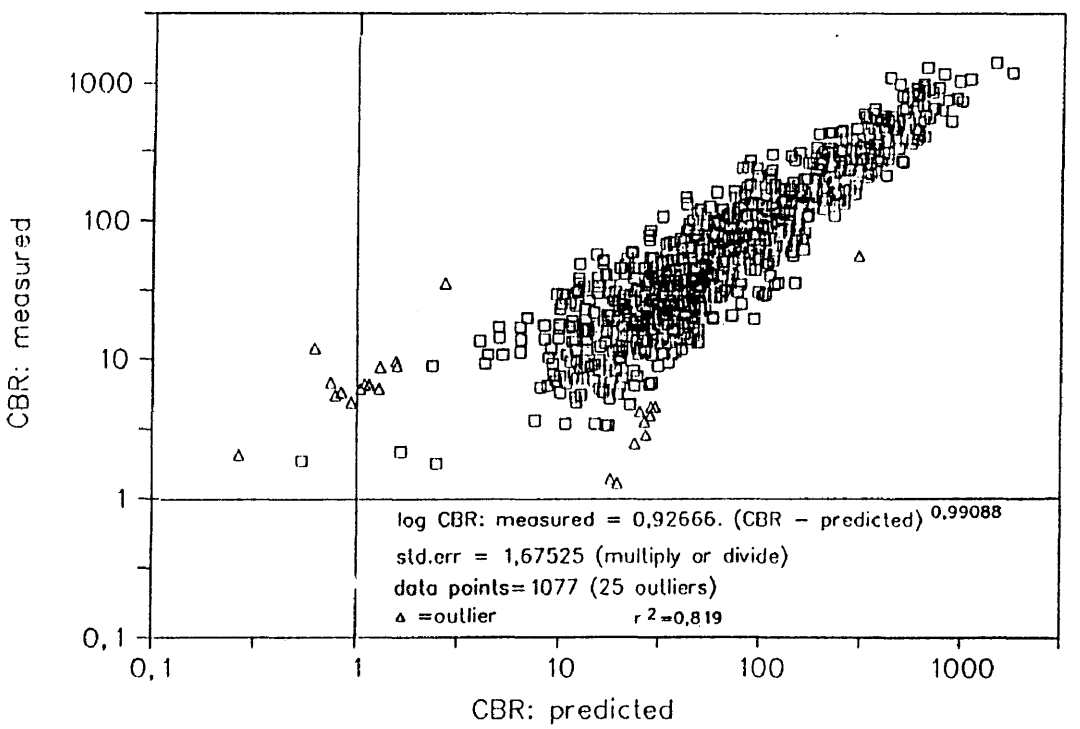

FIGURE 7.7(b) **RELATION BETWEEN LOG (CBR:MEASURED) AND LOG (CBR:PREDICTED) (MODEL B) FOR ALL MATERIALS**

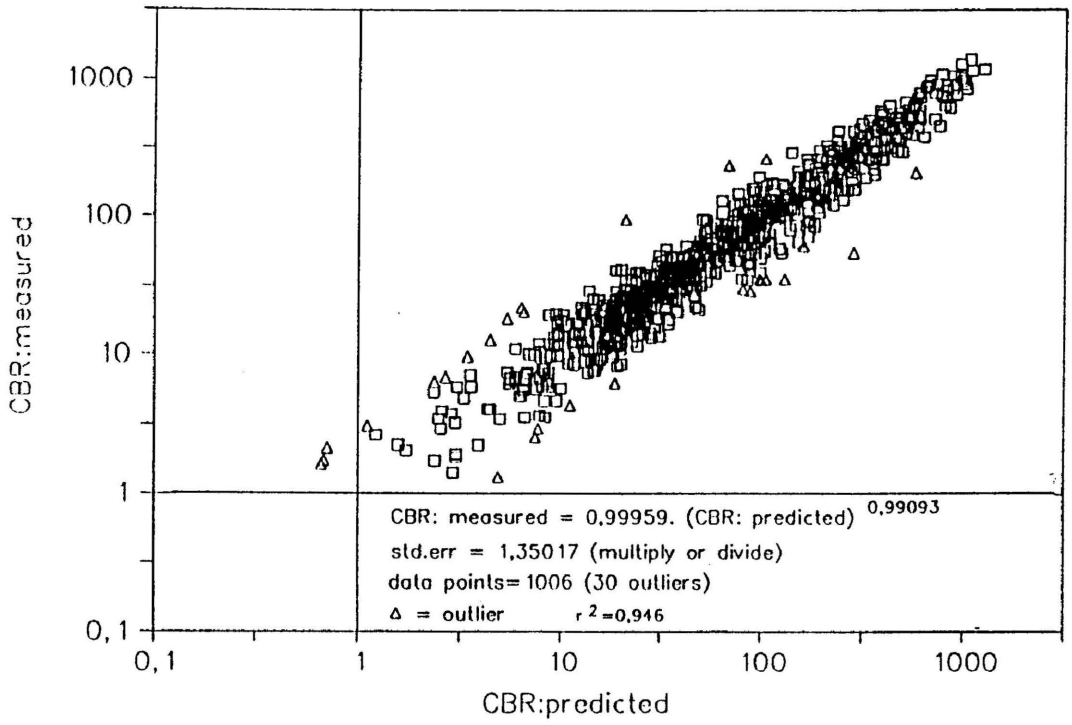

FIGURE 7.8(a) **RELATION BETWEEN LOG (CBR:MEASURED) AND LOG (CBR:PREDICTED) (MODEL A) FOR ALL MATERIALS EXCEPT BLACK CLAY**

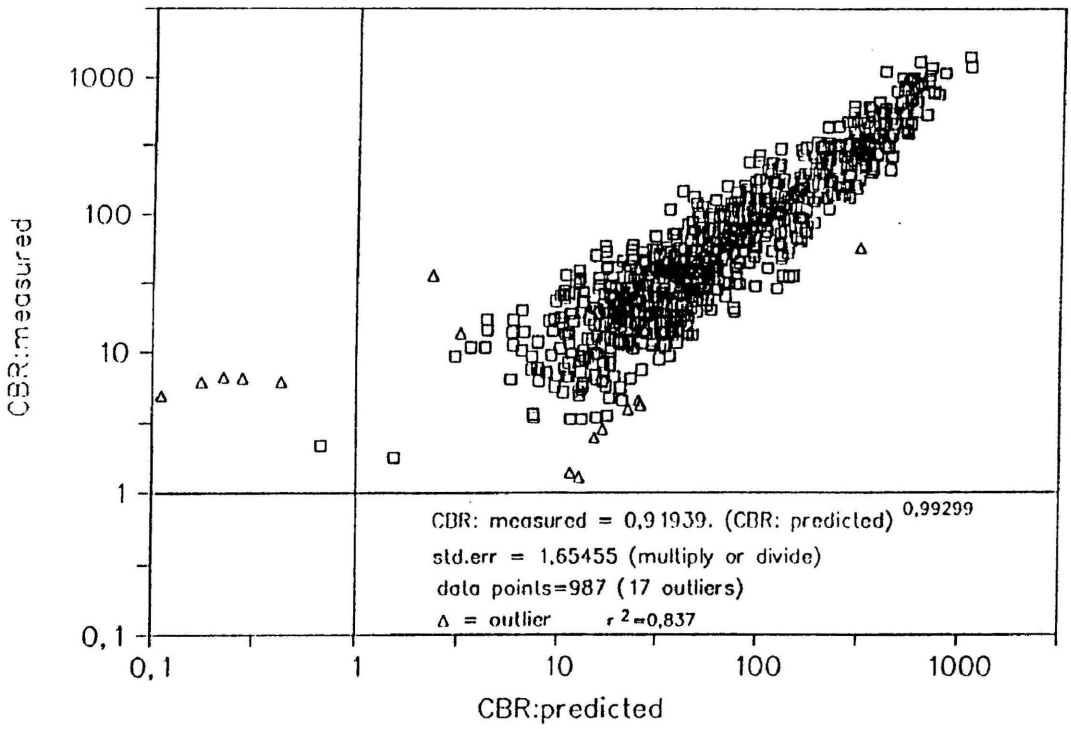

FIGURE 7.8(b) **RELATION BETWEEN LOG (CBR:MEASURED) AND LOG (CBR:PREDICTED) (MODEL B) FOR ALL MATERIALS EXCEPT BLACK CLAY**

The difference in the number of data points between models A and B, as shown in Figures 7.4 to 7.8, is caused by the fact that the logarithmic values of a negative value cannot be determined. The negative values were caused by the fact that for some of the data points the predicted CBR-values became negative just below zero. This was caused by the CBR:decrease being calculated as greater than 100 %. This is naturally not possible in practice. This problem could be overcome by, for example, postulating that the maximum value for CBR:decrease is say 99 %. If a larger value is calculated this could then be replaced with this value. Defining the soaked condition is a slight problem as the CBR samples are allowed to drain for a period when removed from the waterbath which means that the moisture content is lower than ZAVMC. Note that the scatter of data points is always broader at the lower end of the scale (ie. low CBRs, low densities, high moisture content deviations from CMCs). An outlier in these figures was defined as any point more than three standard deviations away from the mean line.

Note that all the r^2-values are high by civil engineering standards and that the slopes of the best fitting lines are all very close to one, showing that very good estimates of the bearing capacities of materials can be determined using models B once the MDD (% SD) and CMC (%) have been determined from the grading factor (GF), LL and LS of the material.

Note that models A had to be determined for the separate materials first and that their predicted CBR values cannot be derived from the indicator tests as in the case with Models B.

7.4 Conclusions

The high r^2-values achieved in the modelling process very clearly indicate that the grading, Atterberg limits and linear shrinkage, together with the shape and texture of the aggregate directly influence the CBR that can be achieved at a particular dry density and moisture content for a particular material.

Once estimates for the MDDs (vibratory and mod. AASHTO), OMCs (vibratory and mod. AASHTO), ZAVMCs (vibratory and mod. AASHTO) as well as CMC have been determined with the models developed in Chapter 6, it should be possible to get estimates of the bearing capacity as well by using these estimates in the models developed in this Chapter (see Appendix F for regression analysis results).

As shape and texture have a substantial influence on the bearing capacity of materials it stands to reason that they will also influence the resistance to compaction. The amount of compactive effort required to compact untreated roadbuilding materials optimally will therefore vary from one material to another. End result specifications for density requirements are recommended for this reason rather than the method specification approach. Because the shape and texture had such a tremendous effect on the CBR:CMC, it was concluded that they were therefore also likely to have an influence on the MDD and the moisture regime as well. The models for the determination of MDD, OMC, ZAVMC and CMC were therefore recalibrated, taking account of these two variables together with the previously identified variables namely the GF, LL and LS. The improvements in the results were small compared to the effect of the SBD and SF on the CBC:CMC. This seems to indicate the shape and texture have a tremendous effect on the resistance to compaction and the ultimate bearing capacity but only a very limited influence on the MDD if the compactive force is large enough to compact the material properly. This is confirmed by the t-values of the regression coefficients for SBD and SF in the compactability models (see Table 7.3).

TABLE 7.3 Listing of regression coefficients, their standard errors and t-values, and r^2-values for the different compaction properties

PROPERTY		$GF^{0,85}$	C	LS	C^3	SBD	SF	Constant	$t_{(0,050)}$	r^2	Degrees of freedom
MDD (vib)	X Coeff	-40,2497	16,74064	-1,63137	-8,37628	0,111113	0,206339	99,37093			
	Std Err	4,299426	3,781997	0,192058	4,036096	0,084488	0,115473	1,581555			
	t-value	9,361651	4,426403	8,494140	2,075343	1,315119	1,786908	62,83113	2,145	0,970	14
OMC (vib)	X Coeff	22,62105	-15,2461	1,076490	10,74169	-0,03708	-0,02650	-4,56070			
	Std Err	2,949191	2,594261	0,131742	2,768560	0,057955	0,079208	1,084868			
	t-value	7,670254	5,876891	8,171175	3,879885	0,639929	0,334567	4,203923	2,145	0,965	14
ZAVMC (vib)	X Coeff	25,23629	-13,4865	1,021651	11,79872	-0,03981	-0,12992	-4,40440			
	Std Err	2,775823	2,441757	0,123997	2,605810	0,054548	0,074552	1,021094			
	t-value	9,091462	5,523286	8,239262	4,527852	0,729877	1,742688	4,313417	2,145	0,971	14
CMC	X Coeff	10,25198	-2,72904	0,408870	-1,12567	-0,02080	0,069362	-0,87252			
	Std Err	1,550195	1,363631	0,069248	1,455249	0,030463	0,041634	0,570243			
	t-value	6,613349	2,001305	5,904411	0,773525	0,683024	1,665969	1,530094	2,145	0,965	14
MDD (mod. AASHTO)	X Coeff	-33,9206	15,34473	-1,28353	-9,30291	0,152339	0,232665	87,96416			
	Std Err	5,984434	5,220130	0,265351	5,665530	0,116471	0,159648	2,180148			
	t-value	5,668150	2,939530	4,837100	1,642019	1,307963	1,457365	40,34777	2,160	0,921	13
OMC (mod. AASHTO)	X Coeff	6,697516	1,878918	0,561881	1,759635	-0,07139	-0,07753	6,559983			
	Std Err	3,014797	2,651971	0,134673	2,830148	0,059244	0,080970	1,109001			
	t-value	2,221547	0,708498	4,172186	0,621746	1,205125	0,957561	5,915215	2,145	0,924	14

TABLE 7.3 (Continued)

PROPERTY		$GF^{0,85}$	C	LS	C^3	SBD	SF	Constant	$t_{(0,050)}$	r^2	Degrees of freedom
ZAVMC (mod. AASHTO)	X Coeff	24,05091	-12,1754	0,891343	10,45804	-0,06374	-0,18022	0,679363			
	Std Err	3,770593	3,289031	0,167189	3,569663	0,073384	0,100588	1,373639			
	t-value	6,378548	3,701849	5,331349	2,929701	0,868680	1,791731	0,494571	2,160	0,936	13
SOMC (vib)	X Coeff	21,54663	-16,1441	1,091149	11,73755	-0,04758	0,010137	-3,13939			
	Std Err	2,779412	2,444914	0,124158	2,609179	0,054618	0,074648	1,022414			
	t-value	7,752227	6,603166	8,788376	4,498562	0,871229	0,135803	3,070566	2,145	0,971	14
SZAVMC (vib)	X Coeff	24,07317	-14,4159	1,032267	12,92494	-0,05089	-0,09206	-2,85787			
	Std Err	2,697479	2,372842	0,120498	2,532265	0,053008	0,072448	0,992275			
	t-value	8,924320	6,075390	8,566656	5,104103	0,960208	1,270811	2,880121	2,145	0,974	14
SCMC	X Coeff	9,443518	-3,22213	0,413319	-0,74310	-0,02730	0,097120	0,106224			
	Std Err	1,697253	1,492991	0,075817	1,593300	0,033353	0,045584	0,624339			
	t-value	5,563999	2,158171	5,451513	0,466392	0,818632	2,130558	0,170139	2,145	0,960	14
SOMC (mod. AASHTO)	X Coeff	5,562672	1,216733	0,567507	2,448490	-0,08124	-0,04371	8,005320			
	Std Err	3,329077	2,928428	0,148712	3,125178	0,065420	0,089411	1,224610			
	t-value	1,670935	0,415490	3,816150	0,783472	1,241822	0,488898	6,537036	2,145	0,913	14
SZAVMC (mod. AASHTO)	X Coeff	22,49622	-13,2274	0,884294	11,68022	-0,07900	-0,13125	2,793415			
	Std Err	3,869083	3,374941	0,171556	3,662904	0,075301	0,103216	1,409519			
	t-value	5,814356	3,919312	5,154548	3,188788	1,049166	1,271689	1,981820	2,160	0,935	13

CHAPTER 8

VERIFICATION OF THE APPLICABILITY OF THE DENSITY-, MOISTURE REGIME- AND CBR-MODELS ON MATERIALS NOT USED TO DEVELOP THE MODELS

In Chapter 6 it was shown that a definite relationship exists between the properties used to define the compactability of untreated roadbuilding materials, namely the MDD, OMC, CMC and ZAVMC, and the particle size distribution of the material defined by the grading, Atterberg limits and linear shrinkage. The fact that the same basic regression model could be used to calculate all the compactability parameters also very clearly indicates that all the compactability parameters are directly related. It therefore seems likely that one can fairly accurately predict the MDDs, OMCs, ZAVMCs and CMC of untreated roadbuilding materials from the basic information of the indicator tests, provided that the grading represents the grading of the material after compaction. Other information that is required are the ARD, BRD and WA of the material so that the densities can be expressed in kg/m^3 and the OMC can be adjusted for possible water absorption by the aggregate particles.

In Chapter 7 it was shown that the bearing capacity of a material is directly influenced by its degree of densification and its moisture content as well as the shape and texture of its aggregate particles as quantified by the SBD and SF. It therefore also seems likely that one can reasonably predict the CBRs for these materials for a range of dry densities (% SD) and moisture contents (%) from the basic information of the indicator tests, and the SBD and SF values.

To ensure that the density-, moisture regime- and CBR-models are universally applicable, it was necessary to compare the actual test results of materials not used to develop these models with the predictions of the respective models. As the main purpose of the investigation was to determine the effect of material properties on the compactability of untreated roadbuilding materials, the verification process also concentrated on the applicability of the density- and moisture regime-models.

8.1 The verification process of the density- and moisture regime-models

8.1.1 General comparison

The compactability models were checked by comparing the MDD (mod. AASHTO) (predicted) and OMC (mod. AASHTO) (predicted) with the measured values of MDD (mod. AASHTO) and OMC (mod. AASHTO) of certain road projects as recorded on the material control data

sheets. As the MDDs (mod. AASHTO) (predicted) are expressed in terms of the space occupied by "solids" (ie % SD) an estimate of the solid density of the material had to be used to convert the MDD (mod. AASHTO) from the data sheets into percentage solid density. The value of 2650 kg/m^3 was used throughout because of a lack of more reliable information. This naturally lead to a broader scatter of the predicted results against the actual results. Another factor that also adversely influenced the comparison was that the grading of the material is usually determined before compaction. Where the material consists of sound rock particles of which the grading will hardly change during construction or fine material of which the structure has already been broken down to its minimum size, this causes no problems for the predicted values. But where the material is not sound and breakdown occurs during compaction the actual value can deviate substantially from the predicted value. The predicted value in these situations will be too high. The difference between the predicted laboratory results and predicted field results in Section 8.1.2 illustrate this point. For this reason it was only possible to assess if there was a significant relation between the actual values and the predicted values (see Figures 8.1 and 8.2 and Table 8.1). The number of data points were 144.

From Table 8.1 and Figures 8.1 and 8.2 it is clear that no definite conclusion can be made. Both the MDDs and OMCs cover a limited range. The fact that the "solid" density of the laboratory results was set at 2650 kg/m^3 for all the materials must have contributed to the wide scatter of the results. The t-value of the coefficient for MDD (predicted) seems to indicate that there is a significant relation between the predicted and actual values, although the slope is far from unity (ie 0,17097) and the r^2-value extremely low. The t-value and r^2-value of the coefficient for OMC (predicted) indicates that there seems to be no relation between OMC (predicted) and OMC (measured). The fact that the OMC (measured) remained relatively constant for the full range of densities measured did not seem normal. The values of MDD (predicted and measured) were then plotted against the values of OMC (predicted and measured) (see Figures 8.3 and 8.4) and the relations were evaluated by means of regression analysis (see Table 8.1). Figure 8.4 and its t-value in Table 8.1 indicate that a significant relation exists between the OMC (measured) and MDD (measured) although the correlation is poor (ie r^2 = 0,222). This poor correlation (ie wide scatter) was most probably partly due to the fixed solid density value of 2650 kg/m^3, which was used to convert the measured results (kg/m^3) to percentage space occupied (ie % SD). If the actual values of the solid density for each of these materials had been known the correlation would most likely have been higher.

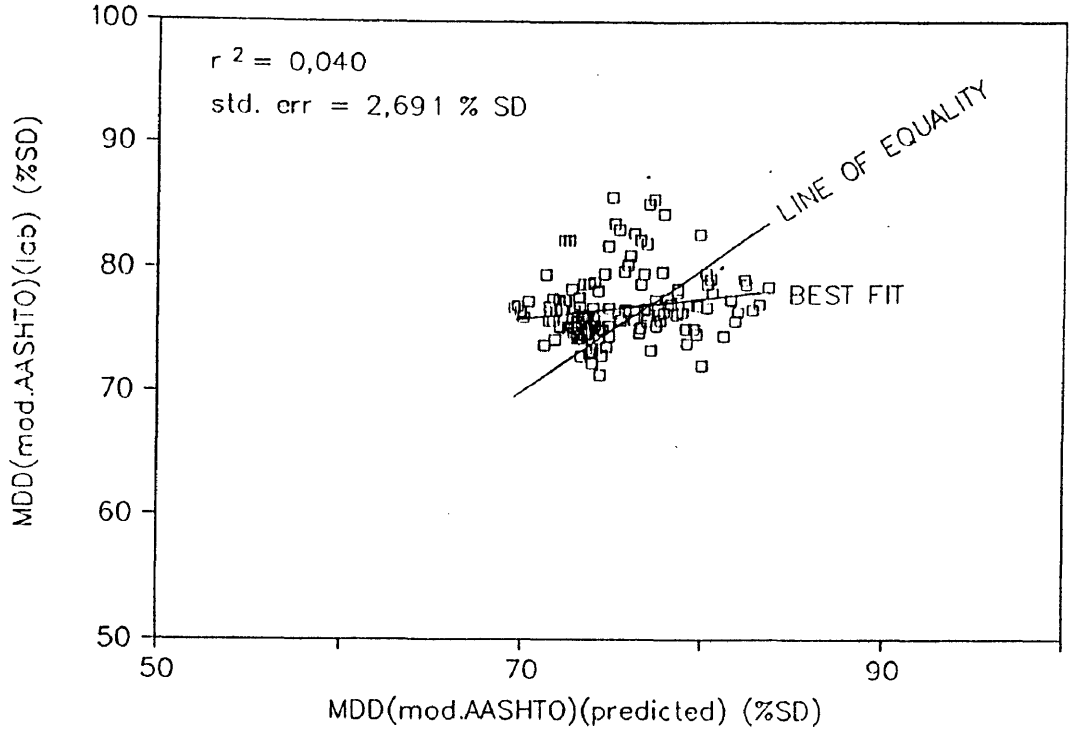

FIGURE 8.1 **RELATION BETWEEN MDD (MOD. AASHTO) (MEASURED) AND MDD (MOD. AASHTO) (PREDICTED) FOR ACTUAL CONSTRUCTION DATA**

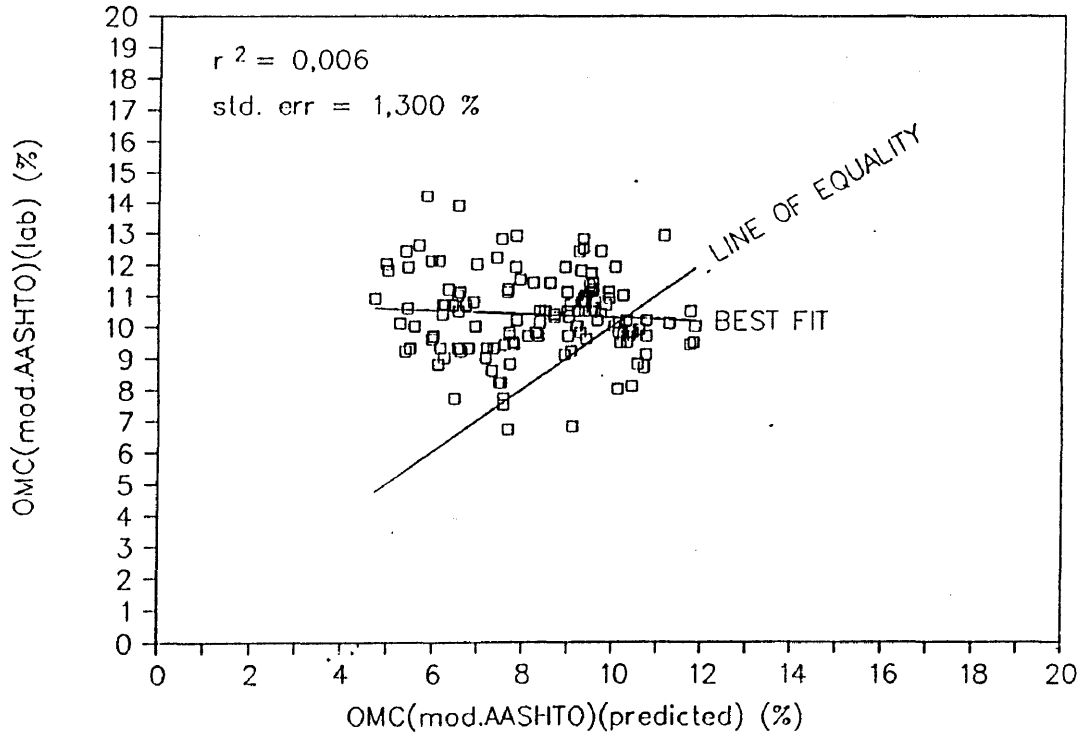

FIGURE 8.2 **RELATION BETWEEN OMC (MOD. AASHTO) (MEASURED) AND OMC (MOD. AASHTO) (PREDICTED) FOR ACTUAL CONSTRUCTION DATA.**

TABLE 8.1 **Listing of regression coefficients, their standard errors and t-values, and r^2-values for the predicted values of different properties as well as the relation between MDD (mod. AASHTO) and OMC (mod. AASHTO) for both the laboratory results and the predicted values**

		x	x^2	Constant	$t_{(0,050)}$·	r^2
MDD (mod) (lab) vs MDD (mod) (predicted) (= x)	X Coefficient(s)	0,170973		63,90669		
	Std Err of Coef.	0,070570		2,691431		
	t-value	2,422728		23,74449	1,984	0,040
OMC (mod) (lab) vs OMC (mod) (predicted) (= x)	X Coefficient(s)	-0,05713		10,86750		
	Std Err of Coef.	0,062592		1,298648		
	t-value	0,912811		8,368319	1,984	0,006
ZAVMC (mod) (lab) vs ZAVMC (mod) (predicted) (= x)	X Coefficient(s)	0,151307		9,630034		
	Std Err of Coef.	0,066107		1,668253		
	t-value	2,288809		5,772524	1,984	0,036
MDD (mod) (lab) vs MDD (vib) (predicted) (= x)	X Coefficient(s)	0,167525		63,67874		
	Std Err of Coef.	0,056987		2,666553		
	t-value	2,939675		23,88054	1,984	0,057
MDD (mod) (lab) vs OMC (mod) (lab) (= x) x^2	X Coefficient(s)	-0,96902	-0,00121	86,98628		
	Std Err of Coef.	0,227688	0,008074	2,430616		
	t-value	4,255908	0,150954	35,78774	1,984	0,222

TABLE 8.1 (Continued)

		x	x^2	Constant	$t_{(0,050)}$*	r^2
MDD (mod) (predicted) vs OMC (mod) predicted) (= x) x^2	X Coefficient(s)	-0,69819	-0,04750	84,76927		
	Std Err of Coef.	0,840629	0,050541	1,890374		
	t-value	0,830556	0,939840	44,84257	1,984	0,654
MDD (mod) (lab) vs OMC (mod) (lab) (= x)	X Coefficient(s)	-0,99397		87,10932		
	Std Err of Coef.	0,156066		2,422238		
	t-value	6,368880		35,96232	1,984	0,222
MDD (mod) (predicted) vs OMC (mod) (predicted)(= x)	X Coefficient(s)	-1,48359		87,87223		
	Std Err of Coef.	0,091074		1,889597		
	t-value	16,28984		46,50314	1,984	0,651
MDD (mod) (lab) (kg/m^3) vs OMC (mod) (lab) (= x)	X Coefficient(s)	-26,3402		2308,397		
	Std Err of Coef.	4,135772		64,18932		
	t-value	6,368880		35,96232	1,984	0,222

* Degrees of freedom = 100

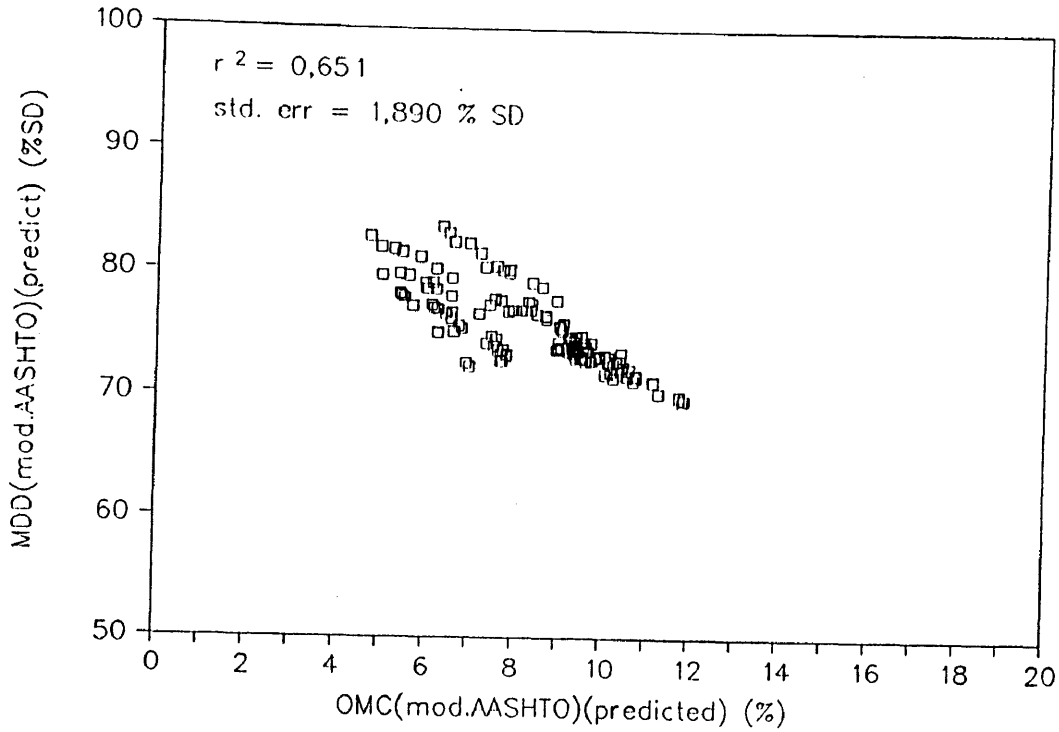

FIGURE 8.3 **RELATION BETWEEN MDD (PREDICTED) (% SD) AND OMC (PREDICTED) (%) FROM THE INDICATOR TESTS OF THE CONSTRUCTION DATA**

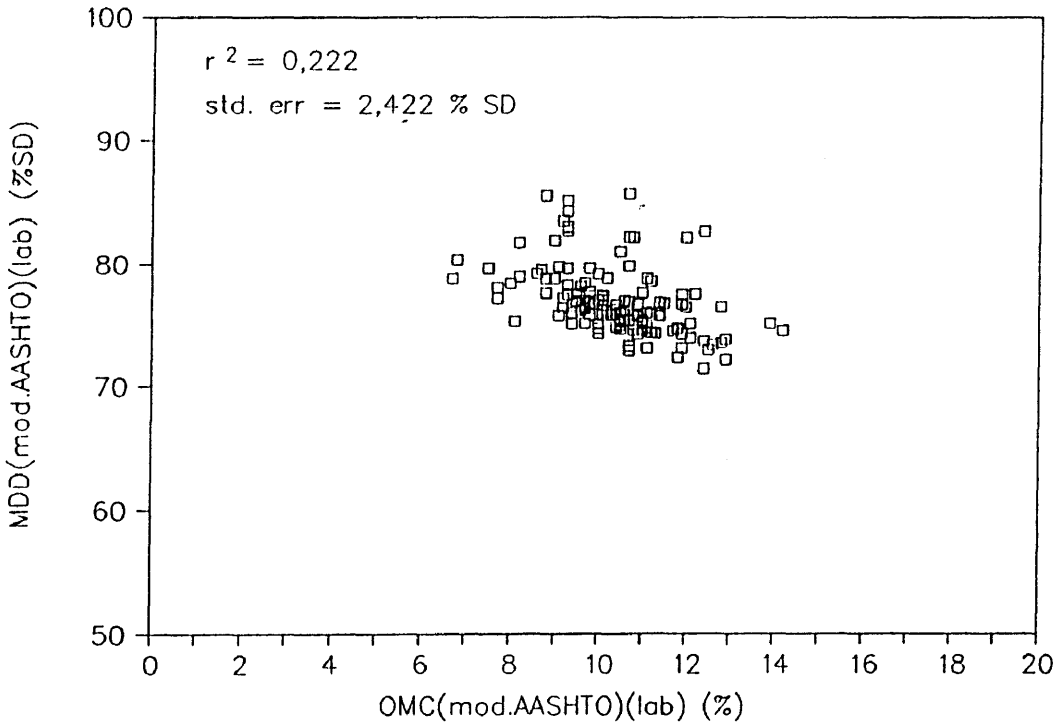

FIGURE 8.4 **RELATION BETWEEN MDD (MEASURED) (% SD) AND OMC (MEASURED) (%) FROM THE CONSTRUCTION DATA**

Even in the case of the actual results obtained on the vibratory compaction table there seems to be a greater amount of scatter of the MDD results in the OMC range from about 6 to 14 per cent (see Figure 4.8 on p 82).

Another possible reason for the poor relation between MDD (measured) (kg/m^3) and OMC (measured) (%) could be that materials which had high densities (ie above 80 % SD) were relatively porous with a water absorption of about 5 %. If this water absorption was subtracted from the OMC (measured) values all these data points would move to the left to be in line with the rest of the data points. This remains pure speculation and one actually needs the actual ARD, BRD and WA values to be able to make a meaningful comparison in this way. Unfortunately this information is not normally recorded. The MDD (predicted) against OMC (predicted) had a much higher r^2-value (ie 0,651). The materials also only covered the selected pavement layers as the gradings, Atterberg limits and linear shrinkages of the in situ materials are not normally recorded. Only the grading moduli, PIs, MDDs and OMCs are listed. To cover a wider range of densities and moisture contents it would be necessary for the normal indicator tests to be recorded, together with the ARD, BRD and WA of these materials. Only then will it be possible to make a good comparison.

8.1.2 Specific verification of the compactability models

As research work was done on the compactability of materials in general the test results obtained were always compared with the theoretical results of the models developed. This included both field results and laboratory results.

8.1.2.1 Solving "density problems" on experimental sections

Problems were experienced with the performance of two experimental test sections on a heavy vehicle simulator (HVS) test site in Natal. The same roadbuilding material, namely a weathered dolerite gravel, had been used to construct all three sections except that different modifying agents had been used in each section to evaluate the effects of the different modifying agents. Section 1 performed well during trafficking by the HVS. The other two sections rutted badly and seemed to be saturated even though they had been constructed at laboratory OMC. According to the field measurements the densities and moisture contents were correct (see Table 8.2). However, when these results are compared with results of the compactability model it was clear that Section 1 had been constructed at OMC, but that both Sections 2 and 3 had been constructed at ZAVMC, which explained their poor performance.

TABLE 8.2 **Comparison of laboratory and field test results with model estimates for 3 sections on a Heavy Vehicle Simulator (HVS) site in Natal**

	MDD (kg/m^3) (measured) (field) (+lab)	OMC (%) (measured) (field) (+lab)	MDD (kg/m^3) (predicted)	OMC (%) (predicted)	ZAVMC (%) (predicted)
SECTION 1					
NAT11			2345	6,3	7,3
NAT12			2328	6,6	7,6
NAT13			2334	6,5	7,5
MEAN(LAB)	2167	9,4	2336	6,5	7,4
ROAD1	2187	9,6	2186	8,9	10,4
ROAD2	2176	10,0	2170	9,2	10,7
ROAD7	2173	9,0	2168	9,2	10,8
ROAD8	2156	8,6	2166	9,2	10,8
ROAD9	2154	9,8	2159	9,4	10,9
ROAD10	2147	9,2	2158	9,4	11,0
ROAD12	2140	9,1	2156	9,4	11,0
ROAD13	2131	9,6	2148	9,6	11,2
MEAN(SITE)	2158	9,4	2164	9,3	10,8
SECTION 2					
NAT21			2313	6,9	7,9
NAT22			2336	6,5	7,4
NAT23			2314	6,8	7,8
MEAN(LAB)	2120	11,7	2321	6,7	7,7
REVER3	2177	11,6	2204	8,6	10,0
REVER5	2132	11,3	2128	9,9	11,6
REVER11	2130	10,6	2116	10,1	11,9
REVER14	2147	11,2	2148	9,6	11,2
REVER15	2129	11,1	2108	10,3	12,1
REVER16	2156	10,8	2160	9,3	10,9
REVER17	2147	11,2	2150	9,6	11,1
MEAN(SITE)	2145	11,1	2145	9,6	11,3

TABLE 8.2 **(continue)**

	MDD (kg/m^3) (measured) (field) (+lab)	OMC (%) (measured) (field) (+lab)	MDD (kg/m^3) (predicted)	OMC (%) (predicted)	ZAVMC (%) (predicted)
SECTION 3					
NAT31			2316	6,8	7,8
NAT32			2368	6,0	6,9
NAT33			2376	5,8	6,7
MEAN (LAB)	2130	11,2	2353	6,2	7,1
LIME4	2130	10,4	2146	9,6	11,2
LIME6	2136	11,2	2174	9,1	10,6
LIME18	2154	10,3	2193	8,9	10,2
LIME19	2142	10,9	2183	8,9	10,4
MEAN (SITE)	2140	10,6	2174	9,1	10,6

The vast differences of approximately 200 kg/m^3 between the measured and predicted results for the laboratory samples were due to the grading before compaction being used to determine the predicted density results. Because the material was a weathered dolerite it broke down fairly extensively during compaction. The predicted site densities were based on the gradings after compaction. The close agreement between the measured and predicted site densities as well as their close agreement with the measured laboratory densities illustrate that the particle size distribution (ie the grading) after compaction actually determines the porosity of the material and, therefore, the actual density that can be achieved.

8.1.2.2 Investigating the effect of the new grading requirements for the target grading of G2 materials as specified by the Cape Provincial Administration

The Cape Provincial Administration (CPA) had experienced compaction problems with G2 materials when the general grading envelope for G1 to G3 materials was used. From experimental work on site new limits for the target grading were laid down, which were particularly aimed at controlling the minus 4,75 mm fraction. There seemed to be a difference of opinion between different road authorities whether these requirements were really

necessary. For this reason the Division was asked to evaluate the effect of the new specification requirements of the CPA on the compactability of G2 materials.

The new CPA specification requirements for the minus 4,75 mm material were the following:

Apart from the target grading after compaction being as near as possible to the mean of the specified grading envelope, the following requirements are specified for the -4,75 mm material:

(a) A target value of between 7 and 9 % for the fraction passing the 0,075 mm sieve.

(b) The percentage by mass of material passing the 2,00 mm sieve shall not exceed 34 % and the percentage by mass of material passing the 0,425 mm sieve shall not exceed 22 %.

(c) The fraction passing the 2,00 mm sieve and which is retained on the 0,425 mm sieve shall not be less than 35 % by mass nor more than 50 % by mass expressed as a percentage of the mass of the total fraction passing the 2,00 mm sieve.

(d) A target value of between 40 and 45 % for the fraction passing the 4,75 mm sieve.

Seven test gradings were compiled as far as the -13,2 mm material was concerned (see Table 8.3). The fraction of the material larger than 13,2 mm was separated from the material smaller than 13,2 mm, and later re-added to make up the particular test gradings.

TABLE 8.3: Specific gradings for different sample gradings

	% < 13,2 mm	% < 4,75 mm	% < 2 mm	% < 0,425 mm	% < 0,075 mm
Target values	59 - 75	40 - 45	< 34	< 22	7 - 9
Grading 1	67	44	32	18	8
Grading 2	70	50	34	18	8
Grading 3	60	36	30	18	8
Grading 4	62	43	36	22	8
Grading 5	63	43	34	24	8
Grading 6	62	43	32	18	11
Grading 7	63	43	30	18	5

Grading 1 was exactly in the middle of the grading envelope. Gradings 2 to 7 were such that one of the controlling parameters was outside the target limits while the rest were in the middle. For example, in grading 2 the percentage passing the 4,75 mm sieve was too high. This was done to evaluate the effect of the deviation on the compactability of the material.

Because the investigation was aimed at the evaluation of the compactability and other engineering properties of G2 materials, the CPA Roads Department was requested to supply G2 materials obtained from different sources.

The materials used in this investigation are listed in Table 8.4.

TABLE 8.4: List of materials to be evaluated

SAMPLE	MATERIAL TYPE	SOURCE	TRB (PRA) CLASS
CPA 4	Crushed alluvial gravel	Montagu-Barrydale	A-1-a(0)
CPA 5	Crushed granite	Derbyshire crushers (George)	A-1-a(0)
CPA 6	Crushed quartzite	Nanaga-Middleton	A-1-a(0)
CPA 7	Crushed dolerite	Graaff Reinet-Aberdeen	A-1-a(0)
CPA 8	Crushed dolerite	Burgersdorp-Aliwal North	A-1-a(0)
CPA 9	Crushed hornfels	Peninsula crushers	A-1-a(0)

Because the quantities of material in each of these sieve sizes had to be controlled as closely as possible, it was necessary to sieve out the separate sieve fractions and recompile the samples to satisfy the grading requirements listed in Table 8.3.

For each of the seven gradings five samples were prepared for each material. The dry mass of the sample was such that at a 100 % mod. AASHTO density the sample height would be 100 mm. The moisture contents used for compaction purposes were 0,75 CMC, CMC, 1,25 CMC, 1,50 CMC and 1,75 CMC of the material. The CMCs were estimated by means of the original compactability model (see Equation 6.7).

The samples were then compacted in a single layer on the vibratory compaction table. The samples were compacted for 180 seconds with the table set at a low frequency (30 Hz), high amplitude (k = 64 %) which generally gave the best compaction results in the past.

The sample height was accurately measured with a vernier height gauge, after which the CBR at moulding moisture content was determined. After testing the whole sample was ovendried to determine the moisture content.

The actual grading after compaction of the wettest sample of each test grading was also determined. Time did not allow for gradings of all the samples of each test grading to be determined. Because it was expected that MDD (vib) would be achieved in the region of 1,75 CMC, it was felt that this grading would be the best approximation of the grading at MDD (vib). The separate sieved fractions were then evaluated to determine the shape factor of the material. The shakedown bulk density was also determined for this sample as a whole.

Estimates of the MDD were calculated using the earlier developed compactability models. The estimates of the MDD were evaluated with both the original model (not incorporating the SBD and SF) and the second model (incorporating the SBD and SF) in an effort to quantify the effect of the grading and the shape and texture of the aggregate particles separately. It was reasoned that the original model would give the effect of the grading only and that the difference between the original and second model could therefore be attributed to the shape and texture of the aggregate (see Appendices E and F for the respective regression coefficients used for determining the theoretical MDD (% DBD or % AD) and OMC (%)).

The actual compaction results were also evaluated. The best function to describe the dry density in terms of moisture content for each grading was determined by means of multiple regression analysis on both the dry side of OMC and the wet side of OMC. OMC was defined as the point at which these two functions intersected, making it possible to determine both the MDD and OMC.

The actual MDD and OMC results obtained on the vibratory table compared to the estimates of the compactability models with and without the influence of the shape factor (SF) and shakedown bulk density (SBD) are given in Table 8.5. From Table 8.5 it is clear that the estimates of both models compare favourably with the actual compaction results. The small differences between the estimates of the original and second models also seem to indicate that the influence of the shape and texture of the aggregate particles on the compactability is small compared to the influence of the grading, Atterberg limits and linear shrinkage. This confirms the findings of the significance test done in Chapter 7 on the compactability models when the SBD and SF were included as input variables.

TABLE 8.5 **The values of OMC (vib) and OMC (predicted) and MDD (vib) and MDD (predicted) for the original model and second model (incorporating SBD and SF) for the different gradings for the different G2 materials**

			SECOND		ORIGINAL			SECOND		ORIGINAL	
Sample (code)	Grading (No.)	OMC (vib) (%)	OMC** (predict) (%)	OMC*** (predict) (%)	OMC** (predict) (%)	OMC*** (predict) (%)	MDD (vib) (%DBD) or (%AD)	MDD** (predict) (%DBD) or (%AD)	MDD*** (predict) (%DBD) or (%AD)	MDD** (predict) (%DBD) or (%AD)	MDD*** (predict) (%DBD) or (%AD)
CPA4	1	4,4	4,0	4,1	4,8	4,8	89,8	87,6	89,9	86,1	88,5
CPA4	2	5,0	4,8	4,9	5,1	5,2	88,5	85,1	87,9	84,5	87,4
CPA4	3	5,1	4,2	4,3	4,6	4,7	88,2	87,8	90,0	86,9	89,3
CPA4	4	4,9	4,2	4,3	4,9	4,9	88,7	87,0	89,7	85,7	88,5
CPA4	5	4,9	4,5	4,6	5,0	5,0	88,6	86,3	89,3	85,4	88,6
CPA4	6	4,9	4,3	4,3	4,7	4,7	88,7	87,4	89,6	86,6	88,9
CPA4	7	4,8	4,1	4,2	4,8	4,8	88,8	87,5	89,8	86,2	88,7
CPA5	1	5,0	4,5	4,5	4,6	4,6	87,5	87,3	89,2	87,0	89,1
CPA5	2	5,1	4,7	4,8	4,9	4,9	87,2	86,0	88,1	85,7	87,9
CPA5	3	4,7	4,5	4,6	4,7	4,7	88,0	87,1	89,1	86,8	89,0
CPA5	4	5,1	4,5	4,6	4,8	4,8	87,1	86,7	88,9	86,2	88,5
CPA5	5	5,2	4,5	4,6	4,8	4,8	87,1	86,9	89,2	86,4	88,9
CPA5	6	4,7	4,6	4,6	4,7	4,7	88,0	86,9	88,7	86,6	88,6
CPA5	7	5,0	4,7	4,8	4,9	4,9	87,4	86,1	88,3	85,8	88,1

** LL = 0,0% for CPA4, CPA5, CPA6, CPA8 and CPA9
*** LL = 0,5% for CPA4, CPA5, CPA6, CPA8 and CPA9

TABLE 8.5 (Continued)

Sample (code)	Grading (No.)	OMC (vib) (%)	SECOND OMC** (predict) (%)	SECOND OMC*** (predict) (%)	ORIGINAL OMC** (predict) (%)	ORIGINAL OMC*** (predict) (%)	MDD (vib) (%DBD) or (%AD)	SECOND MDD** (predict) (%DBD) or (%AD)	SECOND MDD*** (predict) (%DBD) or (%AD)	ORIGINAL MDD** (predict) (%DBD) or (%AD)	ORIGINAL MDD*** (predict) (%DBD) or (%AD)
CPA6	1	4,9	5,2	5,3	5,3	5,3	87,4	85,3	87,5	85,2	87,6
CPA6	2	5,3	5,3	5,4	5,4	5,4	86,9	84,7	87,0	84,6	87,0
CPA6	3	4,8	4,9	4,9	5,0	5,0	86,8	86,8	88,9	86,6	88,8
CPA6	4	5,7	5,3	5,4	5,4	5,4	86,8	84,7	87,3	84,4	87,1
CPA6	5	5,8	5,3	5,4	5,4	5,4	86,6	84,8	87,5	84,7	87,6
CPA6	6	5,1	5,1	5,2	5,1	5,1	86,1	85,9	88,1	85,8	88,2
CPA6	7	5,2	5,0	5,0	5,2	5,2	87,7	86,1	88,3	85,7	88,1
CPA7	1	4,4	5,2	5,2	5,3	5,3	88,1	88,8	88,8	88,4	88,4
CPA7	2	4,6	5,4	5,4	5,6	5,6	87,3	87,6	87,6	87,3	87,3
CPA7	3	4,5	5,3	5,3	5,4	5,4	87,7	88,6	88,6	88,5	88,5
CPA7	4	4,5	5,6	5,6	5,7	5,7	85,9	87,8	87,8	87,6	87,6
CPA7	5	4,9	5,5	5,5	5,5	5,5	86,9	88,2	88,2	88,0	88,0
CPA7	6	4,3	5,2	5,2	5,3	5,3	85,7	88,5	88,5	88,3	88,3
CPA7	7	4,6	5,4	5,4	5,4	5,4	87,4	88,1	88,1	88,0	88,0

** LL = 0,0% for CPA4, CPA5, CPA6, CPA8 and CPA9
*** LL = 0,5% for CPA4, CPA5, CPA6, CPA8 and CPA9

TABLE 8.5 (Continued)

Sample (code)	Grading (No.)	OMC (vib) (%)	SECOND OMC** (predict) (%)	SECOND OMC*** (predict) (%)	ORIGINAL OMC** (predict) (%)	ORIGINAL OMC*** (predict) (%)	MDD (vib) (%DBD) or (%AD)	SECOND MDD** (predict) (%DBD) or (%AD)	SECOND MDD*** (predict) (%DBD) or (%AD)	ORIGINAL MDD** (predict) (%DBD) or (%AD)	ORIGINAL MDD*** (predict) (%DBD) or (%AD)
CPA8	1	4,6	4,5	4,6	4,8	4,8	88,2	86,8	89,0	86,3	88,7
CPA8	2	5,2	4,8	4,9	5,0	5,0	86,7	85,5	88,1	85,0	87,7
CPA8	3	4,9	4,4	4,5	4,6	4,6	87,5	87,3	89,8	86,9	89,5
CPA8	4	5,6	4,8	4,9	4,9	4,9	85,9	86,0	88,8	85,7	88,7
CPA8	5	5,2	4,7	4,8	4,8	4,9	86,7	86,3	89,3	86,0	89,1
CPA8	6	5,2	4,5	4,6	4,7	4,7	86,7	87,1	89,4	86,8	89,2
CPA8	7	4,8	4,7	4,8	4,8	4,8	83,7	86,5	88,8	86,4	88,9
CPA9	1	4,5	5,0	5,1	5,5	5,5	89,2	85,1	87,6	84,2	86,8
CPA9	2	4,8	5,0	5,0	5,7	5,7	87,1	84,6	87,1	83,2	85,9
CPA9	3	4,0	4,7	4,7	5,2	5,2	89,0	86,5	88,7	85,5	87,9
CPA9	4	4,6	4,8	4,9	5,3	5,4	87,6	85,7	88,3	84,8	87,5
CPA9	5	4,7	5,2	5,3	5,5	5,5	87,4	84,7	87,5	84,2	87,2
CPA9	6	4,2	5,1	5,2	5,2	5,2	88,5	85,6	87,7	85,5	87,7
CPA9	7	4,3	4,9	4,9	5,4	5,4	88,2	85,4	87,8	84,3	86,9

** LL = 0,0% for CPA4, CPA5, CPA6, CPA8 and CPA9
*** LL = 0,5% for CPA4, CPA5, CPA6, CPA8 and CPA9

8.1.3 Comparison of models with special materials

As the earlier research on G2 materials had shown that the results compared favourably with the estimates of the models, it was decided also to test the models on two metalliferous materials with much higher solid densities than the usual roadbuilding materials. (The DBDs of the manganese ore and iron ore were 4,002 and 4,232 respectively in comparison with the average value of about 2,65 for most other roadbuilding materials.)

As these materials contained a large proportion of particles larger than 37,5 mm, these particles were broken down individually by means of a hammer until the particles would pass the 37,5 mm sieve. This material was then added to the rest of the material that passed the 37,5 mm sieve. The gradings, Atterberg limits and linear shrinkage of these materials were then determined and fed into the compactability model to estimate the densities and moisture regimes of these materials. These estimates were used to determine the sample sizes of the material that was compacted by means of the vibratory compaction table. The samples were once again compacted over a range of moisture contents so that the OMC could be determined.

The coarse quality of these materials (ie both contained a high percentage of large particles) gave density estimates of 93,73 % SD and 94,25 % SD for the manganese and iron ores respectively. The subsequent results obtained on the vibratory table were much lower, namely 83,99 % SD and 83,79 % SD for the manganese and iron ores respectively.

As these were the first laboratory results obtained that differed substantially from the estimates obtained from the compactability model, the reason for this deviation had to be established. The gradings of the materials showed that they were very coarse, and lying on lower side of the "ideal" grading curve (ie $100.(d/D)^{0,5}$ with D = 37,5 mm) (see Figures 8.5 and 8.6).

Because the only two data points for "coarse" gradings were supplied by the metalliferous ores, extra points were added by taking these ore samples as well as other coarse materials such as crushed stone and natural gravels and sieving out the finer fractions. Because these samples contained a very low amount of fines, the amount of water added to the samples was just enough to wet the entire surface of all aggregate particles thoroughly (ie shiny appearance). The samples were then compacted for three minutes using a frequency of 40 Hz and amplitude setting k equal to 36 %. This was done to limit breakdown of the aggregate during the compaction (ie high frequency - low amplitude combination).

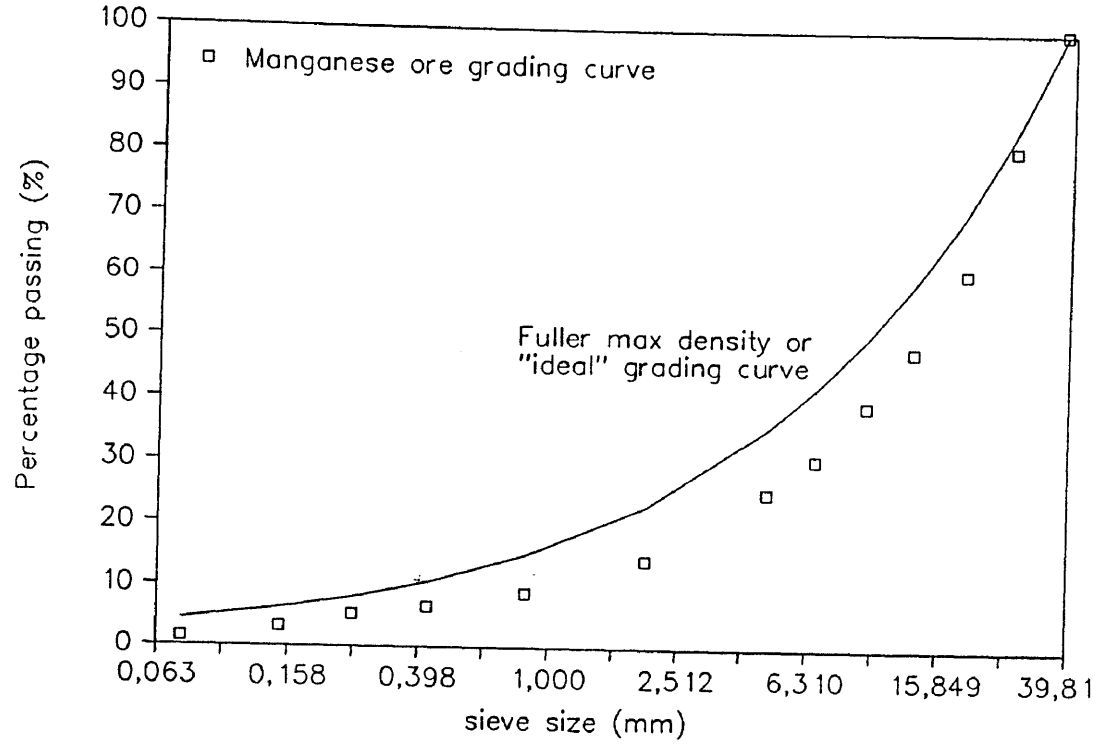

FIGURE 8.6 GRADING CURVES OF MANGANESE ORE SAMPLES

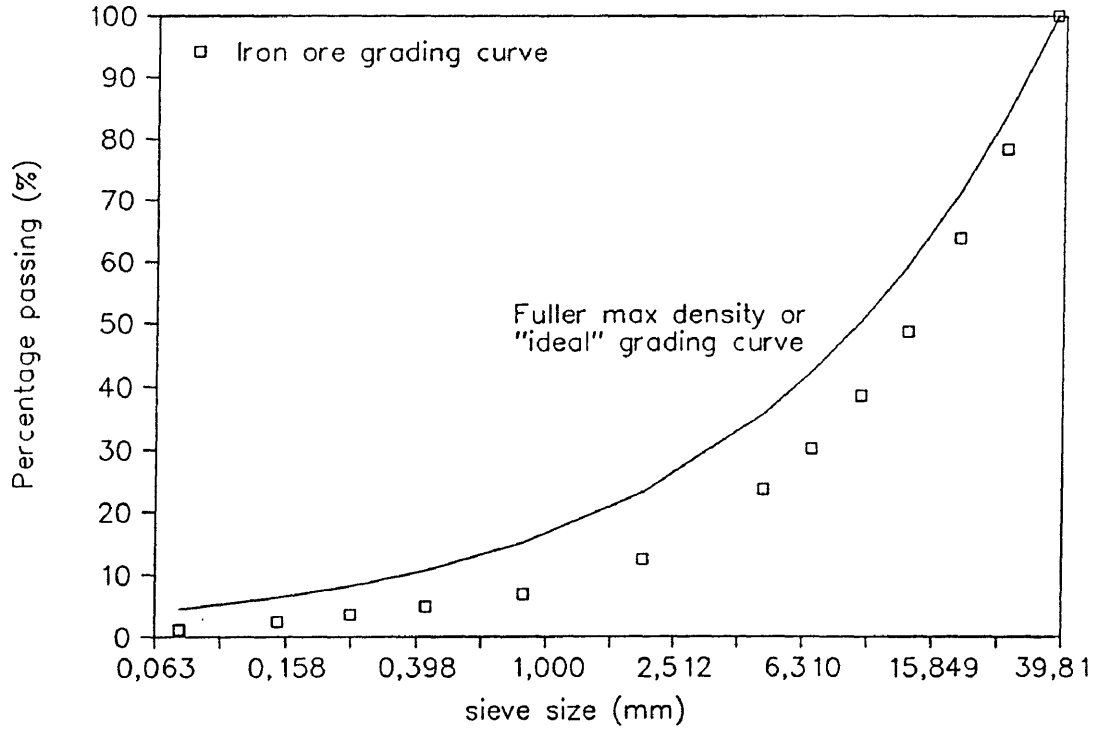

FIGURE 8.7 GRADING CURVES OF IRON ORE SAMPLES

Similarly samples of the metalliferous ores were prepared to be on the "fine" side of the "ideal" grading. This was done by removing some of the larger sieve size fractions (ie + 26,5 mm, + 19 mm and + 13,2 mm) from the samples. These samples were compacted at a moisture content of about 5 %. These samples were compacted for three minutes using a frequency of 30 Hz and amplitude setting k equal to 64 %. This was done to assess whether the compaction properties of metalliferous materials were the same as those of other untreated roadbuilding materials with gradings on the "fine" side of the "ideal" grading.

After compaction of these samples the samples were oven-dried and sieved to determine the gradings from which the grading factors were then determined. The results of all the MDDs (% SD) were then plotted against their respective grading factors. Note that the results of the metalliferous ores are marked differently, to discern them from the other untreated roadbuilding materials (see Figure 8.7). From Figure 8.7 it is clear that metalliferous ores react similar to other roadbuilding materials on both the "coarse" side and the "fine" side of the "ideal" grading.

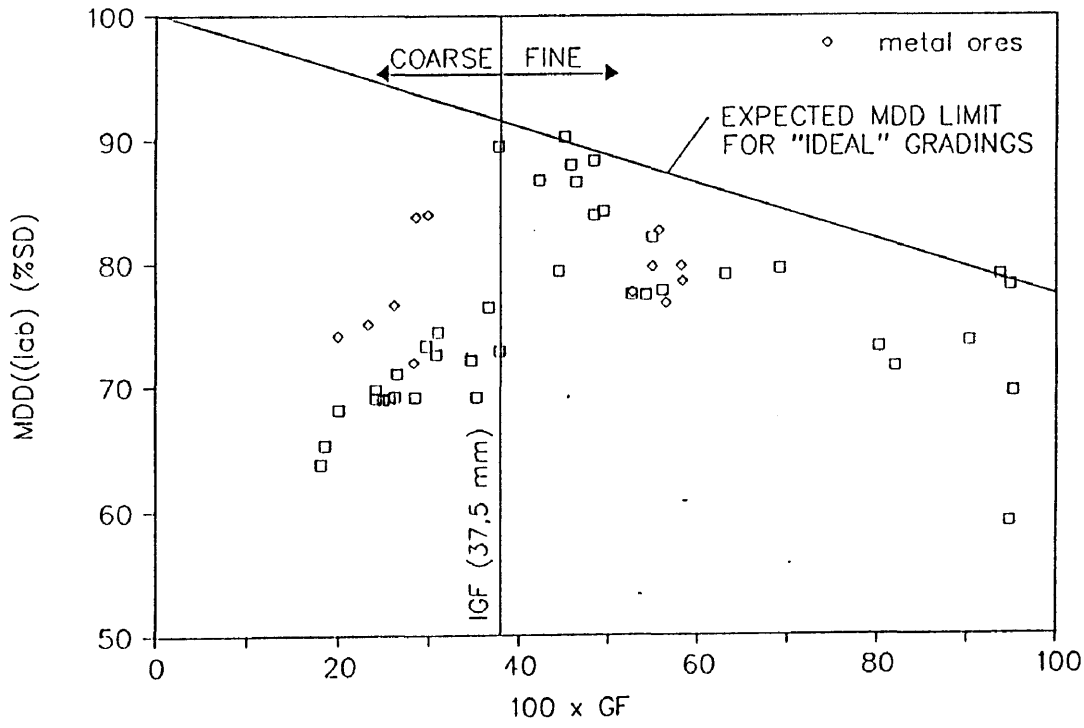

FIGURE 8.7 RELATION BETWEEN MDD (vlb) (% SD) AND GF FOR THE ORIGINAL MATERIALS AND METAL ORES IN BOTH THE "COARSE" AND "FINE" ZONES

Figure 8.7 also shows that there are two distinct zones on the graph; one where the compacted material is lacking fines ("coarse" zone) and one where the compacted material contains ample or too much fines ("fine" zone). The slope tendencies of the data points are also not the same and the two zones meet each other at a distinct point. The value of the GF where these two functions meet is approximately equal to 0,400 (ie 40/100). The value of GF for the Fuller curve or Talbot curve which has often been defined as the "ideal" grading (see Section 2.4) is equal to 0,379 (ie 37,9/100) for a maximum particle size D of 37,5 mm. This graph therefore confirms the findings of many other researchers that there is a distinct grading, the so-called "ideal" grading, which usually gives the maximum density. The steeper slope tendency of the data points of the "coarse" zone also emphasizes the negative influence that a lack of fines can have on the MDD that can be achieved. This last point therefore also supports the approach of ensuring that the amount of fines in the material is slightly higher than required and ridding the layer of the excess fines by means of the slushing process as is done for G1 crushed stone bases in South Africa.

Because of the two distinct zones the compactability models will have to be able to discern whether the material is on the "coarse" side of the ideal grading or on the "fine" side of the "ideal" grading. This can be done by comparing the GF of the actual grading with the ideal grading factor (IGF) of the "ideal" grading for the maximum particle size D of the particular grading. If the GF is smaller than the IGF the material is in the "coarse" zone, and if the GF is larger than the IGF the material is in the "fine" zone. In this investigation the maximum particle size D was equal to 37,5 mm. This is the reason why the curves peaked at the IGF for a maximum particle size of 37,5 mm (ie IGF = 37,9/100), Figure 8.7 also seems to indicate that for each maximum particle size there is an "ideal" grading which will yield the highest MDD for that particular maximum particle size D. This is most probably defined by the line shown in Figure 8.7, which is plotted through the highest MDD results against their respective grading factors. Note that the line passes through 100 % SD for GF equal to zero, that is when the material consist of a solid block. By determining the grading factors of the "ideal" gradings for different maximum particle sizes, it is possible to estimate the MDDs (% SD) that can be achieved (see Table 8.6 and Figure 8.8).

Figure 8.8 shows that the rise in density of the "ideal" grading is extremely rapid at the beginning which means that it should be possible to get reasonable densities and good support from most of the untreated roadbuilding materials, even the fine ones, if we can adjust the natural gradings to approach the "ideal" grading for the given maximum particle size D (see Figure 7.1 for the influence of the dry density on the CBR).

TABLE 8.6 Estimates of MDD for ideal grading for different maximum particle sizes D

D (mm)	MDD (%SD)
2,00	78,3
4,75	82,3
13,20	87,1
19,00	88,6
26,50	90,0
37,50	91,3
53,00	92,5
63,00	93,1
75,00	93,6
150,00	95,5
300,00	96,8

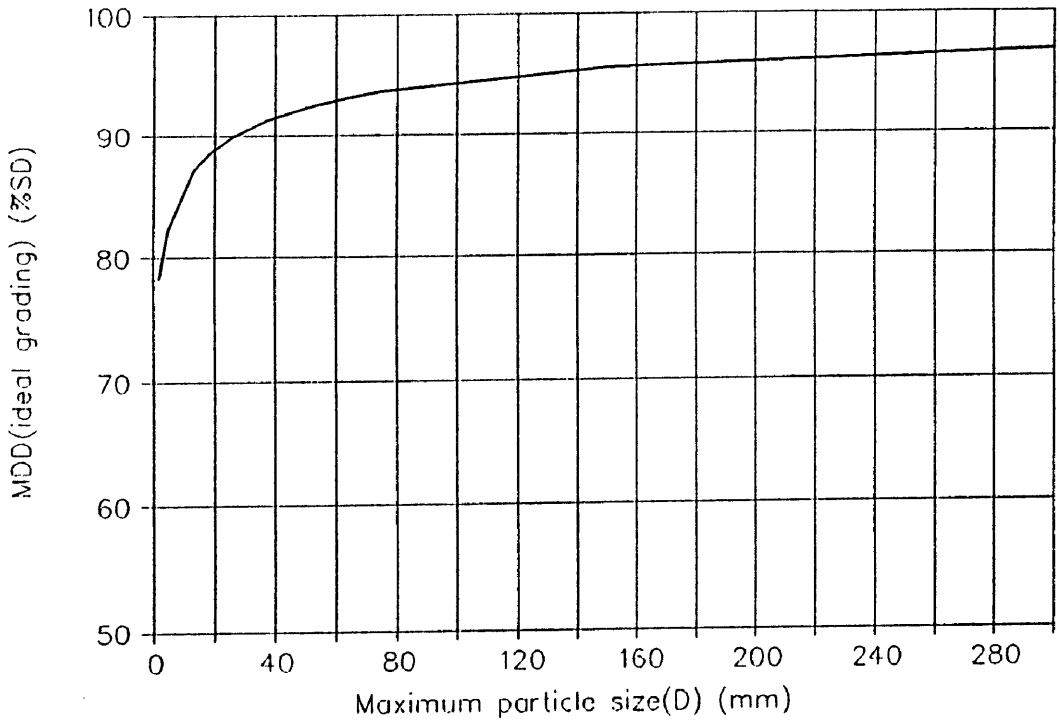

FIGURE 8.8 ESTIMATED MDDs OF IDEAL GRADING FOR DIFFERENT MAXIMUM PARTICLE SIZES

To determine whether these expectations were realistic, the "adjusted" grading for the montmorillonite clay material was fed into the compactability model. Although the amount of material passing the 0,425 mm sieve had substantially been "reduced' from 97 per cent to 29,9 per cent, the improvement in the MDD was only marginal (see Figure 8.9). As the grading factor itself had changed substantially this prediction was rather unexpected. The cause of this unexpected prediction turned out to be the input variable of the linear shrinkage which had not been adjusted even though the amount of material passing the 0,425 mm sieve had substantially been reduced. This input variable was therefore adjusted in a similar manner as the liquid limit so that its effect would be limited by the percentage passing the 0,425 mm sieve (ie the fraction on which LS and LL are determined). This revised model is:

$$X = k_1.(GF)^{0,85} + k_2.C + k_3.Q + k_4C^3 + k_5 \quad \ldots\ldots\ldots\ldots\ldots\ldots\ldots\ldots\ldots\ldots \quad (8.1)$$

where

	X	=	MDD (vib or mod. AASHTO), OMC (vib or mod. AASHTO), ZAVMC (vib or mod. AASHTO) or CMC
	GF	=	grading factor
	C	=	(percentage passing 0,425 mm sieve/100)(LL/100)^{0,1}
	Q	=	(percentage passing 0,425 mm sieve/100)(LS)
	k_n	=	regression coefficients

Although the correlation value was slightly lower for MDD (vib) (ie r^2 = 0,944) the correlation values for all the other properties improved. Apart from this the significance of the LL also improved. Only for the models of ZAVMC (vibratory and mod. AASHTO), and CMC and OMC (mod. AASHTO) did C^3 and C respectively not have a significant influence (see Table 8.7).

For these properties the regression analysis was repeated omitting these respective C-factors. To keep the same basic regression model these coefficients were set to zero (see Table 8.8).

Apart from this adjustment being theoretically more correct, it had the desired effect in that there was a substantial improvement in MDD when the grading was "adjusted" (see Figure 8.10). The gradings of some of the other original materials were also "adjusted" for their original maximum particle sizes. Figure 8.10 clearly shows that they tend towards the line of maximum dry density for ideal gradings which supports the experience in practice that the quality of many untreated roadbuilding materials can substantially be improved by means of mechanical stabilisation.

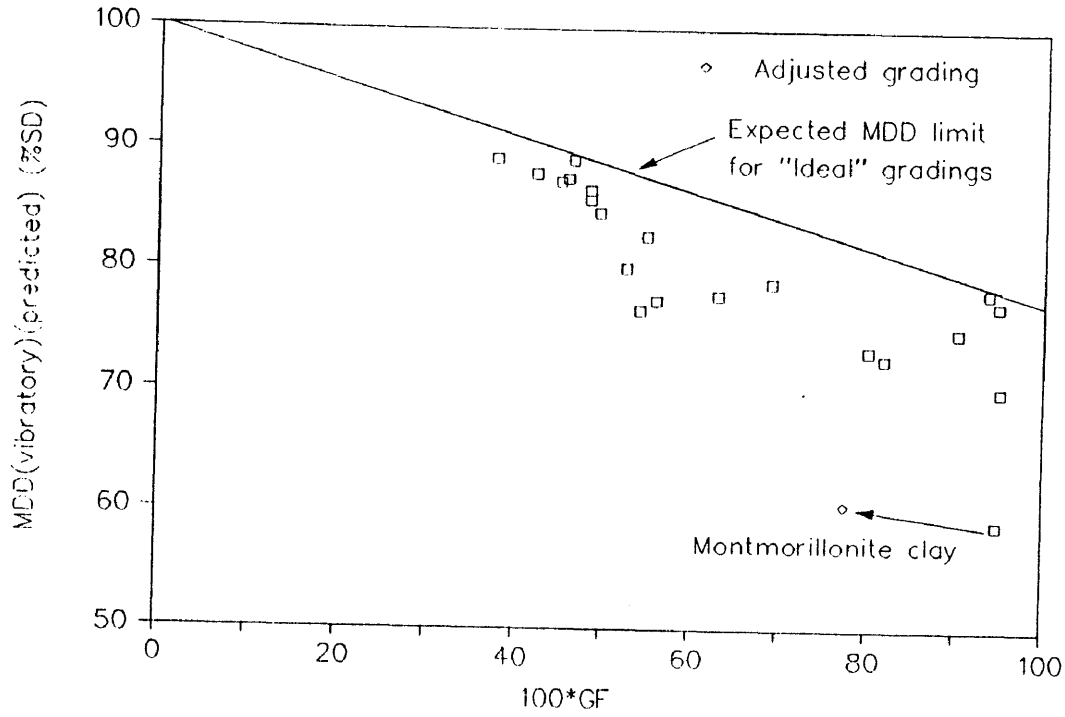

FIGURE 8.9 **PREDICTED CHANGE IN MDD FOR MONTMORILLONITE CLAY WITH ADJUSTED "IDEAL" GRADING USING THE ORIGINAL COMPACTABILITY MODEL**

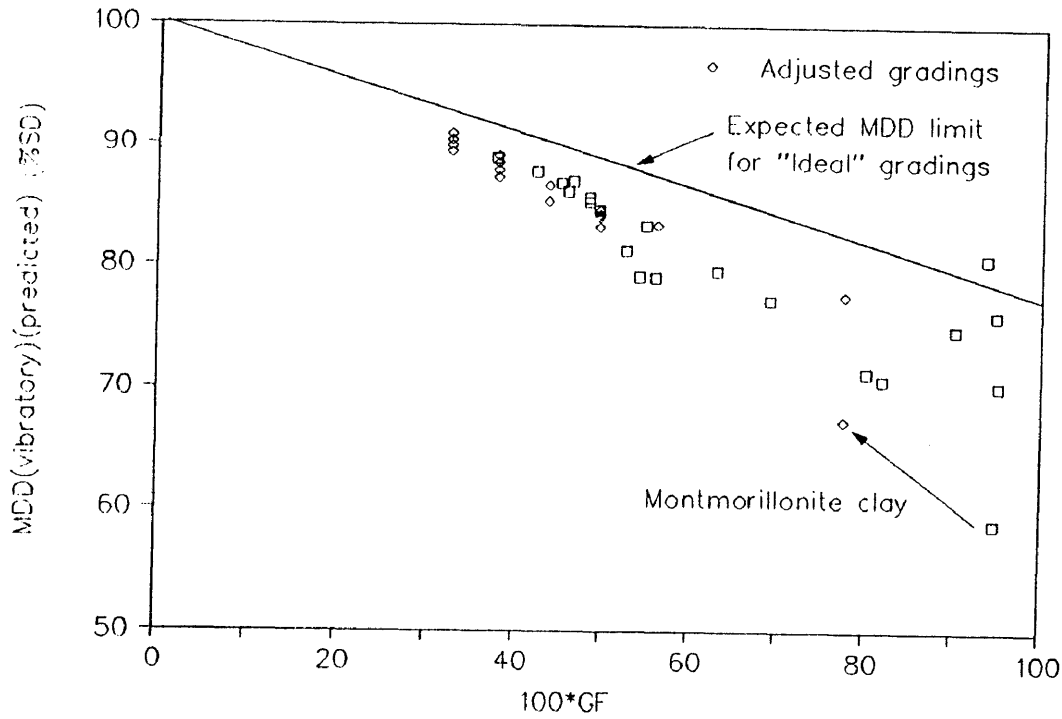

FIGURE 8.10 **PREDICTED CHANGE IN MDD FOR MONTMORILLONITE CLAY AND OTHER MATERIALS WITH ADJUSTED "IDEAL" GRADINGS USING THE FINAL REVISED COMPACTABILITY MODEL NOT INCORPORATING THE SBD AND SF**

Table 8.7 **The regression coefficients, their standard errors and t-values, as well as r^2-values and degrees of freedom for the final revised compactability model not incorporating the SBD and SF as input variables**

$$C = (\% < 0{,}425\ mm/100)(LL/100)^{0,1}$$
$$Q = (\% < 0{,}425\ mm/100)(LS)$$

		$GF^{0,85}$	C	Q	C^3	Constant	t (0,050)	Degrees of freedom	r^2
MDD (vib)	X Coefficient(s)	-35,7891	9,710725	-2,85420	21,80919	104,6374			
	Std Err of Coef.	3,991916	4,056554	0,365447	6,929769	2,030274			
	t-value	8,965394	2,393835	7,810164	3,147174	51,53856	2,120	16	0,944
OMC (vib)	X Coefficient(s)	21,02111	-9,01290	2,105612	-13,1290	-5,59777			
	Std Err of Coef.	1,950995	1,982586	0,178607	3,386831	0,992269			
	t-value	10,77455	4,546032	11,78905	3,876487	5,641381	2,120	16	0,967
ZAVMC (vib)	X Coefficient(s)	21,90103	-9,22285	1,786720	-7,21725	-5,27615			
	Std Err of Coef.	2,191676	2,227164	0,200641	3,804641	1,114678			
	t-value	9,992821	4,141072	8,905061	1,896959	4,733343	2,120	16	0,961
CMC	X Coefficient(s)	11,13116	0,956643	0,928960	-12,4122	-2,14114			
	Std Err of Coef.	1,360621	1,382653	0,124560	2,361971	0,692007			
	t-value	8,180940	0,691889	7,457899	5,255023	3,094109	2,120	16	0,941
MDD (mod. AASHTO)	X Coefficient(s)	-31,2779	11,30244	-2,38409	15,66226	97,66944			
	Std Err of Coef.	4,357959	4,370789	0,392794	7,614549	2,161286			
	t-value	7,177205	2,585904	6,069577	2,056885	45,19041	2,131	15	0,910

Table 8.7 **(continued)**

		$GF^{0,85}$	C	Q	C^3	Constant	t (0,050)	Degrees of freedom	r^2
OMC (mod. AASHTO)	X Coefficient(s)	6,254905	3,797868	1,114521	-10,0146	1,689648			
	Std Err of Coef.	2,049204	2,082385	0,187598	3,557317	1,042217			
	t-value	3,052358	1,823806	5,941004	2,815214	1,621204	2,120	16	0,923
ZAVMC (mod. AASHTO)	X Coefficient(s)	20,97874	-9,63847	1,579367	-5,98295	-2,49032			
	Std Err of Coef.	2,606649	2,614323	0,234944	4,554530	1,292741			
	t-value	8,048166	3,686794	6,722303	1,313627	1,926393	2,131	15	0,935
SOMC (vib)	X Coefficient(s)	20,83809	-9,31739	2,213815	-13,6690	-5,18985			
	Std Err of Coef.	1,910281	1,941213	0,174880	3,316153	0,971562			
	t-value	10,90838	4,799780	12,65904	4,121969	5,341764	2,120	16	0,970
SZAVMC (vib)	X Coefficient(s)	21,67648	-9,57535	1,890087	-7,57417	-4,80564			
	Std Err of Coef.	2,123593	2,157979	0,194408	3,686453	1,080052			
	t-value	10,20745	4,437187	9,722257	2,054597	4,449461	2,120	16	0,965
SCMC	X Coefficient(s)	10,96870	0,878710	0,993553	-12,9908	-1,81518			
	Std Err of Coef.	1,589328	1,615063	0,145498	2,758996	0,808326			
	t-value	6,901468	0,544071	6,828640	4,708542	2,245606	2,120	16	0,923
SOMC (mod. AASHTO)	X Coefficient(s)	5,968437	3,620265	1,199379	-10,5580	2,169750			
	Std Err of Coef.	2,292453	2,329573	0,209866	3,979585	1,165933			
	t-value	2,603515	1,554046	5,714954	2,653042	1,860955	2,120	16	0,910
SZAVMC (mod. AASHTO)	X Coefficient(s)	20,69599	-10,1263	1,681335	-6,28167	-1,87052			
	Std Err of Coef.	2,532798	2,540254	0,228287	4,425492	1,256115			
	t-value	8,171196	3,986349	7,364979	1,419430	1,489131	2,131	15	0,940

Table 8.8 **The corrected regression coefficients, their standard errors and t-values, as well as r^2-values and degrees of freedom for the final revised models not incorporating the SBD and SF as input variables with some insignificant factors**

$$C = (\% < 0{,}425\ mm/100)(LL/100)^{0,1}$$
$$Q = (\% < 0{,}425\ mm/100)(LS)$$

		$(GF)^{0,85}$	C	Q	C^3	Constant	t (0,050)	Degrees of freedom	r^2
MDD (vib)	X Coefficient(s)	-35,7891	9,710725	-2,85420	21,80919	104,6374			
	Std Err of Coef.	3,991916	4,056554	0,365447	6,929769	2,030274			
	t-value	8,965394	2,393835	7,810164	3,147174	51,53856	2,120	16	0,944
OMC (vib)	X Coefficient(s)	21,02111	-9,01290	2,105612	-13,1290	-5,59777			
	Std Err of Coef.	1,950995	1,982586	0,178607	3,386831	0,992269			
	t-value	10,77455	4,546032	11,78905	3,876487	5,641381	2,120	16	0,967
ZAVMC (vib)	X Coefficient(s)	20,90554	-10,7386	1,515342	0,00000	-4,34233			
	Std Err of Coef.	2,284767	2,232106	0,151049	0,00000	1,196840			
	t-value	9,149964	4,811008	10,03211	0,00000	3,628164	2,110	17	0,952
CMC	X Coefficient(s)	11,62205	0,00000	0,947743	-11,8258	-2,28897			
	Std Err of Coef.	1,143055	0,00000	0,119687	2,170641	0,681314			
	t-value	10,16753	0,00000	7,918465	5,448100	3,359640	2,110	17	0,939
MDD (mod. AASHTO)	X Coefficient(s)	-28,7578	14,73411	-1,80369	0,00000	95,31451			
	Std Err of Coef.	4,585016	4,428967	0,299568	0,00000	2,369468			
	t-value	6,272126	3,326761	6,020974	0,00000	40,22612	2,120	16	0,885

Table 8.8 **(Continued)**

		$(GF)^{0,85}$	C	Q	C^3	Constant	t (0,050)	Degrees of freedom	r^2
OMC (mod. AASHTO)	X Coefficient(s)	8,203742	0,00000	1,189091	-7,68682	1,102778			
	Std Err of Coef.	1,864351	0,00000	0,195213	3,540367	1,111240			
	t-value	4,400319	0,00000	6,091229	2,171194	0,992385	2,110	17	0,908
ZAVMC (mod. AASHTO)	X Coefficient(s)	20,01604	-10,9493	1,357654	0,00000	-1,59074			
	Std Err of Coef.	2,557601	2,470555	0,167104	0,00000	1,321730			
	t-value	7,826100	4,431945	8,124576	0,00000	1,203535	2,120	16	0,927
SOMC (vib)	X Coefficient(s)	20,83809	-9,31739	2,213815	-13,6690	-5,18985			
	Std Err of Coef.	1,910281	1,941213	0,174880	3,316153	0,971562			
	t-value	10,90838	4,799780	12,65904	4,121969	5,341764	2,120	16	0,970
SZAVMC (vib)	X Coefficient(s)	20,63176	-11,1661	1,605288	0,00000	-3,82564			
	Std Err of Coef.	2,248699	2,196869	0,148664	0,00000	1,177946			
	t-value	9,174976	5,082757	10,79804	0,00000	3,247722	2,110	17	0,955
SCMC	X Coefficient(s)	11,41960	0,00000	1,010806	-12,4522	-1,95096			
	Std Err of Coef.	1,327770	0,00000	0,139028	2,521410	0,791413			
	t-value	8,600587	0,00000	7,270474	4,938614	2,465170	2,110	17	0,921
SOMC (mod. AASHTO)	X Coefficient(s)	7,826139	0,00000	1,270461	-8,33907	1,610325			
	Std Err of Coef.	2,035895	0,00000	0,213175	3,866127	1,213489			
	t-value	3,844076	0,00000	5,959689	2,156959	1,327020	2,110	17	0,896
SZAVMC (mod. AASHTO)	X Coefficient(s)	19,68522	-11,5026	1,448553	0,00000	-0,92602			
	Std Err of Coef.	2,506530	2,421222	0,163767	0,00000	1,295337			
	t-value	7,853574	4,750777	8,845164	0,00000	0,714892	2,120	16	0,932

Because the influences of LL (the C-factors) had substantially improved in this revised model, it was decided to re-evaluate the effect of the SBD and SF as well. The revised model incorporating the SBD and SF is:

$$X = k_1.(GF)^{0,85} + k_2.C + k_3.Q + k_4C^3 + k_5.SBD + k_6.SF + k_7 \quad \ldots\ldots\ldots\ldots\ldots\ldots \quad (8.2)$$

where

	X	=	MDD (vib or mod. AASHTO), OMC (vib or mod. AASHTO), ZAVMC (vib or mod. AASHTO) or CMC
	GF	=	grading factor
	C	=	(percentage passing 0,425 mm sieve/100)(LL/100)^{0,1}
	Q	=	(percentage passing 0,425 mm sieve/100)(LS)
	SBD	=	shakedown bulk density
	SF	=	shape factor
	k_n	=	regression coefficients

This time it was found that the SBD and SF had a significant effect on the compactability results. The overall correlations of the model also improved (see Table 8.9). It should be noted, however, that influence of the SBD and SF is generally less significant than the influence of the other factors (ie generally smaller t-values).

The regression analysis of models in which certain factors had been found to have a insignificant effect was repeated with the omission of these factors to determine the regression coefficients of the remaining factors. To keep the basic regression model the same for all of the prediction models, the value of the regression coefficients for the insignificant factors were all set to zero (see Table 8.10). Note that with the omission of certain factors the significance of other factors may change. For instance GF becomes significant in the models of OMC (mod. AASHTO) and SOMC (mod. AASHTO) whereas C becomes insignificant in the model of OMC (mod. AASHTO) when SBD and SF are omitted.

The effect of the adjusted gradings using the model incorporating the SBD and SF is shown in Figure 8.11. Figures 8.10 and 8.11 also clearly show that the MDDs of the "adjusted" gradings tend towards the line of maximum dry density for ideal gradings. It is therefore possible to predict the effect of grading adjustments on compactability properties without having to perform actual laboratory experiments. One should therefore be able to determine the mix ratio which will give the highest MDD as well as the moisture regime in the case of mechanical stabilization from the indicator tests of the separate materials without having to perform a vast number of tests.

Table 8.9 **The regression coefficients, their standard errors and t-values, as well as r^2-values and degrees of freedom for the final revised compactability models incorporating the SBD and SF as input variables**

$$C = (\% < 0{,}425/100)(LL/100)^{0,1}$$
$$Q = (\% < 0{,}425/100)(LS)$$

		$GF^{0,85}$	C	Q	C^3	SBD	SF	Constant	t (0,050)	Degrees of freedom	r^2
MDD (vib)	X Coefficient(s)	-32,9593	3,672499	-2,83461	26,65833	0,311038	0,269246	79,42664			
	Std Err of Coef.	4,508662	3,723360	0,406008	6,762449	0,108641	0,115392	1,582250			
	t-value	7,310233	0,986340	6,981661	3,942112	2,862984	2,333307	50,19854	2,145	14	0,970
OMC (vib)	X Coefficient(s)	20,04174	-6,86438	2,100869	-14,8777	-0,10981	-0,09613	3,298296			
	Std Err of Coef.	2,623528	2,166572	0,236250	3,934976	0,063216	0,067145	0,920689			
	t-value	7,63923	3,168315	8,892541	3,780897	1,737170	1,431748	3,582419	2,145	14	0,975
ZAVMC (vib)	X Coefficient(s)	22,33133	-5,52523	1,949901	-12,0201	-0,12322	-0,19100	4,308471			
	Std Err of Coef.	2,492005	2,057957	0,224406	3,737708	0,060047	0,063779	0,874533			
	t-value	8,961190	2,684814	8,689130	3,215920	2,052047	2,994759	4,926594	2,145	14	0,979
CMC	X Coefficient(s)	8,384639	0,343762	0,685267	-9,34864	-0,06274	0,063968	3,509512			
	Std Err of Coef.	1,844158	1,522949	0,166067	2,766014	0,044437	0,047198	0,647180			
	t-value	4,546594	0,225721	4,126433	3,379825	1,411984	1,355316	5,422770	2,145	14	0,955
MDD (mod. AASHTO)	X Coefficient(s)	-29,6133	4,272988	-2,49808	22,66247	0,310915	0,337765	72,70601			
	Std Err of Coef.	4,515234	3,725279	0,404557	6,814623	0,108158	0,115157	1,574897			
	t-value	6,558546	1,147024	6,174870	3,325565	2,874619	2,933079	46,16556	2,16	13	0,959
OMC (mod. AASHTO)	X Coefficient(s)	5,532757	5,884612	1,128464	-11,9072	-0,09953	-0,09613	9,710062			
	Std Err of Coef.	2,840553	2,345796	0,255793	4,260487	0,068446	0,072699	0,996851			
	t-value	1,947774	2,508577	4,411616	2,794800	1,454272	1,322393	9,740734	2,145	14	0,939

Table 8.9 **(Continued)**

		$GF^{0,85}$	C	Q	C^3	SBD	SF	Constant	t (0,050)	Degrees of freedom	r^2
ZAVMC (mod. AASHTO)	X Coefficient(s)	21,21706	-5,82085	1,830919	-10,2244	-0,12290	-0,29063	8,460725			
	Std Err of Coef.	4,028769	3,327053	0,362793	6,04266900	0,097077	0,103110	1,413838			
	t-value	5,266387	1,749551	5,046723	1,692042	1,266090	2,818698	5,984222	2,145	14	0,927
SOMC (vib)	X Coefficient(s)	18,44797	-7,62189	2,079103	-13,6783	-0,13694	-0,05633	6,206848			
	Std Err of Coef.	2,504037	2,067893	0,225490	3,755754	0,060337	0,064087	0,878756			
	t-value	7,367292	3,685827	9,220360	3,641964	2,269577	0,878997	7,063220	2,145	14	0,978
SZAVMC (vib)	X Coefficient(s)	20,61340	-6,34231	1,916205	-10,5536	-0,15248	-0,14962	7,469653			
	Std Err of Coef.	2,457144	2,029168	0,221267	3,685420	0,059207	0,062886	0,862299			
	t-value	8,389172	3,125575	8,660124	2,863634	2,575432	2,379216	8,662482	2,145	14	0,980
SCMC	X Coefficient(s)	7,174404	-0,10444	0,652158	-8,59475	-0,08163	0,095229	5,594437			
	Std Err of Coef.	2,009158	1,659210	0,180926	3,013495	0,048412	0,051421	0,705085			
	t-value	3,570850	0,062949	3,604553	2,852089	1,686316	1,851950	7,934413	2,145	14	0,949
SOMC (mod. AASHTO)	X Coefficient(s)	3,963340	5,260442	1,093926	-10,8271	-0,12292	-0,05820	12,36374			
	Std Err of Coef.	3,246712	2,681212	0,292368	4,869677	0,078233	0,083094	1,139387			
	t-value	1,220724	1,961964	3,741597	2,223388	1,571296	0,700435	10,85122	2,145	14	0,925
SZAVMC (mod. AASHTO)	X Coefficient(s)	20,48837	-5,84459	1,816526	-11,2265	-0,16426	-0,21591	11,15540			
	Std Err of Coef.	2,586120	2,133670	0,231711	3,903105	0,061948	0,065956	0,902029			
	t-value	7,922437	2,739223	7,839589	2,876309	2,651667	3,273623	12,36701	2,16	13	0,973

Table 8.10 **The corrected regression coefficients, their standard errors and t-values, as well as r^2-values and degrees of freedom for the final revised compactability models (incorporating the SBD and SF) with some insignificant factors**

$$C = (\% < 0{,}425\ mm/100)(LL/100)^{0,1}$$
$$Q = (\% < 0{,}425\ mm/100)(LS)$$

		$(GF)^{0,85}$	C	Q	C^3	SBD	SF	Constant	t (0,050)	Degrees of freedom	r^2
MDD (vib)	X Coefficient(s)	-32,0356	0,00000	-2,85341	29,87983	0,335383	0,326000	77,21464			
	Std Err of Coef.	4,406325	0,00000	0,405193	5,916065	0,105704	0,099932	1,580818			
	t-value	7,270366	0,00000	7,042096	5,050625	3,172846	3,262224	48,84472	2,131	15	0,968
OMC (vib)	X Coefficient(s)	21,02111	-9,01290	2,105612	-13,1290	0,00000	0,00000	-5,59777			
	Std Err of Coef.	1,950995	1,982586	0,178607	3,386831	0,00000	0,00000	0,992269			
	t-value	10,77455	4,546032	11,78905	3,876487	0,00000	0,00000	5,641381	2,120	16	0,967
ZAVMC (vib)	X Coefficient(s)	25,15475	-6,48469	2,145249	-13,2616	0,00000	-0,17689	-6,12109			
	Std Err of Coef.	2,289339	2,208249	0,223910	4,064062	0,00000	0,069864	0,963599			
	t-value	8,961190	2,684814	8,689130	3,215920	0,00000	2,994759	4,926594	2,131	15	0,972
CMC	X Coefficient(s)	11,62205	0,00000	0,947743	-11,8258	0,00000	0,00000	-2,28897			
	Std Err of Coef.	1,143055	0,00000	0,119687	2,170641	0,00000	0,00000	0,681314			
	t-value	10,16753	0,00000	7,918465	5,448100	0,00000	0,00000	3,359640	2,110	17	0,939
MDD (mod. AASHTO)	X Coefficient(s)	-28,6075	0,00000	-2,52192	26,49597	0,339207	0,402152	70,20786			
	Std Err of Coef.	4,478923	0,00000	0,408552	6,005377	0,106489	0,101677	1,592553			
	t-value	6,387151	0,00000	6,172819	4,412041	3,185362	3,955184	44,08509	2,145	14	0,955
OMC (mod. AASHTO)	X Coefficient(s)	8,203742	0,00000	1,189091	-7,68682	0,00000	0,00000	1,102778			
	Std Err of Coef.	1,864351	0,00000	0,195213	3,540367	0,00000	0,00000	1,111240			
	t-value	4,400319	0,00000	6,091229	2,171194	0,00000	0,00000	0,992385	2,110	17	0,908

Table 8.10 **(Continued)**

		$(GF)^{0,85}$	C	Q	C^3	SBD	SF	Constant	t (0,050)	Degrees of freedom	r^2
ZAVMC (mod. AASHTO)	X Coefficient(s)	20,01604	-10,9493	1,357654	0,00000	0,00000	0,00000	-1,59074			
	Std Err of Coef.	2,557601	2,470555	0,167104	0,00000	0,00000	0,00000	1,321730			
	t-value	7,826100	4,431945	8,124576	0,00000	0,00000	0,00000	1,203535	2,120	16	0,927
SOMC (vib)	X Coefficient(s)	17,55489	-8,52828	1,975320	-11,8334	-0,13122	0,00000	5,988729			
	Std Err of Coef.	2,271232	1,778820	0,190646	3,090862	0,059529	0,00000	0,872070			
	t-value	7,729235	4,794348	10,36115	3,828519	2,204318	0,00000	6,867252	2,131	15	0,977
SZAVMC (vib)	X Coefficient(s)	20,61340	-6,34231	1,916205	-10,5536	-0,15248	-0,14962	7,469653			
	Std Err of Coef.	2,457144	2,029168	0,221267	3,685420	0,059207	0,062886	0,862299			
	t-value	8,389172	3,125575	8,660124	2,863634	2,575432	2,379216	8,662482	2,145	14	0,980
SCMC	X Coefficient(s)	11,41960	0,00000	1,010806	-12,4522	0,00000	0,00000	-1,95096			
	Std Err of Coef.	1,327770	0,00000	0,139028	2,521410	0,00000	0,00000	0,791413			
	t-value	8,600587	0,00000	7,270474	4,938614	0,00000	0,00000	2,465170	2,110	17	0,921
SOMC (mod. AASHTO)	X Coefficient(s)	7,826139	0,00000	1,270461	-8,33907	0,00000	0,00000	1,610325			
	Std Err of Coef.	2,035895	0,00000	0,213175	3,866127	0,00000	0,00000	1,213489			
	t-value	3,844076	0,00000	5,959689	2,156959	0,00000	0,00000	1,327020	2,110	17	0,896
SZAVMC (mod. AASHTO)	X Coefficient(s)	20,48837	-5,84459	1,816526	-11,2265	-0,16426	-0,21591	11,15540			
	Std Err of Coef.	2,586120	2,133670	0,231711	3,903105	0,061948	0,065956	0,902029			
	t-value	7,922437	2,739223	7,839589	2,876309	2,651667	3,273623	12,36701	2,160	13	0,973

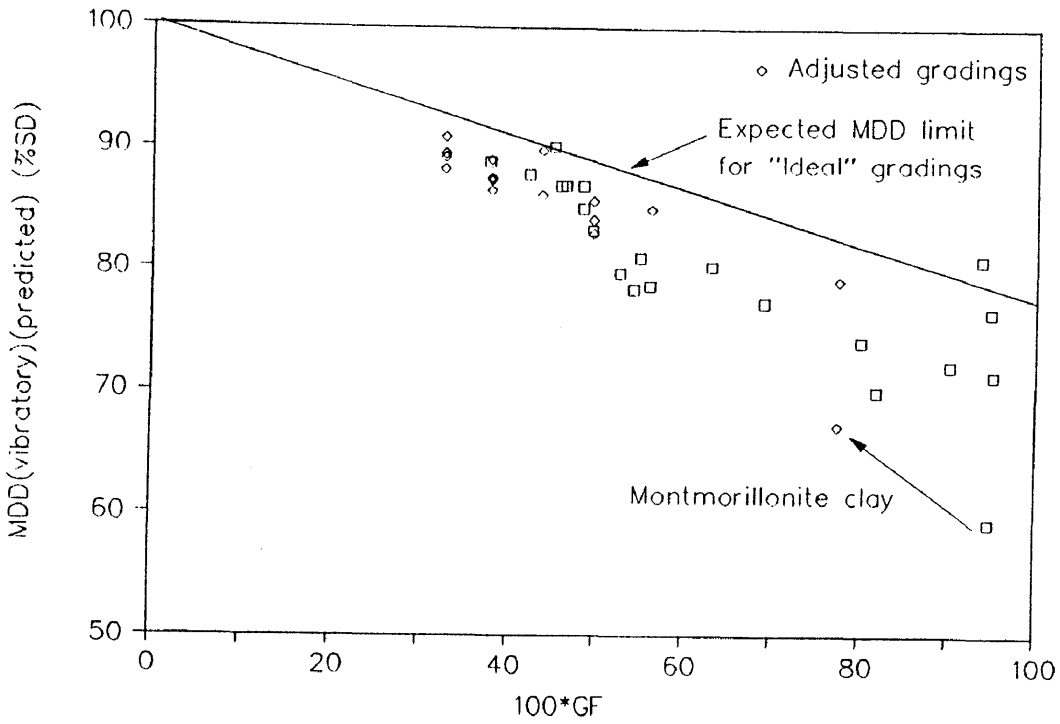

FIGURE 8.11 PREDICTED CHANGE IN MDD FOR MONTMORILLONITE CLAY AND OTHER MATERIALS WITH ADJUSTED "IDEAL" GRADINGS USING THE FINAL REVISED COMPACTABILITY MODEL INCORPORATING THE SBD AND SF

Note that in both Figures 8.10 and 8.11 the adjusted gradings are grouped together below one another. This is because they all have the same "ideal" grading and grading factor GF. The differences in MDD are therefore due to differences in LL and LS. The higher LL and LS the lower the MDD, confirming that the fines in crushed stone base should have a low plasticity. The highest MDDs are achieved for slightly plastic material (ie LL of 5 to 10).

Because of the different models on the "coarse" side a compatibility model for the material on the "coarse" side of the "ideal" grading (ie GF < 37,9/100) was developed. The revised compactability model was used to determine the regression coefficients (see Table 8.11). From Table 8.11 it is clear that the variability is seemingly greater on the "coarse" side of the ideal grading (ie lower r^2-values throughout) and the slope tendency of the data points is also steeper. The fines also have less of an influence as reflected by the low t-value for the regression coefficients of LS. It seems to indicate that one should rather be slightly on the fine side of the IGF than too coarse. Predicted values are plotted against the measured values for MDD (vib) (% SD), OMC (vib) (%) and ZAVMC (vib) (%) (see Figures 8.12 to 8.14). The MDD

TABLE 8.11 **Listing of regression coefficients, their standard errors and t-values, and r^2-values for MDD, OMC and ZAVMC of coarse graded materials**

$C = (\% < 0{,}425\ mm/100)\ (LL/100)^{0,1}$
$Q = (\% < 0{,}425\ mm/100)\ (LS)$

		$GF^{0,85}$	C	Q	C^3	Constant	$t_{(0,050)}$	Degrees of freedom	r^2
MDD (vib)	X Coefficient(s)	73,15136	-148,543	-15,6043	11548,19	52,59602			
	Std Err of Coef.	15,17935	39,83570	15,20867	6256,890	3,714490			
	t-value	4,819136	3,728904	1,026016	1,845676	14,15968	2,086	20	0,680
OMC (vib)	X Coefficient(s)	10,55197	-21,0084	4,464320	560,9068	-1,01611			
	Std Err of Coef.	3,152030	8,271983	3,158120	1299,259	0,771323			
	t-value	3,347673	2,539707	1,413600	0,431712	1,317362	2,086	20	0,828
ZAVMC (vib)	X Coefficient(s)	-44,6293	156,0310	12,15292	-11278,4	23,81786			
	Std Err of Coef.	11,46010	30,07514	11,48224	4723,825	2,804364			
	t-value	4,036612	3,676478	1,579808	4,010296	8,715475	2,086	20	0,708

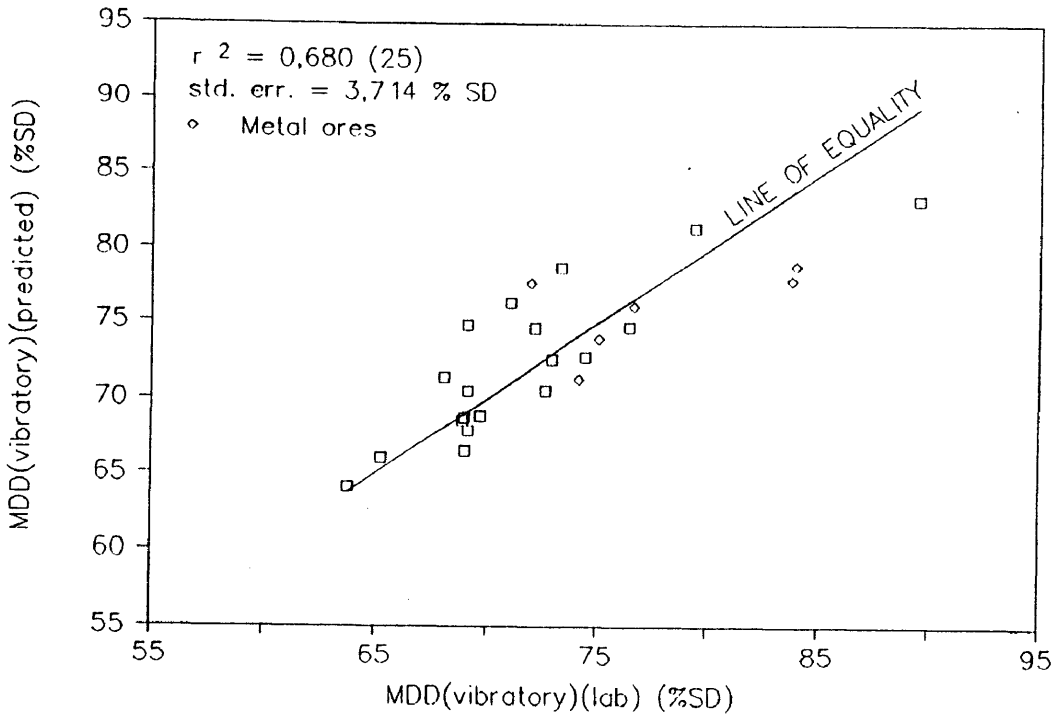

FIGURE 8.12 RELATION BETWEEN MDD (VIB) (PREDICTED) (% SD) AND MDD (VIB) (MEASURED) (% SD) FOR SOME OF THE ORIGINAL MATERIALS AND THE METAL ORES ON THE "COARSE" SIDE OF IGF

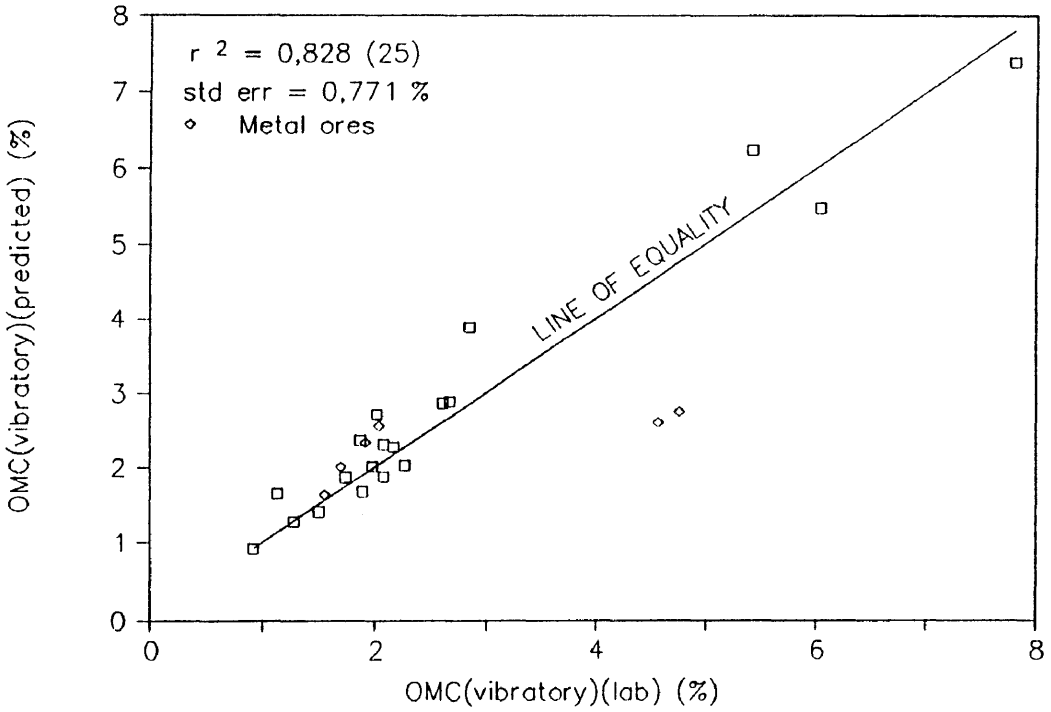

FIGURE 8.13 RELATION BETWEEN OMC (VIB) (PREDICTED) (%) AND OMC (VIB) (MEASURED) (%) FOR SOME OF THE ORIGINAL MATERIALS AND THE METAL ORES ON THE "COARSE" SIDE OF IGF

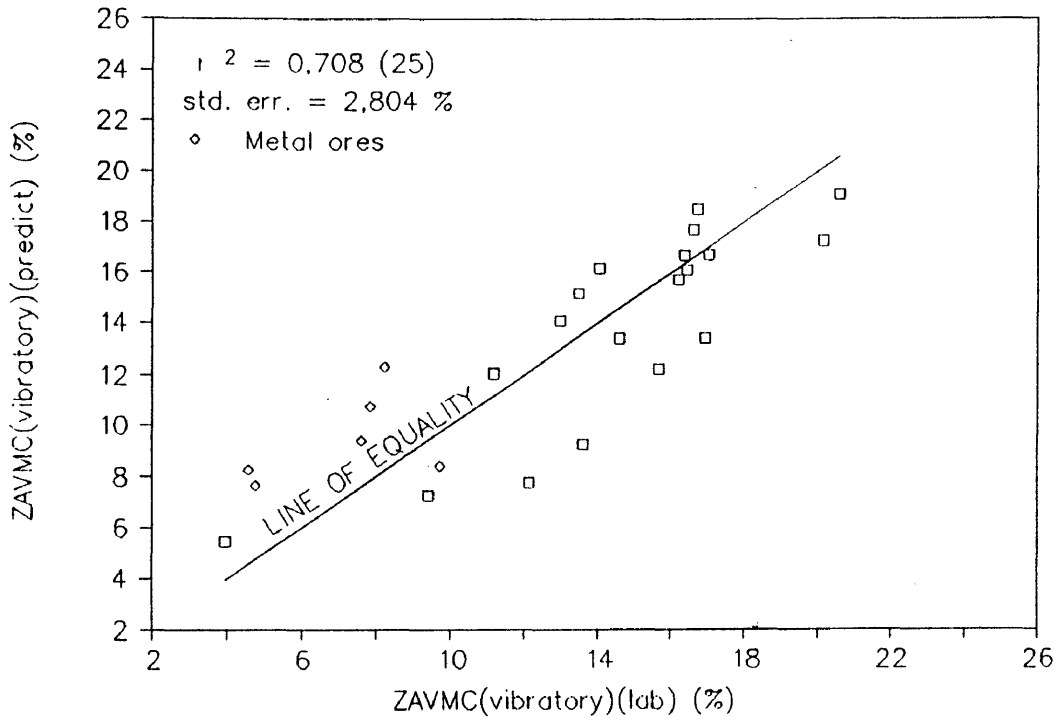

FIGURE 8.14 RELATION BETWEEN ZAVMC (VIB) (PREDICTED) (%) AND ZAVMC (VIB) (MEASURED) (%) FOR SOME OF THE ORIGINAL MATERIALS AND THE METAL ORES ON THE "COARSE" SIDE OF IGF

(mod. AASHTO), OMC (mod. AASHTO), ZAVMC (mod. AASHTO) and CMC were not investigated as time and funds did not allow for this. As far as the OMCs are concerned it is felt that the amount of water that can be held in suspension by the coarse material when thoroughly wetted (ie shiny surface) is most probably the best indication of the OMC. Any excess moisture which cannot be held in suspension by the surface tension will drain away and should therefore not really be considered as part of the OMC. It should be noted that the measured OMC at MDD is lower than this value for coarse materials as the excess water is lost during the compaction phase (ie the appearance of material at OMC is dark and dull and not shiny anymore).

Similarly the predicted values of MDD (vib), OMC (vib), ZAVMC (vib), SOMC (vib) and SZAVMC (vib) of the "fine" metalliferous ore gradings are plotted together with those of the other materials (ie original and G2 (grading 1)) to see whether the compatibility models on the "fine" side of the "ideal" grading are also applicable to them (see figures 8.15 to 8.19). Figures 8.15 to 8.19 indicate that the metalliferous ores react similarly to other untreated roadbuilding materials on the "fine" side.

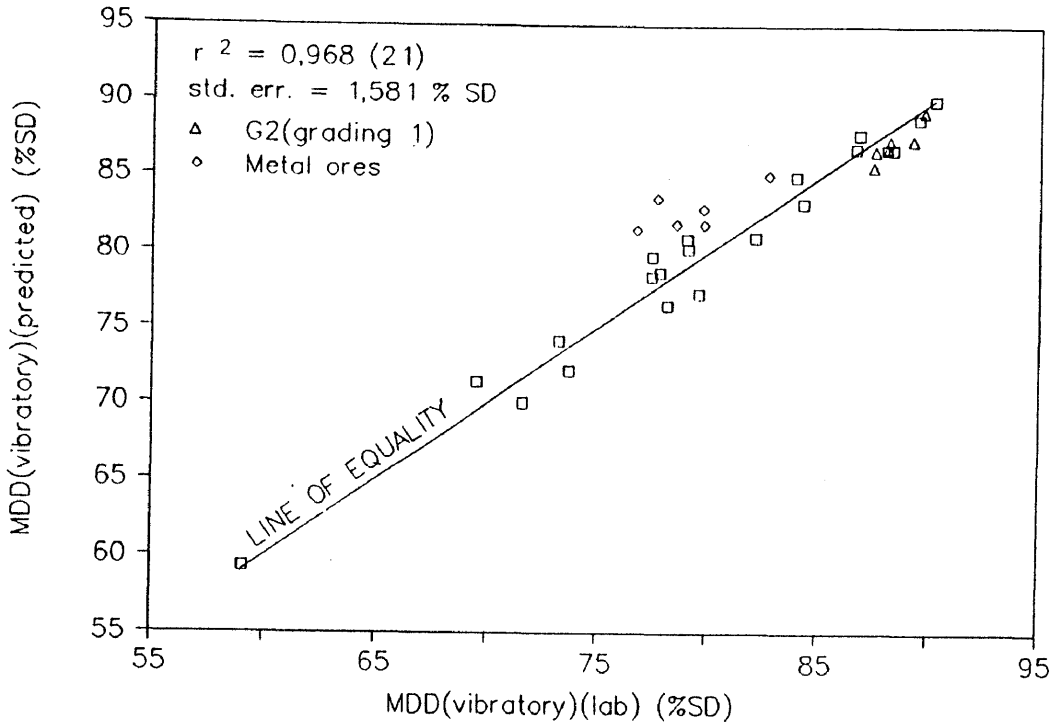

FIGURE 8.15 RELATION BETWEEN MDD (VIB) (PREDICTED) (% SD) AND MDD (VIB) (MEASURED) (% SD) FOR THE ORIGINAL MATERIALS, METAL ORES AND G2 MATERIALS (GRADING 1) ON THE "FINE SIDE OF IGF

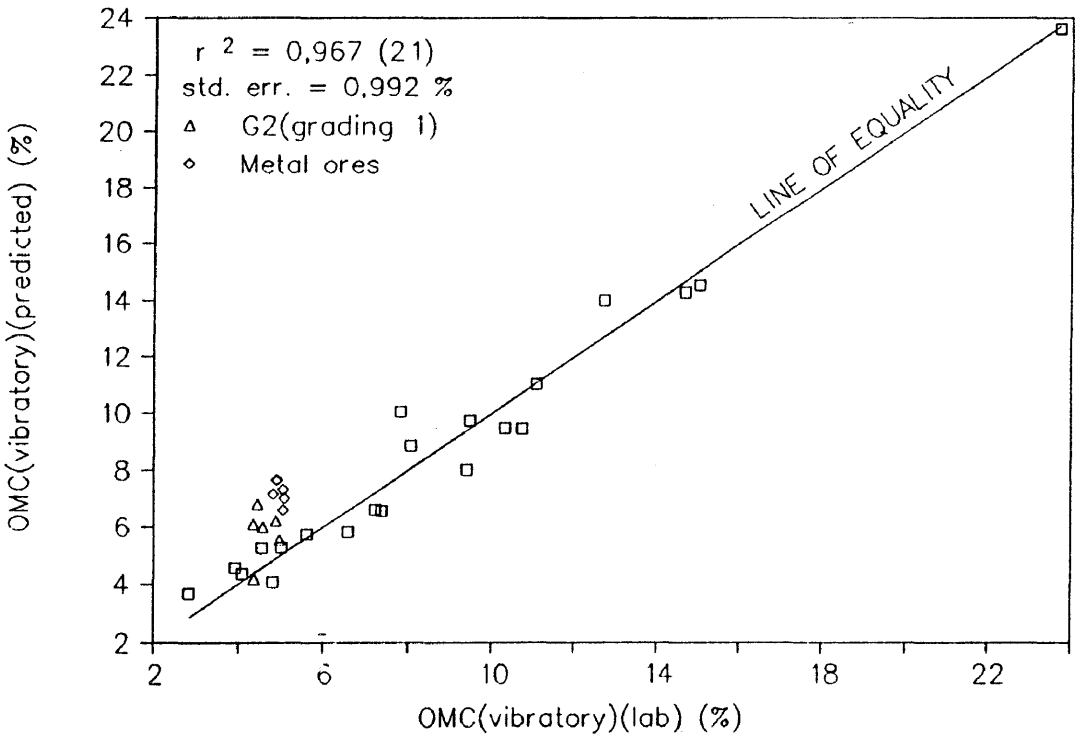

FIGURE 8.16 RELATION BETWEEN OMC (VIB) (PREDICTED) (%) AND OMC (VIB) (MEASURED) (%) FOR THE ORIGINAL MATERIALS, METAL ORES AND G2 MATERIALS (GRADING 1) ON THE "FINE" SIDE OF IGF

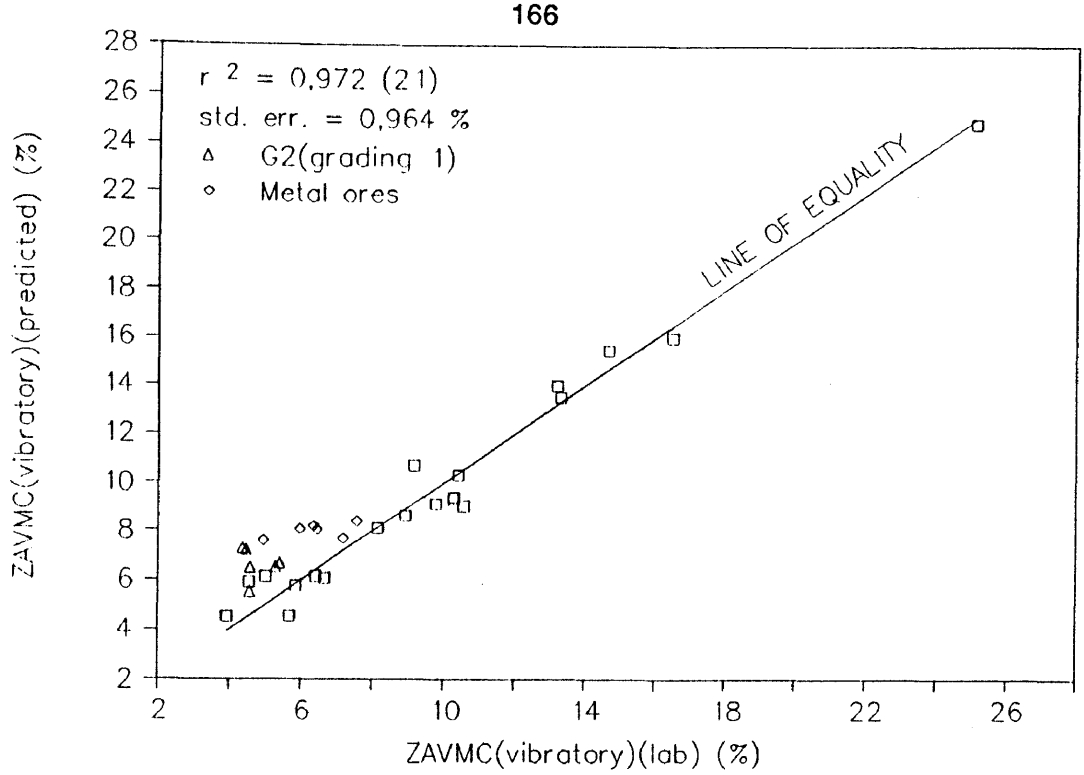

FIGURE 8.17 RELATION BETWEEN ZAVMC (VIB) (PREDICTED) (%) AND ZAVMC (VIB) (MEASURED) (%) FOR THE ORIGINAL MATERIALS, METAL ORES AND G2 MATERIALS (GRADING 1) ON THE "FINE" SIDE OF IGF

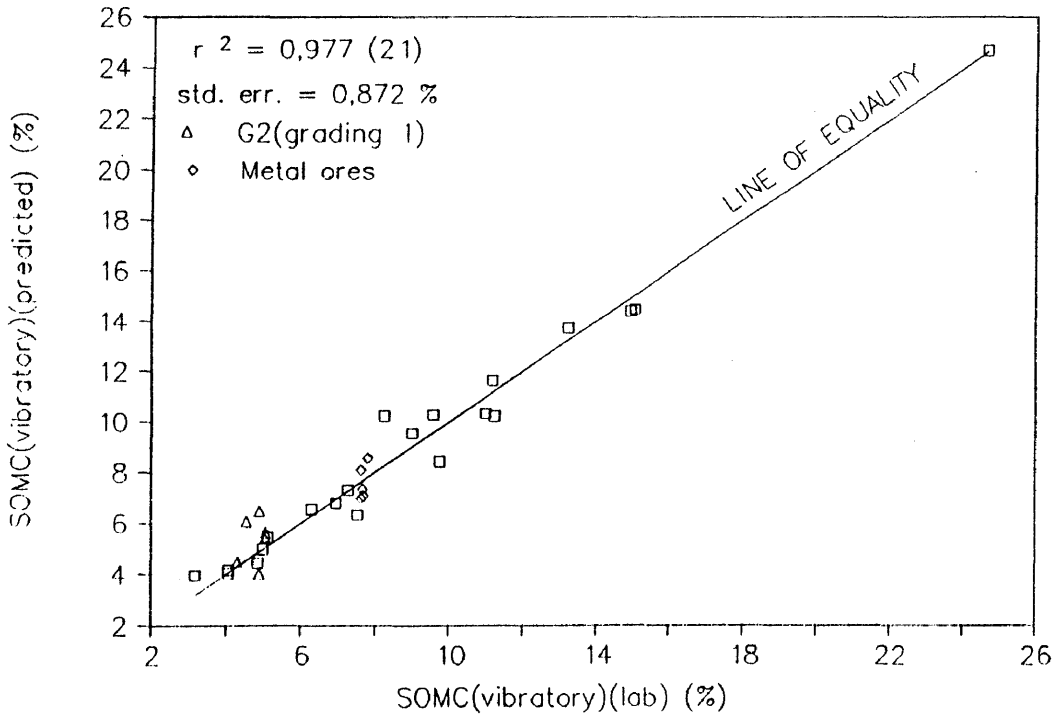

FIGURE 8.18 RELATION BETWEEN SOMC (VIB) (PREDICTED) (%) AND SOMC (VIB) (MEASURED) (%) FOR THE ORIGINAL MATERIALS, METAL ORES AND G2 MATERIALS (GRADING 1) ON THE "FINE" SIDE OF IGF

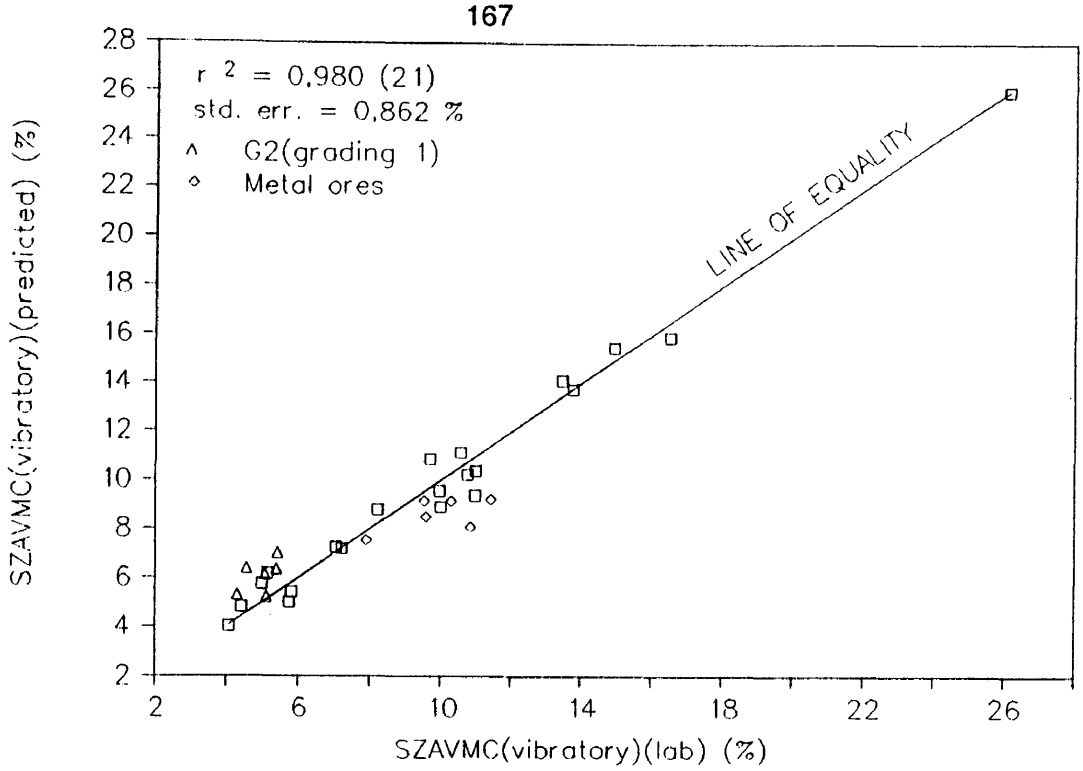

FIGURE 8.19 RELATION BETWEEN SZAVMC (VIB) (PREDICTED) (%) AND SZAVMC (VIB) (MEASURED) (%) FOR THE ORIGINAL MATERIALS, METAL ORES AND G2 MATERIALS (GRADING 1) ON THE "FINE" SIDE OF IGF

From the plots on both the "coarse" and "fine" side of the ideal" grading it would seem that all untreated roadbuilding materials react similarly as far as their compactability are concerned. The predicted values of both the normal and standardised OMC and ZAVMC for a solid density of the material of 2650 kg/m^3 of the metalliferous ores agreed well with the other materials. The fact that the models gave reasonable predictions of OMC (vib) and ZAVMC (vib) shows that the difference in solid density may have less of an influence on the OMC than expected. It therefore seems that it is not really necessary to standardise the moisture regime values (ie SCMC, SOMC, SZAVMC).

8.2 Verification of the CBR-models

8.2.1 General verification of the CBR-models

For the general verification of the CBR-models, the soaked CBR information recorded on the material control data sheets of the road projects used to verify the compactability models, was used. The predicted CBR values were calculated by means of the "CBR:CMC" and "CBR:decrease" models using the dry density prediction of MDD (mod. AASHTO) and CMC determined by means of the compactability models. The moisture content for the soaked

condition was estimated at being equal to ZAVMC (mod. AASHTO). If lower densities were chosen the CBR:decrease value was often greater than hundred per cent. It should also be remembered that the soaked laboratory samples are allowed to drain for 15 minutes after pouring off the excess water on the top surface. The SBD and SF values were estimated by using regression functions, determined for the original 21 materials between SBD and MDD (vib) and SF and MDD (vib) and using MDD (vib) (predicted) as input variable.

From Figures 8.20 and 8.21 and Table 8.8 it would seem that the correlation between "soaked" CBR (predicted) and soaked CBR (measured) is rather poor. Note the shift in the results when the measured values of the soaked CBR are plotted against the values of CBR:CMC (predicted). From Table 8.8 it would seem that even though the correlation is very poor there is a significant relation between the predicted and measured values ($t_{0,100}$ = 1,653 and $t_{0,050}$ = 1,894 for υ = 100).

The problem does not necessarily lie with the predicted value. To mention but one problem with the method of "soaked" CBR (measured), is the fact that the amount of drainage taking place in soaked samples will vary from one material to another. It will also change from one grading to another for the same material. For the sample to be truly tested in a soaked condition one would have to do the penetration test with the sample submerged in a water bath. The soaked CBR (measured) values for the different density requirements were therefore plotted against their respective densities to see whether any relation existed between CBR and specified dry density for the soaked condition (see Figure 8.22). From Figure 8.22 it would seem that there is no definite relation between the soaked CBR and dry density for the soaked condition. This is probably one of the main reasons why some engineers are rather sceptical about the CBR test. However, as shown by the author and others, good relations between the CBR and dry density and moisture content most likely exist for all untreated roadbuilding materials. The moisture content should, however, be changed by compacting the material at different moisture contents and determining the CBR at moulding moisture content rather than soaking it. The "soaked" condition as defined by the test procedure is just too variable to be "fixed".

8.2.2 Verification of the CBR-models using different moulding moisture contents

The CBR prediction models were also verified with the CBR results of materials which had been compacted in the laboratory to different density levels for a range of moisture contents. These materials were not soaked but the CBR at moulding moisture content was determined immediately after compacting the sample. Amongst the materials tested were four of the G2 materials, mentioned under the verification of the compactability models (see Figure 8.23).

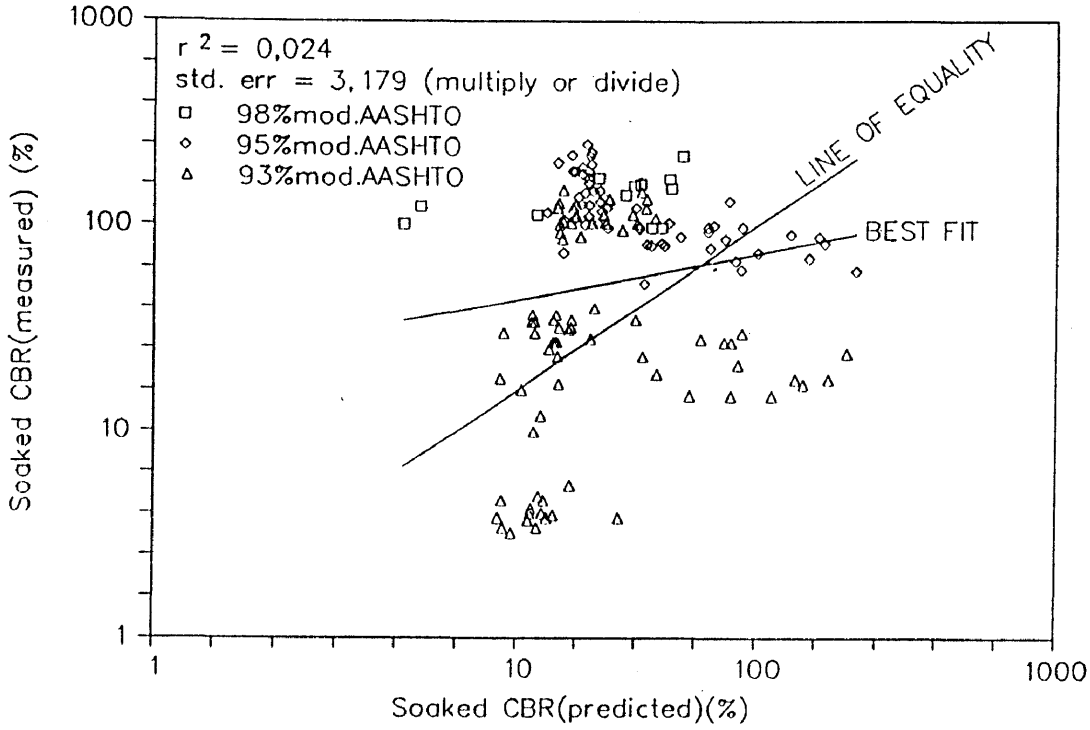

FIGURE 8.20 RELATION BETWEEN SOAKED CBR (MEASURED) AND "SOAKED" CBR (PREDICTED) ON A LOG-LOG SCALE FOR CONSTRUCTION DATA

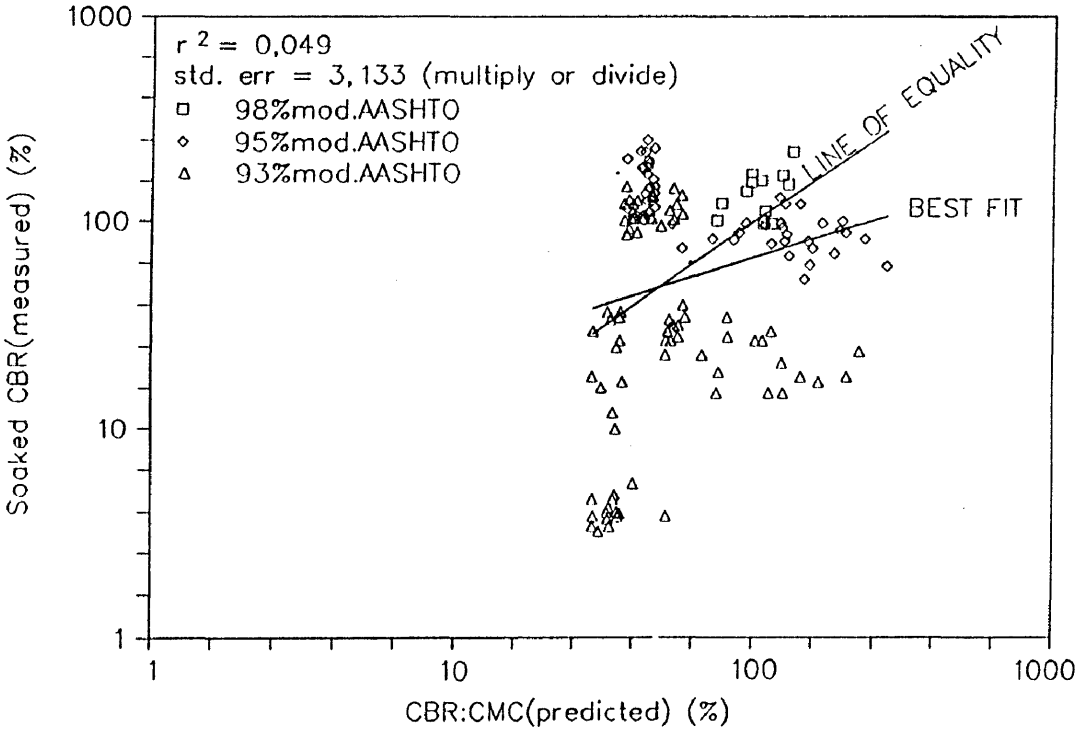

FIGURE 8.21 RELATION BETWEEN SOAKED CBR (MEASURED) AND CBR:CMC (PREDICTED) ON A LOG-LOG SCALE FOR CONSTRUCTION DATA

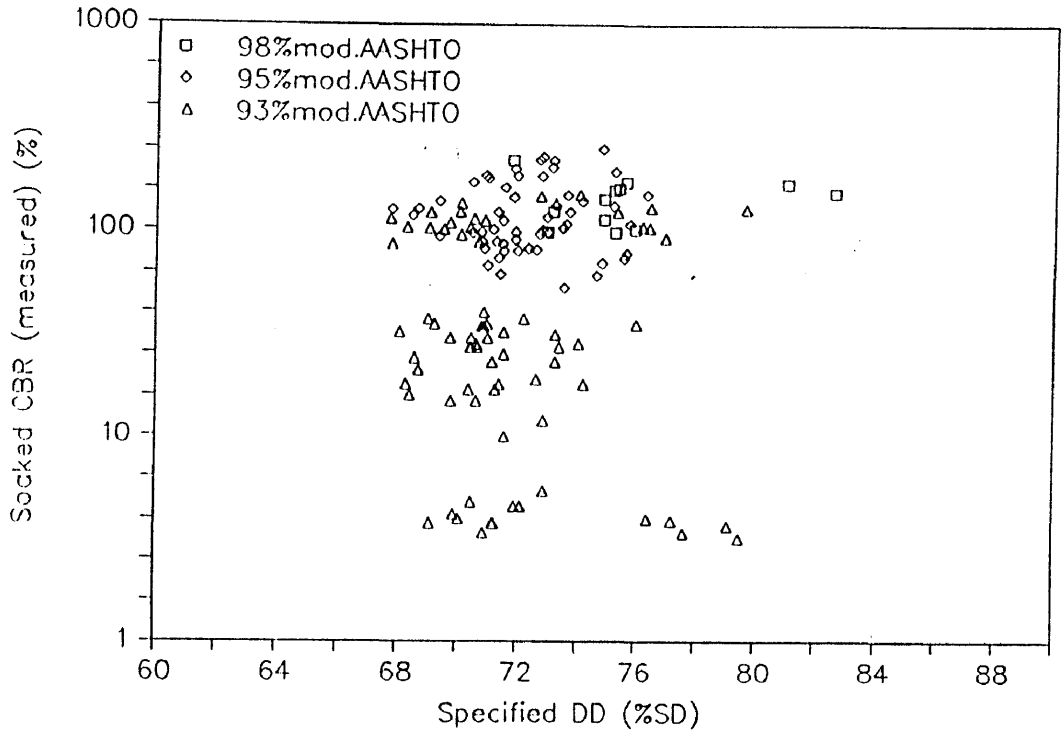

FIGURE 8.22 RELATION BETWEEN SOAKED CBR (MEASURED) AND DRY DENSITY (MEASURED) (% SD) WITH CBR ON A LOGARITHMIC SCALE FOR CONSTRUCTION DATA

TABLE 8.8 The regression coefficients, their standard errors and t-values, and r^2-values for the relation between soaked CBR (measured) and "soaked" CBR (predicted) and CBR:CMC (predicted) for the data obtained from the material control data sheets of certain road construction projects

		Predict	Constant	$t_{(0,050)}$	r^2
CBR(lab) vs CBR(predict)	X Coefficient(s)	0,279655	1,306751		
CBR(pre) = f(logDD(=E),E^2,	Std Err of Coef.	0,148784	0,502324		
logSBD,logSF,logCMC,logMCdev)	t-value	1,879596	2,601411	1,984	0,024
CBR(lab) vs CBR:CMC(predict)	X Coefficient(s)	0,447162	0,932336		
CBR:CMC(pre) = f(logDD(=E),E^2,	Std Err of Coef.	0,165876	0,496000		
logSBD,logSF,logCMC)	t-value	2,695757	1,879706	1,984	0,049

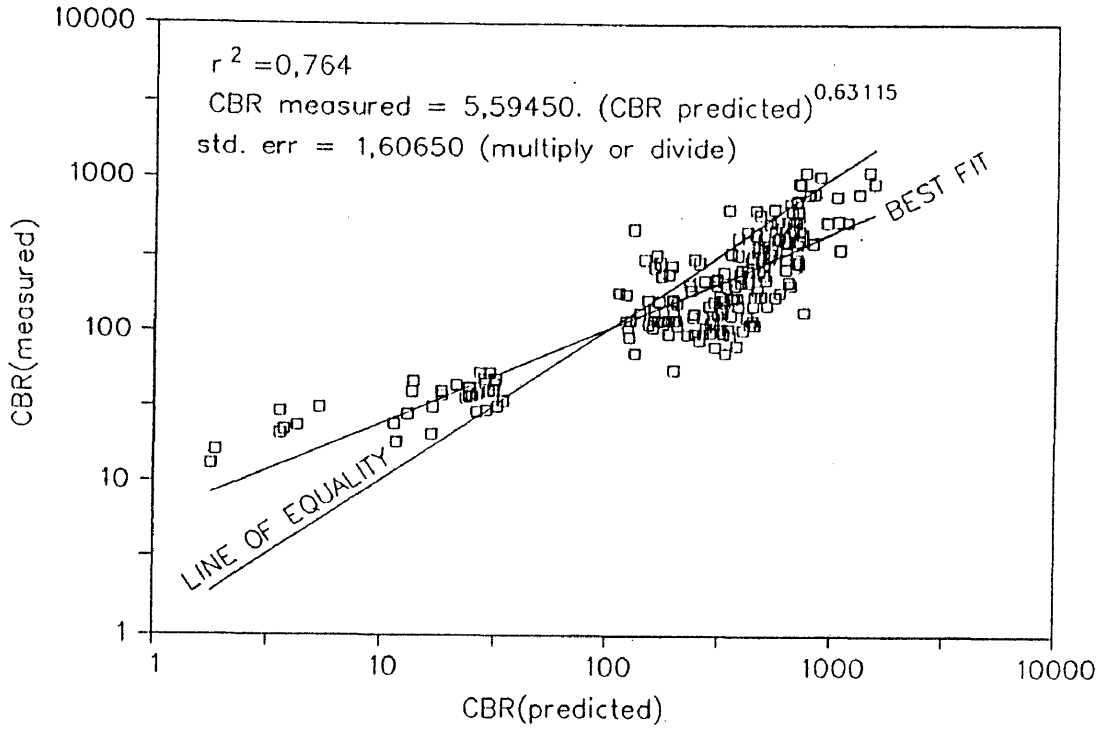

FIGURE 8.23 RELATION BETWEEN CBR (MEASURED) AND CBR (PREDICTED) FOR OTHER UNTREATED ROADBUILDING MATERIALS FOR DIFFERENT DENSITIES AND MOULDING MOISTURE CONTENTS

Although the estimated values were higher than the measured values (ie the data points were mostly below the line of equality), the same trend as found with the original materials investigated, was once again observed. This confirms that as far as the bearing capacity is concerned, both the density and moisture regimes as well as the shape and texture of the aggregate play an important role.

Comparing the results of CBR (predicted) with CBR (measured) for both the "soaked" and "moulding moisture content" conditions, it becomes clear that the "soaked" conditions are highly variable (compare Figures 8.20 and 8.23). The real reason for the poor correlation does not lie in the prediction model but in the inherent variability of the "soaked" condition. If this is taken into account it would seem that the CBR-models gave reasonable estimates for the "soaked" conditions as well. It should be stressed that the same prediction models were used in both cases.

8.3 Conclusions of the verification process

From the estimates obtained with the compactability and bearing capacity models on other materials not used to compile these models, it seems that the material properties of these materials have a similar effect on the densities, moisture regimes and bearing capacities of these materials as the material properties of the materials used in the original investigation.

It would seem that the compactability model even works for modified materials as shown by the example of the experimental sections on an HVS site. The correlation between the "predicted" and "measured" results for the information obtained from the material control data sheets were much lower. A number of factors played a role in this. The grading normally recorded is the grading before compaction. The mod. AASHTO compaction test also specifies that all material larger than 19 mm should be replaced with material in the size bracket of 19 mm to 13,2 mm. The "soaked" condition is also not "fixed", which gives rise to poor correlation with the predicted results.

One possible approach to overcome these problems would be to compare the measured field densities of different layers with the predicted densities using the grading and solid density of the material at the spot of the density measurement. This approach unfortunately also has inherent problems in that most layers are normally not compacted to refusal density but only to a specified level of the mod. AASHTO density. Apart from this the underlying support conditions may not allow the material to be compacted to MDD. Assuming that the compactability models are correct, this approach would at least show what the "predicted" values for MDD and OMC are for the particular grading. If the predicted value of the MDD is lower than the specified density, it is highly unlikely that the specified density will be achieved. Similarly, if the predicted value of the OMC is much lower the material is too wet for proper compaction.

Because the grading, Atterberg limits and linear shrinkage are the normal indicator tests to describe a roadbuilding material, one can only conclude that the likelihood is high that the compactability models would also yield reasonable estimates for the MDD, CMC, OMC and ZAVMC for other untreated roadbuilding materials. It should, however, be determined if the material is on the "coarse" or "fine" side of the IGF to ensure that the correct models are used for prediction purposes.

The shape factor (SF) and shakedown bulk density (SBD) of materials can also be determined according to the methods described in Chapter 3. It is therefore also possible to get

reasonable estimates of the bearing capacity at different densities and moisture contents in terms of bearing capacity models once the MDD, CMC, OMC and ZAVMC have been established by means of the compactability models.

The results of the experimental sections on the HVS test site also warn that even standard test methods such as the modified AASHTO compaction test sometimes yield erroneous results which can lead to construction problems. If one thinks logically about it, it is highly unlikely that the OMC of a particular roadbuilding material can vary by more than 2 % purely because of the use of a different modifying agent. The consequences of such test errors can have serious consequences on the road performance as demonstrated by the premature failure of two of these test sections due to a too high specified OMC.

Lastly, it is gratifying to note that untreated roadbuilding materials react systematically and that it is therefore possible to approach all compaction problems in a scientific manner instead of on an trial and error basis as has usually been the case up till now.

CHAPTER 9
CONCLUSIONS AND RECOMMENDATIONS

9.1 Conclusions

9.1.1 The influence of the grading

From the investigation it is clear that the particle size distribution (ie grading) of untreated roadbuilding materials has an effect on nearly all the other roadbuilding parameters such as the MDD, CMC, OMC, ZAVMC and bearing capacity. What is even more stunning is the fact that these same basic principles are also applicable to treated materials such as asphalt mixes and portland cement concrete in that the particle size distribution also determines the amount of voids available and thus the allowable binder content or OMC for concrete and thus the optimum amount of cement (see findings of Fuller et al[24] in Section 2.4).

This work also confirms the observations of other researchers (see Section 2.4) that the ideal grading curve for material is described by the following particle size distribution (ie the Fuller or Talbot curve):

$$p = 100.(d/D)^{0,5} \quad \ldots\ldots\ldots\ldots\ldots\ldots\ldots\ldots\ldots\ldots\ldots\ldots\ldots\ldots\ldots\ldots\ldots\ldots \quad (9.1)$$

where p = percentage passing sieve size d (%)
d = sieve size (mm)
D = maximum particle size (mm)

Deviating with the grading to either the fine side or the coarse side leads to a lowering of the achievable density. This is illustrated in Figure 8.7.

In many parts of the world a severe shortage of good roadbuilding materials exist, such as in desert areas where the only materials available are often uniformly-graded sands. However, if these materials could be mechanically stabilised by mixing in extra fines (ie calcrete dust or clay) to make up the ideal grading, it should be possible to achieve MDDs in the order of 78 % and 82 % for maximum particle sizes of 2 mm and 4,75 mm respectively.

In a previous research project guided by the author[65] where the stabilisation of desert sand with foamed asphalt was, amongst others, investigated, the original specification for foamed asphalt only required a minimum of 4 % fines (- 0,075 mm material). When tested at this fines

level it was found that this material was highly unstable and could not be compacted properly. The amount of fines was increased by adding calcrete dust in increments to determine the correct amount of fines. The unconfined compressive strength of the material improved dramatically as the fines were increased (see Figure 9.1). At a level of approximately 14 % fines the strength tapered off so that the unconfined compressive strength at 24 % fines was very nearly the same as at 14 %. However, there was a fourfold increase in the strength simply due to the addition of an extra 10 % fines.

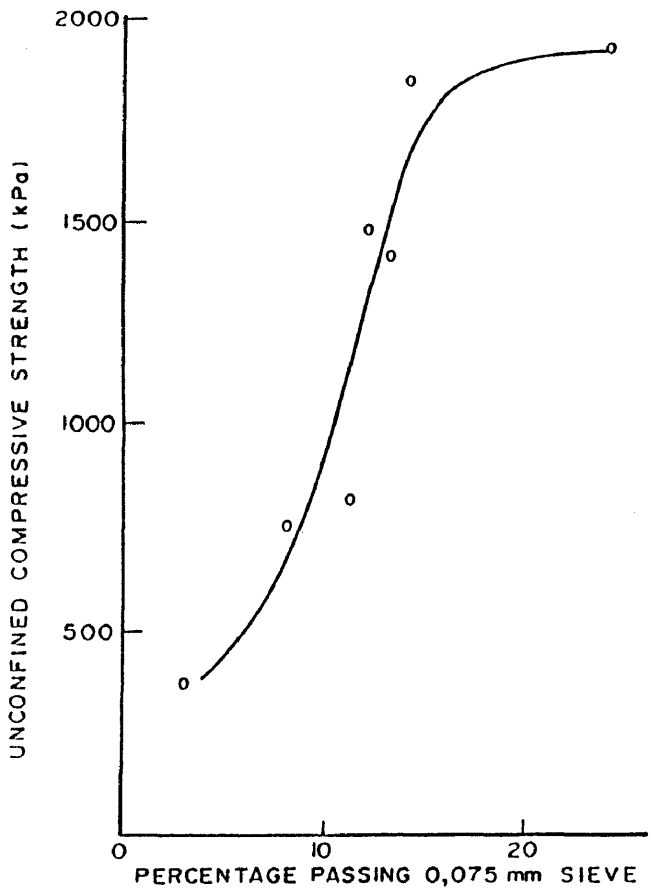

FIGURE 9.1 RELATION BETWEEN UNCONFINED COMPRESSIVE STRENGTH AND PERCENTAGE FINES FOR A MIXTURE OF UNIFORMLY GRADED SAND, CALCRETE DUST AND 5 % FOAMED BITUMEN

9.1.2 The influence of the maximum particle size

Apart from the grading the maximum particle size plays an all important role, provided the grading is correct. The greatest contribution to the final density that can be achieved is due to the particle size distribution (ie for most materials the LBD is 75 % + of MDD (vib)). The contribution of the compactive effort is the balance of this amount. Both these aspects are of cardinal importance for the proper performance of pavement layers (see Table 9.1).

TABLE 9.1 The values of the SBD and LBD as a percentage of the MDD for the materials investigated

SAMPLE	SBD (% SD)	LBD (% SD)	MDD (vib) (% SD)	SBD (% MDD) (vib)	LBD (% MDD) (vib)
BAB	52,89	47,91	59,11	89,47	81,06
SPR2	67,74	57,09	73,26	92,46	77,93
SPR1	64,19	55,53	71,62	89,62	77,53
LABLEN	69,58	60,99	79,05	88,02	77,15
LABDEW	61,14	49,06	78,17	78,21	62,76
OFS1	63,35	53,12	69,53	91,11	76,40
NPAB	64,76	60,15	77,44	83,63	77,67
SIL	61,34	52,17	73,72	83,21	70,77
LABD1	67,44	57,41	79,59	84,74	72,13
TPA3	69,09	62,27	77,47	89,18	80,38
TPA1	64,83	61,74	79,11	81,95	78,04
CPA1	72,57	60,98	90,24	80,42	67,58
DENS7	66,21	52,04	84,28	78,56	61,75
TPA2	67,17	61,14	82,14	81,77	74,43
NPAE	76,26	71,65	88,33	86,34	81,11
FERR1	72,82	63,70	86,79	83,91	73,40
OFS2	67,71	62,07	83,96	80,64	73,92
NPAA	72,94	70,38	88,04	82,85	79,94
ROSS1	76,24	66,09	86,64	87,99	76,28
DENS8	64,95	58,49	77,81	83,48	75,17
OFS3	74,56	70,01	89,52	83,28	78,21
			Average	84,86	74,93
			Std. dev	3,99	5,29

Using a larger maximum particle size therefore also increases the loose bulk density of a well-mixed properly graded material which would indirectly lead to an increase in strength of the layer without any compaction effort being applied. At the same time the fines requirement for the ideal grading curve reduces as the maximum particle size increases and free-draining layers with high strengths can be constructed providing the dry densities are above say 86 % SD as already shown in practice for waterbound macadams with maximum stone sizes of 75 mm and 53 mm and railway ballast. It should be remembered, however, that the shape and texture have a tremendous effect on the strength of the material, therefore smooth rounded particles should preferably be crushed to improve their strength properties and should not be used for free-draining layers.

The overall moisture requirements are also reduced as the maximum particle size increases, which means that one of the ways to overcome the water shortage on construction sites would be to construct thicker layers with a larger maximum particle size, provided that the compactive effort applied is high enough to properly densify the layer to the required density. In some cases it may even be possible to achieve the required level of density (ie 90 % mod. AASHTO in terms of % SD) without any compactive effort apart from the equipment carting in the material if the special compaction standards are maintained. However, the author does not recommend this approach as the under-compaction of material could lead to failures such as the "rock-fill" embankments built with shale as described by Spangler et al[51] (see Section 2.7).

The strength requirements of pavement layers will indicate what sort of a density level must be achieved. This may assist in the selection of materials. However, only by proper compaction of the layers can the required levels of density normally be met. The strength potential of an untreated roadbuilding material will only be fully utilized if the material forms a tight knit matrix. Where labour intensive construction techniques are therefore used and where suitable compaction equipment is lacking it is essential that these materials be placed as densely as possible through hand packing. For labour intensive construction techniques the material should therefore preferably be coarse (see Section 2.4.1 on the pavement designs of the Romans and others when roads were still constructed by means of labour intensive construction techniques without the use of sophisticated compaction equipment).

9.1.3 The influence of the density level

The investigation showed that the mod. AASHTO compaction test and for that matter the standard AASHTO compaction test (ie the Proctor density test) do not compact most materials to their MDDs (see Table 9.2). Because of the all too prevalent misconception that the MDDs achieved by these compaction tests are the MDDs that can be achieved, some layers of the roads being constructed nowadays are under-compacted, which leads to premature distress of these roads due to extensive rutting. Apart from the unnecessary rutting of pavements, under-compaction of pavements also leads to a loss in potential strength of the pavement.

The author is of the opinion that the service life of most roads could be increased substantially if all layers are properly compacted to refusal density (ie the highest density that can be achieved for that material when applying the correct amount of compactive effort at OMC for the material). As refusal density of a layer is partly dependent on the resistance of the supporting layer below, it should be clear that right from the roadbed up every single layer

should be compacted to refusal density if we are to achieve optimal performance from our roads and for that matter other fill structures.

In a report on the permanent deformation in pavements with granular bases and subbases, Shackleton[66] concluded that the amount of rutting taking place during the bedding phase of the pavement could shorten the pavement design life of 20 years (normal rut depth 20 mm) by between one and eight years. This amounts to a loss of service life of between five and forty per cent. Most of this loss could be avoided if all pavement layers are optimally compacted. The author of this dissertation estimates that the extra compaction costs should not exceed one per cent of the project costs. Shackleton also pointed out that apart from the extra service life because of optimal compaction, the optimal compaction will also contribute to:

> "Saving brought about by being able to delay maintenance
> Higher serviceability of the pavement throughout its life
> Reduced vehicle operating costs throughout the pavement's life
> Better safety (less ponding) for the road user"[66]

As it has already been pointed out that the grading and the maximum particle size have a tremendous effect on the MDD, OMC and CBR, it is hard to comprehend how we as engineers have accepted the results of the modified AASHTO and standard AASHTO compaction tests as well as the CBR values when the gradings of the samples compacted and tested differed from the actual gradings of the materials. This is due to the test method stipulation that all material larger than 19 mm should be reduced to material smaller than 19 mm or be replaced with a similar proportion of material smaller than 19 mm. The serious consequence of this stipulation for coarse granular material is that both the measured MDDs and CBRs are too low and the measured OMCs are too high. Even materials which do not contain particles larger than 19 mm are not optimally compacted by the mod. AASHTO test. This is because the material adjacent to the compaction hammer position is continually disturbed because the hammer does not cover the whole surface of the sample (see Table 9.2).

Where the MDD (mod. AASHTO) is, therefore, accepted as the optimum density of the material, this can lead to unnecessary rutting of the pavement structures during the bedding phase because of incomplete compaction as well as substantial loss in service life (see earlier findings by Shackleton).

TABLE 9.2 **The values of MDD, OMC and ZAVMC for the vibratory table and the mod. AASHTO compaction tests and the ratio between the mod. AASHTO and the vibratory table values for the original materials**

SAMPLE	MDD (mod) (% SD)	OMC (mod) (%)	ZAVMC (mod) (%)	MDD (vib) (% SD)	OMC (vib) (%)	ZAVMC (vib) (%)	MDD (mod) (% vib)	OMC (mod) (% vib)	ZAVMC (mod) (% vib)
BAB*	59,58	18,05	24,62	59,11	23,71	25,10	100,79	76,13	98,07
SPR2	71,32	11,40	14,58	73,26	12,73	13,23	97,35	89,55	110,17
SPR1	69,10	11,40	16,57	71,62	14,68	14,68	96,48	77,66	112,85
LABLEN	77,47	7,80	10,74	79,05	7,38	9,79	98,01	105,69	109,71
LABDEW	76,42	8,75	11,51	78,17	9,47	10,42	97,76	92,40	110,50
OFS1	67,38	7,80	18,23	69,53	15,04	16,51	96,91	51,86	110,46
NPAB	76,05	10,10	11,14	77,44	10,31	10,30	98,21	97,96	108,09
SIL	70,42	12,50	15,70	73,72	11,08	13,33	95,53	112,82	117,82
LABD1	74,89	9,80	11,97	79,59	7,82	9,16	94,10	125,32	130,73
TPA3	75,47	9,20	11,81	77,47	9,40	10,57	97,42	97,87	111,75
TPA1	75,45	8,70	10,99	79,11	8,06	8,92	95,37	107,94	123,24
CPA1	86,03	4,10	5,89	90,24	3,92	3,92	95,34	104,59	150,13
DENS7	79,81	7,80	9,03	84,28	6,58	6,65	94,69	118,54	135,65
TPA2	77,20	5,60	11,06	82,14	7,22	8,14	93,99	77,56	135,83
NPAE	85,52	5,90	6,42	88,33	5,01	5,01	96,82	117,76	128,16
FERR1	81,12	5,30	8,68	86,79	4,82	5,68	93,47	109,96	152,92
OFS2	79,44	3,80	8,68	83,96	5,61	6,41	94,62	67,74	135,45
NPAA	82,23	6,30	7,23	88,04	4,55	4,54	93,41	138,46	159,02
ROSS1	82,77	6,20	7,89	86,64	4,09	5,84	95,53	151,59	135,04
DENS8*	78,37	7,90	9,95	77,81	10,74	10,28	100,72	73,56	96,78
OFS3	74,07	3,90	11,80	89,52	2,85	3,95	82,74	136,84	298,99

* Cohesive materials

The fact that crushed stone is not compacted effectively with the mod. AASHTO density test has been recognised in South Africa for a considerable period and the density requirement is now specified in terms of percentage solid density. But as far as all other materials are concerned, the old requirements are still being applied to the detriment of the roads constructed.

9.1.4 The influence of the grading on the moisture regime

The moisture regime (CMC, OMC and ZAVMC) are all influenced by the grading of the material. If the material becomes finer the moisture requirements increase due to an increase in surface area and void space. It is therefore of the utmost importance to compact material properly while avoiding unnecessary breakdown which normally occurs when the compaction procedure is not stopped timeously when maximum density is reached. Similarly, the unnecessary breakdown of compacted laboratory samples also leads to an increase in the specified moisture requirements. This leads to the specification of unnecessary high OMCs which give rise to construction problems as it is more difficult to compact materials above OMC in most cases because of pore pressure built-up and lower stability. It also leads to unnecessary waste of a scarce commodity in many parts of the world.

Where the grading of the material also has such a direct bearing on the moisture regime, it should be clear why the material in a particular section which is treated as a unit should be as uniform as possible. Variation in the quality of the material (ie grading, etc) will lead to variable moisture requirements throughout the section, making it virtually impossible to deliver satisfactory work. For this reason material used on a particular section should preferably come from one source only, or where two or more sources are used (ie mechanical stabilisation), these materials should be very thoroughly mixed to ensure uniform moisture requirements throughout the section.

9.1.5 Concluding remarks

The high correlation values of the compactability and CBR models indicate that untreated roadbuilding materials react systematically. Good estimates of both the MDD and the moisture regime can be determined from the grading and the Atterberg limits and the linear shrinkage of the minus 0,425 mm material. It is also possible to determine reasonable estimates of the bearing capacity (CBR) when the SBD and SF are known as well.

The fact that untreated roadbuilding materials react systematically as far as their compactability and bearing capacity are concerned, means that compaction problems can now be approached in a scientific manner, rather than by trial and error as is presently the case. Better understanding of the factors that influence the compactability of untreated roadbuilding materials should also lead to improved construction practices as well as more effective utilization of these materials, which should hopefully lead to improved road performance (ie a higher benefit/cost ratio).

9.2 Recommendations

It was shown in Chapter 8 that there is a "coarse" grouping and "fine" grouping for materials which react differently and should therefore be treated separately. It was also found that the two groupings meet each other at the "ideal grading" (ie $p = 100.(d/D)^{0,5}$). As the maximum particle size is not fixed it means that each maximum particle size D will most likely have a "coarse" and "fine" grouping. It is therefore recommended that this be investigated for maximum particle sizes D equal to 26,5 mm, 19 mm, 13,2 mm and 4,75 mm. Once this has been properly established it is probable that the compactability models can be modified so that they can also be applied to larger particle sizes such as 53 mm, 63 mm, 75 mm, 150 mm and 300 mm. These refined models will then allow us to estimate the MDD and moisture regime (CMC, OMC and ZAVMC) from the grading, Atterberg limits and linear shrinkage for any maximum particle size D. For the structural layers, where D is normally 37,5 mm the models developed can immediately be applied in practice for materials which are not too coarse.

The fact that the ideal grading curve yields the best results as far as density and bearing capacity are concerned, and the fact that the bearing capacity generally increases dramatically for densities above 80 % SD, seem to point to the fact that we stand to gain a lot by using larger maximum particle sizes than the presently used 37,5 mm. Research leading to the effective construction of layers with maximum particle sizes larger than 37,5 mm would therefore yield large dividends in the form of improved performance.

Many underdeveloped areas have a severe shortage of good roadbuilding materials. This means that more effort needs to be spent to determine how the performance of the locally available materials can be drastically improved through the proper selection and mixing of several of these materials. Mechanical stabilisation of these roadbuilding materials is most likely the most cost-effective approach for constructing roads in many of these areas and should therefore be seriously considered. Where many third world countries are saddled with

this problem, research in this field should also yield high dividends.

It is recommended that in the case of mod. AASHTO density standards the compactability models be used on site to determine the density standard instead of determining separate "dry density-moisture content" curves for each position where field densities are determined. These answers should be available much more rapidly and there should also be a substantial saving in laboratory costs.

The predicted MDDs (vib) (% SD) for the separate sampling positions, as determined from the gradings and Atterberg limits of the material, should also be compared with one another as well as the original mod. AASHTO density (% SD) to see whether they all belong to the same population (ie similar MDDs in terms of % SD). If the predicted MDDs (vib) vary substantially it points to the fact that the material is not uniform in quality and has not been properly mixed. If the predicted MDDs (vib) are generally lower than the MDD (mod. AASHTO) (lab) substantial breakdown occurred during the compaction, possibly due to "over-rolling". In the case of coarse granular materials the predicted MDDs (vib) may in actual fact be greater than the MDD (mod. AASHTO) (lab), pointing to the fact that the material could actually be compacted to a substantially higher density. In the latter situation a higher level of density would therefore be expected from the contractor as this can readily be achieved.

In the compaction of crushed stone materials contractors sometimes experience great difficulty in achieving the specified dry density. Where this is due to the shape and texture of the aggregate particles and not due to problems with the grading every effort should be made to achieve the specified dry density. It is, however, recommended that the contractor be rewarded for the extra effort required in view of the superior performance of the road later on.

This research also showed that the actual moisture content of an untreated roadbuilding material has got a tremendous influence on both the compactability and the bearing capacity of the material. The highest density and best bearing capacity during construction will normally be achieved at a moisture content somewhere between the CMC and OMC depending on the compaction equipment itself. Actual compaction should therefore preferably take place in this range. The closer the moisture content is to the CMC, the greater the achievable bearing capacity will be for the specified density.

However, during wet conditions on site it is not always possible to keep the moisture content between these limits. It is proposed that the maximum allowable moisture content for materials to be compacted to the mod. AASHTO standard should be equal to the moisture content at

which the material, if compacted to 100 % mod. AASHTO density, would still contain two per cent air voids. This will prevent the situation arising where the materials cannot be compacted to the required density because of saturation. In the case of coarse granular materials such as G1, G2 and G3 materials, the maximum allowable moisture content should be equal to the saturation moisture content for the specified density requirement in terms of SD. Where the crushed stone is porous in nature (ie a significant difference in the values of ARD and BRD), the maximum allowable moisture content should be equal to the saturation moisture content for the specified dry density requirement (in terms of DBD) plus a correction for the water absorbed by the porous aggregate (ie the water absorption percentage determined during the laboratory determination of the ARDs and BRDs multiplied by their respective fractional contributions to the total grading). The reason why the coarse materials may be compacted at saturation moisture content is because they are more free draining by nature and tend to lose moisture far more rapidly during compaction than the finer materials where pore pressure build-up and instability is far more likely to occur.

If the in-situ moisture content of the material is, therefore, greater than the maximum allowable moisture content the material may not be compacted before the in-situ moisture content has dropped to a level equal to or less than the maximum allowable moisture content (MAMC). A subsequent layer should also not be placed if the moisture content of the previously approved layer has risen to above MAMC due to exposure to the elements. Construction should therefore preferably take place during the dry season to avoid long delays.

Because of the inherent differences in the apparent densities of different untreated roadbuilding materials, this variable was eliminated in the compactability models that were developed by expressing the MDD as a percentage of the solid density of the material.

Therefore, before converting the MDD (% SD) to kg/m^3 it is important to compare the values of the ARD and BRD with one another. A close approximation would be to use the DBD in all cases as the values of the DBD and AD for non-porous materials will approximately be the same. In the case of finer roadbuilding materials or materials which break down completely, the AD value should be used as all the voids in the soil particles are normally accessible to the filled with soil fines.

Where the material comes from more than one source, either it its natural state or by mechanical mixing, it is recommended that the BRD and ARD of the fraction larger than 4,75 mm (coarse fraction) as well as the BRD and ARD of the material smaller than 4,75 mm (fine fraction) be determined. The solid density is then determined using both the BRD of the

coarse fraction and the BRD of the fine fraction in terms of their contribution by mass to the total grading. The water absorption is determined from the BRDs and ARDs of both fractions and their contribution by mass to the total grading.

Soil exploration and testing during the planning and design phases of a road can also cost a substantial amount of money. Because the indicator test values are normally recorded as part of this information, it is recommended that the predicted results from the compactability models be compared with the results achieved in the laboratory. Once it has been established that the predicted values compare favourably with the laboratory results, it will be possible to cut back on a lot of this testing. The field moisture content and season should also be recorded. This is done to get an estimate of the equilibrium moisture content in the pavement. If the design allows for proper drainage of the pavement structure it is expected that the equilibrium moisture content in a surfaced pavement will be close to the CMC. Designing the pavement for CBR:CMC or even CBR:OMC should lead to substantial reduction in total pavement thickness compared to soaked CBR.

Apart from this it will become possible to use so-called "substandard" materials which do meet the CBR requirements at the EMC or OMC but not in the soaked condition. Tertiary road construction particularly stands to benefit from this design approach as it will be possible to construct more roads for the same amount of funds. Although these roads have a higher risk of failure, this approach has already been used with success in South Africa by some of the road authorities[67].

The author feels strongly that the soaked CBR should be eliminated as it very seldom reflects in situ conditions in South Africa. It is realised, however, that engineers have to be convinced of the advantages of the new approach. Therefore, instead of only determining the soaked CBR it is recommended that the CBRs at moulding moisture content should also be determined in the evaluation period. It is also recommended that the SBD and SF of the materials be determined to evaluate the CBR-models. Both these tests are extremely simple, but have shown that they can be used to quantify the effects of shape and texture of the aggregate particles on the bearing capacity of the material. The moulding moisture content should also be recorded.

The investigation has also shown that impact compaction tests (ie modified AASHTO and standard AASHTO) are not suitable to determine the MDDs and OMCs of most materials. Much better results were obtained with a vibratory compaction table. It is strongly recommended that the mod. AASHTO and std. AASHTO compaction tests be replaced by a

vibratory compaction test. Samples should be compacted in a single layer without any adjustments to the sample grading. The sample should also not be scraped off and levelled, but the sample volume should rather be determined by accurate height measurement. The dry mass of the sample should approximately be equal to a sample which should be 100 mm high if compacted to 82 % of solid density for coarse granular materials (ie crushed stone and natural gravels) and 72 % of solid density for fine granular and cohesive materials (ie sands and clays).

The tremendous improvements in bearing capacity for slight increases in densities when these untreated roadbuilding materials approach their MDDs, seriously questions the policy of compacting layers to a certain uniform level of density (ie 90 % mod. AASHTO) instead of compacting each layer to refusal density. More research should also be done in this field so that both the costs of the extra compaction effort as well as the benefits of improved road performance can be quantified.

The only situations in which it is not recommended to compact to refusal density, are highly expansive soils and materials which are susceptible to frost heave. The discussion of this falls outside the scope of this dissertation.

The high degree of accuracy with which both the density, moisture regime and bearing capacity can be estimated from the grading, Atterberg limits, linear shrinkage, SBD and SF of untreated roadbuilding materials seem to indicate that granular materials react systematically to certain physical laws and the likelihood is great that these empirical models will also yield reasonable estimates for durable untreated roadbuilding materials from other parts of the globe. Where materials with a low durability, such as mudrocks, have to be used, the prediction should always be based on the grading, Atterberg limits, linear shrinkage, SBD and SF after breakdown has occurred. These models could therefore most probably speed up the evaluation process of roadbuilding materials and also cut down on standard testing. The fact that the CMC and ZAVMC of the material are also determined by these models, can assist the engineer in avoiding compaction problems as far as possible. Where compaction problems are experienced these models can be of great value in determining the cause of the problem. The only way to find out whether these models are universally applicable is by comparing the results of these models with actual results, and this is only possible if people elsewhere are willing to try them out.

9.2.1 Specific recommendations on the use of the compactability and bearing capacity models

For the prediction of the compactability properties (ie MDDs, OMCs, ZAVMCs and CMC) it is recommended that the following models be used:

$$X = k_1.GF^{0,85} + k_2.C + k_3.Q + k_4.C^3 + k_5 \quad \ldots\ldots\ldots\ldots\ldots\ldots\ldots\ldots \quad (9.2)$$

or

$$X = k_{11}.GF^{0.85} + k_{12}.C + k_{13}.Q + k_{14}.C^3 + k_{15}.SBD + k_{16}.SF + K_{17} \quad \ldots\ldots\ldots \quad (9.3)$$

where	X	=	MDD (vib or mod. AASHTO), OMC (vib or mod. AASHTO), ZAVMC (vib or mod. AASHTO) or CMC
and	GF	=	grading factor = Σ (percentage passing sieve size/nominal sieve size (mm))/100 for the 75 mm, 53 mm, 37,5 mm, 26,5 mm, 19 mm, 13,2 mm, 4,75 mm and 2,0 mm sieve sizes
	C	=	(percentage passing 0,425 mm sieve/100).$(LL/100)^{0,1}$
	Q	=	(percentage passing 0,425 mm sieve/100).(LS)
	SBD	=	shakedown bulk density (% SD)
	SF	=	shape factor (%)
	k_n	=	regression coefficients

Equation 9.2 should be used if the SBD and SF values are unknown. The values of the regression coefficients from Table 9.3 should be used together with this equation for materials on the fine side of the IGF and Table 9.4 for material on the coarse side of the IGF. Note that the predicted property values for materials on the coarse side of the IGF are less accurate than the predicted properties on the fine side of the IGF.

Equation 9.3 should be used if the SBD and SF values have been determined. The values of the regression coefficients from Table 9.5 should be used together with this equation for materials on the fine side of the IGF.

When the SBD and SF values are known it is also possible to make reasonable predictions of the bearing capacity (CBR) by using equations 9.4 and 9.5 as follows:

$$\log(CBR{:}CMC) = k_{21}.E + k_{22}.E^2 + k_{23}.F + k_{24}.G + k_{25}.H + k_{26} \quad \ldots\ldots\ldots\ldots \quad (9.4)$$

Table 9.3: Regression coefficients for the different compactability properties for materials on the fine side of the IGF when the SBD and SF are unknown

PROPERTY	UNITS	$(GF)^{0.85}$	C	Q	C^3	Constant
MDD (vib)	(% SD)	-35,7891	9,710725	-2,85420	21,80919	104,6374
OMC (vib)	(%)	21,02111	-9,01290	2,105612	-13,1290	-5,59777
ZAVMC (vib)	(%)	20,90554	-10,7386	1,515342	0,00000	-4,34233
CMC	(%)	11,62205	0,00000	0,947743	-11,8258	-2,28897
MDD (mod. AASHTO)	(% SD)	-28,7578	14,73411	-1,80369	0,00000	95,31451
OMC (mod. AASHTO)	(%)	8,203742	0,00000	1,189091	-7,68682	1,102778
ZAVMC (mod. AASHTO)	(%)	20,01604	-10,9493	1,357654	0,00000	-1,59074

Table 9.4: Regression coefficients for the different compactability properties for materials on the coarse side of the IGF when the SBD and SF are unknown

PROPERTY	UNITS	$GF^{0.85}$	C	Q	C^3	Constant
MDD (vib)	(%SD)	73.15136	-148.543	-15.6043	11548.19	52.59602
OMC (vib)	(%)	10.55197	-21.0084	4.464320	560.9068	-1.01611
ZAVMC (vib)	(%)	-44.6293	156.0310	12.15292	-11278.4	23,81786

Table 9.5: **Regression coefficients for the different compactability properties for materials on the fine side of the IGF when the SBD and SF are known**

PROPERTY	UNITS	$(GF)^{0,85}$	C	Q	C^3	SBD	SF	Constant
MDD (vib)	(% SD)	-32,0356	0,00000	-2,85341	29,87983	0,335383	0,326000	77,21464
OMC (vib)	(%)	21,02111	-9,01290	2,105612	-13,1290	0,00000	0,00000	-5,59777
ZAVMC (vib)	(%)	25,15475	-6,48469	2,145249	-13,2616	0,00000	-0,17689	-6,12109
CMC	(%)	11,62205	0,00000	0,947743	-11,8258	0,00000	0,00000	-2,28897
MDD (mod. AASHTO)	(% SD)	-28,6075	0,00000	-2,52192	26,49597	0,339207	0,402152	70,20786
OMC (mod. AASHTO)	(%)	8,203742	0,00000	1,189091	-7,68682	0,00000	0,00000	1,102778
ZAVMC (mod. AASHTO)	(%)	20,01604	-10,9493	1,357654	0,00000	0,00000	0,00000	-1,59074

where log(CBR:CMC) = logarithm of the CBR at CMC for a particular level of density
E = log (dry density)(% SD)
F = log (SBD)(% SD)
G = log (SF)(%)
H = log (CMC)(%)
k_n = regression coefficient

and

$$\log(\text{CBR:decrease}) = k_{31}.H + k_{32}.L + k_{33} \quad \ldots\ldots\ldots\ldots\ldots\ldots\ldots \quad (9.5)$$

where log(CBR:decrease) = logarithm of the percentage decrease in bearing capacity (% CBR:CMC)
H = log (CMC)(%)
L = log (absolute moisture content deviation from CMC)(% CMC)
k_n = regression coefficient

The values for the regression coefficients for equations 9.4 and 9.5 should be taken from Table 9.6 and Table 9.7 respectively. Select the coefficients according to the material classification; if uncertain, use the "All materials" category coefficients.

The predicted bearing capacity for a particular material at dry density DD1 (% SD) and moisture content MC1, is determined by using equation 9.4 to determine log(CBR:CMC) for the dry density level of DD1, and using equation 9.5 to determine log(CBR:decrease) for the moisture content MC1. The moisture content deviation (MCDEV) is determined as follows:

$$\text{MCDEV (\%)} = \text{absolute value of } [100.(MC1 - CMC)/CMC] \quad \ldots\ldots\ldots\ldots\ldots \quad (9.6)$$

where MC1 = moisture content of the material
CMC = critical moisture content of the material as determined with compactability model in equation 9.3.

The natural values of CBR:CMC and CBR:decrease are determined and from these values the predicted CBR-value at DD1 and MC1 is determined as follows:

Table 9.6: Regression coefficients for log(CBR:CMC) for different categories of materials

MATERIALS	E	E^2	F	G	H	Constant
Crushed stone	-59,9536	17,94450	7,265313	0,731499	-3,25459	39,29038
Natural gravel	-139,200	39,61879	13,66789	-1,90879	6,819824	95,17697
Sandy material	-7,69326	3,702538	1,451194	-0,91779	2,018085	0,007049
All materials except clay	-51,8394	15,65623	1,608016	0,325161	-1,62131	42,15851
All materials	-176,655	48,91816	0,267347	0,352645	-1,82238	161,7910

Table 9.7: Regression coefficients for log (CBR:decrease) for different categories of materials

MATERIALS	H	L	Constant
Crushed stone	1,178208	0,986691	-0,69168
Natural gravel	1,085141	0,933824	-0,82473
Sandy material	-0,61633	0,990730	0,568200
All materials except clay	0,150996	0,998355	-0,16016
All materials	0,127356	0,993750	-0,13852

$$CBR:CMC = 10^{\log (CBR:CMC)} \quad \ldots\ldots\ldots\ldots\ldots\ldots\ldots\ldots\ldots\ldots\ldots\ldots \quad (9.7)$$

$$CBR:decrease = 10^{\log (CBR:decrease)} \quad \ldots\ldots\ldots\ldots\ldots\ldots\ldots\ldots\ldots\ldots\ldots\ldots \quad (9.8)$$

If the moisture content deviation is very large, the predicted CBR:decrease values may sometimes exceed 100 per cent, which is not possible in practice. It is proposed that the maximum decrease should be about 95 per cent, because the soaked CBR samples are allowed to drain for 15 minutes which means that the samples will not be totally saturated.

$$CBR = (CBR:CMC).(100 - CBR:decrease)/100 \quad \ldots\ldots\ldots\ldots\ldots\ldots\ldots\ldots\ldots\ldots \quad (9.9)$$

It is very important to remember that the "after compaction" grading should be used to determine the compactability properties and that the SBD and SF values are also determined from the same sample which was used to determine the "after compaction" grading. In the case of unstable materials such as mudrocks it may even be advisable to do a durability test on the material before compaction so as to take account of the rapid weathering properties of these materials. However, no unnecessary breakdown of the material to reduce the maximum particle size, as in the case of the mod. AASHTO, should be done. If a sample is compacted in the laboratory, the compaction should preferably be done on a vibratory compaction table in a single layer. If this is not available, a sample of about 4 kg should be compacted in a single layer with the normal mod. AASHTO compaction effort. The moisture content of the material should be close to the expected OMC; an experienced technician can estimate this fairly accurately. In the case of actual construction, the sample may be obtained from a layer that has already been compacted. The grading of the material is determined by wet sieving. The sieve fractions are kept separate to firstly determine the weighted SF value

(see Section 3.8), after which the fractions are added together and mixed to determine the SBD value (see Section 3.9).

As SBD and SF only have a limited effect on the compactability of untreated roadbuilding materials, these properties should only be determined if one is interested in the bearing capacity or when compaction problems are experienced.

To convert the predicted MDD values (% SD) to kg/m^3 it is important that the solid density be determined accurately. Particularly in the case of natural gravels or where materials are mixed together it is proposed that the relative solid density (RSD) be determined as follows. Sieve the material through the 4,75 mm sieve. Determine the BRD and ARD of the fraction larger than 4,75 mm, and the BRD and ARD of the fraction smaller than 4,75 mm.

The relative solid density (RSD) and water absorption (WA)(%) are determined as follows:

$$RSD = ((100 - P).BRD_1 + P.BRD_2)/100 \quad \ldots\ldots\ldots\ldots\ldots\ldots\ldots\ldots \quad (9.10)$$

and

$$WA(\%) = (100 - P).(1/BRD_1 - 1/ARD_1) + P.(1/BRD_2 - 1/ARD_2) \quad \ldots\ldots\ldots \quad (9.11)$$

and

$$SD\ (kg/m^3) = 1000 \times RSD \quad \ldots\ldots\ldots\ldots\ldots\ldots\ldots\ldots\ldots\ldots \quad (9.12)$$

where P = percentage passing the 4,75 mm sieve
BRD_1 = bulk relative density of the fraction larger than 4,75 mm
ARD_1 = apparent relative density of the fraction larger than 4,75 mm
BRD_2 = bulk relative density of the fraction smaller than 4,75 mm
ARD_2 = apparent relative density of the fraction smaller than 4,75 mm
SD = solid density

It is important to realise that the absorbed water WA is absorbed into the porous structure of the aggregate and is not freely available to lubricate or lower cohesive forces. The predicted OMCs, ZAVMCs and CMC should therefore be increased by this amount to determine the range of field moisture contents in which compaction should take place; preferably between OMC (vib) and OMC (mod. AASHTO).

As the maximum particle size in the investigation was normally 37,5 mm (some larger particles present in the natural gravels), it is recommended that for the present one should be careful in using the compactability models on materials with larger particle sizes. Where used, one should always verify the predicted values by field measurements.

The Atterberg limits and linear shrinkage also have a significant influence on the compactability properties. It should be emphasized that the liquid limit should be determined with the Casagrande apparatus. A definite relation between the LL (Casagrande method) (bowl method) and the LS was found during the investigation. Unfortunately the LL (cone method) does not follow the same relationship and may therefore not be used. When the material is classified as non-plastic (NP) the value of the LL is taken to be zero. When the material is classified as slightly plastic (SP) the value of the LL is taken to be 0,25.

REFERENCES

1. JOHNSON, A.W. and SALLBERG, J.R. - Factors influencing test results. Bull. Highw. Res. Bd. No. 319, Washington, D.C., 1962, pp 1-2.

2. HER MAJESTY'S STATIONARY OFFICE - Soil mechanics for road engineers, London, 1964, pp 157-158.

3. ALLEN, H. (Ed.) - Compaction of earth embankments. Proc. Highw. Res. Bd. Washington, D.C., Vol 18(2), 1938, pp 142-184, Table on p 149.

4. JOSLIN, J.G. - Ohio's typical moisture-density curves, Symposium on Application of Soil Testing in Highway Design and Construction, ASTM Spec. Tech. Publ. 239, Philadelphia, 1959, pp 111-118.

5. TRANSPORTATION TECHNOLOGY SUPPORT FOR DEVELOPING COUNTRIES. - Compaction of roadway soils (Compendium 10) TRB, Washington, D.C., 1979, pp 20-68.

6. HER MAJESTY'S STATIONARY OFFICE - Soil mechanics for road engineers, London, 1964, pp 66-88, table between pp 66 and 67.

7. MAREK, C.R. and JONES, T.R. - Compaction - an essential ingredient for good base performance - Proc. Conf. on Utilization of Graded Aggregate Base Materials in Flexible Pavements (sponsored by NCSA and NSA) Oak Brook, Ill. 1974, pp IX-1 to IX-32, quote on p IX-3.

8. JOHNSON, A.W. and SALLBERG, J.R. - Factors influencing compaction test results, Bull. Highw. Res. Bd., No. 319, Washington, D.C., 1967, pp 81-98.

9. NOORANY, I. - Discussion of "Compaction control and the index unit weight" by Steve J Poulos. Geotechnical Testing Journal, GTJODJ, Vol. 13, No. 2, June 1990, pp 146-147.

10. ALLEN, H. (Ed) - Compaction of earth embankments . Proc. Highw. Res. Bd., Washington, D.C., Vol 18(2), 1938, pp 142-181, quotes on pp 142-143.

11. TURNBULL, W.J. and FOSTER, C.R. - Compaction of graded crushed stone base course. Proc. 4th Internat. Conf. on Soil Mechanics and Foundation Engineering, London, 1957, Vol. 2, pp 181-185.

12. LEE, P.J. and SUEDKAMP, R.J. - Characteristics of irregularly shaped compaction curves of soils. Highw. Res. Rec. No. 381, Washington, D.C., 1972, pp 1-9.

13. PIKE, D.C. - Compactability of graded aggregates: Standard laboratory tests. TRRL Laboratory Report 447, Crowthorne, Berkshire, 1972.

14. POULOS, S.J. - Compaction control and the index unit weight. Geotechnical Testing Journal, GTJODJ, Vol. 11, No. 2, June 1988, pp 100-108.

15. OLSON, R.E. - Effective stress theory of soil compaction. Journ. of Soil Mechanics and Foundation Division, Proc. Amer. Soc. Civ. Engrs., Vol. 89, 1963, pp 27-45.

16. ARQUIé, G. - Theorie generale de l'influence de la teneur en eau sur les resultats du compactage. Revue Generale des Pontes en des Aerodromes, No. 489, February 1973, pp 91-99. Dutch translation of article under the title Verdichting van grond. Wegen, The Hague, Vol. 47(8), 1973, pp 693-213 to 693-225.

17. MAREE, J.H. - Aspekte van die ontwerp en gedrag van plaveisels met korrelmateriaal kroonlae. D.Eng. Thesis, University of Pretoria, Pretoria, 1982, pp 4.1-4.34.

18. LEES, G. - The rational design of aggregate gradings for dense asphaltic compositions. Proc. of Assoc. of Asphalt Paving Technologists (Feb. 1970) (Vol. 34), Cushing-Malloy Inc, Ann Arbor, Michigan, 1971, pp 60-97.

19. HINDLEY, G. - A History of Roads. Peter Davies, London, 1971, quote on pp 30-31.

20. HINDLEY, G. - A History of Roads. Peter Davies, London, 1971, quote on p 75.

21. ENCYCLOPEDIA BRITTANICA, William Benton, London, 1963, Vol. 19, quote on p 341.

22. ENCYCLOPEDIA BRITTANICA, William Benton, London, 1963, Vol. 19, quote on p 342.

23. CASAGRANDE, A. - Classification and identification of soils, Trans. Amer. Soc. Civ. Engrs. Vol. 73(6), 1947, pp 783-810. Information on pp 784-787.

24. FULLER, W.B. and THOMPSON, S.E. - The laws of proportioning concrete. Trans. Amer. Soc. Civ. Engrs, Vol. 59, 1907, pp 67-143. Discussion 144-172, quotes on pp 71-72.

25. HUANG, E.Y., SQUIER, L.R. and TRIFFO, R.P. - Effect of geometric characteristics of coarse aggregates on compaction characteristics of soil-aggregate mixtures. Highw. Res. Rec. No. 22, 1963, pp 38-47.

26. HOGENTOGLER, C.A. and TERZAGHI, C. - Interrelationship of road, load and subgrade. Publ. Rds., Washington, D.C., Vol 10(3), 1929, pp 31-64.

27. ROTHFUCHS, G. - Wie sind möglichst dicthe (hohlraumarme) Asphalt- und Bitumenmischungen zu erzielen? Bitumen Vol. 5(3), 1935, pp 57-61.

28. TAYLOR, W. - Fundamentals of soil mechanics. John Wiley & Sons, New York, 1962, quote on p 70.

29. NATIONAL INSTITUTE FOR TRANSPORT AND ROAD RESEARCH - Guidelines for road construction material. TRH14, Pretoria, CSIR, 1985.

30. SWEERE, G.T.H. - Unbound granular bases for roads. Doctoral Thesis, Technical University of Delft, The Netherlands, 1990, pp 146-147.

31. LEES, G. - The measurement of particle shape and its influence in engineering materials. Reprinted from Journal of the British Granite and Whinstone Federation, 16 Berkeley Street, London, W.1., Vol, 4, No. 2, Autumn 1964, World Copyright A.4446.

32. VALLERGA, B.A., SEED, H.B., MONISMITH, C.L. and COOPER, R.S. - Effect of shape, size and surface roughness of aggregate particles on the strength of granular materials. A paper prepared for presentation at the 2nd Pacific Area Nat. Meeting on the Am. Soc. for Test. Materials, Los Angeles, California, Sept. 17-21, 1956 (elsewhere listed as ASTM STP 212, pp 63-76).

33. GUR, Y., SHLARSKY, E. and LIVNEH, M. - Effect of course-fraction flakiness on the strength of graded materials. Proc. of Third Asian Regional Conf. on Soil Mech. and Fndn Engng, Haifa, 25-28 Sept. 1967, Jerusalem Academic Press, Vol. 1, pp 276-281.

34. PIKE, D.C. - Shear-box tests on graded aggregates. TRRL Laboratory Report 584, Crowthorne, Berkshire, 1973.

35. HOLUBEC, I. and D'APPOLONIA, E. - Effect of particle shape on the engineering properties of granular soils in evaluation of relative density and its role in geotechnical projects involving cohesiveless soils. (Editors Selig, E.J. and Ladd, R.S.), ASTM Publication STP 523, Baltimore, 1973, pp 304-318.

36. HOLTZ, W.G. and GIBBS, H.J. - Triaxial shear tests on gravelly soils. Jl of Soil Mech, and Fndn Engng Div. ASCE, Vol. 82, No. SM1, Proc. Paper 867, January 1956, pp 1-22.

37. MARACHI, D.N., CHAN, C.K. and SEED, H.B. - Evaluation of properties of rockfill materials. Jl of Soil Mech. and Fndn Engng Div. ASCE, Vol. 98, No. SM1, Proc. Paper 8672, January 1972, pp 95-114.

38. KOERNER, R.M. - Effects of particle characteristics on soil strength. Jl of Soil Mech. and Fndn Engng Div. ASCE, Vol. 96, No. SM4, Proc. Paper 7393, July 1970, pp 1221-1234.

39. MARSAL, R.J. - Large scale testing of rockfill materials. Jl of Soil Mech. and Fndn Engng Div. ASCE, Vol. 93, No. SM2, Proc. Paper 5128, March 1967, pp 27-43.

40. GEORGE, K.P. and STARK, N.S. - Dilatancy of granular media in triaxial shear. Transp. Res. Rec. No 497, pp 88-95.

41. BARKSDALE, R.D. and ITANI, S.Y. Influence of aggregate shape on base behaviour. Paper No. 830573, prepared for presentation at the 1989 TRB Meeting, April 1989.

42. BRITISH STANDARDS INSTITUTION - Methods of sampling and testing of mineral aggregates, sands and fillers. British Standard BS. 812, London, 1967.

43. ISHAI, I. and TONS, E. - Concept and test method for a unified characterization of the geometric irregularities of aggregate particles. ASTM Journ. of Testing and Evaluation, Vol 5(1), 1977, pp 3-15.

44. VAN DER MERWE, C.J. - Factors affecting the compaction of crushed stone. M.Sc (Eng) Thesis, University of Pretoria, 1984, pp 118-141.

45. HOGENTOGLER, C.A. and TERZAGHI, C. - Interrelationship of load, road and subgrade, Publ. Rds. Washington, D.C., Vol 10(3), 1929, pp 31-64.

46. SWAMINATHAN, C.G., LAL, N.B. and BINDRA, S.R. - A study on the compaction characteristics of soils in India. Proc. int. conf. on compaction, Paris, 1980, Vol. 1, pp 81-85.

47. YUDHBIR, RAYMAHASHAY, B.C. and SAHU, B.K. - Compaction characteristics of clay-mineral mixtures. Proc. int. conf. on compaction, Paris 1980, Vol. 1, pp 93-98.

48. LAMBE, T.W. - Soil stabilization In: Foundation Engineering. Leonards, G. (Ed.), McGraw-Hill, New York, 1962, pp 354-363.

49. SCOTT, R.F. - Principles of soil mechanics. Addison-Wesiley, Reading, Massachusetts, 1963, pp 291-294.

50. PINTO, A.V. - Research applied to rockfill materials. LNEC Proc. 3/13/7384, Lisbon, 1987, pp 65-92.

51. SPANGLER, M.G. and HANDY, R.L. - Soil Engineering. Harper & Row, New York, 1982, p 320.

52. MAREE, H.J. - Aspekte van die ontwerp en gedrag van plaveisels met korrelmateriaal kroonlae. D.Eng. Thesis, University of Pretoria, Pretoria, 1982, p 4.17.

53. VENTER, J.P. - The engineering properties and roadbuilding characteristics of mudrocks, with special reference to Southern Africa. D.Sc Thesis, University of Pretoria, Pretoria, 1980, pp 288-296.

54. COMMITTEE FOR STATE ROAD AUTHORITIES (CSRA). Standard specifications for road and bridge works (Vol. 2) (Ed. 1). Clause 3305, Treating the roadbed, December 1987, ISBN 0 7991 0422-1, pp 3300-3 to 3300-4.

55. ALLEN, H. (Ed.) - Compaction of earth embankments. Proc. High. Res. Bd. Washington, D.C., Vol. 18(2), 1938, pp 142-181, quote on p 174.

56. PORTER, O.J. - Foundations for flexible pavements. Proc. High. Res. Bd., Vol. 22, 1942, pp 100-143, quote on p 108.

57. EMERY, S.J. - Prediction of moisture content for use in pavement design. PhD Thesis, University of the Witwatersrand, Johannesburg, 1985, pp 107-142.

58. LUBKING, P., JANSE, E., JONKER, J.F. and DE JAGER, W.F.J. - Investigation of the variation of density, rigidity and bearing capacity measuring results on behalf of the acceptance control of sand subbases. Proc. int. conf. on compaction, Paris, 1980, Vol. 2, pp 515-521.

59. HER MAJESTY'S STATIONARY OFFICE - Soil mechanics for road engineers. London, 1964, p 169.

60. SWEERE, G.T.H. - Unbound granular bases for roads. Doctoral Thesis, Technical University of Delft, the Netherlands, 1990, p 196.

61. MAREE, J.H. - Aspekte van die ontwerp en gedrag van plaveisels met korrelmateriaal kroonlae. D.Eng. Thesis, University of Pretoria, Pretoria, 1978, p 4.20 (Table 4.10).

62. SPANGLER, M.G. and HANDY, R.L. - Soil engineering. Harper & Row, New York, 1982, p 194.

63. MAREE, J.H. - Ontwerpparameters vir klipslag in plaveisels. M.Sc (Eng) Thesis, University of Pretoria, Pretoria, 1978, pp 58-62.

64. SPANGLER, M.G. and HANDY, R.L. - Soil engineering. Harper & Row, Yew York, 1982, pp 185-188.

65. HORAK, E. (Compiler). - Ondersoek na die stabilisasie van sande en kleie vir operasionele paaie en stofdigting van vliegvelde en helikopterlandingstroke. Report C/PAD/20.1, NITRR, CSIR, Pretoria, March 1981.

66. SHACKLETON, M.C. - Permanent deformation in pavements with granular bases and subbases. Draft Contract Report DPVT/C 164.1, DRTT, CSIR, July 1990.

67. SEMMELINK, C.J. - Designing lightly trafficked roads - Lets change our attitudes. Report TC/43/80, NITRR, CSIR, Pretoria, 1980.

APPENDIX A

LIST OF TERMS AND THEIR MEANINGS

The Britanica World Language Edition of the Oxford Dictionary defines the terms "compact" and "ability" or "ibility" as follows:

Compact:	to join or knit (things) firmly and tightly together or to each other, to consolidate; to condense; solidify.
Consolidate:	(1) to make solid; to form into a solid mass; to solidify.
	(2) to make firm or strong; to strengthen.
Condense:	to make dense; increase the density of; to reduce in volume; to compress.
Solidify:	to render solid; to make firm, hard or compact.
Ability:	capacity in an agent, bodily or mental power.
Capacity:	the power, ability or faculty for anything in particular.

Webster's Third International Dictionary defines the terms as follows:

Compact:	to press together (as parts, components), dense, suggesting firmness, roundness and a degree of strength.
Ability:	the quality of state of being able.
	-ability; -ibiliity: capacity, fitness or tendency to act or be acted on in a (specified) way.

McGraw-Hill's Dictionary of Science and Technical Terms (Second Edition) has the following definitions:

Compaction:	(Geological) Process by which soil and sediment mass loses pore space in response to increasing weight of overlying material; (Engineering) Increasing the dry density of granular material, particularly soil, by means such as impact or by rolling the surface layers.
Compactor:	(Mechanical Engineering) Machine designed to consolidate earth and paving materials by kneading, weight, vibration, or impact, to sustain loads greater than those sustained in an uncompacted state.

APPENDIX B

CALIBRATION OF THE VIBRATORY COMPACTION TABLE

B.1 General

Because the aim of the investigation was to determine the effect of the different material properties on the compactability, it was very important that the laboratory method of compaction should simulate practice as closely as possible. This meant that laboratory samples would have to be compacted in a single layer instead of five or three thin layers as is the case with the mod. AASHTO and std. AASTHO compaction tests respectively. The only method which complied with this test requirement was the vibratory compaction test.

A large range of vibratory rollers are available on the market with a range of "frequency-amplitude" combinations. To determine the separate effects of frequency and amplitude of vibratory compaction on the compactability of roadbuilding materials it was also necessary to test materials at different "frequency-amplitude" combinations. For this reason it was decided to build a vibratory compaction table on which both the frequency and amplitude could be adjusted to cover the basic range of "frequency-amplitude" combinations of the different vibratory rollers (see Chapter 4 for discussion of this aspect).

As this is not a standard piece of laboratory equipment, it had to be custom-built and calibrated. The basic vibratory table was manufactured by VIBRAMECH, a company which specializes in the design and manufacture of vibratory equipment for the industry such as vibrating screens and conveyer systems used by the mining industry.

The purpose of the calibration process was to be able to set the two input variables of the vibratory compaction table, namely the frequency and amplitude, in relation to the total mass of the mould, sample and surcharge on the table.

B.2 Description of the vibratory table

A schematic diagram of the vibratory table is shown in Figure B.1. It basically consists of three sections namely a base, spring system and vibrating table top. The table top consists of a thick metal plate (600 mm by 600 mm) mounted on a steel frame with the electric motor supplying the vibratory force mounted on the bottom side of the top frame. The vibratory motor is a standard electric motor built specifically for vibratory purposes, with extra heavy duty bearings and two eccentric weights mounted on the drive shaft on each side of the electric motor itself. The eccentric weights provide an eccentric force which causes the table top to vibrate. The 1,1 kW motor can deliver a maximum force of 23,5 kN. The spring system consists of four torsional springs which assist in limiting the horizontal movement of the table

top while leaving it free to move up and down in a vertical direction. The base consists of 600 mm by 600 mm square footing of hollow square tubing which has been filled with lead shot and which is mounted on four rubber footings to limit transfer of the vibration to the surroundings. The speed control unit is a standard unit manufactured by Danfoss which makes it possible to vary the speed of the motor between approximately 720 rpm (12 Hz) and 3600 rpm (60 Hz). The magnitude of the amplitude of the table is controlled by the angle between the two eccentric weights on each side of the drive motor and can be set accurately by means of the k-setting scale (see discussion later on).

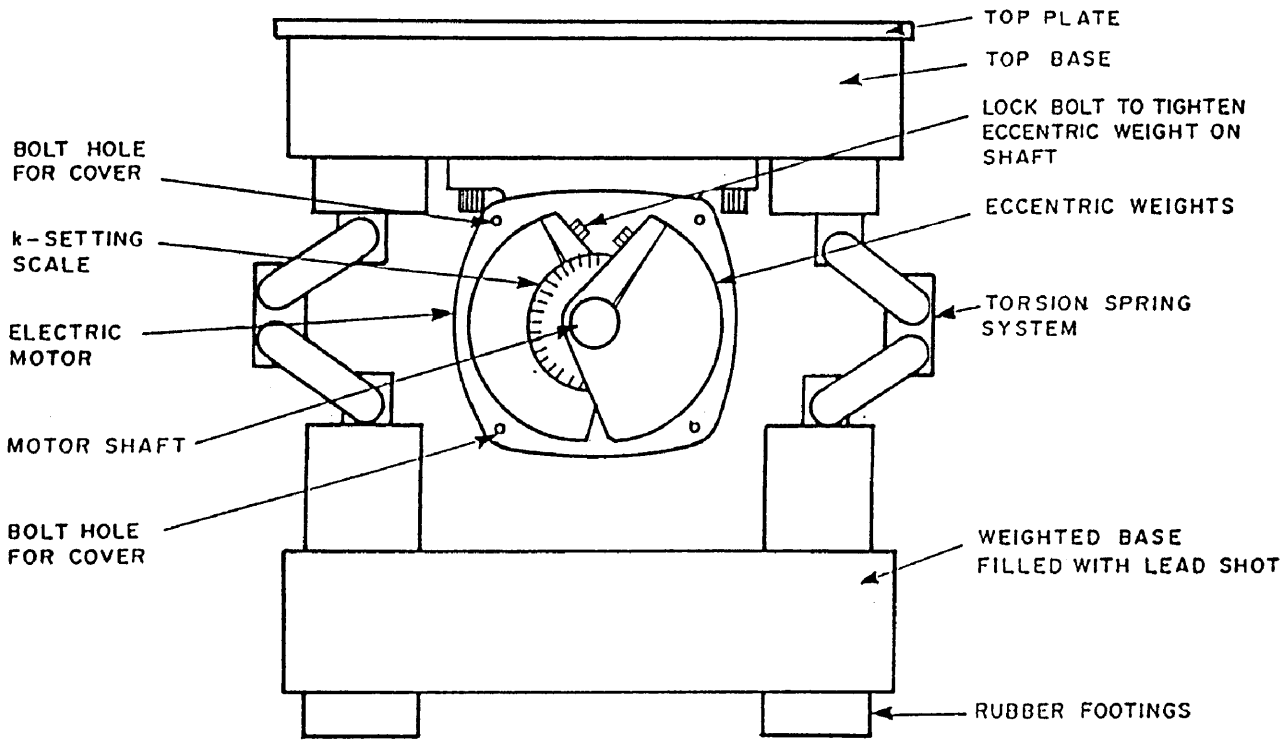

FIGURE B.1 SCHEMATIC ILLUSTRATION OF VIBRATORY COMPACTION TABLE

B.3 Method of calibration

B.3.1 Frequency calibration

The frequency calibration was fairly straight forward as the frequency is practically solely dependent on the gauge-setting of the vernier dial gauge rheostat on top of the speed control unit.

However, because the initial torque requirements to get the motor started varied with the percentage of the eccentric moment being used (position of weights on motor drive shaft) (ie k-setting), it was not possible to use one calibration curve for the frequency setting for all the k-settings.

Two frequency curves were determined for initial use:

(i) One for maximum k-settings between 55 % and 100 %
(ii) One for maximum k-settings between 0 % and 55 %.

Apart from the vernier dial gauge rheostat mounted on top of the speed control unit, the speed control unit uses a number of other rheostats which are mounted inside the control box to control the turning speed of the motor.

For the adjustment of the initial torque requirement of the drive motor the uppermost rheostat on the control unit panel inside the box had to be adjusted (between 100 % and 200 %). However, the maximum frequency of the table was influenced by this setting (the lower this value, the lower the maximum frequency). This meant that for each setting of this rheostat a separate calibration curve was required.

Because the only "fixed" points on the scale, namely 100 % and 200 %, were not satisfactory for our requirements as far as frequency-amplitude combinations were concerned, a small vernier dial gauge was mounted over this rheostat to enable fairly accurate setting in between the 100 % and 200 % marks. For the first frequency calibration scale (k-settings between 55 % and 100 %) the reading on this vernier scale was set to 15. For the second frequency calibration scale (k-settings between 0 % and 55 %) the reading on this vernier scale was set to 90.

The exact frequency of the vibratory table was then determined by means of an accelerometer, mounted on the vibrating surface, coupled to a spectrum analyser, for dial gauge-settings of the vernier dial gauge on top of the speed control unit from 0 to 1000 in steps of 50 units.

To test whether repeated vernier dial guage-settings of the rheostat inside the control box to the values of 15 and 90 gave similar readings as before, four sets of readings (alternating between these two settings) were taken at each dial gauge-setting. The repeatability was found to be excellent (as can be seen in Tables B.1(a) and B.1(b)). It was therefore assumed that for a particular gauge-setting on this internal dial gauge one would have a "fixed" calibration curve for dial gauge-settings of the external vernier dial gauge.

The mathematical function of the dial gauge-setting for a particular frequency was then determined by means of polynomial regression from the mean frequency values for the two internal dial gauge-settings (ie 15 and 90). In both cases separate functions had to be determined for dial gauge-settings from 0 to 500 and 500 to 1000 respectively (see Figures B.2(a) and B.2(b)). All four mathematical functions (ie for 0 - 500 (15), 500 - 1000 (15), 0 - 500 (90), 500 - 1000 (90)) were very highly correlated (the lowest r^2-value was 0,99995). With these functions it was possible to compile a table of dial gauge-settings for particular frequency values. To ensure that the drive motor was not damaged, the maximum allowable percentage (k) of the maximum eccentric moment also had to be specified (see Tables B.2(a) and B.2(b)).

It was subsequently found that the eccentric weight-setting (k) had a slight influence on the frequency value. A new calibration was done for the internal dial setting of 15 with the eccentric weight-setting at 55 % (to enable it to cover the full lower frequency range), because the first calibrations for both internal dial settings had been done at an eccentric weight-setting of 20 % (see Table B.3).

Table B.1(a) - Frequency measurements for internal dial gauge-setting = 15

Dial-setting	Test 1 (Hz)	Test 2 (Hz)	Test 3 (Hz)	Test 4 (Hz)	Mean (Hz)	Std.dev (Hz)
0	11,3223	11,4714	11,5000	11,5076	11,450325	0,086761
50	12,3461	12,8474	12,5198	12,5196	12,558225	0,209434
100	13,3223	13,4810	13,5168	13,7230	13,510775	0,164808
150	14,3170	14,4573	14,4858	14,5203	14,445100	0,089200
200	15,2946	15,4265	15,4512	15,4561	15,407100	0,076110
250	16,2429	16,3922	16,4207	16,4213	16,369275	0,085337
300	17,1942	17,3086	17,3523	17,3446	17,299925	0,073011
350	18,1460	18,2600	18,3044	18,3005	18,252725	0,073928
400	19,0977	19,2097	19,2578	19,2388	19,201000	0,071651
450	20,0835	20,1614	20,2058	20,1943	20,161250	0,055143
500	21,0337	21,1062	21,1353	21,1567	21,107975	0,053668
550	21,9807	22,0925	22,1125	22,1228	22,077125	0,065503
600	22,9453	23,0513	23,0698	23,1060	23,043100	0,069044
650	23,9287	24,0686	24,0784	24,0759	24,037900	0,072919
700	24,9512	25,0728	25,0601	25,1084	25,048125	0,067774
750	26,1304	26,0513	26,1113	26,0639	26,089225	0,037693
800	26,9829	27,1694	27,0796	27,1372	27,092275	0,081833
850	28,0908	28,2139	28,1831	28,2231	28,177725	0,060422
900	29,1987	29,3457	29,2949	29,3550	29,298575	0,071631
950	30,4019	30,5342	30,4556	30,5435	30,483800	0,067348
1000	31,5806	31,7275	31,7129	31,7349	31,688975	0,072826

Table B.1(b) - Frequency measurements for internal dial gauge-setting = 90

Dial-setting	Test 1 (Hz)	Test 2 (Hz)	Test 3 (Hz)	Test 4 (Hz)	Mean (Hz)	Std.dev (Hz)
0	17,6152	17,6771	17,5966	17,6490	17,634475	0,035749
50	19,5197	19,2131	19,1724	19,2151	19,280075	0,160957
100	20,7466	20,7896	20,7090	20,7874	20,758150	0,038270
150	22,2766	22,3250	22,2405	22,3044	22,286625	0,036591
200	23,7886	23,8223	23,7119	23,7773	23,775025	0,046221
250	25,2524	25,2871	25,1885	25,2458	25,243450	0,040867
300	26,7383	26,7646	26,5908	26,6733	26,691750	0,077471
350	28,2207	28,2241	28,0039	28,0947	28,135850	0,106602
400	29,5786	29,6030	29,3984	29,4888	29,517200	0,093187
450	30,9834	31,0024	30,7959	30,8711	30,913200	0,097325
500	32,3042	32,3848	32,2187	32,2812	32,297225	0,068656
550	33,7422	33,8340	33,6260	33,7114	33,728400	0,085861
600	35,0952	35,2271	35,0830	35,1338	35,134775	0,065247
650	36,6030	36,6201	36,5762	36,6519	36,612800	0,031716
700	38,1333	38,1270	38,1230	38,1938	38,144275	0,033288
750	39,6348	39,7134	39,7124	39,8091	39,717425	0,071350
800	41,2622	41,3555	41,3687	41,4507	41,359275	0,077212
850	42,9580	43,1260	43,0713	43,1611	43,079100	0,088787
900	44,6787	44,8623	44,8076	44,8857	44,808575	0,092562
950	46,5244	46,6807	46,6729	46,7646	46,660650	0,099869
1000	48,4199	48,5693	48,5967	48,7148	48,575175	0,121248

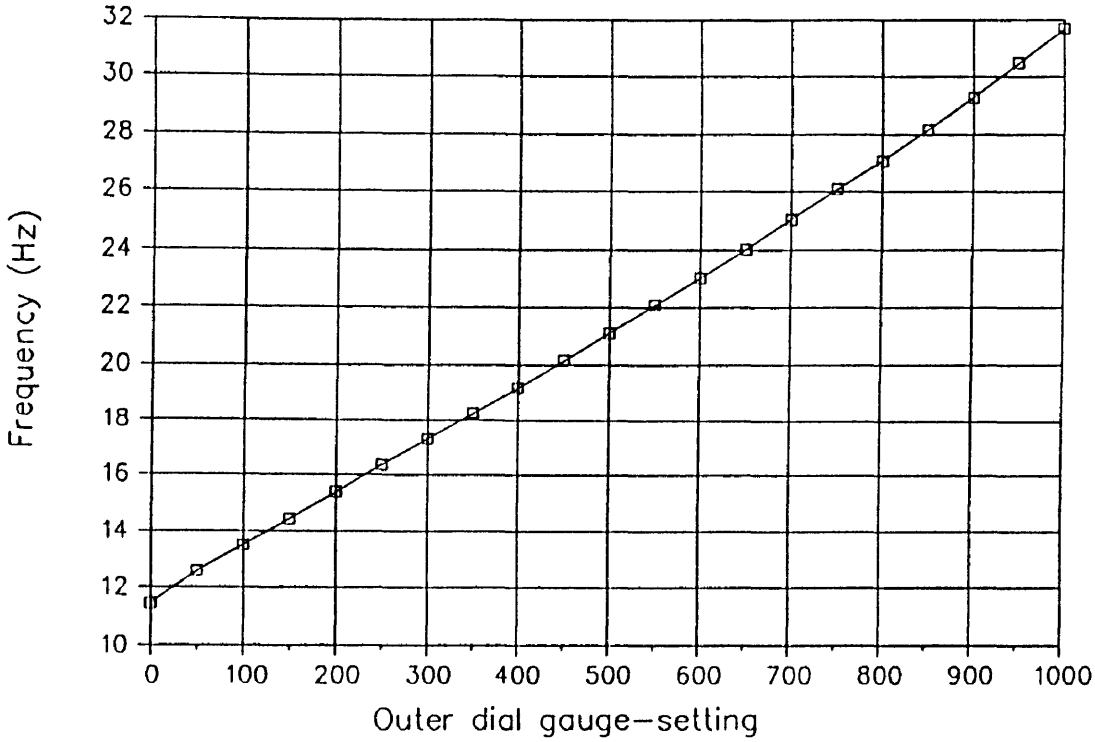

FIGURE B.2(a) **VIBRATORY TABLE FREQUENCY AGAINST OUTER DIAL GAUGE-SETTING FOR DIAL GAUGE-SETTING FOR RHEOSTAT INSIDE CONTROL BOX = 15**

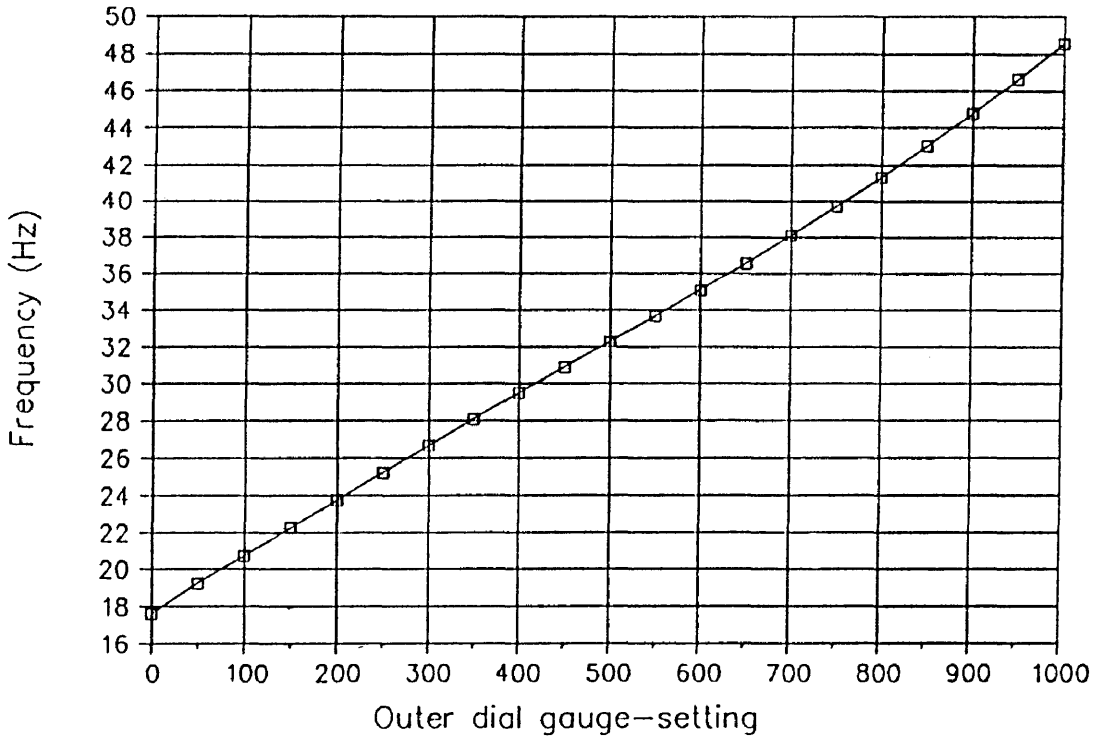

FIGURE B.2(b) **VIBRATORY TABLE FREQUENCY AGAINST OUTER DIAL GAUGE-SETTING FOR DIAL GAUGE-SETTING FOR THEOSTAT INSIDE CONTROL BOX = 90**

Table B.2(a) - Outer dial gauge-setting for required frequency
(internal dial gauge-setting = 15)(k = 20)

Frequency (Hz)	Dial-setting	Max. k-setting
12,0	24,7	100,0
12,5	50,1	100,0
13,0	75,7	100,0
13,5	101,3	100,0
14,0	127,1	100,0
14,5	152,9	100,0
15,0	178,7	100,0
15,5	204,7	100,0
16,0	230,7	100,0
16,5	256,8	100,0
17,0	283,0	100,0
17,5	309,3	100,0
18,0	335,6	100,0
18,5	362,0	100,0
19,0	388,5	100,0
19,5	415,1	100,0
20,0	441,8	100,0
20,5	468,5	100,0
21,0	495,3	100,0
21,5	519,8	100,0
22,0	546,2	100,0
22,5	572,3	100,0
23,0	598,1	100,0
23,5	623,7	100,0
24,0	648,9	100,0
24,5	673,9	96,0
25,0	698,6	92,2
25,5	723,0	88,6
26,0	747,1	85,2
26,5	770,9	82,0
27,0	794,4	79,0
27,5	817,6	76,2
28,0	840,6	73,5
28,5	863,2	70,9
29,0	885,6	68,5
29,5	907,8	66,2
30,0	929,5	64,0
30,5	951,0	61,9
31,0	972,2	59,9
31,5	993,1	58,0

Table B.2(b) - Outer dial gauge-setting for required frequency

(internal dial gauge-setting = 90)(k = 20)

Frequency (Hz)	Dial-setting	Max. k-setting
18,0	10,7	100,0
19,0	42,6	100,0
20,0	74,9	100,0
21,0	107,5	100,0
22,0	140,5	100,0
23,0	173,8	100,0
24,0	207,5	100,0
25,0	241,5	92,2
26,0	275,9	85,2
27,0	310,6	79,0
28,0	345,7	73,5
29,0	381,1	68,5
30,0	416,9	64,0
31,0	453,0	59,9
32,0	489,4	56,3
33,0	525,0	52,9
34,0	560,4	49,8
35,0	595,1	47,0
36,0	629,1	44,4
37,0	662,5	42,1
38,0	695,1	39,9
39,0	727,1	37,9
40,0	758,5	36,0
41,0	789,2	34,3
42,0	819,2	32,7
43,0	848,5	31,2
44,0	877,2	29,8
45,0	905,1	28,4
46,0	932,5	27,2
47,0	959,1	26,1
48,0	985,1	25,0

Table B.3 - Outer dial gauge-setting for required frequency

(internal dial gauge-setting = 15)(k = 55)

Frequency (Hz)	Dial-setting	Max. k-setting
11,5	6,3	100,0
12,0	31,9	100,0
12,5	57,5	100,0
13,0	83,2	100,0
13,5	109,1	100,0
14,0	135,0	100,0
14,5	161,1	100,0
15,0	187,2	100,0
15,5	213,5	100,0
16,0	239,8	100,0
16,5	266,2	100,0
17,0	292,8	100,0
17,5	319,4	100,0
18,0	346,2	100,0
18,5	373,1	100,0
19,0	400,0	100,0
19,5	427,1	100,0
20,0	454,2	100,0
20,5	481,5	100,0
21,0	505,9	100,0
21,5	533,1	100,0
22,0	559,9	100,0
22,5	586,4	100,0
23,0	612,5	100,0
23,5	638,2	100,0
24,0	663,6	100,0
24,5	688,7	96,0
25,0	713,3	92,2
25,5	737,6	88,6
26,0	761,6	85,2
26,5	785,2	82,0
27,0	808,4	79,0
27,5	831,2	76,2
28,0	853,7	73,5
28,5	875,9	70,9
29,0	897,6	68,5
29,5	919,0	66,2
30,0	940,1	64,0
30,5	960,8	61,9
31,0	981,1	59,9
31,5	1001,0	58,0

B.3.2 Amplitude calibration

To determine the amplitude of the vibrating table for a particular eccentric weight-setting use was made of the same accelerometer and spectrum analyser to measure the rate of acceleration from which the amplitude could then be calculated.

B.3.2.1 Theory used to determine the amplitude

Assuming that both m and r are constant for the eccentric weights the value of the "fixed eccentric moment" is as follows:

Eccentric moment (fixed) = m.r

where m = total mass of the eccentric weights (kg)
and r = eccentricity of the centre of gravity of the eccentric weights from the centre line of the shaft (mm)

Variable eccentric moment = k.m.r

where k = (percentage weight-setting)/100

Nominal amplitude of the vibratory table = A

$$= (k.m.r)/M$$

where M = mass of table top plus motor plus mass on top of table

Centrifugal force $= k.m.r.\omega^2$

$= k.m.r.4\pi^2.f^2$

where ω = speed of rotation (radians/sec)
and f = turning frequency of the motor (Hz)

Table acceleration "a" $= (k.m.r.4\pi^2.f^2)/M$

$= (M.A.4\pi^2.f^2)/M$ (because M.A = k.m.r)

$= A.4\pi^2.f^2$

Therefore $A = a/(4\pi^2.f^2)$

With both the values of M and A known it is possible to determine the fixed eccentric moment

$m.r = (M.A)/k$

$= [(243+m1).A]/k$

where $m1$ = mass on top of table and the mass of the table top plus motor is equal to 243 kg.

The output signal of the accelerometer is in terms of volts. Because the signals are often very small and vary over a wide range the spectrum analyser converts the output signal to dBr (a logarithmic scale).

$dBr = 20 \log [(\text{measured V})/(\text{reference V})]$

$= 20 [\log V_m - \log V_{ref}]$

Therefore $\log V_m = dBr/20 + \log V_{ref}$

and $V_m = 10^{(dBr/20 + \log Vref)}$

where V_m = measured voltage, and

V_{ref} = reference voltage

The accelerometer measures a certain number of millivolts per "g"(g=9,81 m/s^2). For the particular accelerometer used the value is 9,77 millivolts/g. Therefore the rate of acceleration "a"(m/s^2) of the table was determined by dividing V_m by 0,00977 and multiplying this value by 9,81.

B.3.2.2 Practical execution of the calibration process

In the practical execution of the amplitude calibration use was made of five weights which each had a mass of approximately 40 kg and were fixed to the table top by means of a simple bracket system whereby the mass on the table could be varied from 0 kg to approximately 200 kg. For each weight-setting of the eccentric weights a full set of readings were taken through the whole allowable frequency range measuring the acceleration at each frequency-setting for the different amounts of mass on the table. From the rate of acceleration it was then possible to determine the amplitude and with the amplitude known it was possible to determine the "fixed eccentric moment".

Because the original weight-setting scales mounted on the ends of the drive shaft of the vibratory motor were very rough (scale in steps of 10 %) larger scales were manufactured by the Division Workshop. Basically the scale value is zero when the two eccentric weights mounted on one side of the electric motor are exactly opposite each other (180° apart) and

at 100 % when they are exactly on top of one another. The angle between the two weights on the right hand side of the motor can therefore be determined for any percentage by the following simple equation (see Figure B.3).

Angle between the two weights $= 2\theta$

$= 2.\cos^{-1}(\text{percentage}/100)$

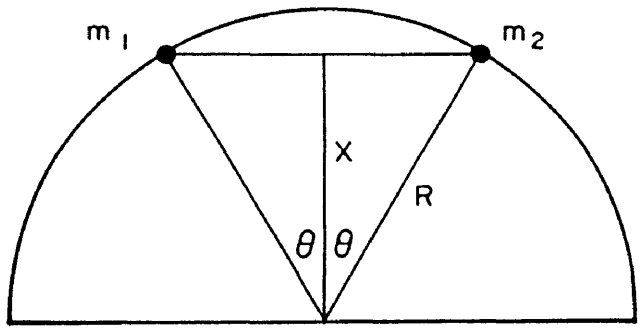

k = percentage/100 =X/R

FIGURE B.3 DIAGRAMMATIC ILLUSTRATION OF WEIGHT-SETTING SCALE THEORY.

A scale was therefore manufactured for percentage intervals of one per cent. It should be noted that the scales at opposite ends of the electric motor are not the same because the direction of rotation is the opposite from the other side. The scale on the left hand side of the motor is in actual fact a mirror image of the right hand side scale. Therefore the angle between the two weights for the scale on the left hand side of the drive motor is equal to the following (see Figure B.4).

Angle between the two weights $= 180 - 2\theta$

$= 180 - 2.\cos^{-1}(\text{percentage}/100)$

B.3.2.3 Determination of the amplitude calibration from the practical measurements

Theoretically the amplitude is not dependent on the frequency. This is verified by our measurements because the measured amplitudes differed by a fraction of a millimetre through the whole frequency range (the larger values occurring at the low frequency side).

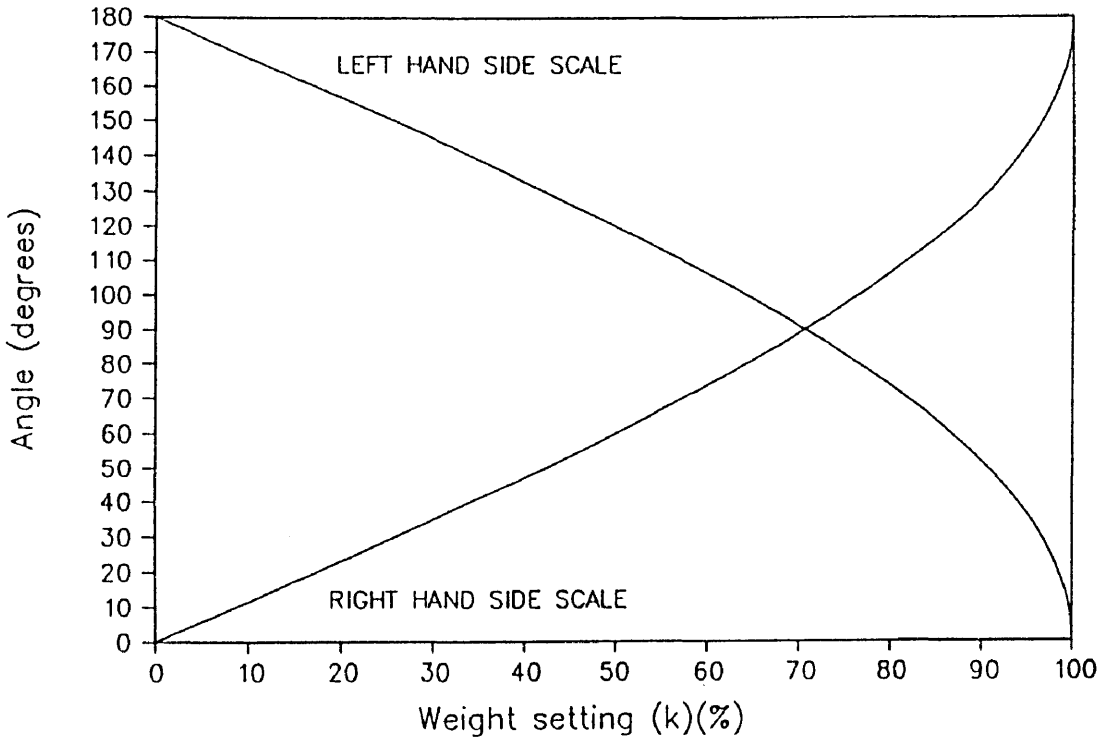

FIGURE B.4 ANGLES BETWEEN WEIGHTS FOR DIFFERENT WEIGHT-SETTINGS

Theoretically the fixed eccentric moment should also be constant. However our measurements showed that this was not the case. It changed with the percentage weight-setting from 0 % to approximately 35 % after which it remained more or less constant (see Figure B.5). The most likely cause for this variation is the damping effect of the torsional spring system. According to manufacturers' specifications the "fixed eccentric moment" of the motor is equal to 4167 kg-mm. The measured maximum effective "fixed eccentric moment" of the vibratory table is approximately 1729 kg-mm. The theoretical equation of the first part of the "fixed eccentric moment" was also determined by polynomial regression. The theoretical value of the second part was taken to be the mean of the measured values. Once the value of the fixed eccentric moment was known for any percentage weight-setting it was possible to determine the variable eccentric moment for any percentage weight-setting.

Because k.m.r = (243+m1).A, it is possible to determine the value of k.m.r for any value of m1 and "A" respectively and from the required value of k.m.r the required value of k (the percentage weight-setting). A table was then compiled for the required weight-setting k for values of "A" varying from 0,5 mm to 4,0 mm in steps of 0,5 mm and m1 varying from 50 kg to 300 kg in steps of 5 kg (see Table B.4).

After this random checks were made to verify whether the calibration was correct (see Figures B.6(a) and B.6(b)). From Figures B.6(a) and B.6(b) it is clear that the initial amplitude calibration of the vibratory table agreed very closely with the specified amplitude values (the

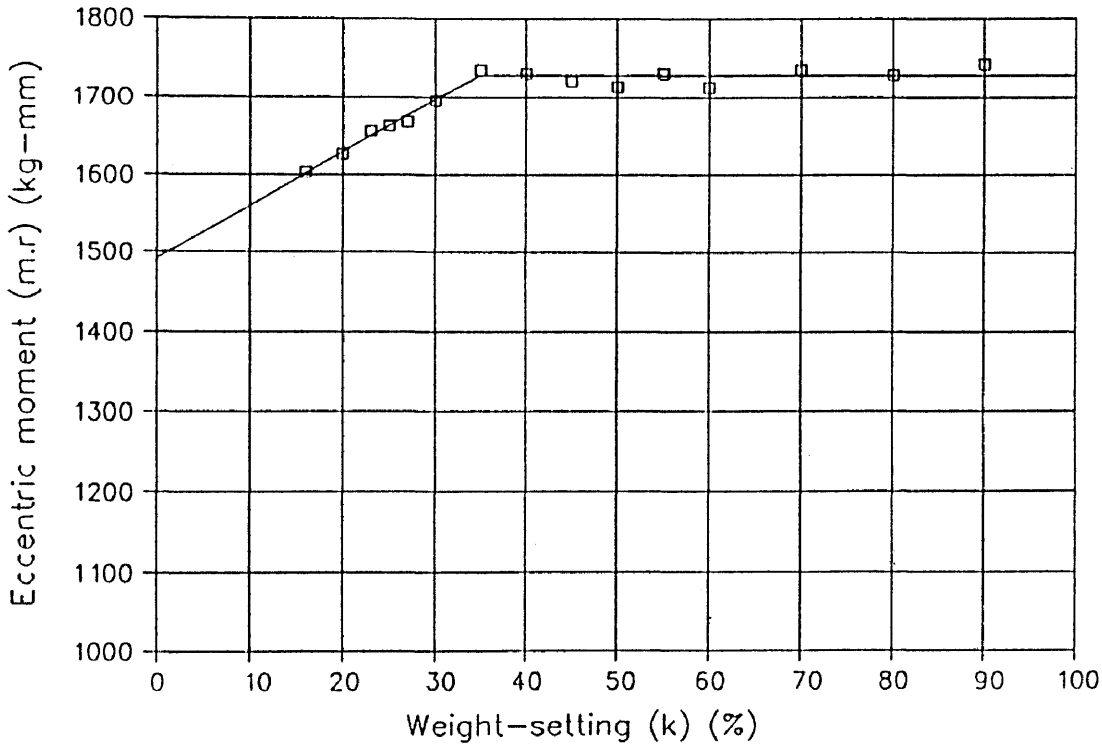

FIGURE B.5 VALUE OF "FIXED ECCENTRIC MOMENT" FOR DIFFERENT WEIGHT-SETTINGS (k)

r^2-value for the full frequency range is 0,995 and the r^2-value for 20 Hz and above was 0,999). However the measured amplitude values were slightly lower than the specified values for the frequency range above 20 Hz ($A_{measured}$ = 0,990292. $A_{specified}$ - 0,01879). The calibration table was therefore adjusted to take account of this small difference (see Table B.5).

B.3 Concluding remarks

Because of the variation in the "fixed eccentric moment" for k-settings up to 35 % k-settings greater than 35 were used most times for different frequency-amplitude combinations to ensure that the total compactive energy per unit time would be the same for the different combinations. The combinations mostly used were 30Hz - 64 %, 35Hz - 47 % and 40 Hz - 36 % for which $k.f^2$ is constant.

TABLE B.4 **Original calibration table for the values of k depending on the mass on the table and required amplitude**

	Required amplitude(mm)							
	0,5	1,0	1,5	2,0	2,5	3,0	3,5	4,0
mass(kg)								
50,0	9,4	18,1	26,3	34,0	42,4	50,8	59,3	67,8
55,0	9,6	18,4	26,7	34,5	43,1	51,7	60,3	68,9
60,0	9,7	18,7	27,1	35,0	43,8	52,6	61,3	70,1
65,0	9,9	19,0	27,5	35,6	44,5	53,4	62,3	71,3
70,0	10,0	19,3	27,9	36,2	45,3	54,3	63,4	72,4
75,0	10,2	19,6	28,3	36,8	46,0	55,2	64,4	73,6
80,0	10,3	19,8	28,7	37,4	46,7	56,0	65,4	74,7
85,0	10,5	20,1	29,1	37,9	47,4	56,9	66,4	75,9
90,0	10,6	20,4	29,5	38,5	48,1	57,8	67,4	77,0
95,0	10,8	20,7	29,9	39,1	48,9	58,6	68,4	78,2
100,0	10,9	21,0	30,3	39,7	49,6	59,5	69,4	79,4
105,0	11,1	21,2	30,7	40,3	50,3	60,4	70,4	80,5
110,0	11,2	21,5	31,1	40,8	51,0	61,2	71,5	81,7
115,0	11,4	21,8	31,5	41,4	51,8	62,1	72,5	82,8
120,0	11,6	22,1	31,8	42,0	52,5	63,0	73,5	84,0
125,0	11,7	22,4	32,2	42,6	53,2	63,9	74,5	85,1
130,0	11,9	22,6	32,6	43,1	53,9	64,7	75,5	86,3
135,0	12,0	22,9	33,0	43,7	54,7	65,6	76,5	87,5
140,0	12,2	23,2	33,4	44,3	55,4	66,5	77,5	88,6
145,0	12,3	23,5	33,8	44,9	56,1	67,3	78,5	89,8
150,0	12,5	23,7	34,2	45,5	56,8	68,2	79,6	90,9
155,0	12,6	24,0	34,6	46,0	57,5	69,1	80,6	92,1
160,0	12,8	24,3	34,9	46,6	58,3	69,9	81,6	93,2
165,0	12,9	24,6	35,4	47,2	59,0	70,8	82,6	94,4
170,0	13,1	24,8	35,8	47,8	59,7	71,7	83,6	95,5
175,0	13,2	25,1	36,3	48,4	60,4	72,5	84,6	96,7
180,0	13,4	25,4	36,7	48,9	61,2	73,4	85,6	97,9
185,0	13,5	25,7	37,1	49,5	61,9	74,3	86,6	99,0
190,0	13,7	25,9	37,6	50,1	62,6	75,1	87,7	****
195,0	13,8	26,2	38,0	50,7	63,3	76,0	88,7	****
200,0	14,0	26,5	38,4	51,2	64,1	76,9	89,7	****
205,0	14,1	26,7	38,9	51,8	64,8	77,7	90,7	****
210,0	14,2	27,0	39,3	52,4	65,5	78,6	91,7	****
215,0	14,4	27,3	39,7	53,0	66,2	79,5	92,7	****
220,0	14,5	27,5	40,2	53,6	66,9	80,3	93,7	****
225,0	14,7	27,8	40,6	54,1	67,7	81,2	94,7	****
230,0	14,8	28,1	41,0	54,7	68,4	82,1	95,8	****
235,0	15,0	28,3	41,5	55,3	69,1	82,9	96,8	****
240,0	15,1	28,6	41,9	55,9	69,8	83,8	97,8	****
245,0	15,3	28,9	42,3	56,4	70,6	84,7	98,8	****
250,0	15,4	29,1	42,8	57,0	71,3	85,5	99,8	****
255,0	15,6	29,4	43,2	57,6	72,0	86,4	****	****
260,0	15,7	29,7	43,6	58,2	72,7	87,3	****	****
265,0	15,9	29,9	44,1	58,8	73,5	88,1	****	****
270,0	16,0	30,2	44,5	59,3	74,2	89,0	****	****
275,0	16,2	30,5	44,9	59,9	74,9	89,9	****	****
280,0	16,3	30,7	45,4	60,5	75,6	90,7	****	****
285,0	16,5	31,0	45,8	61,1	76,3	91,6	****	****
290,0	16,6	31,2	46,2	61,7	77,1	92,5	****	****
295,0	16,7	31,5	46,7	62,2	77,8	93,3	****	****
300,0	16,9	31,8	47,1	62,8	78,5	94,2	****	****

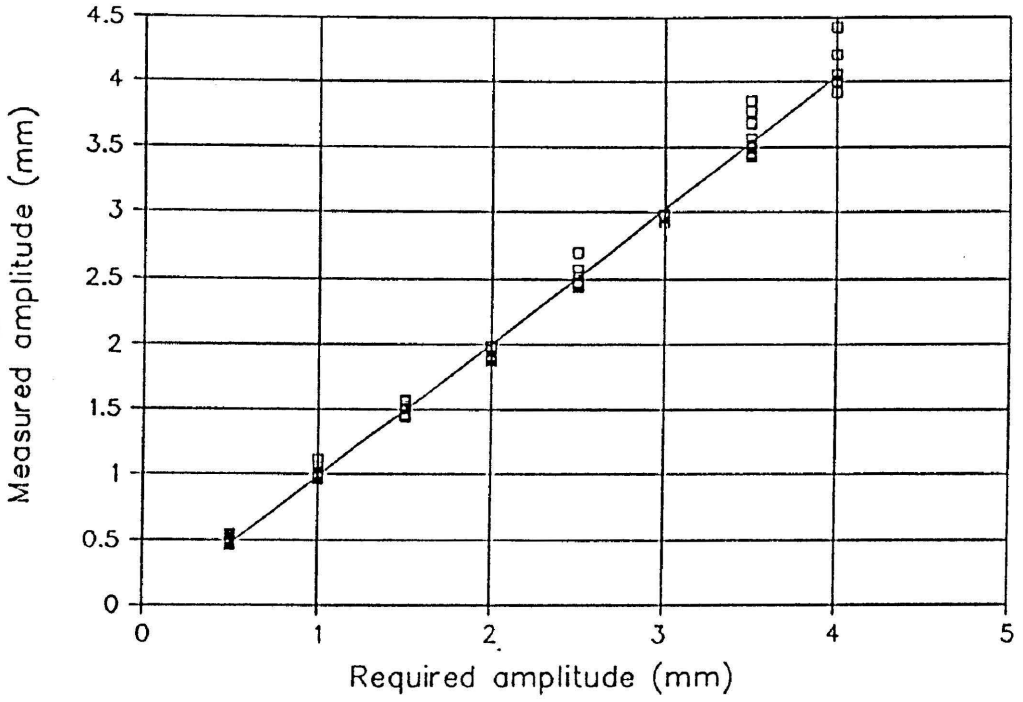

FIGURE B.6(a) **COMPARISON OF MEASURED AMPLITUDE AND REQUIRED AMPLITUDE FOR ORIGINAL AMPLITUDE CALIBRATION (WHOLE FREQUENCY RANGE)**

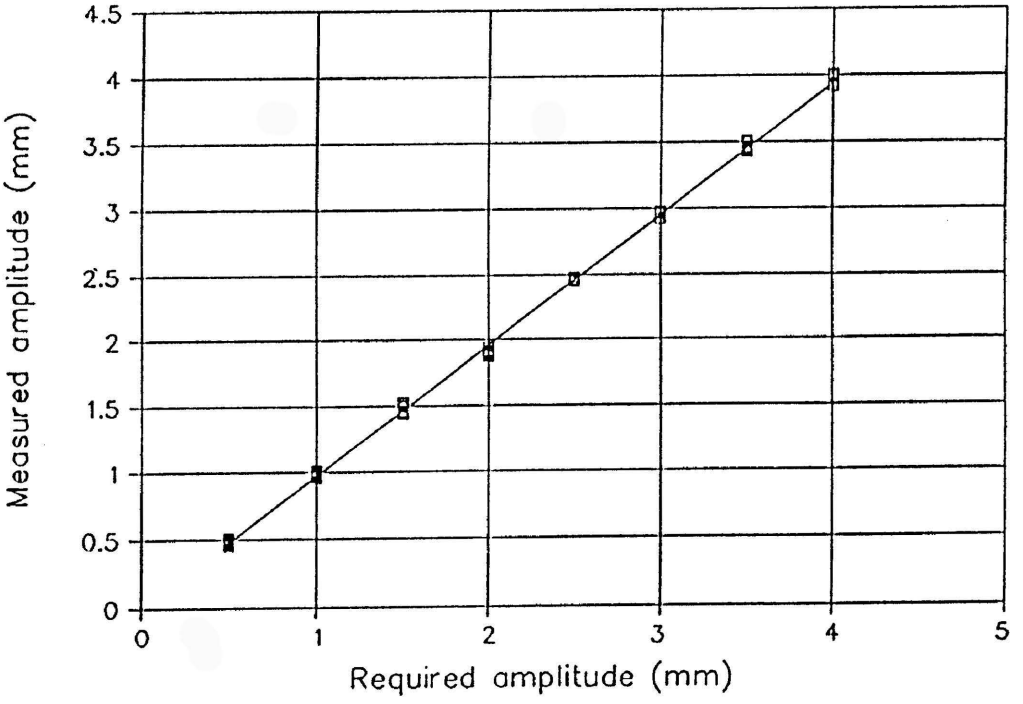

FIGURE B.6(b) **COMPARISON OF MEASURED AMPLITUDE AND REQUIRED AMPLITUDE FOR ORIGINAL AMPLITUDE CALIBRATION (FREQUENCIES > 20 Hz)**

Table B.5 **Final calibration table for the values of k depending on the mass on the table and required amplitude**

	Required amplitude(mm)							
	0,5	1,0	1,5	2,0	2,5	3,0	3,5	4,0
mass(kg)								
50,0	9,9	18,6	26,8	34,6	43,1	51,7	60,2	68,8
55,0	10,0	18,9	27,2	35,1	43,8	52,5	61,2	70,0
60,0	10,2	19,2	27,6	35,7	44,6	53,4	62,3	71,1
65,0	10,3	19,5	28,1	36,3	45,3	54,3	63,3	77,0
70,0	10,5	19,8	28,5	36,9	46,1	55,2	64,3	73,5
75,0	10,7	20,1	28,9	37,5	46,8	56,1	65,4	74,6
80,0	10,8	20,4	29,3	38,1	47,5	57,0	66,4	75,8
85,0	11,0	20,7	29,7	38,7	48,3	57,8	67,4	77,0
90,0	11,1	21,0	30,1	39,3	49,0	58,7	68,4	78,2
95,0	11,3	21,2	30,5	39,9	49,7	59,6	69,5	79,3
100,0	11,5	21,5	30,9	40,4	50,5	60,5	70,5	80,5
105,0	11,6	21,8	31,3	41,0	51,2	61,4	71,5	81,7
110,0	11,8	22,1	31,7	41,6	51,9	62,2	72,6	82,9
115,0	11,9	22,4	32,1	42,2	52,7	63,1	73,6	84,0
120,0	12,1	22,7	32,5	42,8	53,4	64,0	74,6	85,2
125,0	12,3	23,0	32,9	43,4	54,1	64,9	75,6	86,4
130,0	12,4	23,2	33,3	44,0	54,9	65,8	76,7	87,6
135,0	12,6	23,5	33,7	44,6	55,6	66,7	77,7	88,7
140,0	12,7	23,8	34,1	45,2	56,4	67,5	78,7	89,9
145,0	12,9	24,1	34,5	45,8	57,1	68,4	79,7	91,1
150,0	13,0	24,4	34,9	46,3	57,8	69,3	80,8	92,2
155,0	13,2	24,7	35,3	46,9	58,6	70,2	81,8	93,4
160,0	13,4	24,9	35,8	47,5	59,3	71,1	82,8	94,6
165,0	13,5	25,2	36,2	48,1	60,0	71,9	83,9	95,8
170,0	13,7	25,5	36,6	48,7	60,8	72,8	84,9	96,9
175,0	13,8	25,8	37,1	49,3	61,5	73,7	85,9	98,1
180,0	14,0	26,1	37,5	49,9	62,2	74,6	86,9	99,3
185,0	14,1	26,3	38,0	50,5	63,0	75,5	88,0	****
190,0	14,3	26,6	38,4	51,1	63,7	76,4	89,0	****
195,0	14,4	26,9	38,9	51,7	64,4	77,2	90,0	****
200,0	14,6	27,2	39,3	52,2	65,2	78,1	91,0	****
205,0	14,8	27,4	39,8	52,8	65,9	79,0	92,1	****
210,0	14,9	27,7	40,2	53,4	66,6	79,9	93,1	****
215,0	15,1	28,0	40,6	54,0	67,4	80,8	94,1	****
220,0	15,2	28,3	41,1	54,6	68,1	81,6	95,2	****
225,0	15,4	28,5	41,5	55,2	68,9	82,5	96,2	****
230,0	15,5	28,8	42,0	55,8	69,6	83,4	97,2	****
235,0	15,7	29,1	42,4	56,4	70,3	84,3	98,2	****
240,0	15,8	29,4	42,9	57,0	71,1	85,2	99,3	****
245,0	16,0	29,6	43,3	57,5	71,8	86,0	****	****
250,0	16,1	29,9	43,7	58,1	72,5	86,9	****	****
255,0	16,3	30,2	44,2	58,7	73,3	87,8	****	****
260,0	16,5	30,4	44,6	59,3	74,0	88,7	****	****
265,0	16,6	30,7	45,1	59,9	74,7	89,6	****	****
270,0	16,8	31,0	45,5	60,5	75,5	90,5	****	****
275,0	16,9	31,3	46,0	61,1	76,2	91,3	****	****
280,0	17,1	31,5	46,4	61,7	76,9	92,2	****	****
285,0	17,2	31,8	46,8	62,3	77,7	93,1	****	****
290,0	17,4	32,1	47,3	62,9	78,4	94,0	****	****
295,0	17,5	32,3	47,7	63,4	79,2	94,9	****	****
300,0	17,7	32,6	48,2	64,0	79,9	95,7	****	****

APPENDIX C

INFORMATION PERTAINING TO CHAPTER 4

MAXIMUM DRY DENSITIES AND OPTIMUM MOISTURE CONTENTS OF THE MATERIALS AS DETERMINED ON THE VIBRATORY COMPACTION TABLE FOR DIFFERENT FREQUENCY-AMPLITUDE (F/A) COMBINATIONS

MATERIAL	F/A	MDD(vib) (%mod)	MDD(mod.) (kg/m^3)	SD (kg/m^3)	MDD(vib) (%SD)	OMC(vib) (%)	ZAVD(vib) (%SD)	MDD(mod.) (%SD)	F/A	MATERIAL
BAB2(1+2)	40/36	97,20	1631,0	2756,0	57,52	25,35	58,87	59,18	40/36	BAB2(1+2)
BAB2(1+2)	35/47	97,77	1631,0	2756,0	57,86	25,00	59,21	59,18	35/47	BAB2(1+2)
BAB2(1+2)	30/64	99,89	1631,0	2756,0	59,11	23,71	60,48	59,18	30/64	BAB2(1+2)
BAB2(2)	40/36	98,47	1631,0	2756,0	58,27	24,63	59,57	59,18	40/36	BAB2(2)
BAB2(2)	35/47	98,54	1631,0	2756,0	58,32	24,58	59,61	59,18	35/47	BAB2(2)
BAB2(2)	30/64	99,84	1631,0	2756,0	59,09	23,80	60,39	59,18	30/64	BAB2(2)
SPR2	40/36	98,48	1967,0	2758,0	70,23	14,84	70,96	71,32	40/36	SPR2
SPR2	35/47	102,72	1967,0	2758,0	73,26	12,73	74,02	71,32	35/47	SPR2
SPR2	30/64	102,03	1967,0	2758,0	72,77	13,05	73,53	71,32	30/64	SPR2
SPR1	40/36	106,75	1865,0	2780,0	71,62	14,68	71,01	67,09	40/36	SPR1
SPR1	35/47	106,44	1865,0	2780,0	71,41	14,84	70,80	67,09	35/47	SPR1
SPR1	30/64	106,59	1865,0	2780,0	71,51	14,76	70,90	67,09	30/64	SPR1
SPR1(2)	40/36	106,76	1865,0	2780,0	71,62	14,68	71,01	67,09	40/36	SPR1(2)
SPR1(2)	35/47	106,49	1865,0	2780,0	71,44	14,84	70,79	67,09	35/47	SPR1(2)
SPR1(2)	30/64	106,62	1865,0	2780,0	71,53	14,77	70,89	67,09	30/64	SPR1(2)
LABLEN2	40/36	98,37	2097,0	2800,0	73,67	10,62	77,08	74,89	40/36	LABLEN2
LABLEN2	35/47	99,42	2097,0	2800,0	74,46	10,12	77,92	74,89	35/47	LABLEN2
LABLEN2	30/64	105,55	2097,0	2800,0	79,05	7,38	82,87	74,89	30/64	LABLEN2
LABDEW1	40/36	101,42	2048,0	2680,0	77,51	9,87	79,09	76,42	40/36	LABDEW1
LABDEW1	35/47	102,30	2048,0	2680,0	78,17	9,47	79,76	76,42	35/47	LABDEW1
LABDEW1	30/64	102,02	2048,0	2680,0	77,96	9,59	79,55	76,42	30/64	LABDEW1
OFS1	40/36	100,32	1789,0	2655,0	67,60	18,60	66,95	67,38	40/36	OFS1
OFS1	35/47	106,29	1789,0	2655,0	71,62	15,04	71,46	67,38	35/47	OFS1
OFS1	30/64	105,11	1789,0	2655,0	70,83	15,68	70,60	67,38	30/64	OFS1
NPAB	40/36	98,36	2150,0	2827,0	74,81	11,90	74,82	76,05	40/36	NPAB
NPAB	35/47	100,51	2150,0	2827,0	76,44	10,90	76,45	76,05	35/47	NPAB
NPAB	30/64	101,82	2150,0	2827,0	77,44	10,31	77,44	76,05	30/64	NPAB

MATERIAL	F/A	MDD(vib) (%mod)	MDD(mod.) (kg/m^3)	SD (kg/m^3)	MDD(vib) (%SD)	OMC(vib) (%)	ZAVD(vib) (%SD)	MDD(mod.) (%SD)	F/A	MATERIAL
SIL1	40/36	104,37	1884,0	2675,3	73,50	11,23	76,90	70,42	40/36	SIL1
SIL1	35/47	104,69	1884,0	2675,3	73,72	11,08	77,13	70,42	35/47	SIL1
SIL1	30/64	103,96	1884,0	2675,3	73,21	11,42	76,60	70,42	30/64	SIL1
LABD1	40/36	103,63	2097,0	2800,0	77,61	8,93	80,00	74,89	40/36	LABD1
LABD1	35/47	105,27	2097,0	2800,0	78,84	8,23	81,27	74,89	35/47	LABD1
LABD1	30/64	106,27	2097,0	2800,0	79,59	7,82	82,04	74,89	30/64	LABD1
TPA3	40/36	102,04	2077,0	2752,0	77,01	9,67	78,99	75,47	40/36	TPA3
TPA3	35/47	102,22	2077,0	2752,0	77,15	9,58	79,13	75,47	35/47	TPA3
TPA3	30/64	102,64	2077,0	2752,0	77,47	9,40	79,45	75,47	30/64	TPA3
TPA1	40/36	103,28	2234,0	2961,0	77,92	8,70	79,51	75,45	40/36	TPA1
TPA1	35/47	104,74	2234,0	2961,0	79,03	8,11	80,64	75,45	35/47	TPA1
TPA1	30/64	104,86	2234,0	2961,0	79,11	8,06	80,73	75,45	30/64	TPA1
CPA1	40/36	103,13	2371,0	2756,0	88,73	4,61	88,73	86,03	40/36	CPA1
CPA1	35/47	103,43	2371,0	2756,0	88,98	4,49	88,98	86,03	35/47	CPA1
CPA1	30/64	104,90	2371,0	2756,0	90,24	3,92	90,24	86,03	30/64	CPA1
DENS7	40/36	102,46	2237,0	2803,0	81,77	7,84	81,98	79,81	40/36	DENS7
DENS7	35/47	104,22	2237,0	2803,0	83,17	7,13	83,34	79,81	35/47	DENS7
DENS7	40/36	103,60	2237,0	2803,0	82,68	7,38	82,86	79,81	40/36	DENS7
DENS7	35/47	105,34	2237,0	2803,0	84,07	6,69	84,21	79,81	35/47	DENS7
DENS7	20/64	105,61	2237,0	2803,0	84,28	6,58	84,42	79,81	20/64	DENS7
TPA2	40/36(1)	105,04	2062,0	2671,0	81,09	7,80	82,75	77,20	40/36(1)	TPA2
TPA2	40/36(2)	104,39	2062,0	2671,0	85,90	8,08	82,24	77,20	40/36(2)	TPA2
TPA2	40/36(3)	106,40	2062,0	2671,0	82,14	7,22	83,82	77,20	40/36(3)	TPA2
NPAE	40/36	102,28	2256,0	2638,0	87,47	5,43	87,48	85,52	40/36	NPAE
NPAE	35/47	102,84	2256,0	2638,0	87,95	5,19	87,95	85,52	35/47	NPAE
NPAE	30/64	103,29	2256,0	2638,0	88,33	5,01	88,33	85,52	30/64	NPAE
FERR1	40/36	105,90	2174,0	2680,0	85,91	5,25	87,66	81,12	40/36	FERR1
FERR1	35/47	106,34	2174,0	2680,0	86,26	5,08	88,03	81,12	35/47	FERR1
FERR1	30/64	106,99	2174,0	2680,0	86,79	4,82	88,57	81,12	30/64	FERR1

MATERIAL	F/A	MDD(vib) (%mod)	MDD(mod.) (kg/m^3)	SD (kg/m^3)	MDD(vib) (%SD)	OMC(vib) (%)	ZAVD(vib) (%SD)	MDD(mod.) (%SD)	F/A	MATERIAL
OFS2	40/36	102,42	2369,0	2982,0	81,36	6,87	82,99	79,44	40/36	OFS2
OFS2	35/47	105,66	2369,0	2982,0	83,94	5,62	85,65	79,44	35/47	OFS2
OFS2	30/64	105,69	2369,0	2982,0	83,96	5,61	85,67	79,44	30/64	OFS2
NPAA	40/36	107,98	2458,0	3018,9	87,92	4,60	87,81	81,42	40/36	NPAA
NPAA	35/47	107,63	2458,0	3018,9	87,63	4,72	87,52	81,42	35/47	NPAA
NPAA	30/64	108,13	2458,0	3018,9	88,04	4,55	87,93	81,42	30/64	NPAA
ROSS1	40/36	104,08	2185,0	2640,0	86,14	4,34	89,73	82,77	40/36	ROSS1
ROSS1	35/47	103,67	2185,0	2640,0	85,80	4,50	89,38	82,77	35/47	ROSS1
ROSS1	30/64	104,68	2185,0	2640,0	86,64	4,09	90,25	82,77	30/64	ROSS1
DENS8	40/36	96,85	2174,0	2774,0	75,90	11,92	75,15	78,37	40/36	DENS8
DENS8	35/47	97,07	2174,0	2774,0	76,07	11,81	75,32	78,37	35/47	DENS8
DENS8	30/64	99,25	2174,0	2774,0	77,79	10,76	77,02	78,37	30/64	DENS8
DENS8(2)	40/36	99,16	2174,0	2774,0	77,72	10,80	76,95	78,37	40/36	DENS8(2)
DENS8(2)	35/47	97,97	2174,0	2774,0	76,78	11,37	76,02	78,37	35/47	DENS8(2)
DENS8(2)	30/64	99,29	2174,0	2774,0	77,81	10,74	77,05	78,37	30/64	DENS8(2)
OFS3	40/36	19,92	2197,0	3055,0	86,24	4,25	88,52	71,92	40/36	OFS3
OFS3	35/47	124,47	2197,0	3055,0	89,52	2,85	91,98	71,92	35/47	OFS3
OFS3	30/64	122,94	2197,0	3055,0	88,41	3,31	90,82	71,92	30/64	OFS3

APPENDIX D

INFORMATION PERTAINING TO CHAPTER 5

CBR, DD AND MC RESULTS OF THE MATERIALS

BAB - BLACK CLAY (MONTMORILLONITE) TEST RESULTS

CMC = 12 %
mod. AASHTO density = 1642 kg/m^3
Apparent density = 2756 kg/m^3

CBR (%)	MC (%)	DD (kg/m^3)	DD (% mod)	DD (% AD)	T(0,050) 3,254 T
51,6	10,70	1494,2	91,00	54,22	0,228
67,6	10,80	1498,7	91,27	54,38	1,344
53,6	10,94	1447,7	88,17	52,53	0,832
71,7	11,00	1547,4	94,24	56,15	1,235
31,7	11,30	1434,0	87,33	52,03	1,336
36,0	11,50	1451,7	88,41	52,67	1,489
48,2	11,60	1472,1	89,65	53,41	0,767
22,9	12,83	1442,3	87,84	52,33	2,435
83,1	12,83	1548,7	94,32	56,19	2,325
77,9	13,23	1544,7	94,07	56,05	2,068
31,5	13,25	1469,6	89,50	53,32	1,937
30,5	13,47	1451,4	88,39	52,66	1,495
58,8	15,30	1542,7	93,95	55,98	1,373
46,9	15,30	1477,1	89,96	53,59	0,714
16,2	15,40	1398,5	85,17	50,74	1,074
37,7	15,50	1492,1	90,87	54,14	0,381
26,3	15,50	1478,3	90,03	53,64	1,405
30,1	15,50	1419,6	86,45	51,51	0,054
23,7	15,50	1444,2	87,95	52,40	1,096
30,0	15,60	1497,6	91,21	54,34	1,219
24,2	15,70	1450,2	88,32	52,62	1,071
30,1	15,75	1396,8	85,07	50,68	0,515
27,1	15,80	1474,3	89,79	53,50	1,116
21,9	15,80	1469,9	89,52	53,34	1,603
34,7	15,90	1411,2	85,94	51,20	0,810
36,2	15,90	1485,0	90,44	53,88	0,247
24,9	15,90	1447,9	88,18	52,54	0,876
22,0	15,90	1422,3	86,62	51,61	0,736
31,0	15,90	1513,5	92,18	54,92	1,112
34,1	15,94	1420,2	86,49	51,53	0,604
39,6	16,03	1473,9	89,76	53,48	0,331
33,9	16,10	1436,0	87,46	52,10	0,363
36,2	16,10	1422,8	86,65	51,62	0,832
42,5	16,20	1471,8	89,63	53,40	0,748
29,4	16,20	1449,5	88,27	52,59	0,306
34,3	16,60	1471,6	89,62	53,40	0,045
20,2	16,60	1436,3	87,47	52,12	0,941
26,9	17,10	1508,2	91,85	54,72	0,919
26,6	17,30	1512,5	92,11	54,88	0,891
31,4	17,38	1384,6	84,32	50,24	0,999
30,6	17,40	1460,8	88,96	53,00	0,097
47,3	17,42	1497,7	91,21	54,34	1,488
25,5	17,43	1379,5	84,02	50,06	0,393
22,1	17,50	1451,9	88,42	52,68	0,668

CBR (%)	MC (%)	DD (kg/m^3)	DD (% mod)	DD (% AD)	T(0,050) 3,254 T
41,5	17,51	1474,6	89,81	53,51	1,137
38,4	17,54	1429,6	87,07	51,87	1,357
42,0	17,59	1434,2	87,34	52,04	1,700
24,8	17,60	1497,6	91,21	54,34	0,839
33,9	17,61	1415,3	86,19	51,35	1,050
45,0	17,67	1471,2	89,60	53,38	1,608
29,4	17,70	1427,5	86,93	51,79	0,459
26,1	17,70	1396,1	85,03	50,66	0,392
44,7	17,77	1458,0	88,79	52,90	1,760
45,4	17,80	1444,1	87,95	52,40	2,004
18,0	17,80	1470,3	89,54	53,35	1,218
27,1	17,80	1429,0	87,03	51,85	0,219
26,2	17,90	1429,6	87,07	51,87	0,139
50,8	18,00	1534,9	93,48	55,69	1,900
38,6	18,14	1544,2	94,04	56,03	0,642
23,6	18,20	1433,9	87,33	52,03	0,113
21,9	18,30	1483,0	90,32	53,81	0,749
24,5	18,30	1387,5	84,50	50,34	0,296
24,9	18,30	1394,1	84,90	50,59	0,324
31,4	18,40	1442,4	87,84	52,34	0,686
44,9	18,50	1472,7	89,69	53,44	1,868
18,1	18,60	1427,7	86,95	51,80	0,561
25,6	18,91	1389,2	84,61	50,41	0,429
26,1	19,00	1474,1	89,77	53,49	0,009
20,7	19,17	1380,1	84,05	50,08	0,125
48,1	19,18	1550,1	94,40	56,24	2,080
26,4	19,20	1454,7	88,59	52,78	0,248
16,8	20,70	1497,5	91,20	54,34	0,602
29,3	20,80	1522,8	92,74	55,25	0,688
15,9	20,90	1452,0	88,43	52,69	0,487
29,1	21,10	1488,7	90,66	54,02	0,855
11,6	21,30	1428,4	86,99	51,83	0,87′
16,0	21,40	1420,9	86,54	51,56	0,41.
15,9	21,60	1382,4	84,19	50,16	0,792
17,4	21,90	1475,4	89,85	53,53	0,167
9,0	23,50	1527,7	93,04	55,43	0,698
8,8	23,70	1637,5	99,72	59,41	0,756
9,0	23,70	1565,8	95,36	56,81	0,644
9,7	23,90	1487,3	90,58	53,97	0,556
6,6	23,90	1560,1	95,01	56,61	0,846
12,0	24,10	1587,0	96,65	57,59	0,228
6,9	24,20	1449,4	88,27	52,59	0,972
3,2	24,50	1611,5	98,15	58,47	1,119
4,9	27,40	1564,5	95,28	56,77	0,133
8,1	27,40	1530,5	93,21	55,53	0,196
3,1	27,90	1548,9	94,33	56,20	0,184
5,6	27,90	1504,2	91,61	54,58	0,061
2,7	28,00	1543,7	94,01	56,01	0,203
4,8	28,20	1538,1	93,67	55,81	0,067
3,9	28,40	1539,3	93,75	55,85	0,026
3,9	28,60	1450,7	88,35	52,64	0,786

CBR (%)	MC (%)	DD (kg/m^3)	DD (% mod)	DD (% AD)	T(0,050) 3,254 T		
3,5	31,30	1478,6	90,05	53,65	0,354		
1,8	31,30	1481,2	90,21	53,74	0,205		
1,3	31,80	1463,5	89,13	53,10	0,180		
2,5	31,90	1459,2	88,87	52,95	0,311		
1,4	32,00	1455,4	88,63	52,81	0,207		
0,8	32,10	1462,5	89,07	53,07	0,299		
1,0	32,10	1447,2	88,14	52,51	0,124		
38,2	15,40	1532,5	93,33	55,61	0,737		
30,6	16,90	1538,3	93,69	55,82	0,774		
22,1	10,87	1507,4	91,80	54,69	3,685	#	*
29,5	10,89	1505,3	91,67	54,62	2,881		*
25,3	11,11	1460,6	88,95	53,00	2,618		*
22,9	11,20	1482,9	90,31	53,81	3,427	#	*
16,6	11,20	1445,5	88,03	52,45	3,212		*
60,6	11,30	1422,7	86,65	51,62	2,078		*
36,0	12,77	1541,5	93,88	55,93	2,737		*
24,9	14,60	1541,0	93,85	55,91	2,665		*
19,2	14,60	1592,6	96,99	57,79	3,057		*
29,6	17,56	1564,0	95,25	56,75	0,566		*
22,1	11,85	1484,7	90,42	53,87	4,010	#	*

Statistical outlier * Visual outlier

SPR2 - WHITE SANDY CLAY TEST RESULTS

CMC = 9,5 %
mod. AASHTO density = 1967 (kg/m^3)
Apparent density = 2758 (kg/m^3)

CBR (%)	MC (%)	DD (kg/m^3)	DD (% mod)	DD (% AD)	T(0,050) 3,044 T
14,3	6,00	1786,7	90,83	64,78	0,712
11,0	6,40	1702,6	86,56	61,73	0,866
15,3	6,80	1735,4	88,23	62,92	0,209
24,2	6,80	1798,9	91,46	65,23	0,264
19,5	7,40	1742,1	88,57	63,17	0,266
33,9	8,70	1801,1	91,57	65,31	0,020
25,0	9,10	1780,1	90,50	64,54	1,165
19,3	9,10	1742,6	88,59	63,18	0,726
33,7	9,20	1820,1	92,53	65,99	1,409
20,5	9,30	1757,4	89,34	63,72	1,258
22,1	9,50	1711,0	86,98	62,04	0,532
38,7	9,70	1791,3	91,07	64,95	0,419
18,1	9,70	1732,7	88,09	62,83	0,740
17,6	9,90	1694,8	86,16	61,45	0,440
25,1	9,90	1782,8	90,64	64,64	1,252
30,2	10,10	1783,0	90,65	64,65	0,178

CBR (%)	MC (%)	DD (kg/m^3)	DD (% mod)	DD (% AD)	T(0,050) 3,044 T		
31,6	10,10	1788,6	90,93	64,85	0,150		
40,0	10,60	1837,2	93,40	66,61	0,202		
38,1	11,00	1859,6	94,54	67,43	0,227		
38,1	11,00	1831,8	93,13	66,42	0,579		
26,8	11,20	1796,0	91,31	65,12	0,040		
19,4	11,50	1699,8	86,42	61,63	0,780		
16,5	11,50	1728,7	87,88	62,68	0,035		
18,7	11,50	1672,2	85,01	60,63	0,717		
36,6	11,60	1807,2	91,88	65,53	1,654		
38,0	11,80	1906,5	96,93	69,13	0,198		
50,6	12,20	1965,5	99,92	71,26	1,671		
26,4	12,30	1811,4	92,09	65,68	0,453		
48,6	12,50	1973,5	100,33	71,56	1,730		
21,5	12,60	1769,0	89,93	64,14	0,536		
44,8	12,70	1889,5	96,06	68,51	2,428		
17,8	12,80	1783,3	90,66	64,66	0,182		
28,0	13,10	1795,4	91,28	65,10	1,509		
21,6	13,10	1742,8	88,60	63,19	0,867		
15,9	13,90	1922,5	97,74	69,71	1,369		
18,1	14,00	1977,0	100,51	71,68	1,259		
15,5	14,00	1911,7	97,19	69,31	1,215		
16,1	14,20	1958,3	99,56	71,00	1,235		
9,1	15,00	1901,6	96,67	68,95	1,096		
11,3	15,00	1966,9	99,99	71,32	1,055		
9,4	16,10	1889,7	96,07	68,52	0,157		
9,7	16,30	1867,5	94,94	67,71	0,393		
7,7	16,30	1837,4	93,41	66,62	0,055		
10,7	16,60	1854,8	94,29	67,25	0,794		
7,6	16,70	1747,7	88,85	63,37	1,201		
9,5	16,80	1956,8	99,48	70,95	1,004		
5,8	16,90	1872,7	95,21	67,90	0,367		
7,0	17,00	1856,8	94,40	67,32	0,570		
11,4	14,00	1865,3	94,83	67,63	1,417		
10,1	14,00	1831,7	93,12	66,42	1,296		
40,8	8,40	1842,4	93,66	66,80	0,168		
23,3	13,90	1860,2	94,57	67,45	0,525		
47,0	8,60	1824,9	92,78	66,17	1,498		
33,1	10,40	1730,7	87,98	62,75	2,283		*
44,6	9,80	1754,0	89,17	63,60	2,978		*
47,9	11,30	1791,7	91,09	64,96	3,674	#	*
41,9	6,90	1801,7	91,60	65,33	3,076	#	*
38,0	6,80	1824,4	92,75	66,15	2,027		*
43,6	7,10	1834,2	93,25	66,50	2,448		*
13,4	9,10	1840,4	93,56	66,73	5,391	#	*
44,6	6,80	1845,3	93,81	66,91	2,676		*
15,5	13,40	2008,5	102,11	72,83	2,605		*
19,8	8,00	2025,1	102,95	73,43	3,061	#	*

Statistical outlier * Visual outlier

SPR1 - RED SANDY CLAY TEST RESULTS

CMC = 9,25 %
mod. AASHTO density = 1865 (kg/m^3)
Apparent density = 2699 (kg/m^3)

CBR (%)	MC (%)	DD (kg/m^3)	DD (% mod)	DD (% AD)	T(0,050) 2,992 T	
1,7	20,40	1795,4	96,27	66,52	0,190	
3,0	20,30	1806,0	96,84	66,92	0,352	
2,6	20,30	1771,7	95,00	65,64	0,257	
2,0	20,20	1760,0	94,37	65,21	0,052	
3,9	20,00	1792,9	96,13	66,43	0,248	
2,2	20,00	1898,8	101,81	70,35	0,320	
2,9	20,00	1804,7	96,76	66,86	0,067	
3,2	19,90	1803,9	96,72	66,83	0,037	
4,0	19,70	1852,1	99,31	68,62	0,062	
13,5	18,00	1856,4	99,54	68,78	0,208	
10,8	17,90	1861,4	99,81	68,97	0,419	
9,4	17,80	1770,6	94,94	65,60	0,272	
16,9	17,80	1888,7	101,27	69,98	0,348	
14,3	17,80	1890,6	101,38	70,05	0,162	
10,8	17,60	1830,4	98,15	67,82	0,407	
11,2	17,50	1908,6	102,34	70,72	1,269	
19,7	17,50	1940,1	104,03	71,88	0,264	
17,0	17,50	1908,7	102,34	70,72	0,187	
13,8	17,40	1882,8	100,96	69,76	0,502	
25,0	16,60	1924,9	103,21	71,32	0,170	
27,3	16,50	1926,0	103,27	71,36	0,482	
13,9	16,50	1774,6	95,15	65,75	0,183	
14,1	16,40	1871,8	100,36	69,35	1,094	
18,7	16,40	1941,1	104,08	71,92	1,576	
11,8	16,40	1814,8	97,31	67,24	0,896	
23,1	16,40	1882,1	100,92	69,73	0,433	
30,6	16,30	1953,5	104,75	72,38	0,216	
30,0	16,30	1942,6	104,16	71,97	0,399	
31,4	16,20	1942,1	104,13	71,96	0,575	
30,0	15,60	1955,0	104,83	72,43	0,647	
17,3	15,50	1773,8	95,11	65,72	0,062	
33,4	15,50	1873,6	100,46	69,42	1,811	
24,2	15,50	1816,5	97,40	67,30	0,863	
51,5	15,40	1959,0	105,04	72,58	3,039	#
33,6	15,40	1933,2	103,66	71,63	0,465	
40,5	15,30	1956,3	104,90	72,48	0,972	
34,0	15,20	1966,8	105,46	72,87	0,698	
26,6	15,10	1850,0	99,19	68,54	0,639	
16,6	15,00	1806,0	96,84	66,92	0,734	
40,4	15,00	1965,1	105,37	72,81	0,350	
16,0	15,00	1748,7	93,77	64,79	0,382	
29,0	14,90	1996,8	107,07	73,98	3,140	#
41,2	14,80	1993,0	106,87	73,84	0,812	
39,3	14,80	1913,4	102,59	70,89	1,523	
29,7	14,80	1930,0	103,49	71,51	0,719	
53,1	14,70	1993,7	106,90	73,87	1,269	

CBR (%)	MC (%)	DD (kg/m^3)	DD (% mod)	DD (% AD)	T(0,050) 2,992 T		
44,3	14,60	1957,0	104,93	72,51	0,961		
26,4	12,70	1639,9	87,93	60,76	1,118		
19,3	12,40	1819,0	97,53	67,40	1,923		
18,6	12,40	1596,5	85,60	59,15	0,404		
17,7	12,40	1544,0	82,79	57,21	0,653		
25,6	12,20	1544,0	82,79	57,20	0,743		
44,4	12,10	1682,9	90,24	62,35	4,083	#	*
38,1	12,50	1551,1	83,17	57,47	3,215	#	*
35,9	12,40	1647,0	88,31	61,02	2,760		*

Statistical outlier * Visual outlier

LABLEN - RED SILTY SAND TEST RESULTS

CMC = 7 %
mod. AASHTO density = 2098 (kg/m^3)
Apparent density = 2708 (kg/m^3)

CBR (%)	MC (%)	DD (kg/m^3)	DD (% mod)	DD (% AD)	T(0,050) 3,000 T
16,6	8,03	1789,2	85,28	66,07	0,790
23,1	7,79	1826,6	87,06	67,45	0,458
19,5	8,04	1826,7	87,07	67,46	0,720
28,0	7,80	1859,7	88,64	68,68	0,242
6,3	13,75	1917,3	91,38	70,80	0,482
3,7	13,87	1941,7	92,55	71,70	0,101
13,7	10,10	1945,8	92,75	71,85	1,466
5,0	13,36	1950,6	92,98	72,03	0,160
56,6	7,66	1953,5	93,11	72,14	1,115
35,9	10,06	1959,7	93,41	72,37	0,951
5,4	13,43	1966,0	93,71	72,60	0,138
7,3	13,41	1968,4	93,82	72,69	0,065
6,8	13,58	1972,2	94,01	72,83	0,109
18,3	11,75	1974,2	94,10	72,90	0,020
17,7	13,68	1974,7	94,12	72,92	1,509
38,0	9,88	1976,9	94,23	73,00	0,635
49,2	10,03	1985,6	94,64	73,32	1,940
19,0	12,73	1986,7	94,70	73,37	0,770
17,6	12,09	1991,5	94,92	73,54	0,046
17,7	11,91	1992,2	94,96	73,57	0,214
53,9	9,40	2003,8	95,51	74,00	1,246
14,8	11,91	2004,8	95,56	74,03	0,817
13,9	11,79	2032,0	96,85	75,04	1,730
17,8	11,62	2033,9	96,94	75,11	1,509
77,1	9,84	2047,8	97,61	75,62	2,928
6,2	13,49	2065,5	98,45	76,27	1,536
75,6	9,93	2091,6	99,69	77,24	0,577

CBR (%)	MC (%)	DD (kg/m^3)	DD (% mod)	DD (% AD)	T(0,050) 3,000 T
77,9	7,39	2005,0	95,57	74,04	1,408
50,3	7,73	1979,7	94,36	73,11	0,452
88,1	8,24	2083,2	99,29	76,93	0,336
78,9	8,85	2089,8	99,61	77,17	0,801
58,7	9,41	2047,8	97,61	75,62	0,052
43,6	7,38	1888,5	90,01	69,74	0,815
59,9	7,78	1968,6	93,83	72,69	1,182
52,5	8,11	1998,1	95,24	73,78	0,374
47,3	8,84	2004,0	95,52	74,00	0,273
41,7	9,50	2005,3	95,58	74,05	0,178
50,1	7,27	1955,2	93,19	72,20	0,224
40,2	7,56	1912,2	91,15	70,61	0,085
51,3	7,91	1911,7	91,12	70,59	1,816
32,5	8,76	1941,4	92,54	71,69	0,305
42,0	9,28	1952,2	93,05	72,09	1,123
40,6	7,40	1897,5	90,44	70,07	0,286
40,3	7,63	1897,4	90,44	70,07	0,482
23,3	8,19	1910,7	91,07	70,56	1,324
21,6	8,44	1918,0	91,42	70,83	1,444
24,7	9,49	1920,5	91,54	70,92	0,190
66,0	7,24	2030,7	96,79	74,99	1,581
72,8	7,61	2025,6	96,55	74,80	0,129
58,4	8,14	2026,1	96,57	74,82	0,838
52,6	8,79	2029,9	96,76	74,96	0,767
49,8	7,58	1966,7	93,74	72,63	0,247
49,2	8,22	1967,5	93,78	72,66	0,444
18,3	6,11	1631,8	77,78	60,26	0,373
20,7	5,76	1678,4	80,00	61,98	0,143
14,0	6,07	1718,3	81,90	63,45	0,880

LABDEW - SLIGHTLY PLASTIC SAND TEST RESULTS

CMC = 8,75 %
mod. AASHTO density = 2048 (kg/m^3)
Apparent density = 2680 (kg/m^3)

CBR (%)	MC (%)	DD (kg/m^3)	DD (% mod)	DD (% AD)	T(0,050) 3,006 T
10,7	12,50	1968,8	96,13	73,46	1,142
11,2	12,34	1973,7	96,37	73,64	1,593
13,9	13,12	2061,9	100,68	76,94	0,517
16,7	12,92	2060,4	100,60	76,88	0,031
18,3	12,86	2056,8	100,43	76,75	0,031
18,8	12,39	1969,9	96,19	73,50	0,476
21,6	8,91	1825,1	89,12	68,10	0,625
22,2	12,25	1959,9	95,70	73,13	0,323
23,3	11,91	1865,4	91,09	69,61	0,007

CBR (%)	MC (%)	DD (kg/m^3)	DD (% mod)	DD (% AD)	T(0,050) 3,006 T		
23,8	8,14	1840,9	89,89	68,69	0,764		
24,7	12,24	1944,2	94,93	72,55	0,128		
25,6	10,57	1853,2	90,49	69,15	0,824		
26,1	9,01	1851,2	90,39	69,07	0,551		
26,2	9,97	1857,8	90,72	69,32	0,852		
29,7	12,11	1873,9	91,50	69,92	1,093		
33,0	11,92	1853,6	90,51	69,17	1,296		
33,7	11,91	2093,0	102,20	78,10	1,561		
33,8	7,21	1959,1	95,66	73,10	1,485		
34,0	10,85	1901,9	92,87	70,97	0,287		
35,3	11,08	1965,2	95,96	73,33	0,831		
36,5	9,94	1893,9	92,48	70,67	0,136		
36,7	8,26	1890,4	92,30	70,54	0,000		
37,3	10,93	1904,5	92,99	71,06	0,140		
38,4	9,01	1891,3	92,35	70,57	0,224		
39,7	10,99	1973,4	96,36	73,64	0,509		
40,5	11,26	1952,7	95,35	72,86	0,194		
42,0	8,36	1950,2	95,23	72,77	0,519		
43,8	10,39	1950,6	95,24	72,78	0,064		
43,9	10,00	1973,8	96,38	73,65	0,612		
44,9	12,05	2104,7	102,77	78,53	0,004		
45,3	8,17	1910,5	93,29	71,29	0,674		
46,7	8,02	1950,7	95,25	72,79	0,074		
47,4	7,24	1970,3	96,21	73,52	0,020		
47,5	11,88	2079,3	101,53	77,59	0,278		
49,4	8,12	2042,0	99,70	76,19	1,524		
50,3	9,21	1964,7	95,94	73,31	0,206		
52,2	11,91	1958,0	95,60	73,06	2,613		
52,5	7,21	2009,6	98,13	74,99	0,091		
53,3	8,21	1954,1	95,41	72,91	0,803		
58,2	8,84	2072,5	101,20	77,33	1,351		
60,0	11,21	2088,1	101,96	77,91	0,371		
61,7	8,00	1963,8	95,89	73,28	1,664		
63,6	10,02	2097,9	102,43	78,28	0,642		
63,9	10,13	2092,2	102,16	78,07	0,410		
64,1	8,00	2052,7	100,23	76,59	0,098		
64,4	10,78	2108,0	102,93	78,66	0,040		
64,5	9,88	1996,0	97,46	74,48	1,462		
65,3	8,86	2100,8	102,58	78,39	1,142		
67,5	8,18	1989,0	97,12	74,22	1,832		
72,2	8,78	1990,3	97,18	74,27	2,276		
73,3	10,91	2115,7	103,30	78,94	1,079		
78,6	10,36	2106,4	102,85	78,60	1,300		
43,6	11,25	1980,0	96,68	73,88	0,169		*
62,7	11,80	1981,5	96,75	73,94	3,389	#	*
33,3	8,87	1958,4	95,62	73,07	1,787		*
25,8	9,35	1946,9	95,07	72,65	2,436		*
25,1	7,81	1966,8	96,03	73,39	2,872		*

Statistical outlier * Visual outlier

OFS1 - WINDBLOWN SAND TEST RESULTS

CMC = 8,5 %
mod. AASHTO density = 1789 (kg/m^3)
Apparent density = 2655 (kg/m^3)

CBR (%)	MC (%)	DD (kg/m^3)	DD (% mod)	DD (% AD)	T(0,050) 2,978 T
5,3	12,17	1630,8	91,16	61,42	0,554
6,8	4,93	1638,6	91,59	61,72	0,775
2,9	7,75	1641,4	91,75	61,82	0,933
2,5	6,81	1651,4	92,31	62,20	0,930
1,4	12,00	1652,3	92,36	62,23	0,287
1,3	5,48	1660,4	92,81	62,54	0,677
6,5	6,76	1660,5	92,82	62,54	0,184
3,4	4,89	1661,1	92,85	62,57	0,173
3,6	7,73	1663,6	92,99	62,66	0,817
6,8	8,58	1663,8	93,00	62,67	0,203
4,6	8,46	1693,4	94,65	63,78	0,918
15,9	9,47	1693,9	94,69	63,80	1,211
13,4	9,44	1697,0	94,86	63,92	0,689
6,1	12,00	1708,6	95,50	64,35	0,116
16,4	8,80	1715,2	95,88	64,60	0,853
3,4	4,76	1715,8	95,91	64,63	0,298
16,5	8,63	1717,3	95,99	64,68	0,813
8,3	6,75	1719,2	96,10	64,75	0,628
9,7	5,75	1719,5	96,12	64,76	0,019
11,8	7,67	1721,2	96,21	64,83	0,151
13,6	6,66	1725,8	96,47	65,00	0,217
11,4	11,84	1732,8	96,86	65,27	0,407
10,7	8,66	1742,3	97,39	65,62	1,135
7,3	5,79	1743,9	97,48	65,68	1,193
21,4	6,80	1744,8	97,53	65,72	0,998
22,4	9,49	1745,2	97,55	65,73	1,028
19,7	7,68	1751,4	97,90	65,96	0,223
21,4	6,87	1752,0	97,93	65,99	0,673
11,8	9,38	1752,3	97,95	66,00	1,302
20,5	4,93	1756,0	98,16	66,14	1,503
17,2	6,90	1757,0	98,21	66,18	0,363
21,7	6,15	1759,1	98,33	66,26	0,668
23,9	9,64	1760,0	98,38	66,29	0,635
34,1	7,53	1761,6	98,47	66,35	2,442
19,1	5,85	1761,7	98,47	66,35	0,217
15,3	8,70	1762,6	98,52	66,39	1,270
17,1	6,68	1762,7	98,53	66,39	0,606
24,5	5,74	1766,3	98,73	66,53	1,068
20,6	4,64	1770,4	98,96	66,68	1,155
15,3	4,99	1773,5	99,13	66,80	0,418
8,1	5,15	1776,3	99,29	66,91	2,104
8,4	11,84	1778,5	99,41	66,99	2,188
25,9	12,05	1792,4	100,19	67,51	0,378
24,4	11,83	1800,3	100,63	67,81	0,784
44,6	7,77	1809,7	101,16	68,16	0,575
17,6	9,66	1608,4	89,90	60,58	1,571

CBR (%)	MC (%)	DD (kg/m^3)	DD (% mod)	DD (% AD)	T(0,050) 2,978 T		
11,9	5,72	1646,8	92,05	62,03	1,195		*
11,2	8,82	1650,7	92,27	62,17	0,651		*
43,5	7,67	1754,8	98,09	66,09	4,541	#	*
49,1	4,75	1712,9	95,74	64,51	8,382	#	*
46,4	5,66	1734,8	96,97	65,34	6,564	#	*
18,6	11,67	1713,1	95,75	64,52	2,113		*
26,7	8,66	1694,5	94,72	63,82	3,226	#	*

Statistical outlier * Visual outlier

NPAB - BROWN DECOMPOSED DOLERITE TEST RESULTS

CMC = 8 %
mod. AASHTO density = 2150 (kg/m^3)
Apparent density = 2827 (kg/m^3)

CBR (%)	MC (%)	DD (kg/m^3)	DD (% mod)	DD (% AD)	T(0,050) 3,044 T
48,8	6,00	1949,9	90,69	68,98	0,886
39,4	6,10	2016,7	93,80	71,34	0,998
82,0	6,50	2018,6	93,89	71,40	1,880
33,3	6,60	2008,1	93,40	71,03	1,424
44,3	6,60	1995,5	92,82	70,59	0,401
44,7	6,80	1960,3	91,18	69,34	0,188
43,0	6,80	1929,0	89,72	68,24	0,559
34,7	7,40	1932,7	89,89	68,36	0,247
36,7	8,40	1913,6	89,01	67,69	0,126
97,7	8,50	2062,7	95,94	72,97	1,756
31,7	8,60	1981,4	92,16	70,09	1,270
63,8	8,70	1996,3	92,85	70,62	0,775
78,7	8,70	2035,8	94,69	72,01	1,052
28,7	8,90	1968,1	91,54	69,62	1,169
44,7	9,10	2010,9	93,53	71,13	0,754
78,6	9,20	2051,7	95,43	72,58	0,851
33,7	9,30	1914,3	89,04	67,72	0,136
36,7	9,40	1984,0	92,28	70,18	0,734
53,4	9,50	2004,7	93,24	70,91	0,106
21,5	9,70	1870,6	87,00	66,17	0,056
33,6	9,70	1959,5	91,14	69,31	0,445
26,7	9,80	1937,4	90,11	68,53	0,560
24,8	10,00	1947,7	90,59	68,90	0,792
110,4	10,00	2214,3	102,99	78,33	1,042
86,0	10,10	2064,3	96,01	73,02	1,400
72,8	10,20	2109,9	98,14	74,63	0,596
21,6	10,20	1998,3	92,94	70,69	1,818
28,6	10,20	1931,3	89,83	68,32	0,207
93,6	10,60	2181,4	101,46	77,16	0,938

CBR (%)	MC (%)	DD (kg/m^3)	DD (% mod)	DD (% AD)	T(0,050) 3,044 T		
110,6	10,70	2129,1	99,03	75,31	1,806		
70,2	10,90	2045,0	95,12	72,34	0,996		
99,0	11,00	2128,7	99,01	75,30	1,122		
22,7	11,00	1916,1	89,12	67,78	0,130		
27,1	11,10	1973,6	91,79	69,81	0,655		
26,4	11,10	1897,3	88,25	67,12	0,422		
47,6	11,30	2065,1	96,05	73,05	0,874		
69,6	11,50	2070,8	96,32	73,25	0,664		
53,9	12,20	2041,5	94,96	72,22	0,531		
53,7	12,30	2064,2	96,01	73,02	0,099		
58,0	12,70	2008,4	93,41	71,04	1,755		
24,2	13,40	2049,6	95,33	72,50	0,972		
12,4	13,40	1903,7	88,55	67,34	0,567		
25,6	13,50	2083,2	96,89	73,69	1,513		
18,6	13,60	1970,7	91,66	69,71	0,204		
19,7	13,80	2066,3	96,11	73,09	1,325		
19,2	14,20	1973,2	91,78	69,80	0,699		
22,8	14,60	2047,6	95,24	72,43	0,005		
25,3	15,00	2060,8	95,85	72,90	0,333		
35,8	12,70	2131,8	99,15	75,41	2,533		*
101,7	6,50	1996,1	92,84	70,61	3,718	#	*
121,7	8,40	2032,6	94,54	71,90	4,102	#	*
59,9	8,60	2094,3	97,41	74,08	1,667		*
39,5	9,30	2165,6	100,72	76,60	4,839	#	*
69,2	9,50	2184,1	101,59	77,26	3,209	#	*
79,4	9,70	2155,8	100,27	76,26	1,556		*
19,1	9,70	2042,1	94,98	72,24	3,030		*
41,7	9,90	2102,4	97,79	74,37	2,740		*
55,8	10,00	2047,0	95,21	72,41	0,412		*
42,9	10,20	2051,3	95,41	72,56	1,357		*
19,2	10,40	2046,0	95,16	72,37	2,862		*
27,6	10,60	2003,1	93,17	70,86	1,335		*
29,7	10,90	2078,7	96,68	73,53	2,637		*
16,2	11,30	2001,8	93,11	70,81	1,842		*

Statistical outlier * Visual outlier

SIL - SILTY SAND TEST RESULTS

CMC = 7 %
mod. AASHTO density = 1884 (kg/m^3)
Apparent density = 2675,3 (kg/m^3)

CBR (%)	MC (%)	DD (kg/m^3)	DD (% mod)	DD (% AD)	T(0,050) 3,107 T
28,3	5,88	1597,3	84,78	59,71	2,467
19,7	5,90	1588,1	84,29	59,36	1,101

CBR (%)	MC (%)	DD (kg/m^3)	DD (% mod)	DD (% AD)	T(0,050) 3,107 T
24,2	5,90	1668,9	88,59	62,38	0,562
21,2	5,96	1693,5	89,89	63,30	0,535
12,7	5,97	1650,6	87,61	61,70	1,138
20,1	5,99	1620,7	86,03	60,58	0,624
15,6	6,01	1569,4	83,30	58,66	0,550
19,1	6,07	1592,7	84,54	59,53	0,808
29,4	6,83	1738,6	92,28	64,99	1,785
39,2	6,84	1708,8	90,70	63,87	0,714
36,8	6,92	1727,9	91,71	64,59	0,391
29,8	6,92	1746,4	92,70	65,28	2,133
44,4	6,95	1742,6	92,50	65,14	0,410
66,9	6,97	1782,5	94,61	66,63	2,988
51,4	6,98	1731,1	91,89	64,71	1,885
24,1	7,14	1672,5	88,77	62,52	0,930
42,9	7,17	1737,1	92,21	64,93	0,564
21,1	7,89	1714,1	90,98	64,07	1,243
55,6	7,97	1868,0	99,15	69,82	0,748
32,9	8,02	1749,5	92,86	65,39	0,138
23,8	8,02	1703,7	90,43	63,68	0,341
12,9	8,03	1724,4	91,53	64,46	2,659
23,1	8,12	1726,8	91,65	64,55	0,828
23,3	8,12	1669,7	88,63	62,41	0,418
35,9	8,12	1819,9	96,60	68,02	0,963
29,3	8,16	1779,1	94,43	66,50	0,958
32,6	9,27	1837,3	97,52	68,68	0,267
36,1	9,34	1920,7	101,95	71,80	0,826
49,5	9,38	1921,3	101,98	71,81	1,535
42,2	9,38	1933,2	102,61	72,26	0,022
16,3	9,40	1723,2	91,47	64,41	0,221
18,9	9,41	1803,8	95,74	67,42	1,167
14,6	9,48	1760,4	93,44	65,80	1,018
41,0	9,57	1882,6	99,93	70,37	1,289
36,7	10,37	2010,0	106,69	75,13	0,380
37,1	10,46	1990,5	105,65	74,40	0,227
38,6	10,48	1992,0	105,73	74,46	0,494
10,3	10,48	1715,4	91,05	64,12	0,241
12,4	10,50	1802,3	95,66	67,37	0,828
14,7	10,52	1837,8	97,55	68,69	0,916
12,3	10,57	1758,4	93,33	65,73	0,244
21,5	10,64	1911,9	101,48	71,47	0,753
28,9	11,72	1971,7	104,65	73,70	1,278
24,0	11,74	1941,4	103,05	72,57	0,851
25,4	11,82	1957,6	103,91	73,17	0,998
14,9	11,82	1771,3	94,02	66,21	0,917
7,3	11,83	1705,8	90,54	63,76	0,237
21,4	11,85	1851,2	98,26	69,20	1,499
13,2	11,85	1800,4	95,56	67,30	0,485
17,2	11,91	1884,9	100,05	70,46	0,521
8,3	12,14	1928,2	102,35	72,07	1,191
8,5	12,27	1855,6	98,49	69,36	0,398
9,6	12,31	1796,9	95,38	67,17	0,130

CBR (%)	MC (%)	DD (kg/m^3)	DD (% mod)	DD (% AD)	T(0,050) 3,107 T	
3,5	12,33	1730,9	91,88	64,70	0,824	
9,2	12,35	1941,7	103,06	72,58	0,936	
7,2	12,42	1768,7	93,88	66,11	0,175	
8,8	12,43	1924,3	102,14	71,93	0,757	
8,9	12,43	1941,8	103,07	72,58	0,900	
9,4	12,74	1797,4	95,40	67,19	0,254	
11,7	12,74	1932,9	102,60	72,25	0,028	
6,5	12,76	1718,1	91,19	64,22	0,370	
10,3	12,77	1762,3	93,54	65,87	0,415	
13,4	12,77	1934,1	102,66	72,30	0,281	
13,4	12,81	1931,8	102,54	72,21	0,336	
7,8	12,85	1840,1	97,67	68,78	0,078	
16,7	12,95	1901,6	100,94	71,08	1,218	
6,2	14,35	1758,1	93,32	65,72	0,396	
6,6	14,41	1866,2	99,06	69,76	0,174	
6,7	14,42	1864,0	98,94	69,67	0,186	
6,2	14,43	1867,4	99,12	69,80	0,111	
5,0	14,44	1837,9	97,55	68,70	0,204	
5,9	14,44	1713,7	90,96	64,06	0,477	
5,6	14,46	1798,5	95,46	67,23	0,324	
7,3	14,64	1870,5	99,28	69,92	0,328	
3,4	5,83	1654,9	87,84	61,86	2,645	*

Statistical outlier * Visual outlier

LABD - RED CHERT SOIL TEST RESULTS

CMC = 7 %
mod. AASHTO density = 2097 (kg/m^3)
Apparent density = 2800 (kg/m^3)

CBR (%)	MC (%)	DD (kg/m^3)	DD (% mod)	DD (% AD)	T(0,050) 2,992 T	
20,5	6,10	1928,0	91,94	68,86	1,736	
60,0	6,42	2036,2	97,10	72,72	0,566	
32,5	6,51	1883,3	89,81	67,26	0,068	
85,0	6,63	2074,6	98,93	74,09	2,322	
72,9	7,08	2057,8	98,13	73,49	0,699	
38,0	7,28	1987,9	94,80	71,00	1,586	
55,0	7,33	1965,6	93,73	70,20	1,283	
25,1	7,61	1913,1	91,23	68,32	1,248	
65,4	7,75	2050,5	97,78	73,23	1,172	
33,0	7,77	1967,3	93,81	70,26	1,013	
36,6	7,96	1999,3	95,34	71,40	0,961	
75,3	8,45	2142,3	102,16	76,51	0,816	
67,5	8,48	2217,6	105,75	79,20	3,226	#
77,7	8,71	2144,6	102,27	76,59	1,569	

CBR (%)	MC (%)	DD (kg/m^3)	DD (% mod)	DD (% AD)	T(0,050) 2,992 T
74,3	8,81	2135,9	101,85	76,28	1,615
69,3	8,81	2170,7	103,52	77,53	0,311
57,9	8,92	2105,3	100,39	75,19	0,624
52,5	9,02	2076,1	99,00	74,15	0,910
15,4	9,11	1903,7	90,78	67,99	0,667
31,2	9,17	1995,3	95,15	71,26	0,135
16,6	9,23	1920,6	91,59	68,59	0,586
60,8	9,29	2166,1	103,30	77,36	0,316
24,2	9,35	1951,8	93,08	69,71	0,138
33,9	9,39	2007,5	95,73	71,70	0,550
43,0	9,40	2038,2	97,20	72,79	1,148
28,8	9,45	2051,6	97,84	73,27	0,968
16,5	9,53	1961,5	93,54	70,05	0,826
27,4	9,56	2029,4	96,78	72,48	0,520
39,3	9,96	2131,7	101,65	76,13	0,859
35,6	10,29	2100,3	100,16	75,01	0,003
25,0	10,39	2032,8	96,94	72,60	0,142
23,4	10,52	2103,8	100,32	75,13	1,374
27,9	10,52	2113,8	100,80	75,49	1,023
24,3	10,59	1968,1	93,85	70,29	1,186
36,3	10,60	2116,9	100,95	75,60	0,133
25,3	10,62	2063,2	98,39	73,69	0,106
31,4	10,68	2075,7	98,98	74,13	0,529
22,5	11,06	2011,6	95,93	71,84	0,844
12,9	11,08	1912,7	91,21	68,31	0,489
11,6	11,18	1910,6	91,11	68,23	0,384
20,5	11,81	2047,0	97,61	73,11	0,789
11,7	12,00	1968,4	93,87	70,30	0,530
7,6	12,08	2062,9	98,38	73,68	0,909
17,1	12,22	2022,6	96,45	72,23	0,947
5,7	12,47	2039,9	97,28	72,85	0,573
5,9	12,75	2031,5	96,88	72,55	0,287
3,5	12,85	2013,4	96,01	71,91	0,412
7,0	12,89	2018,4	96,25	72,08	0,039
5,6	13,22	2036,1	97,10	72,72	0,114
1,8	14,40	2003,3	95,53	71,55	0,163
2,2	14,49	1969,4	93,92	70,34	0,084
1,9	14,65	2014,6	96,07	71,95	0,151
2,1	14,68	1961,7	93,55	70,06	0,185
1,7	14,77	1999,8	95,37	71,42	0,090
1,6	15,13	1979,3	94,39	70,69	0,125

Statistical outlier * Visual outlier

TPA3 - CHERT GRAVEL TEST RESULTS

CMC = 6,75 %
mod. AASHTO density = 2077 (kg/m^3)
Apparent density = 2752 (kg/m^3)

CBR (%)	MC (%)	DD (kg/m^3)	DD (% mod)	DD (% AD)	T(0,050) 3,006 T
26,2	5,69	1833,8	88,29	66,64	0,917
44,4	5,58	1898,8	91,42	69,00	0,440
14,2	10,73	1902,3	91,59	69,13	0,165
28,1	9,86	1904,0	91,67	69,19	0,104
31,7	8,61	1905,7	91,75	69,25	0,511
12,2	11,30	1906,9	91,81	69,29	0,035
44,4	7,32	1909,5	91,94	69,39	1,142
61,5	6,62	1910,1	91,97	69,41	0,855
52,2	7,71	1928,2	92,84	70,07	0,599
72,9	5,78	1932,8	93,06	70,23	0,308
77,4	5,08	1937,8	93,30	70,42	1,145
54,5	6,52	1942,4	93,52	70,58	1,542
123,6	6,03	1949,4	93,86	70,84	2,128
92,9	5,67	1957,5	94,25	71,13	1,002
77,0	6,96	1960,2	94,38	71,23	0,849
90,5	5,62	1961,3	94,43	71,27	0,890
118,2	6,70	1972,5	94,97	71,67	0,582
24,4	11,14	1983,2	95,48	72,06	0,261
42,9	10,03	1984,1	95,53	72,10	0,417
19,7	12,33	1985,1	95,57	72,13	0,607
44,3	9,72	1987,8	95,71	72,23	0,201
11,1	12,12	1990,6	95,84	72,33	0,070
65,9	7,84	1993,6	95,98	72,44	0,863
95,4	5,62	1996,7	96,13	72,55	0,486
11,4	11,41	2000,7	96,32	72,70	0,279
55,7	9,05	2006,2	96,59	72,90	0,153
13,9	11,21	2009,6	96,76	73,02	0,328
51,8	10,03	2013,9	96,96	73,18	0,504
97,0	6,72	2017,4	97,13	73,31	1,545
20,9	10,54	2019,7	97,24	73,39	0,564
104,1	7,36	2023,3	97,41	73,52	0,467
99,1	8,45	2027,2	97,60	73,66	0,741
13,5	11,31	2036,3	98,04	73,99	0,493
18,8	12,53	2036,7	98,06	74,01	0,469
141,9	7,10	2039,3	98,18	74,10	0,398
107,2	5,35	2042,2	98,33	74,21	0,340
158,0	7,36	2047,4	98,57	74,40	1,316
13,5	11,81	2048,2	98,61	74,43	0,253
11,1	11,81	2049,4	98,67	74,47	0,373
113,1	6,23	2054,4	98,91	74,65	1,132
14,8	11,33	2059,4	99,15	74,83	0,671
39,2	11,68	2060,9	99,23	74,89	0,716
31,6	11,09	2074,1	99,86	75,37	0,322
99,9	8,95	2078,6	100,08	75,53	0,151
96,2	9,39	2084,7	100,37	75,75	0,431
81,4	9,55	2089,2	100,59	75,92	0,156

CBR (%)	MC (%)	DD (kg/m^3)	DD (% mod)	DD (% AD)	T(0,050) 3,006 T	
204,2	7,50	2130,6	102,58	77,42	0,362	
111,2	9,43	2133,6	102,73	77,53	0,435	
143,1	8,80	2135,4	102,81	77,59	0,137	
101,5	9,37	2140,5	103,06	77,78	1,259	
176,4	8,33	2141,8	103,12	77,83	0,215	
168,0	8,84	2154,4	103,73	78,28	0,219	
222,5	7,10	2155,4	103,78	78,32	1,051	
45,5	9,74	2099,2	101,07	76,28	1,831	
121,5	7,58	2075,0	99,91	75,40	0,924	
155,8	8,77	2056,8	99,03	74,74	3,070	#
234,7	6,97	2077,6	100,03	75,50	3,087	#

Statistical outlier * Visual outlier

TPA1 - NORITE GRAVEL TEST RESULTS

CMC = 6,75 %
mod. AASHTO density = 2234 (kg/m^3)
Apparent density = 2961 (kg/m^3)

CBR (%)	MC (%)	DD (kg/m^3)	DD (% mod)	DD (% AD)	T(0,050) 3,006 T
24,1	6,48	1928,4	86,32	65,13	0,270
16,2	5,48	1970,0	88,18	66,53	0,906
18,5	6,58	1971,5	88,25	66,58	1,146
24,7	5,11	1972,7	88,30	66,62	0,331
19,8	5,94	1977,3	88,51	66,78	0,652
17,2	7,73	2001,2	89,58	67,59	0,986
22,8	5,05	2002,3	89,63	67,62	0,046
21,0	5,23	2002,4	89,63	67,63	0,259
35,6	7,31	2008,1	89,89	67,82	1,159
16,0	5,00	2016,1	90,25	68,09	0,855
18,1	6,14	2022,4	90,53	68,30	1,159
17,0	7,59	2023,9	90,59	68,35	1,181
10,2	11,21	2028,7	90,81	68,51	0,455
29,0	6,30	2030,6	90,89	68,58	0,112
12,2	9,44	2031,9	90,95	68,62	1,012
13,1	11,72	2041,0	91,36	68,93	0,289
38,3	4,70	2049,5	91,74	69,22	2,063
35,5	6,19	2054,8	91,98	69,39	0,859
37,7	7,18	2058,3	92,14	69,51	1,027
34,0	5,00	2060,1	92,21	69,57	1,314
22,2	5,27	2065,9	92,47	69,77	0,394
32,0	7,95	2069,1	92,62	69,88	0,698
18,9	10,10	2072,7	92,78	70,00	0,109
30,9	6,11	2081,9	93,19	70,31	0,079
17,9	8,65	2084,1	93,29	70,39	0,832

CBR (%)	MC (%)	DD (kg/m^3)	DD (% mod)	DD (% AD)	T(0,050) 3,006 T
23,1	7,92	2090,2	93,56	70,59	0,645
9,9	12,09	2092,5	93,66	70,67	0,383
34,0	7,76	2093,0	93,69	70,68	0,637
39,4	6,55	2093,2	93,70	70,69	0,710
27,8	7,34	2101,6	94,07	70,98	0,575
13,3	10,72	2117,4	94,78	71,51	0,278
47,9	7,64	2118,0	94,81	71,53	2,077
28,6	8,56	2124,0	95,07	71,73	0,190
28,5	8,99	2129,3	95,31	71,91	0,430
27,5	6,97	2138,5	95,72	72,22	1,489
25,9	8,73	2142,4	95,90	72,35	0,227
15,9	11,06	2143,3	95,94	72,38	0,304
35,1	9,79	2161,5	96,75	73,00	1,622
25,3	9,67	2169,3	97,10	73,26	0,174
11,7	11,38	2170,6	97,16	73,31	0,025
4,3	11,44	2175,6	97,38	73,47	0,883
18,8	10,67	2181,7	97,66	73,68	0,158
26,3	8,95	2191,7	98,11	74,02	0,648
19,2	11,30	2195,2	98,26	74,14	0,820
14,1	10,87	2203,0	98,61	74,40	0,395
8,9	11,12	2208,7	98,87	74,59	0,820
11,0	10,94	2211,1	98,97	74,67	0,784
16,6	10,93	2214,8	99,14	74,80	0,102
24,8	11,29	2223,6	99,53	75,10	1,343
13,6	11,76	2225,6	99,62	75,16	0,525
61,6	8,64	2241,6	100,34	75,70	2,538
55,3	8,42	2249,7	100,70	75,98	1,206
9,5	11,18	2253,7	100,88	76,11	1,138
29,6	9,69	2257,9	101,07	76,26	0,678
38,2	9,55	2271,4	101,67	76,71	0,097
30,9	9,22	2301,9	103,04	77,74	2,528
88,7	8,13	2358,6	105,58	79,65	0,167

CPA1 - HORNFELS CRUSHED STONE TEST RESULTS

CMC = 2,75 %
mod. AASHTO density = 2371 (kg/m^3)
Apparent density = 2756 (kg/m^3)

CBR (%)	MC (%)	DD (kg/m^3)	DD (% mod)	DD (% AD)	T(0,050) 2,644 T
103,9	1,63	2042,8	86,16	74,12	0,789
93,9	1,23	2085,9	87,98	75,69	0,633
110,0	0,91	2087,2	88,03	75,73	0,305
76,3	2,87	2119,1	89,38	76,89	0,942
256,2	2,19	2180,1	91,95	79,10	0,311
300,1	1,23	2198,7	92,73	79,78	0,265

CBR (%)	MC (%)	DD (kg/m^3)	DD (% mod)	DD (% AD)	T(0,050) 2,644 T		
376,7	3,95	2250,3	94,91	81,65	0,758		
381,9	3,22	2250,8	94,93	81,67	1,294		
255,3	3,21	2279,3	96,13	82,70	1,145		
377,1	3,88	2280,0	96,16	82,73	0,424		
381,8	4,12	2358,4	99,47	85,57	0,140		
418,1	4,67	2402,7	101,34	87,18	0,531		
334,4	5,52	2403,8	101,38	87,22	0,430		
252,7	4,72	2410,4	101,66	87,46	2,166		
393,3	4,31	2429,2	102,45	88,14	0,024		
309,7	4,55	2434,9	102,70	88,35	1,270		
409,1	4,78	2449,9	103,33	88,89	0,595		
442,8	4,27	2453,7	103,49	89,03	0,942		
336,2	5,11	2509,6	105,85	91,06	0,239		
575,6	4,41	2468,1	104,09	89,55	3,250	#	*
568,2	5,04	2428,2	102,41	88,11	3,435	#	*
548,6	5,06	2431,0	102,53	88,21	3,147	#	*
945,6	3,82	2420,3	102,08	87,82	9,236	#	*
141,7	4,27	2396,8	101,09	86,97	4,194	#	*

Statistical outlier * Visual outlier

DENS7 - DOLOMITIC SOIL TEST RESULTS

CMC = 5 %
mod. AASHTO density = 2237 (kg/m^3)
Apparent density = 2803 (kg/m^3)

CBR (%)	MC (%)	DD (kg/m^3)	DD (% mod)	DD (% AD)	T(0,050) 2,698 T
28,2	6,89	2023,8	90,47	72,20	0,714
43,2	4,93	2025,3	90,54	72,25	0,371
52,1	4,54	2054,0	91,82	73,28	0,634
71,7	5,04	2060,9	92,13	73,53	0,299
19,3	8,19	2068,3	92,46	73,79	0,047
13,1	8,47	2078,2	92,90	74,14	0,497
6,4	9,74	2094,1	93,61	74,71	0,055
22,4	8,18	2105,2	94,11	75,10	0,202
15,0	8,75	2110,0	94,32	75,28	0,214
5,8	9,98	2117,6	94,66	75,55	0,325
118,8	5,12	2119,2	94,73	75,60	0,994
25,5	8,57	2139,7	95,65	76,34	0,392
59,9	6,57	2141,8	95,75	76,41	0,997
14,5	8,81	2149,8	96,10	76,70	0,531
109,7	4,88	2151,7	96,19	76,76	1,592
4,6	9,56	2166,8	96,86	77,30	0,433
6,6	9,69	2176,7	97,30	77,66	0,009
39,4	8,54	2186,0	97,72	77,99	1,755

CBR (%)	MC (%)	DD (kg/m^3)	DD (% mod)	DD (% AD)	T(0,050) 2,698 T	
83,3	6,21	2186,3	97,73	78,00	0,146	
4,8	9,94	2190,1	97,90	78,13	0,176	
19,3	8,74	2200,9	98,39	78,52	0,161	
24,9	8,06	2206,2	98,62	78,71	0,976	
4,0	9,87	2228,7	99,63	79,51	0,053	
30,4	7,94	2242,0	100,22	79,99	0,018	
105,9	5,92	2246,5	100,43	80,15	3,150	#
19,3	8,22	2256,5	100,87	80,50	0,493	
40,1	5,54	2116,4	94,61	75,50	6,312	# *

Statistical outlier * Visual outlier

TPA2 - QUARTZITE GRAVEL TEST RESULTS

CMC = 4,5 %
mod. AASHTO density = 2062 (kg/m^3)
Apparent density = 2671 (kg/m^3)

CBR (%)	MC (%)	DD (kg/m^3)	DD (% mod)	DD (% AD)	T(0,050) 3,061 T	
59,8	2,97	1955,2	94,82	73,20	0,456	
92,9	3,09	1959,4	95,03	73,36	2,074	
75,0	3,19	1952,1	94,67	73,08	1,207	
37,0	3,20	1827,1	88,61	68,40	0,371	
94,1	3,21	1947,6	94,45	72,92	2,251	
13,2	3,27	1836,3	89,05	68,75	0,930	
47,8	3,94	2002,8	97,13	74,98	1,367	
31,4	4,13	1885,7	91,45	70,60	0,560	
111,6	4,30	2074,4	100,60	77,66	0,014	
96,2	4,34	2029,1	98,40	75,97	0,357	
113,8	4,37	2080,3	100,89	77,88	0,125	
28,1	4,42	1842,0	89,33	68,96	0,387	
56,1	4,46	1969,0	95,49	73,72	0,551	
96,3	4,54	2038,3	98,85	76,31	0,065	
20,6	4,75	1912,7	92,76	71,61	1,466	
37,3	4,79	1891,8	91,75	70,83	0,340	
136,6	4,85	2111,7	102,41	79,06	0,220	
98,1	5,04	2082,8	101,01	77,98	0,720	
108,9	5,11	2083,8	101,06	78,01	0,138	
166,5	5,15	2072,1	100,49	77,58	3,216	#
108,7	5,18	2109,7	102,32	78,99	0,903	
97,3	5,18	2086,3	101,18	78,11	0,765	
147,9	5,20	2149,4	104,24	80,47	0,270	
40,0	5,25	1952,4	94,69	73,10	0,824	
119,4	5,31	2093,1	101,51	78,36	0,275	
90,1	5,32	2058,5	99,83	77,07	0,281	
131,6	5,33	2114,7	102,55	79,17	0,243	
20,0	5,34	1873,2	90,84	70,13	0,920	

CBR (%)	MC (%)	DD (kg/m^3)	DD (% mod)	DD (% AD)	T(0,050) 3,061 T
87,3	5,38	2058,4	99,83	77,06	0,386
63,6	5,39	1987,4	96,38	74,41	0,102
97,0	5,44	2082,0	100,97	77,95	0,472
117,3	5,46	2079,1	100,83	77,84	0,678
118,0	5,49	2075,1	100,64	77,69	0,843
121,3	5,54	2067,8	100,28	77,42	1,242
78,8	5,57	2053,9	99,61	76,90	0,597
107,9	5,60	2043,6	99,11	76,51	1,176
78,6	5,70	2083,3	101,03	78,00	1,286
84,5	5,71	2043,0	99,08	76,49	0,037
89,7	5,80	2070,7	100,42	77,53	0,305
106,7	5,98	2083,6	101,05	78,01	0,359
17,6	6,44	1884,1	91,37	70,54	0,890
162,1	6,45	2173,5	105,41	81,38	0,689
76,9	6,59	2000,5	97,02	74,90	0,930
150,1	6,65	2097,0	101,70	78,51	2,739
18,0	6,76	1866,0	90,50	69,86	0,675
163,3	6,80	2199,4	106,66	82,34	0,057
92,5	6,86	2065,9	100,19	77,34	0,660
16,1	6,98	1903,1	92,29	71,25	0,962
125,5	7,00	2140,6	103,81	80,14	0,471
37,1	7,18	1959,8	95,04	73,37	0,316
126,2	7,33	2197,7	106,58	82,28	1,219
39,3	7,52	1972,6	95,67	73,85	0,182
106,6	7,61	2162,3	104,86	80,95	0,629
95,4	7,64	2119,9	102,81	79,37	0,097
103,1	7,86	2156,7	104,59	80,75	0,369
35,6	7,88	1995,8	96,79	74,72	0,447
59,2	7,95	2074,6	100,61	77,67	0,446
12,2	7,99	1840,8	89,27	68,92	0,551
38,2	9,00	1980,7	96,06	74,15	0,612
48,8	9,19	2133,2	103,45	79,87	1,035
35,3	9,36	2163,1	104,90	80,99	2,301
36,3	9,71	2044,9	99,17	76,56	0,509
36,5	9,78	2113,0	102,47	79,11	0,483
21,2	9,84	1914,1	92,83	71,66	0,772
10,8	9,89	1853,7	89,90	69,40	0,609
32,4	9,93	2093,5	101,53	78,38	0,142
40,9	10,17	2056,7	99,74	77,00	1,145

Statistical outlier * Visual outlier

NPAE - TILLITE CRUSHED STONE TEST RESULTS

CMC = 4 %
mod. AASHTO density = 2256 (kg/m^3)
Apparent density = 2638 (kg/m^3)

CBR (%)	MC (%)	DD (kg/m^3)	DD (% mod)	DD (% AD)	T(0,050) 3,130 T
56,9	1,63	2041,6	90,50	77,39	0,112
122,6	1,64	2061,3	91,37	78,14	2,703
48,9	1,80	2032,4	90,09	77,04	3,060
85,2	1,92	2075,3	91,99	78,67	0,802
184,1	3,84	2074,0	91,93	78,62	2,295
240,4	3,85	2088,1	92,56	79,15	1,281
309,7	3,88	2106,2	93,36	79,84	0,370
271,2	3,92	2133,1	94,55	80,86	1,941
487,6	3,94	2196,1	97,34	83,25	0,043
157,2	4,09	2035,6	90,23	77,16	0,515
225,3	4,13	2106,9	93,39	79,87	1,102
659,1	4,72	2296,8	101,81	87,06	1,254
532,1	4,81	2314,1	102,58	87,72	1,260
340,5	4,90	2211,5	98,03	83,83	0,243
276,9	5,08	2155,9	95,56	81,73	0,918
386,3	5,08	2236,9	99,15	84,80	0,512
130,1	5,13	2072,3	91,86	78,56	0,914
137,1	5,27	2101,9	93,17	79,68	2,571
257,1	5,28	2280,4	101,08	86,45	0,069
122,1	5,35	2050,6	90,89	77,73	0,734
220,6	5,53	2240,6	99,32	84,93	0,987
252,1	5,53	2298,0	101,86	87,11	0,578
136,6	5,74	2176,7	96,49	82,51	1,316
269,6	5,89	2250,9	99,78	85,33	0,266
242,6	5,89	2250,7	99,77	85,32	0,310
247,1	6,05	2255,4	99,97	85,50	0,547
243,9	6,06	2223,2	98,55	84,28	0,547
70,5	6,06	2093,2	92,78	79,35	0,201
90,9	6,09	2078,7	92,14	78,80	0,370
272,9	6,12	2283,5	101,22	86,56	0,014
292,2	6,25	2235,8	99,10	84,75	0,145
212,9	6,27	2273,0	100,76	86,17	0,109
72,5	6,50	2135,9	94,68	80,97	1,385
90,3	6,65	2150,5	95,32	81,52	0,723
238,2	6,67	2228,6	98,78	84,48	0,140
72,4	6,69	2043,8	90,60	77,48	0,472
120,5	6,70	2105,1	93,31	79,80	0,445
133,4	6,78	2149,3	95,27	81,47	0,590
100,5	6,81	2080,3	92,21	78,86	0,030
193,0	6,82	2228,6	98,79	84,48	0,053
173,4	6,84	2171,9	96,27	82,33	0,371
106,0	6,86	2254,5	99,94	85,46	0,116
130,2	7,04	2188,8	97,02	82,97	0,208
127,7	7,45	2159,0	95,70	81,84	0,884
72,1	7,75	2062,1	91,41	78,17	0,426
76,1	7,77	2118,6	93,91	80,31	0,147

CBR (%)	MC (%)	DD (kg/m^3)	DD (% mod)	DD (% AD)	T(0,050) 3,130 T		
106,6	7,82	2153,9	95,48	81,65	0,233		
70,6	8,06	2114,6	93,73	80,16	0,174		
105,4	8,22	2119,7	93,96	80,35	0,565		
56,8	8,42	2055,2	91,10	77,91	0,369		
52,5	2,50	1928,2	85,47	73,09	0,418		
39,1	6,63	1932,1	85,64	73,24	0,484		
35,2	8,66	1945,4	86,23	73,75	3,006		
28,3	2,51	1945,6	86,24	73,75	0,661		
75,0	1,67	1949,9	86,43	73,91	0,120		
87,5	1,52	1950,6	86,46	73,94	0,405		
73,8	7,53	1957,2	86,75	74,19	0,004		
84,7	4,07	1958,0	86,79	74,22	0,234		
52,0	6,39	1958,7	86,82	74,25	0,554		
71,1	2,43	1961,5	86,94	74,35	1,108		
87,6	5,46	1961,5	86,94	74,35	1,303		
51,1	2,68	1964,0	87,05	74,45	0,895		
46,4	5,60	1967,9	87,23	74,60	1,017		
34,2	2,66	1971,3	87,38	74,73	0,193		
72,9	2,46	1972,4	87,43	74,77	1,044		
34,4	2,62	1975,0	87,54	74,87	0,604		
105,7	1,64	1976,4	87,61	74,92	0,742		
128,1	1,61	1977,4	87,65	74,96	0,031		
35,1	2,72	1980,0	87,77	75,06	0,174		
55,0	2,46	1986,8	88,07	75,31	0,014		
62,5	6,75	1990,2	88,22	75,44	1,436		
55,3	7,83	1993,0	88,34	75,55	0,460		
45,4	8,21	1994,2	88,40	75,60	0,661		
58,0	1,28	2002,4	88,76	75,91	0,381		
64,9	2,70	2005,7	88,91	76,03	0,964		
230,2	1,66	2010,9	89,13	76,23	0,889		
141,9	4,33	2028,8	89,93	76,91	0,134		
64,7	5,71	2028,9	89,94	76,91	0,500		
50,3	4,38	2212,5	98,07	83,87	5,121	#	*
40,7	5,14	2199,4	97,49	83,37	3,721	#	*

Statistical outlier * Visual outlier

FERR1 - QUARTZITE CRUSHED STONE TEST RESULTS

CMC = 4 %
mod. AASHTO density = 2174 (kg/m^3)
Apparent density = 2680 (kg/m^3)

CBR (%)	MC (%)	DD (kg/m^3)	DD (% mod)	DD (% AD)	T(0,050) 2,745 T		
223,0	3,07	2042,5	93,95	76,21	0,625		
132,9	3,22	2051,8	94,38	76,56	0,896		
224,7	3,81	2058,5	94,69	76,81	0,195		
222,2	4,00	2060,1	94,76	76,87	0,066		
213,8	4,41	2073,2	95,36	77,36	0,038		
162,0	2,30	2077,9	95,58	77,53	0,228		
168,4	2,59	2098,6	96,53	78,31	0,183		
202,5	5,32	2099,9	96,59	78,35	0,244		
251,7	5,09	2108,7	97,00	78,68	0,713		
161,3	4,67	2114,8	97,28	78,91	1,030		
163,2	4,99	2116,1	97,34	78,96	0,814		
181,1	5,45	2118,0	97,43	79,03	0,161		
358,7	4,82	2127,0	97,84	79,37	1,953		
265,3	3,39	2140,1	98,44	79,85	0,202		
151,9	2,87	2155,0	99,12	80,41	1,446		
208,2	3,58	2156,1	99,17	80,45	1,034		
238,7	5,22	2172,8	99,95	81,08	0,351		
359,3	4,57	2180,9	100,32	81,38	0,914		
321,7	2,96	2183,4	100,43	81,47	0,576		
257,7	4,52	2185,7	100,54	81,55	0,781		
465,2	4,53	2225,7	102,38	83,05	1,495		
451,1	5,39	2256,5	103,80	84,20	1,044		
442,1	3,49	2263,3	104,11	84,45	0,061		
370,5	4,58	2269,8	104,41	84,69	1,211		
401,2	5,30	2308,8	106,20	86,15	1,556		
629,0	4,97	2324,2	106,91	86,72	1,108		
345,1	5,12	2317,4	106,60	86,47	2,902	#	*
333,3	4,96	2318,3	106,64	86,50	3,242	#	*
206,9	4,67	2251,8	103,58	84,02	3,141	#	*
244,7	3,85	2264,0	104,14	84,48	3,183	#	*

Statistical outlier * Visual outlier

OFS2 - WEATHERED DOLERITE TEST RESULTS

CMC = 3,75 %
mod. AASHTO density = 2369 (kg/m^3)
Apparent density = 2982 (kg/m^3)

CBR (%)	MC (%)	DD (kg/m^3)	DD (% mod)	DD (% AD)	T(0,050) 3,087 T
62,9	0,61	2101,7	88,72	70,48	0,246
68,4	0,95	2115,8	89,31	70,95	0,088
117,3	0,88	2116,9	89,36	70,99	0,835
58,8	1,90	2118,7	89,44	71,05	0,562
34,6	1,80	2121,4	89,55	71,14	0,961
121,2	1,80	2122,4	89,59	71,17	0,681
68,3	1,29	2124,2	89,66	71,23	0,121
143,5	0,61	2124,2	89,66	71,23	1,279
85,6	5,90	2125,7	89,73	71,28	0,106
127,9	3,60	2134,9	90,12	71,59	1,104
69,2	1,80	2137,8	90,24	71,69	0,307
60,5	2,00	2143,6	90,49	71,89	0,600
102,4	4,40	2143,8	90,49	71,89	0,906
103,2	1,40	2144,0	90,50	71,90	0,511
111,1	3,00	2147,5	90,65	72,01	0,620
62,2	1,50	2147,9	90,67	72,03	0,301
90,1	4,10	2150,1	90,76	72,10	1,552
75,6	1,50	2151,4	90,81	72,15	0,048
62,8	1,26	2153,0	90,88	72,20	0,221
169,1	4,80	2159,7	91,16	72,42	0,812
137,8	3,60	2164,3	91,36	72,58	0,972
92,4	2,00	2169,6	91,58	72,76	0,017
43,7	1,80	2169,6	91,58	72,76	0,809
54,6	2,00	2172,5	91,71	72,85	0,738
152,4	3,70	2187,4	92,33	73,35	0,940
110,2	2,10	2187,7	92,35	73,36	0,214
151,8	5,10	2193,2	92,58	73,55	0,719
138,6	4,30	2199,4	92,84	73,75	0,518
80,8	1,70	2199,4	92,84	73,76	0,087
92,5	3,20	2210,4	93,30	74,12	1,453
89,5	2,00	2211,0	93,33	74,14	0,156
75,9	1,40	2211,5	93,35	74,16	0,051
144,8	3,20	2218,0	93,63	74,38	0,509
111,5	5,30	2218,8	93,66	74,41	0,060
71,9	3,10	2230,3	94,14	74,79	1,835
92,5	1,80	2230,9	94,17	74,81	0,011
122,1	4,00	2236,2	94,39	74,99	1,546
128,8	3,30	2238,2	94,48	75,06	1,120
149,9	5,80	2244,9	94,76	75,28	1,096
164,0	2,90	2245,2	94,77	75,29	0,076
325,1	3,40	2257,7	95,30	75,71	2,241
85,6	1,50	2258,4	95,33	75,73	0,045
165,1	5,20	2258,5	95,33	75,74	0,752
193,1	2,80	2263,4	95,54	75,90	0,601
247,7	4,00	2268,1	95,74	76,06	0,470
193,9	3,20	2271,0	95,86	76,16	0,080

CBR (%)	MC (%)	DD (kg/m^3)	DD (% mod)	DD (% AD)	T(0,050) 3,087 T	
191,2	1,60	2275,5	96,05	76,31	1,798	
225,5	4,20	2281,7	96,32	76,52	0,204	
304,6	3,40	2282,4	96,34	76,54	1,520	
132,9	5,70	2286,2	96,50	76,67	0,443	
178,9	3,30	2290,6	96,69	76,81	0,817	
239,8	3,40	2297,4	96,98	77,04	0,042	
318,7	4,10	2301,4	97,15	77,18	1,465	
208,7	4,70	2303,0	97,22	77,23	0,394	
228,1	4,70	2305,0	97,30	77,30	0,730	
311,0	4,00	2322,7	98,05	77,89	0,682	
295,4	3,50	2334,5	98,54	78,29	0,096	
232,1	4,40	2350,6	99,22	78,83	0,707	
119,2	7,06	2363,5	99,77	79,26	0,354	
303,1	4,70	2371,5	100,10	79,53	0,648	
195,2	5,20	2374,2	100,22	79,62	0,522	
75,3	7,40	2385,5	100,70	80,00	0,644	
199,9	5,60	2409,2	101,70	80,79	0,796	
129,9	7,13	2418,8	102,10	81,11	0,377	
140,9	7,27	2430,6	102,60	81,51	0,364	
304,6	5,20	2455,6	103,65	82,35	1,736	
526,6	5,40	2503,9	105,69	83,97	0,185	
413,8	4,00	2328,2	98,28	78,07	2,501	
413,7	3,40	2297,4	96,98	77,04	3,340	#
96,5	3,20	2277,1	96,12	76,36	2,008	*
116,2	4,50	2339,1	98,74	78,44	2,414	*

Statistical outlier * Visual outlier

NPAA - DOLERITE CRUSHED STONE TEST RESULTS

CMC = 3,75 %
mod. AASHTO density = 2458 (kg/m^3)
Apparent density = 2989 (kg/m^3)

CBR (%)	MC (%)	DD (kg/m^3)	DD (% mod)	DD (% AD)	T(0,050) 3,049 T
259,1	2,20	2398,3	97,57	80,24	0,400
268,7	2,30	2443,3	99,40	81,74	0,106
148,6	2,40	2357,6	95,92	78,88	0,554
328,7	2,50	2429,1	98,82	81,27	0,441
341,1	2,50	2407,4	97,94	80,54	0,823
223,3	2,50	2384,4	97,01	79,77	0,134
136,7	2,60	2346,6	95,47	78,51	0,774
268,7	2,70	2420,7	98,48	80,99	0,316
54,9	2,80	2397,2	97,53	80,20	2,331
307,7	3,00	2383,3	96,96	79,74	0,150
226,1	3,00	2354,8	95,80	78,78	0,371

CBR (%)	MC (%)	DD (kg/m^3)	DD (% mod)	DD (% AD)	T(0,050) 3,049 T
130,4	3,10	2329,7	94,78	77,94	1,219
344,0	3,10	2422,9	98,57	81,06	0,130
532,8	3,20	2434,8	99,06	81,46	1,462
553,5	3,20	2457,6	99,98	82,22	1,305
869,6	3,60	2531,9	103,01	84,71	2,262
721,7	3,60	2577,4	104,86	86,23	0,424
258,8	3,70	2347,6	95,51	78,54	0,863
776,0	3,80	2501,4	101,77	83,69	1,811
583,0	3,90	2471,9	100,57	82,70	0,651
198,9	3,90	2369,8	96,41	79,28	1,609
432,9	4,00	2509,9	102,11	83,97	1,473
641,9	4,10	2511,6	102,18	84,03	0,809
434,2	4,10	2430,9	98,90	81,33	0,206
1017,6	4,40	2650,4	107,83	88,67	1,547
172,6	4,60	2379,7	96,81	79,62	1,058
505,1	5,10	2647,2	107,70	88,56	1,981
494,1	5,10	2575,3	104,77	86,16	0,246
388,0	5,20	2593,1	105,50	86,75	1,556
323,1	5,20	2435,8	99,10	81,49	0,540
565,2	5,30	2601,1	105,82	87,02	0,236
507,4	5,40	2604,4	105,96	87,13	0,255
260,3	5,40	2337,8	95,11	78,21	0,966
319,6	5,60	2443,1	99,39	81,74	0,847
427,2	5,60	2556,9	104,03	85,55	0,259
496,4	5,60	2517,4	102,42	84,22	1,650
267,6	5,60	2534,7	103,12	84,80	0,963
336,5	5,70	2508,1	102,04	83,91	0,290
320,1	5,70	2568,9	104,51	85,94	0,916
426,1	5,70	2563,4	104,29	85,76	0,267
476,6	5,70	2593,4	105,51	86,77	0,174
189,0	5,80	2380,9	96,86	79,66	0,229
357,0	5,90	2576,3	104,81	86,19	0,405
473,6	5,90	2574,0	104,72	86,12	0,823
347,1	6,00	2621,1	106,64	87,69	1,297
467,9	6,10	2537,8	103,25	84,91	1,626
131,8	6,20	2342,3	95,29	78,36	0,025
253,2	6,20	2560,2	104,16	85,65	0,807
294,1	6,20	2545,3	103,55	85,16	0,152
130,4	6,40	2345,0	95,40	78,46	0,040
193,7	6,40	2406,7	97,91	80,52	0,410
298,8	6,40	2459,1	100,04	82,27	1,092
257,7	6,40	2504,4	101,89	83,79	0,209
301,1	6,70	2499,1	101,67	83,61	0,894
295,5	6,80	2525,0	102,73	84,48	0,608
119,3	6,90	2519,3	102,49	84,28	1,071
115,7	7,20	2485,5	101,12	83,16	0,725
126,2	7,30	2387,0	97,11	79,86	0,201
130,4	7,60	2304,4	93,75	77,10	0,044
707,8	4,50	2636,6	107,26	88,21	0,927
743,8	4,60	2630,1	107,00	87,99	0,140
339,3	2,40	2346,9	95,48	78,52	1,470

CBR (%)	MC (%)	DD (kg/m^3)	DD (% mod)	DD (% AD)	T(0,050) 3,049 T	
37,8	2,30	2394,3	97,41	80,10	1,911	*
502,0	2,10	2432,7	98,97	81,39	2,616	*

Statistical outlier * Visual outlier

ROSS1 - GRANITE CRUSHED STONE TEST RESULTS

CMC = 3,25 %
mod. AASHTO density = 2185 (kg/m^3)
Apparent density = 2640 (kg/m^3)

CBR (%)	MC (%)	DD (kg/m^3)	DD (% mod)	DD (% AD)	T(0,050) 2,698 T
773,4	2,87	2187,5	100,11	82,86	0,480
809,5	3,26	2204,4	100,89	83,50	0,011
633,1	4,27	2230,6	102,09	84,49	1,024
905,3	4,66	2294,0	104,99	86,90	0,552
749,1	4,87	2276,2	104,17	86,22	0,992
205,4	2,92	2147,5	98,28	81,34	2,401
797,8	3,29	2201,0	100,73	83,37	0,044
827,5	4,41	2255,0	103,20	85,42	0,243
1045,1	4,82	2237,3	102,39	84,75	1,908
822,6	4,22	2286,1	104,63	86,59	1,225
885,9	4,37	2260,8	103,47	85,64	0,033
941,6	3,04	2171,1	99,36	82,24	1,857
864,7	3,26	2201,3	100,75	83,38	0,455
1231,6	4,07	2266,0	103,71	85,83	1,896
939,6	4,48	2282,7	104,47	86,47	0,160
1111,0	3,97	2294,1	104,99	86,90	0,268
345,9	2,97	2087,1	95,52	79,06	0,254
299,3	3,54	2080,1	95,20	78,79	0,425
284,1	4,18	2069,3	94,70	78,38	0,029
288,5	4,90	2082,1	95,29	78,87	0,151
283,2	5,50	2071,2	94,79	78,45	0,417
516,1	2,96	2117,5	96,91	80,21	0,278
475,9	3,30	2125,3	97,27	80,50	0,317
444,3	3,81	2130,5	97,51	80,70	0,290
420,4	5,00	2119,2	96,99	80,27	0,406
295,2	5,77	2130,2	97,49	80,69	0,466
283,1	4,05	2055,7	94,08	77,87	0,182

DENS8 - COARSE SHALE TEST RESULTS

CMC = 7,25 %
mod. AASHTO density = 2174 (kg/m^3)
Apparent density = 2774 (kg/m^3)

CBR (%)	MC (%)	DD (kg/m^3)	DD (% mod)	DD (% AD)	T(0,050) 2,580 T		
11,8	6,00	1921,6	88,39	69,27	0,375		
14,0	6,32	1889,5	86,92	68,12	0,483		
28,5	6,42	2012,2	92,56	72,54	0,294		
24,8	6,49	1986,5	91,38	71,61	0,268		
35,6	6,59	1998,7	91,94	72,05	1,417		
23,8	6,76	1976,8	90,93	71,26	0,612		
13,1	8,00	1939,4	89,21	69,91	1,231		
38,3	8,57	2068,3	95,14	74,56	0,617		
20,1	8,60	1963,5	90,32	70,78	0,410		
15,3	9,31	2000,2	92,01	72,11	0,701		
13,8	9,38	1945,9	89,51	70,15	0,433		
38,3	9,45	2113,5	97,22	76,19	0,690		
24,8	9,58	2021,8	93,00	72,89	1,079		
30,1	9,64	2147,2	98,77	77,41	1,930		
37,1	9,84	2118,5	97,45	76,37	1,001		
13,2	10,27	2027,7	93,27	73,10	0,704		
31,5	10,99	2152,4	99,01	77,59	0,606		
18,3	11,35	2125,8	97,78	76,63	0,989		
19,4	12,19	2109,4	97,03	76,04	0,366		
10,3	10,51	2103,2	96,74	75,82	3,144	#	*
17,6	10,00	2111,2	97,11	76,11	2,644	#	*

Statistical outlier * Visual outlier

OFS3 - DOLERITE CRUSHED STONE TEST RESULTS

CMC = 3,0 %
mod. AASHTO density = 2197 (kg/m^3)
Apparent density = 2966 (kg/m^3)

CBR (%)	MC (%)	DD (kg/m^3)	DD (% mod)	DD (% AD)	T(0,050) 3,179 T
260,3	0,51	2236,3	101,79	75,40	1,421
210,6	0,65	2273,8	103,49	76,66	0,557
107,1	0,74	2166,7	98,62	73,05	0,228
231,2	0,77	2136,8	97,26	72,04	1,481
176,3	0,90	2242,9	102,09	75,62	0,243
288,9	0,90	2229,9	101,50	75,18	1,360
87,7	0,93	2085,2	94,91	70,30	0,269
41,4	0,98	1968,9	89,62	66,38	0,194
144,8	1,00	2270,1	103,33	76,54	0,339
30,5	1,04	2035,4	92,64	68,62	0,154
262,7	1,10	2274,3	103,52	76,68	0,613

T(0,050)
3,179

CBR (%)	MC (%)	DD (kg/m^3)	DD (% mod)	DD (% AD)	T
167,3	1,10	2164,2	98,51	72,97	0,498
166,0	1,20	2222,0	101,14	74,91	0,050
107,4	1,62	2078,4	94,60	70,07	0,025
146,1	1,64	2183,4	99,38	73,61	0,185
249,3	1,75	2244,0	102,14	75,66	0,246
39,6	1,80	2038,6	92,79	68,73	0,535
183,0	1,84	2156,4	98,15	72,70	0,193
29,4	1,86	1979,1	90,08	66,73	0,469
310,3	1,90	2323,4	105,75	78,33	0,045
294,7	1,96	2268,6	103,26	76,49	0,307
188,1	2,00	2323,1	105,74	78,33	1,228
406,4	2,01	2235,1	101,74	75,36	1,576
114,6	2,22	2074,9	94,44	69,96	0,212
65,9	2,25	2098,5	95,51	70,75	0,782
275,9	2,27	2245,6	102,21	75,71	0,138
275,6	2,32	2188,1	99,60	73,77	0,553
613,6	2,36	2453,0	111,65	82,70	0,609
574,1	2,38	2344,9	106,73	79,06	1,764
243,0	2,39	2205,3	100,38	74,35	0,091
508,0	2,45	2389,8	108,77	80,57	0,533
154,9	2,46	2257,9	102,77	76,13	1,191
622,4	2,55	2363,2	107,57	79,68	1,853
218,2	2,70	2304,2	104,88	77,69	1,231
244,3	2,72	2297,8	104,59	77,47	0,938
441,9	2,80	2401,3	109,30	80,96	0,504
55,2	2,84	1969,2	89,63	66,39	0,637
250,3	2,85	2151,7	97,94	72,55	0,280
519,3	2,85	2378,3	108,25	80,18	0,492
61,8	2,93	2045,4	93,10	68,96	0,899
168,7	2,93	2151,3	97,92	72,53	0,503
725,6	2,96	2450,6	111,54	82,62	1,164
842,4	2,98	2467,2	112,30	83,18	1,917
151,1	2,98	2198,1	100,05	74,11	1,030
360,4	3,00	2368,6	107,81	79,86	0,935
258,3	3,03	2191,9	99,77	73,90	0,000
104,1	3,05	2061,1	93,81	69,49	0,595
35,1	3,11	1975,2	89,90	66,59	0,861
710,2	3,12	2442,3	111,16	82,34	1,231
130,1	3,12	2113,1	96,18	71,24	0,593
1329,9	3,14	2640,1	120,17	89,01	2,526
174,4	3,23	2169,4	98,75	73,14	0,487
59,3	3,26	1973,2	89,81	66,53	0,569
80,3	3,27	2087,3	95,01	70,38	0,833
374,9	3,36	2266,3	103,16	76,41	0,620
99,1	3,39	1990,8	90,61	67,12	0,207
85,6	3,42	2054,0	93,49	69,25	0,556
772,0	3,49	2464,8	112,19	83,10	1,724
889,1	3,50	2533,3	115,31	85,41	1,493
442,5	3,53	2317,8	105,50	78,14	0,817

CBR (%)	MC (%)	DD (kg/m^3)	DD (% mod)	DD (% AD)	T(0,050) 3,179 T		
545,6	3,59	2349,2	106,93	79,20	1,432		
294,5	3,60	2400,1	109,25	80,92	1,516		
367,5	3,61	2363,0	107,56	79,67	0,346		
429,0	3,67	2281,7	103,86	76,93	1,162		
292,5	3,70	2421,2	110,21	81,63	1,763		
315,9	3,70	2384,4	108,53	80,39	1,027		
558,3	3,78	2416,6	109,99	81,48	0,790		
81,0	3,81	2077,6	94,56	70,05	0,515		
529,0	3,90	2485,0	113,11	83,78	0,481		
506,7	4,00	2469,8	112,42	83,27	0,330		
1134,4	4,10	2731,3	124,32	92,09	0,900		
377,2	4,20	2518,8	114,65	84,92	2,199		
157,2	4,24	2214,3	100,79	74,66	0,372		
413,4	4,30	2419,0	110,10	81,56	0,127		
93,9	4,38	2101,3	95,64	70,85	0,199		
446,7	4,50	2436,0	110,88	82,13	0,112		
989,6	4,70	2668,7	121,47	89,98	0,478		
610,3	4,80	2639,3	120,13	88,98	2,062		
505,1	5,00	2550,8	116,11	86,00	0,781		
252,7	5,00	2333,7	106,22	78,68	0,067		
447,6	5,40	2519,6	114,68	84,95	0,221		
582,0	5,60	2589,5	117,86	87,30	0,060		
451,2	5,90	2669,8	121,52	90,01	2,639		
93,4	6,10	2226,0	101,32	75,05	0,659		
127,1	4,07	2011,5	91,56	67,82	0,289		
225,5	2,30	2507,8	114,15	84,55	3,847	#	*
471,9	3,40	2548,5	116,00	85,92	2,725		*
48,8	3,60	2293,7	104,40	77,33	2,463		*
94,5	3,70	2367,5	107,76	79,82	2,821		*
809,1	3,90	2667,7	121,42	89,94	2,132		*
628,4	3,90	2615,0	119,03	88,17	2,351		*
963,2	4,00	2525,4	114,95	85,14	2,809		*

Statistical outlier * Visual outlier

REGRESSION ANALYSIS OF CBR AS A FUNCTION OF DRY DENSITY AND MOISTURE CONTENT

BAB - BLACK CLAY(MONTMORILLONITE) RESULTS

REGRESSION ANALYSIS (% SD)

11 OUTLIERS DELETED

First approximation

Regression Output:

Constant	-1157,66 (k_4)
Std Err of Y Est	10,23081
R Squared	0,651403
No. of Observations	104
Degrees of Freedom	100

	(k_1)	(k_2)	(k_3)
X Coefficient(s)	25,59695	-0,13552	-2,68625
Std Err of Coef.	13,21104	0,072965	0,200547

Second approximation

Regression Output:

Constant	38,08868 (k_9)
Std Err of Y Est	9,364216
R Squared	0,710878
No. of Observations	104
Degrees of Freedom	99

	(k_5)	(k_6)	(k_7)	(k_8)
X Coefficient(s)	-2,02971	0,051093	0,941845	-0,00869
Std Err of Coef.	0,872899	0,014359	0,991759	0,003466

NO OUTLIERS DELETED

Regression Output:

Constant	-971,847
Std Err of Y Est	11,39783
R Squared	0,542045
No. of Observations	115
Degrees of Freedom	111

X Coefficient(s)	21,85388	-0,11739	-2,33244
Std Err of Coef.	14,19077	0,078285	0,207672

Regression Output:

Constant	0,577448
Std Err of Y Est	11,42519
R Squared	0,543990
No. of Observations	115
Degrees of Freedom	110

X Coefficient(s)	1,185000	-0,00413	-0,52561	0,001571
Std Err of Coef.	1,521405	0,025488	1,393768	0,004730

REGRESSION ANALYSIS (% mod. AASHTO)

11 OUTLIERS DELETED

Regression Output:

Constant	-1157,66
Std Err of Y Est	10,23081
R Squared	0,651403
No. of Observations	104
Degrees of Freedom	100
X Coefficient(s)	25,59695 -0,13552 -2,68625
Std Err of Coef.	13,21104 0,072965 0,200547

Regression Output:

Constant	38,08868
Std Err of Y Est	9,364216
R Squared	0,710878
No. of Observations	104
Degrees of Freedom	99
X Coefficient(s)	-2,02971 0,051093 0,941845 -0,00869
Std Err of Coef.	0,872899 0,014359 0,991759 0,003466

NO OUTLIERS DELETED

Regression Output:

Constant	-971,847
Std Err of Y Est	11,39783
R Squared	0,542045
No. of Observations	115
Degrees of Freedom	111
X Coefficient(s)	21,85388 -0,11739 -2,33244
Std Err of Coef.	14,19077 0,078285 0,207672

Regression Output:

Constant	0,577448
Std Err of Y Est	11,42519
R Squared	0,543990
No. of Observations	115
Degrees of Freedom	110
X Coefficient(s)	1,185000 -0,00413 -0,52561 0,001571
Std Err of Coef.	1,521405 0,025488 1,393768 0,004730

SPR2 - WHITE SANDY CLAY RESULTS

REGRESSION ANALYSIS (% SD)

MINUS 10 OUTLIERS

Regression Output:

Constant	-906,122
Std Err of Y Est	7,346614
R Squared	0,652228
No. of Observations	53
Degrees of Freedom	49
X Coefficient(s)	26,08765 -0,17830 -4,83332
Std Err of Coef.	14,76251 0,111027 0,515777

Regression Output:

Constant	15,84318
Std Err of Y Est	6,015099
R Squared	0,771624
No. of Observations	53
Degrees of Freedom	48
X Coefficient(s)	-1,16158 0,049074 2,938735 -0,06930
Std Err of Coef.	0,455432 0,009948 1,020897 0,019134

NO OUTLIERS DELETED

Regression Output:

Constant	-1553,33
Std Err of Y Est	9,123271
R Squared	0,519933
No. of Observations	63
Degrees of Freedom	59
X Coefficient(s)	46,06758 -0,33204 -4,67147
Std Err of Coef.	14,68043 0,109537 0,611259

Regression Output:

Constant	28,81384
Std Err of Y Est	9,628468
R Squared	0,474356
No. of Observations	63
Degrees of Freedom	58
X Coefficient(s)	-0,34241 0,003384 -1,85653 -0,02815
Std Err of Coef.	0,541993 0,003130 1,314802 0,024202

REGRESSION ANALYSIS (% mod. AASHTO)

MINUS 10 OUTLIERS

Regression Output:

Constant	-906,122
Std Err of Y Est	7,346614
R Squared	0,652228
No. of Observations	53
Degrees of Freedom	49
X Coefficient(s)	18,60565 -0,09069 -4,83332
Std Err of Coef.	10,52859 0,056474 0,515777

Regression Output:

Constant	15,84318
Std Err of Y Est	6,015099
R Squared	0,771624
No. of Observations	53
Degrees of Freedom	48
X Coefficient(s)	-1,16158 0,049074 2,938735 -0,06930
Std Err of Coef.	0,455432 0,009948 1,020897 0,019134

NO OUTLIERS DELETED

Regression Output:

Constant	-1553,33
Std Err of Y Est	9,123271
R Squared	0,519933
No. of Observations	63
Degrees of Freedom	59
X Coefficient(s)	32,85530 -0,16889 -4,67147
Std Err of Coef.	10,47005 0,055716 0,611259

Regression Output:

Constant	7,213594
Std Err of Y Est	8,884315
R Squared	0,552467
No. of Observations	63
Degrees of Freedom	58
X Coefficient(s)	-0,00944 0,020780 2,562966 -0,05841
Std Err of Coef.	0,732920 0,014955 1,532851 0,028451

SPR1 - RED SANDY CLAY RESULTS

REGRESSION ANALYSIS (% SD)

MINUS 3 OUTLIERS

Regression Output:

Constant	500,9524
Std Err of Y Est	5,726803
R Squared	0,825187
No. of Observations	52
Degrees of Freedom	48
X Coefficient(s)	-15,7824 0,133282 -3,72966
Std Err of Coef.	6,452769 0,048378 0,475634

Regression Output:

Constant	8,437631
Std Err of Y Est	5,354630
R Squared	0,850354
No. of Observations	52
Degrees of Freedom	47
X Coefficient(s)	-0,07852 0,020173 1,542591 -0,01803
Std Err of Coef.	0,407559 0,007205 1,292111 0,010166

NO OUTLIERS DELETED

Regression Output:

Constant	486,3552
Std Err of Y Est	6,496287
R Squared	0,784795
No. of Observations	55
Degrees of Freedom	51
X Coefficient(s)	-14,8716 0,124111 -4,26706
Std Err of Coef.	6,723719 0,050481 0,500000

Regression Output:

Constant	21,33191
Std Err of Y Est	6,281781
R Squared	0,802718
No. of Observations	55
Degrees of Freedom	50
X Coefficient(s)	0,138308 0,014858 -1,28020 -0,00419
Std Err of Coef.	0,474678 0,008344 1,337468 0,011397

REGRESSION ANALYSIS (% mod. AASHTO)

MINUS 3 OUTLIERS

Regression Output:

Constant	500,9524
Std Err of Y Est	5,726803
R Squared	0,825187
No. of Observations	52
Degrees of Freedom	48
X Coefficient(s)	-10,9056 0,063639 -3,72966
Std Err of Coef.	4,458842 0,023099 0,475634

Regression Output:

Constant	8,437631
Std Err of Y Est	5,354630
R Squared	0,850354
No. of Observations	52
Degrees of Freedom	47
X Coefficient(s)	-0,07852 0,020173 1,542591 -0,01803
Std Err of Coef.	0,407559 0,007205 1,292111 0,010166

NO OUTLIERS DELETED

Regression Output:

Constant	486,3552
Std Err of Y Est	6,496287
R Squared	0,784795
No. of Observations	55
Degrees of Freedom	51
X Coefficient(s)	-10,2762 0,059260 -4,26706
Std Err of Coef.	4,646067 0,024103 0,500000

Regression Output:

Constant	21,33191
Std Err of Y Est	6,281781
R Squared	0,802718
No. of Observations	55
Degrees of Freedom	50
X Coefficient(s)	0,138308 0,014858 -1,28020 -0,00419
Std Err of Coef.	0,474678 0,008344 1,337468 0,011397

LABLEN - RED SILTY SAND RESULTS

REGRESSION ANALYSIS (% SD)

NO OUTLIERS DELETED

Regression Output:

Constant	1110,291
Std Err of Y Est	9,161172
R Squared	0,846184
No. of Observations	56
Degrees of Freedom	52
X Coefficient(s)	-35,1086 0,283859 -8,35666
Std Err of Coef.	9,412528 0,067500 0,597222

Regression Output:

Constant	15,69181
Std Err of Y Est	8,156095
R Squared	0,880427
No. of Observations	56
Degrees of Freedom	51
X Coefficient(s)	0,136949 0,010369 -0,15523 -0,03325
Std Err of Coef.	0,273042 0,003009 1,529823 0,040850

REGRESSION ANALYSIS (% mod. AASHTO)

NO OUTLIERS DELETED

Regression Output:

Constant	1110,291
Std Err of Y Est	9,161172
R Squared	0,846184
No. of Observations	56
Degrees of Freedom	52
X Coefficient(s)	-27,2001 0,170379 -8,35666
Std Err of Coef.	7,292276 0,040515 0,597222

Regression Output:

Constant	15,69181
Std Err of Y Est	8,156095
R Squared	0,880427
No. of Observations	56
Degrees of Freedom	51
X Coefficient(s)	0,136949 0,010369 -0,15523 -0,03325
Std Err of Coef.	0,273042 0,003009 1,529823 0,040850

LABDEW - SLIGHTLY PLASTIC SAND RESULTS

REGRESSION ANALYSIS (% SD)

MINUS 5 OUTLIERS

Regression Output:

Constant	-506,988
Std Err of Y Est	10,44925
R Squared	0,672654
No. of Observations	52
Degrees of Freedom	48
X Coefficient(s)	11,64167 -0,05415 -8,92216
Std Err of Coef.	22,69572 0,152454 1,161309

Regression Output:

Constant	7,811143
Std Err of Y Est	8,117989
R Squared	0,806540
No. of Observations	52
Degrees of Freedom	47
X Coefficient(s)	0,115468 0,010568 10,61166 -0,69635
Std Err of Coef.	0,416296 0,004717 2,304291 0,128314

NO OUTLIERS DELETED

Regression Output:

Constant	-214,933
Std Err of Y Est	11,98602
R Squared	0,553719
No. of Observations	57
Degrees of Freedom	53
X Coefficient(s)	3,697473 -0,00079 -7,49340
Std Err of Coef.	24,98930 0,167836 1,279062

Regression Output:

Constant	71,78962
Std Err of Y Est	9,700854
R Squared	0,713182
No. of Observations	57
Degrees of Freedom	52
X Coefficient(s)	1,489072 -0,00900 11,31176 -0,75295
Std Err of Coef.	0,334498 0,004647 2,571463 0,148177

REGRESSION ANALYSIS (% mod. AASHTO)

MINUS 5 OUTLIERS

Regression Output:

Constant	-506,988
Std Err of Y Est	10,44925
R Squared	0,672654
No. of Observations	52
Degrees of Freedom	48
X Coefficient(s)	8,957136 -0,03205 -8,92216
Std Err of Coef.	17,46215 0,090250 1,161309

Regression Output:

Constant	7,811143
Std Err of Y Est	8,117989
R Squared	0,806540
No. of Observations	52
Degrees of Freedom	47
X Coefficient(s)	0,115468 0,010568 10,61166 -0,69635
Std Err of Coef.	0,416296 0,004717 2,304291 0,128314

NO OUTLIERS DELETED

Regression Output:

Constant	-214,933
Std Err of Y Est	11,98602
R Squared	0,553719
No. of Observations	57
Degrees of Freedom	53
X Coefficient(s)	2,844847 -0,00047 -7,49340
Std Err of Coef.	19,22684 0,099356 1,279062

Regression Output:

Constant	6,078509
Std Err of Y Est	9,646699
R Squared	0,716376
No. of Observations	57
Degrees of Freedom	52
X Coefficient(s)	0,024323 0,011634 12,94292 -0,77774
Std Err of Coef.	0,489071 0,005535 2,613561 0,148116

OFS1 - WINDBLOWN SAND RESULTS

REGRESSION ANALYSIS (% SD)

MINUS 8 OUTLIERS

Regression Output:

Constant	3100,903
Std Err of Y Est	5,416660
R Squared	0,675352
No. of Observations	45
Degrees of Freedom	41
X Coefficient(s)	-99,4868 0,800305 -2,07520
Std Err of Coef.	35,67020 0,276093 0,673262

Regression Output:

Constant	1,476967
Std Err of Y Est	5,308143
R Squared	0,695834
No. of Observations	45
Degrees of Freedom	40
X Coefficient(s)	0,559637 0,013853 1,828624 -0,14034
Std Err of Coef.	0,334805 0,010162 1,855549 0,122661

NO OUTLIERS DELETED

Regression Output:

Constant	1341,949
Std Err of Y Est	9,924684
R Squared	0,294063
No. of Observations	53
Degrees of Freedom	49
X Coefficient(s)	-44,4571 0,370557 -1,14946
Std Err of Coef.	52,14399 0,404805 1,093638

Regression Output:

Constant	4,999918
Std Err of Y Est	10,08363
R Squared	0,286143
No. of Observations	53
Degrees of Freedom	48
X Coefficient(s)	0,648162 0,006403 0,691323 -0,01997
Std Err of Coef.	0,614165 0,018900 3,189781 0,214181

REGRESSION ANALYSIS (% mod. AASHTO)

MINUS 8 OUTLIERS

Regression Output:

Constant	3100,903
Std Err of Y Est	5,416660
R Squared	0,675352
No. of Observations	45
Degrees of Freedom	41
X Coefficient(s)	-67,0365 0,363368 -2,07520
Std Err of Coef.	24,03540 0,125356 0,673262

Regression Output:

Constant	1,476967
Std Err of Y Est	5,308143
R Squared	0,695834
No. of Observations	45
Degrees of Freedom	40
X Coefficient(s)	0,559637 0,013853 1,828624 -0,14034
Std Err of Coef.	0,334805 0,010162 1,855549 0,122661

NO OUTLIERS DELETED

Regression Output:

Constant	1341,949
Std Err of Y Est	9,924684
R Squared	0,294063
No. of Observations	53
Degrees of Freedom	49
X Coefficient(s)	-29,9562 0,168246 -1,14946
Std Err of Coef.	35,13582 0,183796 1,093638

Regression Output:

Constant	3,047504
Std Err of Y Est	10,00945
R Squared	0,296606
No. of Observations	53
Degrees of Freedom	48
X Coefficient(s)	0,578123 0,012808 0,044287 -0,00859
Std Err of Coef.	1,038074 0,030752 3,167214 0,211484

NPAB - BROWN DECOMPOSED DOLERITE RESULTS

REGRESSION ANALYSIS (% SD)

MINUS 15 OUTLIERS

Regression Output:

Constant	846,6028
Std Err of Y Est	14,13612
R Squared	0,738133
No. of Observations	48
Degrees of Freedom	44
X Coefficient(s)	-29,8951 0,265798 -7,08581
Std Err of Coef.	32,07377 0,223367 1,181758

Regression Output:

Constant	-0,09501
Std Err of Y Est	14,00404
R Squared	0,748844
No. of Observations	48
Degrees of Freedom	43
X Coefficient(s)	0,844810 0,001141 3,099420 -0,08015
Std Err of Coef.	0,311301 0,002509 2,983191 0,064736

NO OUTLIERS DELETED

Regression Output:

Constant	-391,408
Std Err of Y Est	20,83116
R Squared	0,458155
No. of Observations	63
Degrees of Freedom	59
X Coefficient(s)	6,859756 -0,00668 -6,92390
Std Err of Coef.	41,60622 0,288607 1,609439

Regression Output:

Constant	5,514632
Std Err of Y Est	20,98511
R Squared	0,459437
No. of Observations	63
Degrees of Freedom	58
X Coefficient(s)	0,774829 0,002175 -0,14888 -0,00219
Std Err of Coef.	0,633032 0,005881 3,949230 0,088939

REGRESSION ANALYSIS (% mod AASHTO)

MINUS 15 OUTLIERS

Regression Output:

Constant	846,6028
Std Err of Y Est	14,13612
R Squared	0,738133
No. of Observations	48
Degrees of Freedom	44
X Coefficient(s)	-22,7359 0,153736 -7,08581
Std Err of Coef.	24,39286 0,129194 1,181758

Regression Output:

Constant	-0,09501
Std Err of Y Est	14,00404
R Squared	0,748844
No. of Observations	48
Degrees of Freedom	43
X Coefficient(s)	0,844810 0,001141 3,099420 -0,08015
Std Err of Coef.	0,311301 0,002509 2,983191 0,064736

NO OUTLIERS DELETED

Regression Output:

onstant	-391,408
Std Err of Y Est	20,83116
R Squared	0,458155
No. of Observations	63
Degrees of Freedom	59
X Coefficient(s)	5,217006 -0,00386 -6,92390
Std Err of Coef.	31,64251 0,166929 1,609439

Regression Output:

Constant	5,514632
Std Err of Y Est	20,98511
R Squared	0,459437
No. of Observations	63
Degrees of Freedom	58
X Coefficient(s)	0,774829 0,002175 -0,14888 -0,00219
Std Err of Coef.	0,633032 0,005881 3,949230 0,088939

SIL - SILTY SAND RESULTS

REGRESSION ANALYSIS (% SD)

MINUS 1 OUTLIER

Regression Output:

Constant	-256,092
Std Err of Y Est	7,609215
R Squared	0,715895
No. of Observations	74
Degrees of Freedom	70
X Coefficient(s)	6,897218 -0,03683 -5,68948
Std Err of Coef.	6,882820 0,050957 0,434428

Regression Output:

Constant	10,74612
Std Err of Y Est	5,853235
R Squared	0,834292
No. of Observations	74
Degrees of Freedom	69
X Coefficient(s)	-0,52004 0,037517 0,280034 -0,01436
Std Err of Coef.	0,319249 0,006651 0,789500 0,017918

NO OUTLIERS DELETED

Regression Output:

Constant	-306,890
Std Err of Y Est	7,888675
R Squared	0,696969
No. of Observations	75
Degrees of Freedom	71
X Coefficient(s)	8,322556 -0,04683 -5,66986
Std Err of Coef.	7,111316 0,052667 0,450310

Regression Output:

Constant	80,82823
Std Err of Y Est	6,050693
R Squared	0,824236
No. of Observations	75
Degrees of Freedom	70
X Coefficient(s)	2,822826 -0,02990 -1,66623 0,009074
Std Err of Coef.	0,331180 0,005193 0,720983 0,016004

REGRESSION ANALYSIS (% mod. AASHTO)

MINUS 1 OUTLIER

Regression Output:

Constant	-256,092
Std Err of Y Est	7,609215
R Squared	0,715895
No. of Observations	74
Degrees of Freedom	70
X Coefficient(s)	4,857159 -0,01826 -5,68948
Std Err of Coef.	4,847020 0,025271 0,434428

Regression Output:

Constant	10,74612
Std Err of Y Est	5,853235
R Squared	0,834292
No. of Observations	74
Degrees of Freedom	69
X Coefficient(s)	-0,52004 0,037517 0,280034 -0,01436
Std Err of Coef.	0,319249 0,006651 0,789500 0,017918

NO OUTLIERS DELETED

Regression Output:

Constant	-306,890
Std Err of Y Est	7,888675
R Squared	0,696969
No. of Observations	75
Degrees of Freedom	71
X Coefficient(s)	5,860911 -0,02322 -5,66986
Std Err of Coef.	5,007932 0,026119 0,450310

Regression Output:

Constant	9,907661
Std Err of Y Est	6,077672
R Squared	0,822666
No. of Observations	75
Degrees of Freedom	70
X Coefficient(s)	-0,51440 0,038385 -0,37320 0,196637
Std Err of Coef.	0,284251 0,006082 0,636335 0,202040

LABD - RED CHERT SOIL RESULTS

REGRESSION ANALYSIS (% SD)

NO OUTLIERS DELETED

Regression Output:		Regression Output:	
Constant	-50,4299	Constant	20,32097
Std Err of Y Est	9,765361	Std Err of Y Est	7,519645
R Squared	0,837371	R Squared	0,905460
No. of Observations	55	No. of Observations	55
Degrees of Freedom	51	Degrees of Freedom	50
X Coefficient(s)	-1,50173 0,040761 -7,31065	X Coefficient(s)	0,098094 0,012103 -3,40003 0,020542
Std Err of Coef.	22,82601 0,156883 0,628888	Std Err of Coef.	0,310807 0,003628 1,182153 0,025519

REGRESSION ANALYSIS (%mod.AASHTO)

NO OUTLIERS DELETED

Regression Output:		Regression Output:	
Constant	-50,4299	Constant	20,32097
Std Err of Y Est	9,765361	Std Err of Y Est	7,519645
R Squared	0,837371	R Squared	0,905460
No. of Observations	55	No. of Observations	55
Degrees of Freedom	51	Degrees of Freedom	50
X Coefficient(s)	-1,12469 0,022862 -7,31065	X Coefficient(s)	0,098094 0,012103 -3,40003 0,020542
Std Err of Coef.	17,09505 0,087994 0,628888	Std Err of Coef.	0,310807 0,003628 1,182153 0,025519

TPA3 - CHERT GRAVEL RESULTS

REGRESSION ANALYSIS (% SD)

NO OUTLIERS

Regression Output:

Constant	1903,847
Std Err of Y Est	25,10491
R Squared	0,817423
No. of Observations	57
Degrees of Freedom	53
X Coefficient(s)	-61,3005 0,505757 -23,2003
Std Err of Coef.	56,80480 0,387953 2,006042

Regression Output:

Constant	38,51345
Std Err of Y Est	21,68706
R Squared	0,866323
No. of Observations	57
Degrees of Freedom	52
X Coefficient(s)	0,115213 0,004781 -4,48291 -0,02266
Std Err of Coef.	0,237011 0,001169 4,307341 0,154588

REGRESSION ANALYSIS (%mod.AASHTO)

NO OUTLIERS

Regression Output:

Constant	1903,847
Std Err of Y Est	25,10491
R Squared	0,817423
No. of Observations	57
Degrees of Freedom	53
X Coefficient(s)	-46,2649 0,288083 -23,2003
Std Err of Coef.	42,87193 0,220981 2,006042

Regression Output:

Constant	38,51345
Std Err of Y Est	21,68706
R Squared	0,866323
No. of Observations	57
Degrees of Freedom	52
X Coefficient(s)	0,115213 0,004781 -4,48291 -0,02266
Std Err of Coef.	0,237011 0,001169 4,307341 0,154588

TPA1 - NORITE GRAVEL RESULTS

REGRESSION ANALYSIS (% SD)

NO OUTLIERS

Regression Output:

Constant	840,6045
Std Err of Y Est	8,997341
R Squared	0,624297
No. of Observations	57
Degrees of Freedom	53
X Coefficient(s)	-25,2054 0,195871 -6,96135
Std Err of Coef.	15,03941 0,104185 0,909379

Regression Output:

Constant	20,85469
Std Err of Y Est	7,693548
R Squared	0,730476
No. of Observations	57
Degrees of Freedom	52
X Coefficient(s)	-0,41540 0,021249 1,206949 -0,13257
Std Err of Coef.	0,332783 0,004726 1,799980 0,074186

REGRESSION ANALYSIS (% mod. AASHTO)

NO OUTLIERS

Regression Output:

Constant	840,6045
Std Err of Y Est	8,997341
R Squared	0,624297
No. of Observations	57
Degrees of Freedom	53
X Coefficient(s)	-19,0168 0,111496 -6,96135
Std Err of Coef.	11,34686 0,059305 0,909379

Regression Output:

Constant	20,85469
Std Err of Y Est	7,693548
R Squared	0,730476
No. of Observations	57
Degrees of Freedom	52
X Coefficient(s)	-0,41540 0,021249 1,206949 -0,13257
Std Err of Coef.	0,332783 0,004726 1,799980 0,074186

CPA1 - HORNFELS CRUSHED STONE RESULTS

REGRESSION ANALYSIS (% SD)

MINUS 5 OUTLIERS

Regression Output:

Constant	-14715,2
Std Err of Y Est	63,40979
R Squared	0,763998
No. of Observations	19
Degrees of Freedom	15
X Coefficient(s)	346,9165 -1,99377 -0,33218
Std Err of Coef.	124,5844 0,760830 29,98297

Regression Output:

Constant	-37,2744
Std Err of Y Est	60,37888
R Squared	0,800285
No. of Observations	19
Degrees of Freedom	14
X Coefficient(s)	0,910836 0,000239 58,02037 -8,93017
Std Err of Coef.	0,908140 0,001977 48,03659 5,812780

NO OUTLIERS DELETED

Regression Output:

Constant	-6617,84
Std Err of Y Est	154,2922
R Squared	0,438939
No. of Observations	24
Degrees of Freedom	20
X Coefficient(s)	142,2264 -0,69356 -50,9903
Std Err of Coef.	286,8384 1,747062 65,04069

Regression Output:

Constant	84,53730
Std Err of Y Est	160,1282
R Squared	0,425908
No. of Observations	24
Degrees of Freedom	19
X Coefficient(s)	-0,27545 0,003366 16,97096 -5,95816
Std Err of Coef.	2,338968 0,005027 125,2649 14,77098

REGRESSION ANALYSIS (% mod. AASHTO)

MINUS 5 OUTLIERS

Regression Output:

Constant	-14715,2
Std Err of Y Est	63,40979
R Squared	0,763998
No. of Observations	19
Degrees of Freedom	15
X Coefficient(s)	298,4539 -1,47564 -0,33218
Std Err of Coef.	107,1806 0,563108 29,98297

Regression Output:

Constant	-37,2744
Std Err of Y Est	60,37888
R Squared	0,800285
No. of Observations	19
Degrees of Freedom	14
X Coefficient(s)	0,910836 0,000239 58,02037 -8,93017
Std Err of Coef.	0,908140 0,001977 48,03659 5,812780

NO OUTLIERS DELETED

Regression Output:

Constant	-6617,84
Std Err of Y Est	154,2922
R Squared	0,438939
No. of Observations	24
Degrees of Freedom	20
X Coefficient(s)	122,3580 -0,51332 -50,9903
Std Err of Coef.	246,7684 1,293043 65,04069

Regression Output:

Constant	84,53730
Std Err of Y Est	160,1282
R Squared	0,425908
No. of Observations	24
Degrees of Freedom	19
X Coefficient(s)	-0,27545 0,003366 16,97096 -5,95816
Std Err of Coef.	2,338968 0,005027 125,2649 14,77098

DENS7 - DOLOMITIC SOIL RESULTS

REGRESSION ANALYSIS (% SD)

MINUS 1 OUTLIER

Regression Output:

Constant	-10058,1
Std Err of Y Est	11,58049
R Squared	0,901603
No. of Observations	26
Degrees of Freedom	22
X Coefficient(s)	261,3792 -1,67989 -21,5392
Std Err of Coef.	64,15838 0,419336 1,518269

Regression Output:

Constant	18,77738
Std Err of Y Est	8,402319
R Squared	0,950555
No. of Observations	26
Degrees of Freedom	21
X Coefficient(s)	-0,08876 0,010347 1,930865 -0,20606
Std Err of Coef.	0,292960 0,002522 3,475981 0,132728

NO OUTLIERS DELETED

Regression Output:

Constant	-7776,63
Std Err of Y Est	14,66573
R Squared	0,835086
No. of Observations	27
Degrees of Freedom	23
X Coefficient(s)	201,5208 -1,28875 -19,7925
Std Err of Coef.	78,84026 0,515303 1,835297

Regression Output:

Constant	20,86372
Std Err of Y Est	13,33487
R Squared	0,869587
No. of Observations	27
Degrees of Freedom	22
X Coefficient(s)	-0,08160 0,009113 1,459663 -0,20326
Std Err of Coef.	0,464938 0,003989 5,515072 0,210645

REGRESSION ANALYSIS (% mod. AASHTO)

MINUS 1 OUTLIER

Regression Output:

Constant	-10058,1
Std Err of Y Est	11,58049
R Squared	0,901603
No. of Observations	26
Degrees of Freedom	22
X Coefficient(s)	208,5998 -1,06996 -21,5392
Std Err of Coef.	51,20310 0,267084 1,518269

Regression Output:

Constant	18,77738
Std Err of Y Est	8,402319
R Squared	0,950555
No. of Observations	26
Degrees of Freedom	21
X Coefficient(s)	-0,08876 0,010347 1,930865 -0,20606
Std Err of Coef.	0,292960 0,002522 3,475981 0,132728

NO OUTLIERS DELETED

Regression Output:

Constant	-7776,63
Std Err of Y Est	14,66573
R Squared	0,835086
No. of Observations	27
Degrees of Freedom	23
X Coefficient(s)	160,8284 -0,82083 -19,7925
Std Err of Coef.	62,92032 0,328208 1,835297

Regression Output:

Constant	18,55307
Std Err of Y Est	12,58129
R Squared	0,883910
No. of Observations	27
Degrees of Freedom	22
X Coefficient(s)	-0,23694 0,012683 3,138744 -0,25148
Std Err of Coef.	0,485445 0,004505 5,290131 0,200918

TPA2 - QUARTZITE GRAVEL RESULTS

REGRESSION ANALYSIS (% SD)

NO OUTLIERS

Regression Output:

Constant	693,6289
Std Err of Y Est	21,16575
R Squared	0,769425
No. of Observations	67
Degrees of Freedom	63
X Coefficient(s)	-25,3251 0,230182 -12,6030
Std Err of Coef.	28,94947 0,192707 1,661920

Regression Output:

Constant	16,79980
Std Err of Y Est	19,24224
R Squared	0,812454
No. of Observations	67
Degrees of Freedom	62
X Coefficient(s)	0,230993 0,005369 4,520759 -0,21605
Std Err of Coef.	0,235088 0,001595 3,568645 0,120051

REGRESSION ANALYSIS (% mod. AASHTO)

NO OUTLIERS

Regression Output:

Constant	693,6289
Std Err of Y Est	21,16575
R Squared	0,769425
No. of Observations	67
Degrees of Freedom	63
X Coefficient(s)	-19,5508 0,137183 -12,6030
Std Err of Coef.	22,34886 0,114849 1,661920

Regression Output:

Constant	16,79980
Std Err of Y Est	19,24224
R Squared	0,812454
No. of Observations	67
Degrees of Freedom	62
X Coefficient(s)	0,230993 0,005369 4,520759 -0,21605
Std Err of Coef.	0,235088 0,001595 3,568645 0,120051

NPAE - TILLITE CRUSHED STONE RESULTS

REGRESSION ANALYSIS (% SD)

MINUS 2 OUTLIERS

Regression Output:

Constant	6072,841
Std Err of Y Est	65,83300
R Squared	0,711488
No. of Observations	78
Degrees of Freedom	74
X Coefficient(s)	-166,179 1,163307 -40,1172
Std Err of Coef.	77,10310 0,481878 6,713608

Regression Output:

Constant	105,0719
Std Err of Y Est	56,35989
R Squared	0,791403
No. of Observations	78
Degrees of Freedom	73
X Coefficient(s)	0,091494 0,002387 -35,0636 1,500732
Std Err of Coef.	0,264853 0,000643 11,96485 0,642455

NO OUTLIERS DELETED

Regression Output:

Constant	7112,025
Std Err of Y Est	74,61073
R Squared	0,626405
No. of Observations	80
Degrees of Freedom	76
X Coefficient(s)	-191,426 1,313304 -34,5280
Std Err of Coef.	87,16966 0,544913 7,490405

Regression Output:

Constant	100,7730
Std Err of Y Est	68,82554
R Squared	0,686278
No. of Observations	80
Degrees of Freedom	75
X Coefficient(s)	0,073713 0,002477 -30,2010 1,271662
Std Err of Coef.	0,362492 0,000907 14,32443 0,772295

REGRESSION ANALYSIS (% mod. AASHTO)

MINUS 2 OUTLIERS

Regression Output:

Constant	6072,841
Std Err of Y Est	65,83300
R Squared	0,711488
No. of Observations	78
Degrees of Freedom	74
X Coefficient(s)	-142,115 0,850791 -40,1172
Std Err of Coef.	65,93806 0,352424 6,713608

Regression Output:

Constant	105,0719
Std Err of Y Est	56,35989
R Squared	0,791403
No. of Observations	78
Degrees of Freedom	73
X Coefficient(s)	0,091494 0,002387 -35,0636 1,500732
Std Err of Coef.	0,264853 0,000643 11,96485 0,642455

NO OUTLIERS DELETED

Regression Output:

Constant	7112,025
Std Err of Y Est	74,61073
R Squared	0,626405
No. of Observations	80
Degrees of Freedom	76
X Coefficient(s)	-163,706 0,960492 -34,5280
Std Err of Coef.	74,54691 0,398525 7,490405

Regression Output:

Constant	100,7730
Std Err of Y Est	68,82554
R Squared	0,686278
No. of Observations	80
Degrees of Freedom	75
X Coefficient(s)	0,073713 0,002477 -30,2010 1,271662
Std Err of Coef.	0,362492 0,000907 14,32443 0,772295

FERR1 - QUARTZITE CRUSHED STONE RESULTS

REGRESSION ANALYSIS (% SD)

MINUS 4 OUTLIERS

Regression Output:

Constant	16684,03
Std Err of Y Est	63,32482
R Squared	0,767226
No. of Observations	26
Degrees of Freedom	22
X Coefficient(s)	-437,531 2,906330 -44,5075
Std Err of Coef.	230,2052 1,416615 29,79358

Regression Output:

Constant	0,542700
Std Err of Y Est	64,72659
R Squared	0,767860
No. of Observations	26
Degrees of Freedom	21
X Coefficient(s)	0,956599 0,000052 16,09472 -6,38783
Std Err of Coef.	0,903116 0,001297 74,91867 26,65900

NO OUTLIERS DELETED

Regression Output:

Constant	7189,706
Std Err of Y Est	83,78773
R Squared	0,535206
No. of Observations	30
Degrees of Freedom	26
X Coefficient(s)	-194,462 1,347710 -19,1729
Std Err of Coef.	273,5543 1,677226 36,85410

Regression Output:

Constant	-59,1911
Std Err of Y Est	85,00732
R Squared	0,539978
No. of Observations	30
Degrees of Freedom	25
X Coefficient(s)	1,321070 -0,00056 38,17378 -14,4533
Std Err of Coef.	1,853052 0,002997 88,83761 32,59716

REGRESSION ANALYSIS (% mod. AASHTO)

MINUS 4 OUTLIERS

Regression Output:

Constant	16684,03
Std Err of Y Est	63,32482
R Squared	0,767226
No. of Observations	26
Degrees of Freedom	22
X Coefficient(s)	-354,923 1,912469 -44,5075
Std Err of Coef.	186,7411 0,932183 29,79358

Regression Output:

Constant	0,542700
Std Err of Y Est	64,72659
R Squared	0,767860
No. of Observations	26
Degrees of Freedom	21
X Coefficient(s)	0,956599 0,000052 16,09472 -6,38783
Std Err of Coef.	0,903116 0,001297 74,91867 26,65900

NO OUTLIERS DELETED

Regression Output:

Constant	7189,706
Std Err of Y Est	83,78773
R Squared	0,535206
No. of Observations	30
Degrees of Freedom	26
X Coefficient(s)	-157,747 0,886841 -19,1729
Std Err of Coef.	221,9056 1,103674 36,85410

Regression Output:

Constant	-59,1911
Std Err of Y Est	85,00732
R Squared	0,539978
No. of Observations	30
Degrees of Freedom	25
X Coefficient(s)	1,321070 -0,00056 38,17378 -14,4533
Std Err of Coef.	1,853052 0,002997 88,83761 32,59716

OFS2 - WEATHERED DOLERITE RESULTS

REGRESSION ANALYSIS (% SD)

MINUS 2 OUTLIERS

Regression Output:

Constant	10389,04
Std Err of Y Est	58,01894
R Squared	0,671338
No. of Observations	69
Degrees of Freedom	65
X Coefficient(s)	-286,452 2,010777 -54,4582
Std Err of Coef.	104,6680 0,687146 8,227777

Regression Output:

Constant	141,5883
Std Err of Y Est	52,73209
R Squared	0,732683
No. of Observations	69
Degrees of Freedom	64
X Coefficient(s)	-0,28873 0,003148 -32,3916 1,293097
Std Err of Coef.	0,356693 0,000827 18,94492 1,349786

NO OUTLIERS DELETED

Regression Output:

Constant	11170,20
Std Err of Y Est	60,83120
R Squared	0,630570
No. of Observations	71
Degrees of Freedom	67
X Coefficient(s)	-306,419 2,136845 -52,6150
Std Err of Coef.	109,4291 0,718488 8,601159

Regression Output:

Constant	147,4303
Std Err of Y Est	55,57540
R Squared	0,696252
No. of Observations	71
Degrees of Freedom	66
X Coefficient(s)	-0,37149 0,003280 -33,0145 1,398727
Std Err of Coef.	0,374774 0,000871 19,93143 1,420734

REGRESSION ANALYSIS (% mod. AASHTO)

MINUS 2 OUTLIERS

Regression Output:

Constant	10389,04
Std Err of Y Est	58,01894
R Squared	0,671338
No. of Observations	69
Degrees of Freedom	65
X Coefficient(s)	-227,567 1,269050 -54,4582
Std Err of Coef.	83,15178 0,433674 8,227777

Regression Output:

Constant	141,5883
Std Err of Y Est	52,73209
R Squared	0,732683
No. of Observations	69
Degrees of Freedom	64
X Coefficient(s)	-0,28873 0,003148 -32,3916 1,293097
Std Err of Coef.	0,356693 0,000827 18,94492 1,349786

NO OUTLIERS DELETED

Regression Output:

Constant	11170,20
Std Err of Y Est	60,83120
R Squared	0,630570
No. of Observations	71
Degrees of Freedom	67
X Coefficient(s)	-243,429 1,348614 -52,6150
Std Err of Coef.	86,93412 0,453455 8,601159

Regression Output:

Constant	148,7795
Std Err of Y Est	56,28741
R Squared	0,688419
No. of Observations	71
Degrees of Freedom	66
X Coefficient(s)	-0,33957 0,003273 -35,0107 1,486267
Std Err of Coef.	0,403465 0,000940 20,52089 1,455872

NPAA - DOLERITE CRUSHED STONE RESULTS

REGRESSION ANALYSIS (% SD)

MINUS 3 OUTLIERS

Regression Output:

Constant	1315,824
Std Err of Y Est	113,4983
R Squared	0,702334
No. of Observations	61
Degrees of Freedom	57
X Coefficient(s)	-61,8969 0,631577 -107,599
Std Err of Coef.	264,3257 1,592562 15,24437

Regression Output:

Constant	166,8397
Std Err of Y Est	98,31923
R Squared	0,780547
No. of Observations	61
Degrees of Freedom	56
X Coefficient(s)	0,081187 0,001264 -34,7615 2,248692
Std Err of Coef.	0,331107 0,000401 29,38538 2,772950

NO OUTLIERS DELETED

Regression Output:

Constant	1452,194
Std Err of Y Est	118,7686
R Squared	0,673548
No. of Observations	64
Degrees of Freedom	60
X Coefficient(s)	-64,6812 0,645522 -107,245
Std Err of Coef.	272,4310 1,641808 15,94722

Regression Output:

Constant	177,2892
Std Err of Y Est	105,9296
R Squared	0,744641
No. of Observations	64
Degrees of Freedom	59
X Coefficient(s)	0,025640 0,001314 -28,5202 1,492191
Std Err of Coef.	0,358830 0,000436 31,50079 2,926145

REGRESSION ANALYSIS (% mod. AASHTO)

MINUS 3 OUTLIERS

Regression Output:

Constant	1315,824
Std Err of Y Est	113,4983
R Squared	0,702334
No. of Observations	61
Degrees of Freedom	57

X Coefficient(s)	-50,9008 0,427109 -107,599
Std Err of Coef.	217,3679 1,076981 15,24437

Regression Output:

Constant	166,8397
Std Err of Y Est	98,31923
R Squared	0,780547
No. of Observations	61
Degrees of Freedom	56

X Coefficient(s)	0,081187 0,001264 -34,7615 2,248692
Std Err of Coef.	0,331107 0,000401 29,38538 2,772950

NO OUTLIERS DELETED

Regression Output:

Constant	1452,194
Std Err of Y Est	118,7686
R Squared	0,673548
No. of Observations	64
Degrees of Freedom	60

X Coefficient(s)	-53,1905 0,436539 -107,245
Std Err of Coef.	224,0332 1,110285 15,94722

Regression Output:

Constant	177,2892
Std Err of Y Est	105,9296
R Squared	0,744641
No. of Observations	64
Degrees of Freedom	59

X Coefficient(s)	0,025640 0,001314 -28,5202 1,492191
Std Err of Coef.	0,358830 0,000436 31,50079 2,926145

ROSS1 - GRANITE CRUSHED STONE RESULTS

REGRESSION ANALYSIS (% SD)

NO OUTLIERS

Regression Output:

Constant	-14055,9
Std Err of Y Est	148,8665
R Squared	0,786950
No. of Observations	27
Degrees of Freedom	23
X Coefficient(s)	270,6583 -1,11077 -70,8178
Std Err of Coef.	748,7600 4,535392 45,09597

Regression Output:

Constant	157,7683
Std Err of Y Est	150,6623
R Squared	0,791267
No. of Observations	27
Degrees of Freedom	22
X Coefficient(s)	0,453517 0,000451 -38,8983 4,613699
Std Err of Coef.	0,822940 0,000670 101,5098 17,81791

REGRESSION ANALYSIS (%mod.AASHTO)

NO OUTLIERS

Regression Output:

Constant	-14055,9
Std Err of Y Est	148,8665
R Squared	0,786950
No. of Observations	27
Degrees of Freedom	23
X Coefficient(s)	224,0107 -0,76089 -70,8178
Std Err of Coef.	619,7124 3,106775 45,09597

Regression Output:

Constant	157,7683
Std Err of Y Est	150,6623
R Squared	0,791267
No. of Observations	27
Degrees of Freedom	22
X Coefficient(s)	0,453517 0,000451 -38,8983 4,613699
Std Err of Coef.	0,822940 0,000670 101,5098 17,81791

DENS8 - COARSE SHALE RESULTS

REGRESSION ANALYSIS (% SD)

MINUS 2 OUTLIERS

Regression Output:

Constant	-647,914
Std Err of Y Est	4,639253
R Squared	0,793333
No. of Observations	19
Degrees of Freedom	15
X Coefficient(s)	11,59061 -0,04547 -6,59050
Std Err of Coef.	17,28406 0,092760 1,241749

Regression Output:

Constant	8,318642
Std Err of Y Est	4,662514
R Squared	0,805172
No. of Observations	19
Degrees of Freedom	14
X Coefficient(s)	0,288645 0,015427 -1,01527 0,048065
Std Err of Coef.	0,847084 0,017905 2,096276 0,087511

NO OUTLIERS DELETED

Regression Output:

Constant	-463,638
Std Err of Y Est	6,301165
R Squared	0,617269
No. of Observations	21
Degrees of Freedom	17
X Coefficient(s)	10,07728 -0,04421 -6,92099
Std Err of Coef.	29,87314 0,204586 1,672066

Regression Output:

Constant	19,14916
Std Err of Y Est	5,935815
R Squared	0,680344
No. of Observations	21
Degrees of Freedom	16
X Coefficient(s)	-0,69660 0,039105 -2,44652 0,117826
Std Err of Coef.	1,237493 0,027396 2,421527 0,103864

REGRESSION ANALYSIS (% mod. AASHTO)

MINUS 2 OUTLIERS

Regression Output:

Constant	-647,914
Std Err of Y Est	4,639253
R Squared	0,793333
No. of Observations	19
Degrees of Freedom	15
X Coefficient(s)	11,59061 -0,04547 -6,59050
Std Err of Coef.	17,28406 0,092760 1,241749

Regression Output:

Constant	8,318642
Std Err of Y Est	4,662514
R Squared	0,805172
No. of Observations	19
Degrees of Freedom	14
X Coefficient(s)	0,288645 0,015427 -1,01527 0,048065
Std Err of Coef.	0,847084 0,017905 2,096276 0,087511

NO OUTLIERS DELETED

Regression Output:

Constant	-463,638
Std Err of Y Est	6,301165
R Squared	0,617269
No. of Observations	21
Degrees of Freedom	17
X Coefficient(s)	7,897629 -0,02715 -6,92099
Std Err of Coef.	23,41176 0,125655 1,672066

Regression Output:

Constant	19,14916
Std Err of Y Est	5,935815
R Squared	0,680344
No. of Observations	21
Degrees of Freedom	16
X Coefficient(s)	-0,69660 0,039105 -2,44652 0,117826
Std Err of Coef.	1,237493 0,027396 2,421527 0,103864

OFS3 - DOLERITE CRUSHED STONE RESULTS

REGRESSION ANALYSIS (% SD)

MINUS 7 OUTLIERS

Regression Output:

Constant	3284,142
Std Err of Y Est	115,4512
R Squared	0,811297
No. of Observations	85
Degrees of Freedom	81
X Coefficient(s)	-111,011 0,952033 -81,9356
Std Err of Coef.	43,04091 0,276736 16,08255

Regression Output:

Constant	66,94825
Std Err of Y Est	109,8816
R Squared	0,831175
No. of Observations	85
Degrees of Freedom	80
X Coefficient(s)	0,536296 0,000553 5,877340 -3,32327
Std Err of Coef.	0,165675 0,000186 32,29990 4,515792

D-69

NO OUTLIERS DELETED

Regression Output:

Constant	3284,16
Std Err of Y Est	136,4696
R Squared	0,751792
No. of Observations	92
Degrees of Freedom	88
X Coefficient(s)	-109,608 0,929757 -70,5737
Std Err of Coef.	48,48604 0,310395 18,79488

Regression Output:

Constant	58,42800
Std Err of Y Est	133,7294
R Squared	0,764368
No. of Observations	92
Degrees of Freedom	87
X Coefficient(s)	0,555483 0,000447 7,323201 -2,05050
Std Err of Coef.	0,194335 0,000212 38,95224 5,427975

REGRESSION ANALYSIS (% mod. AASHTO)

MINUS 7 OUTLIERS

Regression Output:

Constant	3284,142
Std Err of Y Est	115,4512
R Squared	0,811297
No. of Observations	85
Degrees of Freedom	81
X Coefficient(s)	-82,2294 0,522360 -81,9356
Std Err of Coef.	31,88162 0,151839 16,08255

Regression Output:

Constant	66,94825
Std Err of Y Est	109,8816
R Squared	0,831175
No. of Observations	85
Degrees of Freedom	80
X Coefficient(s)	0,536296 0,000553 5,877340 -3,32327
Std Err of Coef.	0,165675 0,000186 32,29990 4,515792

NO OUTLIERS DELETED

Regression Output:

Constant	3284,160
Std Err of Y Est	136,4696
R Squared	0,751792
No. of Observations	92
Degrees of Freedom	88
X Coefficient(s)	-81,1897 0,510137 -70,5737
Std Err of Coef.	35,91498 0,170307 18,79488

Regression Output:

Constant	55,73777
Std Err of Y Est	134,4122
R Squared	0,761956
No. of Observations	92
Degrees of Freedom	87
X Coefficient(s)	0,623810 0,000447 2,571290 -2,13605
Std Err of Coef.	0,210620 0,000239 39,06797 5,455330

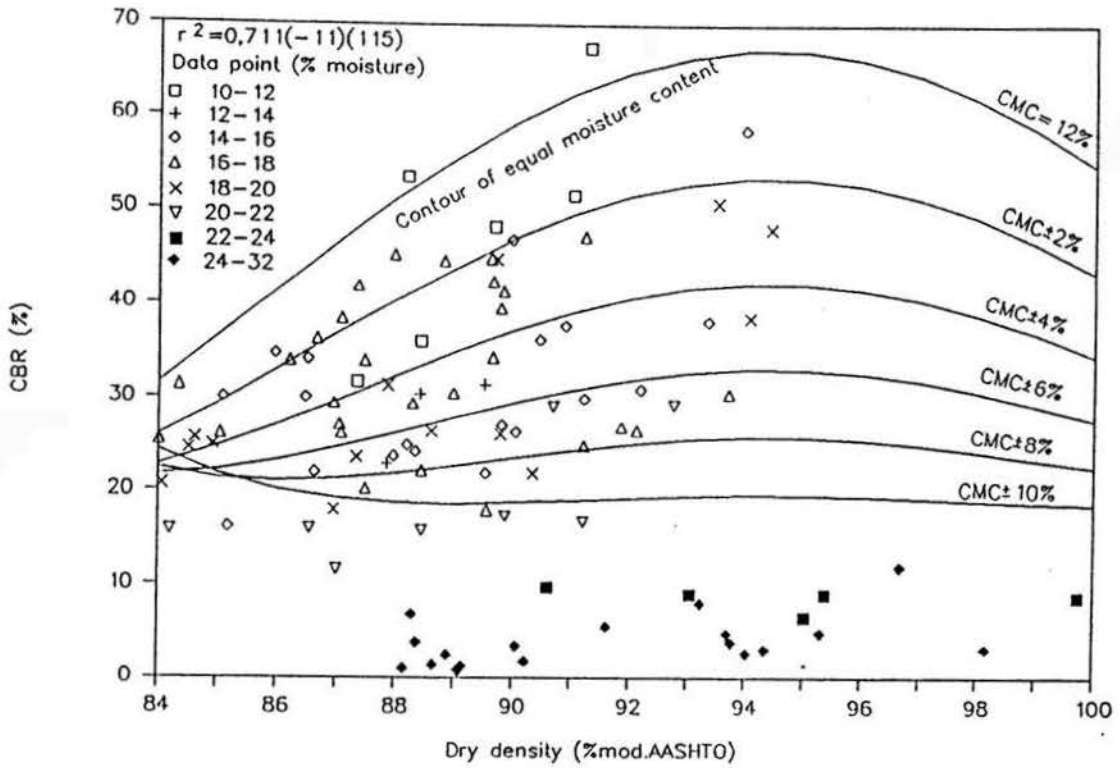

FIGURE D.1(a) **RELATION BETWEEN CBR AND DRY DENSITY FOR DIFFERENT MOISTURE LEVELS (BLACK CLAY) (BAB)**

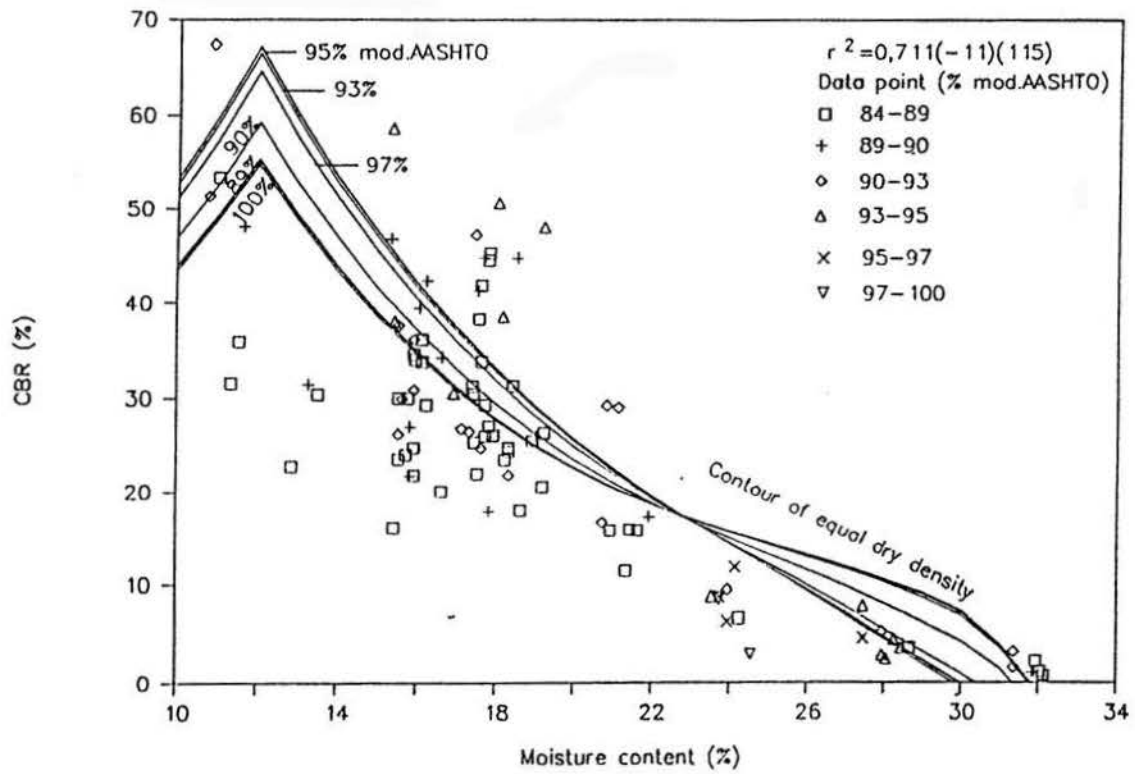

FIGURE D.1(b) **RELATION BETWEEN CBR AND MOISTURE CONTENT FOR DIFFERENT DENSITY LEVELS (BLACK CLAY) (BAB)**

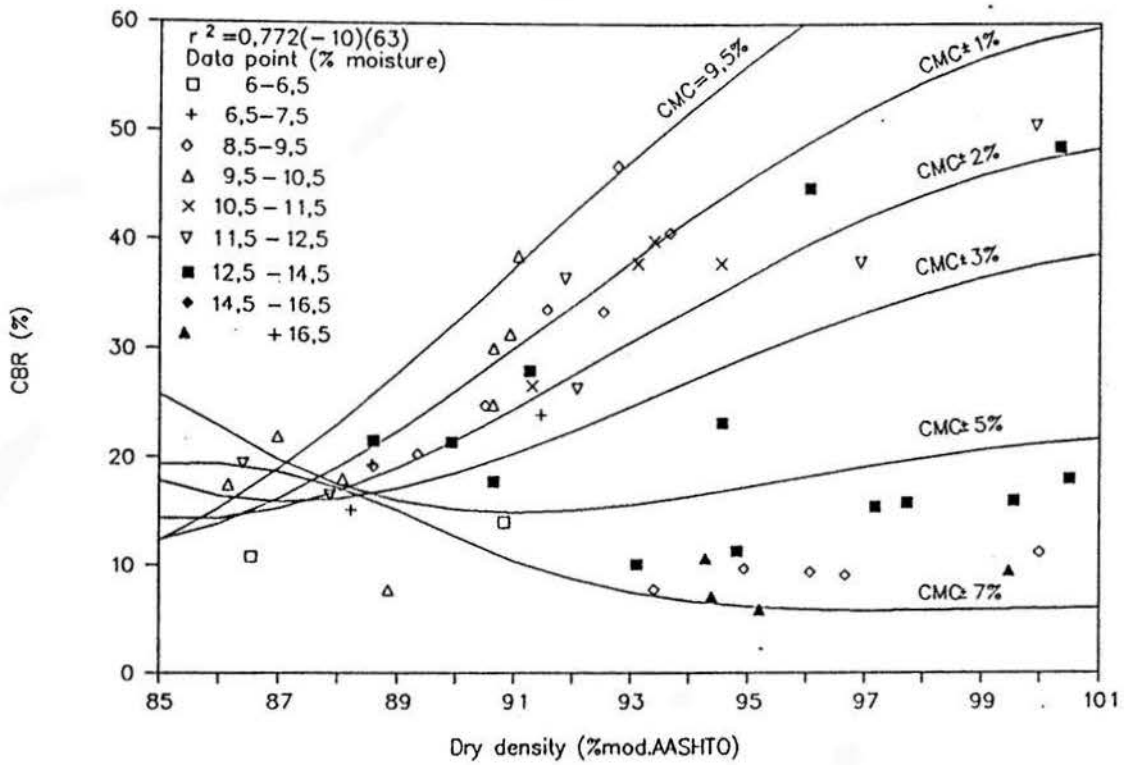

FIGURE D.2(a) **RELATION BETWEEN CBR AND DRY DENSITY FOR DIFFERENT MOISTURE LEVELS (WHITE SANDY CLAY) (SPR2)**

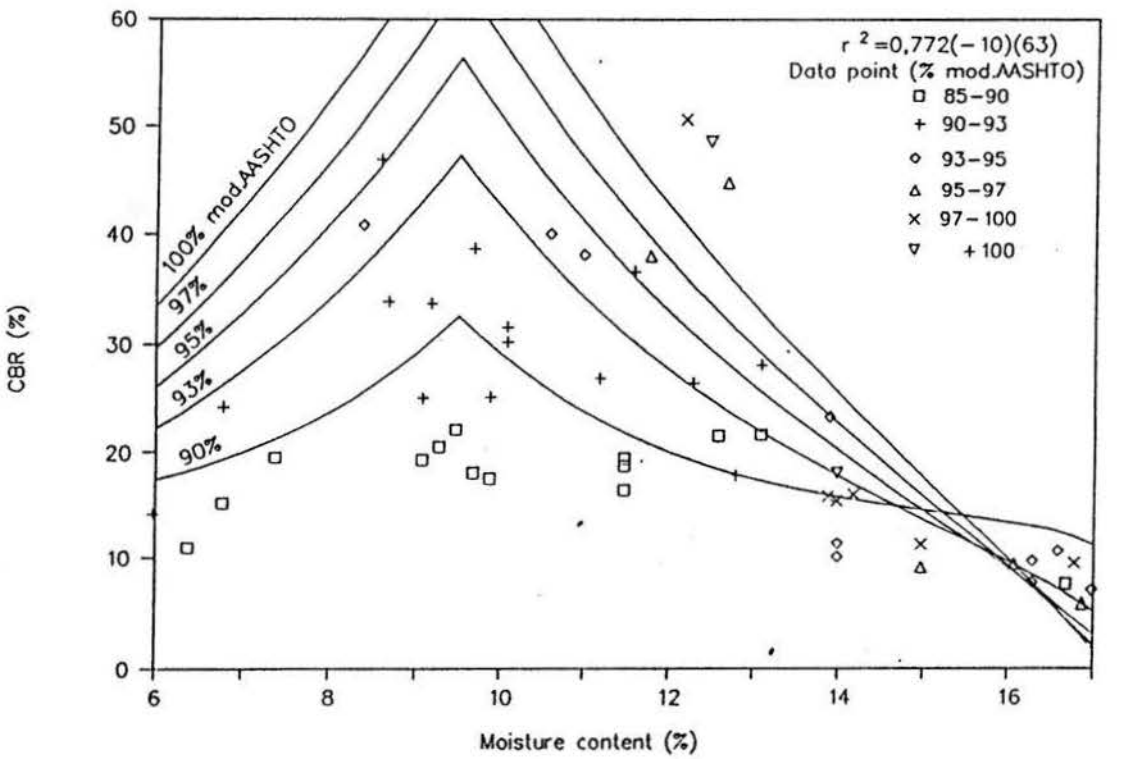

FIGURE D.2(b) **RELATION BETWEEN CBR AND MOISTURE CONTENT FOR DIFFERENT DENSITY LEVELS (WHITE SANDY CLAY) (SPR2)**

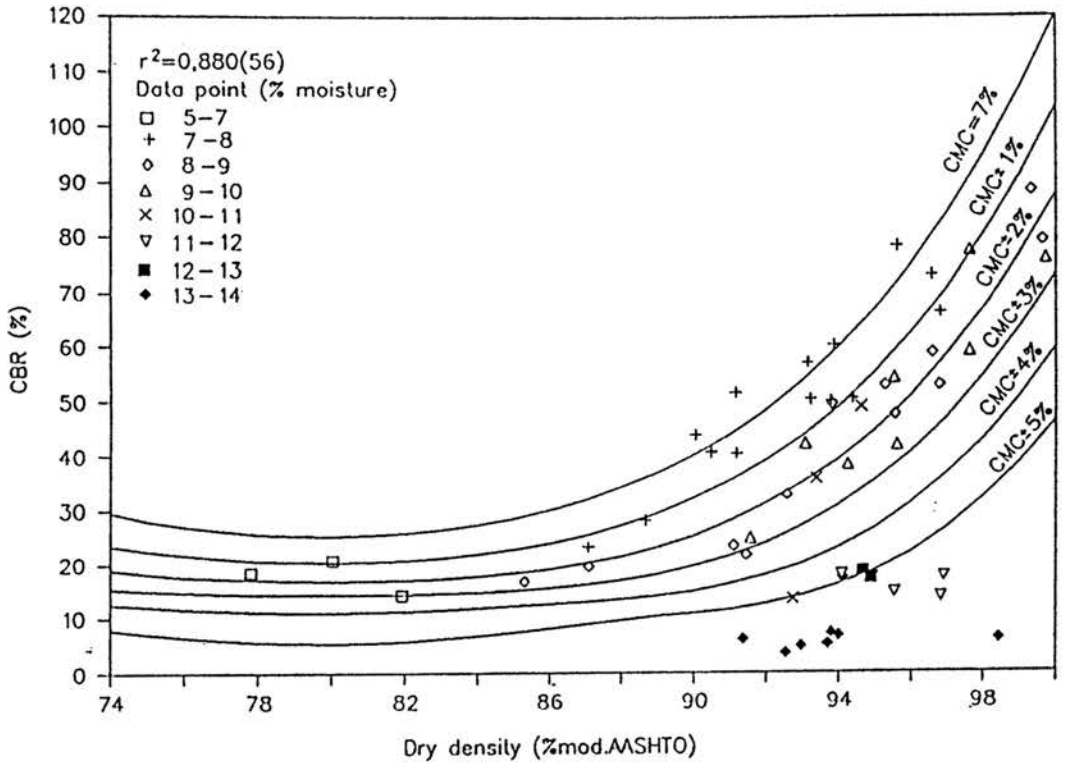

FIGURE D.3(a) **RELATION BETWEEN CBR AND DRY DENSITY FOR DIFFERENT MOISTURE LEVELS (RED SILTY SAND) (LABLEN)**

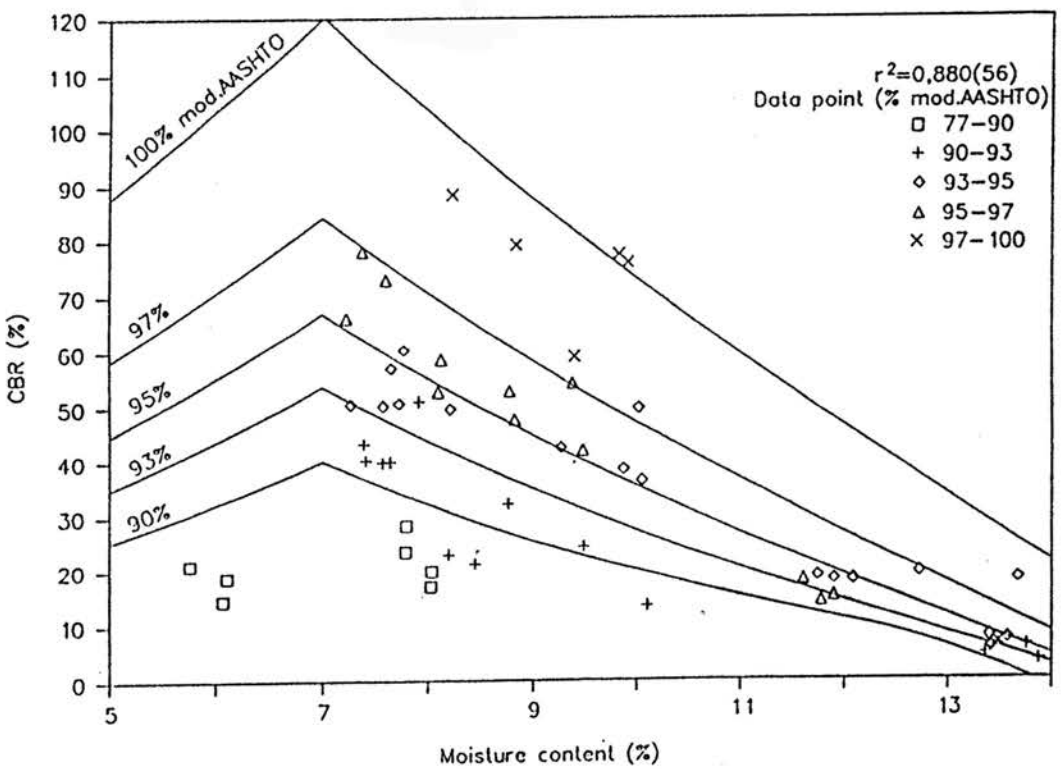

FIGURE D.3(b) **RELATION BETWEEN CBR AND MOISTURE CONTENT FOR DIFFERENT DENSITY LEVELS (RED SILTY SAND) (LABLEN)**

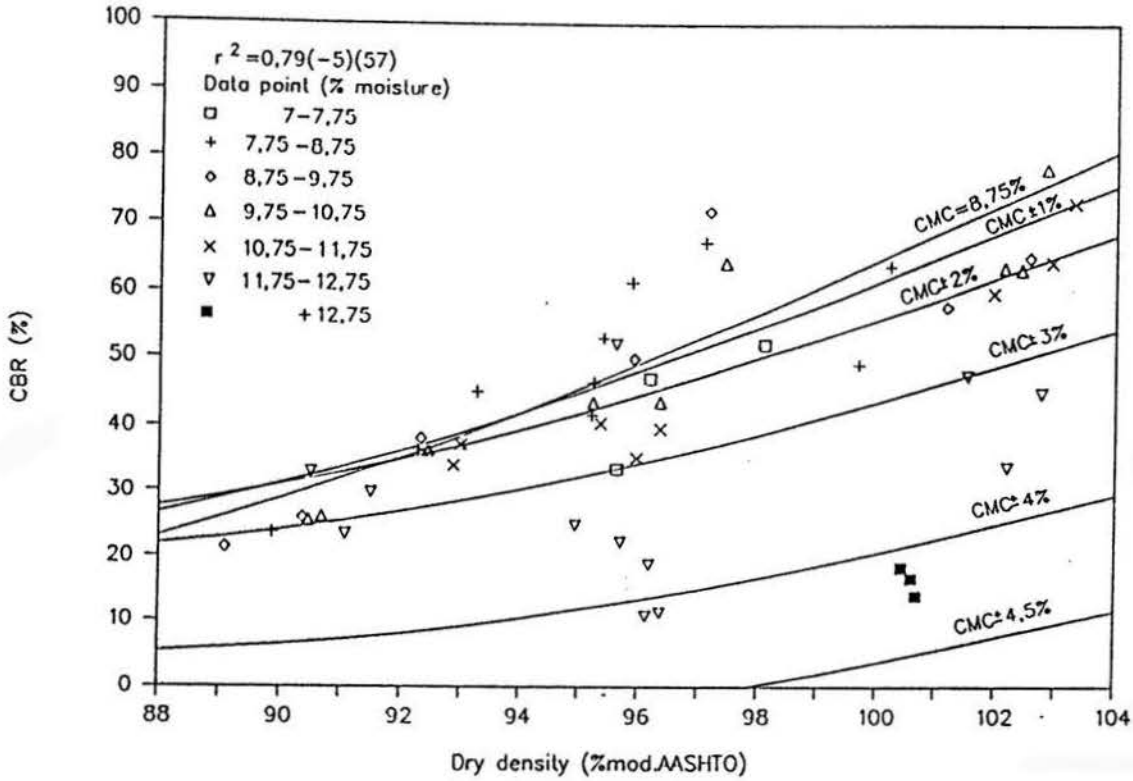

FIGURE D.4(a) **RELATION BETWEEN CBR AND DRY DENSITY FOR DIFFERENT MOISTURE LEVELS (SLIGHTLY PLASTIC SAND) (LABDEW)**

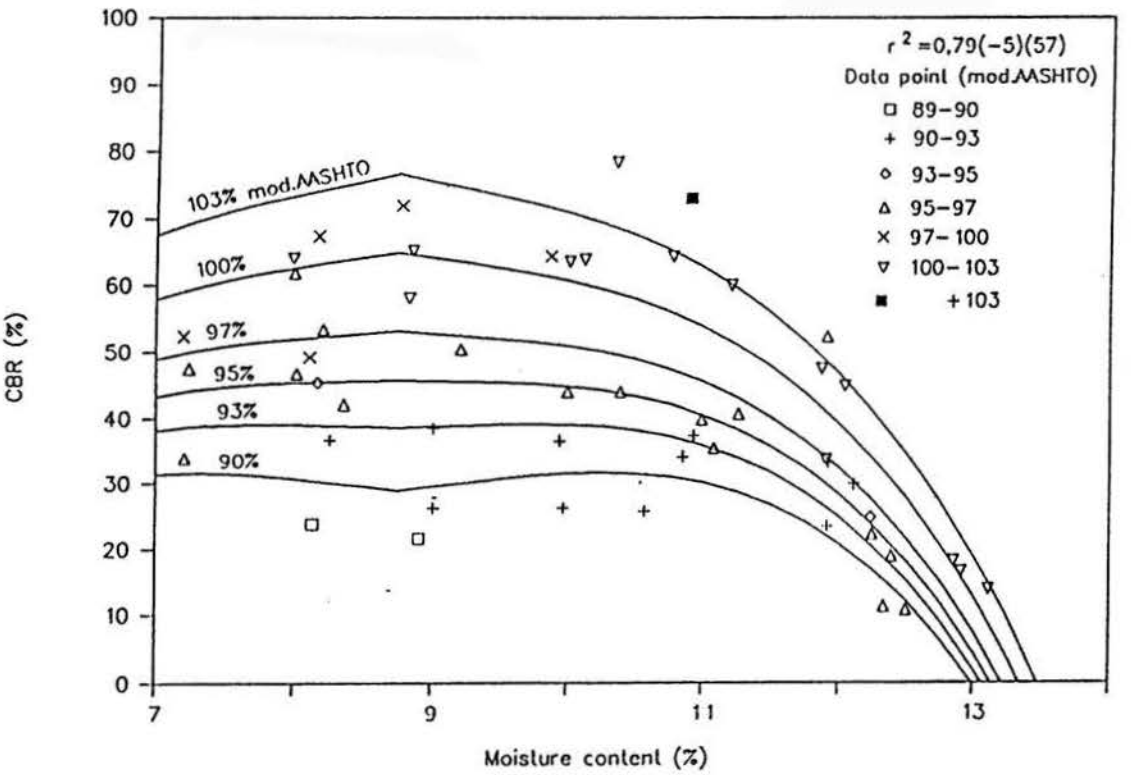

FIGURE D.4(b) **RELATION BETWEEN CBR AND MOISTURE CONTENT FOR DIFFERENT DENSITY LEVELS (SLIGHTLY PLASTIC SAND) (LABDEW)**

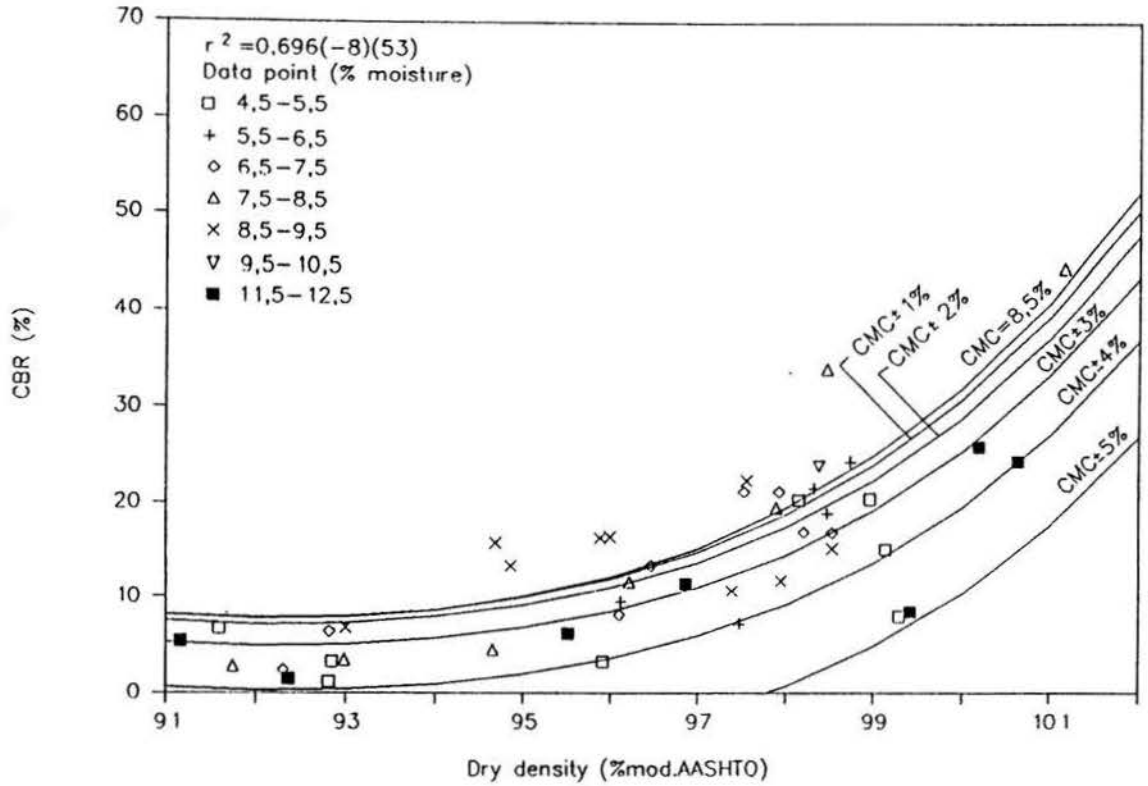

FIGURE D.5(a) **RELATION BETWEEN CBR AND DRY DENSITY FOR DIFFERENT MOISTURE LEVELS (WINDBLOWN SAND) (OFS1)**

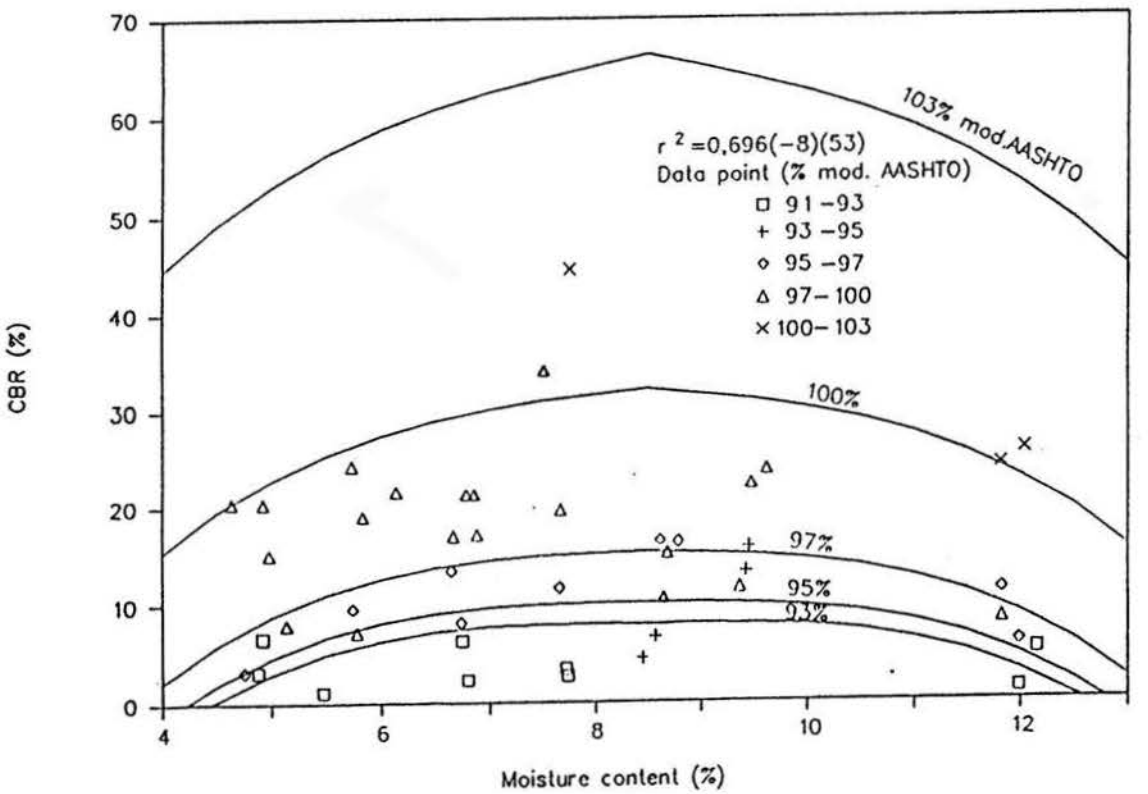

FIGURE D.5(b) **RELATION BETWEEN CBR AND MOISTURE CONTENT FOR DIFFERENT DENSITY LEVELS (WINDBLOWN SAND) (OFS1)**

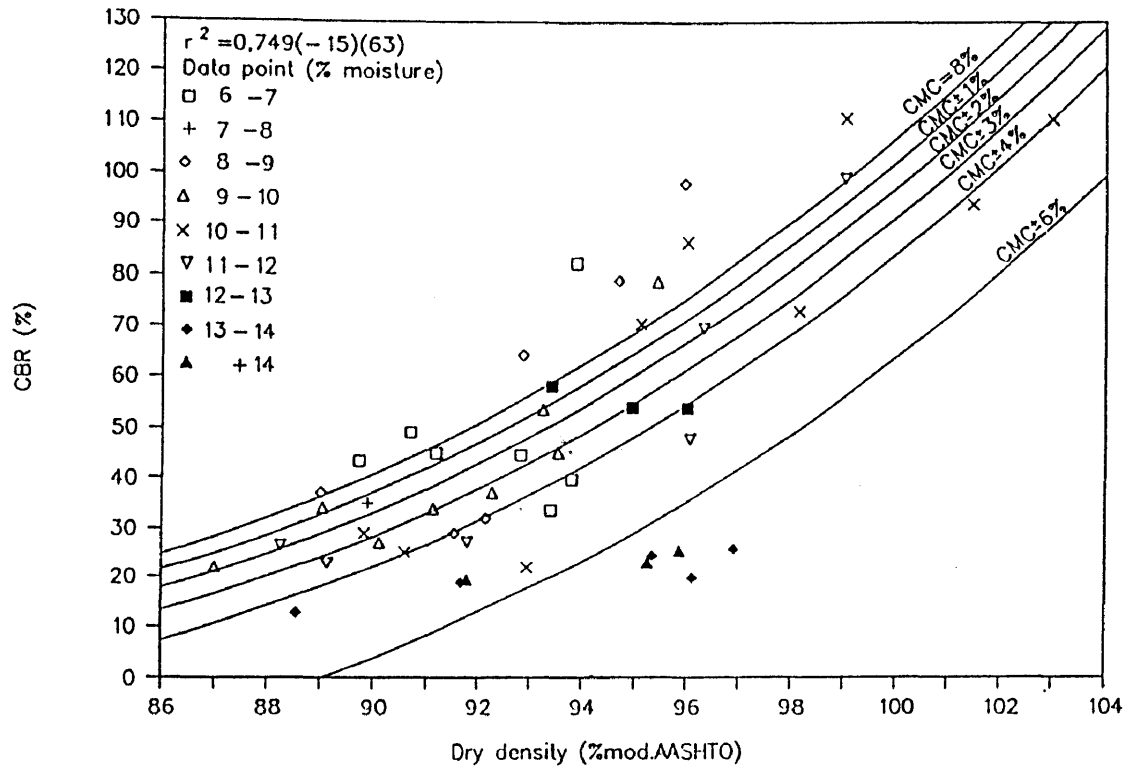

FIGURE D.6(a) **RELATION BETWEEN CBR AND DRY DENSITY FOR DIFFERENT MOISTURE LEVELS (DECOMPOSED DOLERITE) (NPAB)**

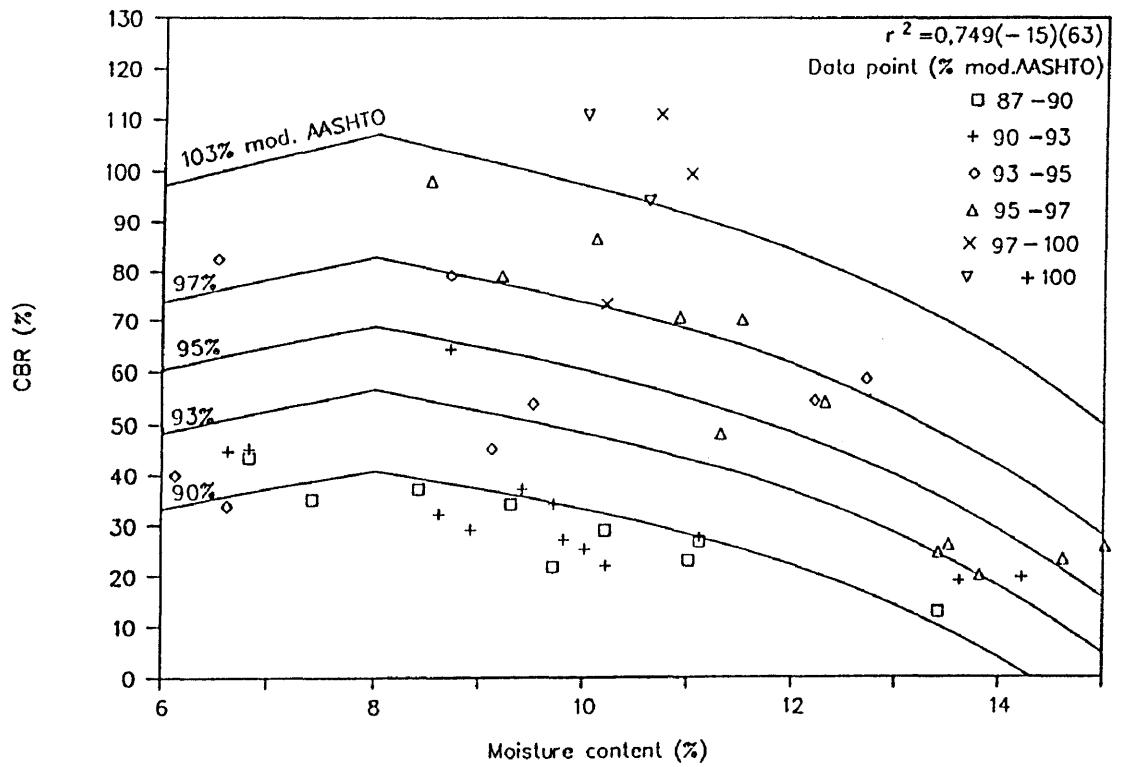

FIGURE D.6(b) **RELATION BETWEEN CBR AND MOISTURE CONTENT FOR DIFFERENT DENSITY LEVELS (DECOMPOSED DOLERITE) (NPAB)**

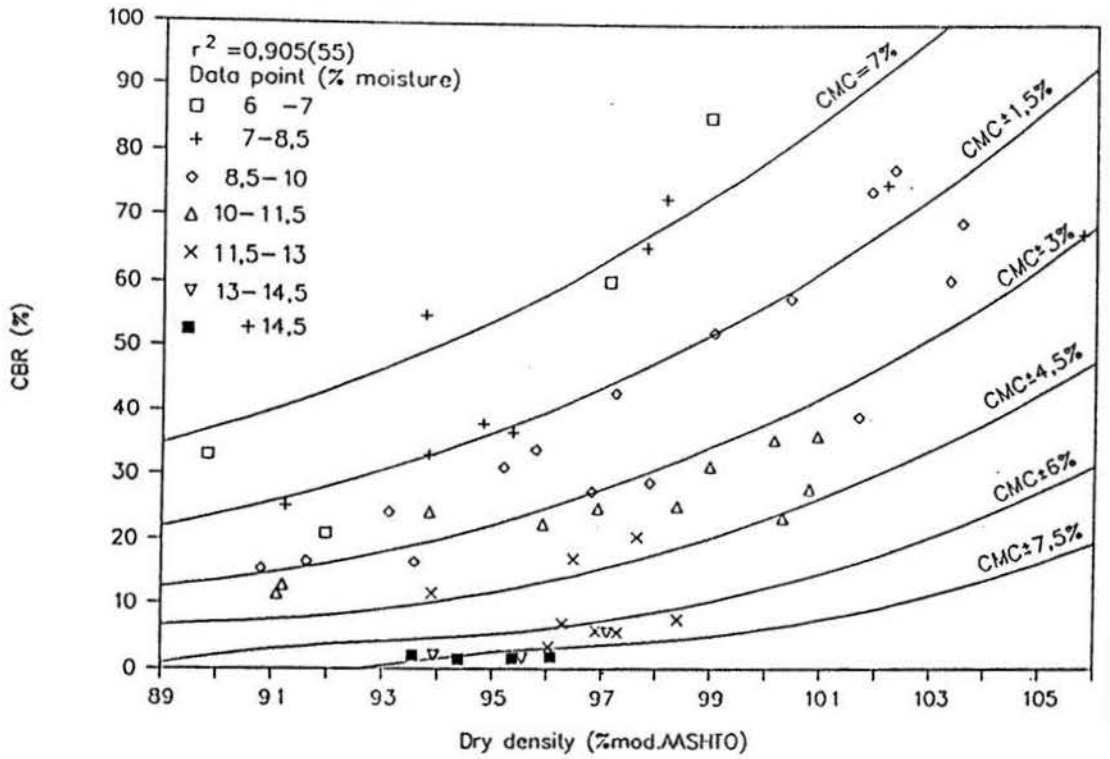

FIGURE D.7(a) **RELATION BETWEEN CBR AND DRY DENSITY FOR DIFFERENT MOISTURE LEVELS (RED CHERT SOIL) (LABD)**

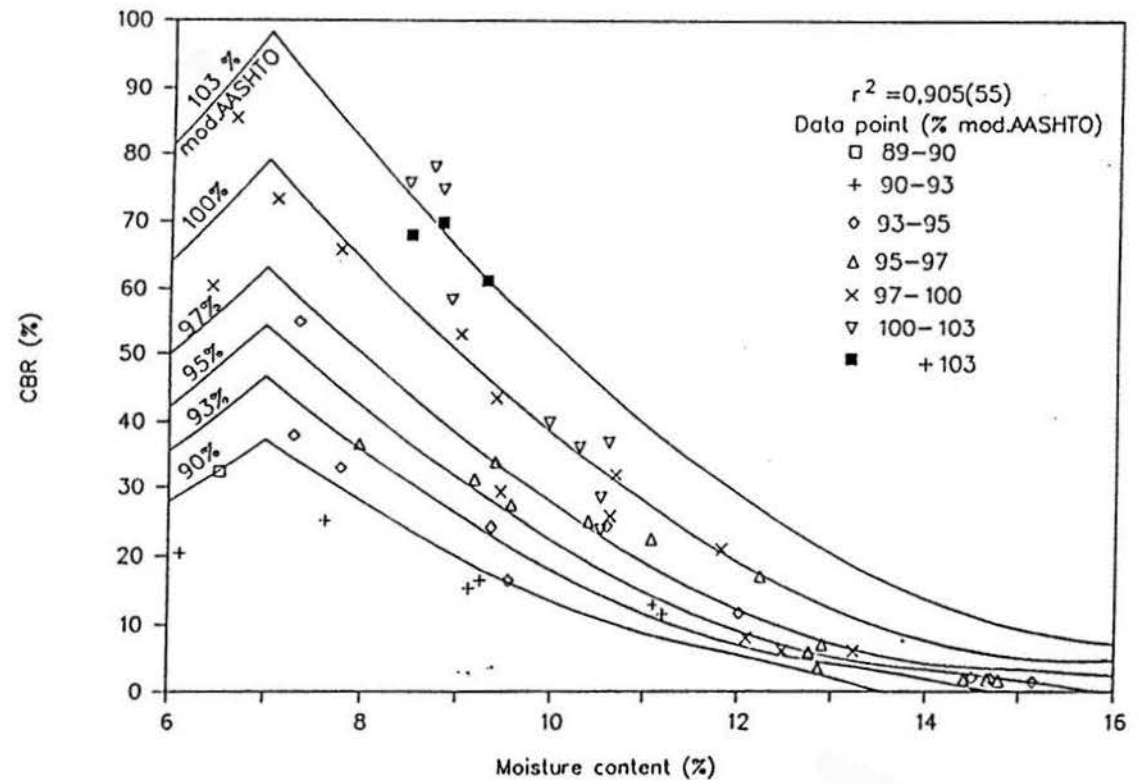

FIGURE D.7(b) **RELATION BETWEEN CBR AND MOISTURE CONTENT FOR DIFFERENT DENSITY LEVELS (RED CHERT SOIL) (LABD)**

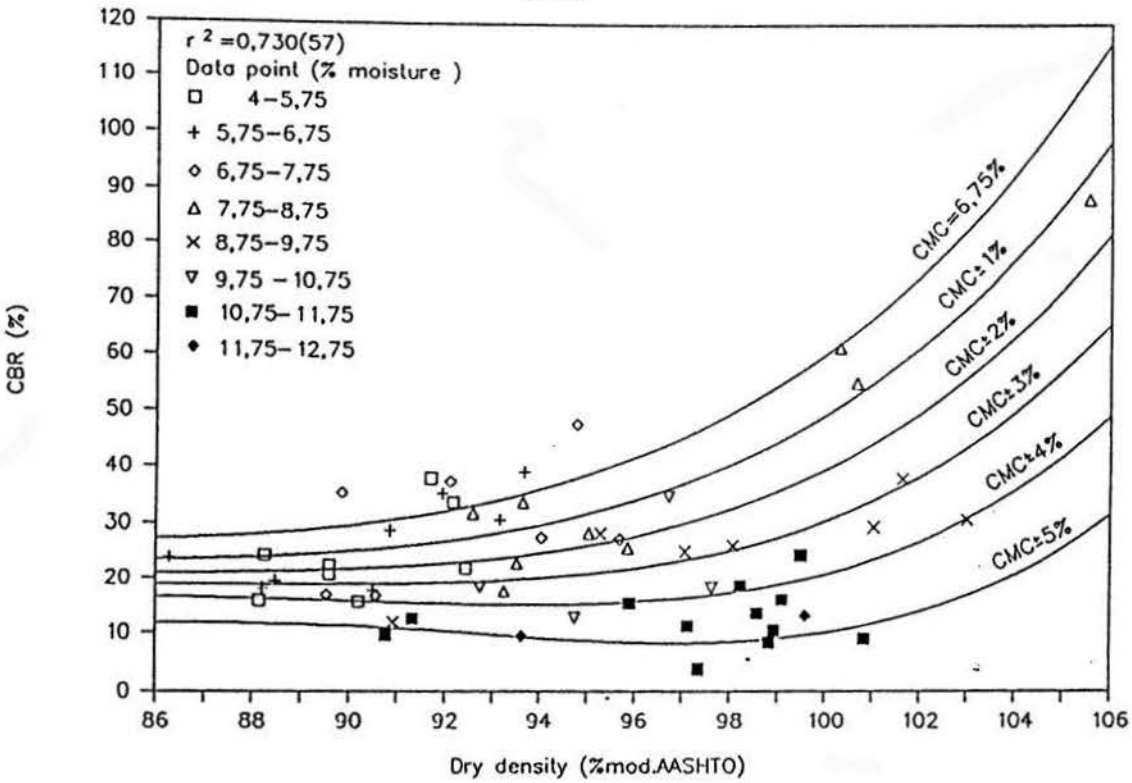

FIGURE D.8(a) **RELATION BETWEEN CBR AND DRY DENSITY FOR DIFFERENT MOISTURE LEVELS (NORITE GRAVEL) (TPA1)**

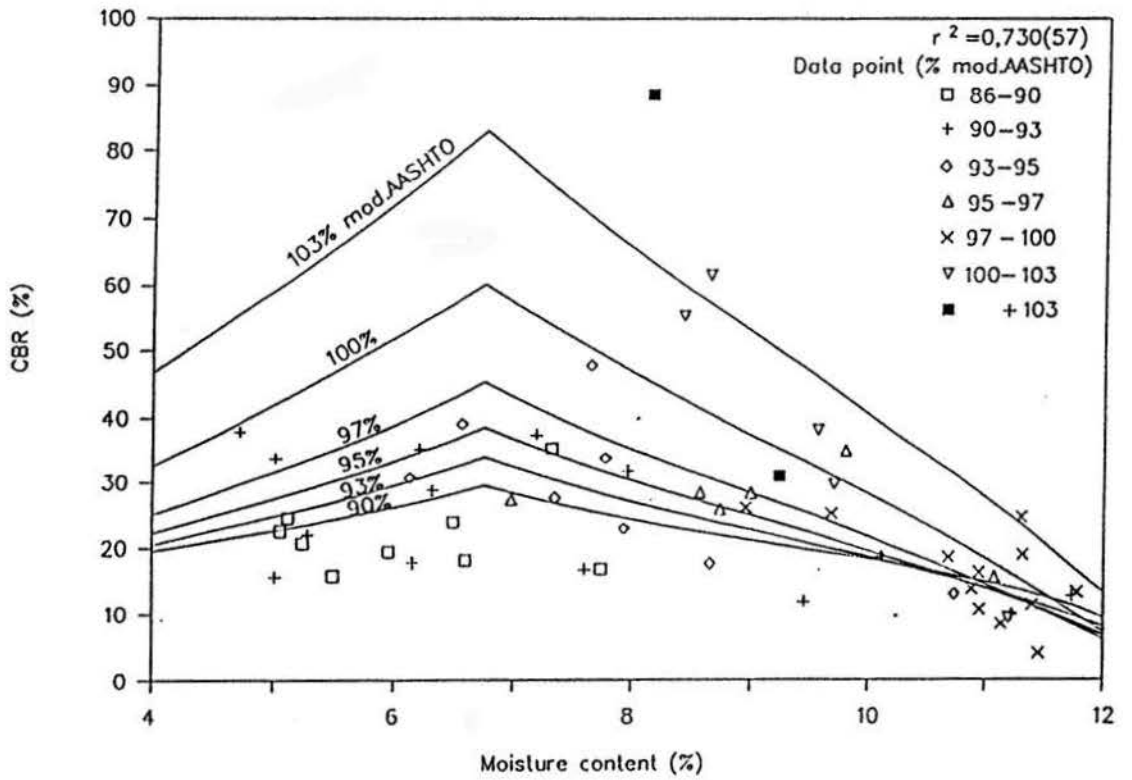

FIGURE D.8(b) **RELATION BETWEEN CBR AND MOISTURE CONTENT FOR DIFFERENT DENSITY LEVELS (NORITE GRAVEL) (TPA1)**

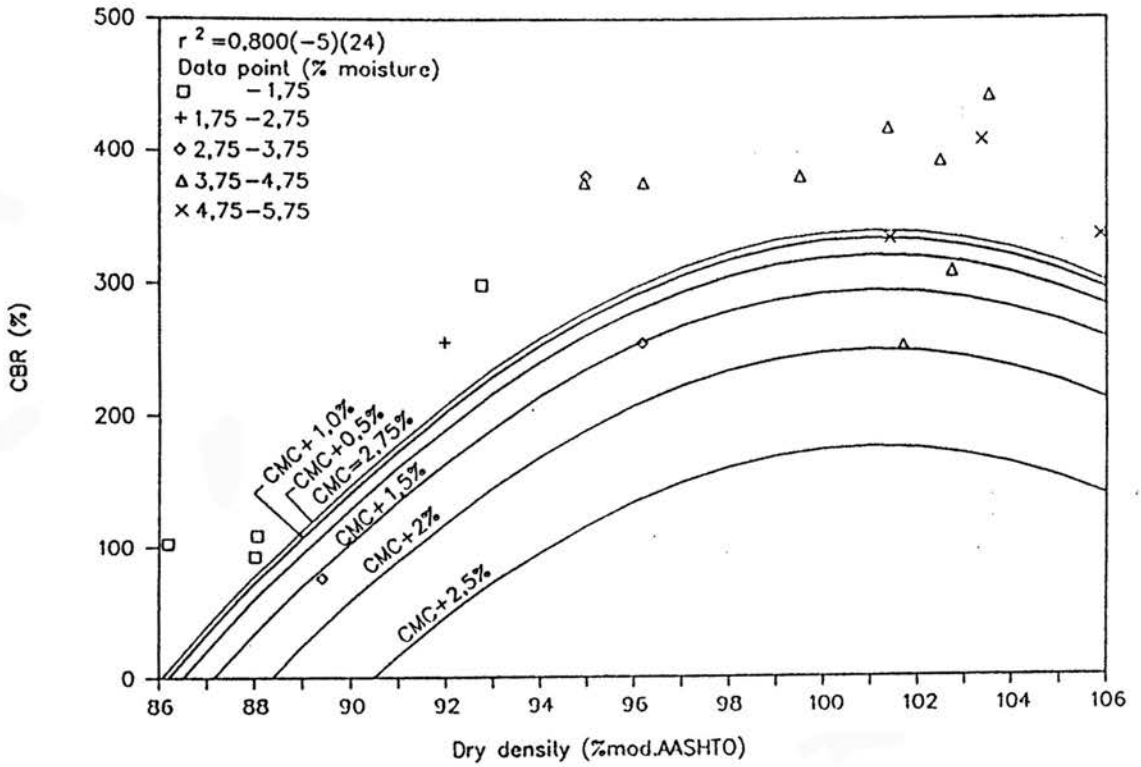

FIGURE D.9(a) **RELATION BETWEEN CBR AND DRY DENSITY FOR DIFFERENT MOISTURE LEVELS (HORNFELS CRUSHED STONE) (CPA1)**

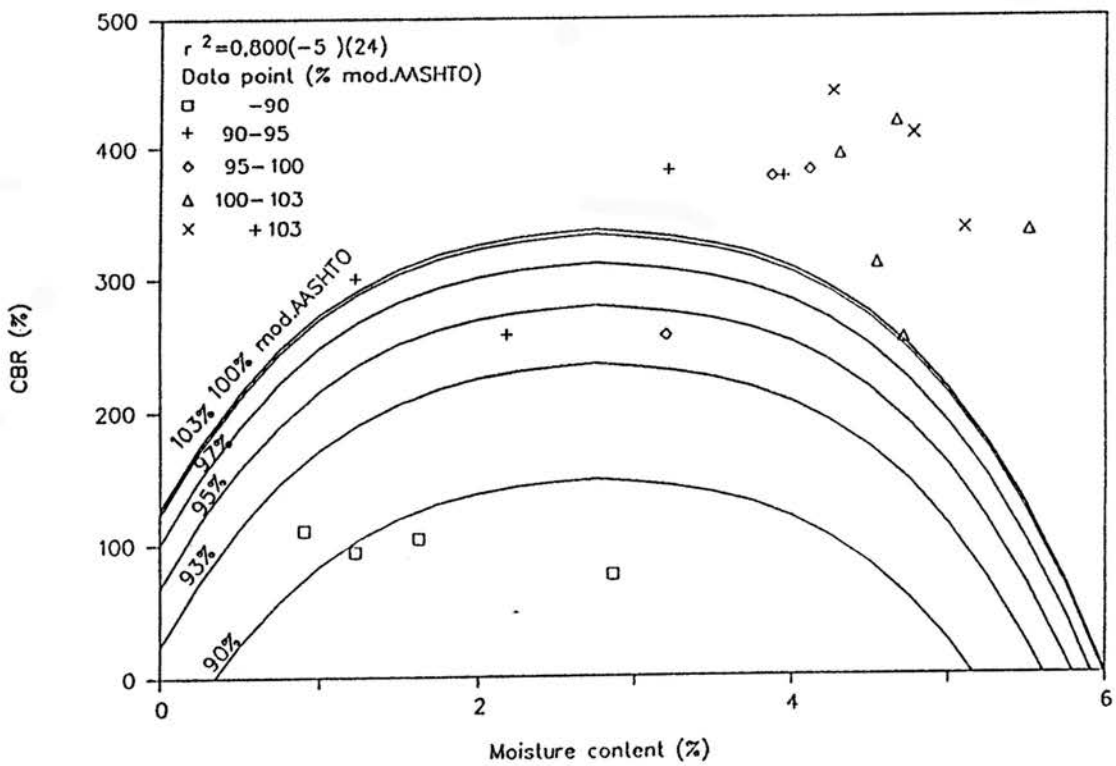

FIGURE D.9(b) **RELATION BETWEEN CBR AND MOISTURE CONTENT FOR DIFFERENT DENSITY LEVELS (HORNFELS CRUSHED STONE) (CPA1)**

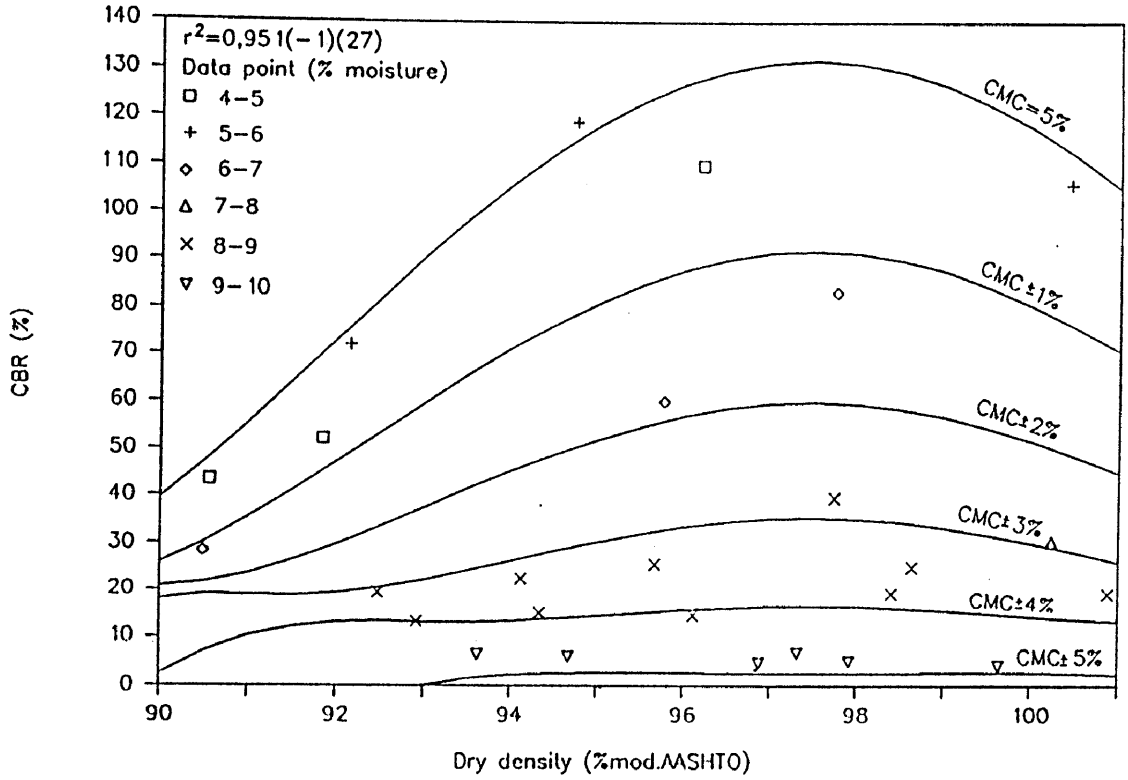

FIGURE D.10(a) **RELATION BETWEEN CBR AND DRY DENSITY FOR DIFFERENT MOISTURE LEVELS (DOLOMITIC SOIL) (DENS7)**

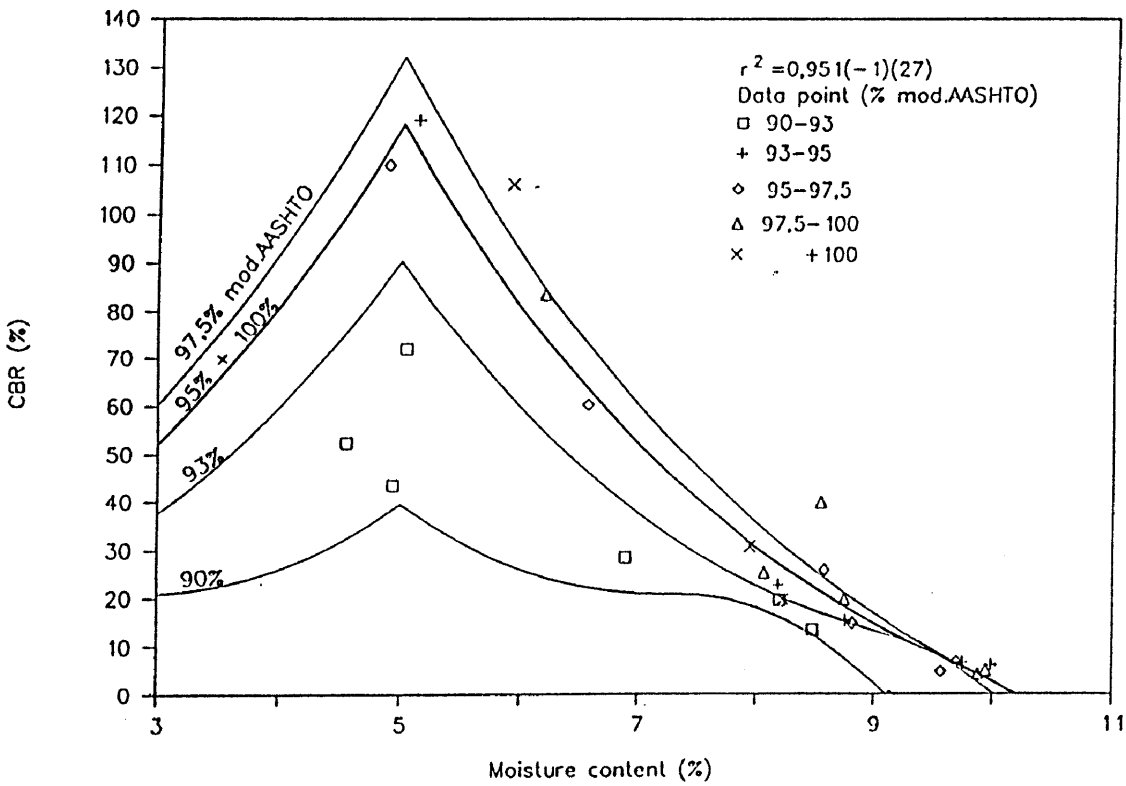

FIGURE D.10(b) **RELATION BETWEEN CBR AND MOISTURE CONTENT FOR DIFFERENT DENSITY LEVELS (DOLOMITIC SOIL) (DENS7)**

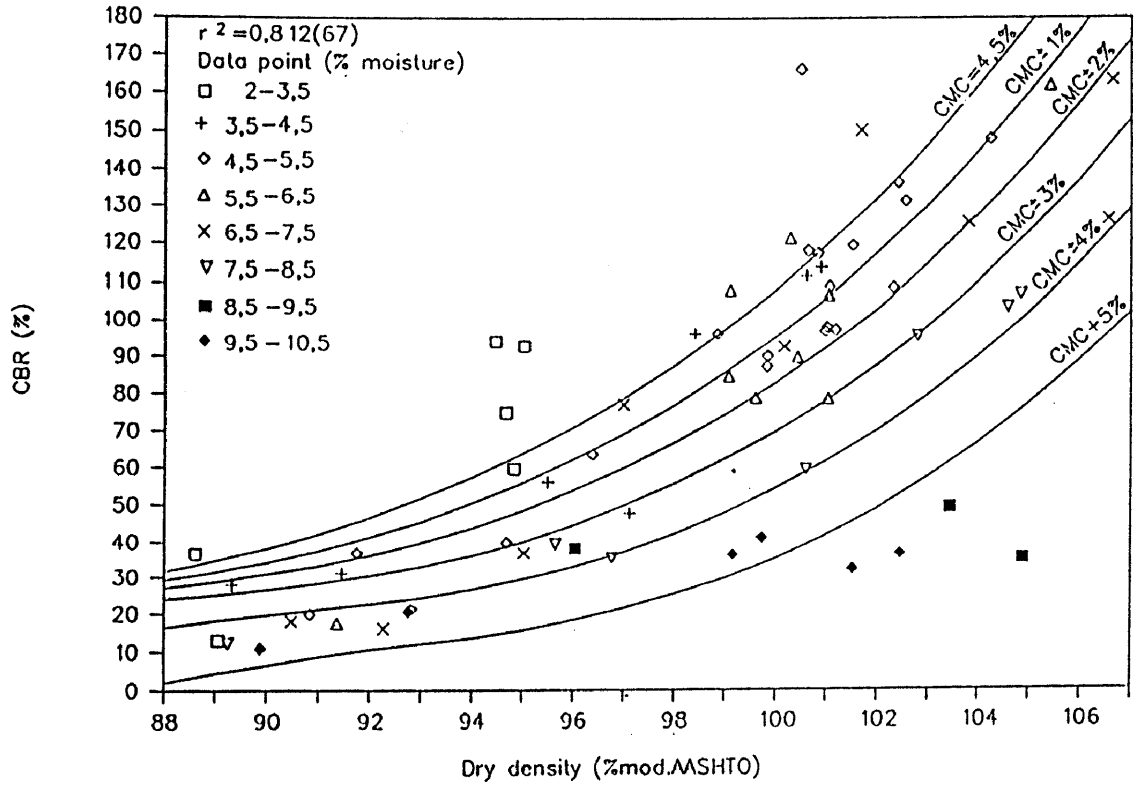

FIGURE D.11(a) **RELATION BETWEEN CBR AND DRY DENSITY FOR DIFFERENT MOISTURE LEVELS (QUARTZITE GRAVEL) (TPA2)**

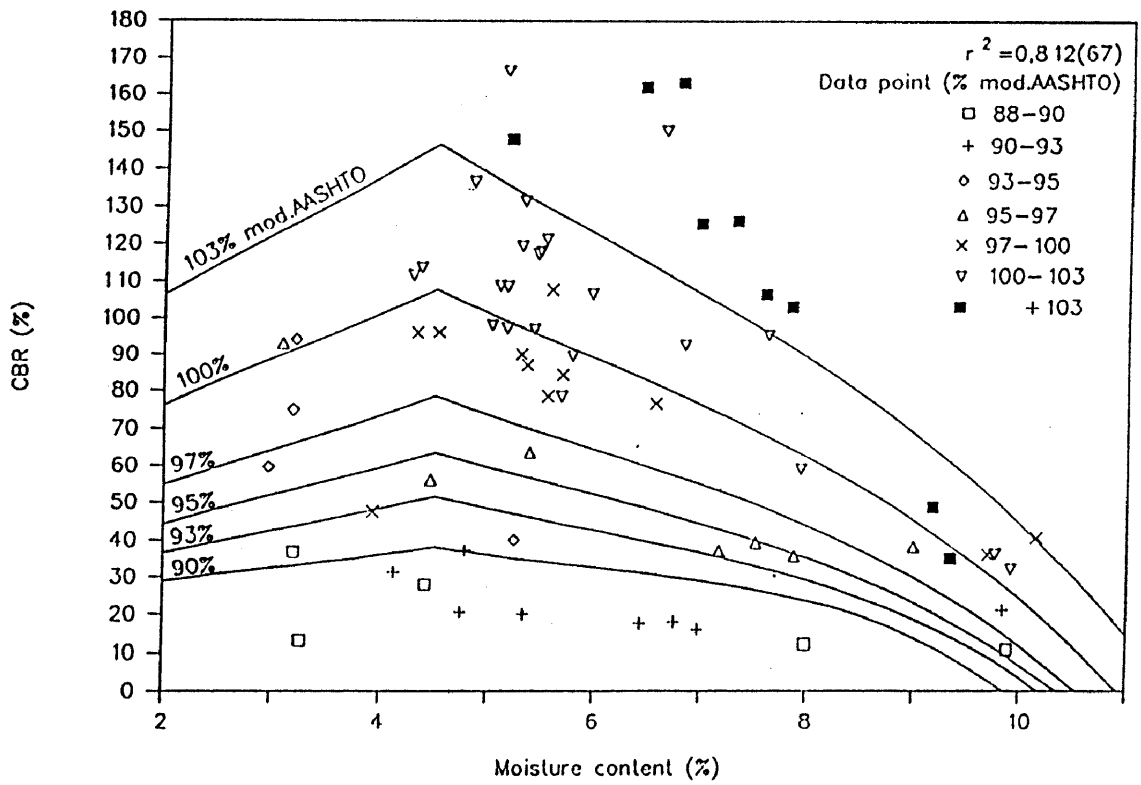

FIGURE D.11(b) **RELATION BETWEEN CBR AND MOISTURE CONTENT FOR DIFFERENT DENSITY LEVELS (QUARTZITE GRAVEL) (TPA2)**

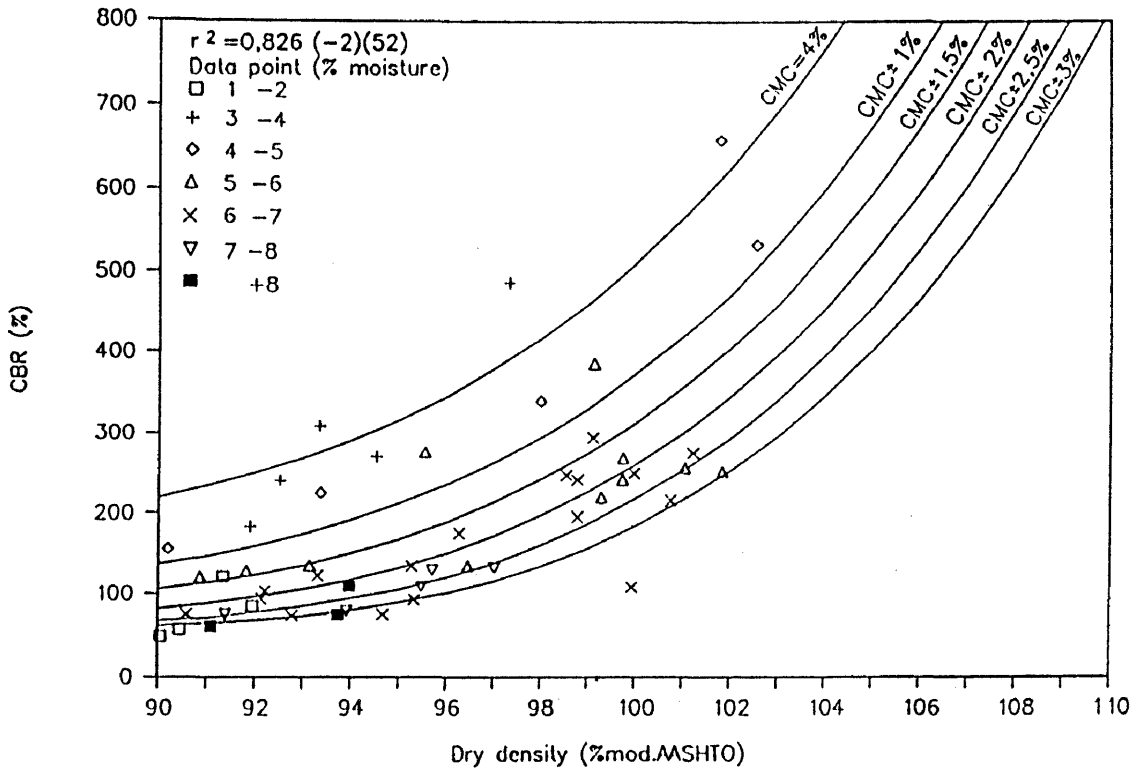

FIGURE D.12(a) **RELATION BETWEEN CBR AND DRY DENSITY FOR DIFFERENT MOISTURE LEVELS (TILLITE CRUSHED STONE) (NPAE)**

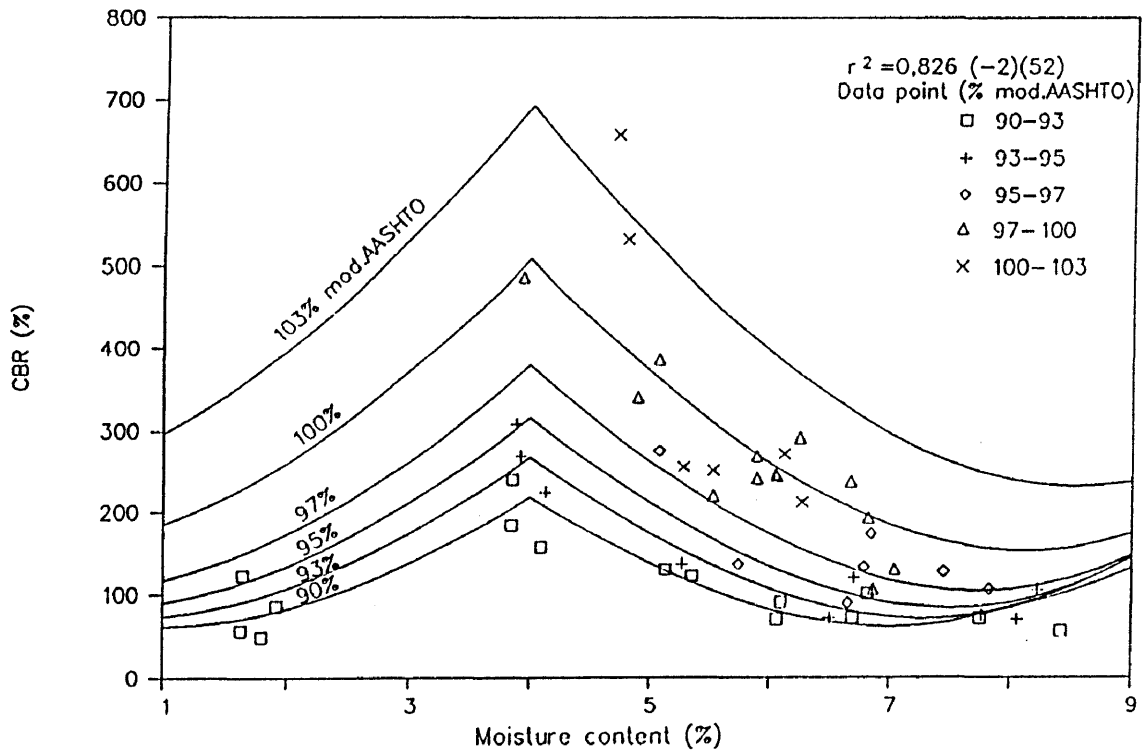

FIGURE D.12(b) **RELATION BETWEEN CBR AND MOISTURE CONTENT FOR DIFFERENT DENSITY LEVELS (TILLITE CRUSHED STONE) (NPAE)**

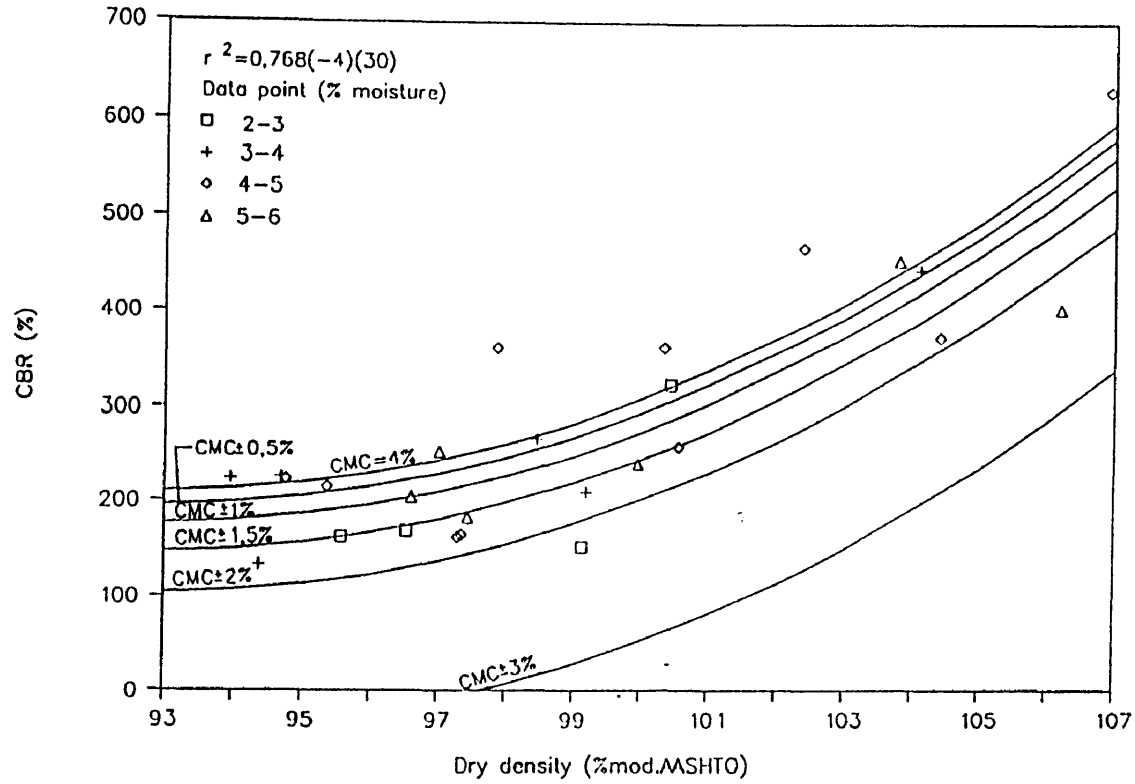

FIGURE D.13(a) **RELATION BETWEEN CBR AND DRY DENSITY FOR DIFFERENT MOISTURE LEVELS (QUARTZITE CRUSHED STONE) (FERR1)**

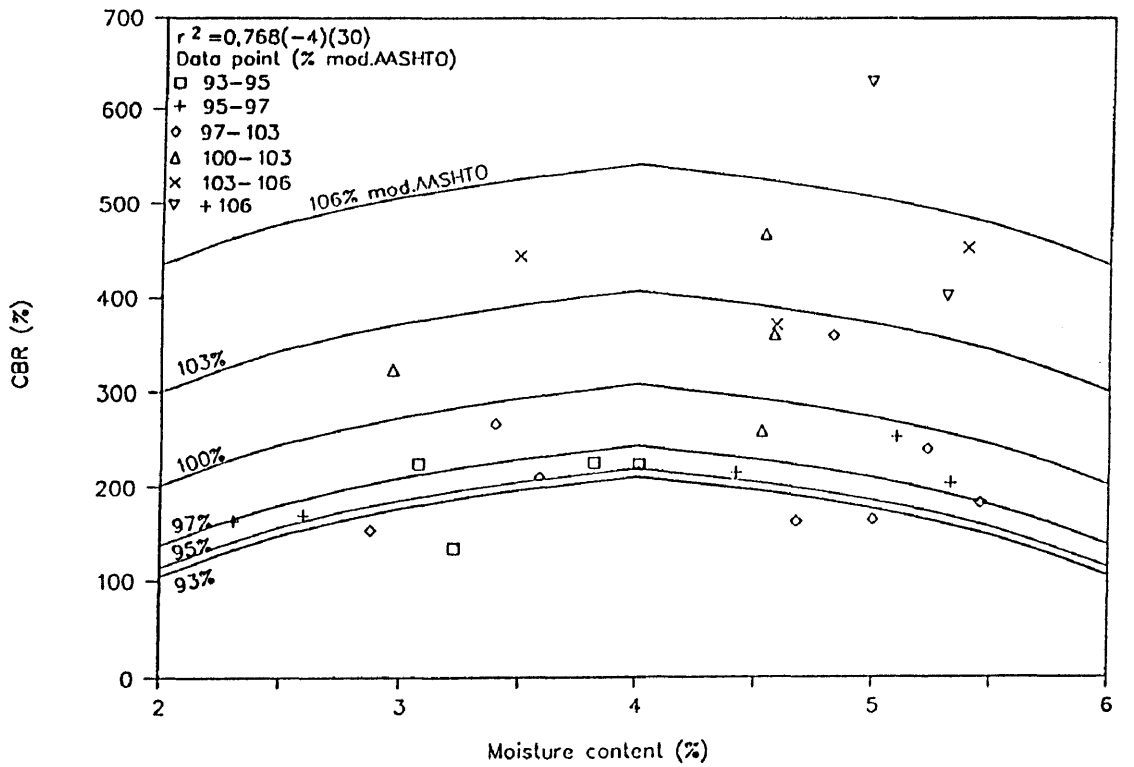

FIGURE D.13(b) **RELATION BETWEEN CBR AND MOISTURE CONTENT FOR DIFFERENT DENSITY LEVELS (QUARTZITE CRUSHED STONE) (FERR1)**

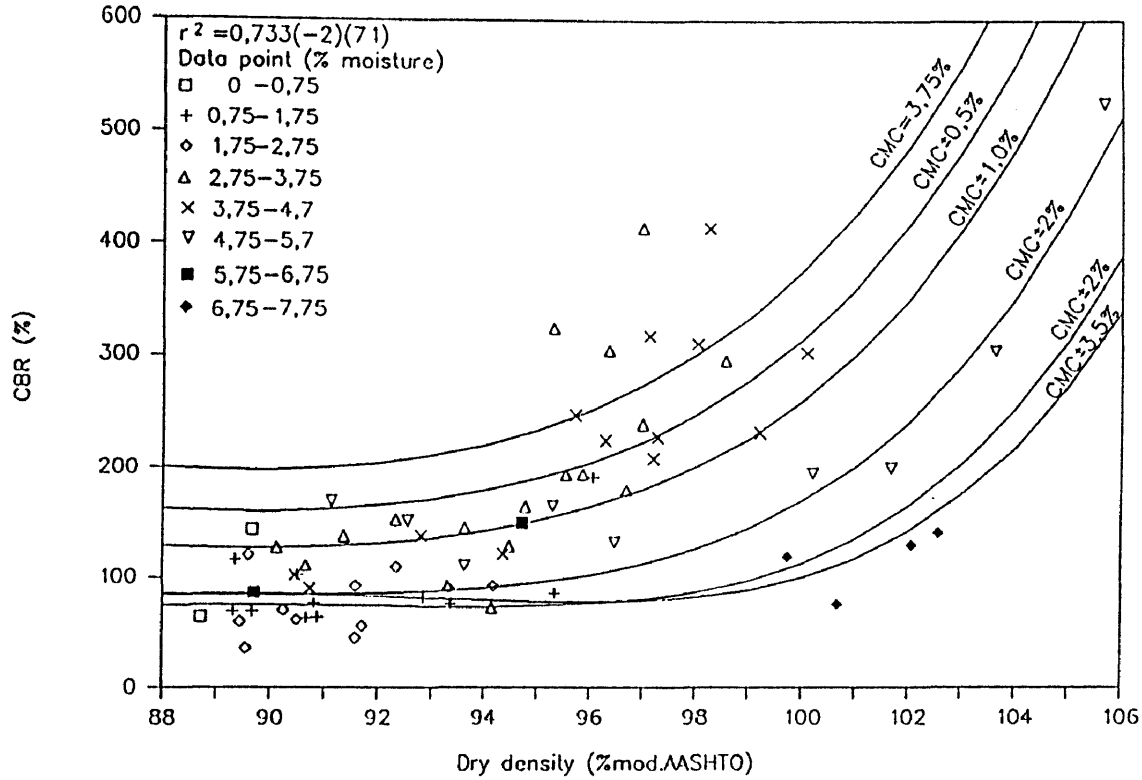

FIGURE D.14(a) **RELATION BETWEEN CBR AND DRY DENSITY FOR DIFFERENT MOISTURE LEVELS (WEATHERED DOLERITE) (OFS2)**

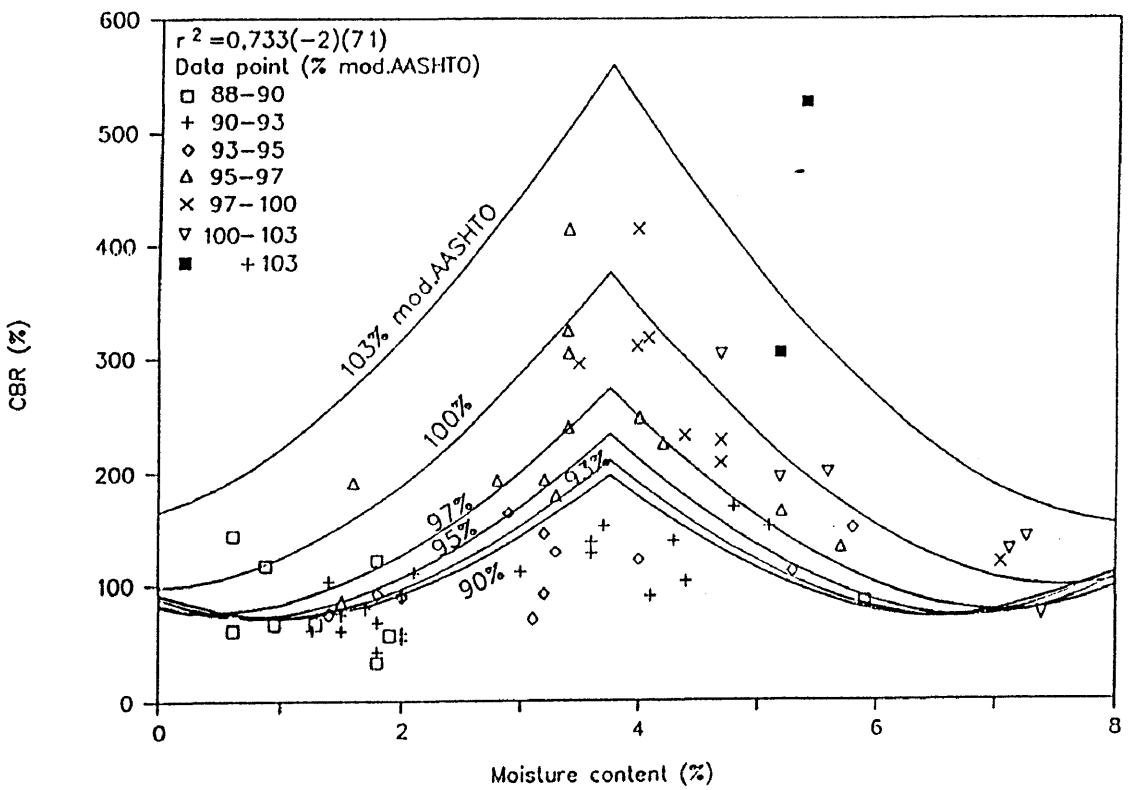

FIGURE D.14(b) **RELATION BETWEEN CBR AND MOISTURE CONTENT FOR DIFFERENT DENSITY LEVELS (WEATHERED DOLERITE) (OFS2)**

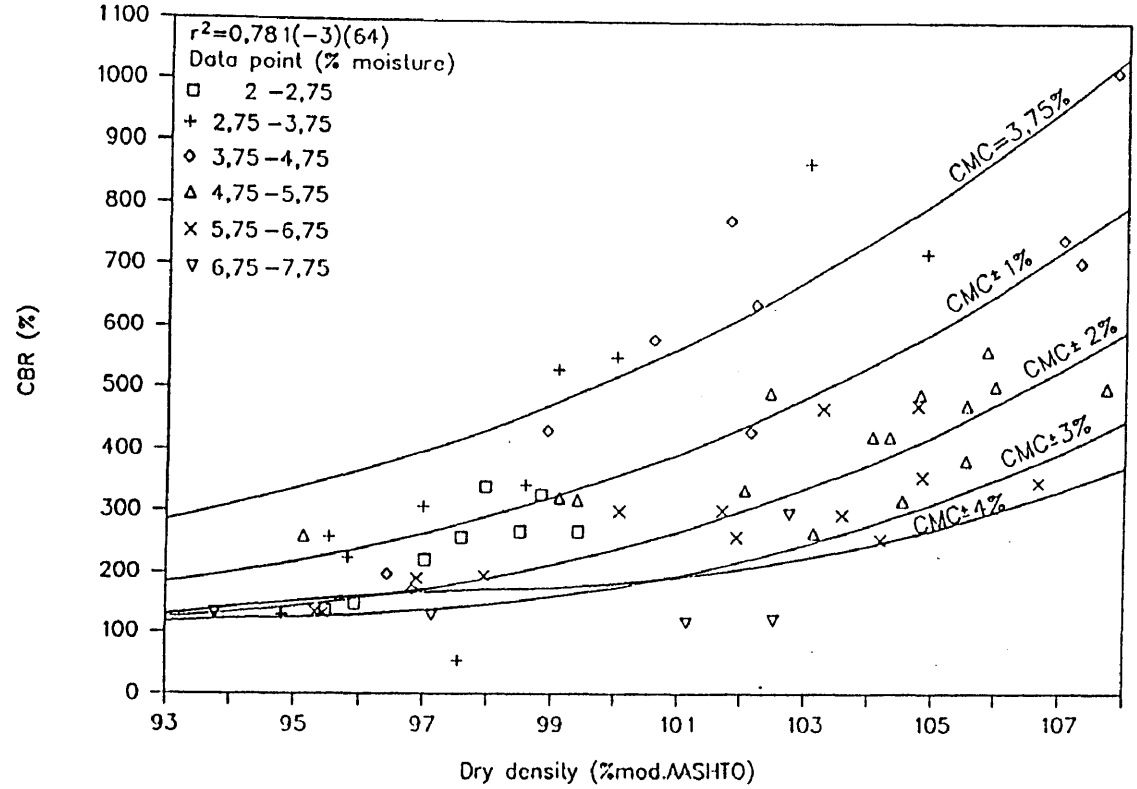

FIGURE D.15(a) **RELATION BETWEEN CBR AND DRY DENSITY FOR DIFFERENT MOISTURE LEVELS (DOLERITE CRUSHED STONE) (NPAA)**

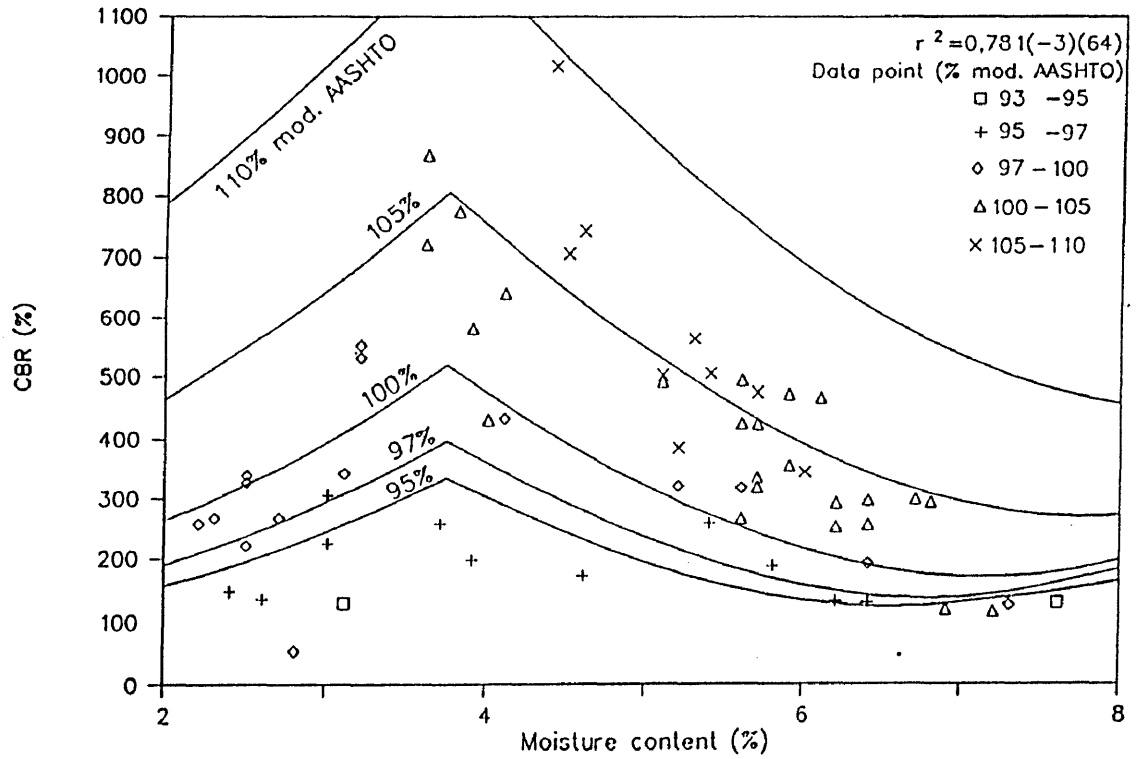

FIGURE D.15(b) **RELATION BETWEEN CBR AND MOISTURE CONTENT FOR DIFFERENT DENSITY LEVELS (DOLERITE CRUSHED STONE) (NPAA)**

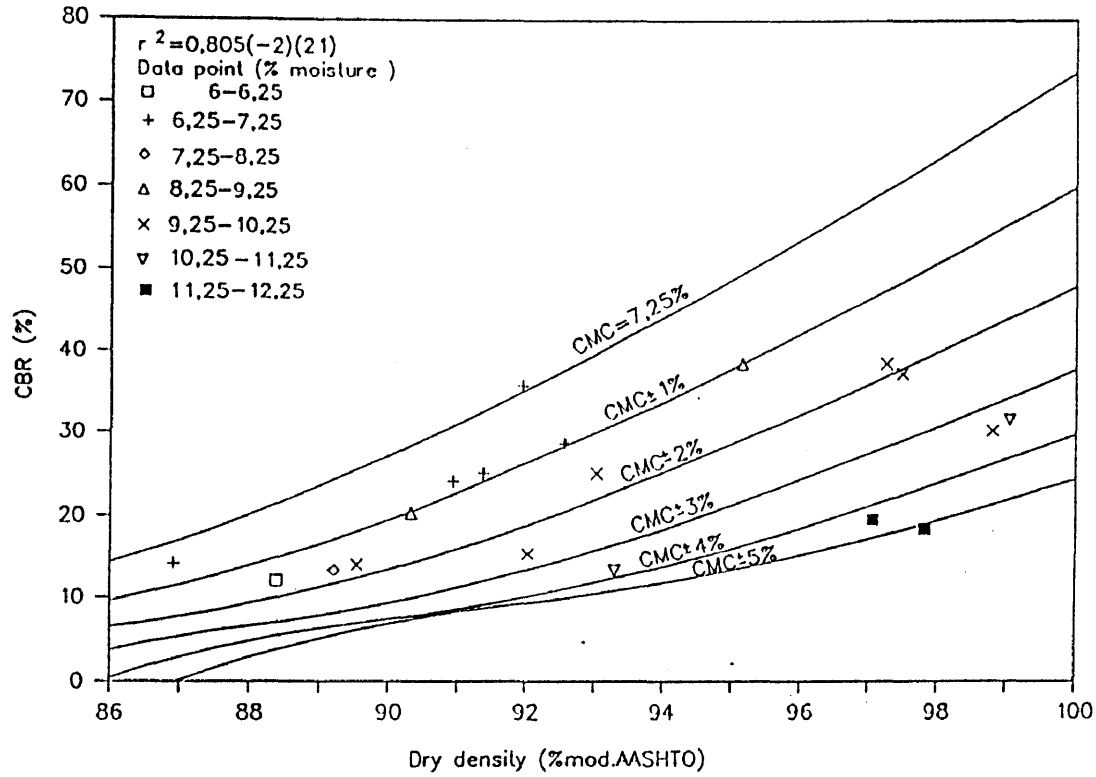

FIGURE D.16(a) **RELATION BETWEEN CBR AND DRY DENSITY FOR DIFFERENT MOISTURE LEVELS (SHALE) (DENS8)**

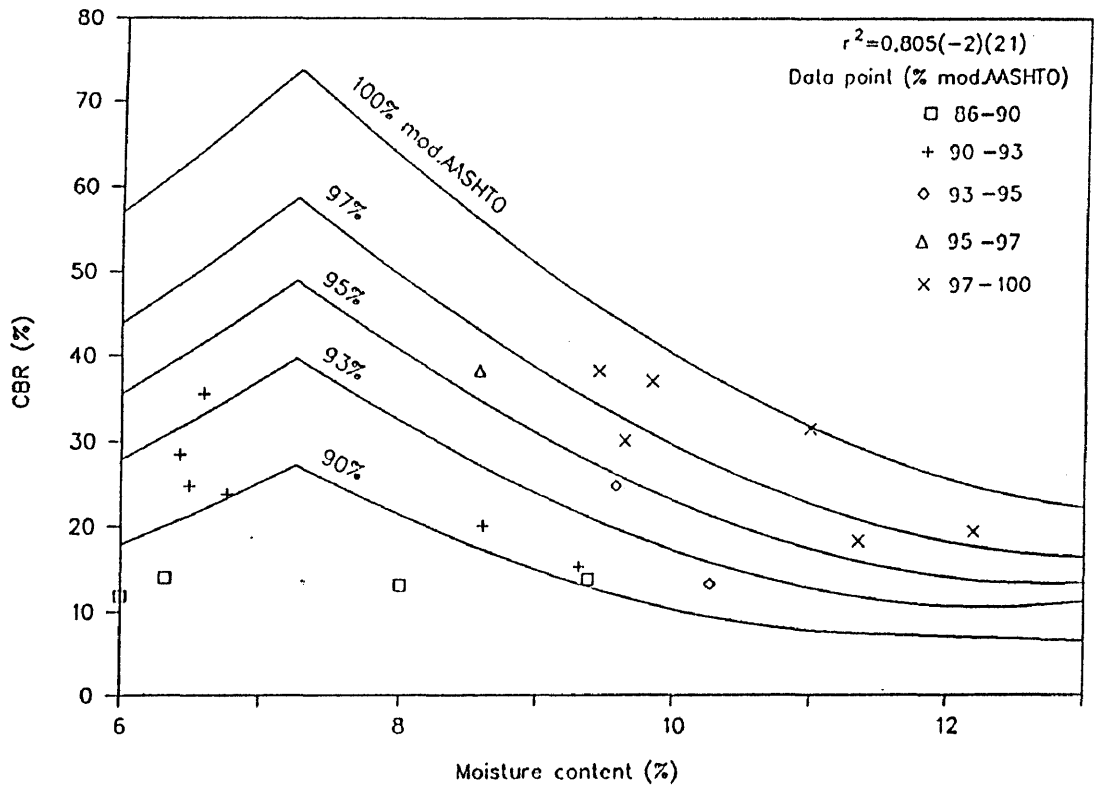

FIGURE D.16(b) **RELATION BETWEEN CBR AND MOISTURE CONTENT FOR DIFFERENT DENSITY LEVELS (SHALE) (DENS8)**

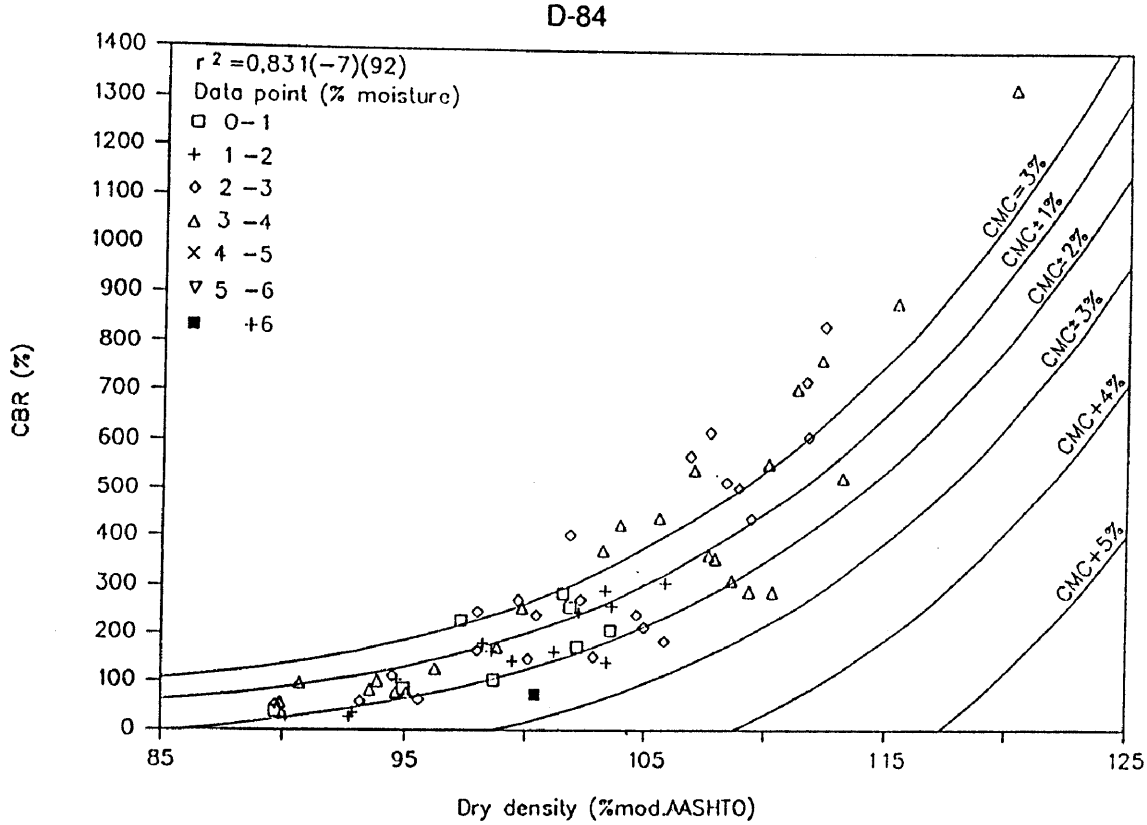

FIGURE D.17(a) **RELATION BETWEEN CBR AND DRY DENSITY FOR DIFFERENT MOISTURE LEVELS (DOLERITE CRUSHED STONE) (OFS3)**

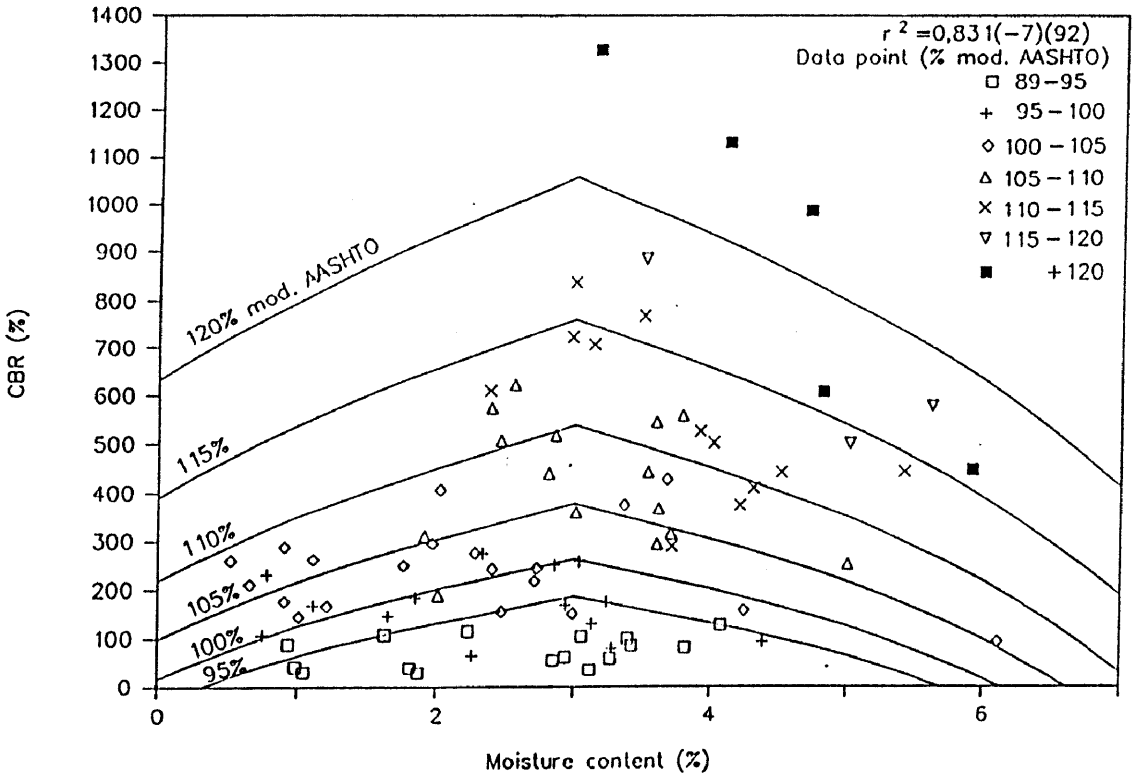

FIGURE D.17(b) **RELATION BETWEEN CBR AND MOISTURE CONTENT FOR DIFFERENT DENSITY LEVELS (DOLERITE CRUSHED STONE) (OFS3)**

APPENDIX E

INFORMATION PERTAINING TO CHAPTER 6

ATTERBERG LIMITS, LINEAR SHRINKAGE, AS WELL AS MDDs AND MOISTURE REGIMES FOR ORIGINAL UNTREATED ROADBUILDING MATERIALS

SAMPLE	LL	PI	LS	RD	MDD (mod) (kg/m^3)	MDD (mod) (%SD)	OMC (mod) (%)	ZAVMC (mod) (%)	MDD (vib) (%SD)	OMC (vib) (%)	ZAVMC (vib) (%)	CMC (%)	SAMPLE
BAB	63,33	31,67	13,67	2,756	1642,0	59,58	18,05	24,62	59,11	23,71	25,10	12,00	BAB
SPR2	38,00	16,00	7,50	2,758	1967,0	71,32	11,40	14,58	73,26	12,73	13,23	9,50	SPR2
SPR1	29,00	15,00	7,00	2,699	1865,0	69,10	11,40	16,57	71,62	14,68	14,68	9,25	SPR1
LABLEN	19,10	2,90	1,60	2,708	2098,0	77,47	7,80	10,74	79,05	7,38	9,79	7,00	LABLEN
LABDEW	18,00	0,50	1,00	2,680	2048,0	76,42	8,75	11,51	78,17	9,47	10,42	8,75	LABDEW
OFS1	0,00	0,00	0,00	2,655	1789,0	67,38	7,80	18,23	69,53	15,04	16,51	8,50	OFS1
NPAB	44,00	13,00	8,50	2,827	2150,0	76,05	10,10	11,14	77,44	10,31	10,30	8,00	NPAB
SIL	24,00	10,00	4,50	2,675	1884,0	70,42	12,50	15,70	73,72	11,08	13,33	7,00	SIL
LABD1	25,50	15,00	5,00	2,800	2097,0	74,89	9,80	11,97	79,59	7,82	9,16	7,00	LABD1
TPA3	30,00	12,00	6,50	2,752	2077,0	75,47	9,20	11,81	77,47	9,40	10,57	6,75	TPA3
TPA1	27,00	10,00	4,50	2,961	2234,0	75,45	8,70	10,99	79,11	8,06	8,92	6,75	TPA1
CPA1	17,00	3,00	2,00	2,756	2371,0	86,03	4,10	5,89	90,24	3,92	3,92	2,75	CPA1
DENS7	25,00	5,20	3,70	2,803	2237,0	79,81	7,80	9,03	84,28	6,58	6,65	5,00	DENS7
TPA2	29,00	6,00	2,50	2,671	2062,0	77,20	5,60	11,06	82,14	7,22	8,14	4,50	TPA2
NPAE	18,00	4,00	2,00	2,638	2256,0	85,52	5,90	6,42	88,33	5,01	5,01	4,00	NPAE
FERR1	20,00	4,00	2,00	2,680	2174,0	81,12	5,30	8,68	86,79	4,82	5,68	4,00	FERR1
OFS2	0,00	0,00	0,00	2,982	2369,0	79,44	3,80	8,68	83,96	5,61	6,41	3,75	OFS2
NPAA	0,00	0,00	0,00	2,989	2458,0	82,23	6,30	7,23	88,04	4,55	4,54	3,75	NPAA
ROSS1	19,00	0,50	0,50	2,640	2185,0	82,77	6,20	7,89	86,64	4,09	5,84	3,25	ROSS1
DENS8	33,40	14,00	7,60	2,774	2174,0	78,37	7,90	9,95	77,81	10,74	10,28	7,25	DENS8
OFS3	0,00	0,50	1,00	2,966	2197,0	74,07	3,90	11,80	89,52	2,85	3,95	3,00	OFS3

GRADING OF ORIGINAL UNTREATED ROADBUILDING MATERIALS

	Sieve size (mm)											
SAMPLE	75	63	53	37,5	26,5	19,0	13,2	4,75	2,0	0,425	0,075	SAMPLE
BAB	100,0	100,0	100,0	100,0	100,0	100,0	100,0	100,0	99,3	97,0	79,0	BAB
SPR2	100,0	100,0	100,0	100,0	100,0	99,3	93,7	87,2	76,3	65,9	42,1	SPR2
SPR1	100,0	100,0	100,0	100,0	100,0	100,0	99,7	90,4	77,6	58,3	23,4	SPR1
LABLEN	100,0	100,0	100,0	100,0	100,0	99,8	99,8	99,5	97,4	81,0	42,2	LABLEN
LABDEW	100,0	100,0	100,0	100,0	100,0	100,0	100,0	99,7	99,5	58,3	9,0	LABDEW
OFS1	100,0	100,0	100,0	100,0	100,0	100,0	100,0	100,0	100,0	99,4	8,2	OFS1
NPAB	100,0	100,0	100,0	93,0	87,0	79,0	73,0	52,0	46,0	30,0	20,0	NPAB
SIL	100,0	100,0	100,0	100,0	100,0	100,0	98,0	94,0	93,0	77,0	28,0	SIL
LABD1	100,0	100,0	100,0	100,0	100,0	99,3	95,0	72,7	60,2	48,3	30,8	LABD1
TPA3	100,0	100,0	100,0	91,0	85,0	78,0	72,0	55,0	42,0	30,0	19,0	TPA3
TPA1	100,0	100,0	100,0	91,0	85,0	79,0	78,0	69,0	56,0	21,0	7,0	TPA1
CPA1	100,0	100,0	100,0	100,0	93,0	82,0	67,0	46,0	30,0	15,0	8,0	CPA1
DENS7	100,0	100,0	100,0	100,0	100,0	98,8	77,8	46,1	34,9	24,8	18,2	DENS7
TPA2	100,0	100,0	100,0	96,0	92,0	88,0	84,0	62,0	40,0	14,0	4,0	TPA2
NPAE	100,0	100,0	100,0	100,0	99,1	96,2	87,5	50,9	29,6	13,6	2,8	NPAE
FERR1	100,0	100,0	100,0	99,7	96,5	85,4	71,2	41,0	25,3	12,4	1,8	FERR1
OFS2	100,0	100,0	100,0	99,6	97,6	96,0	91,6	54,5	27,6	10,3	3,5	OFS2
NPAA	100,0	100,0	100,0	99,0	88,0	76,0	67,0	43,0	34,0	17,0	7,0	NPAA
ROSS1	100,0	100,0	100,0	99,0	83,0	73,0	65,0	48,0	34,0	15,0	6,0	ROSS1
DENS8	100,0	100,0	100,0	100,0	100,0	97,1	85,1	54,6	43,5	31,6	27,2	DENS8
OFS3	100,0	100,0	100,0	100,0	99,0	97,0	83,0	36,0	15,0	5,0	2,0	OFS3

MDD (mod) (% SD) = F((GF > 0,425)^{0,85}), ((% < 0,425)/100)*(LL/100)^{0,1} (= C), LS, C^3) (-OFS3)

Regression Output:

Constant			99,93611 (k_{10})	
Std Err of Y Est			2,263200	
R Squared			0,901795	
No. of Observations			20	
Degrees of Freedom			15	
	(k_6)	(k_7)	(k_8)	(k_9)
X Coefficient(s)	-33,7346	19,27655	-1,20764	-12,3063
Std Err of Coef.	4,723711	4,907930	0,213611	5,567864

OMC (mod) (%) = F ((GF > 0,425)^{0,85}), ((% < 0,425)/100)*(LL/100)^{0,1} (= C), LS, C^3)

Regression Output:

Constant			0,800098 (k_{20})	
Std Err of Y Est			1,107748	
R Squared			0,913513	
No. of Observations			21	
Degrees of Freedom			16	
	(k_{16})	(k_{17})	(k_{18})	(k_{19})
X Coefficient(s)	7,175719	0,346294	0,555493	2,861833
Std Err of Coef.	2,244660	2,394497	0,103395	2,656220

ZAVMC (mod) (%) = F ((GF > 0,425)^{0,85}), ((% < 0,425)/100)*(LL/100)^{0,1} (= C), LS, C^3) (-OFS3)

Regression Output:

Constant			-3,87765 (k_{30})	
Std Err of Y Est			1,438835	
R Squared			0,919196	
No. of Observations			20	
Degrees of Freedom			15	
	(k_{26})	(k_{27})	(k_{28})	(k_{29})
X Coefficient(s)	22,41750	-14,6602	0,780933	12,59359
Std Err of Coef.	3,003111	3,120229	0,135804	3,539784

CMC (%) = F ((GF > 0,425)^{0,85}), ((% < 0,425)/100)*(LL/100)^{0,1} (= C), LS, C^3)

Regression Output:

Constant			-3,09955 (k_{35})	
Std Err of Y Est			0,603354	
R Squared			0,954931	
No. of Observations			21	
Degrees of Freedom			16	
	(k_{31})	(k_{32})	(k_{33})	(k_{34})
X Coefficient(s)	12,16945	-2,22615	0,495747	-1,83665
Std Err of Coef.	1,222593	1,304204	0,056316	1,446756

REGRESSION COEFFICIENTS FOR STANDARDIZED MOISTURE REGIME (MOISTURE REQUIREMENT CONSTANTS STANDARDIZED FOR RD = 2,65)

SOMC (vib) (%) = F ((GF > 0,425)^{0,85}), ((% < 0,425)/100)*(LL/100)^{0,1} (= C), LS, C^3)

Regression Output:

Constant			-7,34696 (k)	
Std Err of Y Est			0,985599	
R Squared			0,968728	
No. of Observations			21	
Degrees of Freedom			16	
	(GF^{0,85})	(C)	(LS)	(C^3)
X Coefficient(s)	23,06058	-16,5273	1,146541	11,77833
Std Err of Coef.	1,997146	2,130461	0,091994	2,363324

SZAVMC (vib) (%) = F ((GF > 0,425)^{0,85}), ((% < 0,425)/100)*(LL/100)^{0,1} (= C), LS, C^3)

Regression Output:

Constant			-6,74470	
Std Err of Y Est			0,995675	
R Squared			0,969852	
No. of Observations			21	
Degrees of Freedom			16	
X Coefficient(s)	23,70265	-15,8884	0,992208	14,12369
Std Err of Coef.	2,017563	2,152240	0,092934	2,387484

SOMC (mod) (%) = F ((GF > 0,425)^{0,85}), ((% < 0,425)/100)*(LL/100)^{0,1} (= C), LS, C^3)

Regression Output:

Constant	1,185852
Std Err of Y Est	1,208963
R Squared	0,902874
No. of Observations	21
Degrees of Freedom	16
X Coefficient(s)	6,967474 -0,06758 0,603192 3,203030
Std Err of Coef.	2,449756 2,613284 0,112842 2,898920

SZAVMC (mod) (%) = F ((GF > 0,425)^{0,85}), ((% < 0,425)/100)*(LL/100)^{0,1} (= C), LS, C^3) (-OFS3)

Regression Output:

Constant	-3,35735
Std Err of Y Est	1,421242
R Squared	0,923699
No. of Observations	20
Degrees of Freedom	15
X Coefficient(s)	22,20080 -15,3738 0,834881 13,35021
Std Err of Coef.	2,966392 3,082077 0,134143 3,496502

SCMC (%) = F ((GF > 0,425)^{0,85}), ((% < 0,425)/100)*(LL/100)^{0,1} (= C), LS, C^3)

Regression Output:

Constant	-2,85255
Std Err of Y Est	0,702348
R Squared	0,941690
No. of Observations	21
Degrees of Freedom	16
X Coefficient(s)	12,07765 -2,49923 0,533210 -1,74455
Std Err of Coef.	1,423187 1,518189 0,065555 1,684130

APPENDIX F

INFORMATION PERTAINING TO CHAPTER 7

SBD, LBD, SF AND S_{rv} VALUES OF ORIGINAL MATERIALS

SAMPLE	SBD (%SD)	LBD (%SD)	SF (%)	Srv (%)
BAB	52,89	47,91	27,76	35,38
SPR2	67,74	57,09	25,89	35,35
SPR1	64,19	55,53	18,13	25,51
LABLEN	69,58	60,99	14,53	23,66
LABDEW	56,70	45,65	23,11	35,21
OFS1	63,35	53,12	11,10	21,88
NPAB	64,76	60,15	15,82	21,74
SIL	61,34	52,17	14,44	25,23
LABD1	67,44	57,41	16,86	25,55
TPA3	69,09	62,27	8,95	15,29
TPA1	64,83	61,74	16,82	26,02
CPA1	78,93	67,02	10,87	20,43
DENS7	58,58	53,66	11,65	23,41
TPA2	67,17	61,14	4,54	13,43
NPAE	76,26	71,65	6,43	12,93
FERR1	72,82	63,70	6,98	17,62
OFS2	67,71	62,07	7,35	17,44
NPAA	72,94	70,38	5,29	16,34
ROSS1	76,24	66,09	3,01	10,74
DENS8	64,95	58,49	16,69	23,90
OFS3	74,56	70,01	- 2,42	9,14

Regression analysis of log (CBR:CMC) against log DD (% SD)) (=E), E^2, log (SBD), log (SF) and log (CMC)
(Only tamped samples) (Improved CMC-values from SAUC5 used) (90/01/08)

log (CBR:CMC) vs log (DD (% SD)) (=E), E^2, log (SBD), log (SF), log (CMC)
Lines 4-349 (G1 + OFS2)

Regression Output:

Constant	67,80743 (k_{16})				
Std Err of Y Est	0,048331				
R Squared	0,957238				
No. of Observations	346				
Degrees of Freedom	340				
	(k_{11})	(k_{12})	(k_{13})	(k_{14})	(k_{15})
X Coefficient(s)	-70,7735	20,80616	-3,01803	-0,48467	0,134345
Std Err of Coef.	10,30969	2,722685	0,241834	0,066673	0,168150

log (CBR:CMC) vs log (DD (% SD)) (=E), E^2, log (SBD),log (SF)
Lines 4-349 (G1 + OFS2)

Regression Output:

Constant	67,57977 (k_{25})				
Std Err of Y Est	0,048305				
R Squared	0,957157				
No. of Observations	346				
Degrees of Freedom	341				
	(k_{21})	(k_{22})	(k_{23})	(k_{24})	
X Coefficient(s)	-70,7392	20,78932	-2,87928	-0,43295	
Std Err of Coef.	10,30413	2,721159	0,168204	0,015943	

log (CBR:CMC) vs log (DD (% SD)) (=E), E^2, log (SBD)
Lines 4-349 (G1 + OFS2)

Regression Output:

Constant	138,5412 (k_{34})			
Std Err of Y Est	0,085779			
R Squared	0,864507			
No. of Observations	346			
Degrees of Freedom	342			
	(K_{31})	(k_{32})	(k_{33})	
X Coefficient(s)	-149,959	41,59211	-0,65539	
Std Err of Coef.	17,54911	4,636714	0,260899	

log (CBR:CMC) vs log (DD (% SD) (=E), E^2
Lines 4-349 (G1 + OFS2)

Regression Output:

Constant	134,9190 (k_{43})		
Std Err of Y Est	0,086441		
R Squared	0,862007		
No. of Observations	346		
Degrees of Freedom	343		
	(k_{41})	(k_{42})	
X Coefficient(s)	-147,302	40,85867	
Std Err of Coef.	17,65230	4,663197	

log (CBR:CMC) vs log (DD (% SD)) (=E), E^2, log (SBD), log (SF), log (CMC)
Lines 4-280 (G1 only)

Regression Output:

Constant	39,29038
Std Err of Y Est	0,046313
R Squared	0,962541
No. of Observations	277
Degrees of Freedom	271
X Coefficient(s)	-59,9536 17,94450 7,265313 0,731499 -3,25459
Std Err of Coef.	10,42351 2,750026 1,656047 0,206720 0,565659

log (CBR:CMC) vs log (DD (% SD)) (=E), E^2, log (SBD), log (SF)
Lines 4-280 (G1 only)

Regression Output:

Constant	48,27211
Std Err of Y Est	0,048970
R Squared	0,957965
No. of Observations	277
Degrees of Freedom	272
X Coefficient(s)	-52,1402 15,92320 -2,05049 -0,45437
Std Err of Coef.	10,92757 2,883969 -,367720 0,016781

log (CBR:CMC) vs log (DD (% SD)) (=E), E^2, log (SBD)
Lines 4-280 (G1 only)

Regression Output:

Constant	130,9048
Std Err of Y Est	0,093963
R Squared	0,844672
No. of Observations	277
Degrees of Freedom	273
X Coefficient(s)	-139,316 38,74522 -1,88508
Std Err of Coef.	20,03678 5,292073 0,705475

log (CBR:CMC) vs log (DD (% SD)) (=E), E^2
Lines 4-280 (G1 only)

Regression Output:

Constant	130,5236
Std Err of Y Est	0,095010
R Squared	0,840609
No. of Observations	277
Degrees of Freedom	274
X Coefficient(s)	-142,718 39,66283
Std Err of Coef.	20,21910 5,339761

log (CBR:CMC) vs log (DD (% SD)) (=E), E^2, log (SBD), log (SF), log (CMC)
Lines 4-1010 (all except BAB)

Regression Output:

Constant	42,15851
Std Err of Y Est	0,135445
R Squared	0,914122
No. of Observations	1007
Degrees of Freedom	1001
X Coefficient(s)	-51,8394 15,65623 1,608016 0,325161 -1,62131
Std Err of Coef.	9,500547 2,548939 0,187429 0,038353 0,07592

log (CBR:CMC) vs log (DD (% SD)) (=E), E^2, log (SBD), log (SF)
Lines 4-1010 (all except BAB)

Regression Output:

Constant	28,75397
Std Err of Y Est	0,163326
R Squared	0,875004
No. of Observations	1007
Degrees of Freedom	1002
X Coefficient(s)	-42,1963 13,52143 2,866164 -0,35190
Std Err of Coef.	11,44319 3,071250 0,214551 0,026019

log (CBR:CMC) vs log (DD (% SD)) (=E), E^2, log (SBD)
Lines 4-1010 (all except BAB)

Regression Output:

Constant	32,00755
Std Err of Y Est	0,177521
R Squared	0,852185
No. of Observations	1007
Degrees of Freedom	1003
X Coefficient(s)	-50,2036 15,88751 4,561181
Std Err of Coef.	12,42110 3,332761 0,189278

log (CBR:CMC) vs log (DD (% SD)) (=E), E^2
Lines 4-1010 (all except BA

Regression Output:

Constant	86,63439
Std Err of Y Est	0,222956
R Squared	0,766607
No. of Observations	1007
Degrees of Freedom	1004
X Coefficient(s)	-101,965 30,32949
Std Err of Coef.	15,36513 4,117519

log (CBR:CMC) vs log (DD (% SD)) (=E), E^2, log (SBD), log (SF), log (CMC)
Lines 350 - 633 (NPAB - LABD)

Regression Output:

Constant	95,17697
Std Err of Y Est	0,035175
R Squared	0,978761
No. of Observations	284
Degrees of Freedom	278
X Coefficient(s)	-139,200 39,61879 13,66789 -1,90879 6,819824
Std Err of Coef.	16,27516 4,366578 0,239005 0,049708 0,165667

log (CBR:CMC) vs log (DD (% SD)) (=E) E^2, log (SBD), log (SF)
Lines 350 - 633 (NPAB - LABD)

Regression Output:

Constant	41,93668
Std Err of Y Est	0,093532
R Squared	0,849296
No. of Observations	284
Degrees of Freedom	279
X Coefficient(s)	-73,2694 21,77480 11,37679 0,079896
Std Err of Coef.	43,06571 11,55341 0,618046 0,031134

log (CBR:CMC) vs log (DD (% SD)) (=E), E^2, log (SBD)
Lines 350 - 633 (NPAB - LABD)

Regression Output:

Constant	14,44055
Std Err of Y Est	0,094460
R Squared	0,845739
No. of Observations	284
Degrees of Freedom	280
X Coefficient(s)	-41,9716 13,29600 10,66549
Std Err of Coef.	41,71248 11,18074 0,557885

log (CBR:CMC) vs log (DD (% SD)) (=E) E^2
Lines 350 - 633 (NPAB - LABD)

Regression Output:

Constant	-70,8046
Std Err of Y Est	0,143166
R Squared	0,644381
No. of Observations	284
Degrees of Freedom	281
X Coefficient(s)	68,81246 -15,9990
Std Err of Coef.	62,60729 16,78587

log (CBR:CMC) vs log (DD (% SD)) (=E), E^2, log (SBD), log (SF), log (CMC)
Lines 350 - 652 (NPAB - DENS8)

Regression Output:

Constant	109,6848
Std Err of Y Est	0,058186
R Squared	0,944269
No. of Observations	303
Degrees of Freedom	297
X Coefficient(s)	-156,037 44,06817 14,57666 -1,79826 6,363698
Std Err of Coef.	26,60195 7,137576 0,388963 0,081818 0,271749

log (CBR:CMC) vs log (DD (% SD)) (=E), E^2, log (SBD), log (SF)
Lines 350 - 652 (NPAB - DENS8)

Regression Output:

Constant	55,76747
Std Err of Y Est	0,098003
R Squared	0,841369
No. of Observations	303
Degrees of Freedom	298
X Coefficient(s)	-89,6046 26,12645 12,20098 0,064340
Std Err of Coef.	44,55004 11,95232 0,632454 0,032303

log (CBR:CMC) vs log (DD (% SD)) (=E), E^2, log (SBD)
Lines 350 - 652 (NPAB - DENS8)

Regression Output:

Constant	33,07391
Std Err of Y Est	0,098488
R Squared	0,839258
No. of Observations	303
Degrees of Freedom	299
X Coefficient(s)	-63,7515 19,12879 11,59041
Std Err of Coef.	42,82804 11,48083 0,555932

log (CBR:CMC) vs log (DD (% SD)) (=E), E^2
Lines 350 - 652 (NPAB - DENS8)

Regression Output:

Constant	-38,6844
Std Err of Y Est	0,154018
R Squared	0,605583
No. of Observations	303
Degrees of Freedom	300
X Coefficient(s)	34,32047 -6,74545
Std Err of Coef.	66,57032 17,84879

log (CBR:CMC) vs log (DD (% SD)) (=E), E^2, log (SBD), log (SF), log (CMC)
Lines 350 - 708 (NPAB - LABLEN)

Regression Output:

Constant	77,83340
Std Err of Y Est	0,075366
R Squared	0,898235
No. of Observations	359
Degrees of Freedom	353
X Coefficient(s)	-115,295 33,19581 10,85031 -2,28175 7,560016
Std Err of Coef.	23,54367 6,333033 0,405295 0,099254 0,339571

log (CBR:CMC) vs log (DD (% SD)) (=E), E^2, log (SBD), log (SF)
Lines 350 - 708 (NPAB - LABLEN)

Regression Output:

Constant	25,01481
Std Err of Y Est	0,116692
R Squared	0,755343
No. of Observations	359
Degrees of Freedom	354
X Coefficient(s)	-44,8575 14,14633 6,251505 -0,12659
Std Err of Coef.	36,12283 9,715744 0,539913 0,033946

log (CBR:CMC) vs log (DD (% SD)) (=E), E^2, log (SBD)
Lines 350 - 708 (NPAB - LABLEN)

Regression Output:

Constant	56,15920
Std Err of Y Est	0,118795
R Squared	0,745731
No. of Observations	359
Degrees of Freedom	355
X Coefficient(s)	-80,0364 23,73777 6,780492
Std Err of Coef.	35,49772 9,537973 0,530334

log (CBR:CMC) vs log (DD (% SD)) (=E), E^2
Lines 350 - 708 (NPAB - LABLEN)

Regression Output:

Constant	66,62936
Std Err of Y Est	0,143361
R Squared	0,628651
No. of Observations	359
Degrees of Freedom	356
X Coefficient(s)	-78,5477 23,49029
Std Err of Coef.	2,83832 11,51037

log (CBR:CMC) vs log (DD (% SD)) (=E), E^2, log (SBD), log (SF), log (CMC)
Lines 653 - 939 (LABLEN - LABDEW)

Regression Output:

Constant	0,007049
Std Err of Y Est	0,068049
R Squared	0,834549
No. of Observations	287
Degrees of Freedom	281
X Coefficient(s)	-7,69326 3,702538 1,451194 -0,91779 2,018085
Std Err of Coef.	14,66805 4,001469 0,147109 0,059872 0,149290

log (CBR:CMC) vs log (DD (% SD) (= E), E^2, Log (SBD), log (SF)
Lines 653 - 939 (LABLEN - L

Regression Output:

Constant	-43,6710
Std Err of Y Est	0,087263
R Squared	0,726959
No. of Observations	287
Degrees of Freedom	282
X Coefficient(s)	43,58686 -10,5751 0,753324 -0,30698
Std Err of Coef.	18,16973 4,949327 0,176648 0,050371

log (CBR:CMC) vs log (DD (% SD)) (=E), E^2, log (SBD)
Lines 653 - 939 (LABLEN - LABDEW)

Regression Output:

Constant	-48,3634
Std Err of Y Est	0,092668
R Squared	0,690998
No. of Observations	287
Degrees of Freedom	283
X Coefficient(s)	47,91169 -11,7407 0,916817
Std Err of Coef.	19,28034 5,251936 0,185413

log (CBR:CMC) vs log (DD (% SD)) (= E) E^2
Lines 653 - 939 (LABLEN - L

Regression Output:

Constant	-63,8506
Std Err of Y Est	0,096418
R Squared	0,664301
No. of Observations	287
Degrees of Freedom	284
X Coefficient(s)	66,79872 -16,9411
Std Err of Coef.	19,66295 5,353781

log (CBR:CMC) vs log (DD (% SD)) (=E), E^2, log (SBD), log (SF), log (CMC)
Lines 653 - 965 (LABLEN - DENS7)

Regression Output:

Constant	11,76772
Std Err of Y Est	0,086972
R Squared	0,785766
No. of Observations	313
Degrees of Freedom	307

X Coefficient(s)	-17,6998 6,330115 0,723353 -0,70404 0,706193
Std Err of Coef.	17,39925 4,743646 0,172464 0,073007 0,140339

log (CBR:CMC) vs log (DD (% SD) (= E) E^2, log (SBD), log (SF)
Lines 940 - 984 (OFS1 only)

Regression Output:

Constant	-14,0526
Std Err of Y Est	0,090341
R Squared	0,768096
No. of Observations	313
Degrees of Freedom	308

X Coefficient(s)	11,47272 -1,75845 0,615324 -0,41292
Std Err of Coef.	17,04041 4,635865 0,177777 0,046256

log (CBR:CMC) vs log (DD (% SD)) (=E), E^2, log (SBD)
Lines 940 - 984 (OFS1 only)

Regression Output:

Constant	-1,27610
Std Err of Y Est	0,101193
R Squared	0,708095
No. of Observations	313
Degrees of Freedom	309

X Coefficient(s)	-3,49053 2,394048 0,714785
Std Err of Coef.	18,99466 5,166495 0,198747

log (CBR:CMC) vs log (DD (% SD)) (= E) E^2
Lines 940 - 984 (OFS1 only)

Regression Output:

Constant	-14,5556
Std Err of Y Est	0,103122
R Squared	0,695876
No. of Observations	313
Degrees of Freedom	310

X Coefficient(s)	12,57905 -2,03528
Std Err of Coef.	18,81366 5,113228

log (CBR:CMC) vs log (DD (% SD)) (=E), E^2, log (SBD), log (SF), log (CMC)
Lines 940 - 965 (DENS7 only)

Regression Output:

Constant	11795,49
Std Err of Y Est	0,004951
R Squared	0,998810
No. of Observations	26
Degrees of Freedom	20

X Coefficient(s)	1631,905	-431,566	2830,297	-9666,05	-11129,3
Std Err of Coef.	19,72193	5,238685	ERR	ERR	2114699,

log (CBR:CMC) vs log (DD (% SD) (= E) E^2, log (SBD), log (SF)
Lines 985 - 1010 (DENS7 onl

Regression Output:

Constant	4439,837
Std Err of Y Est	0,004832
R Squared	0,998810
No. of Observations	26
Degrees of Freedom	21

X Coefficient(s)	1631,905	-431,566	4511,116	-13084,8	
Std Err of Coef.	19,24713	5,112565	ERR	ERR	

log (CBR:CMC) vs log (DD (% SD)) (=E), E^2, log (SBD)
Lines 985 - 1010 (DENS7 only)

Regression Output:

Constant	1966,305
Std Err of Y Est	0,004721
R Squared	0,998810
No. of Observations	26
Degrees of Freedom	22

X Coefficient(s)	1631,905	-431,566	-1983,81	
Std Err of Coef.	18,80477	4,995062	ERR	

log (CBR:CMC) vs log (DD (% SD)) (= E) E^2
Lines 985 - 1010 (DENS7 onl

Regression Output:

Constant	-1540,57
Std Err of Y Est	0,004617
R Squared	0,998810
No. of Observations	26
Degrees of Freedom	23

X Coefficient(s)	1631,905	-431,566	
Std Err of Coef.	18,39150	4,885287	

log (CBR:CMC) vs log (DD (% SD)) (=E), E^2, log (SBD), log (SF), log (CMC)
Lines 966 - 1010 (OFS1 only)

Regression Output:

Constant	-2830,09
Std Err of Y Est	0,015249
R Squared	0,995421
No. of Observations	45
Degrees of Freedom	39

X Coefficient(s)	-1208,24	338,5198	991,2189	242,3307	2009,717
Std Err of Coef.	59,92153	16,55403	ERR 2002667,	2950734,	

log (CBR:CMC) vs log (DD (% SD) (= E) E^2, log (SBD), log (SF)
Lines 966 - 1010 (OFS1 only

Regression Output:

Constant	-928,104
Std Err of Y Est	0,015057
R Squared	0,995421
No. of Observations	45
Degrees of Freedom	40

X Coefficient(s)	-1208,24	338,5198	229,2030	1524,980	
Std Err of Coef.	59,16778	16,34580	ERR	ERR	

log (CBR:CMC) vs log (DD (% SD)) (=E), E^2, log (SBD)
Lines 966 - 1010 (OFS1 only)

Regression Output:

Constant	-2266,61
Std Err of Y Est	0,014872
R Squared	0,995421
No. of Observations	45
Degrees of Freedom	41

X Coefficient(s)	-1208,24	338,5198	1856,886	
Std Err of Coef.	58,44176	16,14523	ERR	

log (CBR:CMC) vs log (DD (% SD)) (= E) E^2
Lines 966 - 1010 (OFS1 only

Regression Output:

Constant	1078,985
Std Err of Y Est	0,014694
R Squared	0,995421
No. of Observations	45
Degrees of Freedom	42

X Coefficient(s)	-1208,24	338,5198	
Std Err of Coef.	57,74183	15,95186	

log (CBR:CMC) vs log (DD (% SD)) (=E), E^2, log (SBD), log (SF), log (CMC)
Lines 1011 - 1114 (BAB only)

Regression Output:

Constant	-827,873
Std Err of Y Est	0,000655
R Squared	0,999944
No. of Observations	104
Degrees of Freedom	98

X Coefficient(s)	450,8820	-129,045	12,07878	231,1043	75,60228
Std Err of Coef.	0,709088	0,205173	ERR	72751,81	91514,76

log (CBR:CMC) vs log (DD (% SD) (= E) E^2, log (SBD), log (SF)
Lines 1011 - 1114 (BAB only

Regression Output:

Constant	-804,891
Std Err of Y Est	0,000652
R Squared	0,999944
No. of Observations	104
Degrees of Freedom	99

X Coefficient(s)	450,8820	-129,045	-1,42737	287,7358	
Std Err of Coef.	0,705498	0,204135	ERR	ERR	

log (CBR:CMC) vs log (DD (% SD)) (=E), E^2, log (SBD)
Lines 1011 - 1114 (BAB only)

Regression Output:

Constant	-871,824
Std Err of Y Est	0,000648
R Squared	0,999944
No. of Observations	104
Degrees of Freedom	100

X Coefficient(s)	450,8820	-129,045	278,4154	
Std Err of Coef.	0,701961	0,203111	ERR	

log (CBR:CMC) vs log (DD (% SD)) (= E) E^2
Lines 1011 - 1114 (BAB only

Regression Output:

Constant	-392,-14
Std Err of Y Est	0,000645
R Squared	0,999944
No. of Observations	104
Degrees of Freedom	101

X Coefficient(s)	450,8819	-129,045
Std Err of Coef.	0,698500	0,202110

log (CBR:CMC) vs log (DD (% SD)) (=E), E^2, log (SBD), log (SF), log (CMC)
Lines 4 - 1114 (All data)

Regression Output:

Constant	161,7910
Std Err of Y Est	0,159110
R Squared	0,874023
No. of Observations	1111
Degrees of Freedom	1105
X Coefficient(s)	-176,655 48,91816 0,267347 0,352645 -1,82238
Std Err of Coef.	4,823213 1,323179 0,207472 0,044898 0,088062

log (CBR:CMC) vs log (DD (% SD) (= E) E^2, log (SBD), log (SF)
Lines 4 - 1114 (All data)

Regression Output:

Constant	177,8976
Std Err of Y Est	0,187339
R Squared	0,825199
No. of Observations	1111
Degrees of Freedom	1106
X Coefficient(s)	-198,772 55,32562 1,493439 -0,41675
Std Err of Coef.	5,537745 1,514677 0,234108 0,029635

log (CBR:CMC) vs log (DD (% SD)) (=E), E^2, log (SBD)
Lines 4 - 1114 (All data)

Regression Output:

Constant	196,5694
Std Err of Y Est	0,203307
R Squared	0,793945
No. of Observations	1111
Degrees of Freedom	1107
X Coefficient(s)	-223,912 62,31252 3,402784
Std Err of Coef.	5,687998 1,552832 0,206970

log (CBR:CMC) vs log (DD (% SD)) (= E) E^2
Lines 4 - 1114 (All data)

Regression Output:

Constant	187,9870
Std Err of Y Est	0,226671
R Squared	0,743631
No. of Observations	1111
Degrees of Freedom	1108
X Coefficient(s)	-209,92159,06805
Std Err of Coef.	6,270316 1,717252

log (CBR:CMC) vs log (DD (% SD)) (=E), E^2, log (SBD), log (SF), log (CMC)
Lines 4 - 965 (NPAE - DENS7)

Regression Output:

Constant	78,41980
Std Err of Y Est	0,124299
R Squared	0,917408
No. of Observations	962
Degrees of Freedom	956

X Coefficient(s)	-89,9688 25,76649 1,417096 0,142092 -1,33473
Std Err of Coef.	9,088248 2,436098 0,172520 0,038329 0,074095

log (CBR:CMC) vs log (DD (% SD) (= E) E^2, log (SBD), log (SF)
Lines 4 - 965 (NPAE - DENS7

Regression Output:

Constant	79,60134
Std Err of Y Est	0,143781
R Squared	0,889374
No. of Observations	962
Degrees of Freedom	957

X Coefficient(s)	-94,4249 27,25336 2,258719 -0,44354
Std Err of Coef.	10,50875 2,816290 0,192192 0,023483

log (CBR:CMC) vs log (DD (% SD)) (=E), E^2, log (SBD)
Lines 4 - 965 (NPAE - DENS7)

Regression Output:

Constant	72,77906
Std Err of Y Est	0,168373
R Squared	0,848136
No. of Observations	962
Degrees of Freedom	958

X Coefficient(s)	-93,0671 27,21422 4,436863
Std Err of Coef.	12,30588 3,297986 0,179913

log (CBR:CMC) vs log (DD (% SD)) (= E) E^2
Lines 4 - 965 (NPAE - DENS7

Regression Output:

Constant	129,8087
Std Err of Y Est	0,215171
R Squared	0,751729
No. of Observations	962
Degrees of Freedom	959

X Coefficient(s)	-147,506 42,33640
Std Err of Coef.	15,47104 4,141129

Regression analysis of log (CBR:drop) (% CBR:CMC) against log (CMC) and log (MC-deviation) (% CMC)
J = log (CBR:decrease): as % of CBR:CMC; H = log (CMC); L = MC deviation from CMC as % of CMC

log (CBR:decrease) vs log (CMC), log (MCdev) (= L), L^3/abs (L)
Lines 4 - 349 (G1 + OFS2)

Regression Output:

Constant	-0,73900 (k_4)		
Std Err of Y Est	0,154254		
R Squared	0,983402		
No. of Observations	346		
Degrees of Freedom	342		
	(k_1)	(k_2)	(k_3)
X Coefficient(s)	1,430041	0,932039	0,004902
Std Err of Coef.	0,121259	0,021620	0,001977

log (E) vs log (CMC), log (MCdev) (= L)
Lines 4 - 349 (G1 + OFS2)

Regression Output:

Constant	-0,77818 (k_7)		
Std Err of Y Est	0,155407		
R Squared	0,983104		
No. of Observations	346		
Degrees of Freedom	343		
	(k_5)	(k_6)	
X Coefficient(s)	1,387697	0,982727	
Std Err of Coef.	0,120948	0,007092	

log (CBR:decrease) vs log (CMC), log (MCdev) (= L), L^3/abs (L)
Lines 4 - 280 (G1 only)

Regression Output:

Constant	-0,67318		
Std Err of Y Est	0,164402		
R Squared	0,984548		
No. of Observations	277		
Degrees of Freedom	273		
X Coefficient(s)	1,203091	0,960898	0,002449
Std Err of Coef.	0,140092	0,024830	0,002245

log (E) vs log (CMC), log (MCdev) (= L)
Lines 4 - 280 (G1 only)

Regression Output:

Constant	-0,69168		
Std Err of Y Est	0,164459		
R Squared	0,984481		
No. of Observations	277		
Degrees of Freedom	274		
X Coefficient(s)	1,178208	0,986691	
Std Err of Coef.	0,138271	0,007596	

log (CBR:decrease) vs log (CMC), log (MCdev) (= L), L^3/abs (L)
Lines 4 - 1010 (all except BAB)

Regression Output:

Constant	-0,17347
Std Err of Y Est	0,237888
R Squared	0,936591
No. of Observations	1007
Degrees of Freedom	1003
X Coefficient(s)	0,150889 1,009676 -0,00124
Std Err of Coef.	0,042586 0,019351 0,001925

log (E) vs log (CMC), log (MCdev) (= L)
Lines 4 - 1010 (all except BAB)

Regression Output:

Constant	-0,16016
Std Err of Y Est	0,237819
R Squared	0,936564
No. of Observations	1007
Degrees of Freedom	1004
X Coefficient(s)	0,150996 0,998355
Std Err of Coef.	0,042573 0,008221

log (CBR:decrease) vs log (CMC), log (MCdev) (= L), L^3/abs (L)
Lines 350 - 633 (NPAB - LABD)

Regression Output:

Constant	-0,77415
Std Err of Y Est	0,176110
R Squared	0,853366
No. of Observations	284
Degrees of Freedom	280
X Coefficient(s)	1,121915 0,770404 0,068673
Std Err of Coef.	0,146870 0,090798 0,036832

log (E) vs log (CMC), log (MCdev) (= L)
Lines 350 - 633 (NPAB - LABD)

Regression Output:

Constant	-0,82473
Std Err of Y Est	0,176884
R Squared	0,851545
No. of Observations	284
Degrees of Freedom	281
X Coefficient(s)	1,085141 0,933824
Std Err of Coef.	0,146180 0,023813

log (CBR:decrease) vs log (CMC), log (MCdev) (= L), L^3/abs (L)
Lines 350 - 652 (NPAB - DENS8)

Regression Output:

Constant	-0,87339
Std Err of Y Est	0,177145
R Squared	0,845109
No. of Observations	303
Degrees of Freedom	299
X Coefficient(s)	1,247979 0,807582 0,048218
Std Err of Coef.	0,144372 0,090849 0,036719

log (E) vs log (CMC), log (MCdev) (= L)
Lines 350 - 652 (NPAB - DENS8)

Regression Output:

Constant	-0,90678
Std Err of Y Est	0,177359
R Squared	0,844216
No. of Observations	303
Degrees of Freedom	300
X Coefficient(s)	1,218312 0,922823
Std Err of Coef.	0,142766 0,023525

log (CBR:decrease) vs log (CMC), log (MCdev) (= L), L^3/abs (L)
Lines 350 - 708 (NPAB - LABLEN)

Regression Output:

Constant	-0,88901
Std Err of Y Est	0,165378
R Squared	0,856999
No. of Observations	359
Degrees of Freedom	355
X Coefficient(s)	1,271976 0,838439 0,031200
Std Err of Coef.	0,134151 0,082089 0,032613

log (E) vs log (CMC), log (MCdev) (= L)
Lines 350 - 708 (NPAB - LABLEN)

Regression Output:

Constant	-0,91248
Std Err of Y Est	0,165358
R Squared	0,856630
No. of Observations	359
Degrees of Freedom	356
X Coefficient(s)	1,252344 0,914522
Std Err of Coef.	0,132556 0,020337

log (CBR:decrease) vs log (CMC), log (MCdev) (= L), L^3/abs (L)
Lines 653 - 939 (LABLEN - LABDEW)

Regression Output:

Constant	0,570880
Std Err of Y Est	0,244386
R Squared	0,940457
No. of Observations	287
Degrees of Freedom	283
X Coefficient(s)	-0,58758 0,966590 0,002696
Std Err of Coef.	0,315104 0,035645 0,003621

log (E) vs log (CMC), log (MCdev) (= L)
Lines 653 - 939 (LABLEN - LABDEW)

Regression Output:

Constant	0,568200
Std Err of Y Est	0,244195
R Squared	0,940340
No. of Observations	287
Degrees of Freedom	284
X Coefficient(s)	-0,61633 0,990730
Std Err of Coef.	0,312484 0,014812

log (CBR:decrease) vs log (CMC), log (MCdev) (= L), L^3/abs (L)
Lines 653 - 965 (LABLEN - DENS7)

Regression Output:

Constant	0,609475
Std Err of Y Est	0,235133
R Squared	0,941563
No. of Observations	313
Degrees of Freedom	309
X Coefficient(s)	-0,60502 0,948581 0,004258
Std Err of Coef.	0,195104 0,032021 0,003309

log (E) vs log (CMC), log (MCdev) (= L)
Lines 653 - 965 (LABLEN - DENS7)

Regression Output:

Constant	0,580066
Std Err of Y Est	0,235382
R Squared	0,941250
No. of Observations	313
Degrees of Freedom	310
X Coefficient(s)	-0,62149 0,985631
Std Err of Coef.	0,194889 0,014020

log (CBR:decrease) vs log (CMC), log (MCdev) (= L), L^3/abs (L)
Lines 940 - 965 (DENS7 only)

CANNOT INVERT MATRIX

log (E) vs log (CMC), log (MCdev) (= L)
Lines 940 - 965 (DENS7 only)

CANNOT INVERT MATRIX

log (CBR:decrease) vs log (CMC), log (MCdev) (= L), L^3/abs (L)
Lines 966 - 1010 (OFS1 only)

Regression Output:

Constant	-1,69758
Std Err of Y Est	0,230479
R Squared	0,934900
No. of Observations	45
Degrees of Freedom	41
X Coefficient(s)	0,671896 0,803758 0,520993
Std Err of Coef.	ERR 0,241360 0,131631

log (E) vs log (CMC), log (MCdev) (= L)
Lines 966 - 1010 (OFS1 only)

Regression Output:

Constant	3,916110
Std Err of Y Est	0,267711
R Squared	0,910026
No. of Observations	45
Degrees of Freedom	42
X Coefficient(s)	-5,60331 1,715960
Std Err of Coef.	ERR 0,083255

log (CBR:decrease) vs log (CMC), log (MCdev) (= L), L^3/abs (L)
Lines 1011 - 1114 (BAB only)

Regression Output:

Constant	-1,15546
Std Err of Y Est	0,056011
R Squared	0,960525
No. of Observations	104
Degrees of Freedom	100

X Coefficient(s)	1,159709	1,162914	-0,13818
Std Err of Coef.	ERR	0,086731	0,028306

log (E) vs log (CMC), log (MCdev) (= L)
Lines 1011 - 1114 (BAB only)

Regression Output:

Constant	-1,57657
Std Err of Y Est	0,062019
R Squared	0,951118
No. of Observations	104
Degrees of Freedom	101

X Coefficient(s)	1,822719	0,746075
Std Err of Coef.	ERR	0,016829

log (CBR:decrease) vs log (CMC), log (MCdev) (= L), L^3/abs (L)
Lines 4 - 1114 (All data)

Regression Output:

Constant	-0,13591
Std Err of Y Est	0,229091
R Squared	0,936268
No. of Observations	1111
Degrees of Freedom	1107

X Coefficient(s)	0,127649	0,991374	0,000264
Std Err of Coef.	0,035677	0,018095	0,001817

log (E) vs log (CMC), log (MCdev) (= L)
Lines 4 - 1114 (All data)

Regression Output:

Constant	-0,13852
Std Err of Y Est	0,228990
R Squared	0,936267
No. of Observations	1111
Degrees of Freedom	1108

X Coefficient(s)	0,127356	0,993750
Std Err of Coef.	0,035604	0,007837

log (CBR:decrease) vs log (CMC), log (MCdev) (= L), L^3/abs (L)
Lines 4 - 965 (NPAE - DENS7)

Regression Output:

Constant	-0,16598
Std Err of Y Est	0,203270
R Squared	0,953290
No. of Observations	962
Degrees of Freedom	958

X Coefficient(s)	0,278452	0,942889	0,004487
Std Err of Coef.	0,037397	0,017040	0,001683

log (E) vs log (CMC), log (MCdev) (= L)
Lines 4 - 965 (NPAE - DENS7)

Regression Output:

Constant	-0,21343
Std Err of Y Est	0,203916
R Squared	0,952943
No. of Observations	962
Degrees of Freedom	959

X Coefficient(s)	0,275976	0,984201
Std Err of Coef.	0,037504	0,007102

Regression constants for MDDs and moisture regime parameters (includes SBD and SF)

MDD (vib) (% SD) = F ((GF > 0,425)^{0,85}), ((% < 0,425)/100)*(LL/100)^{0,1} (= C), LS, C^3, SBD, SF)

Regression Output:

Constant	99,37093
Std Err of Y Est	1,581555
R Squared	0,970361
No. of Observations	21
Degrees of Freedom	14

	(GF^{0,85})	(C)	(LS)	(C^3)	(SBD)	(SF)
X Coefficient(s)	-40,2497	16,74064	-1,63137	-8,37628	0,111113	0,206339
Std Err of Coef.	4,299426	3,781997	0,192058	4,036096	0,084488	0,115473

OMC (vib) (%) = F ((GF > 0,425)^{0,85}), ((% < 0,425)/100)*(LL/100)^{0,1} (= C), LS, C^3, SBD, SF)

Regression Output:

Constant	-4,56070
Std Err of Y Est	1,084868
R Squared	0,965245
No. of Observations	21
Degrees of Freedom	14

X Coefficient(s)	22,62105	-15,2461	1,076490	10,74169	-0,03708	-0,02650
Std Err of Coef.	2,949191	2,594261	0,131742	2,768560	0,057955	0,079208

ZAVMC (vib) (%) = F ((GF > 0,425)^{0,85}), ((% < 0,425)/100)*(LL/100)^{0,1} (= C), LS, C^3, SBD, SF)

Regression Output:

Constant	-4,40440
Std Err of Y Est	1,021094
R Squared	0,971118
No. of Observations	21
Degrees of Freedom	14

X Coefficient(s)	25,23629 -13,4865 1,021651 11,79872 -0,03981 -0,12992
Std Err of Coef.	2,775823 2,441757 0,123997 2,605810 0,054548 0,074552

CMC (%) = F ((GF > 0,425)^{0,85}), ((% < 0,425)/100)*(LL/100)^{0,1} (= C), LS, C^3, SBD, SF)

Regression Output:

Constant	-0,87252
Std Err of Y Est	0,570243
R Squared	0,964774
No. of Observations	21
Degrees of Freedom	14

X Coefficient(s)	10,25198 -2,72904 0,408870 -1,12567 -0,02080 0,069362
Std Err of Coef.	1,550195 1,363631 0,069248 1,455249 0,030463 0,041634

MDD (mod) (% SD) = F ((GF > 0,425)^{0,85}), ((% < 0,425)/100)*(LL/100)^{0,1} (= C), LS, C^3, SBD, SF) (-OFS3)

Regression Output:

Constant	87,96416
Std Err of Y Est	2,180148
R Squared	0,921021
No. of Observations	20
Degrees of Freedom	13
X Coefficient(s)	-33,9206 15,34473 -1,28353 -9,30291 0,152339 0,232665
Std Err of Coef.	5,984434 5,220130 0,265351 5,665530 0,116471 0,159648

OMC (mod) (%) = F ((GF > 0,425)^{0,85}), ((% < 0,425)/100)*(LL/100)^{0,1} (= C), LS, C^3, SBD, SF)

Regression Output:

Constant	6,559983
Std Err of Y Est	1,109001
R Squared	0,924152
No. of Observations	21
Degrees of Freedom	14
X Coefficient(s)	6,697516 1,878918 0,561881 1,759635 -0,07139 -0,07753
Std Err of Coef.	3,014797 2,651971 0,134673 2,830148 0,059244 0,080970

ZAVMC (mod) (%) = F ((GF > 0,425)^{0,85}), ((% < 0,425)/100)*(LL/100)^{0,1} (= C), LS, C^3, SBD, SF) (-OFS3)

Regression Output:

Constant	0,679363
Std Err of Y Est	1,373639
R Squared	0,936172
No. of Observations	20
Degrees of Freedom	13

X Coefficient(s)	24,05091 -12,1754 0,891343 10,45804 -0,06374 -0,18022
Std Err of Coef.	3,770593 3,289031 0,167189 3,569663 0,073384 0,100588

Regression constants for standardized moisture regime parameters (includes SBD and SF)

Moisture requirement constants standardized for RD deviation from 2,65

SOMC (vib) (%) = F ((GF > 0,425)^{0,85}), ((% < 0,425)/100)*(LL/100)^{0,1} (= C), LS, C^3, SBD, SF)

Regression Output:

Constant	-3,13939
Std Err of Y Est	1,022414
R Squared	0,970554
No. of Observations	21
Degrees of Freedom	14

	(GF^{0,85})	(C)	(LS)	(C^3)	(SBD)	(SF)
X Coefficient(s)	21,54663	-16,1441	1,091149	11,73755	-0,04758	0,010137
Std Err of Coef.	2,779412	2,444914	0,124158	2,609179	0,054618	0,074648

SZAVMC (vib) (%) = F ((GF > 0,425)^{0,85}), ((% < 0,425)/100)*(LL/100)^{0,1} (= C), LS, C^3, SBD, SF)

Regression Output:

Constant	-2,85787
Std Err of Y Est	0,992275
R Squared	0,973800
No. of Observations	21
Degrees of Freedom	14

X Coefficient(s)	24,07317	-14,4159	1,032267	12,92494	-0,05089	-0,09206
Std Err of Coef.	2,697479	2,372842	0,120498	2,532265	0,053008	0,072448

SCMC (%) = F ((GF>0,425)^{0,85}), ((% <0,425)/100)*(LL/100)^{0,1} (=C), LS, C^3, SBD, SF)

Regression Output:

Constant	0,106224
Std Err of Y Est	0,624339
R Squared	0,959683
No. of Observations	21
Degrees of Freedom	14

X Coefficient(s)	9,443518 -3,22213 0,413319 -0,74310 -0,02730 0,097120
Std Err of Coef.	1,697253 1,492991 0,075817 1,593300 0,033353 0,045584

SOMC (mod) (%) = F ((GF > 0,425)^{0,85}), ((% <0,425)/100)*(LL/100)^{0,1} (=C), LS, C^3, SBD, SF)

Regression Output:

Constant	8,005320
Std Err of Y Est	1,224610
R Squared	0,912800
No. of Observations	21
Degrees of Freedom	14

X Coefficient(s)	5,562672 1,216733 0,567507 2,448490 -0,08124 -0,04371
Std Err of Coef.	3,329077 2,928428 0,148712 3,125178 0,065420 0,089411

SZAVMC (mod) (%) = F ((GF > 0,425)^{0,85}), ((% <0,425)/100)*(LL/100)^{0,1} (=C), LS, C^3, SBD, SF) (-OFS3)

Regression Output:

Constant	2,793415
Std Err of Y Est	1,409519
R Squared	0,934959
No. of Observations	20
Degrees of Freedom	13

X Coefficient(s)	22,49622 -13,2274 0,884294 11,68022 -0,07900 -0,13125
Std Err of Coef.	3,869083 3,374941 0,171556 3,662904 0,075301 0,103216

APPENDIX G

INFORMATION PERTAINING TO CHAPTER 8

INDICATOR TEST RESULTS FROM MATERIAL CONTROL DATA SHEETS OF ROAD CONSTRUCTION PROJECTS USED FOR VERIFICATION PURPOSES OF COMPACTABILITY AND CBR MODELS

Sample No.	Sieve size (mm) 75	63	53	37,5	26,5	19	13,2	4,75	2,00	0,425	0,075	Sample No.
1	100	100	100	100	97	92	83	57	41	24	13	1
2	100	100	100	100	100	95	89	69	51	29	11	2
3	100	100	100	100	94	88	82	65	49	29	12	3
4	100	100	100	100	98	93	89	67	45	15	7	4
5	100	100	100	100	100	95	91	74	44	15	6	5
6	100	100	100	100	98	94	83	60	49	34	17	6
7	100	100	100	100	97	94	82	57	40	20	7	7
8	100	100	100	100	97	90	80	52	33	13	4	8
9	100	100	100	100	91	78	72	51	41	22	9	9
10	100	100	100	100	98	94	83	60	49	34	17	10
11	100	100	100	100	94	85	76	50	38	22	9	11
12	100	100	100	100	93	87	77	49	36	22	10	12
13	100	100	100	100	96	93	86	64	49	32	16	13
14	100	100	100	100	98	89	80	56	41	23	11	14
15	100	100	100	100	91	83	75	55	43	26	14	15
16	100	100	100	92	90	85	80	62	48	32	18	16
17	100	100	100	100	98	90	81	62	50	34	18	17
18	100	100	100	95	79	69	59	41	33	24	15	18
19	100	100	100	74	60	52	42	30	24	18	12	19
20	100	100	100	89	80	70	63	49	43	34	19	20
21	100	100	100	96	87	76	71	60	54	44	29	21
22	100	100	93	84	78	73	64	47	38	28	18	22
23	100	100	91	87	80	75	65	51	42	31	19	23
24	100	100	100	92	87	81	74	57	49	40	26	24
25	100	100	100	94	80	70	60	42	34	21	13	25
26	100	100	100	90	81	67	60	46	39	32	21	26
27	100	100	100	94	85	79	69	47	37	27	18	27
28	100	100	100	85	81	75	68	49	39	29	20	28
29	100	100	100	84	70	59	64	41	34	25	16	29
30	100	100	100	79	69	59	49	31	24	18	13	30
31	100	100	100	100	100	100	100	99	97	52	16	31
32	100	100	100	100	100	100	100	100	98	59	23	32
33	100	100	100	100	100	100	100	100	98	58	19	33
34	100	100	100	100	100	100	100	99	96	51	15	34
35	100	100	100	100	100	100	100	99	97	48	12	35
36	100	100	100	100	100	100	100	99	95	51	12	36
37	100	100	100	100	100	100	100	100	96	56	21	37
38	100	100	100	100	100	100	100	100	98	51	18	38
39	100	100	100	100	100	100	99	98	95	91	53	39
40	100	100	100	100	100	100	100	99	97	59	19	40
41	100	100	100	100	100	100	99	99	98	50	14	41
42	100	100	100	100	100	100	100	99	97	56	15	42
43	100	100	100	100	100	100	99	98	95	53	18	43
44	100	100	100	100	100	100	100	99	97	50	14	44
45	100	100	100	100	100	100	100	99	98	61	21	45
46	100	100	100	100	100	100	100	99	98	52	14	46
47	100	100	100	100	100	100	100	99	99	60	20	47
48	100	100	100	100	100	100	100	100	99	60	20	48
49	100	100	100	100	100	100	100	99	98	61	19	49

Sample No.	Sieve size (mm) 75	63	53	37,5	26,5	19	13,2	4,75	2,00	0,425	0,075	Sample No.
50	100	100	100	100	100	100	100	99	98	67	17	50
51	100	100	100	100	100	100	99	98	95	59	16	51
52	100	100	100	100	100	100	100	100	92	67	14	52
53	100	100	100	100	100	100	100	100	97	61	18	53
54	100	100	100	100	100	100	100	99	98	57	23	54
55	100	100	100	100	100	100	100	99	98	56	24	55
56	100	100	100	100	100	100	100	99	98	52	21	56
57	100	100	100	100	100	100	100	99	97	57	32	57
58	100	100	100	100	94	94	94	93	92	72	32	58
59	100	100	100	100	100	100	98	96	95	59	25	59
60	100	100	100	100	100	100	100	99	98	59	27	60
61	100	100	100	100	93	91	86	80	77	51	18	61
62	100	100	100	100	100	100	98	95	92	65	29	62
63	100	100	100	100	100	100	100	97	95	59	31	63
64	100	100	100	100	100	100	100	99	98	60	27	64
65	100	100	100	100	100	100	98	97	96	63	29	65
66	100	100	100	100	100	100	100	100	100	73	26	66
67	100	100	100	100	100	100	100	100	99	64	24	67
68	100	100	100	100	100	100	100	100	99	64	23	68
69	100	100	100	100	100	100	100	99	98	69	37	69
70	100	100	100	100	98	97	96	89	63	20	5	70
71	100	100	100	100	100	99	97	90	59	21	6	71
72	100	100	100	100	100	100	100	97	69	23	8	72
73	100	100	100	100	100	100	100	97	67	24	8	73
74	100	100	100	100	100	100	100	95	61	14	4	74
75	100	100	100	100	100	99	95	85	57	18	4	75
76	100	100	100	100	96	94	93	82	56	17	5	76
77	100	100	100	100	100	98	96	88	63	22	7	77
78	100	100	100	100	100	98	96	91	68	23	7	78
79	100	100	100	100	100	99	98	89	55	19	8	79
80	100	100	100	100	100	99	98	88	53	16	6	80
81	100	100	100	100	100	100	100	92	65	23	7	81
82	100	100	100	100	97	89	78	53	37	19	7	82
83	100	100	100	100	100	98	93	74	55	29	12	83
84	100	100	100	100	100	94	90	77	63	37	15	84
85	100	100	100	100	100	98	91	72	51	28	16	85
86	100	100	100	100	100	97	93	69	48	21	6	86
87	100	100	100	100	98	96	91	74	56	25	5	87
88	100	100	100	100	97	95	91	74	57	26	9	88
89	100	100	100	100	100	99	89	87	69	42	7	89
90	100	100	100	100	97	79	74	67	46	30	10	90
91	100	100	100	100	95	89	88	77	60	36	15	91
92	100	100	100	100	100	97	93	79	59	33	13	92
93	100	100	100	100	100	99	98	94	86	44	17	93
94	100	100	100	100	100	100	99	96	87	29	10	94
95	100	100	100	100	100	99	98	95	84	36	12	95
96	100	100	100	100	100	100	99	97	90	38	12	96
97	100	100	100	100	100	100	98	95	89	31	12	97
98	100	100	100	100	100	98	97	94	87	35	11	98
99	100	100	100	100	100	100	98	96	91	40	14	99
100	100	100	100	100	100	100	99	97	87	36	14	100
101	100	100	100	100	90	85	83	78	72	28	11	101
102	100	100	100	100	98	96	95	92	85	42	14	102

Sample No.	Sieve size (mm)											Sample No.
	75	63	53	37,5	26,5	19	13,2	4,75	2,00	0,425	0,075	
103	100	100	100	100	100	100	100	97	88	41	16	103
104	100	100	100	100	98	94	91	86	81	50	14	104
105	100	100	100	100	100	98	96	91	82	32	12	105
106	100	100	100	100	100	100	100	97	93	71	20	106
107	100	100	100	100	100	100	100	99	97	70	29	107
108	100	100	100	100	100	100	100	98	94	62	19	108
109	100	100	100	100	100	100	100	99	96	59	20	109
110	100	100	100	100	100	100	100	99	96	56	19	110
111	100	100	100	100	100	100	100	100	96	52	16	111
112	100	100	100	100	100	100	100	99	96	53	13	112
113	100	100	100	100	100	100	100	98	95	50	14	113
114	100	100	100	100	100	100	100	100	97	62	21	114
115	100	100	100	100	100	100	100	100	96	56	22	115
116	100	100	100	100	100	100	100	100	96	59	23	116
117	100	100	100	100	100	100	100	99	96	60	20	117
118	100	100	100	100	100	100	100	99	96	63	21	118
119	100	100	100	100	100	100	100	100	93	49	13	119
120	100	100	100	100	100	100	100	98	93	58	20	120
121	100	100	100	100	100	100	100	98	93	58	22	121
122	100	100	100	100	100	100	100	100	93	50	16	122
123	100	100	100	100	100	100	100	98	93	63	26	123
124	100	100	100	100	100	100	94	90	86	55	16	124
125	100	100	100	100	100	100	99	94	89	64	19	125
126	100	100	100	100	100	97	95	92	90	74	21	126
127	100	100	100	100	100	100	99	95	91	63	14	127
128	100	100	100	100	100	99	98	96	94	71	14	128
129	100	100	100	100	100	93	93	89	85	56	18	129
130	100	100	100	100	100	100	97	96	93	69	21	130
131	100	100	100	100	100	100	100	99	96	73	27	131
132	100	100	100	100	100	100	100	88	84	60	19	132
133	100	100	100	100	100	95	92	90	86	66	26	133
134	100	100	100	100	100	100	100	100	99	67	28	134
135	100	100	100	100	100	100	100	100	99	61	27	135
136	100	100	100	100	100	100	100	100	99	65	26	136
137	100	100	100	100	100	100	100	99	95	60	28	137
138	100	100	100	100	100	100	100	99	97	67	32	138
139	100	100	100	100	100	100	100	99	97	67	31	139
140	100	100	100	100	100	100	100	99	97	64	29	140
141	100	100	100	100	100	100	100	100	99	72	30	141
142	100	100	100	100	100	100	100	100	98	65	33	142
143	100	100	100	100	100	100	100	100	98	69	32	143
144	100	100	100	100	100	100	100	100	98	72	32	144

G-5

Sample	LL*	PI	LS	RD	MDD (kg/m^3)	MDD (% SD)	OMC (%)	CBR (%)	Sample
1	0,00	0,0	0,0	2,65	1978	74,6	11,8	100,0	1
2	0,00	0,0	0,0	2,65	1942	73,3	12,6	122,0	2
3	0,00	0,0	0,0	2,65	2038	76,9	10,6	53,0	3
4	0,25	0,0	0,0	2,65	2191	82,7	12,4	98,0	4
5	0,00	0,0	0,0	2,65	2234	84,3	9,3	122,0	5
6	0,00	0,0	0,0	2,65	2045	77,2	9,2	80,0	6
7	0,25	0,0	0,0	2,65	2025	76,4	12,0	82,0	7
8	0,25	10,0	4,5	2,65	2053	77,5	12,2	96,0	8
9	0,25	15,0	5,0	2,65	2034	76,8	11,5	98,0	9
10	0,25	12,0	6,5	2,65	2035	76,8	11,4	74,0	10
11	0,25	10,0	4,5	2,65	2025	76,4	12,8	103,0	11
12	0,25	3,0	2,0	2,65	1973	74,5	14,2	90,0	12
13	0,25	5,2	3,7	2,65	2031	76,6	11,9	81,0	13
14	0,25	6,0	2,5	2,65	2056	77,6	11,0	80,0	14
15	0,25	4,0	2,0	2,65	2036	76,8	10,7	74,0	15
16	0,25	4,0	2,0	2,65	1990	75,1	13,9	68,0	16
17	0,25	0,0	0,0	2,65	2052	77,4	11,9	70,0	17
18	27,00	9,0	4,0	2,65	2087	78,8	11,1	17,0	18
19	25,00	11,0	5,0	2,65	2082	78,6	11,2	24,0	19
20	22,00	9,0	4,0	2,65	2054	77,5	9,3	15,0	20
21	26,00	10,0	5,0	2,65	2025	76,4	11,4	15,0	21
22	28,00	11,0	5,0	2,65	2068	78,0	7,7	30,0	22
23	28,00	11,0	5,0	2,65	1910	72,1	12,9	27,0	23
24	27,00	10,0	5,0	2,65	2041	77,0	10,1	28,0	24
25	27,00	11,0	5,0	2,65	2099	79,2	8,6	21,0	25
26	26,00	9,0	4,0	2,65	2098	79,2	10,0	18,0	26
27	29,00	14,0	7,0	2,65	2113	79,7	9,1	19,0	27
28	29,00	14,0	5,0	2,65	2110	79,6	9,8	27,0	28
29	30,00	13,0	6,0	2,65	2087	78,8	10,2	15,0	29
30	28,00	14,0	5,0	2,65	2043	77,1	7,7	18,0	30
31	24,00	3,0	1,7	2,65	1978	74,6	10,0	145,0	31
32	25,00	4,0	2,0	2,65	1975	74,5	11,0	101,0	32
33	19,00	2,0	1,3	2,65	1985	74,9	10,5	149,0	33
34	26,00	4,0	2,0	2,65	1966	74,2	10,9	138,0	34
35	27,00	3,0	1,3	2,65	1935	73,0	11,9	162,0	35
36	26,00	5,0	2,0	2,65	1974	74,5	10,8	127,0	36
37	25,00	4,0	1,9	2,65	1915	72,3	11,8	111,0	37
38	24,00	2,0	1,3	2,65	1935	73,0	11,1	126,0	38
39	28,00	4,0	2,7	2,65	1891	71,4	12,4	107,0	39
40	24,00	4,0	2,0	2,65	1992	75,2	11,0	172,0	40
41	30,00	6,0	3,0	2,65	1966	74,2	11,9	115,0	41
42	21,00	4,0	1,9	2,65	1988	75,0	10,8	127,0	42
43	25,00	6,0	2,7	2,65	2030	76,6	10,4	92,0	43
44	23,00	4,0	2,0	2,65	1977	74,6	10,5	104,0	44
45	25,00	5,0	2,3	2,65	2007	75,7	10,8	103,0	45
46	26,00	5,0	2,3	2,65	1994	75,2	10,5	129,0	46
47	25,00	6,0	2,7	2,65	1980	74,7	11,1	122,0	47
48	24,00	4,0	2,0	2,65	1980	74,7	11,1	122,0	48
49	28,00	6,0	2,8	2,65	2005	75,7	10,9	101,0	49
50	26,00	6,0	2,3	2,65	2008	75,8	10,6	111,0	50
51	28,00	7,0	3,0	2,65	2004	75,6	10,9	86,0	51

Sample	LL*	PI	LS	RD (kg/m^3)	MDD (% SD)	MDD (%)	OMC (%)	CBR	Sample
52	25,00	5,0	2,3	2,65	1995	75,3	10,7	103,0	52
53	27,00	4,0	2,0	2,65	1996	75,3	11,0	88,0	53
54	18,00	4,0	2,0	2,65	2018	76,2	9,6	5,4	54
55	23,00	6,0	3,2	2,65	2053	77,5	9,5	4,0	55
56	24,00	7,0	3,3	2,65	2028	76,5	9,7	10,0	56
57	22,00	6,0	3,5	2,65	2028	76,5	9,7	4,8	57
58	27,00	10,0	4,2	2,65	2006	75,7	9,8	17,0	58
59	23,00	8,0	3,7	2,65	2050	77,4	9,5	3,8	59
60	22,00	8,0	4,0	2,65	2108	79,5	8,7	3,7	60
61	20,00	7,0	3,5	2,65	2129	80,3	6,8	3,8	61
62	21,00	8,0	4,0	2,65	1989	75,1	9,7	3,9	62
63	29,00	12,0	6,0	2,65	2035	76,8	9,5	3,8	63
64	25,00	10,0	4,9	2,65	2050	77,4	10,1	3,2	64
65	28,00	12,0	6,0	2,65	2040	77,0	10,0	18,0	65
66	23,00	6,0	3,7	2,65	2031	76,6	9,9	3,4	66
67	23,00	7,0	3,5	2,65	1994	75,2	8,1	12,0	67
68	24,00	7,0	4,0	2,65	2006	75,7	9,1	4,0	68
69	29,00	10,0	4,7	2,65	1954	73,7	12,9	16,0	69
70	0,25	0,0	0,0	2,65	2147	81,0	10,5	160,0	70
71	0,25	0,0	0,0	2,65	2179	82,2	10,7	98,0	71
72	0,00	0,0	0,0	2,65	2178	82,2	12,0	101,0	72
73	0,00	0,0	0,0	2,65	2178	82,2	10,8	123,0	73
74	0,25	0,0	0,0	2,65	2213	83,5	9,2	172,0	74
75	0,25	0,0	0,0	2,65	2171	81,9	9,0	170,0	75
76	0,25	0,0	0,0	2,65	2266	85,5	8,8	220,0	76
77	0,25	0,0	0,0	2,65	2193	82,8	9,3	98,0	77
78	0,25	0,0	0,0	2,65	2201	83,1	9,3	142,0	78
79	0,00	0,0	0,0	2,65	2270	85,7	10,7	112,0	79
80	0,25	0,0	0,0	2,65	2255	85,1	9,3	153,0	80
81	0,25	0,0	0,0	2,65	2115	79,8	10,7	157,0	81
82	0,25	0,0	0,0	2,65	2031	76,6	10,9	61,0	82
83	0,25	0,0	0,0	2,65	1989	75,1	12,1	86,0	83
84	23,00	5,0	3,0	2,65	2006	75,7	11,4	82,0	84
85	22,00	6,0	3,0	2,65	2008	75,8	11,2	88,0	85
86	0,25	0,0	0,0	2,65	2040	77,0	10,0	62,0	86
87	0,25	0,0	0,0	2,65	2070	78,1	9,6	93,0	87
88	0,25	0,0	0,0	2,65	2078	78,4	9,7	98,0	88
89	24,00	8,0	4,0	2,65	2035	76,8	9,8	97,0	89
90	0,25	0,0	0,0	2,65	2006	75,7	10,1	88,0	90
91	0,25	0,0	0,0	2,65	1958	73,9	12,1	132,0	91
92	0,25	0,0	0,0	2,65	2020	76,2	10,4	78,0	92
93	0,25	0,0	0,0	2,65	2110	79,6	7,5	28,0	93
94	0,25	0,0	0,0	2,65	2013	76,0	11,1	34,0	94
95	0,25	0,0	0,0	2,65	2092	78,9	8,2	32,0	95
96	0,25	0,0	0,0	2,65	2039	76,9	9,5	27,0	96
97	0,25	0,0	0,0	2,65	2024	76,4	9,7	30,0	97
98	0,25	0,0	0,0	2,65	1988	75,0	9,4	32,0	98
99	0,25	0,0	0,0	2,65	2013	76,0	9,4	23,0	99
100	0,25	0,0	0,0	2,65	2088	78,8	6,7	27,0	100
101	0,25	0,0	0,0	2,65	2110	79,6	9,3	35,0	101
102	0,25	0,0	0,0	2,65	2166	81,7	8,2	40,0	102
103	0,25	0,0	0,0	2,65	2087	78,8	8,8	31,0	103
104	0,25	0,0	0,0	2,65	2088	78,8	9,0	23,0	104

Sample	LL*	PI	LS	RD (kg/m^3)	MDD (% SD)	MDD (%)	OMC (%)	CBR	Sample
105	0,25	0,0	0,0	2,65	2073	78,2	9,3	35,0	105
106	28,00	6,0	2,5	2,65	1973	74,5	11,7	131,0	106
107	26,00	5,0	2,3	2,65	1968	74,3	11,2	220,0	107
108	26,00	4,0	2,0	2,65	1950	73,6	12,4	138,0	108
109	29,00	4,0	2,0	2,65	1946	73,4	12,8	148,0	109
110	28,00	4,0	2,0	2,65	1946	73,4	12,8	185,0	110
111	27,00	4,0	2,3	2,65	1997	75,4	10,6	222,0	111
112	27,00	4,0	2,3	2,65	1970	74,3	11,1	184,0	112
113	26,00	4,0	2,3	2,65	1967	74,2	11,3	185,0	113
114	27,00	6,0	3,3	2,65	1989	75,1	11,0	204,0	114
115	27,00	4,0	2,0	2,65	1997	75,4	10,7	250,0	115
116	27,00	4,0	2,0	2,65	1997	75,4	10,7	200,0	116
117	30,00	5,0	2,8	2,65	1930	72,8	10,7	107,0	117
118	29,00	4,0	2,0	2,65	1932	72,9	12,5	102,0	118
119	26,00	4,0	2,0	2,65	2010	75,8	10,5	194,0	119
120	26,00	5,0	2,7	2,65	2018	76,2	10,2	180,0	120
121	26,00	4,0	2,0	2,65	1987	75,0	10,0	118,0	121
122	24,00	2,0	1,7	2,65	1940	73,2	10,7	230,0	122
123	25,00	7,0	3,3	2,65	1967	74,2	10,0	149,0	123
124	20,00	1,0	1,0	2,65	2020	76,2	9,7	135,0	124
125	21,00	2,0	1,0	2,65	2020	76,2	9,7	146,0	125
126	20,00	2,0	1,1	2,65	1996	75,3	10,5	121,0	126
127	23,00	4,0	2,0	2,65	2023	76,3	9,2	103,0	127
128	22,00	4,0	1,7	2,65	2031	76,6	9,7	135,0	128
129	23,00	4,0	1,7	2,65	1992	75,2	10,5	102,0	129
130	21,00	3,0	1,3	2,65	2009	75,8	10,3	95,0	130
131	21,00	3,0	1,5	2,65	2008	75,8	10,3	113,0	131
132	21,00	4,0	2,0	2,65	1981	74,8	10,4	113,0	132
133	22,00	4,0	1,3	2,65	2021	76,3	9,8	108,0	133
134	26,00	9,0	4,0	2,65	2007	75,7	10,2	37,0	134
135	25,00	8,0	3,7	2,65	2056	77,6	8,8	34,0	135
136	22,00	6,0	3,0	2,65	2077	78,4	8,0	35,0	136
137	25,00	9,0	4,3	2,65	2039	76,9	9,7	4,2	137
138	30,00	12,0	5,7	2,65	2014	76,0	10,5	30,0	138
139	30,00	11,0	5,7	2,65	2014	76,0	10,5	3,4	139
140	30,00	11,0	5,7	2,65	2028	76,5	9,4	4,6	140
141	24,00	7,0	3,3	2,65	2014	76,0	10,2	25,0	141
142	30,00	11,0	3,1	2,65	2030	76,6	10,1	27,0	142
143	22,00	6,0	3,6	2,65	2050	77,4	9,8	4,6	143
144	21,00	6,0	3,1	2,65	2058	77,7	9,8	37,0	144

* for SP LL assumed = 0,25
* for NP LL assumed = 0,00

INDICATOR TEST RESULTS AND COMPACTION TEST RESULTS OF COARSE GRADED MATERIALS USED IN CHAPTER 8

Sample	75	63	53	37,5	26,5	19	13,2	4,75	2	0,425	0,075	Sample
CPA13	100,0	100,0	100,0	100,0	81,5	49,7	20,2	5,9	4,4	3,1	1,5	CPA13
ROSS3	100,0	100,0	100,0	98,3	72,7	45,2	22,2	7,9	5,3	3,5	1,7	ROSS3
IRON3	100,0	100,0	100,0	100,0	67,3	43,6	22,9	9,2	7,9	4,1	1,6	IRON3
NPAA3	100,0	100,0	100,0	100,0	78,4	50,0	24,6	9,1	6,5	4,0	1,9	NPAA3
IRON2	100,0	100,0	100,0	100,0	74,7	54,8	40,8	13,9	8,1	4,1	1,5	IRON2
ROSS1	100,0	100,0	100,0	100,0	79,4	55,2	36,5	15,3	9,6	5,3	2,3	ROSS1
FERRO3	100,0	100,0	100,0	100,0	79,6	63,2	35,0	13,3	9,8	6,0	2,7	FERRO3
CPA11	100,0	100,0	100,0	100,0	87,6	66,1	49,9	17,7	6,4	4,1	1,0	CPA11
NPAE3	100,0	100,0	100,0	100,0	100,0	90,6	46,8	11,9	7,2	4,5	1,9	NPAE3
MANG3	100,0	100,0	100,0	100,0	85,4	62,8	37,0	16,8	11,6	5,9	2,0	MANG3
FERRO1	100,0	100,0	100,0	100,0	88,5	64,0	44,5	16,2	10,5	6,3	2,4	FERRO1
NPAA1	100,0	100,0	100,0	100,0	81,7	57,9	42,1	18,7	11,4	6,9	2,8	NPAA1
MANG2	100,0	100,0	100,0	100,0	87,3	74,4	59,1	19,3	10,1	4,6	1,8	MANG2
CPA12	100,0	100,0	100,0	100,0	89,9	76,2	61,2	22,8	8,3	4,9	0,3	CPA12
IRON1	100,0	100,0	100,0	100,0	78,3	63,7	48,7	23,5	12,3	4,8	1,1	IRON1
NPAA2	100,0	100,0	100,0	100,0	88,3	66,7	51,5	23,7	12,8	7,6	3,1	NPAA2
MANG1	100,0	100,0	100,0	100,0	81,2	61,1	48,2	25,4	14,3	6,6	1,4	MANG1
FERRO2	100,0	100,0	100,0	100,0	94,8	75,5	53,2	22,3	14,1	8,2	2,7	FERRO2
ROSS2	100,0	100,0	100,0	100,0	88,3	69,7	53,4	24,0	14,7	7,8	3,0	ROSS2
NPAE1	100,0	100,0	100,0	100,0	100,0	95,9	80,8	30,0	11,8	5,6	1,5	NPAE1
NPAE2	100,0	100,0	100,0	100,0	100,0	97,5	84,8	30,0	12,3	6,0	1,1	NPAE2
TPA33	100,0	100,0	100,0	94,9	80,5	68,4	52,8	31,8	23,8	14,6	1,8	TPA33
TPA32	100,0	100,0	100,0	92,2	81,7	74,3	64,4	34,6	22,8	12,9	4,3	TPA32
OFS3	100,0	100,0	100,0	100,0	99,0	97,0	83,0	36,0	15,0	5,0	2,0	OFS3
TPA31	100,0	100,0	100,0	100,0	96,9	90,7	79,3	41,8	27,5	15,1	5,0	TPA31

Sample	LL	PI	LS	RD	MDD(vib) (%SD)	OMC(vib) (%)	ZAVMC(vib) (%)	Sample
CPA13	17,00	3,00	2,00	2,756	63,78	1,50	20,60	CPA13
ROSS3	19,00	0,50	0,50	2,640	65,26	0,92	20,16	ROSS3
IRON3	0,00	0,00	0,00	4,232	74,17	1,55	8,23	IRON3
NPAA3	0,00	0,00	0,00	2,989	68,08	1,13	15,69	NPAA3
IRON2	0,00	0,00	0,00	4,232	75,08	1,70	7,84	IRON2
ROSS1	19,00	0,50	0,50	2,640	69,72	1,28	16,45	ROSS1
FERRO3	20,00	4,00	2,00	2,680	69,03	1,89	16,74	FERRO3
CPA11	17,00	3,00	2,00	2,756	68,91	1,98	16,37	CPA11
NPAE3	18,00	4,00	2,00	2,638	69,00	2,27	17,03	NPAE3
MANG3	0,00	0,00	0,00	4,002	76,64	1,92	7,62	MANG3
FERRO1	20,00	4,00	2,00	2,680	69,17	2,08	16,63	FERRO1
NPAA1	0,00	0,00	0,00	2,989	71,06	1,87	13,62	NPAA1
MANG2	0,00	0,00	0,00	4,002	71,99	2,04	9,72	MANG2
CPA12	17,00	3,00	2,00	2,756	69,12	2,17	16,21	CPA12
IRON1	0,00	0,00	0,00	4,232	83,79	4,57	4,57	IRON1
NPAA2	0,00	0,00	0,00	2,989	73,36	2,02	12,15	NPAA2
MANG1	0,00	0,00	0,00	4,002	83,99	4,76	4,76	MANG1
FERRO2	20,00	4,00	2,00	2,680	72,66	2,08	14,04	FERRO2
ROSS2	19,00	0,50	0,50	2,640	74,47	1,74	12,99	ROSS2
NPAE1	18,00	4,00	2,00	2,638	72,20	2,61	14,60	NPAE1
NPAE2	18,00	4,00	2,00	2,638	69,10	2,67	16,95	NPAE2
TPA33	30,00	12,00	6,50	2,752	76,47	5,42	11,18	TPA33
TPA32	30,00	12,00	6,50	2,752	72,95	6,04	13,48	TPA32
OFS3	0,00	0,50	1,00	2,966	89,52	2,85	3,95	OFS3
TPA31	30,00	12,00	6,50	2,752	79,41	7,80	9,42	TPA31

Regression constants for MDDs and moisture regime parameters (coarse gradings)

$C = (\% < 0{,}425\ mm/100)(LL/100)^{0,1}$
$Q = (\% < 0{,}425\ mm/100)(LS)$

		$GF^{0,85}$	C	Q	C^3	Constant	t(0,050)	Degrees of freedom	r^2
MDD (vib)	X Coefficient(s)	73,15136	-148,543	-15,6043	11548,19	52,59602			
	Std Err of Coef.	15,17935	39,83570	15,20867	6256,890	3,714490			
	t-value	4,819136	3,728904	1,026016	1,845676	14,15968	2,086	20	0,680
OMC (vib)	X Coefficient(s)	10,55197	-21,0084	4,464320	560,9068	-1,01611			
	Std Err of Coef.	3,152030	8,271983	3,158120	1299,259	0,771323			
	t-value	3,347673	2,539707	1,413600	0,431712	1,317362	2,086	20	0,828
ZAVMC (vib)	X Coefficient(s)	-44,6293	156,0310	12,15292	-11278,4	23,81786			
	Std Err of Coef.	11,46010	30,07514	11,48224	4723,825	2,804364			
	t-value	4,036612	3,676478	1,579808	4,010296	8,715475	2,086	20	0,708

Test results from the laboratory used to verify CBR-models

CPA4 - Crushed alluvial gravel

CBR (%)	DD (% SD)	MC (%)	SBD (%)	SF (%)	CMC (%)
224,03	81,92	2,83	85,92	3,48	2,95
410,98	83,56	3,35	85,92	3,48	2,95
747,75	88,61	3,84	85,92	3,48	2,95
345,90	89,95	4,27	85,92	3,48	2,95
768,31	87,89	4,25	85,92	3,48	2,95
312,12	82,41	3,70	85,92	3,48	2,95
124,40	79,96	3,10	76,62	5,20	3,68
93,24	81,60	3,98	76,62	5,20	3,68
300,59	87,76	4,66	76,62	5,20	3,68
426,72	88,68	4,96	76,62	5,20	3,68
272,17	88,83	5,23	76,62	5,20	3,68
102,26	80,19	2,73	80,20	3,05	2,87
147,86	82,05	3,42	80,20	3,05	2,87
393,45	86,47	3,83	80,20	3,05	2,87
393,10	86,78	4,30	80,20	3,05	2,87
614,09	88,86	5,55	80,20	3,05	2,87
266,21	81,75	3,03	83,81	2,98	3,08
251,70	81,24	3,87	83,81	2,98	3,08
347,22	85,46	4,46	83,81	2,98	3,08
605,30	88,88	4,85	83,81	2,98	3,08
459,69	89,36	4,97	83,81	2,98	3,08
111,91	80,08	2,85	79,68	3,10	3,25
165,55	81,55	3,63	79,68	3,10	3,25
216,08	84,23	4,46	79,68	3,10	3,25
365,84	87,14	4,94	79,68	3,10	3,25
897,92	88,97	4,73	79,68	3,10	3,25
111,27	80,68	2,86	80,22	3,90	2,99
328,16	82,69	3,71	80,22	3,90	2,99
452,73	86,60	4,22	80,22	3,90	2,99
355,87	86,00	4,81	80,22	3,90	2,99
288,41	88,73	4,87	80,22	3,90	2,99
342,38	81,84	2,63	83,49	5,53	2,99
502,95	82,04	3,48	83,49	5,53	2,99
382,39	84,62	4,03	83,49	5,53	2,99
555,95	87,72	4,75	83,49	5,53	2,99
688,54	87,80	4,83	83,49	5,53	2,99

CPA5 - Crushed granite

243,73	80,84	2,61	75,31	3,94	3,04
109,63	81,99	3,43	75,31	3,94	3,04
79,83	82,44	4,14	75,31	3,94	3,04
169,77	84,39	4,82	75,31	3,94	3,04
595,77	88,48	4,73	75,31	3,94	3,04
149,86	79,51	2,87	74,25	5,53	3,47
124,31	82,01	3,76	74,25	5,53	3,47

CBR (%)	DD (% SD)	MC (%)	SBD (%)	SF (%)	CMC (%)
97,88	81,94	4,56	74,25	5,53	3,47
332,95	87,53	4,98	74,25	5,53	3,47
263,86	87,40	4,96	74,25	5,53	3,47
119,92	79,92	2,35	74,47	3,87	3,11
205,25	79,92	3,08	74,47	3,87	3,11
70,86	80,50	3,71	74,47	3,87	3,11
303,75	85,45	4,34	74,47	3,87	3,11
400,29	87,39	4,81	74,47	3,87	3,11
94,77	79,47	2,77	76,61	5,23	3,22
214,37	81,16	3,51	76,61	5,23	3,22
258,61	82,79	4,39	76,61	5,23	3,22
328,05	86,26	4,84	76,61	5,23	3,22
272,78	87,01	5,23	76,61	5,23	3,22
86,68	75,92	2,59	76,44	7,53	3,15
174,16	80,49	3,49	76,44	7,53	3,15
294,10	82,20	4,27	76,44	7,53	3,15
429,94	84,59	4,94	76,44	7,53	3,15
371,50	87,53	4,96	76,44	7,53	3,15
103,07	79,82	2,52	74,52	5,16	3,20
148,48	79,82	3,16	74,52	5,16	3,20
133,84	80,65	4,13	74,52	5,16	3,20
172,16	85,69	4,53	74,52	5,16	3,20
501,55	87,73	4,82	74,52	5,16	3,20
94,55	77,90	2,44	74,56	6,52	3,42
197,54	79,44	3,20	74,56	6,52	3,42
174,16	82,83	3,91	74,56	6,52	3,42
234,22	82,97	4,64	74,56	6,52	3,42
475,14	87,27	4,90	74,56	6,52	3,42

CPA7 - Crushed dolerite

205,97	79,66	3,30	76,29	3,69	3,35
779,02	88,25	4,09	76,29	3,69	3,35
301,73	87,24	4,53	76,29	3,69	3,35
408,90	85,08	4,97	76,29	3,69	3,35
252,27	86,27	4,86	76,29	3,69	3,35
160,00	77,12	3,77	75,25	4,08	3,76
336,46	86,19	4,67	75,25	4,08	3,76
367,64	86,00	4,78	75,25	4,08	3,76
256,42	85,21	4,76	75,25	4,08	3,76
91,22	76,07	5,06	75,25	4,08	3,76
159,61	79,33	3,31	74,69	4,87	3,47
143,72	81,04	4,13	74,69	4,87	3,47
501,48	87,36	4,49	74,69	4,87	3,47
703,03	87,03	4,31	74,69	4,87	3,47
451,83	86,20	4,63	74,69	4,87	3,47
131,89	76,05	3,23	73,88	9,21	3,83
567,63	83,06	4,17	73,88	9,21	3,83
424,53	86,10	4,86	73,88	9,21	3,83
444,27	82,14	3,46	73,88	9,21	3,83
162,57	81,32	4,79	73,88	9,21	3,83

CBR (%)	DD (% SD)	MC (%)	SBD (%)	SF (%)	CMC (%)
219,45	79,39	3,26	74,17	7,84	3,64
173,63	80,04	4,20	74,17	7,84	3,64
516,69	85,54	4,73	74,17	7,84	3,64
914,39	86,54	4,49	74,17	7,84	3,64
241,58	85,08	4,93	74,17	7,84	3,64
97,97	79,06	3,38	75,25	3,78	3,38
118,15	83,97	4,08	75,25	3,78	3,38
471,35	87,01	4,55	75,25	3,78	3,38
320,03	84,05	4,60	75,25	3,78	3,38
329,08	83,39	4,54	75,25	3,78	3,38
125,73	78,72	2,96	73,71	5,51	3,59
128,01	81,38	3,95	73,71	5,51	3,59
513,73	86,49	4,37	73,71	5,51	3,59
318,56	85,68	4,63	73,71	5,51	3,59
226,13	81,80	4,66	73,71	5,51	3,59
CPA9 - Crushed hornfels					
108,99	78,10	2,47	78,71	8,19	3,73
95,21	77,96	3,50	78,71	8,19	3,73
183,78	84,35	4,04	78,71	8,19	3,73
507,90	88,27	4,42	78,71	8,19	3,73
671,30	87,49	5,29	78,71	8,19	3,73
132,09	80,50	2,90	82,29	6,14	3,94
103,80	81,53	3,81	82,29	6,14	3,94
449,04	87,29	4,44	82,29	6,14	3,94
621,43	86,29	4,88	82,29	6,14	3,94
428,18	88,15	5,30	82,29	6,14	3,94
148,41	74,87	2,07	80,92	9,89	3,29
189,85	80,50	2,91	80,92	9,89	3,29
286,22	83,63	3,62	80,92	9,89	3,29
1090,67	88,90	3,83	80,92	9,89	3,29
517,45	87,75	4,25	80,92	9,89	3,29
78,45	79,17	2,55	79,98	10,19	3,51
149,75	81,60	3,63	79,98	10,19	3,51
205,49	84,92	4,39	79,98	10,19	3,51
908,80	91,46	4,89	79,98	10,19	3,51
508,69	91,35	5,52	79,98	10,19	3,51
190,85	80,57	2,54	75,58	5,92	3,79
215,11	81,01	3,59	75,58	5,92	3,79
128,43	80,93	4,23	75,58	5,92	3,79
1023,08	89,27	4,79	75,58	5,92	3,79
780,95	92,98	5,47	75,58	5,92	3,79
54,26	77,99	2,74	72,61	4,71	3,58
96,04	78,35	3,41	72,61	4,71	3,58
383,35	85,82	3,85	72,61	4,71	3,58
382,91	88,15	4,18	72,61	4,71	3,58
406,36	86,09	4,84	72,61	4,71	3,58
105,99	80,79	2,69	81,01	5,29	3,65
157,44	80,66	3,45	81,01	5,29	3,65
605,43	86,33	3,93	81,01	5,29	3,65
1087,61	87,40	4,28	81,01	5,29	3,65
774,70	88,75	4,87	81,01	5,29	3,65

MANG - Manganese ore

CBR (%)	DD (% SD)	MC (%)	SBD (%)	SF (%)	CMC (%)
181,87	72,23	2,19	75,27	3,04	3,23
101,34	71,42	2,68	75,27	3,04	3,23
273,35	75,69	3,42	75,27	3,04	3,23
163,68	74,19	3,80	75,27	3,04	3,23
299,32	78,16	4,97	75,27	3,04	3,23
70,86	74,11	2,26	75,27	3,04	3,23
118,06	76,89	2,69	75,27	3,04	3,23
118,68	75,81	3,32	75,27	3,04	3,23
112,54	76,89	4,09	75,27	3,04	3,23
234,46	81,78	5,46	75,27	3,04	3,23
115,76	77,41	2,01	75,27	3,04	3,23
161,30	75,51	2,65	75,27	3,04	3,23
155,27	75,76	3,24	75,27	3,04	3,23
240,73	76,01	3,65	75,27	3,04	3,23
177,93	75,05	4,67	75,27	3,04	3,23

IRON - Iron ore

116,90	69,67	2,30	75,52	7,78	3,40
119,42	71,72	2,84	75,52	7,78	3,40
204,99	75,63	3,80	75,52	7,78	3,40
303,37	78,96	4,76	75,52	7,78	3,40
265,75	77,94	5,45	75,52	7,78	3,40
117,65	70,94	2,23	75,52	7,78	3,40
136,25	72,44	2,65	75,52	7,78	3,40
118,06	71,93	3,73	75,52	7,78	3,40
110,68	74,19	4,72	75,52	7,78	3,40
318,21	81,12	6,06	75,52	7,78	3,40
132,85	74,40	1,78	75,52	7,78	3,40
119,40	75,14	2,43	75,52	7,78	3,40
94,99	72,79	3,69	75,52	7,78	3,40
164,10	77,58	4,94	75,52	7,78	3,40
220,19	77,40	3,89	75,52	7,78	3,40
105,90	72,77	4,25	75,52	7,78	3,40
285,69	77,98	4,28	75,52	7,78	3,40
134,69	87,03	4,63	75,52	7,78	3,40
217,78	87,75	5,31	75,52	7,78	3,40
169,16	85,65	5,72	75,52	7,78	3,40
286,54	80,56	5,91	75,52	7,78	3,40
457,79	79,73	6,16	75,52	7,78	3,40
611,79	83,58	4,62	75,52	7,78	3,40
114,18	78,44	4,05	75,52	7,78	3,40

BROWIT - Clayey sand

CBR	DD (% SD)	MC	SBD	SF	CMC
41,26	62,61	6,24	63,12	15,40	5,58
46,88	63,79	8,46	63,12	15,40	5,58
51,87	61,58	10,16	63,12	15,40	5,58
45,63	64,01	13,73	63,12	15,40	5,58
30,40	65,66	6,17	63,12	15,40	5,58
28,60	67,57	6,71	63,12	15,40	5,58
35,13	63,07	6,00	63,12	15,40	5,58
51,88	63,38	7,88	63,12	15,40	5,58
47,24	63,46	9,58	63,12	15,40	5,58
39,22	64,72	12,43	63,12	15,40	5,58
23,09	64,30	6,45	63,12	15,40	5,58
21,89	65,83	6,62	63,12	15,40	5,58
36,12	61,16	6,02	63,12	15,40	5,58
43,58	62,29	8,17	63,12	15,40	5,58
36,53	63,81	10,54	63,12	15,40	5,58
36,79	64,17	12,40	63,12	15,40	5,58
38,63	64,98	13,80	63,12	15,40	5,58
20,60	64,15	16,64	63,12	15,40	5,58
28,69	60,67	6,41	63,12	15,40	5,58
31,18	61,54	8,30	63,12	15,40	5,58
39,11	62,18	9,35	63,12	15,40	5,58
30,77	62,45	12,92	63,12	15,40	5,58
23,80	62,78	14,44	63,12	15,40	5,58
15,84	63,13	17,13	63,12	15,40	5,58
37,79	60,00	6,24	63,12	15,40	5,58
33,95	60,11	8,39	63,12	15,40	5,58
29,42	60,42	9,96	63,12	15,40	5,58
20,44	60,08	13,28	63,12	15,40	5,58
18,14	60,97	14,49	63,12	15,40	5,58
12,85	60,74	17,18	63,12	15,40	5,58
36,28	60,97	6,18	63,12	15,40	5,58
39,80	62,30	8,10	63,12	15,40	5,58
44,07	63,00	9,55	63,12	15,40	5,58
42,81	64,97	11,60	63,12	15,40	5,58
27,66	66,30	14,04	63,12	15,40	5,58
23,06	66,83	16,85	63,12	15,40	5,58
14,43	66,62	17,80	63,12	15,40	5,58
17,07	62,31	22,08	63,12	15,40	5,58
10,86	67,06	17,31	63,12	15,40	5,58
11,11	62,33	21,79	63,12	15,40	5,58
29,06	65,41	17,64	63,12	15,40	5,58
6,95	63,08	22,36	63,12	15,40	5,58
13,87	63,76	18,55	63,12	15,40	5,58
4,89	61,89	22,15	63,12	15,40	5,58
15,32	61,66	18,21	63,12	15,40	5,58
4,26	60,53	22,30	63,12	15,40	5,58
13,62	66,85	17,68	63,12	15,40	5,58
3,93	61,66	22,28	63,12	15,40	5,58